

MIT OpenCourseWare

<http://ocw.mit.edu>

Electromechanical Dynamics

For any use or distribution of this textbook, please cite as follows:

Woodson, Herbert H., and James R. Melcher. *Electromechanical Dynamics*. 3 vols. (Massachusetts Institute of Technology: MIT OpenCourseWare). <http://ocw.mit.edu> (accessed MM DD, YYYY). License: Creative Commons Attribution-NonCommercial-Share Alike

For more information about citing these materials or our Terms of Use, visit: <http://ocw.mit.edu/terms>

ELECTROMECHANICAL DYNAMICS

Part II: Fields, Forces, and Motion

ELECTROMECHANICAL DYNAMICS

Part II: Fields, Forces, and Motion

HERBERT H. WOODSON

**Philip Sporn Professor of Energy Processing
Departments of Electrical and Mechanical Engineering**

JAMES R. MELCHER

**Associate Professor of Electrical Engineering
Department of Electrical Engineering
both of Massachusetts Institute of Technology**

JOHN WILEY & SONS, INC., NEW YORK · LONDON · SYDNEY

To our parents

PREFACE

Part II: Fields, Forces, and Motion

In the early 1950's the option structure was abandoned and a common core curriculum was instituted for all electrical engineering students at M.I.T. The objective of the core curriculum was then, and is now, to provide a foundation in mathematics and science on which a student can build in his professional growth, regardless of the many opportunities in electrical engineering from which he may choose. In meeting this objective, core curriculum subjects cannot serve the needs of any professional area with respect to nomenclature, techniques, and problems unique to that area. Specialization comes in elective subjects, graduate study, and professional activities.

To be effective a core curriculum subject must be broad enough to be germane to the many directions an electrical engineer may go professionally, yet it must have adequate depth to be of lasting value. At the same time, the subject must be related to the real world by examples of application. This is true because students learn by seeing material in a familiar context, and engineering students are motivated largely by the relevance of the material to the realities of the world around them.

In the organization of the core curriculum in electrical engineering at M.I.T. electromechanics is one major component. As our core curriculum has evolved, there have been changes in emphasis and a broadening of the topic. The basic text in electromechanics until 1954, when a new departure was made, was *Electric Machinery* by Fitzgerald and Kingsley. This change produced *Electromechanical Energy Conversion* by White and Woodson, which was used until 1961. At that time we started the revision that resulted in the present book. During this period we went through many versions of notes while teaching the material three semesters a year.

Our objective has always been to teach a subject that combines classical mechanics with the fundamentals of electricity and magnetism. Thus the subject offers the opportunity to teach both mechanics and electromagnetic theory in a context vital to much of the electrical engineering community.

Our choice of material was to some extent determined by a desire to give the student a breadth of background sufficient for further study of almost any type of electromechanical interaction, whether in rotating machinery,

plasma dynamics, the electromechanics of biological systems, or magnetoelasticity. It was also chosen to achieve adequate depth while maintaining suitable unity, but, most important, examples were chosen that could be enlivened for the engineering student interested in the interplay of physical reality and the analytical model. There were many examples from which to choose, but only a few satisfied the requirement of being both mathematically lucid *and* physically demonstrable, so that the student could “push it or see it” and directly associate his observations with symbolic models. Among the areas of electrical engineering, electromechanics excels in offering the opportunity to establish that all-important “feel” for a physical phenomenon. Properly selected electromechanical examples can be the basis for discerning phenomena that are remote from human abilities to observe.

Before discussing how the material can be used to achieve these ends, a review of the contents is in order. The student who uses this book is assumed to have a background in electrostatics and magnetostatics. Consequently, Chapter 1 and Appendix B are essentially a review to define our starting point.

Chapter 2 is a generalization of the concepts of inductance and capacitance that are necessary to the treatment of electromechanical systems; it also provides a brief introduction to rigid-body mechanics. This treatment is included because many curricula no longer cover mechanics, other than particle mechanics in freshman physics. The basic ideas of Chapter 2 are repeated in Chapter 3 to establish some properties of electromechanical coupling in lumped-parameter systems and to obtain differential equations that describe the dynamics of lumped-parameter systems.

Next, the techniques of Chapters 2 and 3 are used to study rotating machines in Chapter 4. Physical models are defined, differential equations are written, machine types are classified, and steady-state characteristics are obtained and discussed. A separate chapter on rotating machines has been included not only because of the technological importance of machines but also because rotating machines are rich in examples of the kinds of phenomena that can be found in lumped-parameter electromechanical systems.

Chapter 5 is devoted to the study, with examples, of the dynamic behavior of lumped-parameter systems. Virtually all electromechanical systems are mathematically nonlinear; nonetheless, linear incremental models are useful for studying the stability of equilibria and the nature of the dynamical behavior in the vicinity of an equilibrium. The second half of this chapter develops the classic potential-well motions and loss-dominated dynamics in the context of electromechanics. These studies of nonlinear dynamics afford an opportunity to place linear models in perspective while forming further insights on the physical significance of, for example, flux conservation and state functions.

Chapter 6 represents our first departure from lumped-parameter systems into continuum systems with a discussion of how observers in relative motion will define and measure field quantities and the related effects of material motion on electromagnetic fields. It is our belief that dc rotating machines are most easily understood in this context. Certainly they are a good demonstration of field transformations at work.

As part of any continuum electromechanics problem, one must know how the electric and magnetic fields are influenced by excitations and motion. In quasi-static systems the distribution of charge and current are controlled by magnetic diffusion and charge relaxation, the subjects of Chapter 7. In Chapter 7 simple examples isolate significant cases of magnetic diffusion or charge relaxation, so that the physical processes involved can be better understood.

Chapters 6 and 7 describe the electrical side of a continuum electro-mechanical system with the material motion predetermined. The mechanical side of the subject is undertaken in Chapter 8 in a study of force densities of electric and magnetic origin. Because it is a useful concept in the analysis of many systems, we introduce the Maxwell stress tensor. The study of useful properties of tensors sets the stage for later use of mechanical stress tensors in elastic and fluid media.

At this point the additional ingredient necessary to the study of continuum electromechanics is the mechanical medium. In Chapter 9 we introduce simple elastic continua—longitudinal motion of a thin rod and transverse motion of wires and membranes. These models are used to study simple continuum mechanical motions (nondispersive waves) as excited electro-mechanically at boundaries.

Next, in Chapter 10 a string or membrane is coupled on a continuum basis to electric and magnetic fields and the variety of resulting dynamic behavior is studied. The unifying thread of this treatment is the dispersion equation that relates complex frequency ω with complex wavenumber k . Without material convection there can be simple nondispersive waves, cut off or evanescent waves, absolute instabilities, and diffusion waves. The effect of material convection on evanescent waves and oscillations and on wave amplification are topics that make a strong connection with electron beam and plasma dynamics. The method of characteristics is introduced as a convenient tool in the study of wave propagation.

In Chapter 11 the concepts and techniques of Chapters 9 and 10 are extended to three-dimensional systems. Strain displacement and stress-strain relations are introduced, with tensor concepts, and simple electromechanical examples of three-dimensional elasticity are given.

In Chapter 12 we turn to a different mechanical medium, a fluid. We first study electromechanical interactions with inviscid, incompressible

fluids to establish essential phenomena in the simplest context. It is here that we introduce the basic notions of MHD energy conversion that can result when a conducting fluid flows through a transverse magnetic field. We also bring in electric-field interactions with fluids, in which ion drag phenomena are used as an example. In addition to these basically conducting processes, we treat the electromechanical consequences of polarization and magnetization in fluids. We demonstrate how highly conducting fluids immersed in magnetic fields can propagate Alfvén waves.

In Chapter 13 we introduce compressibility to the fluid model. This can have a marked effect on electromechanical behavior, as demonstrated with the MHD conduction machine. With compressibility, a fluid will propagate longitudinal disturbances (acoustic waves). A transverse magnetic field and high electrical conductivity modify these disturbances to magnetoacoustic waves.

Finally, in Chapter 14 we add viscosity to the fluid model and study the consequences in electromechanical interactions with steady flow. Hartmann flow demonstrates the effect of viscosity on the dc magnetohydrodynamic machine.

To be successful a text must have a theme; the material must be inter-related. Our philosophy has been to get into the subject where the student is most comfortable, with lumped-parameter (circuit) concepts. Thus many of the subtle approximations associated with quasi-statics are made naturally, and the student is faced with the implications of what he has assumed only after having become thoroughly familiar with the physical significance and usefulness of his approximations. By the time he reaches Chapter 4 he will have drawn a circle around at least a class of problems in which electromagnetic fields interact usefully with media in motion.

In dealing with physical and mathematical subjects, as we are here, in which the job is incomplete unless the student sees the physical laws put to work in some kind of physical embodiment, it is necessary for the thread of continuity to be woven into the material in diverse and subtle ways. A number of attempts have been made, to which we can add our early versions of notes, to write texts with one obvious, pedagogically logical basis for evolving the material; for example, it can be recognized that classes of physical phenomena could be grouped according to the differential equation that describes the pertinent dynamics. Thus we could treat magnetic diffusion, diffusion waves on elastic continua, and viscous diffusion waves in one chapter, even though the physical embodiments are entirely different. Alternatively, we could devise a subject limited to certain technological applications or cover superficially a wide range of basically unrelated topics such as "energy conversion" under one heading. This was the prevalent approach in engineering education a decade or so ago, even at the

undergraduate level. It seems clear to us that organizing material in a teachable and meaningful fashion is far more demanding than this. To confess our own mistakes, our material went originally from the general to the specific; it began with the relativistic form of Maxwell's equations, including the effects of motion, and ended with lumped-parameter devices as special cases. Even if this were a pedagogically tenable approach, which we found it was not, what a bad example to set for students who should be learning to distinguish between the essential and the superfluous! Ideas connected with the propagation of electromagnetic waves (relativistic ideas) must be included in the curriculum, but their connection with media in motion should be made after the student is aware of the first-order issues.

A meaningful presentation to *engineers* must interweave and interrelate mathematical concepts, physical characteristics, the modeling process, and the establishment of a physical "feel" for the world of reality. Our approach is to come to grips with each of these goals as quickly as possible (let the student "get wet" within the first two weeks) and then, while reinforcing what he has learned, continually add something new. Thus, if one looks, he will see the same ideas coming into the flow of material over and over again.

For the organization of this book one should look for many threads of different types. We can list here only a few, in the hope that the subtle reinforcing interplay of mathematical and physical threads will be made evident. Probably the essential theme is Maxwell's equations and the ideas of quasi-statics. The material introduced in Chapter 1 is completely abstract, but it is reinforced in the first few chapters with material that is close to home for the student. By the time he reaches Chapter 10 he will have learned that waves exist which intimately involve electric and magnetic fields that are altogether quasistatic. (This is something that comes as a surprise to many late in life.) Lumped-parameter ideas are based on the integral forms of Maxwell's equations, so that the dynamical effects found with lumped-parameter time constants L/R and RC in Chapter 5 are easily associated with the subjects of magnetic diffusion and charge relaxation. A close tie is made between the "speed voltage" of Chapter 5 and the effects of motion on magnetic fields, as described by field transformations in Chapters 6 to 14. Constant flux dynamics of a lumped coil in Chapter 5 are strongly associated with the dynamics of perfectly conducting continuous media; for example, Alfvén waves in Chapter 12.

Consider another thread of continuity. The book begins with the mathematics of circuit theory. The machines of Chapter 4 are essentially circuits in the sinusoidal steady state. In Chapter 5 we linearize to pursue lumped-parameter ideas of stability and other transient responses and then proceed to nonlinear dynamics, potential-well theory, and other approaches that should form a part of any engineer's mathematical background. By the time

the end of Chapter 10 is reached these ideas will have been carried into the continuum with the addition of tensor concepts, simple cases of the method of characteristics, and eigenvalue theory. The ω - k plot and its implication for all sorts of subjects in modern electrical engineering can be considered as a mathematical or a physical objective. The ideas of stability introduced with ordinary differential equations ($\exp st$) in Chapter 5 evolve into the continuum stability studies of Chapter 10 [$\exp j(\omega t - kx)$] and can be regarded as a mathematical or a physical thread in our treatment. We could list many other threads: witness the evolution of energy and thermodynamic notions from Chapters 3 to 5, 5 to 8, and 8 to 13.

We hope that this book is not just one more in the mathematics of electrical engineering or the technical aspects of rotating machines, transducers, delay lines, MHD converters, and so on, but rather that it is the mathematics, the physics, and, most of all, the engineering combined into one.

The material brought together here can be used in a variety of ways. It has been used by Professors C. N. Weygandt and F. D. Ketterer at the University of Pennsylvania for two subjects. The first restricts attention to Chapters 1 to 6 and Appendix B for a course in lumped-parameter electromechanics that both supplants the traditional one on rotating machines in the electrical engineering curriculum and gives the background required for further study in a second term (elective) covering Chapter 7 and beyond. Professors C. D. Hendricks and J. M. Crowley at the University of Illinois have used the material to follow a format that covers up through Chapter 10 in one term but omits much of the material in Chapter 7. Professor W. D. Getty at the University of Michigan has used the material to follow a one-term subject in lumped-parameter electromechanics taught from a different set of notes. Thus he has been able to use the early chapters as a review and to get well into the later chapters in a one-term subject.

At M.I.T. our curriculum seems always to be in a state of change. It is clear that much of the material, Chapters 1 to 10, will be part of our required (core) curriculum for the foreseeable future, but the manner in which it is packaged is continually changing. During the fall term, 1967, we covered Chapters 1 to 10 in a one-semester subject taught to juniors and seniors. The material from Chapters 4 and 6 on rotating machines was used selectively, so that students had "a foot solidly in the door" on this important subject but also that the coverage could retain an orientation toward the needs of all the diverse areas found in electrical engineering today. We have found the material useful as the basis for early graduate work and as a starting point in several courses related to electromechanics.

Finally, to those who open this book and then close it with the benediction, "good material but unteachable," we apologize because to them we have not made our point. Perhaps not as presented here, but certainly as it is

represented here, this material is rich in teaching possibilities. The demands on the teacher to see the subject in its total context, especially the related problems that lie between the lines, are significant. We have taught this subject many times to undergraduates, yet each term has been more enjoyable than the last. There are so many ways in which drama can be added to the material, and we do not need to ask the students (bless them) when we have been successful in doing so.

In developing this material we have found lecture demonstrations and demonstration films to be most helpful, both for motivation and for developing understanding. We have learned that when we want a student to see a particular phenomenon it is far better for us to do the experiment and let the student focus his attention on what he should see rather than on the wrong connections and blown fuses that result when he tries to do the experiment himself. The most successful experiments are often the simplest—those that give the student an opportunity to handle the apparatus himself. Every student should “chop up some magnetic field lines” with a copper “axe” or he will never really appreciate the subject. We have also found that some of the more complex demonstrations that are difficult and expensive to store and resurrect each semester come through very well in films. In addition to our own short films, three films have been produced professionally in connection with this material for the National Committee on Electrical Engineering Films, under a grant from the National Science Foundation, by the Education Development Center, Newton, Mass.

Synchronous Machines: Electromechanical Dynamics by H. H. Woodson

Complex Waves I: Propagation, Evanescence and Instability by J. R. Melcher

Complex Waves II: Instability, Convection and Amplification by J. R. Melcher

An additional film is in the early stages of production. Other films that are useful have been produced by the Education Development Center for the National Committee on Fluid Mechanics Films and for the College Physics Film Program. Of particular interest, from the former series, is *Magnetohydrodynamics* by Arthur Shercliff.

A book like this can be produced only with plenty of assistance. We gratefully acknowledge the help we received from many directions and hope we have forgotten no one after seven years of work. First of all we want to acknowledge our students with whom we worked as the material developed. They are the one most essential ingredient in an effort of this sort. Next we want to thank Dr. S. I. Freedman, Professor H. H. Richardson, and Dr. C. V. Smith, Jr., for their assistance in framing worthwhile approaches to several of our key topics. In seven years we have had the help of many able

teachers in presenting this material to students. Their discussions and advice have been most useful. In this category we want particularly to mention Professors H. A. Haus, P. L. Penfield, D. C. White, G. L. Wilson, R. Gallager, and E. Pierson and Doctors J. Reynolds, W. H. Heiser, and A. Kusko. Professor Ketterer, who has taught this material at M.I.T. and the University of Pennsylvania, Professors C. D. Hendricks and J. M. Crowley, who have taught it at M.I.T. and the University of Illinois, and Professor W. D. Getty, who has taught it at M.I.T. and the University of Michigan, have been most generous with their comments. Messrs. Edmund Devitt, John Dressler, and Dr. Kent Edwards have checked the correctness of many of the mathematical treatments. Such a task as typing a manuscript repeatedly is enough to try the patience of anyone. Our young ladies of the keyboard, Miss M. A. Daly, Mrs. D. S. Figgins, Mrs. B. S. Morton, Mrs. E. M. Holmes, and Mrs. M. Mazroff, have been gentle and kind with us.

A lengthy undertaking of this sort can be successful only when it has the backing of a sympathetic administration. This work was started with the helpful support of Professor P. Elias, who was then head of the Department of Electrical Engineering at M.I.T. It was finished with the active encouragement of Professor L. D. Smullin, who is presently head of the Department.

Finally, and most sincerely, we want to acknowledge the perseverance of our families during this effort. Our wives, Blanche S. Woodson and Janet D. Melcher, have been particularly tolerant of the demands of this work.

This book appears in three separately bound, consecutively paged parts that can be used individually or in any combination. Flexibility is ensured by including with each part a complete Table of Contents and Index. In addition, for convenient reference, Parts II and III are supplemented by brief appendices which summarize the relevant material from the preceding chapters. Part II, Chapters 7 to 10, develops interactions between moving media and fields with simple mechanical models that illustrate the dynamics of continuum electromechanical systems.

H. H. Woodson
J. R. Melcher

CONTENTS

Part I: Discrete Systems

| | | |
|----------|------------------------------------------|-----------|
| 1 | Introduction | 1 |
| 1.0 | Introduction | 1 |
| 1.0.1 | Scope of Application | 2 |
| 1.0.2 | Objectives | 4 |
| 1.1 | Electromagnetic Theory | 5 |
| 1.1.1 | Differential Equations | 6 |
| 1.1.2 | Integral Equations | 9 |
| 1.1.3 | Electromagnetic Forces | 12 |
| 1.2 | Discussion | 12 |
| 2 | Lumped Electromechanical Elements | 15 |
| 2.0 | Introduction | 15 |
| 2.1 | Circuit Theory | 16 |
| 2.1.1 | Generalized Inductance | 17 |
| 2.1.2 | Generalized Capacitance | 28 |
| 2.1.3 | Discussion | 34 |
| 2.2 | Mechanics | 35 |
| 2.2.1 | Mechanical Elements | 36 |
| 2.2.2 | Mechanical Equations of Motion | 49 |
| 2.3 | Discussion | 55 |
| 3 | Lumped-Parameter Electromechanics | 60 |
| 3.0 | Introduction | 60 |
| 3.1 | Electromechanical Coupling | 60 |
| 3.1.1 | Energy Considerations | 63 |
| 3.1.2 | Mechanical Forces of Electric Origin | 67 |
| 3.1.3 | Energy Conversion | 79 |
| 3.2 | Equations of Motion | 84 |
| 3.3 | Discussion | 88 |

| | | |
|----------|----------------------------------------------------|------------|
| 4 | Rotating Machines | 103 |
| 4.0 | Introduction | 103 |
| 4.1 | Smooth-Air-Gap Machines | 104 |
| 4.1.1 | Differential Equations | 106 |
| 4.1.2 | Conditions for Conversion of Average Power | 110 |
| 4.1.3 | Two-Phase Machine | 111 |
| 4.1.4 | Air-Gap Magnetic Fields | 114 |
| 4.1.5 | Discussion | 117 |
| 4.1.6 | Classification of Machine Types | 119 |
| 4.1.7 | Polyphase Machines | 142 |
| 4.1.8 | Number of Poles in a Machine | 146 |
| 4.2 | Salient-Pole Machines | 150 |
| 4.2.1 | Differential Equations | 151 |
| 4.2.2 | Conditions for Conversion of Average Power | 154 |
| 4.2.3 | Discussion of Saliency in Different Machine Types | 156 |
| 4.2.4 | Polyphase, Salient-Pole, Synchronous Machines | 157 |
| 4.3 | Discussion | 165 |
| 5 | Lumped-Parameter Electromechanical Dynamics | 179 |
| 5.0 | Introduction | 179 |
| 5.1 | Linear Systems | 180 |
| 5.1.1 | Linear Differential Equations | 180 |
| 5.1.2 | Equilibrium, Linearization, and Stability | 182 |
| 5.1.3 | Physical Approximations | 206 |
| 5.2 | Nonlinear Systems | 213 |
| 5.2.1 | Conservative Systems | 213 |
| 5.2.2 | Loss-Dominated Systems | 227 |
| 5.3 | Discussion | 233 |
| 6 | Fields and Moving Media | 251 |
| 6.0 | Introduction | 251 |
| 6.1 | Field Transformations | 255 |
| 6.1.1 | Transformations for Magnetic Field Systems | 260 |
| 6.1.2 | Transformations for Electric Field Systems | 264 |
| 6.2 | Boundary Conditions | 267 |
| 6.2.1 | Boundary Conditions for Magnetic Field Systems | 270 |
| 6.2.2 | Boundary Conditions for Electric Field Systems | 277 |
| 6.3 | Constituent Relations for Materials in Motion | 283 |
| 6.3.1 | Constituent Relations for Magnetic Field Systems | 284 |
| 6.3.2 | Constituent Relations for Electric Field Systems | 289 |
| 6.4 | DC Rotating Machines | 291 |

| | | |
|--------------------------------------------------------|---------------------------------------------------------|------------|
| 6.4.1 | Commutator Machines | 292 |
| 6.4.2 | Homopolar Machines | 312 |
| 6.5 | Discussion | 317 |
| Appendix A Glossary of Commonly Used Symbols | | A1 |
| Appendix B Review of Electromagnetic Theory | | B1 |
| B.1 | Basic Laws and Definitions | B1 |
| B.1.1 | Coulomb's Law, Electric Fields and Forces | B1 |
| B.1.2 | Conservation of Charge | B5 |
| B.1.3 | Ampere's Law, Magnetic Fields and Forces | B6 |
| B.1.4 | Faraday's Law of Induction and the Potential Difference | B9 |
| B.2 | Maxwell's Equations | B12 |
| B.2.1 | Electromagnetic Waves | B13 |
| B.2.2 | Quasi-static Electromagnetic Field Equations | B19 |
| B.3 | Macroscopic Models and Constituent Relations | B25 |
| B.3.1 | Magnetization | B25 |
| B.3.2 | Polarization | B27 |
| B.3.3 | Electrical Conduction | B30 |
| B.4 | Integral Laws | B32 |
| B.4.1 | Magnetic Field System | B32 |
| B.4.2 | Electric Field System | B36 |
| B.5 | Recommended Reading | B37 |
| Appendix C Mathematical Identities and Theorems | | C1 |
| Index | | 1 |
| Part II: Fields, Forces, and Motion | | |
| 7 | Magnetic Diffusion and Charge Relaxation | 330 |
| 7.0 | Introduction | 330 |
| 7.1 | Magnetic Field Diffusion | 335 |
| 7.1.1 | Diffusion as an Electrical Transient | 338 |
| 7.1.2 | Diffusion and Steady Motion | 347 |
| 7.1.3 | The Sinusoidal Steady-State in the Presence of Motion | 355 |
| 7.1.4 | Traveling Wave Diffusion in Moving Media | 364 |
| 7.2 | Charge Relaxation | 370 |
| 7.2.1 | Charge Relaxation as an Electrical Transient | 372 |
| 7.2.2 | Charge Relaxation in the Presence of Steady Motion | 380 |
| 7.2.3 | Sinusoidal Excitation and Charge Relaxation with Motion | 392 |
| 7.2.4 | Traveling-Wave Charge Relaxation in a Moving Conductor | 397 |
| 7.3 | Conclusion | 401 |

| | | |
|-----------|------------------------------------------------------------|------------|
| 8 | Field Description of Magnetic and Electric Forces | 418 |
| 8.0 | Introduction | 418 |
| 8.1 | Forces in Magnetic Field Systems | 419 |
| 8.2 | The Stress Tensor | 423 |
| 8.2.1 | Stress and Traction | 424 |
| 8.2.2 | Vector and Tensor Transformations | 434 |
| 8.3 | Forces in Electric Field Systems | 440 |
| 8.4 | The Surface Force Density | 445 |
| 8.4.1 | Magnetic Surface Forces | 447 |
| 8.4.2 | Electric Surface Forces | 447 |
| 8.5 | The Magnetization and Polarization Force Densities | 450 |
| 8.5.1 | Examples with One Degree of Freedom | 451 |
| 8.5.2 | The Magnetization Force Density | 456 |
| 8.5.3 | The Stress Tensor | 462 |
| 8.5.4 | Polarization Force Density and Stress Tensor | 463 |
| 8.6 | Discussion | 466 |
| 9 | Simple Elastic Continua | 479 |
| 9.0 | Introduction | 479 |
| 9.1 | Longitudinal Motion of a Thin Rod | 480 |
| 9.1.1 | Wave Propagation Without Dispersion | 487 |
| 9.1.2 | Electromechanical Coupling at Terminal Pairs | 498 |
| 9.1.3 | Quasi-statics of Elastic Media | 503 |
| 9.2 | Transverse Motions of Wires and Membranes | 509 |
| 9.2.1 | Driven and Transient Response, Normal Modes | 511 |
| 9.2.2 | Boundary Conditions and Coupling at Terminal Pairs | 522 |
| 9.3 | Summary | 535 |
| 10 | Dynamics of Electromechanical Continua | 551 |
| 10.0 | Introduction | 551 |
| 10.1 | Waves and Instabilities in Stationary Media | 554 |
| 10.1.1 | Waves Without Dispersion | 555 |
| 10.1.2 | Cutoff or Evanescent Waves | 556 |
| 10.1.3 | Absolute or Nonconvective Instability | 566 |
| 10.1.4 | Waves with Damping, Diffusion Waves | 576 |
| 10.2 | Waves and Instabilities in the Presence of Material Motion | 583 |
| 10.2.1 | Fast and Slow Waves | 586 |
| 10.2.2 | Evanescence and Oscillation with Convection | 596 |
| 10.2.3 | Convective Instability or Wave Amplification | 601 |
| 10.2.4 | “Resistive Wall” Wave Amplification | 608 |

| | | |
|---------------------------------------------------------|------------------------------------------------|-----------|
| 10.3 | Propagation | 613 |
| 10.3.1 | Phase Velocity | 613 |
| 10.3.2 | Group Velocity | 614 |
| 10.3.3 | Characteristics and the Velocity of Wavefronts | 618 |
| 10.4 | Dynamics in Two Dimensions | 621 |
| 10.4.1 | Membrane Dynamics: Two-Dimensional Modes | 622 |
| 10.4.2 | Moving Membrane: Mach Lines | 624 |
| 10.4.3 | A Kink Instability | 627 |
| 10.5 | Discussion | 636 |
| Appendix D Glossary of Commonly Used Symbols | | D1 |
| Appendix E Summary of Part I and Useful Theorems | | E1 |
| Index | | 1 |

Part III: Elastic and Fluid Media

| | | |
|-----------|--------------------------------------------------------------|------------|
| 11 | Introduction to the Electromechanics of Elastic Media | 651 |
| 11.0 | Introduction | 651 |
| 11.1 | Force Equilibrium | 652 |
| 11.2 | Equations of Motion for Isotropic Media | 653 |
| 11.2.1 | Strain-Displacement Relations | 653 |
| 11.2.2 | Stress-Strain Relations | 660 |
| 11.2.3 | Summary of Equations | 666 |
| 11.3 | Electromechanical Boundary Conditions | 668 |
| 11.4 | Waves in Isotropic Elastic Media | 671 |
| 11.4.1 | Waves in Infinite Media | 671 |
| 11.4.2 | Principal Modes of Simple Structures | 679 |
| 11.4.3 | Elastic Vibrations of a Simple Guiding Structure | 693 |
| 11.5 | Electromechanics and Elastic Media | 696 |
| 11.5.1 | Electromagnetic Stresses and Mechanical Design | 697 |
| 11.5.2 | Simple Continuum Transducers | 704 |
| 11.6 | Discussion | 717 |
| 12 | Electromechanics of Incompressible, Inviscid Fluids | 724 |
| 12.0 | Introduction | 724 |
| 12.1 | Inviscid, Incompressible Fluids | 726 |
| 12.1.1 | The Substantial Derivative | 726 |
| 12.1.2 | Conservation of Mass | 729 |
| 12.1.3 | Conservation of Momentum (Newton's Second Law) | 731 |
| 12.1.4 | Constituent Relations | 735 |

| | | |
|-------------------|----------------------------------------------------------------------|------------|
| 12.2 | Magnetic Field Coupling with Incompressible Fluids | 737 |
| 12.2.1 | Coupling with Flow in a Constant-Area Channel | 739 |
| 12.2.2 | Coupling with Flow in a Variable-Area Channel | 751 |
| 12.2.3 | Alfvén Waves | 759 |
| 12.2.4 | Ferrohydrodynamics | 772 |
| 12.3 | Electric Field Coupling with Incompressible Fluids | 776 |
| 12.3.1 | Ion-Drag Phenomena | 776 |
| 12.3.2 | Polarization Interactions | 783 |
| 12.4 | Discussion | 787 |
| 13 | Electromechanics of Compressible, Inviscid Fluids | 813 |
| 13.0 | Introduction | 813 |
| 13.1 | Inviscid, Compressible Fluids | 813 |
| 13.1.1 | Conservation of Energy | 814 |
| 13.1.2 | Constituent Relations | 815 |
| 13.2 | Electromechanical Coupling with Compressible Fluids | 820 |
| 13.2.1 | Coupling with Steady Flow in a Constant-Area Channel | 821 |
| 13.2.2 | Coupling with Steady Flow in a Variable-Area Channel | 828 |
| 13.2.3 | Coupling with Propagating Disturbances | 841 |
| 13.3 | Discussion | 854 |
| 14 | Electromechanical Coupling with Viscous Fluids | 861 |
| 14.0 | Introduction | 861 |
| 14.1 | Viscous Fluids | 862 |
| 14.1.1 | Mathematical Description of Viscosity | 862 |
| 14.1.2 | Boundary Conditions | 873 |
| 14.1.3 | Fluid-Mechanical Examples | 875 |
| 14.2 | Electromechanical Coupling with Viscous Fluids | 878 |
| 14.2.1 | Electromechanical Coupling with Shear Flow | 878 |
| 14.2.2 | Electromechanical Coupling with Pressure-Driven Flow (Hartmann Flow) | 884 |
| 14.3 | Discussion | 893 |
| Appendix F | Glossary of Commonly Used Symbols | F1 |
| Appendix G | Summary of Parts I and II, and Useful Theorems | G1 |
| Index | | 1 |

ELECTROMECHANICAL DYNAMICS

Part II: Fields, Forces, and Motion

Chapter 7

MAGNETIC DIFFUSION AND CHARGE RELAXATION

7.0 INTRODUCTION

There are two important reasons for introducing a distributed or continuum description of electromechanical interactions. The most obvious is that the mechanical system may be an elastic or fluid medium, with the electric or magnetic force distributed throughout. In this case the electrical and mechanical equations of motion are likely to have both time and space coordinates as independent variables. As we shall see in later chapters, there is a need for this model when the dynamical times of interest (say the period of a sinusoidal excitation) are on the same order as the time required for a disturbance to propagate from one extreme to another in the mechanical system.*

The second reason for introducing a continuum model concerns characteristic times that arise because of competing energy storage and dissipation mechanisms in the electrical system; for example, a lumped inductance L , shunted by a resistance R , constitutes a simple magnetic field system. In the absence of motion (which could change the inductance L) this circuit has a time constant L/R . The response of the circuit to an excitation depends greatly on the time constant (or period) of the excitation relative to L/R . Similarly, the behavior of magnetic field systems involving conducting materials depends considerably on the relative values of times associated with the motion or with electrical excitation and times that characterize the competing energy storage and dissipation phenomena. This point can best be made in terms of a simple example.

* Note that we neglected similar electromagnetic propagational effects starting in Chapter 1, when the quasi-static electric and magnetic field systems were introduced. This is an extremely good approximation in most systems because the velocity of light is usually much greater than any velocity of propagation for a mechanical or an electromechanical disturbance.

Figure 7.0.1 shows what can be thought of as a one-turn inductor (the perfectly conducting plates short-circuited at the end by a perfectly conducting plate) shunted by a resistance (the block with a conductivity σ). Suppose that the plates are excited at the left end by a sinusoidally varying current source with the frequency ω . At very low frequencies (essentially direct current) we know that this current will flow through the perfectly conducting end plate. As the frequency is raised, however, the rate of change of the time-varying magnetic field will induce a voltage across the block and a current will flow through it between the top and bottom plates. In terms of lumped-parameter models, we could determine this current by attributing a resistance to the block. The block itself, however, has finite dimensions, and we could think of breaking it into two sections and modeling each section by

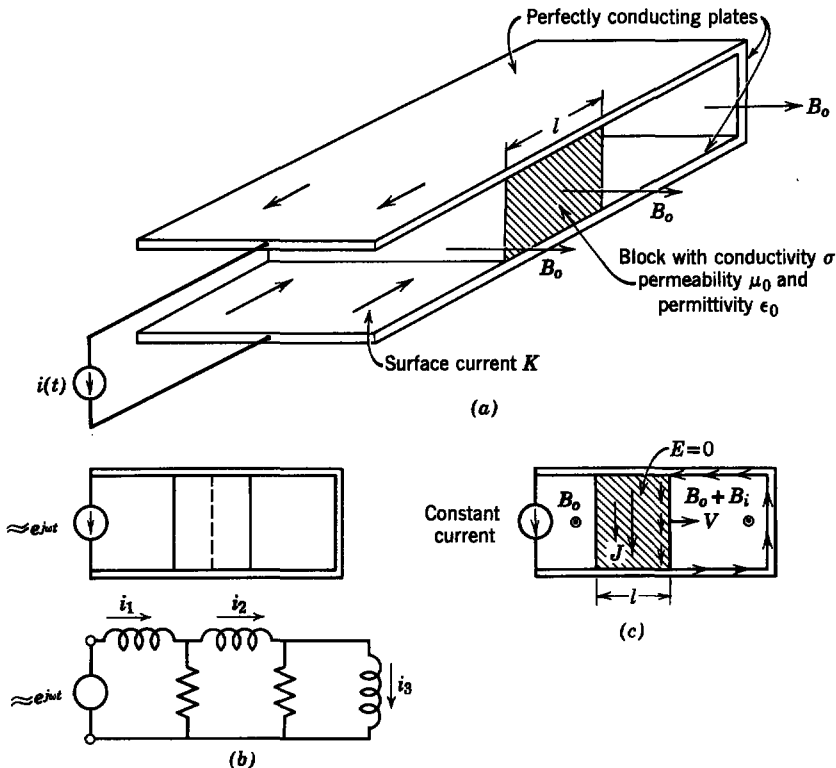


Fig. 7.0.1 (a) A pair of perfectly conducting plates short-circuited at one end by a perfectly conducting plate and driven at the other end by a current source: a block of conductivity σ makes electrical contact between the plates as shown; (b) equivalent circuit that shows the effect of magnetic diffusion on the currents induced in the block when the source is time-varying; (c) block moving with a velocity V induces currents that can alter the imposed magnetic field significantly.

a resistance. We now have the equivalent circuit shown in Fig. 7.0.1*b*, in which it is easy to see that at very low frequencies $i_1 = i_2 = i_3$. As the frequency is raised, the reactances become significant and $i_1 > i_2 > i_3$. In fact, at very high frequencies we expect that current i_3 will be very small. This simple problem points up why a continuum model is required. If the currents i_1 and i_2 are not equal (i.e., if the current through the block is not uniform) to a degree that depends on the dynamical nature of the excitation, what value of resistance do we use to characterize the block? A similar problem exists in attributing one or more equivalent inductances to the system. Our dilemma is brought about by not knowing where the currents flow or, to put it another way, of not knowing how the magnetic field is distributed in space. In the following sections a knowledge of the distribution of magnetic field is our objective, as we discuss the physical phenomenon of *magnetic diffusion*.

In the situation just discussed the time that determined the appropriate system model was $2\pi/\omega$, or the period of excitation. In electromechanical problems the motion is responsible for introducing characteristic times which also play an important role in determining the distribution of magnetic field. This can be illustrated by considering again the system of Fig. 7.0.1, this time with the block moving with the velocity V , as shown in Fig. 7.0.1*c*, and with constant excitation current.

We might model this system by assuming that the constant magnetic flux density B_o , induced by the current source, is the only magnetic field everywhere between the plates. Then, because of the perfectly conducting end plate, the electric field E between the plates would be zero. It follows [from (6.3.5)] (Ohm's law for moving media is $\mathbf{J}' = \sigma\mathbf{E}'$, where field transformations (Table 6.1, Appendix E) require that $\mathbf{E}' = \mathbf{E} + \mathbf{v} \times \mathbf{B}$ and $\mathbf{J}'_f = \mathbf{J}_f$.) that the motion induces a current density J of

$$J = VB_o\sigma. \quad (7.0.1)$$

(Here for purposes of illustration we assume that the plates have sufficient extent to justify plane parallel geometry.) Now, we could use this current, together with the imposed magnetic field B_o , to compute the magnetic force on the block. In doing so, however, we assume that the magnetic field induced by the current J is negligible compared with the imposed field B_o . We can establish when this assumption is valid by computing the addition B_i to the magnetic flux density to the right of the moving block. Constraints on the problem require that J flow through the end plate to the right, where there is an addition to the surface current K of

$$K_i = Jl. \quad (7.0.2)$$

Hence the induced magnetic field in the region to the right is

$$B_i = \mu_0 Jl. \quad (7.0.3)$$

It follows from (7.0.1) and (7.0.3) that the ratio of the induced magnetic field to the imposed magnetic field is

$$\frac{B_i}{B_o} = \mu_0 \sigma V l = R_m. \quad (7.0.4)$$

This dimensionless quantity is called the *magnetic Reynolds number*.^{*} From our example we know that if R_m is significant compared with unity the magnetic field will be altered appreciably by the motion. Of course, this means that the distribution of current within the block will also be dependent on the motion. From (7.0.4) a block with a large dimension l , a large velocity V , or a high conductivity σ will require a continuum model to determine the current distribution. One of our objectives in the sections that follow is to indicate electromechanical models that can be used under various conditions of the excitation and mechanical motion.

In electric field systems we are concerned about the distribution of charge and the associated electric field. Here we can think of a simple system in which a resistance R is connected in series with a capacitance C . The time constant is then RC , and when the period of an excitation is on the order of this time we expect that lumped parameter models may be of dubious significance.

Consider, as an example, the system shown in Fig. 7.0.2. Here, a resistive sheet is placed adjacent to a pair of perfectly conducting electrodes with the potential difference v . A circuit model for this system is shown in Fig. 7.0.2*b*, where the plates form capacitors with the resistive sheet and the sheet is modeled by a single resistance. A more refined model, also shown in Fig. 7.0.2*b*, divides each of the capacitors into two sections and recognizes that the outermost capacitances are connected to a larger series resistance than the inner capacitances.

It is apparent from this latter model that the distribution of charge among the capacitances (hence on the surface of the sheet) is dependent on the frequency of excitation. At very low frequencies the charge would be evenly distributed among the capacitances. As the frequency is raised, the outside capacitances, which have larger series resistances, will support less charge than the inside capacitances. Thus we are in a dilemma about how the capacitances and resistances should be computed and a continuum model is appropriate.

A case in which material motion can have an effect on the charge distribution is shown in Fig. 7.0.2*c*. Here the resistive sheet moves to the right with the velocity V . If the motion has a negligible effect on the surface charge,

^{*} See, for example, W. F. Hughes, and F. J. Young, *The Electromagnetodynamics of Fluids*, Wiley, New York (1966), p. 154.

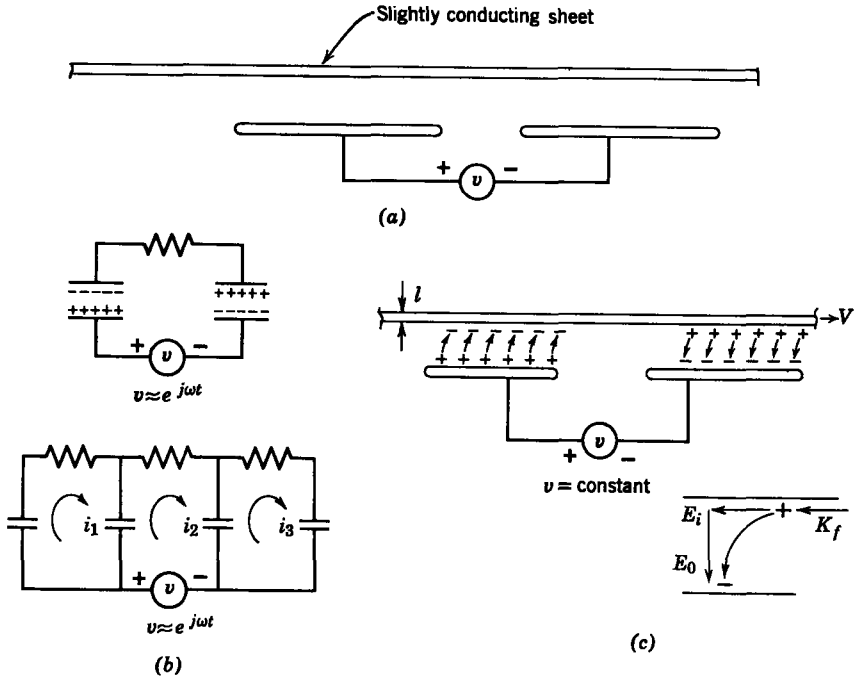


Fig. 7.0.2 (a) A slightly conducting sheet is placed adjacent to a pair of perfectly conducting plates with the potential difference v ; (b) equivalent circuit for case in which excitation is sinusoidal: each section of the sheet can be thought of as forming a capacitor with the opposite electrode, but each capacitance has a different series resistance, as shown by the bottom, more refined, circuit; (c) the motion of the sheet, moving with velocity V and a constant potential difference on the plates, induces a shift in the charge distribution and an electric field E_i .

the electric field intensity E_0 in the section to the right is related to the surface charge density σ_f by

$$\sigma_f = \epsilon_0 E_0. \tag{7.0.5}$$

We model the resistive material as a sheet having conductivity σ ; hence Ohm's law written in the moving frame of the material requires that $\mathbf{K}'_f = \sigma l \mathbf{E}'_i$, where l is the sheet thickness. Field transformations* then require $\mathbf{K}'_f = \mathbf{K}_f - \sigma_f \mathbf{V}$ and $\mathbf{E}'_i = \mathbf{E}_i$ so that

$$K_f = \sigma l E_i - \sigma_f V. \tag{7.0.6}$$

In the steady state there is no current to the right; hence $K_f = 0$. From (7.0.6) there is then an induced electric field intensity given by

$$E_i = \frac{\sigma_f V}{\sigma l}. \tag{7.0.7}$$

* Table 6.1, Appendix E.

It follows from this expression and (7.0.5) that the ratio of the induced electric field intensity E_i to the imposed electric field intensity E_0 is

$$\frac{E_i}{E_0} = \frac{\epsilon_0 V}{\sigma l} = R_e \quad (7.0.8)$$

This dimensionless ratio R_e is called the *electric Reynolds number*.^{*} When this number is significant compared with unity, motion has an appreciable effect on the charge distribution. To understand situations of this kind a continuum model is required.

In the sections that follow we first undertake a study of magnetic field systems (magnetic diffusion) and then electric field systems (charge relaxation). As we have illustrated, our objective is to use a series of examples as vehicles for establishing an understanding of situations in which the distributions of currents and charges are not known until after the problem has been solved.

7.1 MAGNETIC FIELD DIFFUSION

In quasi-static magnetic field systems, which consist primarily of magnetizable and conducting materials, magnetic field diffusion is the principal phenomenon that determines what further approximations can be made. Because a general problem is virtually impossible to solve, we will explore diffusion by using a set of simple examples.

To set the stage for studying these examples we first review the mathematical description of a magnetic field system. We assume all materials (magnetizable and/or conducting) to be electrically linear and isotropic. Thus we write the field equations as [see Table 1.2 and (6.3.5.)]†

$$\nabla \times \mathbf{H} = \mathbf{J}_f, \quad (7.1.1)$$

$$\nabla \cdot \mathbf{B} = 0, \quad (7.1.2)$$

$$\mathbf{B} = \mu \mathbf{H}, \quad (7.1.3)$$

$$\nabla \times \mathbf{E} = - \frac{\partial \mathbf{B}}{\partial t}, \quad (7.1.4)$$

$$\mathbf{J}_f = \sigma(\mathbf{E} + \mathbf{v} \times \mathbf{B}). \quad (7.1.5)$$

In these equations the velocity \mathbf{v} of the conducting material is measured with respect to the inertial coordinate system in which all the field quantities are measured. For our present treatment we assume that the velocity \mathbf{v} is independently specified as a function of space and time. After we have introduced

^{*} O. M. Stuetzer, "Magnetohydrodynamics and Electrohydrodynamics," *Phys. Fluids*, 5, No. 3, 534-544 (May 1962).

† See Table 1.2, Appendix E, and footnote on p. 332.

continuum mechanics, in later chapters, we shall be prepared to treat situations in which the velocity \mathbf{v} is a dependent variable.

To illustrate the different phenomena that can occur it is helpful to eliminate all but one variable from (7.1.1) to (7.1.5) and study the resulting expression. For this purpose we assume that the materials are homogeneous (this means that μ and σ are not functions of space but that they may be functions of time) and eliminate all variables except the flux density \mathbf{B} . We use (7.1.5) to eliminate \mathbf{E} from (7.1.4).

$$\frac{1}{\sigma} \nabla \times \mathbf{J}_f - \nabla \times (\mathbf{v} \times \mathbf{B}) = - \frac{\partial \mathbf{B}}{\partial t}. \quad (7.1.6)$$

Next, we use (7.1.3) to eliminate \mathbf{H} from (7.1.1):

$$\frac{1}{\mu} \nabla \times \mathbf{B} = \mathbf{J}_f. \quad (7.1.7)$$

The curl of this expression, substituted into (7.1.6), yields

$$\frac{1}{\mu\sigma} \nabla \times (\nabla \times \mathbf{B}) - \nabla \times (\mathbf{v} \times \mathbf{B}) = - \frac{\partial \mathbf{B}}{\partial t}. \quad (7.1.8)$$

We use a vector identity* and (7.1.2) to rewrite the first term on the left of (7.1.8) and obtain the desired expression involving a single dependent variable, the magnetic flux density \mathbf{B} :

$$- \frac{1}{\mu\sigma} \nabla^2 \mathbf{B} + \frac{\partial \mathbf{B}}{\partial t} = \nabla \times (\mathbf{v} \times \mathbf{B}). \quad (7.1.9)$$

This equation describes the distribution of magnetic field in the conducting medium.† It includes both the effects of the time-varying magnetic field and the material motion, hence it can be used to analyze the situations shown in Fig. 7.0.1. In a continuum electromechanical problem (7.1.9) plays the same role as the electrical circuit equations played in the lumped-parameter magnetic field systems of the preceding chapters. In fact, there is considerable analogy between (7.1.9) and electrical circuit equations that we encountered in Chapters 3 to 6; for example, the dynamics of a coil in a magnetic field were described in Section 5.1.3 by (5.1.31):

$$-i_1 R - L_1 \frac{di_1}{dt} = AB_o \cos \theta \frac{d\theta}{dt}, \quad (7.1.10)$$

* $\nabla \times (\nabla \times \mathbf{B}) = \nabla(\nabla \cdot \mathbf{B}) - \nabla^2 \mathbf{B}$.

† This equation assumes great importance in the determination of magnetic field origins in the liquid core of the earth. In this context it is sometimes referred to as Bullard's equation. (See T. G. Cowling, *Magnetohydrodynamics*, Interscience, New York, 1957, pp. 4, 77.)

where R and L_1 are the resistance and inductance of a coil that rotates in the flux density B_0 with the angular displacement θ . This expression states that the voltage developed by the motion of the coil in the magnetic field (the "speed voltage" on the right-hand side) is taken up by the voltage drop across the resistance and the inductance of the coil. Similarly, the right-hand side of (7.1.9) is a rate of change of the flux density caused by the motion, and this change is taken up by a flux change due to ohmic dissipation ($-(1/\mu\sigma)\nabla^2\mathbf{B}$) and by a time rate of change of flux density ($\partial\mathbf{B}/\partial t$) at the point.

In the absence of material motion (7.1.9) reduces to the *diffusion equation*.*

$$\frac{1}{\mu\sigma}\nabla^2\mathbf{B} = \frac{\partial\mathbf{B}}{\partial t}. \quad (7.1.11)$$

This expression is appropriate to the analysis of a problem such as that shown in Fig. 7.0.1*b*, in which the conductor is fixed and the distribution of magnetic field is required. We can think of it as a continuum representation of the dynamics of a distributed system of inductances and resistances. In Section 7.1.1 an example is presented to establish the physical phenomena represented by (7.1.11).

A second limiting case of (7.1.9) of considerable importance results when there is motion but steady-state conditions have been established. Then (7.1.9) reduces to

$$-\frac{1}{\mu\sigma}\nabla^2\mathbf{B} = \nabla \times (\mathbf{v} \times \mathbf{B}). \quad (7.1.12)$$

Here the increase in flux density due to the motion is entirely absorbed by the ohmic dissipation in the material. Physical situations consistent with this limit are considered in Section 7.1.2.

Some of the most important engineering applications involving magnetic diffusion are made possible because there are time-varying excitations in the presence of material motion. The induction machine of Section 4.1.6*b* is an example of an interaction of this type. In general, (7.1.9) is required to analyze these problems, which are exemplified in Sections 7.1.3 and 7.1.4. In fact, the example considered in Section 7.1.4 illustrates the significance of the lumped parameter model for an induction machine.

* This form of equation is found to describe a variety of dissipative continuum phenomena, including heat conduction, neutron diffusion, and the diffusion of fluid vorticity. See, for example, R. B. Bird, W. E. Stewart, and E. N. Lightfoot, *Transport Phenomena*, Wiley, New York, 1960, p. 352. A. M. Weinberg and E. P. Wigner, *The Physical Theory of Neutron Chain Reactors*, University of Chicago Press, Chicago, 1958, p. 194. H. Schlichting, *Boundary Layer Theory*, McGraw-Hill, New York, 1960, p. 58.

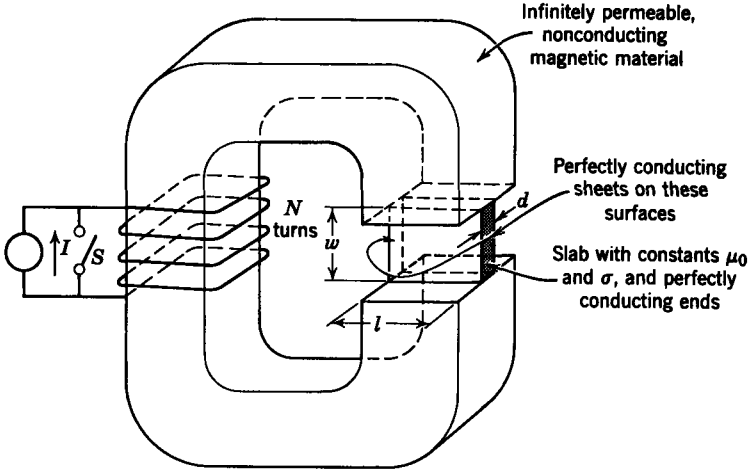


Fig. 7.1.1 System for studying magnetic diffusion as an electrical transient. A slab of conducting material is placed in the gap of a magnetic circuit excited by a step function of current. An end view of the slab is shown in Fig. 7.1.2.

7.1.1 Diffusion as an Electrical Transient

To obtain a firm understanding of the basic electromagnetic phenomena that occur in magnetic field systems we consider first a simple example in which all materials are at rest and we study the diffusion of a magnetic field into (or out of) a rectangular slab of material. The physical situation is shown in Fig. 7.1.1. The system consists of an electromagnet made of

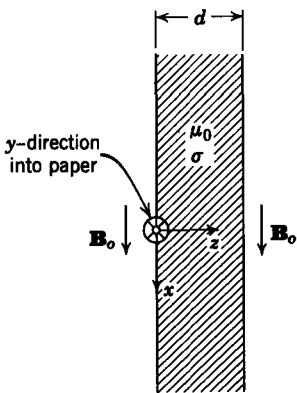


Fig. 7.1.2 Coordinate system for studying one-dimensional diffusion. At time $t = 0^+$ the magnetic field is distributed as shown in Fig. 7.1.3.

infinitely permeable, nonconducting magnetic material with an air gap of length w and excited through the N -turn winding by a constant-current source I which can be turned on or off by the switch S . In the air gap is a slab of non-magnetizable ($\mu = \mu_0$) material of the dimensions shown and with constant electrical conductivity σ .

We assume that the switch S is initially closed so that there is no current through the winding and no flux in the magnet. At $t = 0$ switch S is opened, and we wish to determine the time history of the flux density near the center of the slab. The coordinate system is defined in Fig. 7.1.2. We assume that the slab width w and length l are large enough compared with the thickness d to consider the slab as

infinitely large in the x - and y -directions. Moreover, we neglect fringing at the edges of the air gap; consequently, the flux density will have only an x -component. With switch S opened at $t = 0$, the boundary conditions on the slab are for $t > 0$, $z < 0$, $z > d$,

$$\mathbf{B} = \mathbf{i}_x B_o, \quad (7.1.13)$$

where B_o (see Section 2.1.1) is given by

$$B_o = \frac{\mu_o N I}{w}. \quad (7.1.14)$$

In this one-dimensional problem there is only an x -component of \mathbf{B} and it varies only with z ; thus we write the x -component of (7.1.11) as

$$\frac{1}{\mu_o \sigma} \frac{\partial^2 B_x}{\partial z^2} = \frac{\partial B_x}{\partial t}. \quad (7.1.15)$$

Within the slab ($0 < z < d$) the flux density is zero immediately after the switch S is opened

$$\text{at } t = 0^+; \quad B_x = 0. \quad (7.1.16)$$

This condition follows from (7.1.6) with $\mathbf{v} = 0$, which we integrate around an arbitrary fixed contour within the conductor. Then by Stokes's theorem we have

$$\frac{1}{\sigma} \oint_C \mathbf{J}_f \cdot d\mathbf{l} = - \frac{\partial}{\partial t} \int_S \mathbf{B} \cdot \mathbf{n} \, da.$$

If \mathbf{B} has a finite value just after the switch is opened, the time derivative on the right (assuming that the integral encloses some \mathbf{B} field) will be infinite. It follows that (because the contour of integration is arbitrary) the current density \mathbf{J}_f will be infinite. Because this is not physically reasonable, we argue that the flux density \mathbf{B} remains zero just after the switch S is opened or that the condition of (7.1.16) holds. If the contour encloses the boundary at $z = 0$ or $z = d$, the term on the right is infinite, thus indicating an infinite \mathbf{J}_f , which is actually a finite surface current density necessary to terminate the B_o field. This mathematical idealization results from the assumption that the external flux density B_o is established in zero time. In a real situation the flux density B_o will be established rapidly but at a finite rate. This idealization is better understood after the solution is completed. The process is analogous to the use of singularity functions in circuit theory to simplify mathematical analyses.

It should be clear that after a sufficiently long time all transient currents in the slab will die out and the flux density will be uniform throughout the slab,

$$\text{as } t \rightarrow \infty, \quad B_x = B_o, \quad (7.1.17)$$

for then $\partial B_x / \partial t = 0$ in (7.1.15) for steady-state conditions.

To effect a solution of this problem we assume a separable solution of the form

$$B_x = \hat{B}(z)e^{-\alpha t} + B_0. \quad (7.1.18)$$

Substitution of this expression into 7.1.15 and cancellation of the exponential factor yields

$$\frac{1}{\mu_0\sigma} \frac{d^2\hat{B}}{dz^2} = -\alpha\hat{B}. \quad (7.1.19)$$

This equation has a solution

$$\hat{B} = C_1 \sin \sqrt{\mu_0\sigma\alpha} z + C_2 \cos \sqrt{\mu_0\sigma\alpha} z. \quad (7.1.20)$$

Thus the general solution is

$$B_x = (C_1 \sin \sqrt{\mu_0\sigma\alpha} z + C_2 \cos \sqrt{\mu_0\sigma\alpha} z)e^{-\alpha t} + B_0. \quad (7.1.21)$$

This equation must satisfy the initial conditions illustrated in the sketch of B_x as a function of z in Fig. 7.1.3. We can achieve this by setting

$$C_2 = 0$$

and expanding the rectangular distribution in a Fourier sine series.

Using the initial condition expressed by (7.1.16) and illustrated in Fig. 7.1.3, we write $B_x(z, 0^+)$ as

$$0 = \sum_{n=1}^{\infty} a_n \sin \frac{n\pi z}{d} + B_0. \quad (7.1.22)$$

Comparison of (7.1.21) with $C_2 = 0$ and (7.1.22) shows that each term in the series has

$$\alpha_n = \frac{n^2\pi^2}{\mu_0\sigma d^2} \quad (7.1.23)$$

We evaluate the coefficients a_n in the standard way by multiplying both sides

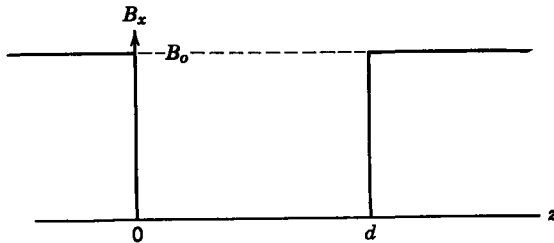


Fig. 7.1.3 Distribution of B_x at $t = 0^+$ in the conducting slab of Fig. 7.1.2. The magnetic field distribution for $t > 0$ is shown in Fig. 7.1.4.

(7.1.22) by $\sin m\pi z/d$ and integrating

$$\int_0^d -B_o \sin \frac{m\pi z}{d} dz = \int_0^d \sum_{n=1}^{\infty} a_n \sin \frac{n\pi z}{d} \sin \frac{m\pi z}{d} dz. \quad (7.1.24)$$

All of the terms on the right for which $m \neq n$ integrate to zero. Thus (7.1.24) reduces to

$$\int_0^d -B_o \sin \frac{n\pi z}{d} dz = \int_0^d a_n \sin^2 \frac{n\pi z}{d} dz. \quad (7.1.25)$$

Evaluation of the integral yields

$$\begin{aligned} a_n &= -\frac{4}{n\pi} B_o, & n \text{ odd,} \\ a_n &= 0, & n \text{ even,} \end{aligned} \quad (7.1.26)$$

and we write the complete solution for B_x as

$$B_x = B_o \left(1 - \sum_{n \text{ odd}} \frac{4}{n\pi} \sin \frac{n\pi z}{d} e^{-\alpha_n t} \right). \quad (7.1.27)$$

In the solution (7.1.27) we see that each space harmonic damps at a different rate, the higher harmonics damping faster. We define the fundamental time constant τ as

$$\tau = \frac{1}{\alpha_1} = \frac{\mu_0 \sigma d^2}{\pi^2} \quad (7.1.28)$$

and write (7.1.27) as

$$B_x = B_o \left(1 - \sum_{n \text{ odd}} \frac{4}{n\pi} \sin \frac{n\pi z}{d} e^{-n^2 t/\tau} \right). \quad (7.1.29)$$

The fundamental time constant of (7.1.28), which is the longest time constant of the series, is usually called the *diffusion time constant* of the system.

The distribution of flux density, as expressed by (7.1.29), is plotted for several instants of time in Fig. 7.1.4. At $t = 0$ the magnetic flux is excluded completely from the interior of the slab. As time progresses the flux diffuses into the slab. Because the higher space harmonics damp out faster, only three terms in the series are needed to calculate the curve at $t = 0.1\tau$; only two terms are necessary for $t = 0.3\tau$; and only the first term has appreciable value for $t > \tau$. Thus it is clear why the fundamental diffusion time τ is the controlling time constant in the diffusion process. It is also clear from Fig. 7.1.4 that the field has almost completely diffused into the slab in a time $t > 3\tau$.

It is also instructive to investigate the behavior of the current density inside the slab during this transient diffusion process. The currents created by

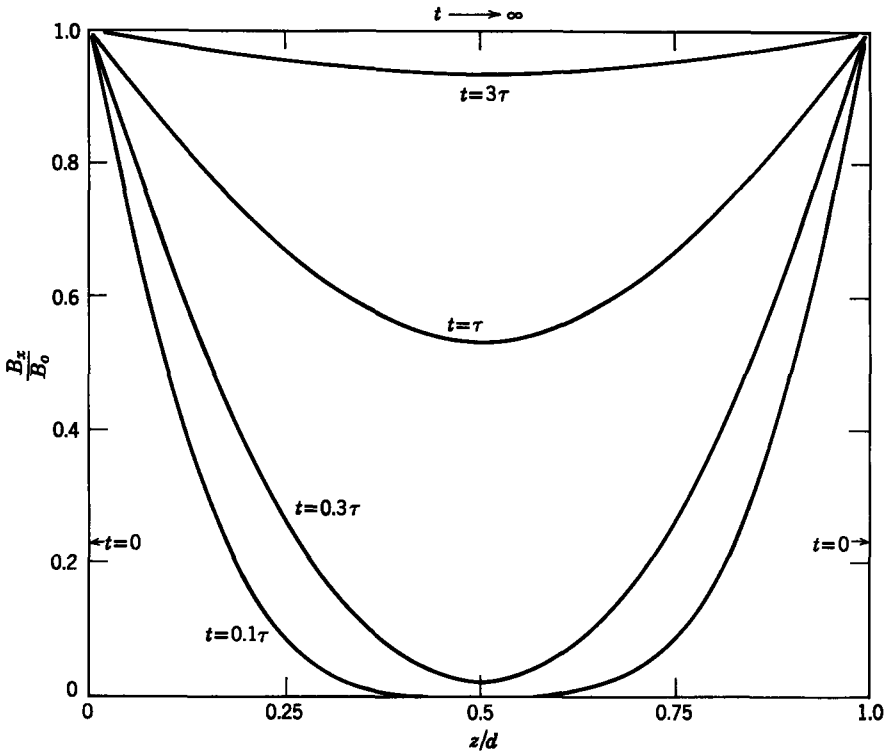


Fig. 7.1.4 Transient, one-dimensional diffusion of a magnetic field into a conducting material. The slab of conductor shown in Figs. 7.1.1 and 7.1.2 is viewed here from the end, as shown in Fig. 7.1.2.

induction in this way are often called *eddy currents*. We use (7.1.7) with the definitions of our present one-dimensional example (see Fig. 7.1.2) to obtain

$$J_y = \frac{1}{\mu_0} \frac{\partial B_x}{\partial z} = -\frac{B_0}{\mu_0 d} \sum_{n \text{ odd}} 4 \cos \frac{n\pi z}{d} e^{-n^2 t/\tau}. \tag{7.1.30}$$

The space distribution of this current density is plotted for several instants of time in Fig. 7.1.5. Note that at $t = 0$ the series does not converge at $z = 0$ and $z = d$. This shows that at $t = 0$ the magnetic field is excluded completely from the slab and, to terminate the external tangential field, a surface current density is required [see (6.2.14)]*. A surface current density implies an infinite volume current density; thus at $t = 0$ there are impulses of J_y at $z = 0$ and $z = d$, as shown in Fig. 7.1.5. As time progresses, the currents diffuse into the slab and decay. At the surface of the slab ($z = 0$ or $z = d$) the current density decays continuously, but at an interior point the current density increases from zero to some maximum value and decays back to zero.

* Table 6.1, Appendix E.

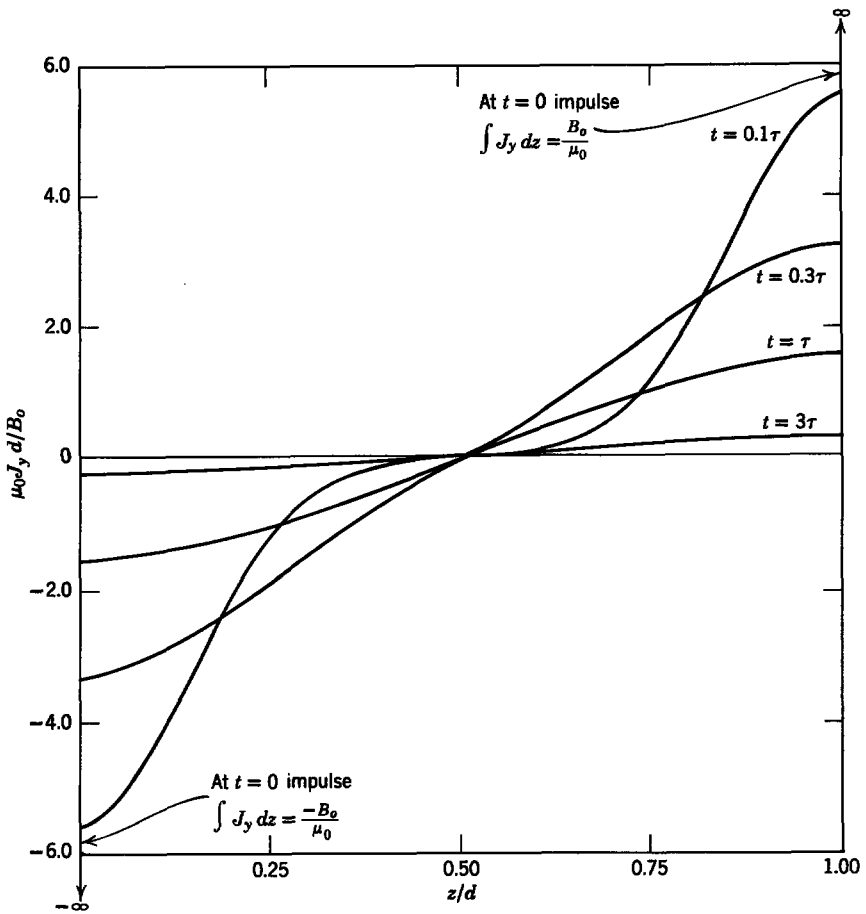


Fig. 7.1.5 Current distribution in transient one-dimensional diffusion.

Conservation of current requires that the current that flows down one side of the block must return on the opposite side. Hence the current distribution of Fig. 7.1.5 has odd symmetry about $z = d/2$. Note that the one-dimensional solution implies perfectly conducting end plates on the slab to provide a return path for the currents.

It should be clear from a study of Figs. 7.1.4 and 7.1.5 that if we are interested in electromagnetic phenomena that occur outside the slab and that have characteristic times much shorter than the diffusion time τ we can approximate the properties of the slab by saying that $\sigma \rightarrow \infty$. In this approximation the flux is excluded from the interior of the slab and currents flow on the surfaces.

On the other hand, when we are concerned with phenomena with characteristic times that are long compared with the diffusion time τ , we can

neglect perturbations due to diffusion effects for field calculations. These two limiting cases are illuminated more thoroughly in additional examples to follow. They are analogous to the constant current and constant flux conditions of the lumped-parameter system described in Section 5.1.3.

We can now state the physical conditions necessary for our mathematical idealization to be accurate. If the flux density B_0 produced by current in the winding in Fig. 7.1.1 builds up in a time much smaller than the diffusion time constant, then our approximation of the boundary conditions at $t = 0^+$ is valid. In any case, the mathematical model is least accurate for very small time, as should be evident from a careful comparison of the results of the analysis with physical reasoning about the sequence of events in a real system.

To illustrate the range of diffusion time constants that may be encountered with conducting media conventionally used in electromechanical systems (7.1.28) is used to obtain the plots of diffusion time constants as functions of slab thickness shown in Fig. 7.1.6. For a slab of copper 1 cm thick the diffusion time constant is approximately 1 msec, whereas for a seeded combustion gas, 1 m thick, the time constant is approximately 10 μ sec. Note that although the conductivity of silicon iron is more than an order of magnitude less than that of copper the diffusion time is longer because the permeability is so high. [In general $\mu_0 \rightarrow \mu$ in (7.1.28) for magnetizable materials.] It is this long diffusion time that makes lamination of iron cores necessary in ac equipment of all types.

Because magnetic diffusion is described basically by Maxwell's equations, it occurs in both lumped-parameter and continuum systems. The analyses of Section 5.1.3 described magnetic diffusion in lumped-parameter systems, although this terminology was not used there. It is often helpful when considering continuum systems to reason qualitatively in terms of lumped-parameter models. Consequently, we consider a lumped-parameter system that provides an approximation of the diffusion process just discussed.

The conducting block of Fig. 7.1.1 is replaced with two perfectly conducting sheets short-circuited at one end and connected at the other end by a conductance G , as shown in Fig. 7.1.7. If, as before, we ignore fringing, the flux densities B_1 and B_2 are related to the currents by

$$B_2 = \frac{\mu_0 N i_2}{w}, \quad (7.1.31)$$

$$B_1 = \frac{\mu_0 N i_2}{w} - \frac{\mu_0 i_1}{w}, \quad (7.1.32)$$

where i_2 is the coil current in Fig. 7.1.1. Then the flux linked by the terminals

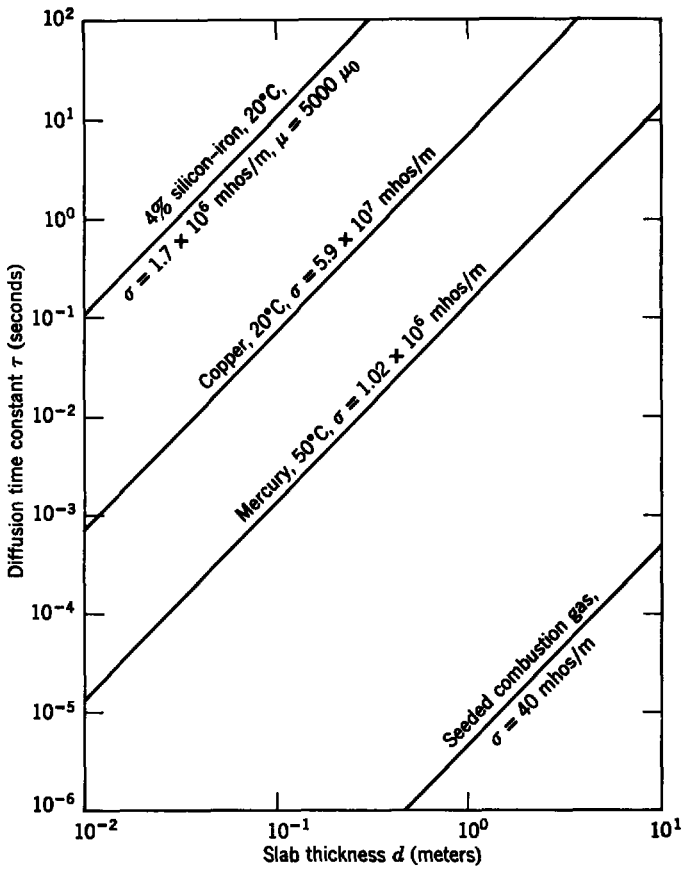


Fig. 7.1.6 Diffusion time constants $\mu\sigma d^2/\pi^2$.

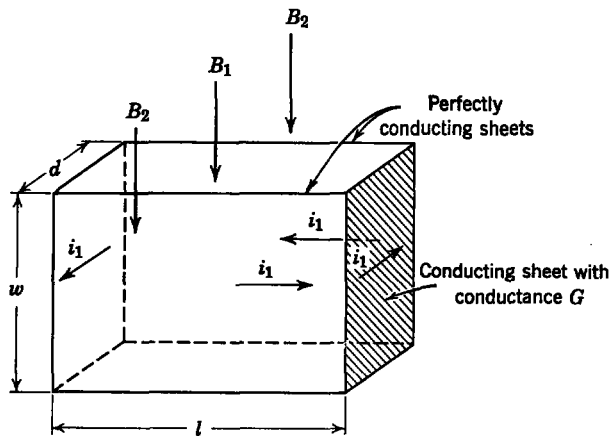


Fig. 7.1.7 A one-turn inductor used to replace the conducting block in Fig. 7.1.1.

of the inductor formed by the conducting sheets is

$$\lambda_1 = -dlB_1 = Li_1 - Mi_2, \tag{7.1.33}$$

where

$$L = \frac{dl\mu_0}{w},$$

$$M = \frac{dl\mu_0 N}{w}.$$

The circuit equation is then

$$GL \frac{di_1}{dt} + i_1 = GM \frac{di_2}{dt}. \tag{7.1.34}$$

In our example the current i_2 is a step function of magnitude I . Hence the solution to (7.1.34) for i_1 is

$$i_1 = INe^{-t/GL}, \tag{7.1.35}$$

where the definitions of L and M have been used.

The flux densities follow from (7.1.31) and (7.1.32). Outside the conductors for $t > 0$,

$$B = B_2 = \frac{\mu_0 NI}{w}, \tag{7.1.36}$$

whereas between the conductors

$$B = B_1 = \frac{\mu_0 NI}{w} (1 - e^{-t/GL}). \tag{7.1.37}$$

This distribution of flux is shown in Fig. 7.1.8. When the switch is closed, there is no magnetic field between the conductors and a current exists to exclude the field. Then the interior region fills up with magnetic field at a

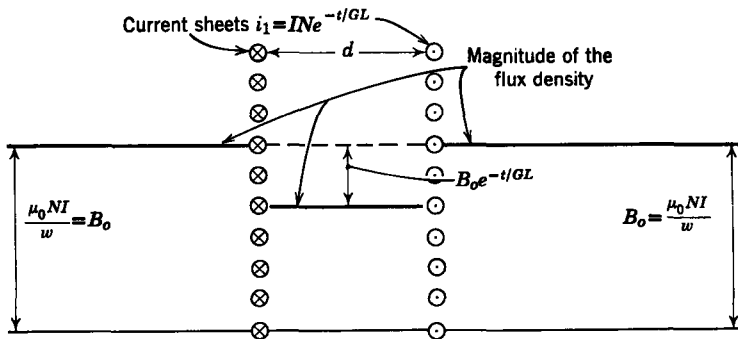


Fig. 7.1.8 Distribution of flux density as predicted by a lumped-parameter model.

rate characterized by the time constant GL . These distributions of current and flux density should be compared with those shown in Figs. 7.1.4 and 7.1.5.

If the equivalent G were computed as the dc conductance of the two sheets with length l and width w by using as the thickness $2d/\pi^2 = 0.203d$, we have

$$G = \left[\frac{\sigma(2d/\pi^2)w}{2l} \right],$$

and using the value of L (7.1.33) the time constant is

$$GL = \frac{\mu_0 \sigma d^2}{\pi^2}.$$

or that predicted by the diffusion equation as the fundamental time constant of the system (7.1.28). Obviously, we would not know what thickness to use unless we had solved the exact problem, hence our lumped-parameter model can at best serve to interpret the diffusion process in terms of familiar lumped-parameter concepts. For engineering purposes, however, judiciously chosen lumped parameters provide a convenient and powerful model for many situations.

7.1.2 Diffusion and Steady Motion

As pointed out in the introduction, if the magnetic Reynolds number (7.0.4) is significant compared with unity, material motion can be responsible for altering current paths, hence redistributing the magnetic field. This type of phenomenon is best emphasized by considering situations in which the fields and motion are in a steady-state condition. Then the appropriate expression for the flux density is (7.1.12) with the velocity \mathbf{v} independent of time.

7.1.2a Steady-State in the Fixed Frame

The system depicted schematically in Fig. 7.1.9 is an example of the kind of steady-state diffusion problem we must consider when studying magneto-hydrodynamic (MHD) generators (see Chapter 12). It involves a continuous strip of material with constant σ , ϵ_0 , μ_0 which slides with constant velocity between a parallel pair of highly conducting electrodes. The sliding strip makes perfect electrical contact with the electrodes. The dimensions and coordinate system used are shown in Fig. 7.1.9. The system is excited at the end $z = l$ by two current sources that supply a total current I to the electrodes. We wish to find the distribution of magnetic flux density in the sliding strip and study how it varies with system parameters.

To simplify the problem we assume that l/d and w/d are large enough

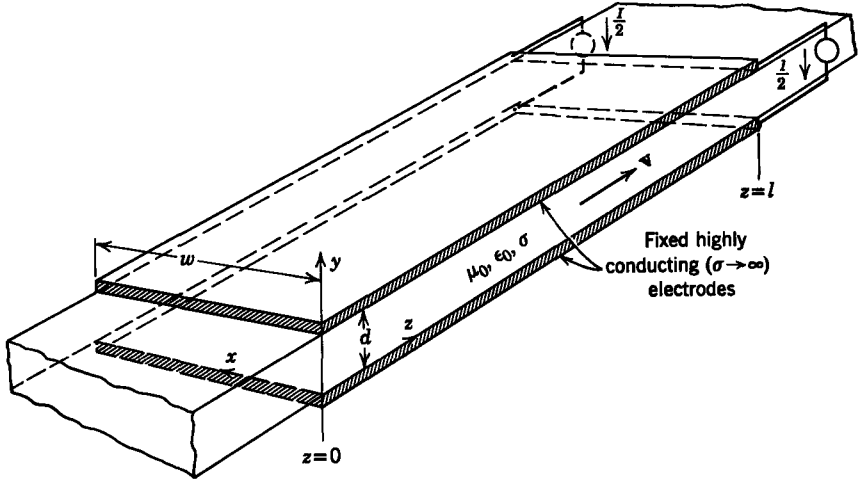


Fig. 7.1.9 Geometry for studying diffusion in the presence of steady motion.

that end and edge effects can be neglected.* Thus the flux density will have only an x -component

$$\mathbf{B} = \mathbf{i}_x B_x, \quad (7.1.38)$$

the electric field intensity and current density will have only y -components

$$\mathbf{J} = \mathbf{i}_y J_y, \quad (7.1.39)$$

$$\mathbf{E} = \mathbf{i}_y E_y, \quad (7.1.40)$$

and the variables will not be functions of x or y ,

$$\frac{\partial}{\partial x} = \frac{\partial}{\partial y} = 0.$$

We have already specified that the strip is moving with constant velocity in the z -direction

$$\mathbf{v} = \mathbf{i}_z v_z. \quad (7.1.41)$$

Finally, interest is confined to a steady-state problem ($\partial/\partial t = 0$).

With the given specifications, the x -component of (7.1.12) is

$$\frac{d^2 B_x}{dz^2} - \mu_0 \sigma v_z \frac{dB_x}{dz} = 0. \quad (7.1.42)$$

We have written total derivatives because B_x is a function only of z .

* Standard practice in the analysis of MHD machines is to assume no fringing, solve the problem, and then add end effects as a perturbation. The end effect analysis is done by using conformal mapping techniques. See, for example, G. W. Sutton and A. Sherman, *Engineering Magnetohydrodynamics*, McGraw-Hill, New York, 1965, pp. 504–508.

Using the excitation of Fig. 7.1.9 and the boundary conditions of Table 6.1*, we arrive at the conditions on the flux density

$$\text{at } z = 0, \quad B_x = 0, \quad (7.1.43a)$$

$$\text{at } z = l, \quad B_x = \frac{\mu_0 I}{w}. \quad (7.1.43b)$$

First consider the system with the velocity equal to zero. The solution for the flux distribution is

$$B_x = \frac{\mu_0 I}{w} \frac{z}{l}. \quad (7.1.44)$$

The distribution of current density is found from the y -component of (7.1.7),

$$J_y = \frac{1}{\mu_0} \frac{dB_x}{dz}, \quad (7.1.45)$$

and for zero velocity it is

$$J_y = \frac{I}{wl}. \quad (7.1.46)$$

This uniform current density and linearly varying flux density are what we expect in the absence of motion

When the velocity is finite, solutions for (7.1.42) are of the form

$$B_x = Ce^{rz}$$

Substitution into (7.1.42) and cancellation of common factors gives

$$r^2 - \mu_0 \sigma v_z r = 0.$$

The solutions for this equation are

$$r = \mu_0 \sigma v_z, 0,$$

which yield the general solution for B_x

$$B_x = C_1 + C_2 e^{R_m(z/l)}, \quad (7.1.47)$$

where we have again defined the *magnetic Reynolds number* R_m as

$$R_m = \mu_0 \sigma v_z l. \quad (7.1.48)$$

The significance of this number in the present context is discussed later.

Using the boundary conditions of (7.1.43), the constants C_1 and C_2 in (7.1.47) are evaluated to obtain the solution

$$B_x = \frac{\mu_0 I}{w} \left[\frac{e^{R_m(z/l)} - 1}{e^{R_m} - 1} \right]. \quad (7.1.49)$$

* See Appendix E.

The distribution of current density is evaluated by using this result in (7.1.45):

$$J_y = \frac{I}{wl} \left[\frac{R_m e^{R_m(z/l)}}{e^{R_m} - 1} \right]. \tag{7.1.50}$$

Note that as $R_m \rightarrow 0$ these expressions reduce to those of (7.1.44) and (7.1.46), which were derived by assuming zero velocity.

The flux density and current density are plotted as functions of position for several values of magnetic Reynolds number R_m in Fig. 7.1.10. It is evident from these curves that the higher R_m , the more flux density and current density are distorted, both being decreased at the entrance to the electrodes. It was shown in Section 7.1.1 that when we try to change the flux density in a conductor eddy currents flow to oppose the flux change. The eddy currents decay and the flux diffuses into the conductor in the process characterized by a diffusion time constant.

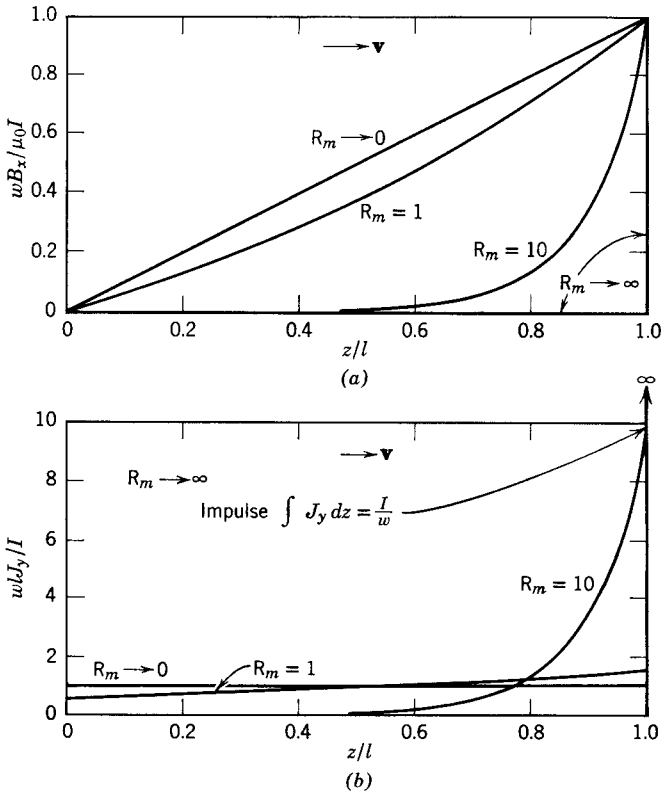


Fig. 7.1.10 Distribution of flux density and current density in the system of Fig. 7.1.9: (a) flux density; (b) current density.

If, in the system of Fig. 7.1.9, we view what happens to a particular sample of the moving strip, we see the competing processes of the sample trying to sweep the flux and current in the direction of motion and the diffusion of flux and current in the opposite direction. The magnitude of the magnetic Reynolds number is an indicator of the relative effectiveness of the two processes; a large R_m indicates a relatively slow diffusion process. We can interpret the magnetic Reynolds number as being proportional to the ratio of the diffusion time constant to the time it takes a sample of material to traverse the length of the electrodes. Equation 7.1.28 is used to write the diffusion time constant for the length l as

$$\tau_d = \frac{\mu_0 \sigma l^2}{\pi^2}.$$

The time taken for a sample of material to traverse the length l with speed v_z is

$$\tau_t = \frac{l}{v_z}.$$

The ratio of diffusion time constant to traversal time is then

$$\frac{\tau_d}{\tau_t} = \frac{\mu_0 \sigma v_z l}{\pi^2} = \frac{R_m}{\pi^2}.$$

The magnetic Reynolds number was defined in a particular way for this example. We find in our further studies of quasi-static magnetic field systems that it is useful to define magnetic Reynolds numbers in other ways; the fundamental interpretation, however, is always the same, namely that a magnetic Reynolds number indicates the relative importance of the diffusion ($\nabla^2 \mathbf{B}$) and convection $\nabla \times (\mathbf{v} \times \mathbf{B})$ terms in (7.1.12).

7.1.2b Steady State in the Moving Frame

The steady-state diffusion situation considered in the preceding subsection could be viewed from a frame moving with the conductor, in which case the magnetic field would be in a transient condition but the velocity v_z would be zero. Here, we turn this relationship around and consider a problem that is in a transient state in the fixed frame but in the steady state in the moving frame. The example provides further insight into the significance of the magnetic Reynolds number.

In the introduction to this chapter (see Fig. 7.0.1c) we discussed an example in which a block of conducting material moves with the velocity V between short-circuited, perfectly conducting parallel plates. If the current excitation in that problem is used to establish the field and is then instantaneously removed, currents will continue to flow through the block and the shorting

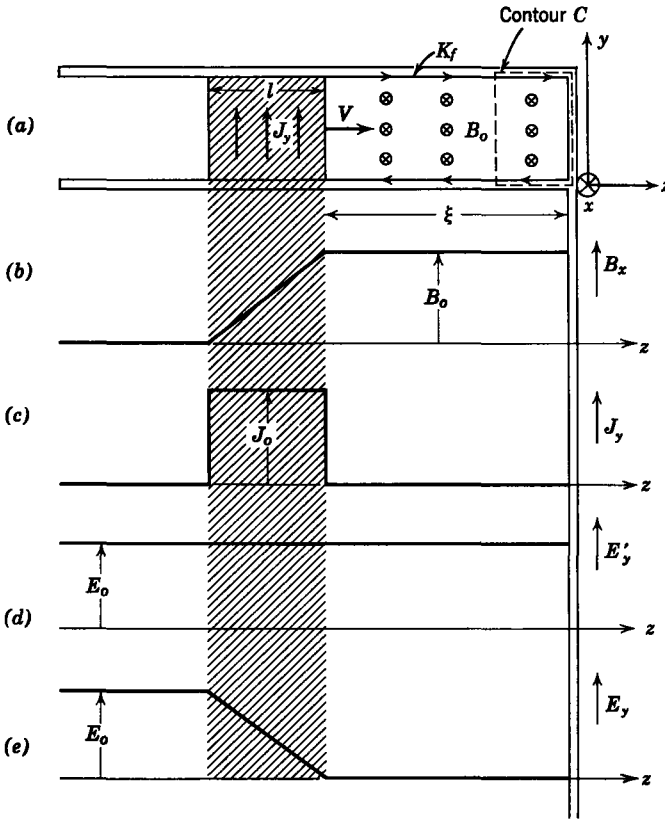


Fig. 7.1.11 The conducting block moves with just the velocity V required to maintain the flux density B_0 constant. This velocity is such that $R_m = 1$.

end plate, as shown in Fig. 7.1.11a. Then there is a magnetic field ahead of the moving block of conductor but none behind.

Now, if the block were stationary, the magnetic field within the “inductor” formed by the block and the perfectly conducting plates would decay, much as in the example in Section 7.1.1. It is possible, however, for the block to move to the right with a sufficient velocity V to maintain the flux density B_0 ahead of the block constant. Under this circumstance the fields can be found by observing that in the frame of the block the situation is no different than for a static case in which the field to the right is constant and the field to the left is zero; that is, in the frame of the moving block,

$$\mathbf{J}' = J'_y \mathbf{i}_y = \text{constant} = \sigma E'_y \mathbf{i}_y \tag{7.1.51}$$

for $-(\xi + l) < z < -\xi$.

Remember that the flux density generated by this current is the same in either the fixed or moving frame (see Table 6.1)*. Hence

$$\mathbf{B}' = \mathbf{B} = \mathbf{i}_x B_o \frac{(z + \xi + l)}{l} \quad (7.1.52)$$

for $-(\xi + l) < z < -\xi$ and

$$\mathbf{B} = B_o \mathbf{i}_x \quad (7.1.53)$$

for $-\xi < z < 0$. The flux density and current density are sketched in Fig. 7.1.11*b, c*. Here the gap length $\xi = -Vt + \text{constant}$, where V is a constant.

There is no time rate of change of the flux enclosed by a fixed contour (such as C in Fig. 7.1.11*a*) that passes through the perfectly conducting plates and the region ahead of the moving block. Hence

$$\oint_C \mathbf{E} \cdot d\mathbf{l} = 0 \quad (7.1.54)$$

around this contour and E_y ahead of the block is zero. It follows from the transformation for the electric field (see Table 6.1)* that

$$E'_y(z = -\xi) = (\mathbf{v} \times \mathbf{B})_y = VB_o. \quad (7.1.55)$$

A sketch of the distribution of E'_y is shown in Fig. 7.1.11*d*.

Of course, the surface current density K_f (which is equal to K'_f in a magnetic field system) is related to the flux density B_o (Ampère's law)

$$B_o = \mu_o K_f \quad (7.1.56)$$

and the surface current density in the perfectly conducting plates is also related to the current density in the block

$$K_f = J_y l. \quad (7.1.57)$$

If we now combine (7.1.51) with these last three equations, we obtain

$$\sigma V B_o = \frac{B_o}{\mu_o l}, \quad (7.1.58)$$

from which it follows that to obtain a constant magnetic flux density ahead of the moving block we must have

$$\mu_o \sigma V l = R_m = 1. \quad (7.1.59)$$

The distribution of electric field in the moving and fixed frames is shown in Fig. 7.1.11*d, e*. Note that in the region to the left $E'_y = E_y$, because there is no magnetic field in that region.

Now that the fields have been found, it is possible to write them in the fixed frame [in which they are functions of (z, t)] and see that they satisfy (7.1.9).

Of course, what we have found is the solution for a particular value of V . The postulated steady-state condition in the moving frame prevails only if

* See Appendix E.

(7.1.59) is satisfied. We know that the field decays to zero if the block is stationary, hence we conclude that if the velocity V is less than required to make $R_m = 1$ the field ahead of the block will decay. More interesting is the fact that if V exceeds the value required to make $R_m = 1$ the magnetic field ahead of the block will increase. In this case the block literally acts as a magnetic piston that compresses the magnetic field in the region bounded by the perfectly conducting plates and increases the flux density. This provides a mechanism for mechanical amplification of flux density which has been used with chemical explosives to achieve amplification by more than a factor of 10 (from 2 Wb/m² to 30 Wb/m²).*

To establish a numerical idea when the conditions of (7.1.59) are met, it is helpful to recognize that this condition can also be written as

$$\frac{l}{V} = \pi^2 \tau,$$

where τ is the diffusion time, defined by (7.1.28), and plotted in Fig. 7.1.6 for several conductors as a function of the material thickness. The quantity l/V is the time required for the material to traverse a distance equal to its thickness. Hence, if we have a copper block with the thickness of 10 cm, it follows from Fig. 7.1.6 that a velocity of

$$V = \frac{l}{\pi^2 \tau} = 0.13 \text{ m/sec}$$

is required just to maintain the flux ahead of the block constant.

The use of a solid block in motion to concentrate magnetic flux mechanically implies a transient situation. For steady-state flux concentration a system has been proposed and tested in which the steady flow of a liquid metal conductor with $R_m > 1$ concentrates the flux.†

Other instances of flux concentration by mechanical motion occur in plasma devices used in research on controlled thermonuclear reactions. In these devices energy from a capacitor bank drives and heats a plasma and the mechanical motion of the plasma compresses the magnetic field and increases the flux density.‡

In a very different physical situation superconducting solids have essentially infinite electrical conductivity; hence at even low velocities the magnetic

* C. M. Fowler et al., "Flux Concentration by Implosion," *High Magnetic Fields*, H. Kolm et al., eds. M.I.T. Press, Cambridge, Mass., and Wiley, New York, 1962, pp. 269–276.

† H. H. Kolm and O. K. Mawardi, "Hydromagnet: A Self-Generating Liquid Conductor Electromagnet," *J. Appl. Phys.*, **32**, No. 7, 1296–1304 (July 1961).

‡ D. J. Rose and Melville Clark, Jr., *Plasmas and Controlled Fusion*, M.I.T. Press and Wiley, New York, 1961, p. 360.

Reynolds number R_m is essentially infinite. As a result, superconducting solids are used for mechanical amplification of flux density.*

7.1.3 The Sinusoidal Steady State in the Presence of Motion

Some of the most significant practical applications of magnetic diffusion phenomena are made possible by introducing two characteristic dynamical times into a single system; for example, in Fig. 7.1.12 a thin sheet of conducting metal (conductivity σ) moves to the right with the constant velocity V .

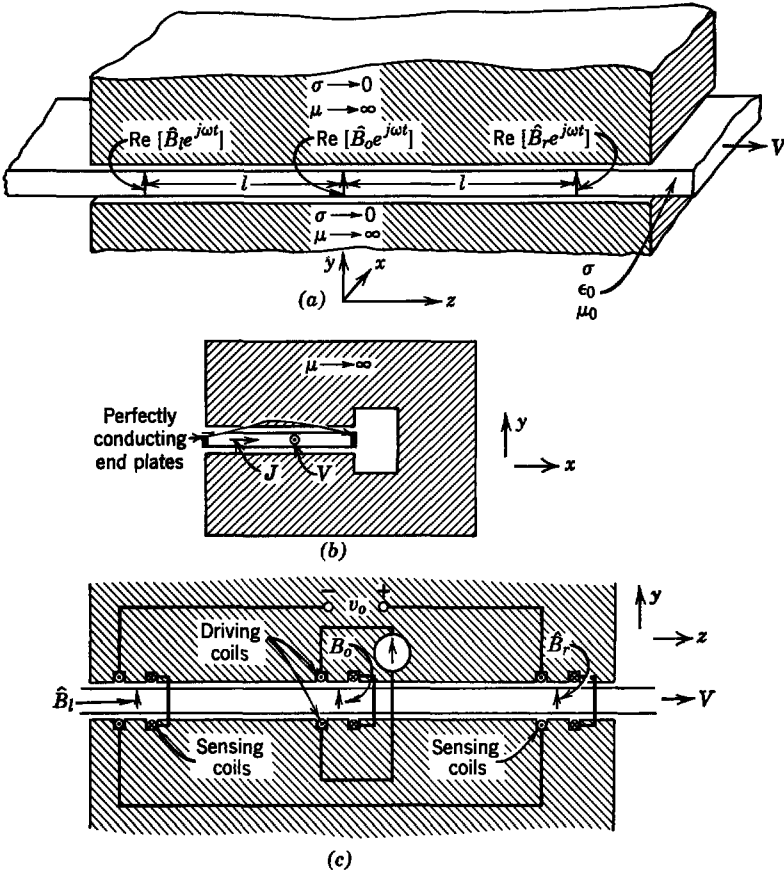


Fig. 7.1.12 (a) A thin slab of conductor moves to the right with velocity V in the air gap of a magnetic circuit; (b) end view of magnetic circuit showing a slab with perfectly conducting end plates moving out of paper; (c) excitation and detection circuits used to measure velocity V of the slab.

* P. S. Swartz and C. H. Rosner, "Characteristics and a New Application of High-Field Superconductors," *J. Appl. Phys.*, 33, No. 7, 2292-2300 (July 1962).

External coils are used to impose the magnetic flux density

$$\mathbf{B} = \mathbf{i}_y \operatorname{Re} \left(\hat{B}_0 e^{j\omega t} \right) \quad (7.1.60)$$

at $z = 0$, as shown in Fig. 7.1.12*a*, *b*, *c*. In addition, coils are arranged symmetrically upstream and downstream from the excitation of (7.1.60). These coils are connected to a high impedance voltmeter, which measures the rms value of v_o , as shown in Fig. 7.1.12*c*. The coils are connected in series and in such a way that the voltage v_o is proportional to the difference between the time rates of change of B_r and B_l . With no motion, the device is symmetrical, and we expect that the output voltage v_o is zero. With motion we expect from the results of the preceding section that the conductor will tend to increase the flux density B_r and decrease B_l . If this is the case, the voltage v_o is a measure of the material velocity. Hence the system shown in Fig. 7.1.12 has the possibility of being a device to measure the velocity of the moving conducting sheet without making mechanical or electrical contact with the sheet.

The problem is particularly appropriate to our present discussion because it can be modeled by a one-dimensional diffusion problem. The sheet is assumed to move in the air gap of an infinitely permeable magnetic circuit so that fields B_y are returned through the circuit. Then currents are in the x -direction through the sheet and for our present purposes we can think of the sheet as having perfectly conducting end plates (Fig. 7.1.12*b*) which allow the currents to return through the sheet at other positions along the z -axis.

There are two characteristic times for the dynamics of this situation. First the excitation has the period $2\pi/\omega$, and we know from Section 7.1.1 that the relative value of this time and the diffusion time will be important. In addition, the motion introduces the characteristic time l/V , and from the studies undertaken in Section 7.1.2 we expect that this time in relation to the diffusion time will also be important.

We are interested in sinusoidal steady-state conditions, hence we require an expression for \mathbf{B} that includes both the effects of time varying fields and material motion. The appropriate equation is the y -component of (7.1.9), written with the assumption that $\partial/\partial x = \partial/\partial y = 0$. (Effects of the slots in which coils are placed are neglected.)

$$\frac{1}{\mu\sigma} \frac{\partial^2 B_y}{\partial z^2} = \frac{\partial B_y}{\partial t} + V \frac{\partial B_y}{\partial z}. \quad (7.1.61)$$

Note that these same assumptions require that a current be in the x -direction which from (7.1.7) is related to B_y by

$$J_x = -\frac{1}{\mu} \frac{\partial B_y}{\partial z}. \quad (7.1.62)$$

It is worthwhile to compare (7.1.61) to the one-dimensional diffusion equation for stationary media (7.1.15). The effect of the motion is to replace the time derivative with the convective derivative. Because B_y is the same, whether measured in the moving or the fixed frame, this result is reasonable. As we learned in Section 6.1, the terms on the right in 7.1.61 constitute the time rate of change of B_y for an observer moving with the material at the velocity V . Hence in the frame of the material (7.1.61) has the same physical significance as (7.1.15). In the present example, of course, the excitation is in the fixed frame and we cannot ignore the effect of the motion by solving the problem in the moving frame.

Because of the sinusoidal steady-state excitation (7.1.60), solutions to (7.1.61) are assumed to have the form

$$B_y = \text{Re} [\hat{B}(z)e^{j\omega t}]. \quad (7.1.63)$$

Substitution into (7.1.61) shows that this assumption is justified if

$$\frac{d^2 \hat{B}}{dz^2} - \mu\sigma V \frac{d\hat{B}}{dz} - j\omega\mu\sigma \hat{B} = 0. \quad (7.1.64)$$

This ordinary constant-coefficient equation can be solved by assuming solutions of the form $\hat{B}(z) = e^{-jkz}$. Then

$$k^2 - jk\mu\sigma V + j\omega\mu\sigma = 0. \quad (7.1.65)$$

Note that we could have obtained this expression, which is called the *dispersion equation*, by assuming both the temporal and spacial dependence at the outset and letting

$$B_y(z, t) = \text{Re} [\hat{B}_y e^{j(\omega t - kz)}]. \quad (7.1.66)$$

Solutions of this form satisfy (7.1.61), provided that ω and k are related by (7.1.65). In the chapters that follow we make extensive use of solutions with this form. In the present situation ω is a given real number. Then it is clear from (7.1.65) that the *wavenumber* k is complex. In solving (7.1.65), it is convenient to normalize k to the length l . There are then two possible wavenumbers ($k = k^-$ and $k = k^+$) for a given frequency ω .

$$l(k^\mp) = \frac{jR_m}{2} \pm j \left[\left(\frac{R_m}{2} \right)^2 + 2j \left(\frac{l}{\delta} \right)^2 \right]^{1/2} \quad (7.1.67)$$

Here the magnetic Reynolds number

$$R_m = \mu\sigma V l \quad (7.1.68)$$

and the *skin depth* δ , defined by

$$\delta = \left(\frac{2}{\omega\mu\sigma} \right)^{1/2}, \quad (7.1.69)$$

have been introduced. By these definitions R_m represents the effect of the material velocity V , whereas δ brings in the excitation frequency ω . As can be seen from (7.1.67), the diffusion with no motion ($R_m = 0$) is described by δ , and it is worthwhile to consider this limiting case so that the effect of the motion can be fully appreciated.

7.1.3a Sinusoidal Steady State with No Motion (Skin Effect)

The sinusoidal steady-state diffusion of a magnetic field into a conductor assumes considerable importance outside the area of electromechanics; for example, the ac resistance of a stationary wire is significantly dependent on frequency,* as are the losses in the walls of a waveguide.† In each of these cases the phenomenon is conventionally referred to as *skin effect* because the currents in the conductor tend to crowd into a region near the surface.

Skin-effect is a magnetic diffusion phenomenon. Section 7.1.1 was concerned with transient skin effect. It is exemplified here as the limiting case in which $V = 0$ ($R_m = 0$). Then from (7.1.67) the wavenumbers are (remember that $\sqrt{j} = (1 + j)/\sqrt{2}$)

$$k^{\mp} = \mp \frac{1 - j}{\delta}. \quad (7.1.70)$$

Now, if we substitute these wavenumbers into (7.1.66), we find that one of the solutions increases exponentially with z as the other decreases. For the present purposes we assume that the extremities of the system in the z -direction are sufficiently remote that the fields there have decayed to zero. Then, in the region to the right in Fig. 7.1.12, the appropriate solution is (here the wavenumber k^+ is used)

$$B_y = \text{Re} [B_0 e^{-z/\delta} e^{j(\omega t - z/\delta)}]. \quad (7.1.71)$$

From this expression it is clear that there are two parts to the solution, as shown in Fig. 7.1.13. To illustrate some of the properties of this *diffusion wave*, the two factors of (7.1.71) are plotted in Fig. 7.1.13. Here, the excitation constant B_0 is assumed to be real. Then the factor $\cos(\omega t - z/\delta)$ represents a wave of constant amplitude, traveling in the positive z -direction. We define a *phase velocity* v_p for this constant-amplitude wave by calculating the velocity of a point of constant phase. The phase of an arbitrary point on the wave (e.g., point A in Fig. 7.1.13) remains constant for an observer at the position z such that

$$\omega t - z/\delta = \text{constant}. \quad (7.1.72)$$

* S. Ramo, J. R. Whinnery, and T. Van Duzer, *Fields and Waves in Communication Electronics*. Wiley, New York, 1965, p. 194.

† *Ibid.* p. 379.

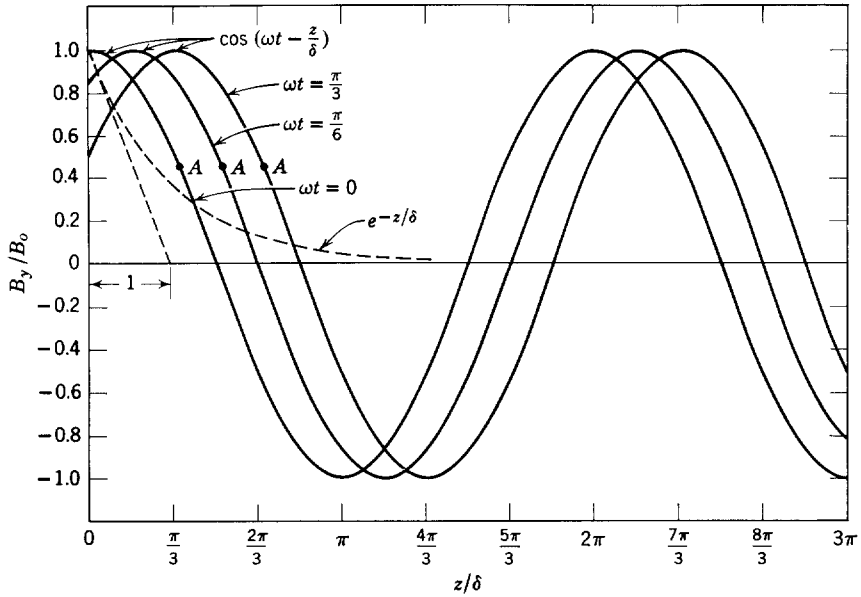


Fig. 7.1.13 Components of a diffusion wave.

To find the phase velocity we differentiate this expression with respect to time to obtain

$$v_p = \omega\delta. \quad (7.1.73)$$

Thus the point *A* or any other point of constant phase on the constant amplitude part of the wave will travel with a phase velocity $\omega\delta$.

The two factors plotted separately in Fig. 7.1.13 are multiplied and replotted to show the complete diffusion wave in Fig. 7.1.14. With the attenuation it is difficult to identify an arbitrary point of constant phase on the wave.

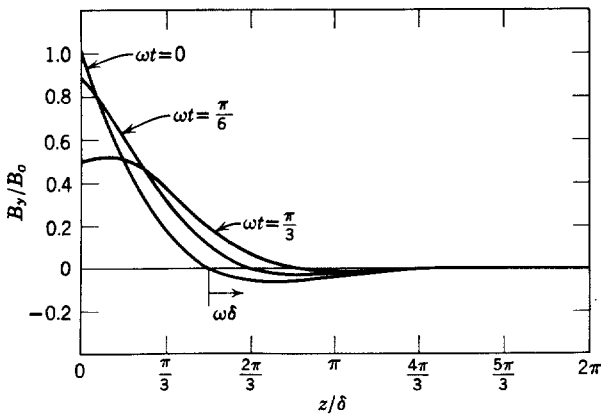


Fig. 7.1.14 A diffusion wave.

We can, however, always be unambiguous by defining the phase velocity in terms of the velocity of a zero-crossing.

A salient property of the diffusion wave is that the spacial rate of decay and the wavelength are both directly proportional to δ ; that is, as can be seen from Fig. 7.1.13, the wave envelope has an extrapolated decay distance equal to the skin depth δ and the wavelength $\lambda = 2\pi\delta$. Hence in Fig. 7.1.14 it is difficult to discern more than one point of zero amplitude.

It is important to recognize that a diffusion wave describes the dynamics of an essentially dissipative interaction. As we shall see in Chapter 10, sinusoidal steady-state waves can be excited in cases in which decay (or evanescence) occurs but there is no dissipation of energy.

In Section 10.1.4 we shall have occasion to return to diffusion waves in another context. There the "mushy" nature of these waves is emphasized.

Because the skin depth δ is such a critical parameter in the electromagnetic

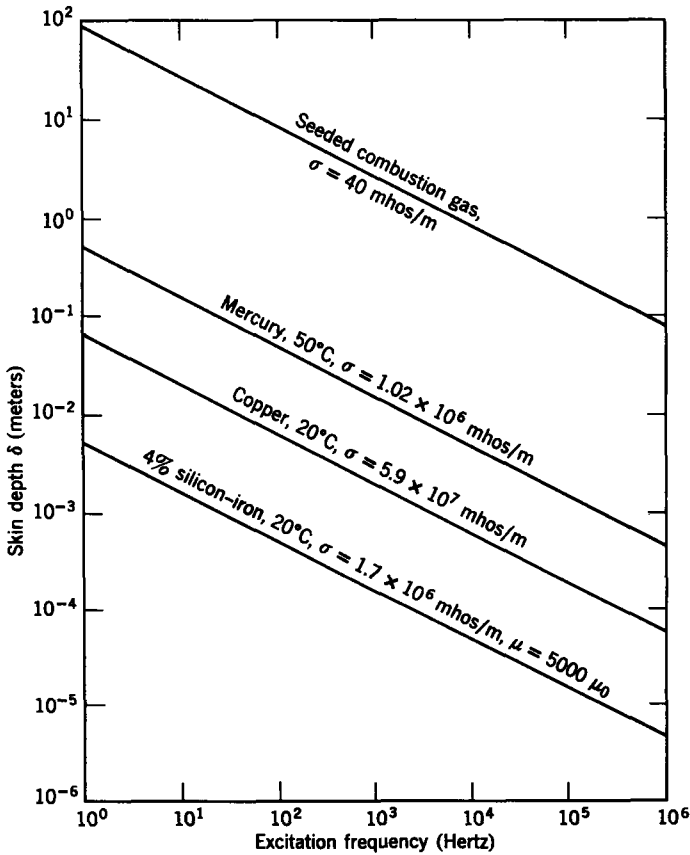


Fig. 7.1.15 Skin depth as a function of frequency for several typical materials.

behavior of conducting materials, it is worthwhile to calculate the skin depth for some typical materials. Equation 7.1.69 is used with the material constants in Fig. 7.1.6 to plot the curves of skin depths as functions of frequency shown in Fig. 7.1.15. Note the tremendous range of skin depths obtainable with useful materials; for example, in silicon iron, even at the low frequency of 1 Hz the skin depth is approximately $\frac{1}{2}$ cm. It is quite clear from these plots that many situations exist in which it is appropriate to assume the material infinitely conducting ($\delta \approx 0$). On the other hand, it is also clear that situations exist in which it is appropriate to neglect the skin effect and the induced currents. A comparison should be made between Figs. 7.1.15 and 7.1.6 because the skin depth and the diffusion time constant are closely related.

7.1.3b The Effect of Motion

To assess the effect of material motion on diffusion waves, the wavenumbers given by (7.1.67) must be considered for finite values of R_m . To determine the relative magnitudes of the real (k_r) and imaginary (k_i) parts of the wavenumber, it is helpful to construct the solution of (7.1.67) graphically (Fig. 7.1.16). From this construction it is clear that the real parts of

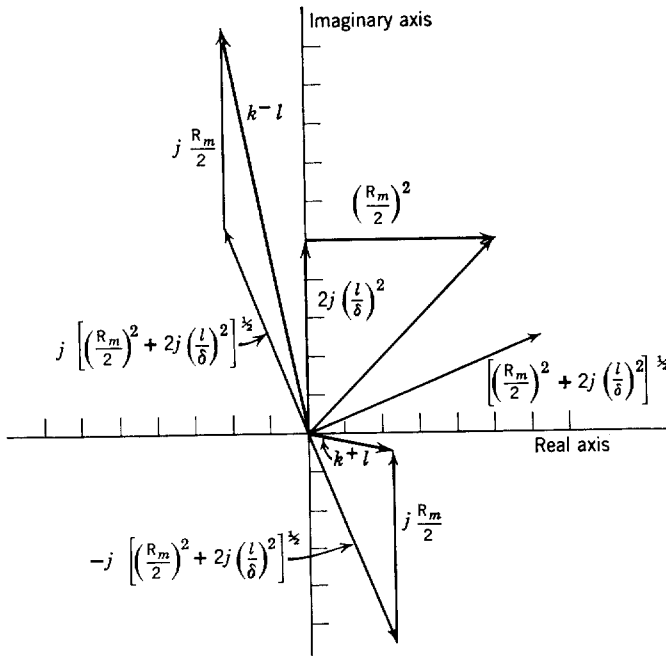


Fig. 7.1.16 Graphical construction of solutions to (7.1.67) for the normalized complex wavenumbers $k+l$ and $k-l$.

k^+ and k^- are negatives,

$$k_r^- = -k_r^+, \quad (7.1.74)$$

that k_i^- is positive and k_i^+ is negative,

$$k_i^- > 0 > k_i^+, \quad (7.1.75)$$

and that the magnitude of k_i^- is greater than that of k_i^+ ,

$$|k_i^-| > |k_i^+|. \quad (7.1.76)$$

The arguments in Section 7.1.3a concerning the extent of the system are then used to arrive at the solutions

$$B_y = \text{Re} [\hat{B}_o e^{-|k_i^+|z} e^{j(\omega t - |k_r^+|z)}] \quad (7.1.77)$$

for $z > 0$ and

$$B_y = \text{Re} [\hat{B}_o e^{|k_i^-|z} e^{j(\omega t + |k_r^-|z)}] \quad (7.1.78)$$

for $z < 0$. From these solutions it is clear that to the right a diffusion wave still propagates in the $+z$ -direction with a phase velocity $\omega/|k_r^+|$ that is modified by the material motion. Moreover, in spite of the motion, a wave propagates to the left with this same phase velocity. The effect of the motion is most apparent in the rate of decay for these waves. The spacial rate of attenuation to the right is decreased by the motion, whereas that to the left is increased. An instantaneous view of the magnetic flux density amplitude to the right and left would appear as shown in Fig. 7.1.17.

As a practical application of the magnetic diffusion phenomenon we have considered in this section, the device shown in Fig. 7.1.12 is now used to measure the velocity of the material. The output voltage from the sensing coils has the form $v_o = \text{Re} (\hat{v}_o e^{j\omega t})$. The coils are connected so that in the absence of motion there is no output signal; that is,

$$\hat{v}_o = j\omega A [\hat{B}_y(l) - \hat{B}_y(-l)], \quad (7.1.79)$$

where A is a geometric constant that depends on the coil area and number of turns. The $j\omega$ in (7.1.79) accounts for the voltage being the time rate of change of the flux. (Here we assume that not only do the coils support a negligible current so that they do not disturb the magnetic field but they have dimensions in the z -direction that are small compared with a wavelength $2\pi/|k_r|$.) In substituting the solutions given by (7.1.77) and (7.1.78) into (7.1.79), it is convenient to use first the complex wavenumbers k^+ and k^- ,

$$\hat{v}_o = j\omega A \hat{B}_o (e^{-jk^+l} - e^{+jk^-l}) \quad (7.1.80)$$

because then we can use (7.1.67) to write this expression as

$$\hat{v}_o = j\omega 2A \hat{B}_o \sinh \left(\frac{R_m}{2} \right) \exp - \left[\left(\frac{R_m}{2} \right)^2 + 2j \left(\frac{l}{\delta} \right)^2 \right]^{1/2}. \quad (7.1.81)$$

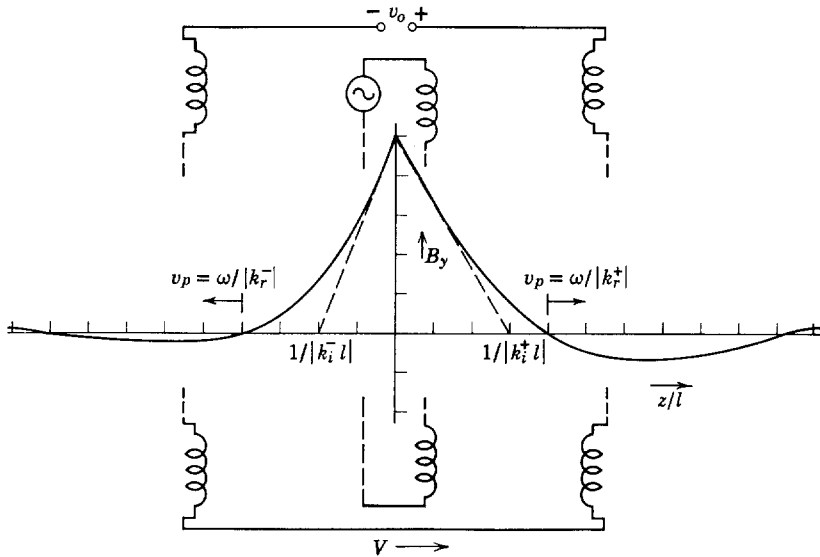


Fig. 7.1.17 Instantaneous distribution of magnetic flux density in the moving slab of conductor shown in Fig. 7.1.12. Points of constant phase move to the right and left with equal velocities but attenuation to the right is decreased by motion, whereas that to the left is increased. Note that detailed account of the excitation at $z = 0$ by the coil has not been made. Hence distribution of B_y at $z = 0$ has a discontinuous slope.

From this equation it is apparent that as R_m approaches zero, the output voltage from the sensing coils does also. For small values of $R_m/2$ compared with unity and l/δ and for fixed frequency ω the output voltage takes the form

$$\hat{v}_o = (\text{constant}) R_m; \quad (7.1.82)$$

that is, in this range of parameters, the voltage v_o is directly proportional to the velocity V of the moving conducting sheet.

The mechanism made available by this phenomenon for measuring the velocity of a material is attractive because it does not require mechanical or electrical contact with the moving medium. Also by varying the frequency the output voltage can be made to give information about the material conductivity.

Devices that exploit the interaction described here are used to measure rotational velocity with drag-cup tachometers* and in flowmeters to measure

* C. W. Blachford, "Induction Cup Parameters from Electromagnetic Field Theory and Experimental Analysis," *IEEE Trans. Power Apparatus Systems*, **PAS. 84**, No. 11, 189-193 (November 1965).

the velocity of liquid metals.* Note that the output voltage is proportional to the conductivity of the moving medium ($R_m = \mu_0 \sigma V l$). Hence there is a lower limit on the material conductivity that will lead to a useful output voltage.

7.1.4 Traveling Wave Diffusion in Moving Media

In Section 7.1.3 attention was given to the effect of material motion on the diffusion of magnetic fields excited in the sinusoidal steady state. These same ingredients are also present in the topic to be undertaken in this section, with attention now being given to currents and forces induced in the moving material. Figure 7.1.18 shows a slab of conducting material that can be moving to the right with velocity V . Adjacent to the lower surface, coils are distributed and interconnected in such a way that a surface current

$$\mathbf{K}_f = \text{Re} [K e^{j(\omega t - kz)} \mathbf{i}_x], \quad (K \text{ real}), \quad (7.1.83)$$

is excited. Hence at any point in the x - z plane this current varies sinusoidally with the frequency ω , whereas at any instant it varies sinusoidally in space. Points of constant phase on the current sheet move to the right with the velocity ω/k , where both ω and k are given.

This example has attributes that make it possible to demonstrate the basic mechanism responsible for several practical magnetic induction-type interactions. As we shall see, currents are induced in the conducting material.

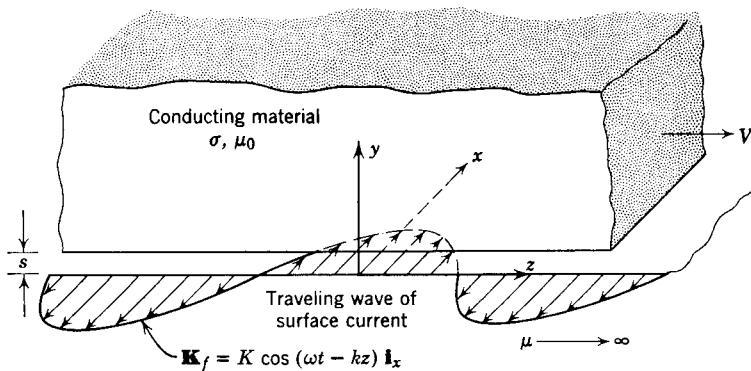


Fig. 7.1.18 A slab of conducting material moves in the z -direction with velocity V . Just below the slab sinusoidally distributed windings are driven by a traveling wave of surface current density which has the phase velocity ω/k to the right. It is assumed that an infinitely permeable material is just below the current sheet and that the extent of the conducting slab in the y -direction is many wavelengths $2\pi/k$.

* For a discussion of magnetohydrodynamic flow measuring devices see J. A. Shercliff, *The Theory of Electromagnetic Flow Measurement*, Cambridge University Press (1962). In particular, the interaction described is basic to material beginning on p. 103.

These currents, and the associated magnetic fields, can produce a time average force on the material in the y -direction. This type of force is often used to levitate solid and liquid metals. Other forces are induced in the z -direction, and under certain conditions this makes it possible to pull the conducting material in the z -direction. This induced force is the basis for the induction machine discussed in Section 4.1.6b and is often used to pump liquid metals.

One of our main objectives in this section is to establish further insight into the manner in which currents and the magnetic fields distribute themselves in a moving conducting medium. The magnetic flux density is given by (7.1.9), which has the y -component

$$\frac{1}{\mu\sigma} \left(\frac{\partial^2 B_y}{\partial y^2} + \frac{\partial^2 B_y}{\partial z^2} \right) = \frac{\partial B_y}{\partial t} + V \frac{\partial B_y}{\partial z} \quad (7.1.84)$$

Hence we assume that the field distribution does not depend on the x -coordinate, and B_y is predicted by a diffusion equation with the same form as (7.1.61), except that now the magnetic field diffusion occurs in two dimensions. Once the component B_y has been found from (7.1.84), the remaining component B_z can be found from the relation $\nabla \cdot \mathbf{B} = 0$, which requires

$$\frac{\partial B_y}{\partial y} + \frac{\partial B_z}{\partial z} = 0. \quad (7.1.85)$$

The magnetic field is driven by the surface current of (7.1.83). Hence we look for solutions with the same traveling wave dependence on (z, t) ; that is, we assume that the flux density and the current density take the forms

$$\mathbf{B} = \text{Re} [(\hat{B}_y(y)\mathbf{i}_y + \hat{B}_z(y)\mathbf{i}_z)e^{j(\omega t - kz)}], \quad (7.1.86)$$

$$\mathbf{J} = \text{Re} [\hat{J}_x(y)\mathbf{i}_x e^{j(\omega t - kz)}].$$

It follows from (7.1.84) that in order for the solutions to take these forms \hat{B}_y must satisfy the equation

$$\frac{d^2 \hat{B}_y}{dy^2} - \alpha^2 \hat{B}_y = 0, \quad (7.1.87)$$

where

$$\alpha = k\sqrt{1 + jS},$$

$$S = \frac{\mu\sigma}{k^2} (\omega - kV).$$

The solutions to (7.1.87) are $\exp \pm \alpha y$. We have defined α as having a positive real part. The y -dimension of the slab is assumed to be very large compared with a wavelength $2\pi/k$, and it is therefore appropriate to assume that the fields approach zero as $y \rightarrow \infty$ with the dependence

$$\hat{B}_y = \hat{A}e^{-\alpha y}. \quad (7.1.88)$$

From (7.1.85) and the assumed form of solutions \hat{B}_z is given by

$$\hat{B}_z = \frac{1}{jk} \frac{d\hat{B}_y}{dy} = -\frac{\alpha\hat{A}}{jk} e^{-\alpha y}. \quad (7.1.89)$$

The constant \hat{A} is determined by the boundary condition imposed by the current sheet at $y = 0$. For purposes of simplicity it is assumed that the distance s between the current sheet and the lower surface of the conducting slab is small compared with the wavelength $2\pi/k$ and that the current sheet is bounded from below by a highly permeable material. This means that

$$\hat{B}_z(0) = \mu_0 K. \quad (7.1.90)$$

These last two equations serve to define the constant \hat{A} , and it follows that the magnetic flux density in the moving conductor is

$$\mathbf{B} = \text{Re} \left[\mu_0 K \left(\frac{-jk}{\alpha} \mathbf{i}_y + \mathbf{i}_z \right) e^{-\alpha y} e^{j(\omega t - kz)} \right]. \quad (7.1.91)$$

The current density implied by this flux density can be found from the relation $\mathbf{J} = \nabla \times \mathbf{H}$. In the present two-dimensional situation the only component of \mathbf{J} is

$$J_x = \frac{1}{\mu_0} (jk\hat{B}_y - \alpha\hat{B}_z), \quad (7.1.92)$$

and it follows from (7.1.91) that this is

$$J_x = \text{Re} \left[\frac{-jKk^2 S}{\alpha} e^{-\alpha y} e^{j(\omega t - kz)} \right] \quad (7.1.93)$$

The component B_z of the flux density and the current density J_x are distributed in the conducting slab, as shown in Fig. 7.1.19. It is clear that the flux and current distributions are strongly dependent on the parameter S . To understand the significance of this parameter recall from Section 7.1.1 that the magnetic diffusion time based on the wavelength $\lambda = 2\pi/k$ is (within a factor of 4)

$$\frac{\mu\sigma}{k^2},$$

whereas the rate of change with respect to time of B_y (say) for an observer moving with the velocity V of the slab is

$$\left(\frac{\partial}{\partial t} + V \frac{\partial}{\partial z} \right) B_y \rightarrow j(\omega - kV) \hat{B}_y;$$

that is, $\omega - kV$ is the frequency of the magnetic flux density for an observer moving with the conducting slab. Hence S is (proportional to) the ratio of the magnetic diffusion time to the period of excitation in the frame of the moving medium.

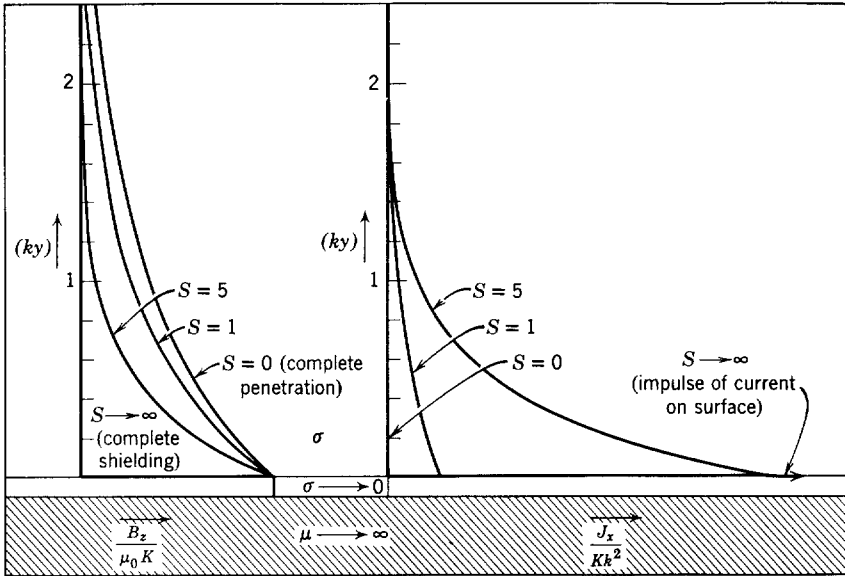


Fig. 7.1.19 Distribution of the instantaneous magnitudes of B_z and J_x in the moving conducting slab of Fig. 7.1.18; S is defined following (7.1.87).

Because the phase velocity of the traveling wave is ω/k , S is zero when the velocity V of the conductor is equal to the phase velocity of the wave. It is clear from (7.1.93) that under this synchronous condition there is no interaction between the conducting slab and the traveling current sheet. No currents are induced and the flux density completely penetrates the medium, with the characteristic exponential decay found in free space (Fig. 7.1.19). This figure shows how finite values of S give rise to currents that tend to exclude the magnetic flux density from the conductor. As S approaches infinity, the magnetic field is completely excluded from the conductor by a current density that is confined to a region very near the lower surface of the conductor. This is as would be expected, for, when $V = 0$, it is similar to the skin effect described in Section 7.1.3a. Here, however, the fields can also be excluded from the conductor because of the motion through a nonuniform field. To illustrate this point suppose that the current sheet is stationary so that $\omega = 0$. Then S is proportional to the velocity V , and it is apparent that a large material velocity leads to a shielding of the fields from the conductor. Note that in this limit S is a magnetic Reynolds number based on the wavelength of the current sheet. Once again a large magnetic Reynolds number indicates that induced field effects are significant.

The currents induced in the conducting slab give rise to time average forces

in the y - and z -directions. Both forces are significant because they are basic to a number of practical applications. The force in the y -direction makes it possible to support or levitate the slab on the magnetic field, whereas the force in the z -direction makes it possible to accelerate the slab in the z -direction.

It is a straightforward matter to compute these forces from the solutions we have obtained, since the force density in the material is $\mathbf{F} = \mathbf{J} \times \mathbf{B}$. The time average force $\langle T_z \rangle$ in the z -direction (per unit x - z area) is

$$\langle T_z \rangle = \int_0^\infty \langle F_z \rangle dy, \quad (7.1.94)$$

where*

$$\langle F_z \rangle = \frac{1}{2} \operatorname{Re} (\mathcal{J}_x \hat{B}_y^*)$$

with \hat{B}_y^* the complex conjugate of \hat{B}_y . The solutions of (7.1.91) and (7.1.93) make it possible to carry out the integration of (7.1.94) to obtain

$$\langle T_z \rangle = \frac{1}{4} \frac{\mu_0 K^2 S}{\sqrt{1 + S^2} \operatorname{Re} \sqrt{1 + jS}}. \quad (7.1.95)$$

As expected, when the currents are not induced in the slab ($S = 0$) there is no force in the z -direction. It is significant that the sign of the z -directed force depends on the sign of S . If S is positive (the traveling wave has a phase velocity that exceeds V), the traveling wave interaction tends to pull the slab in the z -direction. Conversely, if the phase velocity is slower than that of the slab, the induced currents tend to retard the motion of the slab. These properties are similar to those discussed for the induction machine in Section 4.1.6b. In fact, this interaction is the basis for a distributed linear induction machine.

The dependence of the time average force $\langle T_z \rangle$ on the parameter S is shown in Fig. 7.1.20. Here it is apparent that there is an optimum value of S at which the maximum force per unit area $\langle T_z \rangle$ is produced.† This maximum exists between low values of S , in which little current is induced in the medium, and large values of S in which the induced currents have the wrong phase relationship with respect to the imposed current sheet to produce maximum force. Compare this discussion and Fig. 7.1.20 with Fig. 4.1.20 and the associated discussion for an induction machine. There is a direct correspondence between the parameter S used here and the slip s used in the induction-machine analysis. The physical phenomena that govern the shape of the force (or torque) as a function of S (or slip s) are the same.

* Here we use the identity $\langle \operatorname{Re} \hat{A} e^{j\omega t} \operatorname{Re} \hat{B} e^{j\omega t} \rangle \equiv \frac{1}{2} \operatorname{Re} \hat{A} \hat{B}^*$.

† This phenomenon is also used to achieve desired characteristics in deep-bar rotors of induction machines as discussed in Fitzgerald and Kingsley, *op. cit.*, p. 411.

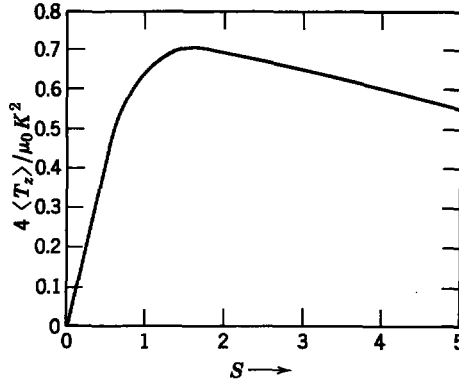


Fig. 7.1.20 Normalized time average force $\langle T_z \rangle$ per unit x - z area on the conducting slab of Fig. 7.1.18; S is defined following (7.1.87).

The time-average force density in the vertical (y)-direction is

$$\langle F_y \rangle = \frac{1}{2} \text{Re} (J_x \hat{B}_z^*) \tag{7.1.96}$$

The force per unit x - z area $\langle T_y \rangle$ can be computed in a manner similar to that used to find (7.1.95):

$$\langle T_y \rangle = \frac{\mu_0 K^2}{4} \left(\frac{\sqrt{1 + S^2} - 1}{\sqrt{1 + S^2}} \right) \tag{7.1.97}$$

The dependence of this levitating force on S is shown in Fig. 7.1.21. As S is increased, the upward force approaches an asymptotic value of $\mu_0 K^2/4$. As discussed in Chapter 8, this is the average magnetic pressure that acts on a perfectly conducting surface. A levitation experiment is shown in Fig. 7.1.22.

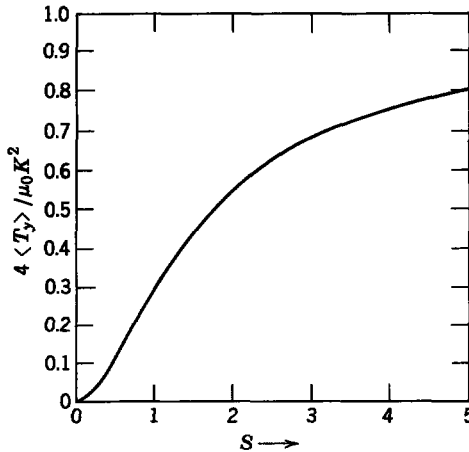


Fig. 7.1.21 Normalized time average force $\langle T_y \rangle$ per unit x - z area.

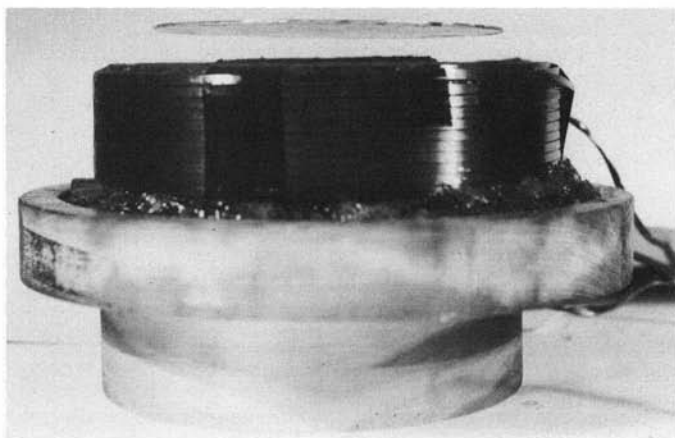


Fig. 7.1.22 Laboratory project in which an aluminum disk (about 6 in. in diameter) is levitated by an alternating magnetic field. The coil is driven by a 400-Hz current. The experiment demonstrates qualitatively the induced force given by (7.1.97) with $V = 0$. Of course, in the experiment the finite thickness of the disk is highly significant (see Fig. 7.1.15) with $\sigma = 3.7 \times 10^7$ mhos/m.

7.2 CHARGE RELAXATION

As discussed in the introduction to this chapter, the relaxation of charge in slightly conducting media constitutes the mechanism by which motion has an effect on electric field distributions in electric field systems. This is illustrated in the following sections by a series of examples. First, the relaxation of charge in systems involving media at rest is considered. Here the relaxation time is of fundamental importance in determining volume and surface charge densities that result from initial conditions and from excitations. In Section 7.2.2 emphasis is given to the effect of steady motion on the relaxation of free charge. In this case the electric Reynolds number based on the material velocity is important. Sections 7.2.3 and 7.2.4 then consider systems in which relaxation is affected by two characteristic times, a time that characterizes an electrical excitation and a time based on the material velocity and characteristic length.

The field equations for an electric field system (see Table 1.2)* are

$$\nabla \times \mathbf{E} = 0, \quad (7.2.1)$$

$$\nabla \cdot \epsilon \mathbf{E} = \rho_f, \quad (7.2.2)$$

$$\nabla \cdot \mathbf{J}_f + \frac{\partial \rho_f}{\partial t} = 0 \quad (7.2.3)$$

where we have assumed $\mathbf{D} = \epsilon \mathbf{E}$.

* See Appendix E.

In this section we confine our attention to situations in which the conduction of free charge can be accounted for by a constitutive law in the form

$$\mathbf{J}_f = \sigma \mathbf{E} + \rho_f \mathbf{v}. \quad (7.2.4)$$

Here we have combined Ohm's law $\mathbf{J}'_f = \sigma \mathbf{E}'$ with the field transformations $\mathbf{E}' = \mathbf{E}$ and $\mathbf{J}'_f = \mathbf{J}_f - \rho_f \mathbf{v}$.^{*} This law describes the conduction process in a wide range of solids, liquids, and gases but is by no means of general applicability.

There is a considerable analogy between the way in which we develop the subject of charge relaxation in this section and the way in which magnetic diffusion is developed in Section 7.1; for example, we begin by developing an equation that, together with appropriate boundary conditions, defines the distribution of the electric field, given the velocity of the medium.[†] From (7.2.3) and (7.2.4)

$$\nabla \cdot \sigma \mathbf{E} + \nabla \cdot \rho_f \mathbf{v} + \frac{\partial \rho_f}{\partial t} = 0. \quad (7.2.5)$$

The free charge density ρ_f can be eliminated from this expression by using (7.2.2).

$$\nabla \cdot \sigma \mathbf{E} + \nabla \cdot (\mathbf{v} \nabla \cdot \epsilon \mathbf{E}) + \frac{\partial}{\partial t} \nabla \cdot \epsilon \mathbf{E} = 0. \quad (7.2.6)$$

Given the velocity \mathbf{v} , this expression involves only the electric field intensity \mathbf{E} . It is a scalar equation, hence does not in general define the three components of \mathbf{E} . From (7.2.1), however, we can define a potential ϕ such that

$$\mathbf{E} = -\nabla \phi. \quad (7.2.7)$$

Then (7.2.6) becomes one equation in one unknown.

$$\nabla \cdot \sigma \nabla \phi + \nabla \cdot (\mathbf{v} \nabla \cdot \epsilon \nabla \phi) = -\frac{\partial}{\partial t} \nabla \cdot \epsilon \nabla \phi. \quad (7.2.8)$$

Physically, this equation accounts for the conservation of free charge. The first term accounts for the flow of free charges into a small volume due to conduction. The second term appears because convection of the medium can give rise to the transport of free charge into a given region. Then the term on the right is the rate of increase of the local free charge density. Equation 7.2.8 serves the same purpose in a distributed electric field system as the electrical equation of motion served in the lumped-parameter descriptions of Chapters 2 to 5. In the sections that follow we confine our attention to the effect of the motion (if there is motion) on the fields; that is, the velocity \mathbf{v} is prescribed. One objective is an indication of models that can

^{*} Table 6.1, Appendix E.

[†] In the development of this section σ and ϵ are assumed to be given functions of the space coordinates.

be used to simplify the analysis of electromechanical coupling, in which the velocity \mathbf{v} is not known until the fields are known.

7.2.1 Charge Relaxation as an Electrical Transient

We first consider the relaxation of charge in the absence of motion. A common situation is one in which the conductivity σ and permittivity ϵ of each medium are uniform; thus changes in conductivity and permittivity occur only at surfaces. In these important situations it is essential to recognize that in the absence of a free charge source in the medium there will be no steady-state volume free-charge density. This is one of the important points to be made in the following subsection.

7.2.1a Media with Uniform Properties

Suppose that we are concerned with the free-charge density in a medium at rest. Then the second term in (7.2.8) is zero and (7.2.2) and (7.2.7) can be used to write this expression as

$$\frac{\partial \rho_f}{\partial t} + \frac{\sigma}{\epsilon} \rho_f = 0. \quad (7.2.9)$$

A more direct derivation of this equation simply combines (7.2.2) to (7.2.4) with $\mathbf{v} = 0$. A general solution to (7.2.9) is

$$\rho_f(x, y, z, t) = \rho_0(x, y, z)e^{-(\sigma/\epsilon)t}, \quad (7.2.10)$$

as can be seen by substitution into (7.2.9); that is, given an initial free-charge distribution ρ_0 at $t = 0$, the free charge density at each point in space decays to zero with the *relaxation time* τ .

$$\tau = \frac{\epsilon}{\sigma}. \quad (7.2.11)$$

Unless there are sources of free charge in the volume of the material [which would contribute a driving term to (7.2.9)], there are no steady-state charges in the bulk. Note that (7.2.9) can be derived without recourse to (7.2.1), so that these conclusions do not depend on the field equations being quasi-static. Of course, in any physical situation the uniformly conducting medium is of finite extent and conservation of charge requires that those charges initially distributed throughout the volume relax to the surfaces that bound the volume. This can best be shown by means of an example.

Example 7.2.1. A conducting shell contains a uniformly conducting sphere at its center (Fig. 7.2.1). The region between the sphere and the shell is perfectly insulating. At time $t = 0$ there is a free charge density ρ_0 distributed uniformly throughout a spherical region of radius R at the center of the conducting sphere; that is, if we call the total charge supported by the center sphere Q ,

$$\rho_f(r < R, t = 0) = \rho_0 = Q/(4/3)\pi R^3. \quad (a)$$

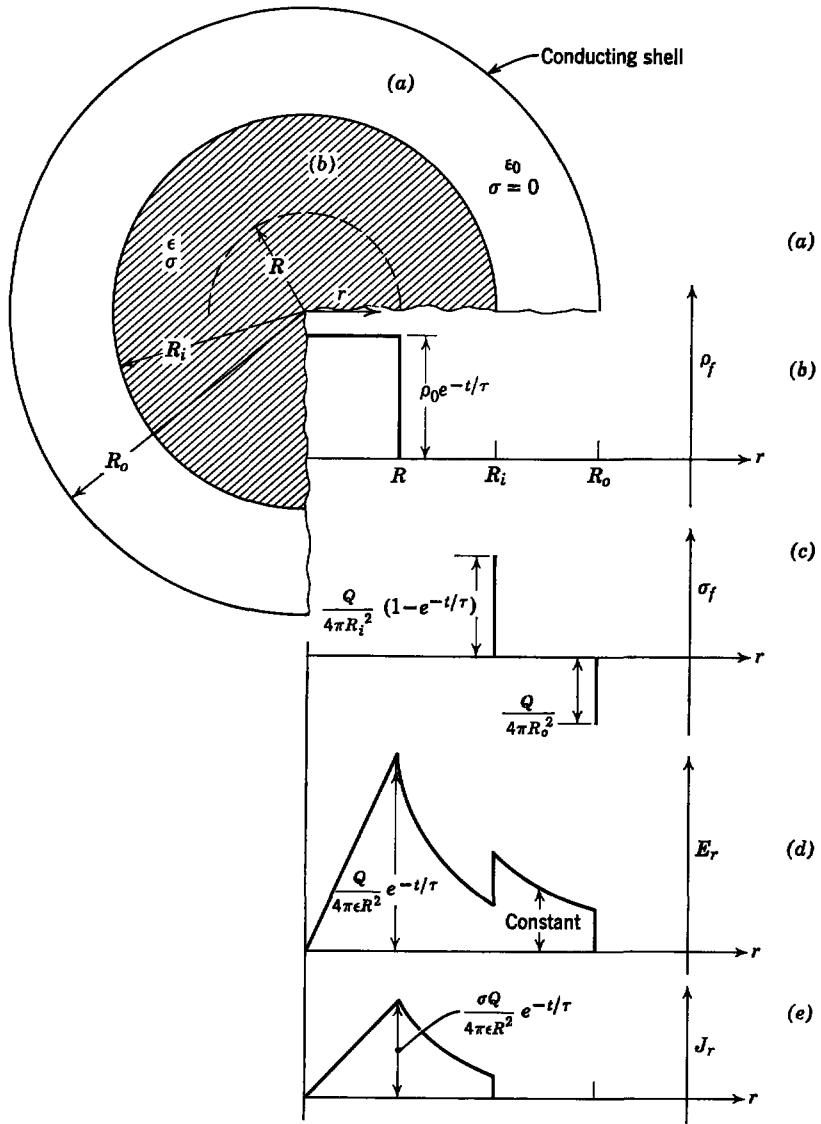


Fig. 7.2.1 (a) A uniformly conducting sphere of radius R_i is bounded by an insulating medium and a perfectly conducting shell of radius R_o ; (b) when $t = 0$, the sphere supports a volume charge distributed uniformly over the region $r < R$; (c) for $t > 0$ charges accumulate at $r = R_i$; (d) radial electric field E_r ; (e) current density J_r .

The transient charge density follows from (7.2.10)

$$\begin{aligned} \rho_f &= \rho_0 e^{-t/\tau} & \text{for } r < R, \\ \rho_f &= 0 & \text{for } r > R. \end{aligned} \quad (b)$$

This distribution of volume charge density is shown in Fig. 7.2.1b.

The problem has radial symmetry. Hence the charge distribution of (b) can be used with (7.2.2) to determine the radial component of the electric field intensity since

$$\frac{1}{r^2} \frac{d}{dr} (r^2 E_r) = \frac{\rho_0}{\epsilon} e^{-t/\tau}. \quad (c)$$

This expression can be integrated to obtain

$$E_r^b = \frac{Q}{4\pi\epsilon R^2} \left(\frac{r}{R}\right) e^{-t/\tau}; \quad r < R \quad (d)$$

The total charge within the radius $r = R$ is $Qe^{-t/\tau}$. Then the integral form of Gauss's theorem shows that

$$E_r^b = \frac{Q}{4\pi\epsilon r^2} e^{-t/\tau}; \quad R < r < R_i \quad (e)$$

Similarly, since the total charge on the sphere must be conserved, the electric field outside the conducting sphere is

$$E_r^a = \frac{Q}{4\pi\epsilon_0 r^2}; \quad R_i < r < R_o \quad (f)$$

These last two electric field intensities can be used to determine the amount of free charge on the surface of the inner sphere, since

$$\sigma_f = \epsilon_0 E_r^a (r = R_i) - \epsilon E_r^b (r = R_i) = \frac{Q}{4\pi R_i^2} (1 - e^{-t/\tau}). \quad (g)$$

Of course, the surface charge on the outer shell is constant, for the electric field in the insulating section adjacent to the shell is constant. The surface charge density and distribution of E_r are shown in Fig. 7.2.1c,d. It is clear from the solutions that the initial free-charge density relaxes to the outer surface of the conducting sphere. In the steady-state condition there is no electric field within the sphere, but rather the field is shielded out of the sphere by the surface charge at $r = R_i$.

Remember that the current density is

$$J_r = \sigma E_r \quad (h)$$

and is therefore distributed as shown in Fig. 7.2.1e. It is this current that accounts for the conduction of free charge to the surface of the sphere. Note that there is a conduction current in the region $R < r < R_i$, even though at no time during the transient is there a free-charge density in this region. Conduction currents modeled by a constitutive law in the form of (7.2.4) can be present in a medium in the absence of ρ_f .

Without injection of charges directly into the bulk of the material, a uniformly conducting medium with uniform permittivity does not support a volume charge density as illustrated by Example 7.2.1. In such systems free charges are confined to surfaces. These surface charges can relax through a

medium and this surface-charge relaxation is accounted for through boundary conditions. Lumped-parameter models often can be used to represent this process, as illustrated by the following example.

Example 7.2.2. The important role of surface-charge relaxation through dielectrics can be demonstrated by means of the experiment shown in Fig. 7.2.2. Three plane parallel metallic electrodes are immersed in a liquid dielectric as shown. A voltage source V_o is used to establish a positive charge on the middle electrode. At time $t = 0$ the switch S connects the battery to the terminal (2), leaving the middle plate isolated from the other two plates except for conduction through the dielectric. We wish to compute the electric fields defined in Fig. 7.2.2 as functions of time, to show the relaxation of charge from the middle plate.

We assume that the fields are uniformly distributed between the plates so that for $t < 0$

$$E_a = \frac{V_o}{a}, \tag{a}$$

$$E_b = 0. \tag{b}$$

We integrate the conservation of charge equation (7.2.3) over the volume that encloses the middle plate to write

$$(J_a - J_b) = -\frac{\partial}{\partial t} \epsilon(E_a - E_b). \tag{c}$$

This equation guarantees that the rate of change of charge on the middle plate is accounted for by current to either of the other plates. The current densities can be replaced by the

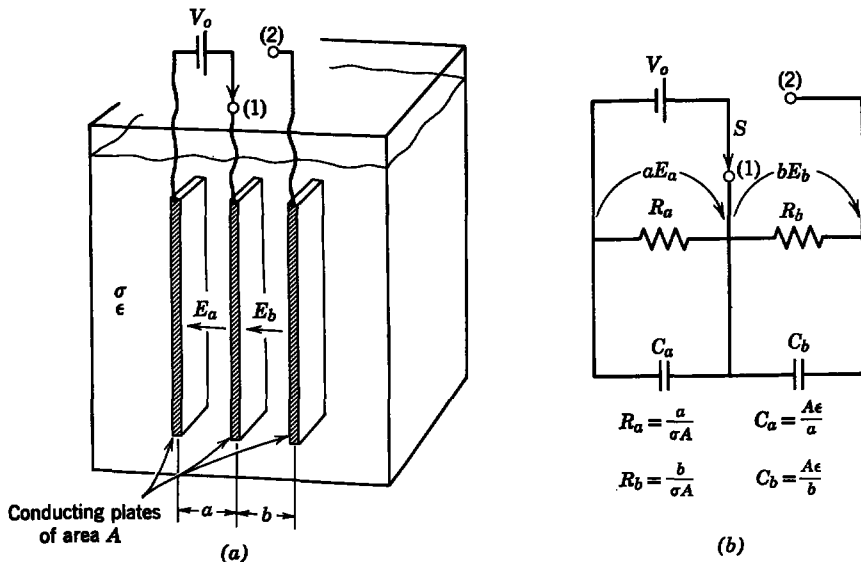


Fig. 7.2.2 System of three parallel-plane metallic electrodes immersed in a dielectric of conductivity σ and permittivity ϵ : at $t = 0$ the switch is connected to terminal (2); (b) equivalent circuit.

electric field intensities by using (7.2.4) with $v = 0$:

$$\sigma(E_a - E_b) = -\frac{d}{dt} \epsilon(E_a - E_b). \quad (d)$$

This expression is recognized as having the same form as (7.2.9) except that the charge density is replaced by the jump in electric field intensity, which is proportional to the charge density on the middle plate. If we use the initial conditions of (a) and (b) the solution to (d) is

$$E_a - E_b = \frac{V_o}{a} e^{-t/\tau}; \quad \tau = \frac{\epsilon}{\sigma}. \quad (e)$$

For $t > 0$ the voltage across the outside plates is constrained to be V_o , hence

$$E_a a + E_b b = V_o. \quad (f)$$

We solve for both E_a and E_b from these last two equations.

$$E_a = \frac{V_o}{a+b} \left(1 + \frac{b}{a} e^{-t/\tau} \right), \quad (g)$$

$$E_b = \frac{V_o}{a+b} (1 - e^{-t/\tau}). \quad (h)$$

These solutions are shown in Fig. 7.2.3. Initially, all of the charge is retained on the middle plate. [Recall that the charge on the middle plate is at first $(A\epsilon V_o/a)$ and is always $A\epsilon(E_a - E_b)$.] All the charge relaxes to the outer plates with the characteristic relaxation time τ . The relaxation of charge is a fundamental way of viewing the decay of the RC circuit shown in Fig. 7.2.2. The solution using this circuit with the equivalent parameter values is the same as the solution just given for the continuum model. This example provides the answer to the question posed in Fig. 7.2.4.

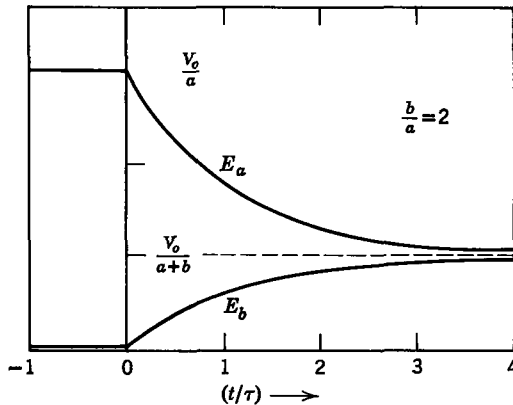


Fig. 7.2.3 Relaxation of the electric field intensities between the plates in Fig. 7.2.2 when S is switched from (1) to (2). The surface charge density on the middle plate is proportional to the difference between E_a and E_b .

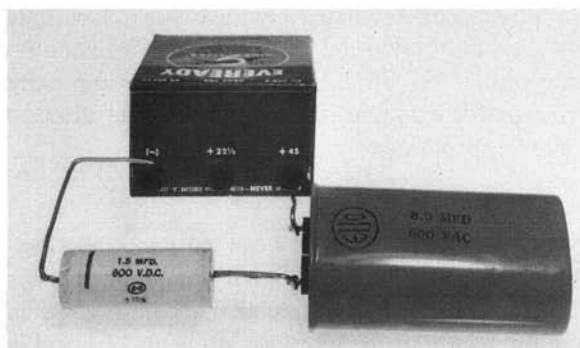


Fig. 7.2.4 The capacitors are connected in series with the battery. The circuit has been completed for a sufficient length of time to establish steady-state conditions. Why is it not possible, on the basis of the given information, to determine the steady-state charge stored in each of the capacitors? (See Example 7.2.2.)

Whether we are concerned with relaxation of charge from the bulk or from an interface, the relaxation time ϵ/σ is of fundamental importance. In Table 7.2.1 we see that the relaxation time depends greatly on the material used. In metals the volume distribution of charge would be difficult to measure, let alone ever be large enough to include in a physical model. On the other hand, there are many materials in which the relaxation time can be measured in minutes or even hours. In slightly conducting materials, however, the conductivity is often extremely sensitive to impurities and sources of

Table 7.2.1 Characteristic Values of Relaxation Time $\tau = \epsilon/\sigma$ for Conductors and Insulators

| Material | σ (mhos/meter) | ϵ | τ (sec) |
|-----------------------|--------------------------|-------------------|------------------------|
| Silver* | 6.17×10^7 | ϵ_0 | 1.43×10^{-19} |
| Copper* | 5.80×10^7 | ϵ_0 | 1.52×10^{-19} |
| Aluminum* | 3.72×10^7 | ϵ_0 | 2.38×10^{-19} |
| Mercury† | 1.06×10^6 | ϵ_0 | 8.35×10^{-18} |
| Seawater* | 4 | $80 \epsilon_0$ | 1.77×10^{-10} |
| Water† | 4×10^{-6} | $80 \epsilon_0$ | 1.77×10^{-4} |
| Nitrobenzene† | 5×10^{-7} | $36.1 \epsilon_0$ | 6.40×10^{-4} |
| Corn oil | 5×10^{-11} | $2.7 \epsilon_0$ | 4.8 |
| Carbon tetrachloride† | 4×10^{-16} | $2.24 \epsilon_0$ | 4.95×10^4 |

* S. Ramo, and J. R. Whinnery, *Fields and Waves in Modern Radio*, Wiley, New York, 1958, pp. 240 and 312.

† N. A. Lange, *Handbook of Chemistry*, Handbook Pub., Inc., Sandusky, Ohio, 1952, pp. 1240 and 1253.

ionization. For this reason tabulated conductivities, especially for liquids, are likely to indicate only the order of magnitude. We should bear in mind also that the constitutive law of (7.2.4) may be a poor approximation for the conduction process; for example, the mobility model discussed in Section 6.3.2 may be more appropriate.

7.2.1b Media with Nonuniform Properties

A steady-state volume charge density can exist in a medium at rest when there are gradients of either the conductivity or permittivity in the bulk of the material. The interface between dissimilar media is a special case of this situation, for in the region of the interface gradients of ϵ and σ are singular. It is for this reason that surface charges accumulate on the surfaces of uniformly conducting media.

With σ and ϵ functions of position the potential in a stationary medium must satisfy the expression

$$\nabla \cdot \sigma \nabla \phi + \frac{\partial}{\partial t} \nabla \cdot \epsilon \nabla \phi = 0, \quad (7.2.12)$$

as we can see from (7.2.8). Note that this expression does not take the simple form of (7.2.9) unless σ and ϵ are constant. A one-dimensional example serves to illustrate the consequences of nonuniform properties in electric field systems.

Example 7.2.3. Plane parallel electrodes bound a material of nonuniform properties shown in Fig. 7.2.5. For purposes of illustration we consider the case in which an external current source drives a current through the material in the x -direction. The material properties depend only on the x -dimension. We wish to determine the free charge density and distribution of electric field intensity between the plates. Physically, this situation would be realized by simply placing electrodes with a temperature difference in an organic liquid. The conductivity is a strong function of temperature in many liquids and there would therefore be a variation in σ as a function of x .

In one dimension the gradient of ϕ in (7.2.12) becomes $(-E_x)$; hence (7.2.12) can be written as

$$\frac{\partial}{\partial x} \left[\frac{\partial}{\partial t} (\epsilon E_x) + \sigma E_x \right] = 0. \quad (a)$$

This expression can be integrated to obtain

$$\frac{\partial}{\partial t} (\epsilon E_x) + \sigma E_x = f(t). \quad (b)$$

This result is not surprising, for it simply states that the sum of the displacement and conduction currents passing any given y - z plane is the same as that found at any other y - z plane; That is, $f(t)$ is simply the current density $i(t)/A$:

$$\frac{\partial}{\partial t} (\epsilon E_x) + \sigma E_x = \frac{i(t)}{A}. \quad (c)$$

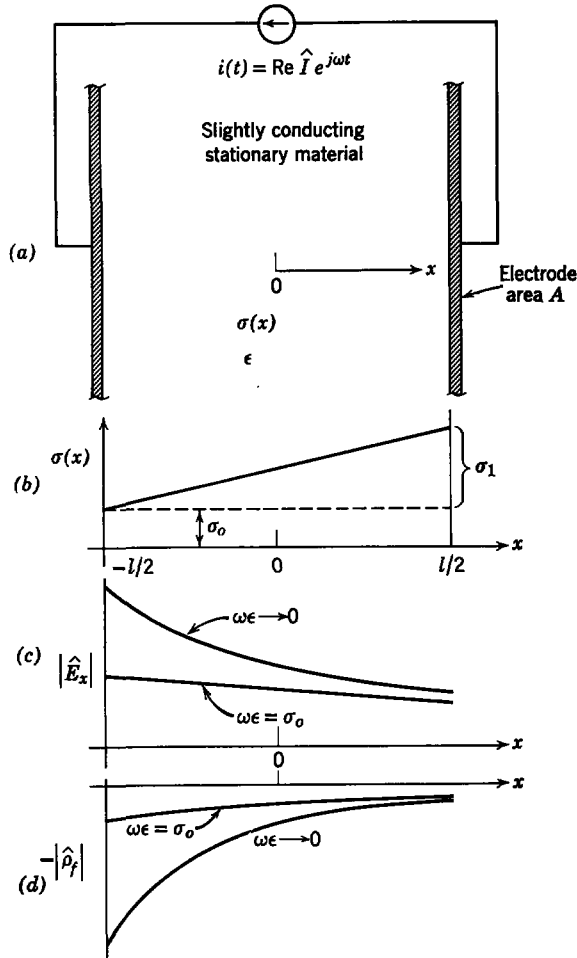


Fig. 7.2.5 (a) A slightly conducting material of uniform permittivity is bounded by plane-parallel electrodes of area A ; (b) conductivity distribution between plates; (c) distribution of the electric field magnitude; (d) free charge density magnitude.

To emphasize the fact that under steady-state conditions there are bulk charges in the nonuniform medium consider a sinusoidal driving current

$$i(t) = \text{Re} (\hat{I} e^{j\omega t}), \tag{d}$$

hence sinusoidal responses in the form

$$E_x = \text{Re} [\hat{E}_x(x) e^{j\omega t}]. \tag{e}$$

Then substitution into (c) shows that

$$\hat{E}_x = \frac{\hat{I}}{A(j\omega\epsilon + \sigma)}. \tag{f}$$

Here σ and ϵ are in general functions of x , hence so also is E_x . The charge density is found by using (7.2.2):

$$\hat{\rho}_f = \frac{d\epsilon \hat{E}_x}{dx} = -\frac{\epsilon \hat{I}}{A} \frac{[j\omega(d\epsilon/dx) + d\sigma/dx]}{(j\omega\epsilon + \sigma)^2} + \frac{\hat{I}(d\epsilon/dx)}{A(j\omega\epsilon + \sigma)}. \quad (g)$$

As a more particular example consider the case in which the conductivity has the linear distribution shown in Fig. 7.2.5*b* and the permittivity is constant.

$$\sigma(x) = \sigma_0 + \frac{\sigma_1}{l}x. \quad (h)$$

Then it follows from (f) and (g) that

$$|\hat{E}_x| = \frac{|\hat{I}|}{A\sqrt{\sigma^2 + (\omega\epsilon)^2}} \quad (i)$$

$$|\hat{\rho}_f| = \frac{\epsilon|\hat{I}|\sigma_1/A}{[\sigma^2 + (\omega\epsilon)^2]}. \quad (j)$$

The distribution of electric field intensity and charge density magnitudes between the plates is shown in Fig. 7.2.5*c, d*. Note that the greatest amount of free charge exists in the bulk of the medium when the frequency is zero (the current is constant). The charge density tends to zero as the frequency is made large compared with the local reciprocal of the relaxation time ϵ/σ . In the high frequency limit one period of excitation is insufficient time for the free charge to accumulate in the bulk of the material.

Bulk charge accumulation due to nonuniform conductivity occurs in many practical situations; for example, in oil-insulated, high-voltage dc cables for the transmission of power a temperature gradient in the oil can make the conductivity vary markedly with position. A bulk charge accumulates; and, when the applied voltage is reversed, the bulk charge may cause overly high electrical stresses and insulation failure before it can relax to a new steady-state distribution.*

7.2.2 Charge Relaxation in the Presence of Steady Motion

We are now in a position to undertake a study of the effects of material motion on charge relaxation. In the sections that follow interest is confined to systems in which changes in material properties occur at surfaces and can be accounted for by the boundary conditions. Then, because σ and ϵ are constant in the bulk of the material, (7.2.8) can be written as

$$\frac{\sigma}{\epsilon} \rho_f + \nabla \cdot \rho_f \mathbf{v} + \frac{\partial \rho_f}{\partial t} = 0, \quad (7.2.13)$$

where use has been made of (7.2.2) and (7.2.7) to state this equation in terms of the free charge density.

A great deal can be said about the implications of (7.2.13) in the important case in which the media are *incompressible*. In such situations the material density remains constant and the net flux of material into a given region is

* See, for example, K. Kojima, S. Tanaka, and K. Matsuura, "Potential Distribution in Dielectrics of Oil-Filled, D-C Cable," *Elec. Eng. Japan*, August 1964.

zero. By analogy with a similar condition on the magnetic flux density ($\nabla \cdot \mathbf{B} = 0$) the condition that the material be incompressible is stated as

$$\nabla \cdot \mathbf{v} = 0. \quad (7.2.14)$$

(More is said about this equation in Chapter 12, in which incompressible fluids are discussed.)

Expansion of the second term in (7.2.13) gives

$$\nabla \cdot \rho_f \mathbf{v} = \mathbf{v} \cdot \nabla \rho_f + \rho_f (\nabla \cdot \mathbf{v}), \quad (7.2.15)$$

where, in view of (7.2.14), the last term is zero. Hence (7.2.13) can be written as

$$\frac{\sigma}{\epsilon} \rho_f + \frac{\partial \rho_f}{\partial t} + \mathbf{v} \cdot \nabla \rho_f = 0. \quad (7.2.16)$$

Written in this form, it is clear that (7.2.16) expresses the same relaxation conditions as (7.2.9) did for stationary media, except that now the charge relaxation occurs with respect to the frame of the moving medium; that is, the last two terms in (7.2.16) (the convective derivative) represent the time rate of change of ρ_f for an observer moving with the velocity \mathbf{v} of the material. Hence the material motion simply serves to transport the free charge as it relaxes with the time constant ϵ/σ .

Example 7.2.4. The relaxation of an initial distribution of charge placed in the fluid stream shown in Fig. 7.2.6 is to be considered. Note that the velocity $\mathbf{v} = v_x(y)\mathbf{i}_x$ satisfies (7.2.14).

Remember that (7.2.16), which must be satisfied by the distribution of ρ_f , expresses the same relaxation phenomenon as (7.2.9), except that the relaxation occurs with respect to the moving medium. Hence we look for a solution to (7.2.16) that has the form of (7.2.10), with x replaced by x' , where

$$x' = x - v_x(y)t. \quad (a)$$

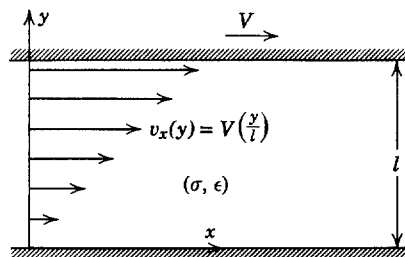


Fig. 7.2.6 A fluid with uniform conductivity and permittivity is confined by parallel plates, one of which is fixed as the other moves to the right with the velocity V . The fluid, which then moves to the right with the velocity profile shown, is given an initial charge distribution which relaxes as shown in Fig. 7.2.7.

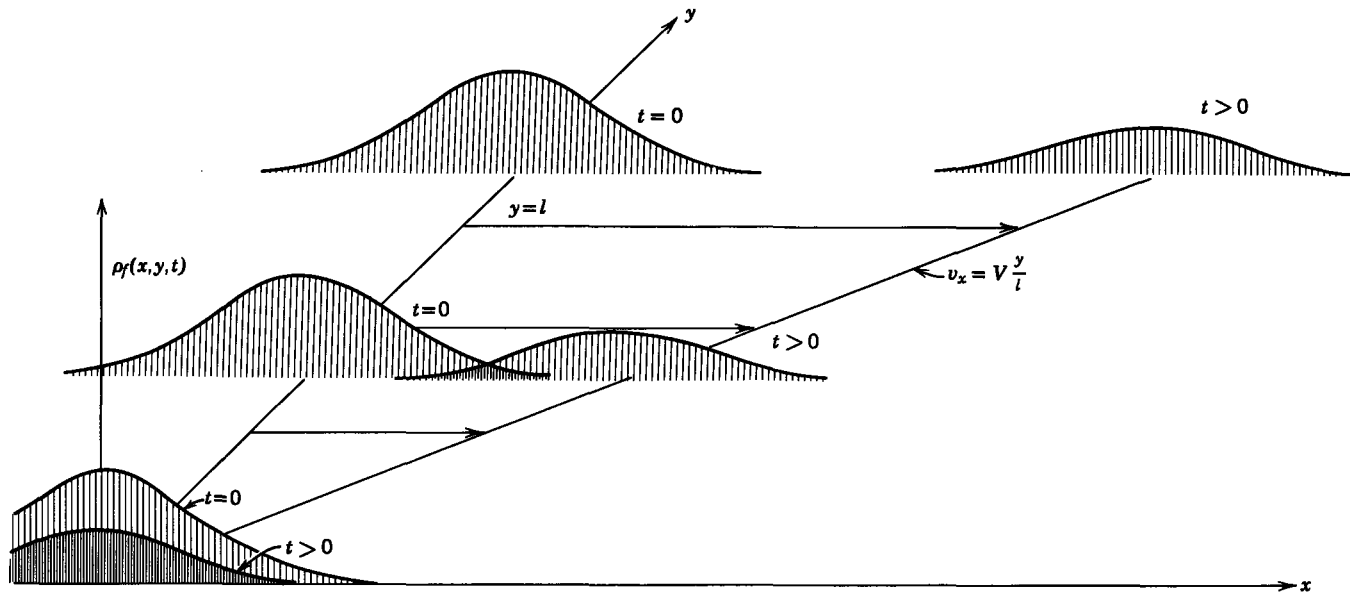


Fig. 7.2.7 An initial distribution of charge is transported downstream with the material velocity as it relaxes with the time constant ϵ/σ .

By this reasoning the desired solution to (7.2.16) is

$$\rho_f = \rho_0[x - v_x(y)t, y]e^{-(\sigma/\epsilon)t}, \quad (b)$$

which can be checked by direct substitution. From this result it is clear that an initial charge distribution is simply translated downstream, attenuating in amplitude with the relaxation time ϵ/σ but otherwise retaining its initial shape; for example, if at $t = 0$ the charge distribution is

$$\rho_f(x, y, t = 0) = \rho_0 e^{-(x/l)^2}, \quad (c)$$

as shown in Fig. 7.2.7, the subsequent charge distribution will be

$$\rho_f(x, y, t) = \rho_0 \exp \left\{ - \left[\frac{x - v_x(y)t}{l} \right]^2 \right\} e^{-(\sigma/\epsilon)t}. \quad (d)$$

This redistribution of the charge is also shown in Fig. 7.2.7. It is important to see that even in the presence of convection the steady-state charge density in source-free media with uniform electrical properties tends to zero.

It must be recognized that there is an electric potential associated with the charge density defined by (7.2.16). In the simple bulk relaxation problem considered here it is possible to determine the charge density without recourse to the boundary conditions, hence to the potential ϕ . Many practical devices exploit the energy conversion process that takes place when the charge is transported from a region of one potential to a region of another. To determine whether energy is taken from the moving medium (a generator) or put into the medium (motor or pump) it is necessary to know the potential distribution. A simple illustration of this kind of problem is made next. The conditions required within the medium for appreciable charge transport are apparent from the developments of this section. The time required for a given initial distribution of charge to relax (with respect to the medium) is ϵ/σ , whereas the time required for the transport of the charge over a distance l with the velocity V is l/V . For an appreciable convection of charge the transport time must be short compared with the relaxation time; that is

$$R_e = \frac{\epsilon/\sigma}{l/V} = \frac{\epsilon V}{\sigma l} \gg 1 \quad (7.2.17)$$

or the electric Reynolds number R_e must be large compared with one if the convection is to compete with the relaxation process in determining the location of the volume charge density.

One highly developed application of the ideas introduced in this section is to the generation of extremely high voltages. Here the basic electro-mechanical system is a Van de Graaff generator that uses the mechanical motion of an insulator to transport free charge against an electric field and generate high-voltage dc power.* A simple model for this generator is the subject of the following example.

* A description of this and other sources of power is given in J. G. Trump, "Electrostatic Sources of Electric Power," *Elec. Eng.*, June 1947.

Example 7.2.5. The basic system, illustrated in Fig. 7.2.8a, consists of a continuous belt made of slightly conducting material, which is driven by rollers at the constant velocity

$$\mathbf{v} = \mathbf{i}_z V.$$

The electrode at $z = 0$ feeds positive ions onto the surface of the belt and the electrode at $z = l$ removes the positive ions. The two electrodes are the electrical terminals that will remain open-circuited for this example. The belt material has a constant conductivity σ and constant permittivity ϵ but the positive ions put on the belt by the electrode are immobile.

The analysis of the system begins with the following assumptions:

1. We consider only that portion of the belt that carries charge from $z = 0$ to $z = l$.
2. The electric field intensity and current density have only z components:

$$\mathbf{E} = \mathbf{i}_z E,$$

$$\mathbf{J}_f = \mathbf{i}_z J.$$

3. All variables are functions of z alone.
4. In the spirit of the one-dimensional model we assume that the net effect of the positive ions applied to the belt and the induced charge in the belt can be represented by an effective free charge density ρ_f which is a function of z only.
5. We assume that the electrode at $z = 0$ maintains the boundary condition

$$\text{at } z = 0, \quad \rho_f = \rho_0. \quad (\text{a})$$

6. The system is operating in the steady state.

With the conductivity constant, the constituent relation for the transport of free charge is (7.2.4)

$$J = \sigma E + \rho_f V. \quad (\text{b})$$

The other equations necessary for the analysis are Gauss's law (7.2.2) written as

$$\epsilon \frac{dE}{dz} = \rho_f \quad (\text{c})$$

and the condition imposed by the open circuit

$$J = 0. \quad (\text{d})$$

We differentiate (b) with respect to z and use (c) to eliminate E and obtain

$$V \frac{d\rho_f}{dz} + \frac{\sigma}{\epsilon} \rho_f = 0. \quad (\text{e})$$

The general solution of this equation is

$$\rho_f = C_1 e^{-\sigma z / \epsilon V}. \quad (\text{f})$$

We use boundary condition (a) to evaluate the constant C_1 and obtain the solution

$$\rho_f = \rho_0 e^{-z/R_e l}; \quad R_e = \frac{\epsilon V}{\sigma l}. \quad (\text{g})$$

Finally, we calculate the open-circuit voltage by using (b) and (d):

$$V_{\text{oc}} = - \int_0^l E_z dz = R_e^2 \frac{\rho_0 l^2}{\epsilon} (1 - e^{-1/R_e}). \quad (\text{h})$$

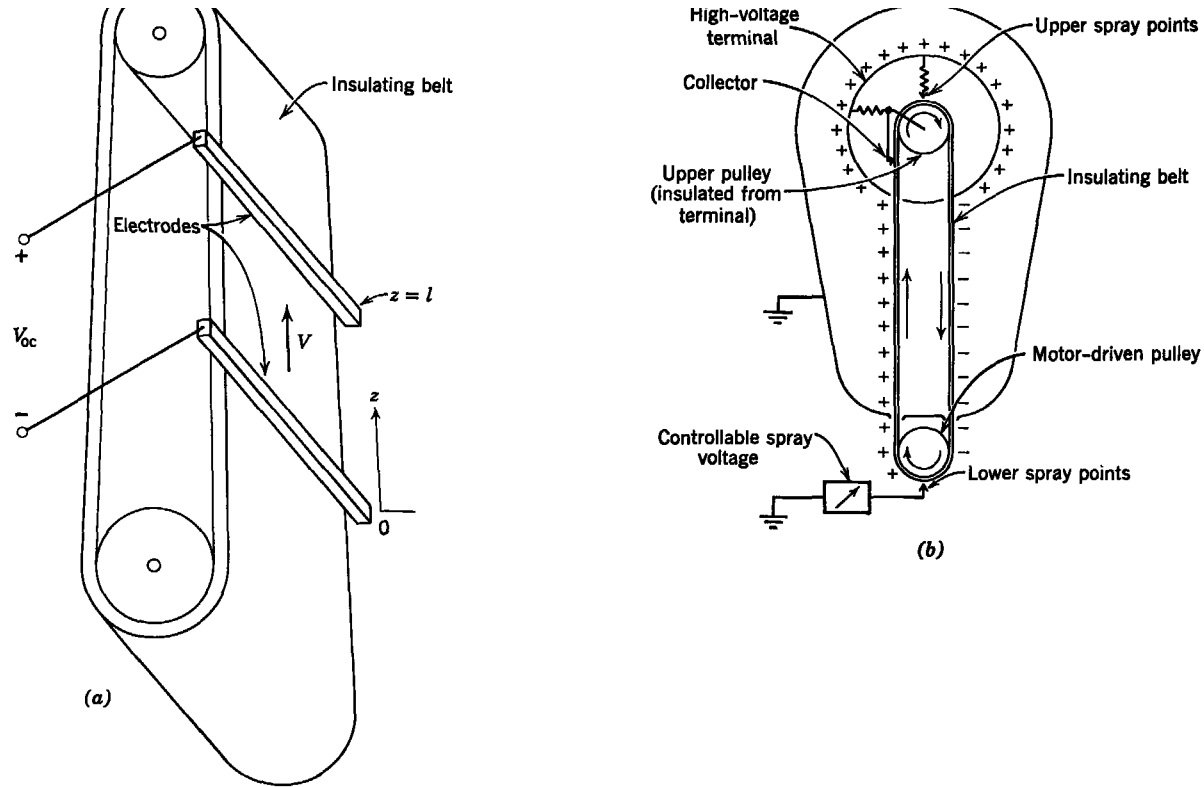


Fig. 7.2.8 (a) A simple model for a Van de Graaff generator. Charges are conveyed to the belt at $z = 0$ and transported in the presence of relaxation to the electrode at $z = l$ through a potential difference V_{0c} . (b) A more realistic schematic diagram of the generator shows how the charge is injected and removed with corona sources. In a practical device the conduction along the belt does not represent a significant limitation.

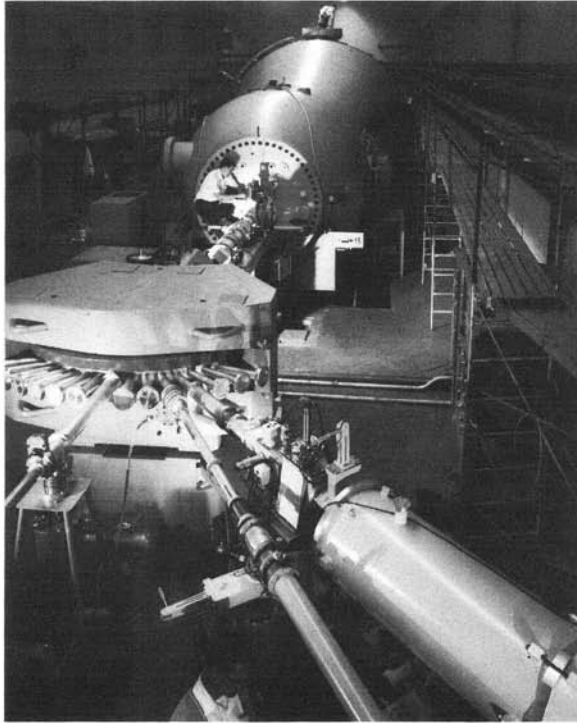


Fig. 7.2.8c Van de Graaff tandem accelerator at High Voltage Engineering Corporation, Burlington, Mass. Capable of a terminal potential of 10 MV, this machine weighs 188 tons, is 18 ft in diameter, and is 81 ft long.

The distributions of free charge density ρ_f and field intensity E along the belt are shown in Figs. 7.2.9 and 7.2.10. To interpret these curves, consider that ϵ and l are fixed and that R_e is changed by varying σ and/or V . The current density J , as given by (b), indicates that free charge is transported by conduction (σE) and by convection ($\rho_f V$). As indicated earlier in this section, the presence of conduction makes the free charge tend to relax to the surfaces of the conductor. Thus in this system we have two competing processes: (a) convection of the charge in the positive z -direction by the moving belt and (b) relaxation of free charge in the belt to neutralize the injected charge. It is apparent from the curves of Fig. 7.2.9 that the electric Reynolds number R_e is a measure of the relative effectiveness of these two processes. For a large R_e the relaxation process is relatively ineffective and the charge density varies very little along the length of the device. On the other hand, for small R_e , the relaxation process predominates and the net charge density decays rapidly along the length because induced charge can build up in the belt to neutralize the injected charge.

It is clear that because the amount of net free charge between the electrodes varies significantly with R_e so will the electric field intensity. As indicated by (b) and (d), E has the same space variation as the charge density but its magnitude is a function of R_e also.

For the three values of R_e for which curves are plotted in Figs. 7.2.9 and 7.2.10 we calculate the open-circuit voltage from (h) and give the values in Table 7.2.2.

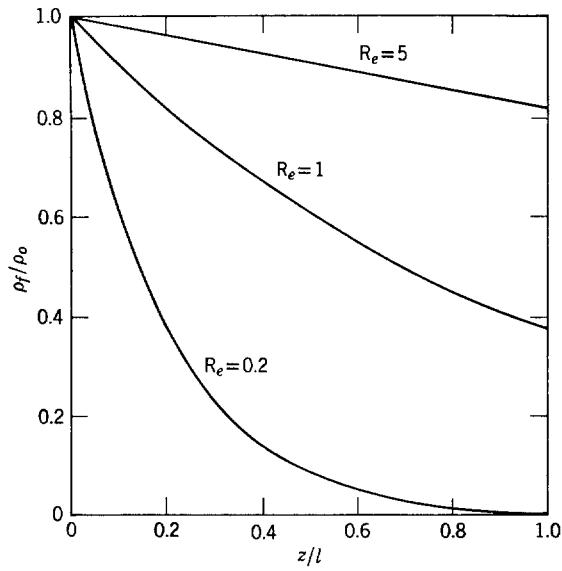


Fig. 7.2.9 Variation of net free charge density with position.

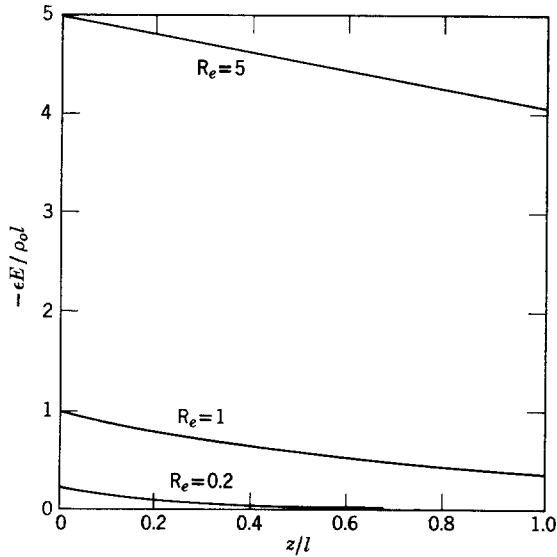


Fig. 7.2.10 Variation of electric field intensity with position.

Table 7.2.2

| R_e | $\frac{\epsilon V_{oc}}{\rho_o l^2}$ |
|-------|--------------------------------------|
| 0.2 | 0.0373 |
| 1.0 | 0.632 |
| 5.0 | 4.55 |

Thus for fixed geometry (l), fixed charge density at $z = 0(\rho_o)$, and fixed permittivity the open-circuit voltage is increased by increasing the velocity (V) of the belt or by decreasing the conductivity (σ) of the belt material. In either case the electric Reynolds number is increased. Note from (h) that the open-circuit voltage increases in proportion to R_e . Thus for the highest possible open-circuit voltage we must make the velocity as high as possible and the conductivity as low as possible.

In the previous example, we assumed that the electric field intensity and material motion were in the same direction. Practical generators are shown in Figs. 7.2.8*b-c*. In these devices, the component of the electric field intensity due to charge on the belt (as compared to that on the terminals) is essentially perpendicular to the direction of motion, and hence a somewhat different model is appropriate for quantitative purposes.

For conceptual simplicity we have so far in this section emphasized the effect of material motion on electric fields in situations in which the material could be essentially characterized by a single electric Reynolds number. Cases in which electric fields interact with continuous media are extremely diverse, both in terms of the mechanism basic to the interaction and in terms of possible applications. This point can be illustrated by considering an example that has some of the basic ingredients of a thunderstorm. This is a system that involves a highly insulating gas (the air, with a relaxation time that can be measured in hours) and water drops (with a relaxation time considerably less than a millisecond). The experiment is an electrohydrodynamic dynamo, in that the motion of the liquid drops is responsible for the generation of extremely high voltages with no external electrical excitations.

Example 7.2.6. The experiment is shown in Fig. 7.2.11. It can be simply constructed from two cans, two pieces of wire, and a pair of pipettes connected to a container of water. Flow of water through the pipettes is adjusted so that the streams break up into drops in the vicinity of the conducting rings. These rings encircle the streams but do not make electrical contact with the drops. The rings are connected, respectively, to the opposite cans, as shown in Fig. 7.2.11. It is extremely important that these cans be carefully insulated from each other. This can be done, as shown in Fig. 7.2.11*a*, by supporting the cans on a dry piece of plastic.

With no external excitations, the apparatus shown in Fig. 7.2.11*a* is capable of producing 10 to 20 kV. This potential difference, which appears between the cans, can be measured with an electrostatic voltmeter, not shown in Fig. 7.2.11*a*.

The formulation of a quantitative model for this experiment affords an opportunity not only to illustrate further the effect on electric fields of media in motion but also to undertake the modeling process itself. In all the examples found in this chapter mathematical models were involved. Here we are involved with the experiment itself and must translate the

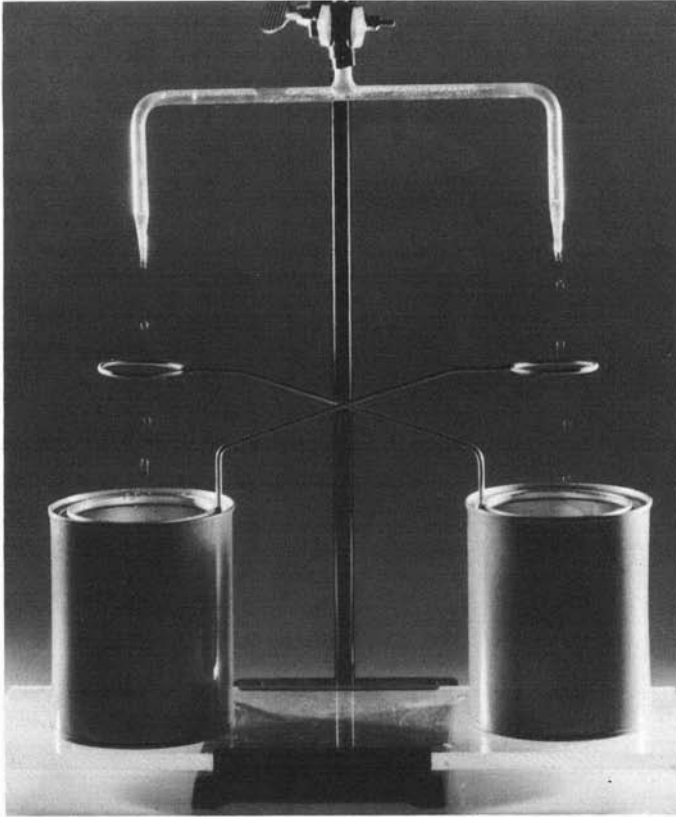


Fig. 7.2.11a Water drops fall into the cans through cross-connected wire loops. A potential difference of more than 20 kV between cans is spontaneously generated by the motion of the drops. For optimum operation the drops should form nearer to the rings than shown. This is accomplished by increasing the flow rate.

observed phenomena into a mathematical explanation. (Of course, actually envisioning the experiment is an even more demanding intellectual process for which we must credit Lord Kelvin.*)

First of all we require a plausible explanation for the generated voltage. Suppose that at a given instant the left ring in Fig. 7.2.11b has a slight excess charge (either due to random fluctuations or to an initial charge purposely placed on the ring). Then charges of the opposite polarity will be induced on the stream passing through the ring, as shown in Fig. 7.2.12. This stream breaks up into drops in the region of the ring; and, as a result, the fully formed drops carry a net induced charge into the container below. But this charge is communicated by means of the wire to the ring encircling the right-hand stream. Hence positive charges are induced on this stream as images of the negative charges on the ring. Now we have the mechanism for regenerative feedback because the positive charge on the right

* L. B. Loeb, *Static Electrification*, Springer, Berlin, 1958, p. 60.

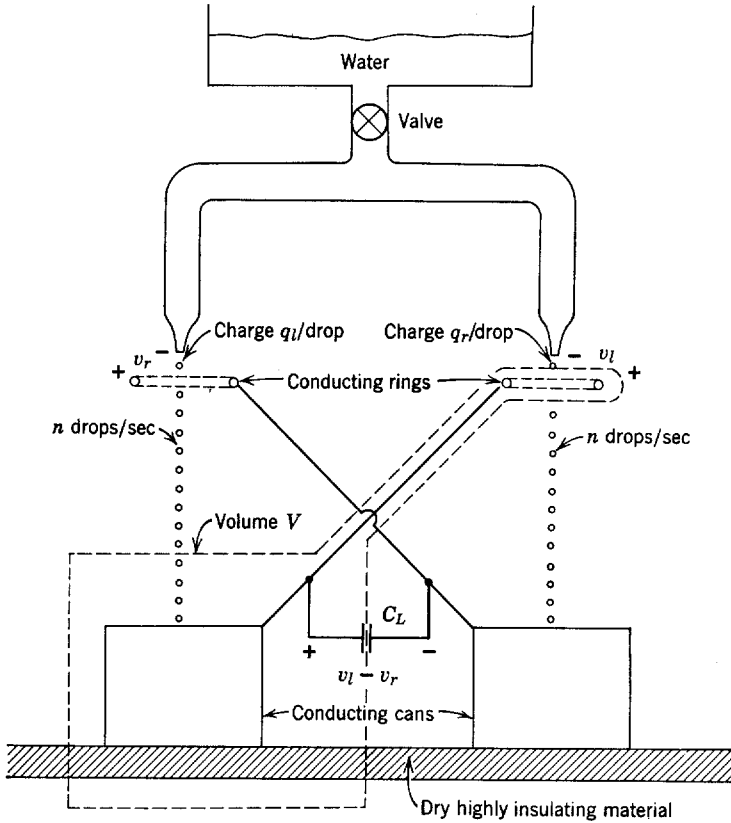


Fig. 7.2.11b Schematic representation of the experiment shown in Fig. 7.2.11a. The capacitance C_L represents the effect of an external electrostatic voltmeter connected between the cans. The volume V is used to define quantitatively the voltages v_r and v_l in Example 7.2.6.

stream falls into the right container, where it is communicated to the left ring by the connecting wire. On the left ring further negative charges are induced on the stream, with a resulting build up of voltage.

In terms of this explanation it is apparent why it is important that there be two relaxation times in the problem. The charge must relax to the surface of the stream before it breaks up. Once the drops are formed, however, the net charge on an individual drop is essentially conserved. These conditions are satisfied here because the water has a relaxation time that is much shorter than the time required for a drop to form, whereas the air has a relaxation time that is much longer than the time required for a drop to reach the container below.

To model the experiment quantitatively we assume that the charge on each drop is proportional to the voltage on the inducing ring with respect to the water in the pipette (which is at ground potential). Thus

$$q_l = -C_i v_r, \tag{a}$$

$$q_r = -C_i v_l, \tag{b}$$

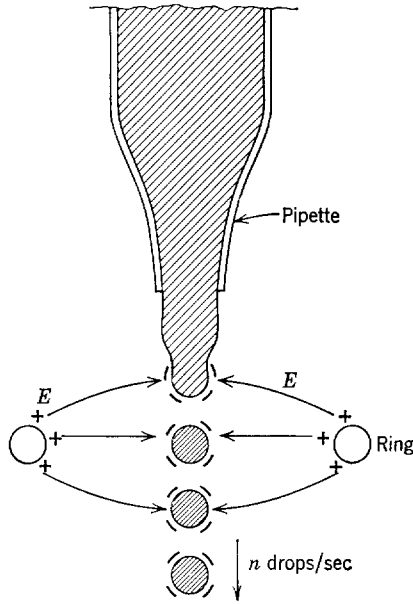


Fig. 7.2.12 As the drops form near the rings in Fig. 7.2.11, image charges are induced on the surface of the water. When the drops are completely formed (and insulated from one another) they carry a net charge, the sign of which is determined by the sign of the charge on the respective rings.

where C_i is the constant of proportionality which has the dimension of capacitance. Because there are two equipotentials in addition to ground (the base and the water in the pipettes), the system can be modeled by the equivalent circuit of Fig. 7.2.13. The two current sources represent the rate of charge transport to the cans by the drops. The capacitances C are capacitances to ground for each can and ring and C_L is the capacitance between cans plus a load such as an electrostatic voltmeter.

From Fig. 7.2.11b conservation of charge for the volume V requires

$$-nC_i v_r = C \frac{dv_l}{dt} + C_L \frac{d(v_l - v_r)}{dt} . \tag{c}$$

This is the node equation for the left node in Fig. 7.2.13. Similarly,

$$-nC_i v_l = C \frac{dv_r}{dt} + C_L \frac{d(v_r - v_l)}{dt} . \tag{d}$$

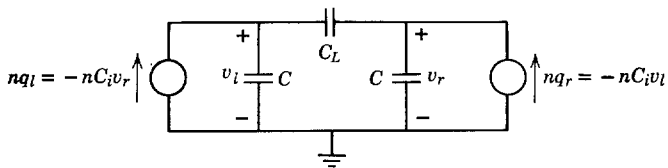


Fig. 7.2.13 Equivalent circuit of electrostatic generator of Fig. 7.2.11.

These expressions could be reduced to a single second-order equation for either of the dependent variables. Hence there are two solutions. By symmetry we expect that one of these solutions is odd, in the sense that $v_l = -v_r$. That this is, in fact, the case can be seen by substituting this condition into (c) and (d) and seeing that they *both* reduce to the form

$$(C + 2C_L) \frac{dv_l}{dt} - nC_l v_l = 0. \quad (e)$$

Similarly, if $v_r = v_l$, both (c) and (d) reduce to the form

$$C \frac{dv_l}{dt} + nC_l v_l = 0. \quad (f)$$

The general solutions are appropriate linear combinations of the solutions of (e) and (f):

$$v_l = A \exp\left(\frac{nC_l}{C + 2C_L} t\right) + B \exp\left(-\frac{nC_l}{C} t\right), \quad (g)$$

$$v_r = -A \exp\left(\frac{nC_l}{C + 2C_L} t\right) + B \exp\left(-\frac{nC_l}{C} t\right). \quad (h)$$

where the constants A and B are determined by initial conditions. Any slight unbalance in initial voltage (such as that supplied by natural noise) will lead to exponential growth of the odd part of the solution and decay of the even part. In practice the potential difference between the cans builds up until there is electrical breakdown between the cans or the electrical force deflects the drops until they hit the inducing rings. The example discussed here illustrates the effect of material motion on the electric field. The drop deflections represent the reverse effect of the fields on the motion.

7.2.3 Sinusoidal Excitation and Charge Relaxation with Motion

A comparison between the developments of Section 7.1, concerned with magnetic diffusion, and those found in this section (Section 7.2) shows a considerable analogy. As might be expected from Section 7.1.3, the introduction of an additional characteristic time by the agent of a sinusoidal excitation makes it possible to tailor the relaxation process to engineering requirements. In this section we undertake to contrast the relaxation process with magnetic diffusion in the presence of motion and with a sinusoidal excitation. The example considered illustrates how charge relaxation can be used to measure the velocity of a moving medium.

A thin slab of slightly conducting material moves to the right with velocity V , as shown in Fig. 7.2.14. This slab passes between plane parallel electrodes which are broken into three sections with different terminations (Fig. 7.2.14*b*). In the section to the left the plates are driven by a sinusoidally varying potential. From the preceding sections we know that because the slab is insulated from the plates by the intervening air, charges will relax to the surfaces of the slab in a way that tends to exclude the imposed electric field. Hence, as the slab leaves this exciter region at $z = 0$, symmetry requires that there be a sinusoidally varying surface charge density σ_0 on the upper slab surface and $-\sigma_0$ on the lower surface.

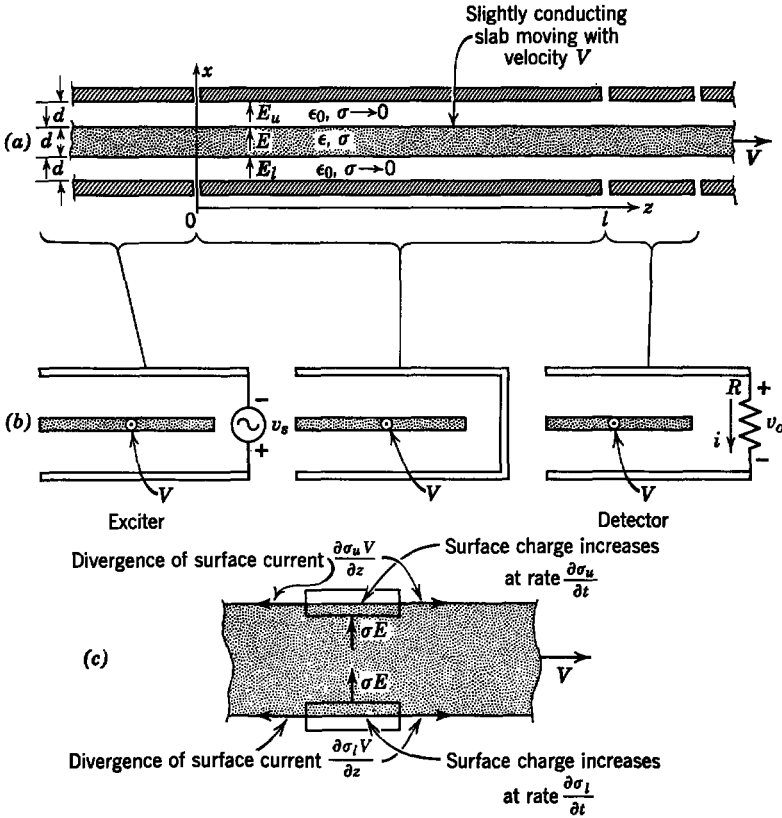


Fig. 7.2.14 (a) A slightly conducting slab moves to the right with velocity V through electric fields imposed or constrained as shown in (b); (c) conduction currents normal to the surfaces lead to an accumulation of surface charge that can be convected away.

As the slab passes through the region $0 < z < l$, the surface charges induced in the exciter region tend to relax so that by the time they reach the detector region to the right the surface charge densities can be considerably attenuated. Those charges that remain induce image charges on the electrodes with a resulting current through the resistance R and a proportionate generated output signal v_o . Because of the charge relaxation this signal can be a measure of the material velocity, as shown in the development that follows.

We know from preceding sections that there is no charge in the bulk of the moving slab. On the surfaces, however, the normal conduction current leads to an accumulation of charge that can be convected away by the motion of the slab. Using the electric field intensities defined in Fig. 7.2.14a,

conservation of charge on the upper surface requires that (see Fig. 7.2.14c)

$$\sigma E = \frac{\partial \sigma_u}{\partial t} + V \frac{\partial \sigma_u}{\partial z}, \quad (7.2.18)$$

where the surface charge density σ_u is related to the field intensities by

$$\sigma_u = \epsilon_0 E_u - \epsilon E. \quad (7.2.19)$$

Equation 7.2.18 is a particular application of boundary condition (6.2.36),* discussed in Section 6.2.2 (see Example 6.2.3).

Similarly, conservation of charge on the lower surface requires

$$-\sigma E = \frac{\partial \sigma_l}{\partial t} + V \frac{\partial \sigma_l}{\partial z}, \quad (7.2.20)$$

where

$$\sigma_l = \epsilon E - \epsilon_0 E_l. \quad (7.2.21)$$

Now, in general, the electric field in the slab, and in the regions above and below, must satisfy the electric field equations with $\rho_f = 0$. We can avoid introducing the complication of solving these equations by making a quasi one-dimensional model based on the distance d , shown in Fig. 7.2.14a, being much smaller than a characteristic (wave) length in the z -direction. Because the plates are short-circuited in the region $0 < z < l$, we not only assume that $\mathbf{E} = E(z, t)\mathbf{i}_x$ but write

$$d(E_u + E + E_l) = 0 \quad (7.2.22)$$

because the integral of the field along a line joining the plates must be zero.

The one-dimensional model implied by (7.2.18) to (7.2.22) ignores any effect introduced by a component of field intensity in the z -direction. This component however, does exist and can be computed from E_x through the condition that the field intensity be irrotational (7.2.1). This second-order effect of one of the field components characterizes "quasi" one-dimensional models as they are found in a variety of physical situations.

At $z = 0$ we assume that the exciter has induced the surface charges

$$\sigma_l = -\sigma_u = \sigma_o \sin \omega t. \quad (7.2.23)$$

For this reason we look for solutions to (7.2.18) to (7.2.22) that satisfy the requirement that $E_u = E_l$. Then, from (7.2.22),

$$E = -(E_u + E_l) = -2E_u, \quad (7.2.24)$$

and it follows from (7.2.19) that the upper surface charge density is related to the field intensity within the moving slab by

$$E = \frac{-2\sigma_u}{\epsilon_0 + 2\epsilon}. \quad (7.2.25)$$

* See Table 6.1, Appendix E.

This relation, together with (7.2.18) then shows that

$$\frac{\partial \sigma_u}{\partial t} + V \frac{\partial \sigma_u}{\partial z} + \frac{2\sigma}{\epsilon_0 + 2\epsilon} \sigma_u = 0. \quad (7.2.26)$$

Once the upper surface charge density has been found from this expression the lower surface charge density and the three field intensities can be found; That is, $\sigma_u = -\sigma_l$ (for the excitation considered here), $E_u = E_l$, and E is given by (7.2.24).

Because the charge is varying sinusoidally at $z = 0$, we assume that the steady-state solution has the form

$$\sigma_u = \text{Re} [\hat{\sigma}_u(z)e^{j\omega t}]. \quad (7.2.27)$$

Substitution into (7.2.26) shows that

$$\frac{d\hat{\sigma}_u}{dz} + \hat{\sigma}_u \left[\frac{2\sigma}{(\epsilon_0 + 2\epsilon)V} + \frac{j\omega}{V} \right] = 0. \quad (7.2.28)$$

The solution to this equation, which satisfies the boundary condition of (7.2.23), is

$$\sigma(z, t) = \sigma_o \exp \left[-\frac{2\sigma l}{(\epsilon_0 + 2\epsilon)V l} z \right] \sin \omega \left(t - \frac{z}{V} \right). \quad (7.2.29)$$

The distribution of surface charge on the moving slab, as given by (7.2.29), is sketched in Fig. 7.2.15. The relaxing charge appears as a wave that propagates to the right with the phase velocity V and with an exponential envelope determined by the electric Reynolds number R_e , defined in this case as

$$R_e = \frac{(\epsilon_0 + 2\epsilon)V}{2\sigma l}. \quad (7.2.30)$$

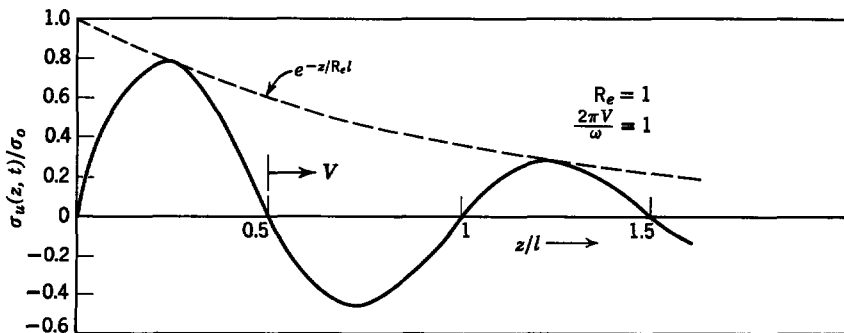


Fig. 7.2.15 Distribution of free charge density on the upper surface of the moving, slightly conducting slab of Fig. 7.2.14. Points of constant phase move with the velocity V of the material.

Note that by contrast with the magnetic diffusion waves of Section 7.1.3 the relaxation wave found here propagates only by virtue of the material motion. There are no waves that propagate upstream, as there were in Section 7.1.3.

We can make practical use of the relaxation interaction by using the section of plates to the right in Fig. 7.2.14*a, b* to detect the charge on the surface. This is done by attaching a resistance R between the plates and measuring the induced voltage. If we assume that this resistance is small enough to ensure that the drop in potential across the resistance is negligible compared with Ed in the section to the left, the induced current is simply

$$i = -A\epsilon_0 \frac{\partial E_x}{\partial t}, \quad (7.2.31)$$

where A is the area of one of the detector plates. Here we have assumed that the detector plates are of sufficiently small extent in the z -direction that the integral of the surface charge over the surface of one of the plates can be approximated by the product of A and the charge at $z = l$. It follows that the voltage v_o from the detector has the magnitude

$$|v_o| = |i| R = \frac{A\epsilon_0\omega\sigma_o}{(\epsilon_0 + 2\epsilon)} e^{-l/R_e}. \quad (7.2.32)$$

The dependence of this signal on the electric Reynolds number is shown in Fig. 7.2.16. As we expected intuitively, the output signal increases with velocity and decreases with conductivity or length l . Unfortunately, the functional dependence is not so convenient as it was in the system discussed

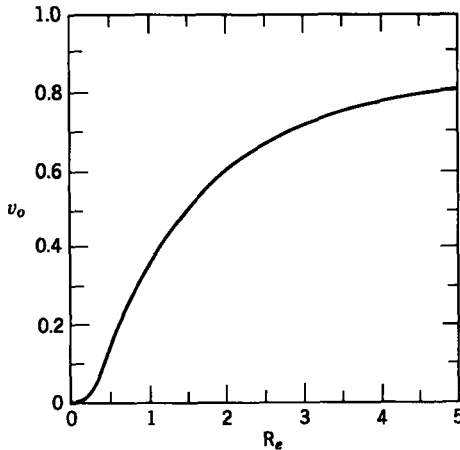


Fig. 7.2.16 Output voltage as a function of electric Reynolds number $R_e = [(\epsilon_0 + 2\epsilon)V]/2\sigma l$ for the system of Fig. 7.2.14.

in Section 7.1.3. It is important in this regard to note that systems in which R_m (magnetic Reynolds number) is on the order of unity and in which R_e is about unity are in entirely different velocity and conductivity ranges. This point is emphasized in Section 7.3.

7.2.4 Traveling-Wave Charge Relaxation in a Moving Conductor

As illustrated in Section 7.1.4, interactions between a periodic traveling wave and moving media provide considerable physical insight into a diversity of situations. In plane geometry the analytical difficulties involved in magnetic field systems were minimal and in the electric field system considered here the mathematical description is even simpler. Even so, as discussed in Section 7.3, a great deal can be learned that is applicable to more complicated situations.

The physical situation to be considered, which is analogous to that discussed in Section 7.1.4, is shown in Fig. 7.2.17. A slightly conducting material moves to the right with a velocity V just below a segmented electrode which supports a traveling wave of potential

$$v = \text{Re } \hat{v} e^{j(\omega t - kz)} \quad (7.2.33)$$

It is assumed that material (a) has negligible electrical conductivity. We wish to determine the effect of the motion on the distribution of potential (hence electric field) above and below the surface (at $x = 0$) of the moving conductor. We know in advance that because electrical conductivity σ is uniform in the moving conductor there is no bulk free charge there. Therefore the interactions between the fields and the media occur at the surface of the moving material where surface charges assume a distribution and magnitude determined by the motion and by the velocity of the imposed traveling wave of potential.

Because there is no free charge in either region (a) or (b), (7.2.8), which follows from (7.2.5), reduces to

$$\nabla^2 \phi = \frac{\partial^2 \phi}{\partial x^2} + \frac{\partial^2 \phi}{\partial z^2} = 0. \quad (7.2.34)$$

Here we assume that the problem is two-dimensional so that $\partial \phi / \partial y = 0$. The traveling wave of potential given by (7.2.33) constitutes a boundary condition on the potential ϕ in the region (a) above the conductor. To match this condition we assume that the potential ϕ takes the form

$$\phi = \text{Re } \hat{\phi}(x) e^{j(\omega t - kz)} \quad (7.2.35)$$

in both regions (a) and (b). Substitution of this form into (7.2.34) shows that in region (a)

$$\hat{\phi}_a = A \sinh kx + B \cosh kx, \quad (7.2.36)$$

where A and B are arbitrary constants to be determined by the boundary

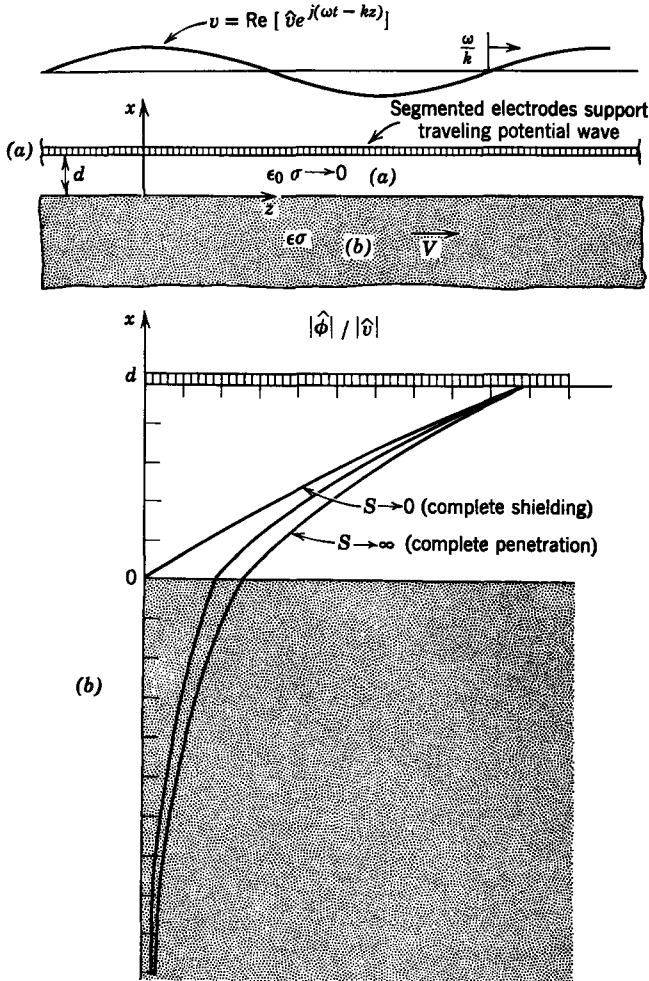


Fig. 7.2.17 (a) A slightly conducting material moves to the right with velocity V just below a segmented electrode which supports a traveling potential wave; (b) distribution of potential above and below the conductor for various values of $S = (\omega - kV)\epsilon_0/\sigma$.

conditions. In region (b) it is more convenient to write the two solutions in the form of exponentials. Then, if we assume that the material in region (b) extends many wavelengths $2\pi/k$ in the $-x$ -direction, one of these solutions becomes unbounded as $x \rightarrow -\infty$ and the appropriate solution is

$$\hat{\phi}_b = Ce^{kx}. \tag{7.2.37}$$

In retaining this half of the solution in region (b) we are assuming that k is a positive number so that the potential will not go to infinity as $x \rightarrow -\infty$.

Three boundary conditions, one of which is (7.2.33), determine the constants A , B , and C . A second condition develops because the potential is continuous at $x = 0$.

$$\hat{\phi}_a(0) = \hat{\phi}_b(0). \quad (7.2.38)$$

The third condition requires conservation of charge on the interface. This equation has the same origins as (7.2.18) in Section 7.2.3. It can be written in terms of the potentials by recognizing that the surface charge density is

$$\sigma_f = \epsilon_0 E_x^a - \epsilon E_x^b = -\epsilon_0 \frac{\partial \phi_a}{\partial x} + \epsilon \frac{\partial \phi_b}{\partial x}. \quad (7.2.39)$$

Then the condition that the conduction current normal to the interface lead to an increase in the surface charge measured in a frame moving with the material is written as

$$-\sigma \frac{\partial \phi_b}{\partial x} = \left(\frac{\partial}{\partial t} + V \frac{\partial}{\partial z} \right) \left(-\epsilon_0 \frac{\partial \phi_a}{\partial x} + \epsilon \frac{\partial \phi_b}{\partial x} \right). \quad (7.2.40)$$

This boundary condition is a particular case of (6.2.36) (see Table 6.1)*. For the assumed traveling-wave solution (7.2.35) it becomes

$$-\sigma \frac{d\hat{\phi}_b}{dx} = j(\omega - kV) \left(-\epsilon_0 \frac{d\hat{\phi}_a}{dx} + \epsilon \frac{d\hat{\phi}_b}{dx} \right). \quad (7.2.41)$$

Now we are in a position to find the constants A , B , and C by requiring that (7.2.36) and (7.2.37) satisfy the boundary conditions of (7.2.33), (7.2.38), and (7.2.41). Substitution gives

$$A \sinh kd + B \cosh kd = \hat{v}, \quad (7.2.42)$$

$$B - C = 0, \quad (7.2.43)$$

$$A(jS) - C \left(1 + jS \frac{\epsilon}{\epsilon_0} \right) = 0, \quad (7.2.44)$$

where S is the normalized frequency (measured in the moving frame of the material) normalized to the relaxation time

$$S = \frac{(\omega - kV)\epsilon_0}{\sigma}. \quad (7.2.45)$$

The constants A , B , and C follow from (7.2.42) to (7.2.44) with the result that the potential distributions above and below the moving medium are

$$\phi_a = \text{Re} \frac{\hat{v}}{\Delta} \left[\left(1 + jS \frac{\epsilon}{\epsilon_0} \right) \sinh kx + jS \cosh kx \right] e^{j(\omega t - kz)}, \quad (7.2.46)$$

$$\phi_b = \text{Re} \frac{\hat{v}}{\Delta} jS e^{kx} e^{j(\omega t - kz)}, \quad (7.2.47)$$

where $\Delta = [1 + jS(\epsilon/\epsilon_0)] \sinh kd + jS \cosh kd$.

* Appendix E.

The magnitude of the potential distribution predicted by these equations is shown in Fig. 7.2.17*b*. The potentials for an intermediate value and an extreme value of S are shown to emphasize two important points. When the frequency in the moving frame of the medium is small compared with the reciprocal relaxation time $S \ll 1$, the fields are excluded from the material and confined to region (*a*). In this extreme charges have a sufficient amount of time [one period $2\pi/(\omega - kV)$, as measured in the frame of the medium] to relax to the surface, where they shield the electric field from the medium; that is, in the limit $S \rightarrow 0$ the potential in the medium is zero, whereas that just above is

$$\phi_a = \text{Re} \left[\hat{v} \frac{\sinh kx}{\sinh kd} e^{j(\omega t - kz)} \right]. \quad (7.2.48)$$

Note that this is simply the potential distribution found when the medium is modeled as a perfectly conducting material.

In the opposite extreme, in which the normalized frequency $|S|$ is very large, the potential distributions become

$$\phi_a = \text{Re} \left[\hat{v} \frac{\cosh kx + \epsilon/\epsilon_0 \sinh kx}{\cosh kd + \epsilon/\epsilon_0 \sinh kd} e^{j(\omega t - kz)} \right], \quad (7.2.49)$$

$$\phi_b = \text{Re} \left[\hat{v} \frac{e^{kx} e^{j(\omega t - kz)}}{\cosh kd + \epsilon/\epsilon_0 \sinh kd} \right]. \quad (7.2.50)$$

From Fig. 7.2.17*b* it is clear that in this limit the electric field completely penetrates the moving medium; that is, the potential distribution is just as it would be if the moving medium were modeled as a perfectly insulating material with no free charge at the surface. (Note that (7.2.49) and (7.2.50) show that there is no free charge at $x = 0$.) In the high-frequency limit one period of excitation (measured in the moving frame of the medium) is not sufficient time for appreciable free charge to relax to the surface. The parameter S can be large either because ω is large or because kV is large; that is, if the material is fixed ($V = 0$) and the imposed wave has a high frequency ω , the fields penetrate the medium with little shielding from free surface charges. Similarly, the frequency ω of the imposed spacially periodic wave could be zero and the same penetration would result by having the material move with a velocity V large enough that the frequency kV observed in the moving medium would be large compared with a reciprocal relaxation time.

Although we do not pursue this point here, the traveling wave of potential results in a time average electric shear on the material surface, hence gives rise to a z -directed force, much as described in Section 7.1.4 for a magnetic field system.*

* For a development of this subject see J. R. Melcher, "Traveling-Wave Induced Electroconvection," *Phys. Fluids* **9**, 1548-1555 (1966).

7.3 CONCLUSION

The subjects of magnetic diffusion and charge relaxation concern themselves with the behavior of fields in the presence of dissipative media. In each case a characteristic time is associated with the dissipation mechanism. In the case in which currents (hence magnetic fields) diffuse in a conducting medium this is the magnetic diffusion time $\mu\sigma l^2$. Similarly, the relaxation time ϵ/σ for free charge governs the dynamical behavior of electric fields in slightly conducting materials.

The nature of the field solutions is determined by the ratio of these times to times that characterize the dynamics of the system; for example, in a magnetic field system excited at the frequency ω , field distributions are determined by the magnetic Reynolds number $\mu\sigma l^2\omega$ (the ratio of diffusion time to the period of excitation). Alternatively, this number can be thought of as the square of the ratio of a characteristic length in the system to the skin depth δ (see Section 7.1.3). A second dynamical time is introduced by motion. With a characteristic velocity V and length l , a second magnetic Reynolds number $\mu\sigma V l$ indicates the importance of material motion in determining the distribution of currents. As we saw in Section 7.1.3, there are situations in which the mechanisms of altering the fields represented by these characteristic numbers are present simultaneously.

In an electric field system excitation at the frequency ω leads to an electric Reynolds number $\omega\epsilon/\sigma$, whereas motion with the velocity V through a characteristic distance l has an effect on the electric field determined by $\epsilon V/\sigma l$. A simple summary example provides the opportunity to review these effects while contrasting the behavior of magnetic and electric field systems.

A cylinder of material with conductivity σ is placed between

the pole faces of a magnet as shown in Fig. 7.3.1a.

With the cylinder stationary, the initially uniform magnetic field completely penetrates the conducting material, as shown in Fig. 7.3.2a.

a pair of plane parallel electrodes, as shown in Fig. 7.3.1b.

With the cylinder stationary, the electric field is completely shielded from the interior of the conducting material by free charges that relax to the cylindrical surface, as shown in Fig. 7.3.2b.

The effect of material motion on the steady-state fields is demonstrated by considering the consequences of making the conductor rotate. If the cylinder has a radius R and angular velocity Ω , a characteristic velocity is ΩR . The

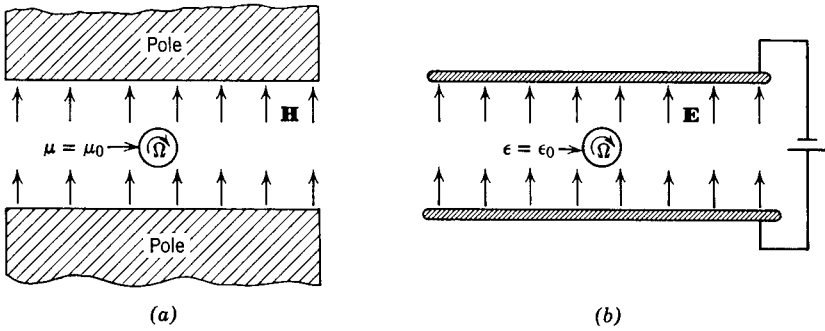


Fig. 7.3.1 (a) Magnetic field system; (b) electric field system.

motion alters the fields of Fig. 7.3.2 if

the magnetic Reynolds number R_m is significant compared with unity

$$R_m = \mu\sigma VR = \mu\sigma\Omega R^2.$$

the electric Reynolds number R_e is significant compared with unity

$$R_e = \frac{\epsilon V}{\sigma R} = \frac{\epsilon\Omega}{\sigma}.$$

The conditions under which R_m and R_e are on the order of unity are very different; for example, suppose that $\Omega = 10$ rad/sec and $R = 10$ cm. Then,

if we let $\mu = \mu_0$, the magnetic Reynolds number is unity if $\sigma = 7.95 \times 10^6$ mhos/m, which is about the conductivity of solder.

if we let $\epsilon = \epsilon_0$, the electric Reynolds number is unity if $\sigma = 8.85 \times 10^{-11}$ mhos/m, which is about the conductivity of corn oil.

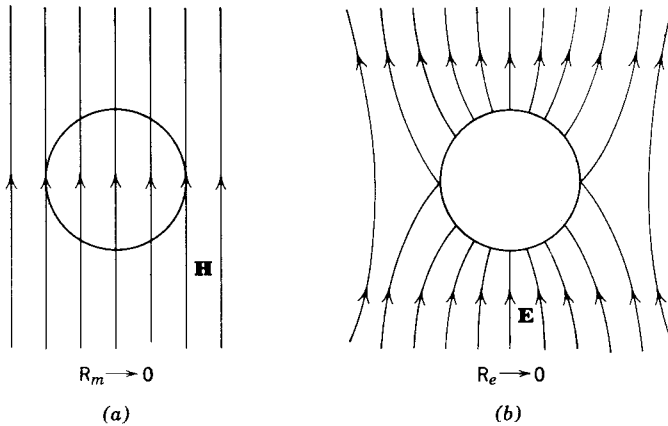


Fig. 7.3.2 (a) Magnetic fields penetrate stationary media; (b) electric fields are excluded from stationary media.

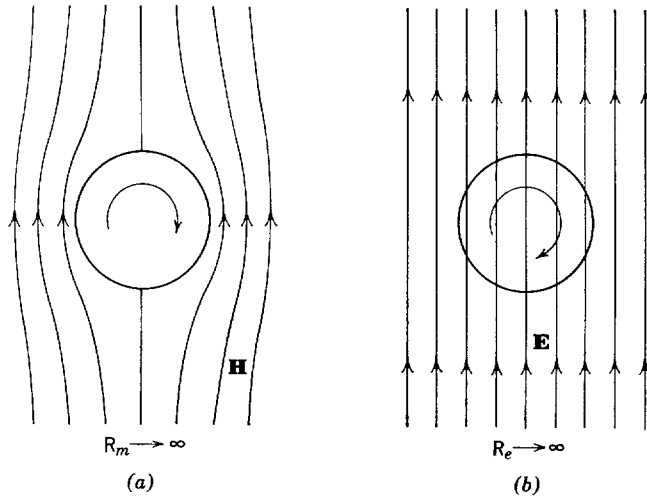


Fig. 7.3.3 (a) Magnetic field completely shielded from cylinder; (b) electric field completely penetrates cylinder.

By making the rotational velocity Ω very large there is a large motional effect on the imposed fields. Hence

for $R_m \gg 1$ the magnetic fields are completely excluded from the rotating cylinder by induced currents, as shown in Fig. 7.3.3a.

for $R_e \gg 1$ the electric field completely penetrates the rotating cylinder because charges are not able to relax to the cylindrical surface, as shown in Fig. 7.3.3b.

The observations that concern the effect of the rotating cylinders on the fields are evident from Sections 7.1.4 and 7.2.4. There we analyzed (a limiting case in which $\omega = 0$) the field effects of material motion in the presence of a temporally constant, spatially periodic wave. The cylinders considered in this summary are simply those problems with one wavelength along the cartesian coordinate z "wrapped around on itself." Of course, the cylindrical geometry requires alterations in the mathematical details. The essential physical features of the problems in cartesian coordinates and those described here, however, are the same.

It should be apparent from the discussions of Sections 7.1.4 and 7.2.4 that we have also developed a picture of what would happen if the cylinders were to be fixed but the fields were to rotate. In the magnetic field case currents would be induced in the rotating cylinder which in turn would develop a torque. This is illustrated in Section 7.1.4 in plane geometry and is a distributed picture of the induction machine discussed in Section 4.1.6b. Situations in which a torque is produced by a rotating electric field are not so common but still exist.

PROBLEMS

7.1. If a short-circuited inductor is modeled by an ideal inductance (no resistance) in series with a resistance R equal to its internal resistance, the time-constant for decay of an initial flux $\lambda = \Lambda$ is $\tau = L/R$. Design an inductor with a time-constant L/R of 100 sec. Specify the dimensions and the material involved; for example, you may wish to use

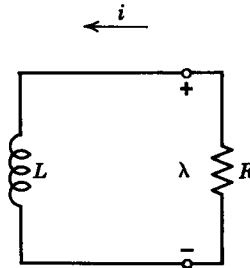


Fig. 7P.1

copper wire, in which case you should specify the size of the wire, the number of turns required, and the size of the winding. You are not allowed to use a superconducting winding.

7.2. This problem is a variation on the situation described in Section 7.1.1. A conducting slab of material with thickness d is positioned between the pole faces of a magnet, as shown in Fig. 7P.2. The switch S has been open for a long time so that the magnetic field in the gap

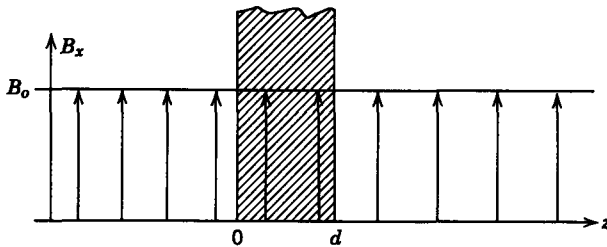


Fig. 7P.2

is as shown. When $t = 0$, the switch is closed and the magnetic field outside the material in the gap collapses.

- (a) Compute the flux density distribution as a function of time in the gap.
- (b) Find the current distribution from the result of (a).

7.3. A fixed block of material with conductivity σ makes electrical contact with a pair of perfectly conducting parallel plates, as shown in Fig. 7P.3. Dimensions are such that $w \ll L$ and $w \ll D$. A current source I (amperes) is distributed along the edge of the plates at $x = -L$. $I(t) = I_0 u_{-1}(t)$, as shown.

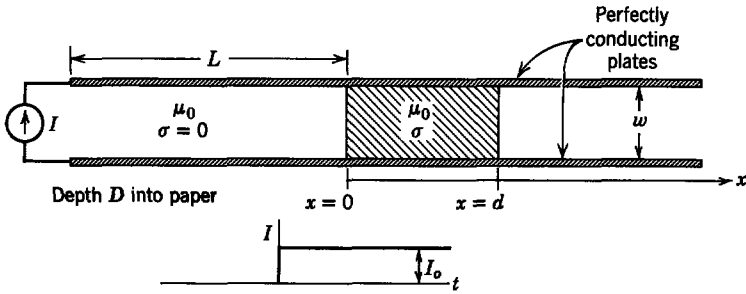


Fig. 7P.3

- (a) Sketch and dimension the distribution of current in the block an instant after the step of current is applied.
- (b) Sketch and dimension the distribution of current as $t \rightarrow \infty$.
- (c) In terms of σ and the system dimensions, how long do you *estimate* that it takes the current to reach essentially the distribution of (b)? (This should be an order of magnitude calculation.)

7.4. A pair of perfectly conducting plates is short-circuited through a conducting block, as shown in Fig. 7P.4a. The block and plates extend a long distance to the right. A current excitation $i(t) = \text{Re}(te^{j\omega t})$ is applied uniformly to the plates along their left edges.

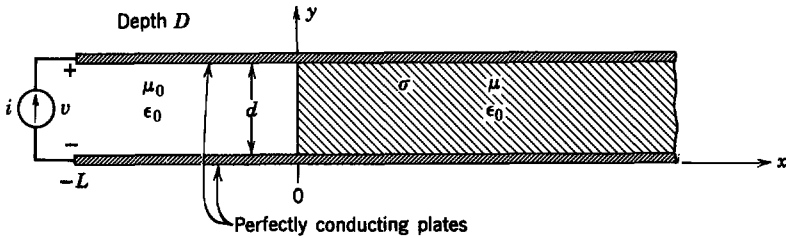


Fig. 7P.4a

- (a) Find the magnetic flux density in the region between the plates.
- (b) Find the current density in the block.
- (c) Sketch the results of (a) and (b).
- (d) Find the equivalent reactance seen at the current source. Using the equivalent circuit shown in Fig. 7P.4b, what are the values of L and R ? How do they depend on frequency?

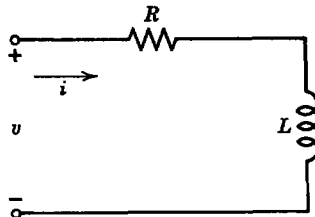


Fig. 7P.4b

7.5. A block of material with conductivity σ is bounded by plane-parallel, perfectly conducting electrodes, as shown in Fig. 7P.5. The plates are driven at the left by the current (amperes) $I_o(t) = \text{Re}(\tilde{I}e^{j\omega t})$, where \tilde{I} is a given complex constant. This current is returned through the block of conductor.

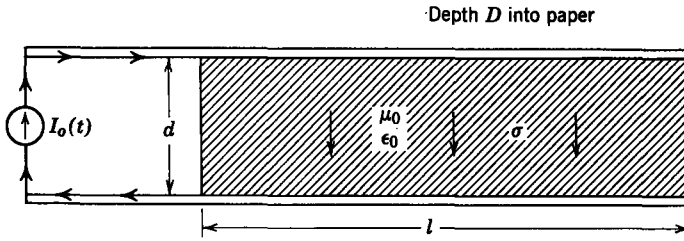


Fig. 7P.5

- (a) Determine the distribution of magnetic field and current within the block.
- (b) Outline how you would find the time-average magnetic force on the block.

7.6. As an example of electromagnetic phenomena that occur in conductors at rest, consider the system in Fig. 7.1.1 with the constant-current sources and switch replaced by an alternating current source, $i(t) = I \cos \omega t$. Make all of the assumptions of Section 7.1.1 and adopt the coordinate system of Fig. 7.1.2. Interest is confined to the sinusoidal steady-state problem.

- (a) Find the magnetic flux density in the conducting slab.
- (b) Find the current density in the slab.
- (c) Sketch the results of parts (a) and (b).

7.7. A pair of plane-parallel, perfectly conducting plates is driven at the left, as shown in Fig. 7P.7a, by a current source $I(t)$, which is a step function. The plates are short-circuited by two conducting slabs spaced a distance l and of thickness Δ . An instant after the current I is established all the current is returned in the left slab; region (1) contains a uniform magnetic field, and region (2) is free of magnetic field. Then, with a characteristic time τ , the field diffuses into region (2).

- (a) Use the "equivalent circuit model" shown in Fig. 7P.7b to establish this characteristic time.
- (b) Physically, why is this characteristic time much longer than the diffusion time based on the thickness Δ of the conducting slabs [(7.1.28) with $d = \Delta$]?

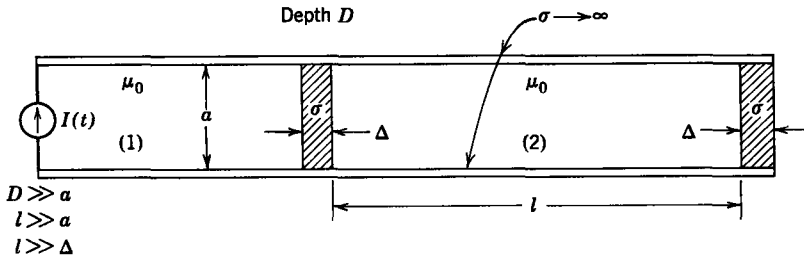


Fig. 7P.7a

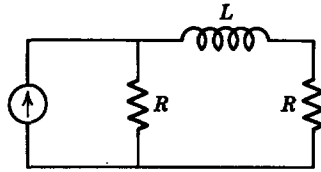


Fig. 7P.7b

(c) Discuss how you would solve this problem by using a field description of the diffusion process.

7.8. The cross section of a cylindrical pair of conductors is shown in Fig. 7P.8a. The current I is a step function and flows azimuthally in the outer conductor. Hence, when $t = 0$, the magnetic field intensity has the distribution of Fig. 7P.8b. The inner conductor acts as a secondary of a transformer and supports an induced current that tends to shield the magnetic

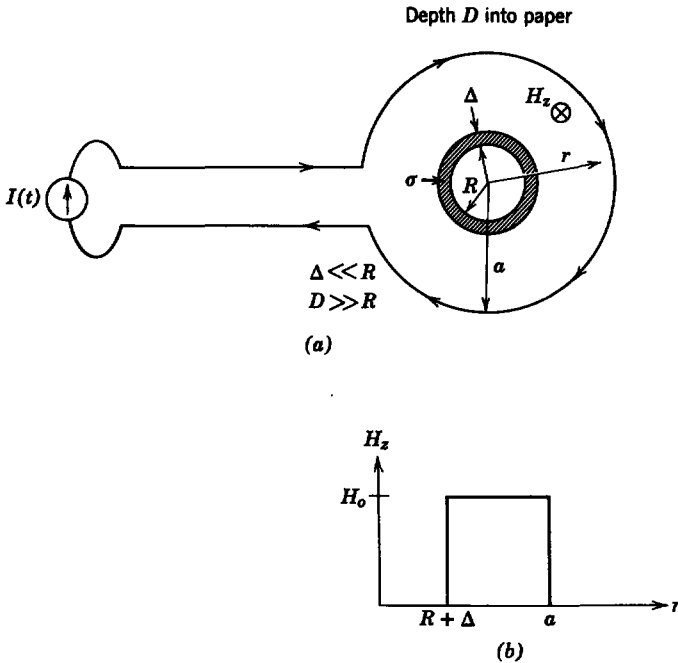


Fig. 7P.8a

field induced by I from the center region. Hence inside the center cylinder the magnetic field rises to its final value with some characteristic time. What is this characteristic time in terms of the system dimensions and σ ? *Hint.* See Problem 7.7.

7.9. As a possible plasma containment scheme, it has been proposed to create a cylindrical column of plasma within a long solenoid. The plasma is created by use of an arc discharge through a gas. After the plasma is formed the solenoid is excited by rapid discharge of a

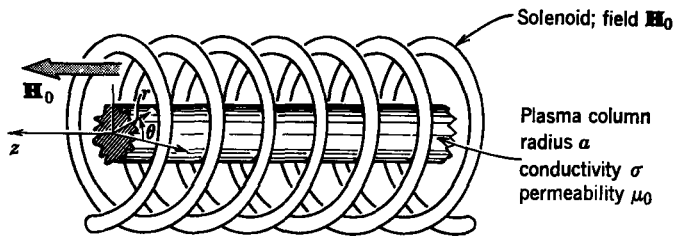


Fig. 7P.9a

capacitor bank connected to the terminals. The magnetic field of the solenoid is initially excluded from the interior of the plasma column by surface currents which flow in the theta direction on the plasma; for this reason the device is called a “Theta-pinch machine.” Because the plasma has only a finite conductivity, the magnetic field diffuses into the interior. Therefore to design the machine it is necessary to determine the time associated with this field diffusion. In Fig. 7P.9a the plasma column is shown in the magnetic field. Neglect end effects by assuming an infinitely long system. Furthermore, assume that the plasma remains stationary during the diffusion process.

- (a) Write an equation governing the magnetic flux density \mathbf{B} inside the plasma.
- (b) Because there are only θ currents independent of θ , assume that $\mathbf{B} = \mathbf{i}_z B(r, t)$, where $B(r, t)$ has the form

$$B(r, t) = \mu_0 H_0 - \hat{B}(r) e^{-\alpha t}, \quad \alpha > 0,$$

which satisfies the condition that $B(r, t) \rightarrow \mu_0 H_0$ as $t \rightarrow \infty$. Using the results of part (a), write an equation for $\hat{B}(r)$.

- (c) The equation obtained in part (b) for $\hat{B}(r)$ is called “Bessel’s equation of zeroth order.” The general solution to this equation is

$$\hat{B}(r) = C_1 J_0(\sqrt{\mu_0 \sigma \alpha} r) + C_2 N_0(\sqrt{\mu_0 \sigma \alpha} r),$$

where J_0 is the Bessel function of zeroth order and the first kind and N_0 is the Bessel

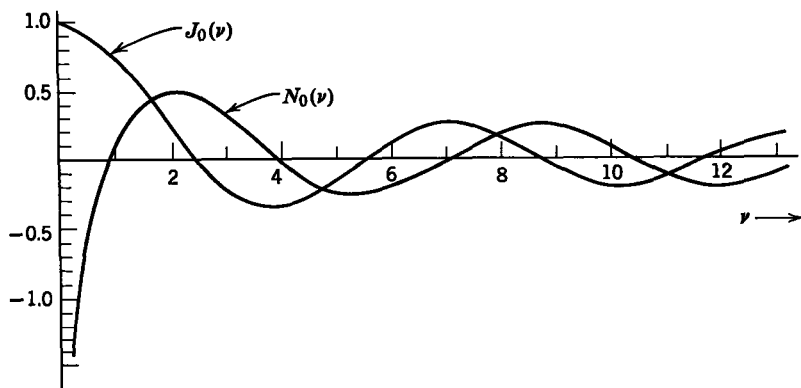


Fig. 7P.9b

function of zeroth order and the second kind (sometimes called a “Neumann function”). See Fig. 7P.9b.

Using the boundary condition at $r = 0$, argue that $C_2 = 0$, hence that $\hat{B}(r) = C_1 J_0(\sqrt{\mu_0 \sigma \alpha} r)$.

- (d) Now apply the boundary condition at $r = a$ that $B(r, t) = \mu_0 H_0$ for all $t > 0$ and show that $J_0(\sqrt{\mu_0 \sigma \alpha} a) = 0$. This transcendental equation determines the allowed values of α .

Roots of $J_0(v_i) = 0$ and the Corresponding Values of $J_1(v_i)$

| i | v_i | $J_1(v_i)$ |
|-----|---------|------------|
| 1 | 2.4048 | 0.5191 |
| 2 | 5.5201 | -0.3403 |
| 3 | 8.6537 | 0.2715 |
| 4 | 11.7915 | -0.2325 |
| 5 | 14.9309 | 0.2065 |
| 6 | 18.0711 | -0.1877 |

The values of α may be obtained from the table as

$$\sqrt{\mu_0 \sigma \alpha} a = v_i; \quad \alpha = \frac{1}{\mu_0 \sigma} \left(\frac{v_i}{a} \right)^2,$$

where $J_0(v_i) = 0$.

- (e) On examination of the results, it is evident that $\hat{B}(r) = C_i J_0[v_i(r/a)]$ is a solution for any of the allowed values of v_i . The most general solution for $B(r, t)$ is obtained by using superposition; hence

$$B(r, t) = \mu_0 H_0 - \sum_{i=1}^{\infty} C_i J_0 \left(v_i \frac{r}{a} \right) \exp \left(- \frac{v_i^2 t}{\mu_0 \sigma a^2} \right),$$

and to evaluate the constants C_i the last boundary condition $B(r, t = 0) \equiv 0$ is used. This condition implies that

$$\sum_{i=1}^{\infty} C_i J_0 \left(v_i \frac{r}{a} \right) = \mu_0 H_0,$$

which is just a series in terms of the functions $J_0[v_i(r/a)]$.

Using the integrals

$$\int_0^a r J_0 \left(v_i \frac{r}{a} \right) J_0 \left(v_j \frac{r}{a} \right) dr = \begin{cases} \frac{a^2}{2} J_1^2(v_i), & v_i = v_j, \\ 0, & v_i \neq v_j, \end{cases}$$

and

$$\int_0^a r J_0 \left(v_i \frac{r}{a} \right) dr = \frac{a^2}{v_i} J_1(v_i),$$

evaluate C_1 , C_2 , and C_3 .

- (f) What is the fundamental time constant for the diffusion? Evaluate this time constant for $a = 5$ cm and $\sigma = 10^4/4\pi(\Omega\text{m})^{-1}$.

7.10. A slab of conducting metal (conductivity σ) moves in the x -direction with the constant velocity U . This slab makes contact with perfectly conducting electrodes which are driven at the left end by a constant current K A/m. This source is distributed along the z -axis but does not get in the way of the moving slab. Assume that there is no fringing and that

$$\mathbf{J} = \mathbf{i}_y J_y(x),$$

$$\mathbf{B} = \mathbf{i}_z B_z(x),$$

$$\mathbf{E} = \mathbf{i}_y E_y(x).$$

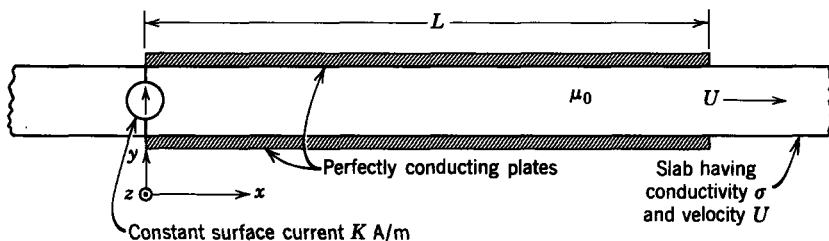


Fig. 7P.10

- Write a single differential equation for $B_z(x)$.
- Write the boundary conditions satisfied by B_z .
- Find an expression for $B_z(x)$ between the perfectly conducting plates.
(Reference: see Section 7.1.2a.)

7.11. In the example in Section 7.1.2a we found the flux density and current density given by (7.1.49) and (7.1.50) for the system in Fig. 7.1.9.

- Calculate the magnetic force density $\mathbf{J} \times \mathbf{B}$ applied to the moving conductor.
- Integrate this force density throughout the volume of the conductor to find the total force that must be supplied by the velocity source. Show that this force is independent of conductivity σ and velocity v .
- Evaluate the power supplied by the velocity source and specify how much power goes to J^2/σ losses in the moving conductor and how much power goes into the current source.

7.12. The electric and magnetic fields were found in Section 7.1.2b for a block of conductor moving between shortcircuited, perfectly conducting plates (see Figs 7.0.1 and 7.1.11). In the fixed frame these fields are functions of both z and t . Show that the fields expressed in the fixed frame satisfy the magnetic diffusion equation (7.1.9).

7.13. A slab of conductor moves in the z -direction with a velocity V , as shown in Figs. 7.1.12 and 7P.13. A perfectly permeable magnetic circuit with the z length L has the same configuration as that in Fig. 7.1.12, except that it has no excitation coils. Instead, an external source is used to constrain $B_y(-L, t)$ to be $B_y(-L, t) = \text{Re } B_0 \exp j\omega t$.

- What physical arguments would you use to show that the condition at $x = 0$, where the moving slab leaves the region between the pole faces, is described approximately by $B_y(0, t) = 0$?
- Find an expression for $B_y(z, t)$, $-L < z < 0$.
- What is J_x in the range $-L < z < 0$?
- Sketch B_y and J_x in the limit at which $\omega \rightarrow 0$. How would you physically arrange the excitation to make these fields a reasonable approximation? (See Section 7.1.2a.)

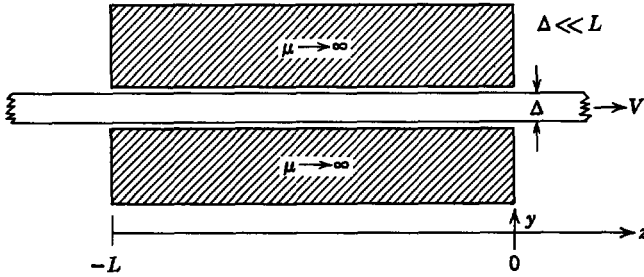


Fig. 7P.13

7.14. You are working on a transportation project and are asked to make an analysis of the following basic method of both levitating and propelling a train. The train rides just above a track which is composed of a slab with conductivity σ . Superconducting coils within the train are arranged to produce a current that can be represented by the current sheet \mathbf{K} (see Fig. 7P.14). This current sheet is backed by a highly permeable magnetic shield ($\mu \rightarrow \infty$) which is also attached to the train. (The shield prevents magnetization of the passengers' watches and the attendant possibility that $t \neq t'$.) Here x' is the distance measured with respect to the moving train. Hence, because the train is moving in the

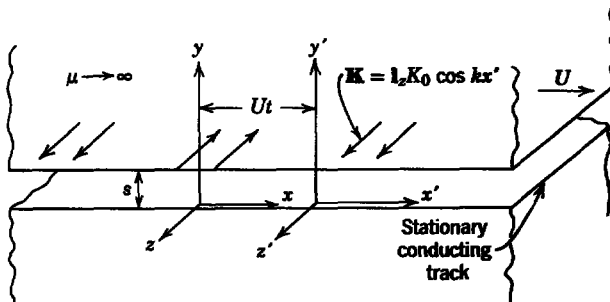


Fig. 7P.14

x -direction with velocity U , $x = Ut + x'$. We wish to compute the time average force per unit area that presumably holds the train a distance s ($ks \ll 1$) above the track.

- Express the surface current in the fixed frame $\mathbf{K}(x, t)$.
 - Assume that the track is infinitely thick in the y -direction (under what conditions is this a good assumption?) and compute the magnetic field and current in the conducting track. Assume that $\partial/\partial z = 0$.
 - Compute the time average force per unit area (in the x - z plane) that holds up the vehicle.
 - Compute the force per unit (x - z) area that tends to propel the train in the x -direction. Do you see any basic problems with the proposed scheme of propulsion?
- 7.15. (a) Compute the fields for the example of Section 7.1.4, taking into account the effect of the spacing s between the moving conductor and the traveling current sheet.

- (b) Check to see that the results of Section 7.1.4 are obtained in the limit $ks \ll 1$.
 (c) Check to see that currents induced in the moving conductor approach zero as $ks \rightarrow \infty$.

7.16. A pair of perfectly conducting electrodes with area A are shown in Fig. 7P.16. Between the plates there is a fluid of depth b , conductivity σ , and permittivity ϵ , bounded from above by an insulating gas. When $t = 0$, there is no charge in the system and the switch S is closed.

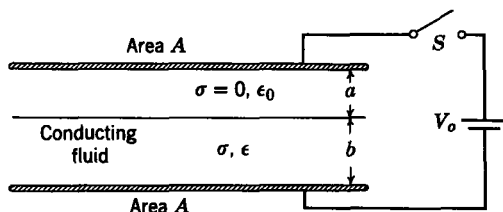


Fig. 7P.16

- (a) What are the electric fields in the liquid (E_l) and in the gas (E_g) an instant after $t = 0$?
 (b) What are these electric fields as $t \rightarrow \infty$?
 (c) Find the charge (q) on the fluid-gas interface as a function of time.

7.17. A spherically symmetric system of free charges and conductors is shown in Fig. 7P.17. A sphere of material of conductivity σ_i is embedded at the center of a second material with conductivity σ_o . When $t = 0$, there is a volume charge density $\rho_o(r)$ in the region $r < R_i$, but no charge density in the outer region. There are no surface charges when $t = 0$.

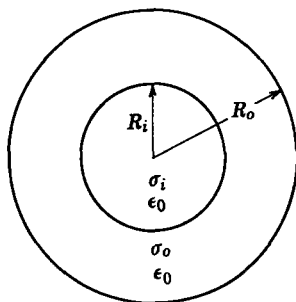


Fig. 7P.17

- (a) Find the charge density at points $r < R_i$ in the center sphere and for $R_i < r < R_o$ in the outer region for $t > 0$.
 (b) Find the surface charges at $r = R_i$ and $r = R_o$ for $t > 0$.
 (c) Sketch the results of (b) for $\sigma_i > \sigma_o$ and $\sigma_i < \sigma_o$.

Hint. You may wish to define the total charge in the inner sphere as

$$q(t) = 4\pi \int_0^{R_i} \rho_o(r) r^2 dr$$

7.18. Three long, cylindrical, highly conducting shells of radius a , b , and c , respectively, are aligned concentrically, as shown in Fig. 7P.18. The space between the cylinders is filled with a material of permittivity ϵ and conductivity σ . Initially, the cylinders of radii a and b are biased with a battery V_0 and switch S in position (1) as shown. At a time $t = 0$, the switch is connected to terminal (2).

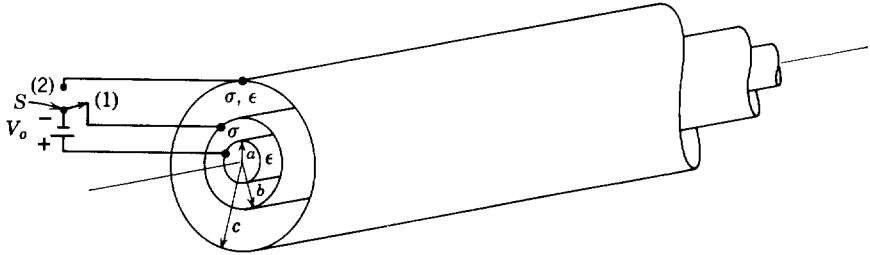


Fig. 7P.18

- Find expressions for the electric field intensity E in the regions between the cylinders.
- Find the expression for the charge per unit length on the cylinder of radius b .
- Find the equivalent circuit for a unit length of the cylinders.

7.19. A pair of metal spheres is suspended in a beaker of slightly conducting liquid, as shown in Fig. 7P.19. The lower sphere is fixed to the bottom, whereas the upper one is free to move (say, with deflection x). The fluid has a constant conductivity σ and permittivity ϵ . An external source of potential v is used to establish the charge q on the upper sphere.

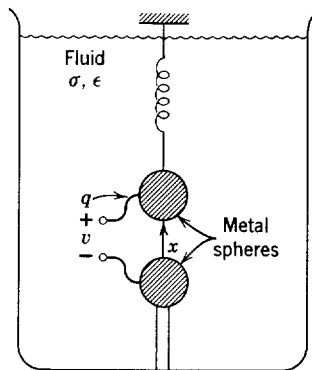


Fig. 7P.19

Then the source of potential is removed, leaving the sphere electrically isolated, except for conduction through the liquid, and free to move. Use the integral laws for an electric field system [(1.1.24) to (1.1.26) and definitions of Table 2.1]* to show that, if the initial charge on the sphere is Q , then as a function of time, the charge q on the sphere is $q = Qe^{-t/\tau}$; $\tau = \epsilon/\sigma$. Your proof should be valid even though the upper sphere is moving [$x = x(t)$].

* Appendix E.

7.20. A pair of parallel slightly conducting plates of conductivity σ and spacing d are insulated from each other, as shown in Fig. 7P.20. When $t = 0$, there is a charge $-Q$ uniformly distributed over the volume of the upper plate and a charge $+Q$ uniformly distributed over the volume of the lower plate. Assume that $d \ll D$:

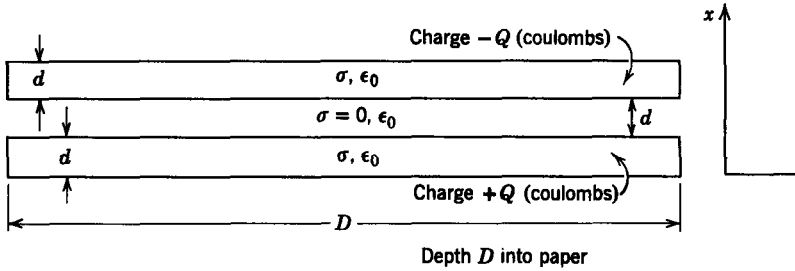


Fig. 7P.20

- (a) Make a dimensioned sketch of the electric field E_x as a function of x when $t = 0$ and as $t \rightarrow \infty$.
- (b) Compute the total force on the lower plate as a function of time.

7.21. Consider the problem of Example 7.2.3 with

$$\epsilon = \epsilon_1 + \frac{\epsilon_2}{l} x,$$

$$\sigma = \sigma_1 + \frac{\sigma_2}{l} x.$$

- (a) Find $E_x(x, t)$ and $\rho_f(x, t)$.
- (b) Discuss the effect of the nonuniform ϵ .

7.22. A fluid moves with the constant velocity $U\mathbf{i}_x$ between parallel plates, as shown in Fig. 7P.22a. The fluid is uncharged ($\rho_f = 0$) for $x < 0$. It has the uniform conductivity σ (which is small) and permittivity ϵ . At $x = 0$ charges are introduced by means of a two-dimensional source midway between the plates. Hence at $x = 0$ the charge has the distribution shown in Fig. 7P.22b, where $\hat{\rho}_0$ is a given complex constant and Δ is the initial thickness of the layer of charge that has been injected.

- (a) Find the charge distribution across the channel at a downstream position $x = l$.
- (b) Describe how you would use the potential induced by this charge on two downstream electrodes to measure the flow velocity U . (Assume that you have control over the frequency. There is more than one way to accomplish this and only a qualitative description is required.)

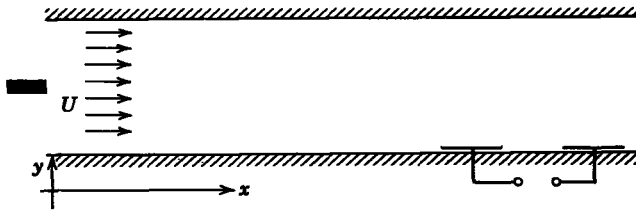


Fig. 7P.22a

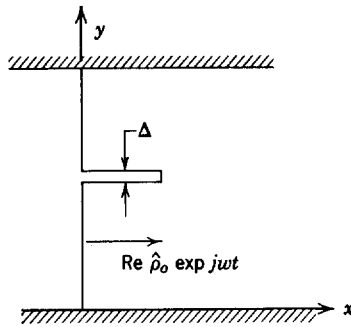


Fig. 7P.22b

7.23. A fluid with conductivity σ flows in the x -direction through a pipe with insulating walls and cross-sectional area A . The velocity of the fluid is approximated as constant (U). Ions are injected into the flow at $x = 0$ with a source that maintains the charge density at $x = 0$ equal to ρ_o (a constant).

- (a) Find the charge density distribution between the screen electrodes.
- (b) Find the distribution of electric field $E_x(x)$ between the electrodes.
- (c) What is the voltage V generated across the load resistance R ?

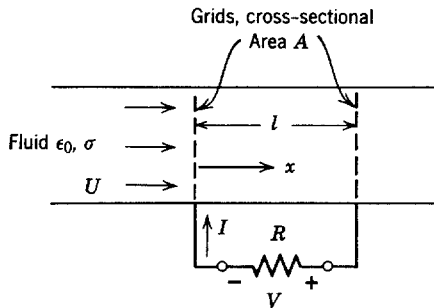


Fig. 7P.23

7.24. When Lord Kelvin invented his electrostatic generator (see Example 7.2.6), he had in mind the generation of dc high voltages. In 1966 William C. Euerle, a student at MIT, elaborated on Lord Kelvin's original idea to make an electrostatic ac generator. This device, with a Y-connected resistive load, is shown in Fig. 7P.24. You can assume that each of the "drippers" is characterized by the same parameters.

- (a) Write three equations for the voltages v_1 , v_2 , and v_3 .
- (b) Use the dynamic description of the potentials found in (a) to show that it is possible for the system to behave as an oscillator; that is, that any one of the voltages would behave as a sinusoid with an exponentially growing amplitude.
- (c) For what values of the parameters will the load limit the oscillations to constant amplitude?
- (d) Under the conditions of (c), what is the oscillation frequency?

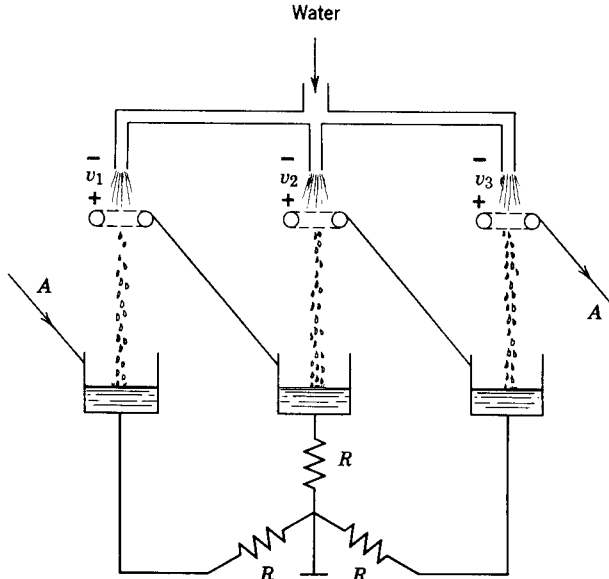


Fig. 7P.24

7.25. Two systems that are proposed to measure the depth d of water in a tank are shown in Fig. 7P.25. In system (a) the depth is indicated by measuring the “inductance” of a loop of copper conductor which encloses a portion of the water; in system (b) the “capacitance” of a pair of copper electrodes is to be used to indicate the depth. You are given that d is on the order of 1 cm., where the properties of the water are about $\sigma = 10^{-2}$ mho/m, $\epsilon = 81 \times \epsilon_0 = 81 \times 8.85 \times 10^{-12}$ F/m, $\mu = \mu_0 = 4\pi \times 10^{-7}$ H/m. Measurements of both the

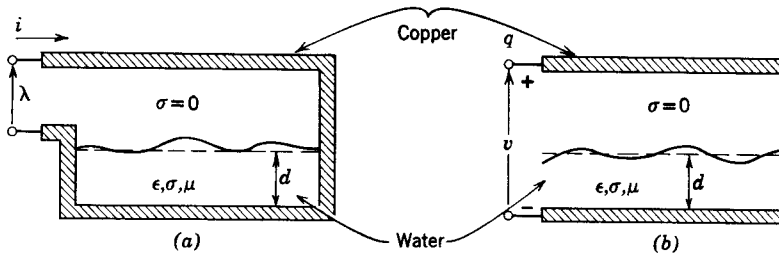


Fig. 7P.25

“capacitance” and “inductance” are to be made with a 100-kc bridge. Which of the two devices would work and why? For what values of σ would both devices be attractive for this application?

7.26. A pair of devices, proposed for measuring the level x of water, is shown in Fig. 7P.26. In case (a) an iron core magnet is driven by a 1-kc signal with the resulting voltage v_0 . In case (b) a pair of plates is parallel to the surface and is driven by a voltage source

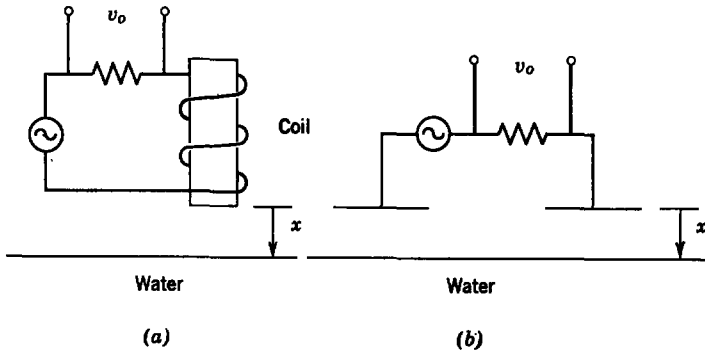


Fig. 7P.26

with a signal v_o across a series resistor. In each case it is desired that v_o be sensitive to the proximity of the water so that the device can be used to indicate the level of the water. Which of the two devices would you use to solve an engineering problem? Give your reasoning.

7.27. Consider the example in Section 7.2.4 but with the additional complication of a perfectly conducting electrode bounding the material (b) from below at $x = -f$.

- (a) Find the potential distribution in regions (a) and (b).
- (b) Check to see that the results of Section 7.2.4 are obtained if $|fk| \gg 1$.

7.28. A sheet of slightly conducting material moves in the z -direction with the constant velocity U . Above and below the sheet electrodes impose the traveling potential waves shown in Fig. 7P.28. The sheet thickness is small compared with c , so that both sheet surfaces can be considered to be at $x = 0$. The constitutive law for a fixed section of the

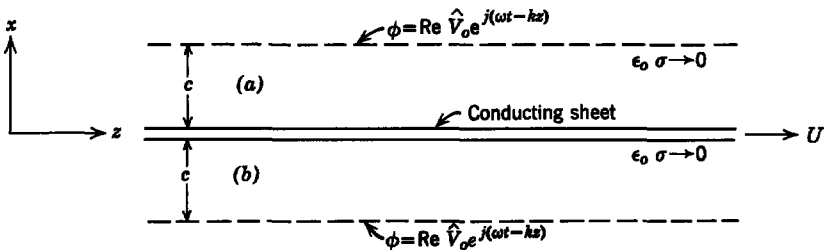


Fig. 7P.28

sheet is $K_f = \sigma_s E_z$, where σ_s is a surface conductivity, K_f is a surface conduction current density, and E_z is the electric field intensity tangential to the sheet.

- (a) Write differential equations and boundary conditions in terms of the potentials $\phi(x, z, t)$ above (a) and below (b) the sheet.
- (b) Determine the time average force/unit length z and unit width y in the z -direction. At what frequency will it have its largest value?
- (c) How would you adjust the traveling potential wave to produce a time average force as $\sigma_s \rightarrow 0$?

Chapter 8

FIELD DESCRIPTION OF MAGNETIC AND ELECTRIC FORCES

8.0 INTRODUCTION

Chapter 7 is restricted to the effects of mechanical motion on magnetic and electric fields. In general, electromechanical interactions involve effects on the mechanical system from the electromagnetic fields as well. These arise from the mechanical forces of electrical origin.

In Chapters 3 through 6 we were concerned with total forces acting on rigid bodies. In systems in which the mechanical medium must be represented by a deformable continuum the details of the force distribution must be known. Hence in continuum electromechanics we are concerned with magnetic or electric force densities, which are, in general, functions of space and time.

Electromagnetic fields are defined by forces composed of two parts: those exerted on free charges by electric fields and those exerted on free currents (moving free charges) by magnetic fields. The relative importance of these forces depends on the type of system being considered. In magnetic field systems, as defined in Section 1.1, the important field excitation is provided by the free current density \mathbf{J}_f . Hence for magnetic field systems the only important forces arise from the interactions of the free current density \mathbf{J}_f with magnetic fields. Similarly, the only forces of significance in electric field systems, as defined in Section 1.1, are the interactions of free charge density ρ_f with electric fields. The validity of these assumptions is checked in particular problems. Following the pattern established in earlier sections, we treat forces in magnetic field and electric field systems separately. Our object is to describe electromagnetic forces mathematically in alternative forms that will prove useful in work with continuum electromechanical systems.

Two other technically important electromagnetic forces are those resulting from the interactions of polarization density \mathbf{P} with electric fields and magnetization density \mathbf{M} with magnetic fields. In Chapters 3 to 5 we calculate total forces on polarizable and magnetizable bodies by using an energy method. We extend this method to account for force densities in polarized or magnetized media that are electrically linear, isotropic, and homogeneous. This limitation in our discussion of polarization and magnetization forces is imposed because use of an energy method requires a knowledge of the mechanical and thermodynamic properties of the material.

8.1 FORCES IN MAGNETIC-FIELD SYSTEMS

Consider first the force resulting from the interaction of moving free charge (i.e., \mathbf{J}_f) and a magnetic field. The Lorentz force (1.1.28) gives the total magnetic force on a charge q moving with velocity \mathbf{v} as

$$\mathbf{f} = q\mathbf{v} \times \mathbf{B}. \quad (8.1.1)$$

The force density \mathbf{F} (newtons per cubic meter) can be obtained from this expression by writing

$$\mathbf{F} = \lim_{\delta V \rightarrow 0} \frac{\sum_i \mathbf{f}_i}{\delta V} = \lim_{\delta V \rightarrow 0} \frac{\sum_i q_i \mathbf{v}_i \times \mathbf{B}_i}{\delta V}, \quad (8.1.2)$$

where \mathbf{f}_i , q_i , and \mathbf{v}_i refer to all the particles in δV and \mathbf{B}_i is the flux density experienced by q_i . If we can say that all particles within δV experience the same flux density \mathbf{B} , we can use the definition of free current density (see Section B.1.2)* to write (8.1.2) as

$$\mathbf{F} = \mathbf{J}_f \times \mathbf{B}. \quad (8.1.3)$$

The general definition of (8.1.2) requires the averaging of products, whereas the result of (8.1.3) is the product of averages. It is not, in general, true for variables x and y that

$$[xy]_{\text{av}} = [x]_{\text{av}}[y]_{\text{av}}.$$

The force density expressed by (8.1.3) however, agrees, to a high degree of accuracy, with all experimental results obtained with common conductors. The relation (8.1.3) is valid because the volume δV can be made small enough to enclose a region of essentially constant magnetic flux density, although still including many free charges.

In fact, we could have used (8.1.3) rather than (8.1.1) as the definition of \mathbf{B} , for the original experiments of Biot and Savart and later Ampère† concerned themselves with relating the force density to the free current density

$$* \mathbf{J}_f = \lim_{\delta V \rightarrow 0} \left[\left(\sum_i q_i \mathbf{v}_i \right) / \delta V \right]$$

† J. D. Jackson, *Classical Electrodynamics*, Wiley, New York 1962, p. 133.

\mathbf{J} . Some writers start with (8.1.3) as the basic definition of the magnetic force on moving free charge.* However, the averaging process used to make (8.1.2) and (8.1.3) consistent is then inherent to the definition.

It is important to remember that (8.1.3) represents the average of forces on the *charges*. This is equivalent to the force on a medium if there is some mechanism by which each charge transmits the Lorentz force to the material. For example, in a conductor, the charges can be thought of as particles moving through a viscous material—in which case the force that acts on each charge is transmitted to the medium by the viscous retarding force and (8.1.3) is the force density experienced by the medium.

There are situations in which the charges do not interact individually with the medium. For example, in a polarized medium, *pairs* of charges (dipoles) transmit a force to the medium—each pair being connected through the structure of an atom or molecule. For these cases it is the dipoles rather than the charges that transmit a force to the medium. Then it is appropriate to consider the average of the forces on individual dipoles as equivalent to the force density on the medium. This class of forces is developed in Section 8.5.

The force density given in (8.1.3) is expressed in terms of source and field quantities. It is useful to have the force expressed as a function of field quantities alone because we often solve field problems without calculating the free current density. We find it useful to define the *Maxwell stress tensor* as a function of the field quantities from which the force density can be obtained by space differentiation. The Maxwell stress tensor is particularly useful for finding electromechanical boundary conditions in a concise form. It is useful also for finding the total electromagnetic force on a body.

A tensor has particular properties that are useful in this and the chapters which follow. We therefore devote Section 8.2 to a discussion of the stress tensor, using magnetic field stresses as an example.

We can write (8.1.3) in terms of the magnetic field intensity and in a particularly useful form when the medium has a constant permeability, that is, with the constituent relation†

$$\mathbf{B} = \mu\mathbf{H}. \quad (8.1.4)$$

We can use (8.1.4) and Ampère's law for magnetic field systems (1.1.1)‡ to write (8.1.3) in the form

$$\mathbf{F} = \mu(\nabla \times \mathbf{H}) \times \mathbf{H}. \quad (8.1.5)$$

It is a vector identity that this expression can be written as

$$\mathbf{F} = \mu(\mathbf{H} \cdot \nabla)\mathbf{H} - \frac{\mu}{2} \nabla(\mathbf{H} \cdot \mathbf{H}), \quad (8.1.6)$$

* See, for example, Jackson, *ibid.*, p. 137.

† Arguments are given in Section 8.5 to show that (8.1.3) is the force density on free currents in the presence of a constant permeability μ . For now we assume that this is the case.

‡ Table 1.2, Appendix E.

There are three components to this vector equation, but we usually do not write them out unless specific situations are under consideration. There are manipulations, however, that become easier to perform when the equations are viewed component by component. They can be carried out without dealing with cumbersome expressions by using *index notation*.*

In what follows we assume a right-hand cartesian coordinate system x_1, x_2, x_3 . The component of a vector in the direction of an axis carries the subscript of that axis. When we write F_m we mean the m th component of the vector \mathbf{F} , where m can be 1, 2, or 3. The mathematical formalism is illustrated by using the force density of (8.1.6) as an example. When we write the differential operator $\partial/\partial x_n$, we mean $\partial/\partial x_1, \partial/\partial x_2, \text{ or } \partial/\partial x_3$. When the index is repeated in a single term, it implies summation over the three values of the index

$$\frac{\partial H_n}{\partial x_n} = \frac{\partial H_1}{\partial x_1} + \frac{\partial H_2}{\partial x_2} + \frac{\partial H_3}{\partial x_3} = \nabla \cdot \mathbf{H}$$

and

$$H_n \frac{\partial}{\partial x_n} = H_1 \frac{\partial}{\partial x_1} + H_2 \frac{\partial}{\partial x_2} + H_3 \frac{\partial}{\partial x_3} = \mathbf{H} \cdot \nabla.$$

This illustrates the *summation convention*. On the other hand, $\partial H_m/\partial x_n$ represents any one of the nine possible derivatives of components of \mathbf{H} with respect to coordinates. We define the *Kronecker delta* δ_{mn} which has the values

$$\delta_{mn} = \begin{cases} 1, & \text{when } m = n, \\ 0, & \text{when } m \neq n. \end{cases} \quad (8.1.7)$$

The Kronecker delta has the property (remember to sum on an index that appears twice)

$$\delta_{mn} H_n = H_m$$

and

$$\delta_{mn} \frac{\partial}{\partial x_n} = \frac{\partial}{\partial x_m},$$

which can be verified by using the definition (8.1.7).

With these definitions we write the m th component of (8.1.6) as

$$F_m = \mu H_n \frac{\partial H_m}{\partial x_n} - \frac{\mu}{2} \frac{\partial}{\partial x_m} (H_k H_k). \quad (8.1.8)$$

* A. J. McConnell, *Applications of the Absolute Differential Calculus*, Blackie, London, 1951, Chapter 1.

We use the property of the Kronecker delta [$\partial/\partial x_m = \delta_{mn}(\partial/\partial x_n)$] and some manipulation to write this expression as

$$F_m = \frac{\partial}{\partial x_n} \left(\mu H_n H_m - \frac{\mu}{2} \delta_{mn} H_k H_k \right) - H_m \frac{\partial \mu H_n}{\partial x_n}. \quad (8.1.9)$$

The last term on the right is

$$H_m (\nabla \cdot \mu \mathbf{H}) = H_m (\nabla \cdot \mathbf{B}) = 0;$$

thus we finally write (8.1.9) in the concise form

$$F_m = \frac{\partial T_{mn}}{\partial x_n}, \quad (8.1.10)$$

where the Maxwell stress tensor T_{mn} is given by

$$T_{mn} = \mu H_n H_m - \frac{\mu}{2} \delta_{mn} H_k H_k. \quad (8.1.11)$$

If we know the magnetic field intensity \mathbf{H} in a region of space, we can calculate the components of the stress tensor T_{mn} . We need only to calculate at most six components because the stress tensor is symmetric:

$$T_{mn} = T_{nm}. \quad (8.1.12)$$

Differentiation of (8.1.11) with respect to the space coordinate according to (8.1.10) gives the force density on the current-carrying matter in that region of space. We should keep in mind that (8.1.10) is simply an alternative way of expressing the m th component of $\mathbf{J} \times \mathbf{B}$. Moreover, we must use the *total* \mathbf{H} to obtain the correct answer from (8.1.10).

Now suppose we wish to find the m th component of the total force \mathbf{f} on material contained within the volume V . We can find it by performing the volume integration:

$$f_m = \int_V F_m dV = \int_V \frac{\partial T_{mn}}{\partial x_n} dV. \quad (8.1.13)$$

When we define the components of a vector \mathbf{A} as

$$A_1 = T_{m1}, \quad A_2 = T_{m2}, \quad A_3 = T_{m3}, \quad (8.1.14)$$

we can write (8.1.13) as

$$f_m = \int_V \frac{\partial A_n}{\partial x_n} dV = \int_V (\nabla \cdot \mathbf{A}) dV. \quad (8.1.15)$$

We now use the divergence theorem to change the volume integral to a surface integral,

$$f_m = \oint_S \mathbf{A} \cdot \mathbf{n} da = \oint_S A_n n_n da, \quad (8.1.16)$$

where n_n is the n th component of the outward-directed unit vector \mathbf{n} normal to the surface S and the surface S encloses the volume V . Substitution from (8.1.14) back into this expression yields

$$f_m = \oint_S T_{mn} n_n da. \quad (8.1.17)$$

Hence we can find the total force of magnetic origin on the matter within a volume V by knowing only the fields along the surface of the volume. This is an important result.

8.2 THE STRESS TENSOR

In the preceding section we introduced the Maxwell stress tensor as an ordered array of nine functions of space and time $T_{mn}(\mathbf{r}, t)$ from which we can calculate magnetic force densities and total forces. The concept of a tensor will be useful to us in later chapters for describing mechanical stresses and deformations in elastic and fluid media. Consequently, we now digress from our study of electromagnetic forces to develop some tensor concepts.

We first consider the tensor representation of stresses with the object of attaching physical significance to the components of a stress tensor. Then mathematical techniques that are used with the stress tensor to find surface stresses (tractions) and volume force densities are introduced. Finally, we introduce some mathematical properties of tensors in general. These properties are introduced in a context in which physical interpretations can be made easily. It is important to remember that tensor analysis is a mathematical formalism that is particularly useful for analyzing a wide variety of physical systems.*

We have remarked that the Maxwell stress tensor is an ordered array of nine functions of space and time. It is conventional to write this array in matrix form as

$$T_{mn}(\mathbf{r}, t) = \begin{bmatrix} T_{11}(\mathbf{r}, t) & T_{12}(\mathbf{r}, t) & T_{13}(\mathbf{r}, t) \\ T_{21}(\mathbf{r}, t) & T_{22}(\mathbf{r}, t) & T_{23}(\mathbf{r}, t) \\ T_{31}(\mathbf{r}, t) & T_{32}(\mathbf{r}, t) & T_{33}(\mathbf{r}, t) \end{bmatrix}. \quad (8.2.1)$$

The first index marks the row and the second, the column in which the element appears. As indicated by (8.1.11) and (8.1.12), the Maxwell stress tensor is symmetric. In the matrix of (8.2.1) the symmetry is about the diagonal. Although the symmetry property has been established only for the Maxwell stress tensor, we find that all the tensors we use in this book are symmetric.

* For a more detailed discussion of tensor calculus than we need in this book see, for example, B. Spain, *Tensor Calculus*, Interscience, New York, 1960.

8.2.1 Stress and Traction

A physical interpretation of the stress tensor follows from (8.1.17) which relates the total force on matter within the volume V enclosed by the surface S to an integral over the surface S . The integrand $T_{mn}n_n$ has the dimension of a force per unit area and, in view of the summation convention with a repeated index, $T_{mn}n_n$ is the m th component of a vector. The vector whose components are $T_{mn}n_n$ has special significance and is therefore given the name *traction* and a symbol τ . Thus the m th component of the traction is written as*

$$\tau_m = T_{mn}n_n = T_{m1}n_1 + T_{m2}n_2 + T_{m3}n_3. \quad (8.2.2)$$

We show subsequently that the traction τ , defined by (8.2.2), is actually the vector force per unit area applied to a surface of arbitrary orientation. For the moment, however, we use (8.2.2) to attach some physical significance to the components of the stress tensor.

Assume that the surface integral of (8.1.17) is to be taken over the rectangular volume whose faces are perpendicular to the coordinate axes illustrated in Fig. 8.2.1. We can express (8.1.17) as the sum of six integrals taken over the six plane faces of the volume. As an example, consider the top face, which has the outward directed normal vector.

$$\mathbf{n} = \mathbf{i}_1.$$

The components of this normal vector are

$$n_1 = 1, \quad n_2 = n_3 = 0.$$

Consequently, the three components of the traction on the top surface are

$$\tau_1 = T_{11}, \quad \tau_2 = T_{21}, \quad \tau_3 = T_{31}.$$

These components and the vector τ are illustrated in Fig. 8.2.1. Next, consider the bottom face, which has the outward directed normal vector

$$\mathbf{n} = -\mathbf{i}_1.$$

The components of this normal vector are

$$n_1 = -1, \quad n_2 = n_3 = 0.$$

* Note that the subscript on the traction τ_m is the same as the *first* subscript on the stress tensor component T_{mn} . This choice for the order of subscripts on T_{mn} is a matter of convention. Although the convention used here is prevalent in the literature, the opposite convention is used. Therefore it is wise to identify the convention used in each case by inspecting equations of the form of (8.1.10) or (8.1.17).

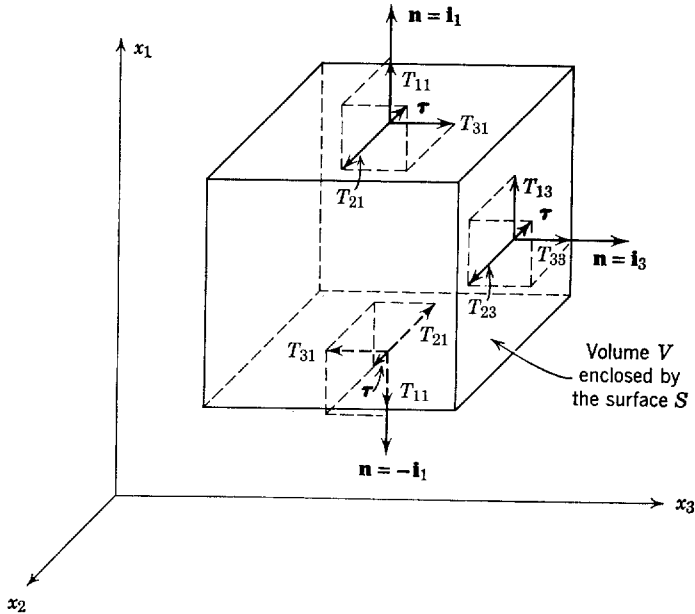


Fig. 8.2.1 A rectangular volume V , acted on by a stress T_{mn} .

Thus the three components of the traction on the bottom face are

$$\tau_1 = -T_{11}, \quad \tau_2 = -T_{21}, \quad \tau_3 = -T_{31}.$$

These components and the vector $\boldsymbol{\tau}$ are illustrated in Fig. 8.2.1.

A similar process can be followed to find the surface traction $\boldsymbol{\tau}$ on each of the other faces. The vector and its components for the face with outward directed normal vector $\mathbf{n} = \mathbf{i}_3$ are also shown in Fig. 8.2.1.

We have shown that *the component T_{mn} of the stress tensor can be physically interpreted as the m th component of the traction applied to a surface with a normal vector in the n -direction.* Thus T_{23} is the x_2 -directed component of the traction applied to a surface whose normal vector is \mathbf{i}_3 .

We use the ideas developed with Fig. 8.2.1 to construct, in component form, the tractions on all six faces of a rectangular volume in Fig. 8.2.2. The faces are perpendicular to the three axes and the position of each face is defined. The corresponding stresses act in opposite directions on opposite faces. Consequently, if each component of the stress tensor is a constant over the whole volume, the stresses exactly oppose one another and no net force is applied to the material inside the volume. The stress tensor must vary with space to produce a net force.

To illustrate this mathematically we assume the dimensions of the volume

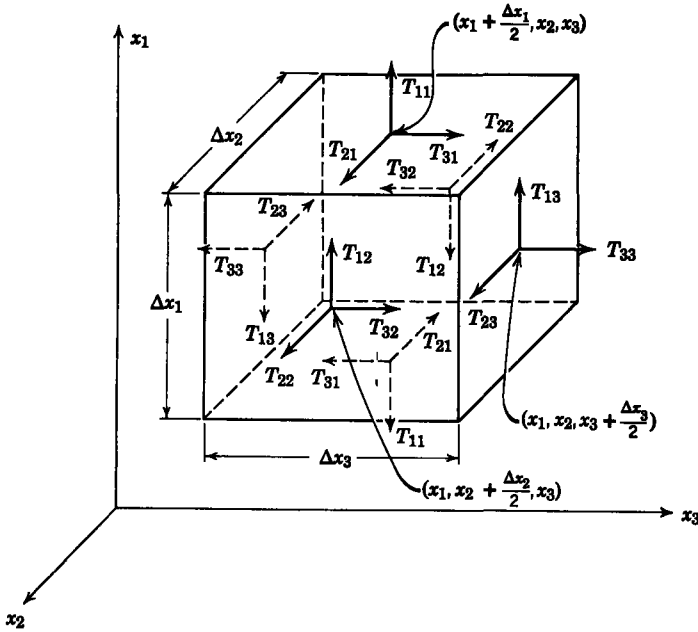


Fig. 8.2.2 Rectangular volume with center at (x_1, x_2, x_3) showing the surfaces and directions of the stresses T_{mn} .

to be small enough that components of the stress tensor do not vary appreciably over one face. We use (8.1.17) to evaluate the x_1 -component of the total force applied to the material within the volume as

$$\begin{aligned}
 f_1 = & T_{11} \left(x_1 + \frac{\Delta x_1}{2}, x_2, x_3 \right) \Delta x_2 \Delta x_3 - T_{11} \left(x_1 - \frac{\Delta x_1}{2}, x_2, x_3 \right) \Delta x_2 \Delta x_3 \\
 & + T_{12} \left(x_1, x_2 + \frac{\Delta x_2}{2}, x_3 \right) \Delta x_1 \Delta x_3 - T_{12} \left(x_1, x_2 - \frac{\Delta x_2}{2}, x_3 \right) \Delta x_1 \Delta x_3 \\
 & + T_{13} \left(x_1, x_2, x_3 + \frac{\Delta x_3}{2} \right) \Delta x_1 \Delta x_2 - T_{13} \left(x_1, x_2, x_3 - \frac{\Delta x_3}{2} \right) \Delta x_1 \Delta x_2.
 \end{aligned}
 \tag{8.2.3}$$

Here we have evaluated the components of the stress tensor at the centers of the surfaces on which they act; for example, the stress component T_{11} acting on the top surface is evaluated at a point having the same x_2 - and x_3 -coordinates as the center of the volume but an x_1 coordinate $\Delta x_1/2$ above the center.

The dimensions of the volume have already been specified as quite small. In fact, we are interested in the limit as the dimensions go to zero. Consequently, each component of the stress tensor is expanded in a Taylor series

about the value at the volume center with only linear terms in each series retained to write (8.2.3) as

$$\begin{aligned} f_1 = & \left(T_{11} + \frac{\Delta x_1}{2} \frac{\partial T_{11}}{\partial x_1} - T_{11} + \frac{\Delta x_1}{2} \frac{\partial T_{11}}{\partial x_1} \right) \Delta x_2 \Delta x_3 \\ & + \left(T_{12} + \frac{\Delta x_2}{2} \frac{\partial T_{12}}{\partial x_2} - T_{12} + \frac{\Delta x_2}{2} \frac{\partial T_{12}}{\partial x_2} \right) \Delta x_1 \Delta x_3 \\ & + \left(T_{13} + \frac{\Delta x_3}{2} \frac{\partial T_{13}}{\partial x_3} - T_{13} + \frac{\Delta x_3}{2} \frac{\partial T_{13}}{\partial x_3} \right) \Delta x_1 \Delta x_2 \end{aligned}$$

or

$$f_1 = \left(\frac{\partial T_{11}}{\partial x_1} + \frac{\partial T_{12}}{\partial x_2} + \frac{\partial T_{13}}{\partial x_3} \right) \Delta x_1 \Delta x_2 \Delta x_3. \quad (8.2.4)$$

All terms in this expression are to be evaluated at the center of the volume (x_1, x_2, x_3) . We have thus verified our physical intuition that space-varying stress tensor components are necessary to obtain a net force.

From (8.2.4) we can obtain the x_1 -component of the force density \mathbf{F} at the point (x_1, x_2, x_3) by writing

$$F_1 = \lim_{\Delta x_1, \Delta x_2, \Delta x_3 \rightarrow 0} \frac{f_1}{\Delta x_1 \Delta x_2 \Delta x_3} = \frac{\partial T_{11}}{\partial x_1} + \frac{\partial T_{12}}{\partial x_2} + \frac{\partial T_{13}}{\partial x_3}. \quad (8.2.5)$$

The limiting process makes the expansion of (8.2.4) exact. The summation convention is used to write (8.2.5) as

$$F_1 = \frac{\partial T_{1n}}{\partial x_n}. \quad (8.2.6)$$

A similar process for the other two components of the force and force density yields the general result that the m th component of the force density at a point is

$$F_m = \frac{\partial T_{mn}}{\partial x_n}. \quad (8.2.7)$$

This is the result obtained in (8.1.10), which was derived for magnetic forces. Thus we have made the transition from the integral in (8.1.17) to the derivative in (8.2.7)—the reverse of the process in which we used the divergence theorem to obtain (8.1.17) from (8.1.10).

Although the formalism presented in this section is based on a result derived with magnetic forces, the stress tensor has a more general significance, as we shall see in later chapters; for example, the rectangular volume in Fig. 8.2.2 can be a block of elastic material with mechanical stresses applied to the surfaces. Our derivation and interpretations are still valid with respect to mechanical forces and force densities. For the moment we restrict our

examples to consider only magnetic forces because they are the only ones we have introduced formally.

Example 8.2.1. To illustrate some properties of the stress tensor and the mathematical techniques used with it, consider the system illustrated schematically in Fig. 8.2.3. The system consists of a long, cylindrical, nonmagnetic ($\mu = \mu_0$) conductor whose axis coincides with the x_3 -axis. The conductor carries a uniform constant current density

$$\mathbf{J} = \mathbf{i}_3 J. \quad (\text{a})$$

An electromagnet, not shown, produces a uniform magnetic field intensity

$$\mathbf{H}_0 = \mathbf{i}_1 H_0, \quad (\text{b})$$

when $J = 0$. The conductor is long enough that we can ignore any variations with x_3 ; thus the problem is two-dimensional.

Because the field problem is linear, we can superimpose the field \mathbf{H}_0 with the field excited by the current density \mathbf{J} . To calculate the two nonzero components H'_1 and H'_2 , due to \mathbf{J} , we establish a cylindrical coordinate system as illustrated in Fig. 8.2.4 and use the integral form of Ampère's law to obtain

$$H_\theta = \frac{Jr}{2} \quad \text{for } r < R, \quad (\text{c})$$

$$H_\theta = \frac{JR^2}{2r} \quad \text{for } r > R. \quad (\text{d})$$

The transformation from cylindrical to cartesian coordinates* is used to find the cartesian components of this field. We then add the externally applied field H_0 to obtain the total field intensity as

$$\left. \begin{aligned} H_1 &= H_0 - \frac{J}{2} x_2 \\ H_2 &= \frac{J}{2} x_1 \end{aligned} \right\} \quad \text{for } x_1^2 + x_2^2 < R^2. \quad (\text{e})$$

$$\left. \begin{aligned} H_1 &= H_0 - \frac{JR^2}{2} \left(\frac{x_2}{x_1^2 + x_2^2} \right) \\ H_2 &= \frac{JR^2}{2} \left(\frac{x_1}{x_1^2 + x_2^2} \right) \end{aligned} \right\} \quad \text{for } x_1^2 + x_2^2 > R^2, \quad (\text{f})$$

The component H_3 is zero; thus we use (8.1.11) and (8.2.1) to write the stress tensor

$$(T_{mn}) = \begin{bmatrix} \frac{\mu_0}{2} (H_1^2 - H_2^2) & \mu_0 H_1 H_2 & 0 \\ \mu_0 H_1 H_2 & \frac{\mu_0}{2} (H_2^2 - H_1^2) & 0 \\ 0 & 0 & -\frac{\mu_0}{2} (H_1^2 + H_2^2) \end{bmatrix}. \quad (\text{g})$$

* H. B. Phillips, *Analytic Geometry and Calculus*, 2nd ed., Wiley, New York, 1946, p. 206.

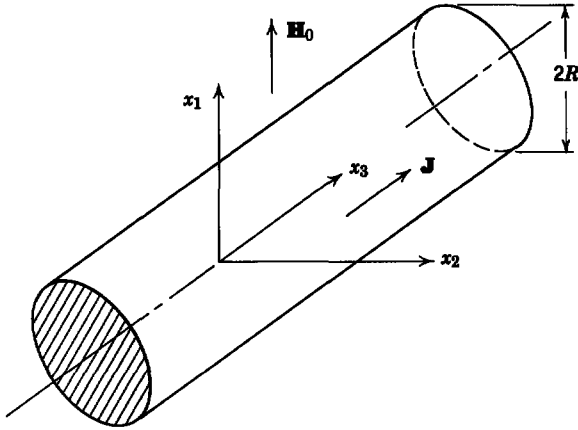


Fig. 8.2.3 A cylindrical conductor carrying uniform current density in the presence of a uniform applied field.

Now (e) or (f) can be used with this expression to find the components of the stress tensor both inside and outside the conductor. First the force density inside the conductor is calculated from (8.1.3):

$$\mathbf{F} = \mathbf{J}_f \times \mathbf{B} = -i_1 J \mu_0 H_2 + i_2 J \mu_0 H_1$$

or

$$\mathbf{F} = -i_1 \frac{\mu_0 J^2 x_1}{2} + i_2 \mu_0 J \left(H_0 - \frac{J x_2}{2} \right). \tag{h}$$

Thus there is a force density term due to the interaction between the current density and the externally applied field and a term due to interaction of the current density with the field it produces.

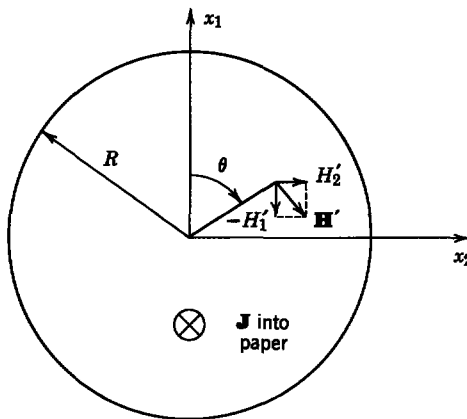


Fig. 8.2.4 Geometry for calculating fields excited by J.

To calculate this same force density from the stress tensor we use (8.1.10) and write for the x_2 -component

$$F_2 = \frac{\partial T_{21}}{\partial x_1} + \frac{\partial T_{22}}{\partial x_2}. \quad (i)$$

By substitution of (e) into (g) this expression becomes

$$F_2 = \frac{\partial}{\partial x_1} \left[\frac{\mu_0 J x_1}{2} \left(H_0 - \frac{J x_2}{2} \right) \right] + \frac{\partial}{\partial x_2} \left\{ \frac{\mu_0}{2} \left[\frac{J^2 x_1^2}{4} - \left(H_0 - \frac{J}{2} x_2 \right)^2 \right] \right\}. \quad (j)$$

Performance of the indicated differentiations yields the x_2 -component of (h), as it should. A similar process can be used to calculate the x_1 -component of the force density and also to show that the x_3 -component of the force density is zero.

It should be evident from a comparison of the effort required to obtain (h) and (j) that the stress tensor is not normally used to calculate force density in a system such as this. We present this example to illustrate the correspondence between the two methods and to illustrate the mathematical processes involved.

It is clear that outside the conductor the force density must be zero because the current density is zero; however, (f) and (g) show that the stress tensor has nonzero components in this region. To show that (8.1.10) yields a zero force density in this region we write the expression for the x_2 -component of (8.1.10) outside the conductor ($x_1^2 + x_2^2 > R^2$):

$$F_2 = \frac{\partial}{\partial x_1} \left\{ \frac{\mu_0 J R^2}{2} \left(\frac{x_1}{x_1^2 + x_2^2} \right) \left[H_0 - \frac{J R^2}{2} \left(\frac{x_2}{x_1^2 + x_2^2} \right) \right] \right\} + \frac{\partial}{\partial x_2} \left\{ \frac{\mu_0}{2} \left[\frac{J^2 R^4}{4} \left(\frac{x_1}{x_1^2 + x_2^2} \right)^2 - \left[H_0 - \frac{J R^2}{2} \left(\frac{x_2}{x_1^2 + x_2^2} \right) \right]^2 \right] \right\}. \quad (k)$$

The indicated differentiation can be carried out to verify that this component of force density is zero. A similar process can be used to show that F_1 and F_3 , calculated from the stress tensor, are zero outside the conductor.

We now turn to the problem of calculating the total magnetic force on a length l of the conductor. First a volume integration of the force density given by (h) is performed. Because there are no variations of the fields with x_3 , we use as a volume element

$$dV = l dx_1 dx_2$$

and use (h) and the geometry of Fig. 8.2.4 to write

$$\mathbf{f} = \int_{-R}^R \int_{-\sqrt{R^2-x_1^2}}^{\sqrt{R^2-x_1^2}} \left[-\mathbf{i}_1 \frac{\mu_0 J^2 x_1}{2} + \mathbf{i}_2 \mu_0 J \left(H_0 - \frac{J x_2}{2} \right) \right] l dx_1 dx_2.$$

We integrate this equation with respect to x_2 , evaluate the result at the limits, and obtain

$$\mathbf{f} = \int_{-R}^R [-\mathbf{i}_1 \mu_0 J^2 x_1 \sqrt{R^2 - x_1^2} + \mathbf{i}_2 2 \mu_0 J H_0 \sqrt{R^2 - x_1^2}] l dx_1$$

Evaluation of this integral with the specified limits yields the final result

$$\mathbf{f} = \mathbf{i}_2 J \mu_0 H_0 \pi R^2 l. \quad (l)$$

This is simply the uniform force density due to the externally applied field H_0 multiplied by the volume $\pi R^2 l$. That the forces due to the self-field canceled out is a result of the cylindrical symmetry. Thus the force density due to the self-fields tends to deform the conductor but produces no net force that tends to move it.

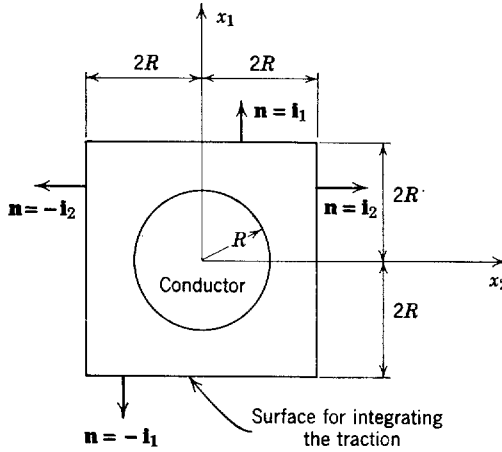


Fig. 8.2.5 Illustrating the surface for integrating the traction.

To use the stress tensor in calculating this same total force we use (8.1.17) with a surface that encloses a length l of the conductor. To make it quite clear that we can use a surface that is totally outside the body we choose a surface of length l and of square cross section with sides $4R$, as shown in end view in Fig. 8.2.5. Because this surface is completely outside the conductor we must use (f) with (g) to calculate the components of the stress tensor.

None of the quantities varies with x_3 ; consequently, we recognize that the contribution to (8.1.17) from the two ends perpendicular to the x_3 -axis is zero. The contribution from one end is the negative of that from the other end. We calculate only the x_2 -component of the force. A similar process can be carried out for the other two components and (l) indicates that they integrate to zero.

We use the four lateral surfaces whose normal vectors are defined in Fig. 8.2.5 to write (8.1.17) for the x_2 -component as

$$f_2 = \int_{-2R}^{2R} T_{21}(2R, x_2)l dx_2 - \int_{-2R}^{2R} T_{21}(-2R, x_2)l dx_2 + \int_{-2R}^{2R} T_{22}(x_1, 2R)l dx_1 - \int_{-2R}^{2R} T_{22}(x_1, -2R)l dx_1. \quad (m)$$

The stress components in the integrands are given by (g) and can be evaluated in terms of the magnetic field components by using (f). Then integration yields the result

$$f_2 = J\mu_0 H_0 \pi R^2 l.$$

This is the same as (l) which was obtained by integrating the volume force density throughout the conductor.

We have verified in an example that we can obtain the total force on current-carrying material within a volume by integrating the traction over a surface enclosing the volume. It is illuminating to investigate the nature of the tractions involved in this integration. For this purpose we refer to Fig. 8.2.2 in which we interpreted the components of the stress tensor as being the components of the traction. Thus we recognize that the first two integrals in (m) involve the x_2 -component of the traction applied to surfaces whose normal vectors

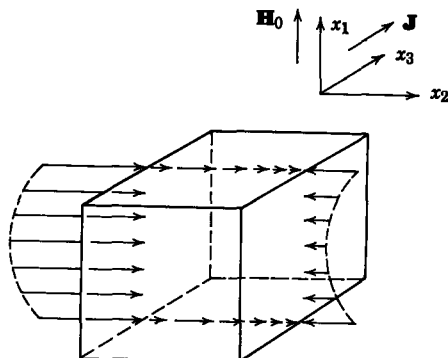


Fig. 8.2.6 Stress distribution.

are in the x_1 -direction. Because these tractions are applied along a surface they are referred to as *shear stresses*. The second two integrals in (m) involve components of the traction that are perpendicular to the surfaces to which they are applied. Such tractions are called *normal stresses*.

If we wish to carry our interpretation a step further and say that there are stresses transmitted through space by the magnetic field as indicated by the Maxwell stress tensor, we can interpret the integrands of (m) as being stresses applied to the four surfaces. We use the integrands to sketch these stresses in Fig. 8.2.6. The shear stresses are equal on top and bottom and are in the direction of the net force. The normal stresses are compressive and there is an excess of stress applied to the left side.

Although the interpretation of the Maxwell stress tensor as representing mechanical stresses transmitted by fields through empty space is often useful it must be employed with understanding; for example, we could add a constant to all components of the stress tensor and not change the results of our calculations of force density and total force. The stress pattern of Fig. 8.2.6, however, would be changed markedly.

In (8.2.2) we defined the m th component τ_m of the traction $\boldsymbol{\tau}$ as

$$\tau_m = T_{mn}n_n. \quad (8.2.8)$$

The traction was interpreted as the vector force per unit area applied to a surface with components n_n of the normal vector \mathbf{n} . The integral force equation (8.1.17) suggests that $\boldsymbol{\tau}$ represents the force per unit area for a surface of arbitrary orientation. This fact is emphasized by the discussion which follows.

Figure 8.2.7 is a tetrahedron with three of its edges parallel to x_1, x_2, x_3 -axes. One surface of the tetrahedron has a normal vector \mathbf{n} and supports the traction $\boldsymbol{\tau}$ (which, in general, is not in the direction of \mathbf{n}). Because three of the surfaces have normal vectors that are in the axis directions, the tractions on these surfaces can be written in terms of the components T_{mn} , whereas the traction on the fourth surface is the unknown $\boldsymbol{\tau}$. Although the surface tractions (and in particular T_{mn}) depend on the space coordinates, it has been

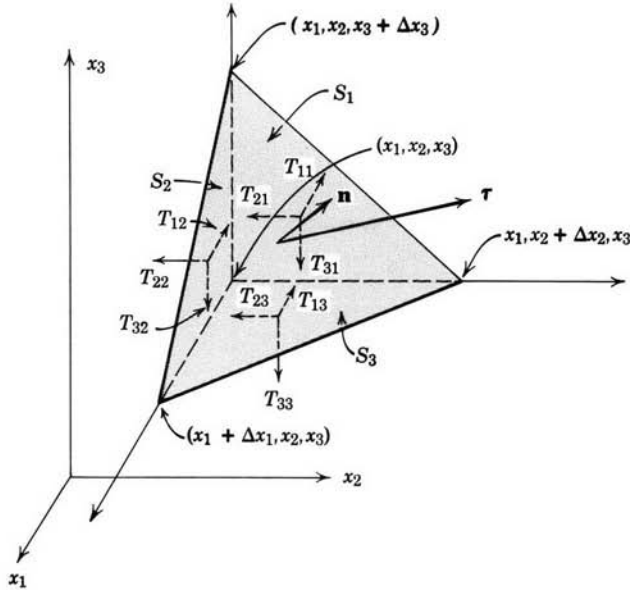


Fig. 8.2.7 The small tetrahedron used to find the surface traction τ on a surface with the normal vector \mathbf{n} in terms of the components of the stress tensor T_{mn} .

implicitly assumed that T_{mn} is a continuous function. Hence, as $\Delta x_1, \Delta x_2, \Delta x_3 \rightarrow 0$, the traction τ must balance the stresses on the negative surfaces. Here we use the fact that the volume forces are proportional to the volume $\Delta x_1 \Delta x_2 \Delta x_3$, whereas the surface tractions produce forces proportional to areas, that is, $\Delta x_1 \Delta x_2$, $\Delta x_2 \Delta x_3$ or $\Delta x_3 \Delta x_1$. Hence in the limit in which $\Delta x_1, \Delta x_2, \Delta x_3 \rightarrow 0$, the prism of material is not in force equilibrium unless the surface forces balance.

If the surface with the normal \mathbf{n} has the area S , the negative surfaces have the areas Sn_1, Sn_2, Sn_3 ,* respectively, and continuity of the stresses which act in the x_1 -direction gives rise to the equation

$$\tau_1 S \cong T_{11} S n_1 + T_{12} S n_2 + T_{13} S n_3. \quad (8.2.9)$$

In the limit in which the dimensions of the tetrahedron become small (8.2.9) becomes exact. Since the equation can also be written for the other components of the stress, (8.2.8) follows.

* A proof of this geometric relation can be made by using Gauss's theorem $\oint_S \mathbf{A} \cdot \mathbf{n} \, da = \int_V (\nabla \cdot \mathbf{A}) \, dV$ with $\mathbf{A} = \mathbf{i}_1$. The volume integral vanishes and the surface integral (integrated over the surface of the tetrahedron) becomes $-S_1 + S n_1 = 0$, where S_1 is the area of the back surface with the normal $-\mathbf{i}_1$. Similar arguments hold using $\mathbf{A} = \mathbf{i}_2$ and $\mathbf{A} = \mathbf{i}_3$.

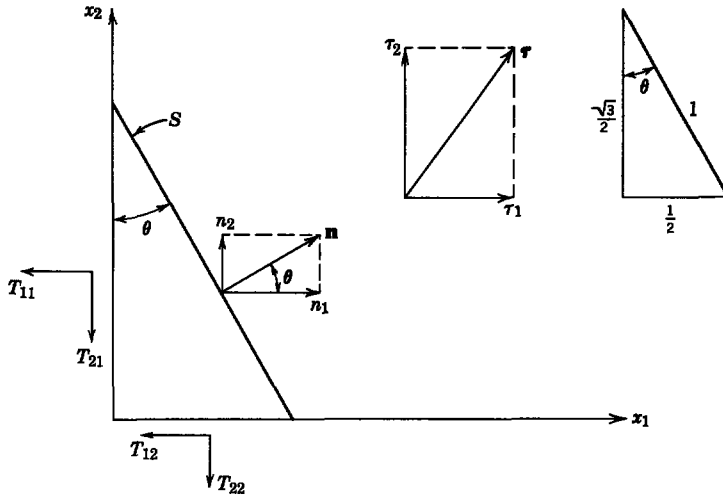


Fig. 8.2.8 Example of surface traction τ acting on a particular surface S .

Example 8.2.2. A brief example will help to fix the meaning of (8.2.8). We wish to derive the traction τ on the surface S shown in Fig. 8.2.8, given the stresses T_{11} , T_{12} , etc. It is assumed that \mathbf{n} lies in the x_1 - x_2 plane, so that from the figure the normal vector is

$$\mathbf{n} = \mathbf{i}_1 \frac{\sqrt{3}}{2} + \mathbf{i}_2 \frac{1}{2}. \quad (\text{a})$$

Note that the components of \mathbf{n} are *not* the unit vectors \mathbf{i}_1 , \mathbf{i}_2 , \mathbf{i}_3 . According to (8.2.8), the components of τ acting on the surface S are

$$\begin{aligned} \tau_1 &= T_{11} \frac{\sqrt{3}}{2} + T_{12} \frac{1}{2}, \\ \tau_2 &= T_{21} \frac{\sqrt{3}}{2} + T_{22} \frac{1}{2}, \\ \tau_3 &= 0, \end{aligned} \quad (\text{b})$$

where we have assumed that T_{31} , T_{32} , and T_{33} are zero or that there are no components of the stress acting in the x_3 -direction. This example should make it clear that all we have done in writing (8.2.8) is to formalize our interpretation of the stress components as forces per unit area acting on surfaces that are perpendicular to the axis directions. The results could be derived from inspection of Fig. 8.2.8 without making use of (8.2.8). Try it!

8.2.2 Vector and Tensor Transformations

In our discussion so far we have interpreted the physical properties of the stress tensor in terms of the vector traction τ whose components are defined by (8.2.2). We now use the mathematical properties of the vector τ to describe some mathematical properties of the stress tensor.

The traction τ is a vector. The components of this vector depend on the coordinate system in which τ is expressed; for example, the vector might be directed in one of the coordinate directions (x_1, x_2, x_3), in which case there would be only one nonzero component of τ . In a second coordinate system (x'_1, x'_2, x'_3), this same vector might have components in all of the coordinate directions. Analyzing a vector into orthogonal components along the coordinate axes is a familiar process. The components in a cartesian coordinate system (x'_1, x'_2, x'_3) are related to those in the cartesian coordinate system (x_1, x_2, x_3) by the three equations

$$\tau'_p = a_{pr}\tau_r, \quad (8.2.10)$$

where a_{pr} is the cosine of the angle between the x'_p -axis and the x_r -axis.

Example 8.2.3. Suppose that we wish to use (8.2.10) to compute the components τ'_m of the vector τ' in the primed coordinate system shown in Fig. 8.2.9, in terms of the known components τ_m of τ in the unprimed coordinate system. (It should be recognized that the x'_1 axis in this figure is in the direction of the normal in Fig. 8.2.8, so that we can consider this example as an extension of the preceding one.) From the geometry the cosine of the angle between

$$\begin{aligned} x'_1 \text{ and } x_1 &= a_{11} = \frac{\sqrt{3}}{2}, & x'_1 \text{ and } x_2 &= a_{21} = \frac{\sqrt{3}}{2}, \\ x'_1 \text{ and } x_3 &= a_{31} = \frac{1}{2}, & x'_2 \text{ and } x_1 &= a_{12} = -\frac{1}{2}, \\ x'_2 \text{ and } x_2 &= a_{22} = \frac{1}{2}, & x'_2 \text{ and } x_3 &= a_{32} = 1, \\ x'_3 \text{ and } x_1 &= a_{13} = -\frac{1}{2}, & x'_3 \text{ and } x_2 &= a_{23} = 0, \\ x'_3 \text{ and } x_3 &= a_{33} = 1, & \text{all others} &= 0. \end{aligned}$$

Hence by definition

$$[a_{mn}] = \begin{bmatrix} \frac{\sqrt{3}}{2} & \frac{1}{2} & 0 \\ -\frac{1}{2} & \frac{\sqrt{3}}{2} & 0 \\ 0 & 0 & 1 \end{bmatrix}.$$

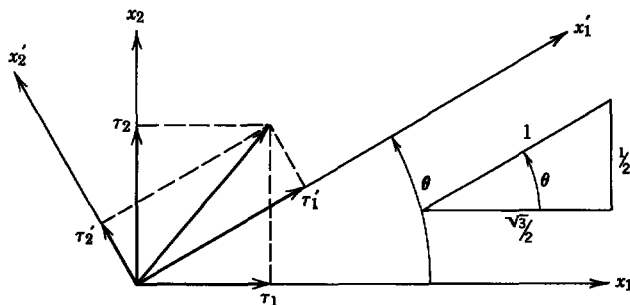


Fig. 8.2.9 Geometrical relationship between the primed and unprimed coordinate systems for Example 8.2.3.

Then (8.2.10) gives

$$\begin{aligned}\tau'_1 &= \frac{\sqrt{3}}{2} \tau_1 + \frac{1}{2} \tau_2, \\ \tau'_2 &= -\frac{1}{2} \tau_1 + \frac{\sqrt{3}}{2} \tau_2.\end{aligned}$$

From this example (8.2.10) should be recognized as a simple statement of vector addition. Again, we could have obtained the result from Fig. 8.2.9 without the formalism of (8.2.10).

Equation 8.2.10 forms the basis for determining how to transform components of the stress tensor from one coordinate system to another.

According to (8.2.2), the components of τ are

$$\tau_r = T_{rs} n_s. \quad (8.2.11)$$

Now we consider a particular cartesian coordinate system (x'_1, x'_2, x'_3) established in such a way that one of the axes (say x'_1) has the same direction as \mathbf{n} . A pictorial representation of the two coordinate systems is given in Fig. 8.2.10. The components (n_1, n_2, n_3) of the normal vector are the cosines of the angles between the (x_1, x_2, x_3) axes and the normal direction, which is also the direction of x'_1 . Hence from the definition following (8.2.10) $(n_1, n_2, n_3) = (a_{11}, a_{12}, a_{13})$ and (8.2.11) can also be written as

$$\tau_r = T_{rs} a_{1s}. \quad (8.2.12)$$

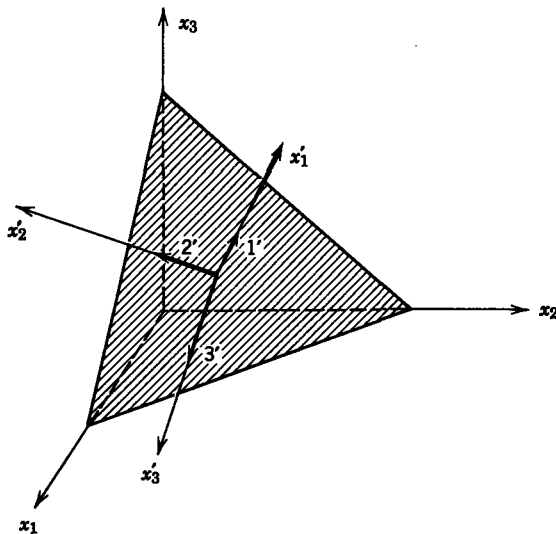


Fig. 8.2.10 Relationship between the primed and unprimed coordinates showing the x'_1 -axis coincident with the normal vector.

Because x'_1 is perpendicular to the surface, x'_2 and x'_3 lie in the surface. We see that $(\tau'_1, \tau'_2, \tau'_3)$ are just the components of the stress acting on a surface with a normal in the direction of the x'_1 -axis, that is,

$$\tau'_p = T'_{p1}, \quad (8.2.13)$$

but we can also use (8.2.10) to express τ'_p as

$$\tau'_p = a_{pr} \tau_r, \quad (8.2.14)$$

which by (8.2.12) gives a relation for τ'_p in terms of the stress components in the unprimed coordinates.

$$\tau'_p = a_{pr}(T_{rs} a_{1s}) \quad (8.2.15)$$

Then from 8.2.13

$$T'_{p1} = a_{pr} a_{1s} T_{rs}. \quad (8.2.16)$$

Finally, the designation of the normal direction by the x'_1 -axis is arbitrary, and the preceding arguments could be repeated with 1 replaced by 2 or 1 replaced by 3. Hence we have shown that

$$T'_{pq} = a_{pr} a_{qs} T_{rs}. \quad (8.2.17)$$

This relation provides the rule for finding the components of the stress in the primed coordinates, given the components in the unprimed coordinates. It serves the same purpose in dealing with tensors that (8.2.10) serves in dealing with vectors. In much of the literature a vector or *first-order tensor* is defined as an array of three numbers that transforms according to an equation in the form of (8.2.10). In the same way, a *second-order tensor* is defined as an array of numbers that transforms according to an equation in the form of (8.2.17).*

Example 8.2.4. Suppose we wish to find the stress component T'_{11} expressed in the primed coordinate system of Fig. 8.2.9 in terms of the components T_{mn} in the unprimed system. Then (8.2.17) gives

$$T'_{11} = a_{11} a_{11} T_{11} + a_{11} a_{12} T_{12} + a_{11} a_{13} T_{13} + a_{12} a_{11} T_{21} + a_{12} a_{12} T_{22} + a_{12} a_{13} T_{23} \\ + a_{13} a_{11} T_{31} + a_{13} a_{12} T_{32} + a_{13} a_{13} T_{33}$$

or, in particular, from the values of a_{mn} given in Example 8.2.3,

$$T'_{11} = \frac{\sqrt{3}}{2} \frac{\sqrt{3}}{2} T_{11} + \frac{\sqrt{3}}{2} \left(\frac{1}{2}\right) T_{12} + \left(\frac{1}{2}\right) \frac{\sqrt{3}}{2} T_{21} + \left(\frac{1}{2}\right) \left(\frac{1}{2}\right) T_{22}.$$

A second example provides a useful result.

Example 8.2.5. Given the stress components T_{mn} expressed in a cylindrical coordinate system with the coordinates r , θ , and z , what are the components of the stress tensor

* See, for example, Spain, *op. cit.*, pp. 6-9.

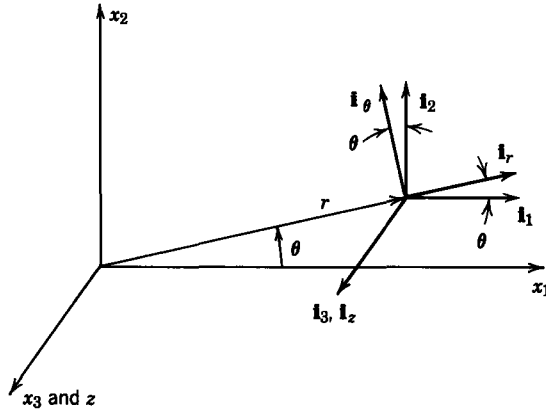


Fig. 8.2.11 Geometrical relationship between cartesian and cylindrical coordinate systems.

expressed in a cartesian coordinate system with axes x_1 , x_2 , and x_3 , as illustrated in Fig. 8.2.11.*

The relationship between the unit vectors is shown in Fig. 8.2.11. The cartesian coordinate system plays the role of the "primed" system. We can see by inspection that the cosine of the angle between

$$\begin{aligned} \mathbf{i}_1 \text{ and } \mathbf{i}_r &= \cos \theta, \\ \mathbf{i}_1 \text{ and } \mathbf{i}_\theta &= \cos(\theta + 90^\circ) = -\sin \theta, \\ \mathbf{i}_2 \text{ and } \mathbf{i}_r &= \cos(90^\circ - \theta) = \sin \theta, \\ \mathbf{i}_2 \text{ and } \mathbf{i}_\theta &= \cos \theta, \\ \mathbf{i}_3 \text{ and } \mathbf{i}_z &= 1, \\ \text{all others} &= 0. \end{aligned}$$

Therefore we can write

$$(a_{mn}) = \begin{bmatrix} \cos \theta & -\sin \theta & 0 \\ \sin \theta & \cos \theta & 0 \\ 0 & 0 & 1 \end{bmatrix}.$$

The components of the stress now follow directly by making use of (8.2.17):

$$\begin{aligned} T_{11} &= T_{rr} \cos^2 \theta - 2T_{r\theta} \sin \theta \cos \theta + T_{\theta\theta} \sin^2 \theta, \\ T_{12} &= T_{rr} \sin \theta \cos \theta + T_{r\theta}(\cos^2 \theta - \sin^2 \theta) - T_{\theta\theta} \sin \theta \cos \theta, \\ T_{13} &= T_{rz} \cos \theta - T_{z\theta} \sin \theta, \\ T_{22} &= T_{rr} \sin^2 \theta + 2T_{r\theta} \sin \theta \cos \theta + T_{\theta\theta} \cos^2 \theta, \\ T_{23} &= T_{rz} \sin \theta + T_{z\theta} \cos \theta, \\ T_{33} &= T_{zz}. \end{aligned}$$

* When the components of a stress tensor are expressed in polar coordinates or any other curvilinear coordinates, care must be exercised in taking space derivatives. This is analogous to taking derivatives of vectors in curvilinear coordinates.

Before we leave the subject of tensor transformations we must make a final important observation. The direction cosines a_{mn} which transformed the vector in (8.2.10) were defined with the understanding that the components of τ were expressed in an *orthogonal* coordinate system. There were therefore implicit trigonometric relations between these direction cosines. If we state them formally, it is possible to extend the concept of a tensor to situations in which the transformations (8.2.10) and (8.2.17) are not geometrical in origin.* These relations are easily established by means of (8.2.10).

Equation 8.2.10 is the transformation of a vector τ from an unprimed to a primed coordinate system. There is, in general, nothing to distinguish the two coordinate systems. We could just as well define a transformation from the primed to the unprimed coordinates by

$$\tau_s = b_{sp}\tau'_p, \quad (8.2.18)$$

where b_{sp} is the cosine of the angle between the x_s -axis and the x'_p -axis. But b_{sp} , from the definition following (8.2.10), is then also

$$b_{sp} \equiv a_{ps}; \quad (8.2.19)$$

that is, the transformation which reverses the transformation (8.2.10) is

$$\tau_s = a_{ps}\tau'_p. \quad (8.2.20)$$

Now we can establish an important property of the direction cosines a_{ps} by transforming the vector τ to an arbitrary primed coordinate system and then transforming the components τ'_m back to the unprimed system in which they must be the same as those we started with. Equation 8.2.10 provides the first transformation, whereas (8.2.20) provides the second; that is, we substitute (8.2.10) into (8.2.20) to obtain

$$\tau_s = a_{ps}a_{pr}\tau_r. \quad (8.2.21)$$

Remember that we are required to sum on both p and r ; for example, consider the case in which $s = 1$:

$$\begin{aligned} \tau_1 &= (a_{11}a_{11} + a_{21}a_{21} + a_{31}a_{31})\tau_1 \\ &\quad + (a_{11}a_{12} + a_{21}a_{22} + a_{31}a_{32})\tau_2 \\ &\quad + (a_{11}a_{13} + a_{21}a_{23} + a_{31}a_{33})\tau_3. \end{aligned} \quad (8.2.22)$$

This relation must hold in general. We have not specified either a_{ps} or τ_m . Hence the second two bracketed quantities must vanish and the first must be unity. We can express this fact much more concisely by stating that in general

$$a_{ps}a_{pr} = \delta_{sr} \quad (8.2.23)$$

* J. C. Slater and N. H. Frank, *Mechanics*, 1st ed., McGraw-Hill, New York, 1947, Appendix V.

[this is the Kronecker delta as defined in (8.1.7)], for then (8.2.21) is reduced to the identity $\tau_s = \tau_s$.

8.3 FORCES IN ELECTRIC FIELD SYSTEMS

We now consider the forces that develop in electric field systems. The Lorentz force (1.1.28) gives the force on a charge q in an electric field \mathbf{E} as

$$\mathbf{f} = q\mathbf{E}. \quad (8.3.1)$$

The force density \mathbf{F} can be found by averaging (8.3.1) over a small volume:

$$\mathbf{F} = \lim_{\delta V \rightarrow 0} \frac{\sum_i \mathbf{f}_i}{\delta V} = \lim_{\delta V \rightarrow 0} \frac{\sum_i q_i \mathbf{E}_i}{\delta V}, \quad (8.3.2)$$

where q_i represents all the charges in δV , \mathbf{E}_i is the electric field acting on the i th charge, and \mathbf{f}_i is the force on the i th charge. It is found experimentally that free charges are almost never dense enough to make the microscopic field \mathbf{E}_i seen by a charge appreciably different from the average (macroscopic) field \mathbf{E} . Consequently, because all charges in the volume δV experience the same electric field \mathbf{E} , we use the definition $\rho_f = \lim_{\delta V \rightarrow 0} \sum_i q_i / \delta V$ to write (8.3.2) as

$$\mathbf{F} = \rho_f \mathbf{E}. \quad (8.3.3)$$

Once again, remember that this is the force density on the charges and (as for the magnetic force density (8.1.3)) can be construed as the material force density only if each of the charges transmits its force to the medium.

The constituent relation is

$$\mathbf{D} = \epsilon \mathbf{E}. \quad (8.3.4)$$

For this development we assume that ϵ is a constant, but this restriction is relaxed in Section 8.5*. In this case we write (8.3.3) in terms of the electric field intensity by using Gauss's law (1.1.12)†:

$$\mathbf{F} = (\nabla \cdot \epsilon \mathbf{E}) \mathbf{E}. \quad (8.3.5)$$

We now express (8.3.5) as the space derivative of a stress tensor by recognizing that for electric field systems $\nabla \times \mathbf{E} = 0$. Hence (8.3.5) can be written as

$$\mathbf{F} = (\nabla \cdot \epsilon \mathbf{E}) \mathbf{E} + (\nabla \times \mathbf{E}) \times \epsilon \mathbf{E}. \quad (8.3.6)$$

* Arguments are given in Section 8.5 to show that this is the force density on free charges embedded in a material with a constant permittivity. For now we *assume* that the only effect of a uniform linear dielectric on the free charge force density is to replace $\epsilon_0 \rightarrow \epsilon$.

† Table 1.2, Appendix E.

We now use a vector identity on the last term to obtain*

$$\mathbf{F} = (\nabla \cdot \epsilon \mathbf{E})\mathbf{E} + \epsilon(\mathbf{E} \cdot \nabla)\mathbf{E} - \frac{1}{2}\epsilon \nabla(\mathbf{E} \cdot \mathbf{E}). \quad (8.3.7)$$

Using the index notation introduced in Section 8.1, we combine the first two terms and write the m th component of this equation as

$$F_m = \frac{\partial}{\partial x_n} (\epsilon E_m E_n) - \frac{\epsilon}{2} \frac{\partial}{\partial x_m} (E_k E_k). \quad (8.3.8)$$

The Kronecker delta is now used to write

$$\frac{\partial}{\partial x_m} = \delta_{mn} \frac{\partial}{\partial x_n}$$

and to put (8.3.8) in the desired form,

$$F_m = \frac{\partial T_{mn}}{\partial x_n}, \quad (8.3.9)$$

where the Maxwell stress tensor T_{mn} for electric field systems is given by

$$T_{mn} = \epsilon E_m E_n - \frac{\epsilon}{2} \delta_{mn} E_k E_k. \quad (8.3.10)$$

Note that this expression has the same form as (8.1.11) if we replace ϵ with μ and \mathbf{E} with \mathbf{H} . The stress tensor here has all the general properties discussed in Section 8.2.2.

Both electric and magnetic forces are usually included in the Maxwell stress tensor†; however, we have not combined these forces because they usually do not occur in appreciable amounts in the same system. We use the term Maxwell stress tensor to denote that function from which electromagnetic force densities can be obtained by differentiation, as in (8.3.9). In different systems the Maxwell stress tensor represents different functions.

Example 8.3.1. To illustrate the use of the different expressions for force density and total force consider the electrostatic problem defined in Fig. 8.3.1.

The system consists of two regions of vacuum separated by a nonpolarizable ($\epsilon = \epsilon_0$) slab of thickness δ in the x_1 -direction and of infinite extent in the other two directions. The slab contains a volume charge density

$$\rho_f = \rho_f^0 \left(1 - \frac{x_1}{\delta}\right) \quad (a)$$

for $0 < x_1 < \delta$. The electric field in the region

$$x_1 < 0$$

is constrained to be

$$\mathbf{E} = \mathbf{i}_1 E_1^0 + \mathbf{i}_2 E_2^0 + \mathbf{i}_3 E_3^0. \quad (b)$$

* $(\nabla \times \mathbf{A}) \times \mathbf{A} = (\mathbf{A} \cdot \nabla)\mathbf{A} - \frac{1}{2}\nabla(\mathbf{A} \cdot \mathbf{A})$.

† J. A. Stratton, *Electromagnetic Theory*, McGraw-Hill, New York, 1941, pp. 97–103.

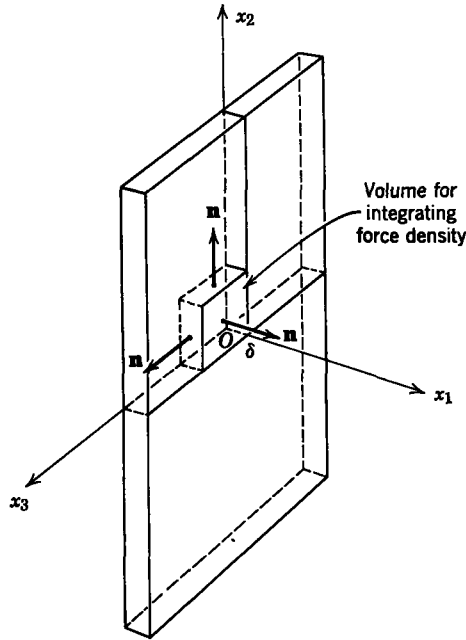


Fig. 8.3.1 Slab of material supporting a volume charge density.

After finding the electric field in the remainder of the system, we wish to compute in two ways the total force per unit area on the slab, first by doing a volume integration of the force density and then by doing a surface integration of the stress tensor.

To find the fields in the system we use the differential equations

$$\nabla \times \mathbf{E} = 0, \quad (\text{c})$$

$$\nabla \cdot \epsilon_0 \mathbf{E} = \rho_f. \quad (\text{d})$$

Because the slab has infinite extent in the x_2 - x_3 plane, we can (for purposes of illustration) assume no variation of \mathbf{E} in the x_2 - and x_3 -directions.

$$\frac{\partial}{\partial x_2} = \frac{\partial}{\partial x_3} = 0.$$

Then (c) shows that everywhere

$$E_2 = E_2^0,$$

$$E_3 = E_3^0.$$

Equations a and d give

$$\frac{\partial E_1}{\partial x_1} = \frac{\rho_f^0}{\epsilon_0} \left(1 - \frac{x_1}{\delta} \right).$$

Integration of this expression yields

$$E_1 = \frac{\rho_f^0}{\epsilon_0} \left(x_1 - \frac{x_1^2}{2\delta} \right) + C_1.$$

We use the boundary condition on the normal component of \mathbf{E} at $x_1 = 0$ to evaluate the constant of integration.

$$C_1 = E_1^0.$$

Thus

$$E_1 = E_1^0 + \frac{\rho_f^0}{\epsilon_0} \left(x_1 - \frac{x_1^2}{2\delta} \right), \quad \text{for } 0 < x_1 < \delta,$$

and use of the boundary condition on the normal component of \mathbf{E} at $x_1 = \delta$ yields

$$E_1 = E_1^0 + \frac{\rho_f^0 \delta}{2\epsilon_0}, \quad \text{for } x_1 > \delta.$$

The only region in which free charge exists is for $0 < x_1 < \delta$, where we can write

$$\mathbf{F} = \rho_f \mathbf{E} = \rho_f^0 \left(1 - \frac{x_1}{\delta} \right) \left\{ \mathbf{i}_1 \left[E_1^0 + \frac{\rho_f^0}{\epsilon_0} \left(x_1 - \frac{x_1^2}{2\delta} \right) \right] + \mathbf{i}_2 E_2^0 + \mathbf{i}_3 E_3^0 \right\}.$$

Taking a volume with unit dimension in the x_2 - and x_3 -directions, we write for the total force per unit area in an x_2 - x_3 plane:

$$\mathbf{f} = \int_0^\delta \mathbf{F} dx_1.$$

Performance of the indicated integration yields

$$\mathbf{f} = \mathbf{i}_1 \rho_f^0 \left(\frac{E_1^0 \delta}{2} + \frac{\rho_f^0 \delta^2}{8\epsilon_0} \right) + \mathbf{i}_2 \frac{\rho_f^0 E_2^0 \delta}{2} + \mathbf{i}_3 \frac{\rho_f^0 E_3^0 \delta}{2}.$$

We can obtain this same result by using the stress tensor, which we need only along the surface that encloses the slab.

The surface selected for integrating (8.1.17) is the one shown in Fig. 8.3.1 which has unit area in the x_2 - x_3 plane and thickness δ in the x_1 -direction. Because the fields are independent of x_2 and x_3 , the contributions from the surfaces perpendicular to x_2 and x_3 add to zero. We need only consider the surfaces of unit area perpendicular to x_1 . Thus we have

$$\begin{aligned} f_1 &= T_{11}(\delta) - T_{11}(0), \\ f_2 &= T_{21}(\delta) - T_{21}(0), \\ f_3 &= T_{31}(\delta) - T_{31}(0). \end{aligned}$$

Using the components T_{mn} defined with the fields derived earlier, we have [remember that $E_2(0) = E_2(\delta)$ and $E_3(0) = E_3(\delta)$]

$$\begin{aligned} f_1 &= \frac{\epsilon_0}{2} [E_1^2(\delta) - E_1^2(0)] = \frac{\epsilon_0}{2} \left[\frac{E_1^0 \rho_f^0 \delta}{\epsilon_0} + \frac{(\rho_f^0)^2 \delta^2}{4\epsilon_0^2} \right], \\ f_2 &= \epsilon_0 [E_1(\delta) E_2(\delta) - E_1(0) E_2(0)] = \epsilon_0 E_2^0 \frac{\rho_f^0 \delta}{2\epsilon_0}, \\ f_3 &= \epsilon_0 [E_1(\delta) E_3(\delta) - E_1(0) E_3(0)] = \epsilon_0 E_3^0 \frac{\rho_f^0 \delta}{2\epsilon_0}. \end{aligned}$$

Thus the result is the same as that obtained by the volume integration. Note that in the surface integration we needed only the fields outside the space occupied by the charge. The fields, of course, are affected by the presence of the charge.

The most significant advantages of a formulation that uses the stress tensor arise because forces on the material within a volume can be determined without knowing the details of the volume force distribution (i.e., the distribution of currents or charges). Moreover, in many problems we are at liberty to choose the surface of integration and this can further simplify the computation. The next example illustrates how the choice of the surface of integration that is most convenient (or makes the integration possible) depends on symmetry and boundary conditions and further shows how the stress tensor can be used to obtain a total force in a situation in which a more direct approach would be difficult if not impossible.

Example 8.3.2. A pair of perfectly conducting plates at the potential difference V_0 is shown in Fig. 8.3.2. One of these plates is flat and the other has a step at the middle, as shown. Both plates extend far enough in the x_3 -direction that we can consider the problem as two-dimensional ($\partial/\partial x_3 = 0$). We wish to find the force in the x_1 -direction on a section of length l (in the x_3 -direction) of the bottom plate, including the effect of the fringing fields. To do this it is assumed that both $c \gg a$ and $d \gg b$, so that the regions of nonuniform electric field near the ends and near the step are separated by regions of essentially uniform electric field intensity.

To carry out the surface integration [the x_1 -component of (8.1.17)]

$$f_1 = \oint_S T_{1n} n_n da \tag{a}$$

we choose the surface shown in Fig. 8.3.2. Surfaces (1), (3) and (5) have the normal vector $\mathbf{n} = \mathbf{i}_2$, whereas surfaces (2) and (4) have the normal $\mathbf{n} = \mp \mathbf{i}_1$, respectively. Hence we can write (a) as

$$f_1 = \int_{(1)(5)} T_{12} da + \int_{(3)} T_{12} da - \int_{(2)} T_{11} da + \int_{(4)} T_{11} da + \int_{(6)} T_{1n} n_n da. \tag{b}$$

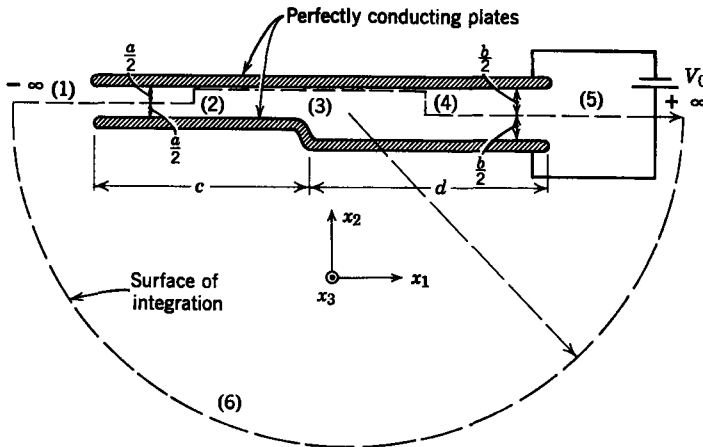


Fig. 8.3.2 Conducting plates at the potential difference V_0 .

The contributions from the surfaces with normals $\pm i_3$ have been ignored, for they cancel. Because the surface of integration (6) is far from the plates (at infinity), we expect the contribution of the last integral to be zero. We can argue that this is the case by making (6) the surface of a cylinder of radius R , with the plates at the origin. Far from the plates the electric field distribution is essentially that of a dipole.* Hence $|E| \approx 1/R^2$ and $|T_{1n}| \approx 1/R^4$. It follows that although the surface area of integration is proportional to R^2 the integral (6) decreases as $1/R^2$ and vanishes as $R \rightarrow \infty$. From (8.3.10)

$$T_{12} = \epsilon E_1 E_2. \quad (c)$$

Surfaces (1) and (5) are half way between the plates where by symmetry $E_1 = 0$. Hence the first term in (b) is also zero. Moreover, because $E_1 = 0$ along the perfectly conducting plate where surface (3) is located, the second integral vanishes also.

From (8.3.10)

$$T_{11} = \frac{1}{2} \epsilon (E_1^2 - E_2^2 - E_3^2). \quad (d)$$

Surfaces (2) and (4) are in regions of uniform electric field intensity. Hence

$$\mathbf{E} = \frac{V_0}{a} \mathbf{i}_2; \quad \text{on surface (2),} \quad (e)$$

$$\mathbf{E} = \frac{V_0}{b} \mathbf{i}_2; \quad \text{on surface (4).}$$

Because these surfaces make the only contribution to the surface integral, (b), (d), and (e) become

$$f_1 = \int_{(2)} \frac{1}{2} \epsilon \left(\frac{V_0}{a} \right)^2 da - \int_{(4)} \frac{1}{2} \epsilon \left(\frac{V_0}{b} \right)^2 da. \quad (f)$$

The stresses are constant over the surfaces of integration and therefore the integral is performed by multiplication of the appropriate areas:

$$f_1 = \frac{1}{2} \epsilon \left(\frac{V_0}{a} \right)^2 \left(\frac{la}{2} \right) - \frac{1}{2} \epsilon \left(\frac{V_0}{b} \right)^2 \left(\frac{lb}{2} \right) \quad (g)$$

or

$$f_1 = \frac{\epsilon V_0^2 l}{4} \left(\frac{1}{a} - \frac{1}{b} \right). \quad (h)$$

The electric force on the lower plate (for $a < b$, as shown in Fig. 8.3.2) tends to pull in the x_1 -direction. If we had closed the surface above the top plate, the signs of the normal vectors involved would have been reversed to give an equal and opposite force on the top plate.

8.4 THE SURFACE FORCE DENSITY

Magnetic and electric fields in many situations are found by modeling the current or charge distributions by surface currents or surface charges. In these systems surface forces of electrical origin must be considered; for

* R. M. Fano, L. J. Chu, and R. B. Adler, *Electromagnetic Fields, Energy, and Forces*, Wiley, New York, 1960, p. 92.

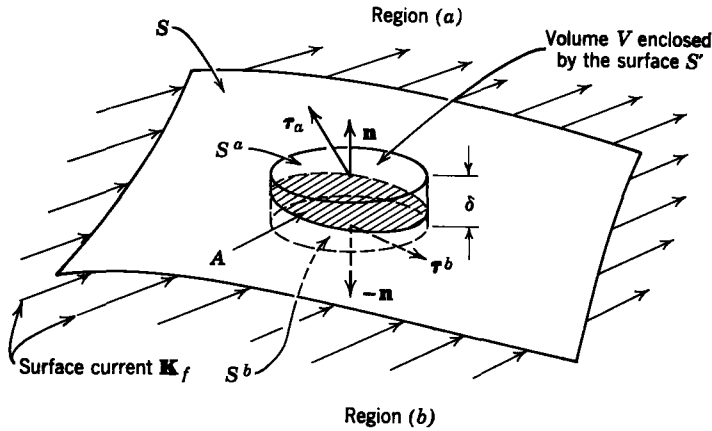


Fig. 8.4.1 Small thin volume V which encloses a section A of a surface S supporting the surface current \mathbf{K}_f .

example, if the surface S supports a surface current density \mathbf{K}_f , as shown in Fig. 8.4.1, and is immersed in a magnetic field \mathbf{H} , we expect a surface force similar in form to (8.1.3) with \mathbf{K}_f playing the role of \mathbf{J}_f .

The surface force density \mathbf{T} (newtons per square meter) is defined in terms of the force \mathbf{f} on the material within the small thin volume shown in Fig. 8.4.1. It is the force per unit area A on the surface S intersected by the volume V in the limit in which first the thickness δ and then the area A become small. The stress tensor provides a convenient means of evaluating \mathbf{T} , for the total force can be written as a surface integral (8.1.17). In the limit in which $\delta \rightarrow 0$ the contribution to this integral along the sides (of height δ) of the volume V becomes vanishingly small and the only contributions come from the tractions acting on the surfaces S^a and S^b . In the limit $S^a \rightarrow S^b \rightarrow A$ we have

$$T_m = \tau_m^a + \tau_m^b, \tag{8.4.1}$$

where $\boldsymbol{\tau}^a$ and $\boldsymbol{\tau}^b$ are the tractions acting on the surfaces S^a and S^b , respectively.

If we define \mathbf{n} as the unit vector *normal to the surface S* and directed from region (b) to region (a), the surface tractions can be evaluated by using (8.2.8):

$$T_m = (T_{mn}^a - T_{mn}^b)\mathbf{n}_n. \tag{8.4.2}$$

Remember that in (8.2.8) \mathbf{n} is the unit vector normal to a surface that *encloses* the volume of integration in Fig. 8.4.1. Over the top surface the normal vector is \mathbf{n} , but over the bottom surface it is $-\mathbf{n}$. Hence the minus sign in (8.4.2).

The Maxwell stresses T_{mn} are functions of either the magnetic or electric fields. Therefore (8.4.2) is a convenient expression for the surface force density on either a surface current or a surface charge.

8.4.1 Magnetic Surface Forces

As already pointed out, the magnetic surface force should be equivalent to the cross product of the surface current with a magnetic field. In this cross product, however, do we use the value of \mathbf{H} from region (a) or from region (b)? In fact the average value of \mathbf{H} should be used and the force per unit area \mathbf{T} acting on a surface current \mathbf{K}_f is

$$\mathbf{T} = \mu \mathbf{K}_f \times \frac{(\mathbf{H}^a + \mathbf{H}^b)}{2}. \quad (8.4.3)$$

We can prove that this relation is, in fact, valid by showing that it is equivalent to (8.4.2).

The surface current density from (6.2.14)* is

$$\mathbf{K}_f = \mathbf{n} \times (\mathbf{H}^a - \mathbf{H}^b) \quad (8.4.4)$$

and (8.4.3) becomes

$$\mathbf{T} = \mu [\mathbf{n} \times (\mathbf{H}^a - \mathbf{H}^b)] \times \frac{(\mathbf{H}^a + \mathbf{H}^b)}{2}. \quad (8.4.5)$$

We now use a vector identity† to rewrite this expression in component form as

$$T_m = \mu (H_m^a - H_m^b) \mathbf{n} \cdot \frac{(\mathbf{H}^a + \mathbf{H}^b)}{2} - \frac{\mu n_m}{2} (\mathbf{H}^a \cdot \mathbf{H}^a - \mathbf{H}^b \cdot \mathbf{H}^b). \quad (8.4.6)$$

The first term of this equation can be simplified by using (6.2.7)* $\mathbf{n} \cdot \mu \mathbf{H}^a = \mathbf{n} \cdot \mu \mathbf{H}^b$, whereas we replace n_m with $n_n \delta_{mn}$ in the second term.

$$T_m = (\mu H_m^a H_n^a - \frac{1}{2} \delta_{mn} \mu H_k^a H_k^a) n_n - (\mu H_m^b H_n^b - \frac{1}{2} \delta_{mn} \mu H_k^b H_k^b) n_n. \quad (8.4.7)$$

Our expression is now identical with (8.4.2), if we note that the magnetic stress is given by (8.1.11). We can alternatively write the surface force in terms of the fields alone (stresses) by using (8.4.2) or in terms of surface currents and an average magnetic field (8.4.3).

8.4.2 Electric Surface Forces

The surface force in an electric field system can be expressed as the product of the surface charge density σ_f and the average electric field intensity.

$$\mathbf{T} = \sigma_f \frac{(\mathbf{E}^a + \mathbf{E}^b)}{2}. \quad (8.4.8)$$

* Table 6.1, Appendix E.

† $(\mathbf{A} \times \mathbf{B}) \times \mathbf{C} = \mathbf{B}(\mathbf{A} \cdot \mathbf{C}) - \mathbf{A}(\mathbf{C} \cdot \mathbf{B})$.

8.1 Electromagnetic Force Densities, Stress Tensors, and Surface Force Densities for Quasi-Static Magnetic and Electric Field Systems*

| Description | Force Density \mathbf{F} | Stress Tensor T_{mn} $F_m = \frac{\partial T_{mn}}{\partial x_n}$ (8.1.10) | Surface Force Density $T_m = [T_{mn}]n_n$ |
|-----------------------------------------------------------------------------------------------------------------------------------|----------------------------------------------------------------------------------------------------------------------------------------------------------------------------------------------------------------|-------------------------------------------------------------------------------------------------------------------------------------------------------|----------------------------------------------------------------------------------------------------------------------|
| Force on media carrying free current density \mathbf{J}_f , μ constant | $\mathbf{J}_f \times \mathbf{B}$ (8.1.3) | $T_{mn} = \mu H_m H_n - \delta_{mn} \frac{1}{2} \mu H_k H_k$ (8.1.11) | $\mathbf{T} = \mathbf{K}_f \times \mathbf{l}$ $\mathbf{K}_f = \mathbf{n} \times [\mathbf{J}]$ (8.4.3) |
| Force on media supporting free charge density ρ_f , ϵ constant | $\rho_f \mathbf{E}$ (8.3.3) | $T_{mn} = \epsilon E_m E_n - \delta_{mn} \frac{1}{2} \epsilon E_k E_k$ (8.3.10) | $\mathbf{T} = \sigma_f \langle \mathbf{E} \rangle$ $\sigma_f = \mathbf{n} \cdot [\epsilon \mathbf{E}]$ (8.4.8) |
| Force on free current plus magnetization force in which $\mathbf{B} = \mu \mathbf{H}$ both before and after media are deformed | $\mathbf{J}_f \times \mathbf{B} - \frac{1}{2} \mathbf{H} \cdot \mathbf{H} \nabla \mu$ $+ \frac{1}{2} \nabla \left(\mathbf{H} \cdot \mathbf{H} \rho \frac{\partial \mu}{\partial \rho} \right)$ (8.5.38) | $T_{mn} = \mu H_m H_n$ $- \frac{1}{2} \delta_{mn} \left(\mu - \rho \frac{\partial \mu}{\partial \rho} \right) H_k H_k$ (8.5.41) | |
| Force on free charge plus polarization force in which $\mathbf{D} = \epsilon \mathbf{E}$ both before and after media are deformed | $\rho_f \mathbf{E} - \frac{1}{2} \mathbf{E} \cdot \mathbf{E} \nabla \epsilon$ $+ \frac{1}{2} \nabla \left(\mathbf{E} \cdot \mathbf{E} \rho \frac{\partial \epsilon}{\partial \rho} \right)$ (8.5.45) | $T_{mn} = \epsilon E_m E_n$ $- \frac{1}{2} \delta_{mn} \left(\epsilon - \rho \frac{\partial \epsilon}{\partial \rho} \right) E_k E_k$ (8.5.46) | |

$$\equiv \frac{\mathbf{A}^a + \mathbf{A}^b}{2}$$

$$\equiv \mathbf{A}^a - \mathbf{A}^b$$

This result expresses the surface force in a form that is similar to that of the force density (8.3.3). We can show that this equation is correct by demonstrating that it is equivalent to (8.4.2). First, we write (8.4.8) in terms of the electric fields, using Gauss's law to express σ_f (6.2.33)*

$$\mathbf{T} = \epsilon \mathbf{n} \cdot (\mathbf{E}^a - \mathbf{E}^b) \frac{(\mathbf{E}^a + \mathbf{E}^b)}{2}. \quad (8.4.9)$$

By use of a vector identity,† this becomes

$$\mathbf{T} = \epsilon \mathbf{n} (\mathbf{E}^a - \mathbf{E}^b) \cdot \frac{(\mathbf{E}^a + \mathbf{E}^b)}{2} - \epsilon (\mathbf{E}^a - \mathbf{E}^b) \times \left[\mathbf{n} \times \frac{(\mathbf{E}^a + \mathbf{E}^b)}{2} \right]. \quad (8.4.10)$$

This looks like the long way to go about it, but in this form the expression can be factored by using the condition (6.2.31)*, $\mathbf{n} \times \mathbf{E}^a = \mathbf{n} \times \mathbf{E}^b$.

$$\mathbf{T} = \frac{1}{2} \epsilon \mathbf{n} (\mathbf{E}^a \cdot \mathbf{E}^a - \mathbf{E}^b \cdot \mathbf{E}^b) - \epsilon [\mathbf{E}^a \times (\mathbf{n} \times \mathbf{E}^a) - \mathbf{E}^b \times (\mathbf{n} \times \mathbf{E}^b)]. \quad (8.4.11)$$

If we now use this same vector identity again,‡

$$\mathbf{T} = \epsilon [\mathbf{E}^a (\mathbf{n} \cdot \mathbf{E}^a) - \mathbf{E}^b (\mathbf{n} \cdot \mathbf{E}^b)] - \frac{1}{2} \epsilon \mathbf{n} (\mathbf{E}^a \cdot \mathbf{E}^a - \mathbf{E}^b \cdot \mathbf{E}^b), \quad (8.4.12)$$

and this equation is equivalent to the traction in terms of the stress (8.4.2), as can be seen by writing the m th component of \mathbf{T} from (8.4.12)

$$T_m = [(\epsilon E_m^a E_n^a - \frac{1}{2} \delta_{mn} \epsilon E_k^a E_k^a) - (\epsilon E_m^b E_n^b - \frac{1}{2} \delta_{mn} \epsilon E_k^b E_k^b)] n_n \quad (8.4.13)$$

and using (8.3.10). Surface forces and their corresponding stresses are summarized in Table 8.1.

Example 8.4.1. The three plane parallel electrodes of Fig. 8.4.2. provide an example of a force on a surface charge. The plates are assumed to be perfectly conducting, with the outer plates connected together. If we ignore the fringing fields, we have

$$\begin{aligned} \mathbf{E}^a &= \frac{v}{d-x} \mathbf{i}_1, \\ \mathbf{E}^b &= \frac{-v}{x} \mathbf{i}_1, \end{aligned} \quad (a)$$

for the fields between the plates.

We now use several methods to compute the force acting on the middle plate.

First, we use the stress, as given in (8.4.2). The force of electrical origin on the middle plate in the \mathbf{i}_1 -direction is

$$f^e = AT_1 = A(T_{11}^a - T_{11}^b), \quad (b)$$

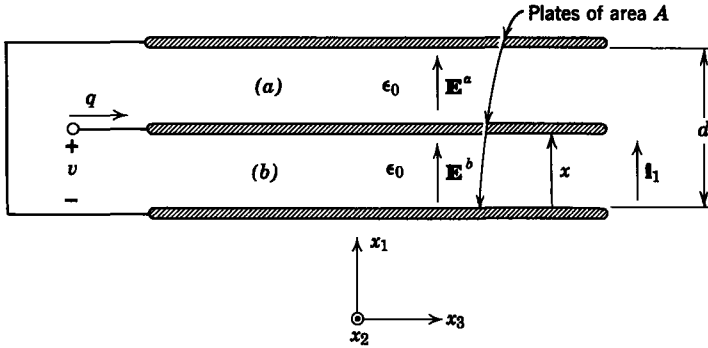
which in view of (a) becomes

$$f^e = \frac{A\epsilon_0}{2} [(E_1^a)^2 - (E_1^b)^2] = \frac{A\epsilon_0}{2} \left[\frac{v^2}{(d-x)^2} - \frac{v^2}{x^2} \right]. \quad (c)$$

* Table 6.1, Appendix E.

† $(\mathbf{C} \cdot \mathbf{A})\mathbf{B} = \mathbf{C}(\mathbf{A} \cdot \mathbf{B}) - \mathbf{A} \times (\mathbf{C} \times \mathbf{B})$.

‡ $\mathbf{A} \times (\mathbf{B} \times \mathbf{A}) = \mathbf{B}(\mathbf{A} \cdot \mathbf{A}) - \mathbf{A}(\mathbf{A} \cdot \mathbf{B})$.

Fig. 8.4.2 Plane-parallel electrodes with Area A .

This same force can be calculated from (8.4.8). We first compute the surface charge density as

$$\sigma_f = \epsilon_0(\mathbf{E}^a - \mathbf{E}^b) \cdot \mathbf{i}_1 = \epsilon_0 \left(\frac{v}{d-x} + \frac{v}{x} \right) \quad (d)$$

and then use (8.4.8)

$$f^e = AT_1 = \frac{A\epsilon_0}{2} \left(\frac{v}{d-x} + \frac{v}{x} \right) \left(\frac{v}{d-x} - \frac{v}{x} \right) = \frac{A\epsilon_0}{2} \left[\frac{v^2}{(d-x)^2} - \frac{v^2}{x^2} \right]. \quad (e)$$

This is the same expression as in (c).

Finally, we use the energy method introduced in Chapter 3* to find the force on the middle plate by noting that the system has one mechanical terminal pair (f^e, x). The capacitance of the electrical terminal pair (v, q) (Fig. 8.4.2) is

$$C = \frac{A\epsilon_0}{x} + \frac{A\epsilon_0}{d-x}. \quad (f)$$

Hence the stored coenergy (which is the same as the energy, since the system is electrically linear) is

$$W'(v, x) = \frac{1}{2} C v^2 = \frac{1}{2} A \epsilon_0 \left(\frac{1}{x} + \frac{1}{d-x} \right) v^2, \quad (g)$$

and we have

$$f^e = \frac{\partial W'}{\partial x} = \frac{1}{2} A \epsilon_0 \left[\frac{1}{(d-x)^2} - \frac{1}{x^2} \right] v^2, \quad (h)$$

where we have used (h) of Table 3.1; of course, this result is also the same as given by (c).

8.5 THE MAGNETIZATION AND POLARIZATION FORCE DENSITIES

So far in this chapter the discussion has been limited to electric and magnetic forces on media that support free charges and free currents. In Chapter 3 examples often involve forces on magnetized or polarized media. In these examples the electric or magnetic fields are excited by means of free charges

* See Table 3.1, Appendix E.

or free currents. However, in many cases, the media subjected to the forces of electric origin do not themselves support free charges or free currents. Such forces, which are found by means of the energy method, must be attributed to the magnetization or polarization of the media.

When an atom or molecule of a substance is subjected to an external electric or magnetic field, the physical microscopic structure is distorted. Although the medium may be electrically neutral on a macroscopic scale, on an atomic scale it is composed in part of charged particles. It is the reaction of these charged particles to the Lorentz force that gives rise to the distortion of the microscopic structure. On a macroscopic level these effects are observed as a magnetization or polarization of the medium. For a wide range of substances it is possible to characterize the magnetization or polarization by simple constitutive laws, such as those introduced in Section 1.1.1; for example, certain isotropic materials can be characterized by a linear relation between the magnetic flux density \mathbf{B} and the field intensity \mathbf{H} , $\mathbf{B} = \mu\mathbf{H}$. Similarly, for many isotropic dielectrics, $\mathbf{D} = \epsilon\mathbf{E}$.

In Chapter 3 we found forces of electrical origin by first establishing the electrical terminal relations for the system, then computing the electrical energy (or coenergy) stored in the system and finally using the energy function and the principle of conservation of energy to find the force of electric origin. In problems involving magnetization or polarization the first step in this procedure is made possible by knowing the appropriate electrical constitutive law.

In this section we wish to derive the force density by using the energy approach introduced in Chapter 3. Hence the derivation begins with the constitutive laws. Because these laws hold only for particular classes of material, the resulting force expressions are also restricted in validity. In particular, we consider media that are isotropic both before and after the magnetic or electric field is applied. Liquids and gases are most clearly in this category, some types of interaction with solids can be so modeled. Attention is given first to magnetization forces. The derivation is then easily revised to account for polarization forces.

8.5.1 Examples with One Degree of Freedom

Two simple examples help to establish the nature of the magnetization force density and show how its derivation relates to the energy method of Chapter 3. Figure 8.5.1 shows a slab of magnetizable material that is free to slide between the pole faces of a magnetic yoke. The force of electric origin tends to make the slab move into the region between the pole faces. This problem involves the rigid body motion of the material. By contrast, a second example (in Fig. 8.5.2) involves a medium that has an interface at ξ

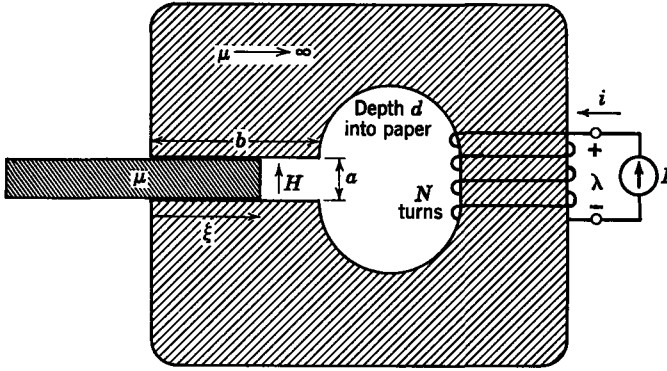


Fig. 8.5.1 A magnetic field intensity H is produced in the gap of the magnetic yoke. As a result, a magnetization force tends to pull the slab of magnetic material into the region between the pole faces.

but is otherwise surrounded by rigid walls. Hence a deflection of the interface must lead to a change in the volume occupied by the material. For the present purposes we assume that the material can deform only in the x_1 -direction.

These two examples have been selected for discussion because they characterize situations in which the magnetization force density is commonly operative. In the first case the force arises because the region occupied by the magnetic field includes a magnetically inhomogeneous material (the air and the magnetic solid). In the example of Fig. 8.5.2 there is an additional contribution to the force, caused by the change in volume of the material. This contribution is called the magnetostriction force.

The force in these examples can be computed by using the energy method of Chapter 3, since in each case there is only one degree of freedom. We first

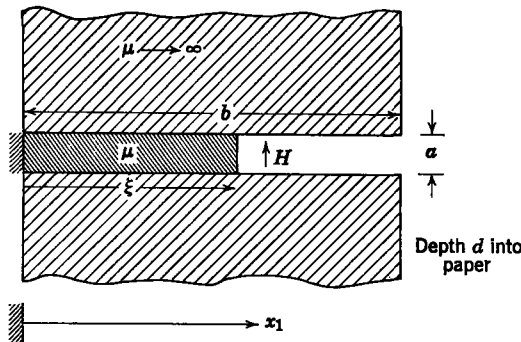


Fig. 8.5.2 The gap in the magnetic yoke of Fig. 8.5.1, with an experiment that demonstrates the magnetostrictive force. The surface at ξ is free to move. Because the material is otherwise surrounded by rigid walls, the motions of the surface must involve a compression or expansion of the medium.

review the energy approach by finding the force in each case associated with the displacement ξ . Then in the next section the same technique is extended to find the continuum force density and we return to these examples to illustrate its significance.

In each of the examples conservation of energy in the electromechanical coupling requires that

$$\lambda \delta i = \delta W' - f \delta \xi, \quad (8.5.1)$$

where W' is the total coenergy, as defined in Chapter 3*, and f is the total force of electrical origin associated with the displacement ξ . The symbol δ is used to indicate incremental changes in the independent variables i and ξ . It has the same significance as d in Chapter 3 and is introduced to avoid confusion with integration symbols such as da and dV , which indicate surface and volume elements.

We can establish the coenergy W' by integrating (8.5.1) in such a way that it is not necessary to know f . First we integrate on ξ (put the system together mechanically) with $i = 0$, but because the force of electrical origin is then zero, this integration makes no contribution. Here, of course, we preclude the possibility that the material is initially magnetized. The remaining integration takes the familiar form

$$W' = \int \lambda \delta i. \quad (8.5.2)$$

If the magnetic material is electrically linear, λ and i are related by the inductance and (8.5.2) yields

$$W' = \frac{1}{2} i^2 L(\xi). \quad (8.5.3)$$

Hence we have established the function W' from information about the electrical system, essentially the $\lambda-i$ relation.

We now hold the independent electrical variable i fixed (say by means of a constant current source). Then the left-hand side of (8.5.1) makes no contribution to the energy balance and this equation becomes,

$$\left(\frac{1}{2} i^2 \frac{\partial L}{\partial \xi} - f \right) \delta \xi = 0. \quad (8.5.4)$$

Here it is important to recognize that in this context ξ is an independent variable. Incremental displacements $\delta \xi$ are arbitrary. It therefore follows from (8.5.4) that the quantity in parentheses is zero.

$$f = \frac{1}{2} i^2 \frac{\partial L}{\partial \xi}. \quad (8.5.5)$$

In the next section we use this procedure to find the continuum force density at each point in the movable medium. Before embarking on that

* See Tables 2.1 and 3.1, Appendix E.

development we consider the specific examples shown in Figs. 8.5.1. and 8.5.2.

In the example of Fig. 8.5.1 the yoke is assumed to be perfectly permeable, hence in the gap $H = Ni/a$. In addition, $B = \mu H$ in the movable slab. It follows that the inductance L is

$$L = \frac{N^2 d}{a} [b\mu_0 + \xi(\mu - \mu_0)]. \quad (8.5.6)$$

Then from (8.5.5) the force is

$$f = (da)\frac{1}{2}H^2(\mu - \mu_0). \quad (8.5.7)$$

In deriving this expression we have assumed that μ in the movable slab is independent of the displacement ξ . This is reasonable as long as the material moves as a rigid body. In the example in Fig. 8.5.2 a displacement of the interface at ξ clearly is accompanied by a change in the density of the material. We expect that there is an associated change in the permeability which can be expressed as

$$\mu = \mu(\rho), \quad (8.5.8)$$

where ρ is the density (mass per unit volume) of the material. It is clear that ρ is in turn a function of ξ , for conservation of mass requires that

$$\rho \xi ad = \text{total mass of material} = \text{constant}. \quad (8.5.9)$$

Differentiation of this expression with respect to ξ gives

$$\frac{\partial \rho}{\partial \xi} = -\frac{\rho}{\xi}, \quad (8.5.10)$$

which shows how changes in density arise from motions of the surface at ξ .

We now use (8.5.6) to find the total force, including the dependence of μ on ξ (through the density ρ).

$$f = da\frac{1}{2}H^2 \left[(\mu - \mu_0) + \xi \frac{\partial \mu}{\partial \rho} \frac{\partial \rho}{\partial \xi} \right]. \quad (8.5.11)$$

From (8.5.10) this force can also be written as

$$f = da\frac{1}{2}H^2 \left[(\mu - \mu_0) - \rho \frac{\partial \mu}{\partial \rho} \right]. \quad (8.5.12)$$

The compressibility of the material gives rise to an additional term, as can be seen by comparing (8.5.7) and (8.5.12). This magnetostrictive force is significant when material deformations that lead to changes in the density are important.

We have considered these special cases to make it clear that the basic thermodynamic techniques introduced in Chapter 3 provide the fundamental means by which magnetization and polarization forces can be derived. The derivations of the next two sections are something new in our development only because the objective is a force density rather than a finite number of total forces. One way to consider the continuum situation is shown schematically in Fig. 8.5.3. A magnet is excited by a current i and a magnetizable material is subjected to the resulting magnetic field. Now, if we divide the material into small volume elements, deformations can be described by simply indicating the displacement ξ^i of each element.

There are three degrees of freedom for each volume element and therefore the i th displacement must be represented by three terminal pairs, which are summarized by vector terminal variables ξ^i and \mathbf{f}^i . Say that the medium has been divided into m regions. Then conservation of energy for the electromechanical coupling requires that

$$i \delta \lambda = \delta W + \sum_{i=1}^m \mathbf{f}^i \cdot \delta \xi^i; \quad (8.5.13)$$

that is, an increment of energy $i \delta \lambda$ introduced through the electrical terminals either increases the magnetic energy stored by the amount δW or does work $\mathbf{f}^i \cdot \delta \xi^i$ on one or more of the elements of volume.

In terms of the coenergy (as discussed in Section 3.1.2b)* this statement of conservation of energy becomes

$$\lambda \delta i = \delta W' - \sum_{i=1}^m \mathbf{f}^i \cdot \delta \xi^i. \quad (8.5.14)$$

Now, if we used a large number of elements m , the force \mathbf{f}^i divided by the volume of the i th element would constitute the force density acting in the neighborhood of the i th element. Hence it should be clear that in principle we can find the force density by using this familiar energy method. Rather than using the summation, we take the limit in which $m \rightarrow \infty$ at the outset and represent the summation by an integration.

One significant point can be made without further mathematical developments. In Section 8.1 we claim (without proof) that the force density $\mathbf{J}_f \times \mathbf{B}$ on free currents remains valid even if the currents are immersed in a material

* See Table 3.1, Appendix E.

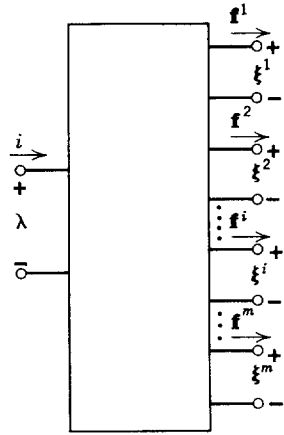


Fig. 8.5.3 Schematic representation of electromechanical coupling in which deformations of a continuum are represented by m vector displacements.

with a uniform and constant μ . We can use the energy method of finding forces to see that this must be true.

Suppose for a moment that we had a system that did not involve magnetization and used the energy method to find the force density $\mathbf{F} = \mathbf{J}_f \times \mathbf{B}$. Now, we do not need to carry out this formalism because we already know the answer. The point is this. Consider the same system, but with a uniform permeability μ . The energy function W' , from which the force density is found, is computed from an electrical terminal relation that in turn is found by using Maxwell's equations. The only change in the laws governing the fields is that $\mu_0 \rightarrow \mu$. Hence the only change in the energy function W' is that $\mu_0 \rightarrow \mu$, and the force density remains the same as in the form without the uniform $\mu: \mathbf{J}_f \times \mathbf{B}$. Of course, \mathbf{B} is computed by using Maxwell's equations with $\mu_0 \rightarrow \mu$.

Note that this conclusion is consistent with the derivation of the Maxwell stress tensor given in Section 8.1. In what follows we concern ourselves with finding the magnetization force on material in which $\mathbf{J}_f = 0$.

8.5.2 The Magnetization Force Density

The force density on magnetizable material can be found by following the same procedure outlined in Section 8.5.1. For this purpose we consider the experiment shown in Fig. 8.5.4. A perfectly permeable magnetic yoke is excited by the current i . Our experiment is carried out in the region between the rigid pole faces, where the magnetic field is concentrated (just as it was in Fig. 8.5.1). In this region a deformable magnetic material has a displacement from the coordinate position \mathbf{r} given by $\delta \boldsymbol{\xi}(\mathbf{r})$.

We define the force per unit volume $\mathbf{F}(\mathbf{r})$ as acting on the material at $\mathbf{r} + \delta \boldsymbol{\xi}$. This makes it possible to write (8.5.14) as

$$\lambda \delta i = \int_V \delta w' dV - \int_V \mathbf{F} \cdot \delta \boldsymbol{\xi} dV. \quad (8.5.15)$$

The function w' is defined as the *coenergy density* and can be integrated over the volume V to find the total coenergy W' . Although the specific geometry of the magnetic circuit is superfluous, it does help to fix attention on a physically reasonable system. For convenience we have included only a single one-turn electrical excitation in the system, with the magnetic circuit arranged to concentrate the magnetic field in the volume V . It is convenient to define this volume V as being enclosed by three surfaces S' , S'' , and S''' , shown in Fig. 8.5.4. The surface S' is bounded by the current path for i and encloses the magnetic circuit to the left. (It covers the pole face to the left like a sock on a foot with the current path i as the garter.) The surface S'' plays a similar role for the remaining section of magnetic circuit to the right (the other foot). Finally, the surface S''' encloses the entire system, with a slit

the potential evaluated on the surface S' , these last two equations are used to write the incremental input of coenergy as

$$\lambda \delta i = - \int_{S'} \mu \delta \phi \nabla \phi \cdot \mathbf{n} da. \quad (8.5.18)$$

The surface S'' shown in Fig. 8.5.4 also has the current path for i as its periphery but is coincident with the remaining part of the magnetic circuit. The integration of (8.5.18) over S'' gives no contribution because ϕ is defined as zero over the surface S'' . A similar integration over S''' makes no contribution, for S''' is greatly removed from the magnetic circuit and $\mathbf{n} \cdot \mathbf{B} = 0$ in the neighborhood of S''' and the terminals. We can just as well use a surface of integration S in (8.5.18) that completely encloses the volume V . It follows that

$$\lambda \delta i = \int_V \nabla \cdot [(\mu \nabla \phi)(\delta \phi)] dV. \quad (8.5.19)$$

Here the surface integral has been converted to a volume integral by using Gauss's theorem. Note that there is a sign change in going from the surface integral to the volume integral. The normal vector \mathbf{n} in Fig. 8.5.4 points into the volume V rather than outward as required in the usual statement of Gauss's theorem.

Because $\nabla \cdot \mathbf{B} = -\nabla \cdot \mu \nabla \phi = 0$, we can use an identity* to convert (8.5.19) to

$$\lambda \delta i = \int_V \frac{1}{2} \mu \delta (\nabla \phi)^2 dV. \quad (8.5.20)$$

It is now possible to write all the terms of (8.5.15) as volume integrals and express conservation of energy as

$$\int_V \frac{1}{2} \mu \delta (\nabla \phi)^2 dV = \int_V \delta w' dV - \int_V \mathbf{F} \cdot \delta \boldsymbol{\xi} dV. \quad (8.5.21)$$

We now put the system together, first mechanically and then electrically to find w' . As in Section 8.5.1, the last term in (8.5.21) makes no contribution to the coenergy stored during this process. We must remember that because the material is deformable the permeability at a given point is a function of deflection (e.g., the permeability at a given point in the gap of the magnetic circuit shown in Fig. 8.5.1 could be μ or μ_0 , depending on the position of the slab); that is, $\mu = \mu(\boldsymbol{\xi})$. Once the system is assembled mechanically, however, μ is constant and the remaining integration of (8.5.21) becomes

$$\int_V \delta [\frac{1}{2} \mu (\nabla \phi)^2] dV = \int_V \delta w' dV. \quad (8.5.22)$$

* $\nabla \cdot \mathbf{A}\psi = \psi \nabla \cdot \mathbf{A} + \mathbf{A} \cdot \nabla \psi$.

Rather than carrying out the integration, it serves our purpose to recognize that if we integrate the quantity

$$\delta w' = \delta \left[\frac{1}{2} \mu (\nabla \phi)^2 \right] \quad (8.5.23)$$

over the volume V , the incremental change in total coenergy will have been computed. This completes the first step in finding the force density \mathbf{F} in that the coenergy has been found from the electrical properties of the material. Note that we have assumed that $\mathbf{B} = \mu \mathbf{H}$ both before and after the material is deformed.

As in the preceding section, the next step uses the coenergy density to determine the force density. This is done by constraining the current i to be a constant so that the left-hand side of (8.5.15), and hence (8.5.21), is zero. From (8.5.16) this means that ϕ is held constant on S' . Changes in coenergy now occur because of changes $\delta \boldsymbol{\xi}$ in the material displacement.

A few manipulations on $\delta w'$ make the remaining terms assume a familiar form. From (8.5.23)

$$\delta w' = \frac{1}{2} (\nabla \phi)^2 \delta \mu + \frac{1}{2} \mu \delta (\nabla \phi)^2. \quad (8.5.24)$$

The integral over the volume of the second term in this equation vanishes, as can be seen by first using an identity to write it as

$$\frac{1}{2} \mu \delta (\nabla \phi)^2 = \mu \nabla \phi \cdot \nabla (\delta \phi) = \nabla \cdot (\delta \phi \mu \nabla \phi) - \delta \phi \nabla \cdot (\mu \nabla \phi). \quad (8.5.25)$$

Because $\nabla \cdot \mathbf{B} = 0$, the last term is zero, whereas the integral over the volume of the remaining term can be transformed by Gauss's theorem to an integral over S , where ϕ is constant, hence $\delta \phi = 0$.

Because the last term in (8.5.24) makes no contribution, the conservation of energy equation (8.5.15) becomes (remember, $\mathbf{H} = -\nabla \phi$)

$$\int_V \left(\frac{1}{2} \mathbf{H} \cdot \mathbf{H} \delta \mu - \mathbf{F} \cdot \delta \boldsymbol{\xi} \right) dV = 0. \quad (8.5.26)$$

This equation is the generalization of (8.5.4). Note that the permeability plays the same role as the inductance in determining the dependence of the coenergy on the displacement of the material. To determine the force density we must relate the permeability μ to the material displacement. (This is analogous to finding the inductance L of (8.5.6) as a function of ξ .)

There are two ways in which the permeability at a point \mathbf{r} can change. Either the material is initially inhomogeneous, in which case a displacement can transport material of different permeability into the region of \mathbf{r} , or the density of the material can change with a resulting change in permeability.

Consider first the effect of inhomogeneities. After the displacement $\delta \boldsymbol{\xi}$, the permeability at \mathbf{r} is that of the material that was at $\mathbf{r} - \delta \boldsymbol{\xi}$ before the displacement. Hence

$$\delta \mu = \lim_{\delta \boldsymbol{\xi} \rightarrow 0} [\mu(\mathbf{r} - \delta \boldsymbol{\xi}) - \mu(\mathbf{r})]. \quad (8.5.27)$$

Taylor's expansion makes it possible to write this as

$$\delta\mu = \lim_{\delta\xi \rightarrow 0} \left[\mu(\mathbf{r}) - \delta\xi_i \frac{\partial\mu}{\partial x_i}(\mathbf{r}) + \cdots - \mu(\mathbf{r}) \right]. \tag{8.5.28}$$

In the limit

$$\delta\mu = -\delta\xi \cdot \nabla\mu. \tag{8.5.29}$$

If this is the only mechanism by which the permeability can change, (8.5.26) becomes

$$\int_V \left(-\frac{1}{2} \mathbf{H} \cdot \mathbf{H} \nabla\mu - \mathbf{F} \right) \cdot \delta\xi \, dV = 0. \tag{8.5.30}$$

It is now crucial to recognize that the displacement $\delta\xi$ is arbitrary, in that ξ is an independent variable in the same sense as in the analogous lumped parameter derivation [see (8.5.4)]. Hence to satisfy (8.5.30) the quantity in parentheses must vanish.

$$\mathbf{F} = -\frac{1}{2} \mathbf{H} \cdot \mathbf{H} \nabla\mu. \tag{8.5.31}$$

This contribution to the magnetization force density results because of inhomogeneities in the magnetic material. An example involving a force of this type, considered in Section 8.5.1 (Fig. 8.5.1), serves to illustrate the significance of (8.5.31).

Example 8.5.1. The slab of magnetic material and adjacent pole faces for the problem of Fig. 8.5.1 is shown in Fig. 8.5.5. Here the distribution of μ in the gap is plotted as a function of x_1 with the transition from μ to μ_0 at the surface (s) expanded over a thickness Δ . The magnetic field intensity H is uniform throughout the gap. The gradient of μ in the x_1 -direction is zero in the bulk of the slab but has the value

$$\nabla\mu = \frac{\mu_0 - \mu}{\Delta} \mathbf{i}_1 \tag{a)}$$

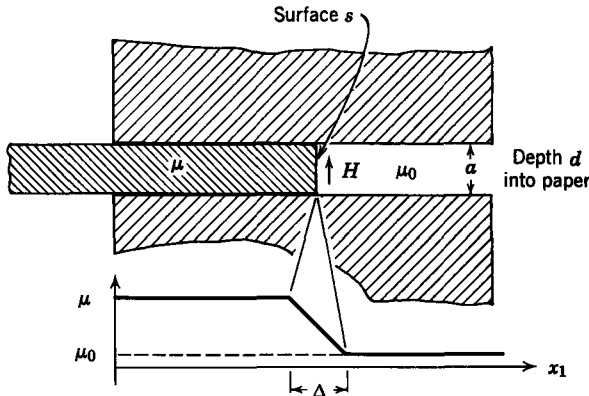


Fig. 8.5.5 Magnetic slab of Fig. 8.5.1 free to slide in the x_1 -direction. Near the surface s the permeability undergoes a rapid change. This region is shown (expanded) to have a thickness Δ over which the permeability varies linearly from μ to μ_0 .

in the expanded region of the surface (s). Hence the force per unit volume acting near the surface s is constant and given by

$$F_1 = -\frac{1}{2}H^2 \frac{(\mu_0 - \mu)}{\Delta} \mathbf{i}_1. \quad (b)$$

The total force is the integral of the force density over the volume of the slab. Because $\nabla\mu$ is constant over the volume Δad and zero elsewhere, this integration reduces to

$$f_1 = -\frac{1}{2}H^2 \frac{(\mu_0 - \mu)}{\Delta} (\Delta ad) \mathbf{i}_1. \quad (c)$$

Note that this result is in agreement with (8.5.7). We may view the force density given by (8.5.31) as the generalization of (8.5.5). The force on the slab does not depend on the thickness Δ , as can be seen from (c). We could have used a distribution of $\mu(x_1)$ other than that shown in Fig. 8.5.5 to arrive at the same answer. Certainly the answer holds in the limit in which $\Delta \rightarrow 0$. This point is easily seen if the force density is represented in terms of a stress tensor, a point to which we return in the next section.

There remains the task of computing the force density that results from changes in the density of the material. As we saw in Section 8.5.1, compression of the material leads to a magnetostriction force. There it was accounted for by including the effect of changes in density on the inductance L . Here it is incorporated as it leads to a change in μ ; that is, in addition to the change in μ given by (8.5.29), there is a change

$$\delta\mu = \frac{\partial\mu}{\partial\rho} \delta\rho. \quad (8.5.32)$$

The decrease in density $-\delta\rho$ is proportional to the density ρ and the increase in the volume occupied by the material $\nabla \cdot \delta\xi$. Hence*

$$-\delta\rho = \rho\nabla \cdot \delta\xi. \quad (8.5.33)$$

Now, if we combine these last two equations, the first term in (8.5.26) can be written as

$$\int_V \frac{1}{2} \mathbf{H} \cdot \mathbf{H} \delta\mu \, dV = \int_V -\frac{1}{2} \mathbf{H} \cdot \mathbf{H} \frac{\partial\mu}{\partial\rho} \rho \nabla \cdot \delta\xi \, dV. \quad (8.5.34)$$

In order to find the force density, we must write the integrand of this expression in the form $(\quad) \cdot \delta\xi$. With this end in mind, we use an identity† to write

* A statement that the decrease in mass within the volume V_e is equal to the mass transported out of the volume through the surface S_e is given by $-\int_{V_e} \delta\rho \, dV = \oint_{S_e} \rho \delta\xi \cdot \mathbf{n} \, da$.

Gauss's theorem converts the surface integral to a volume integral. To first order in $\delta\rho$ and $\delta\xi$, $\nabla \cdot \rho \delta\xi = \rho \nabla \cdot \delta\xi$ and (8.5.33) follows.

† $\psi \nabla \cdot \mathbf{A} = \nabla \cdot \psi \mathbf{A} - \mathbf{A} \cdot \nabla \psi$.

(8.5.34) as

$$\int_V \frac{1}{2} \mathbf{H} \cdot \mathbf{H} \delta\mu \, dV = - \int_V \nabla \cdot \left(\frac{1}{2} \mathbf{H} \cdot \mathbf{H} \frac{\partial\mu}{\partial\rho} \rho \delta\xi \right) dV \\ + \int_V \nabla \left(\frac{1}{2} \mathbf{H} \cdot \mathbf{H} \frac{\partial\mu}{\partial\rho} \rho \right) \cdot \delta\xi \, dV. \quad (8.5.35)$$

The first integral is in a form in which by Gauss's theorem it can be written as an integral over the surface S of the volume V . On the surface S either the fields \mathbf{H} are zero (the surface is outside the field region in Fig. 8.5.4) or $\delta\xi \cdot \mathbf{n}$ is zero (because the surface is adjacent to the rigid pole faces). Hence the first term in (8.5.35) makes no contribution and the last term is in the desired form.

It is now possible to write (8.5.26) with the effects of inhomogeneity and changes in density included. There is a contribution to $\delta\mu$ from (8.5.29) (due to inhomogeneity) and from (8.5.32) which has already been incorporated into (8.5.35):

$$\int_V \left[-\frac{1}{2} \mathbf{H} \cdot \mathbf{H} \nabla\mu + \nabla \left(\frac{1}{2} \mathbf{H} \cdot \mathbf{H} \frac{\partial\mu}{\partial\rho} \rho \right) - \mathbf{F} \right] \cdot \delta\xi \, dV = 0. \quad (8.5.36)$$

As before, we use the arbitrary nature of $\delta\xi$ to conclude that the force density is

$$\mathbf{F} = -\frac{1}{2} \mathbf{H} \cdot \mathbf{H} \nabla\mu + \nabla \left(\frac{1}{2} \mathbf{H} \cdot \mathbf{H} \frac{\partial\mu}{\partial\rho} \rho \right). \quad (8.5.37)$$

Of course, the first term is the same as that given by (8.5.31). The second term is added to account for forces that accompany (or cause) changes in the density of the material and is referred to as the *magnetostriction force density*.

8.5.3 The Stress Tensor

It is often convenient to express the force density in terms of a stress tensor. This is done in this section, with both forces on free currents and magnetization forces included. Thus the appropriate force density is the superposition of (8.1.3) and (8.5.37):

$$\mathbf{F} = \mathbf{J}_f \times \mu \mathbf{H} - \frac{1}{2} \mathbf{H} \cdot \mathbf{H} \nabla\mu + \nabla \left(\frac{1}{2} \mathbf{H} \cdot \mathbf{H} \frac{\partial\mu}{\partial\rho} \rho \right). \quad (8.5.38)$$

The m th component of this equation can be written [using (8.1.8) to express $\mathbf{J}_f \times \mathbf{B}$] as

$$F_m = \mu H_n \frac{\partial H_m}{\partial x_n} - \frac{\mu}{2} \frac{\partial}{\partial x_m} H_k H_k - \frac{1}{2} H_k H_k \frac{\partial\mu}{\partial x_m} + \frac{\partial}{\partial x_m} \left(\frac{1}{2} H_k H_k \frac{\partial\mu}{\partial\rho} \rho \right). \quad (8.5.39)$$

Because $\partial\mu H_n/\partial x_n = 0$, the first term in this equation can be written as $\partial\mu H_n H_m/\partial x_n$. The second and third terms combine. Then, by introducing the Kronecker delta δ_{mn} (8.1.7), (8.5.39) can be written as

$$F_m = \frac{\partial T_{mn}}{\partial x_n}, \quad (8.5.40)$$

where

$$T_{mn} = \mu H_n H_m - \frac{1}{2} \delta_{mn} H_k H_k \left(\mu - \frac{\partial\mu}{\partial\rho} \rho \right). \quad (8.5.41)$$

Note that except for the magnetostriction term the stress tensor takes the same form as it did in Section 8.1, in which only the force on the free current \mathbf{J}_f is considered. This similarity is deceptive unless it is remembered that the magnetic field intensity \mathbf{H} [in (8.5.41)] is not the same with and without the current density \mathbf{J}_f . Moreover, μ in (8.5.41) is a function of position rather than a constant, as it was in (8.1.11).

Example 8.5.2. The problem shown in Fig. 8.5.2 serves as an illustration for the application of the stress tensor. In this example the slab of magnetic material is free to slide in the x_1 -direction but is constrained at $x_1 = 0$ so that the left end of the slab is fixed. The magnetic field intensity \mathbf{H} is uniform throughout the slab and adjacent region of free space. It is therefore apparent from (8.5.38) that the force density in the x_1 -direction is present only at the left and right extremes of the slab in which the permeability μ and magnetostriction constant ρ $\partial\mu/\partial\rho$ undergo rapid variations. Deformations are independent of forces at the left end because it is fixed. At the right end there is a surface force that can be found by using the stress tensor. From (8.4.2) the force per unit area acting on the right end of the slab is

$$T_1 = T_{11}^a - T_{11}^b, \quad (a)$$

where (a) and (b) indicate the regions to the right and left of the surface. From (8.5.41) (a) becomes

$$T_1 = -\frac{1}{2}\mu_0 H^2 + \frac{1}{2} \left(\mu - \frac{\partial\mu}{\partial\rho} \rho \right) H^2. \quad (b)$$

Here we have taken the $\partial\mu/\partial\rho$ as zero in the free-space region (a). The total force on the end of the slab is (b) multiplied by the area ad , and this result agrees with that found in Section 8.5.1 (8.5.12) by using a model with a single degree of freedom.

Force densities, stress tensors, and surface force densities in magnetic field systems are summarized in Table 8.1. Note that the superposition of the free current force density and the magnetization force density leads to the same stress tensor as for the magnetization force density alone.

8.5.4 Polarization Force Density and Stress Tensor

So far we have limited our discussion to forces induced in magnetic materials by magnetic fields. Polarization forces, induced in dielectric materials

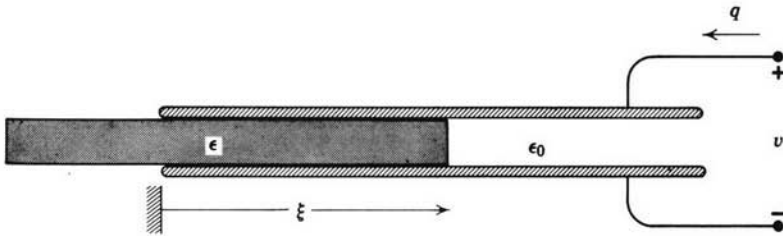


Fig. 8.5.6 A voltage v applied to perfectly conducting electrodes leads to a polarization force that tends to draw the block of dielectric into the region between the plates.

subjected to electric fields, are similar to magnetization forces. The lumped-parameter example shown in Fig. 8.5.6 is analogous to that shown in Fig. 8.5.1. A potential between the perfectly conducting electrodes induces a polarization force in the dielectric material which tends to draw it into the region between the plates. We could find this force by again using the energy methods introduced in Chapter 3* and writing a conservation of energy equation analogous to (8.5.1).

$$q \delta v = \delta W' - f \delta \xi. \quad (8.5.42)$$

Now, W' is the electric coenergy, q is the charge on the upper electrode, and v is the potential of the upper electrode with the potential of the lower electrode defined as zero.

We are interested here in finding the polarization force density and so generalize (8.5.42) to write a conservation of energy expression analogous to (8.5.15) (the physical system is shown in Fig. 8.5.7).

$$q \delta v = \int_V \delta w' dV - \int_V \mathbf{F} \cdot \delta \boldsymbol{\xi} dV. \quad (8.5.43)$$

If we define the potential $\phi (\mathbf{E} = -\nabla \phi)$ as being zero on the lower electrode, then $v = \phi$ evaluated on the upper electrode, whereas the total charge q is the integral of the surface charge $-\epsilon \mathbf{n} \cdot \nabla \phi$ over the surface of the upper electrode. Hence (8.5.43) becomes

$$-\int_{S'} \epsilon \nabla \phi \cdot \mathbf{n} \delta \phi da = \int_V \delta w' dV - \int_V \mathbf{F} \cdot \delta \boldsymbol{\xi} dV. \quad (8.5.44)$$

As in Section 8.5.2, the surface of integration S' can be extended to enclose a volume V that includes all the deformable material with no further contribution to the integral. This is true because ϕ is zero on the lower electrode which is enclosed by a surface S'' . Moreover, there is no contribution to an integration over a surface S''' that encloses the entire system, for this surface

* Table 3.1, Appendix E.

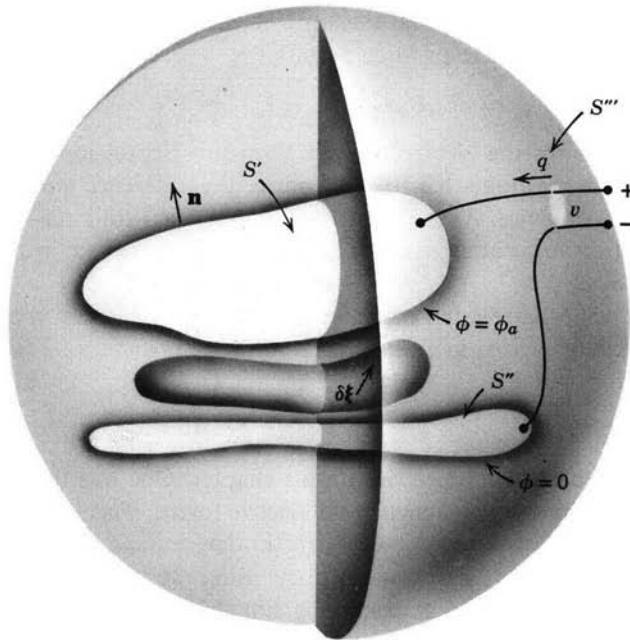


Fig. 8.5.7 A pair of perfectly conducting rigid electrodes imposes an electric field $\mathbf{E} = -\nabla\phi$ on a polarizable deformable dielectric medium. The surface S' encloses the upper electrode which is at the potential $\phi = v$.

is either far from the system or arranged (in the neighborhood of the terminals) so that $\mathbf{n} \cdot \mathbf{D} = 0$. The surface $S = S' + S'' + S'''$ completely encloses the volume V , and we can make use of Gauss's theorem to convert the left-hand side of (8.5.44) to a volume integral over V .

As a consequence of these manipulations, the left-hand side of (8.5.44) takes the same form as (8.5.19) with $\mu \rightarrow \epsilon$. Of course, ϕ now has the physical significance of being the potential for the electric field rather than for the magnetic field. All of the mathematical steps following (8.5.19) are valid, however, and we are led to a polarization force density with the same form as (8.5.37), with $\mathbf{H} \rightarrow \mathbf{E}$ and $\mu \rightarrow \epsilon$. If we superimpose on this force density, the force density on free charges ρ_f , the force density is

$$\mathbf{F} = \rho_f \mathbf{E} - \frac{1}{2} \mathbf{E} \cdot \mathbf{E} \nabla \epsilon + \nabla \left(\frac{1}{2} \mathbf{E} \cdot \mathbf{E} \frac{\partial \epsilon}{\partial \rho} \rho \right). \quad (8.5.45)$$

The first term is the free charge force density, the second is due to inhomogeneities in the dielectric, and the last results from changes in the material density. This last term is called the *electrostriction force density*.

Manipulations of (8.5.45) that incorporate the irrotational nature of the electric field intensity show that the stress tensor representation of combined free charge and polarization force densities is

$$T_{mn} = \epsilon E_m E_n - \frac{1}{2} \delta_{mn} E_k E_k [\epsilon - (\partial\epsilon/\partial\rho)\rho]. \quad (8.5.46)$$

Note that without the electrostriction term this expression is as obtained for the free charge alone (8.3.10). Of course, the difference now is that ϵ can be a function of space. At the same time the electric field intensity that must be used in (8.5.46) is affected by the presence of free charge in the material, for $\nabla \cdot \epsilon \mathbf{E} = \rho_f$.

Force densities, stress tensors, and surface force densities in electric field systems are summarized in Table 8.1.

8.6 DISCUSSION

There have been two objectives in this chapter. One was the development of a field description of magnetic and electric forces. This led to the concept of a stress tensor, which was convenient in determining total forces from a knowledge of the fields over a surface enclosing the volume of interest. The stress tensor is also useful in describing singular force distributions such as surface forces. The stress tensor, as developed here, is of interest as a basic mathematical representation. As illustrated in the chapters that follow, it can be used to represent a variety of physical quantities.

Our second objective has been to develop a picture of the distribution of forces due to magnetization and polarization. This was done while illustrating the important fact that the energy methods which form the theme of Chapter 3 are of equal significance in formulating a continuum description of electro-mechanical interactions.

From our derivations and discussion it should be clear that attention has been confined to a simple class of materials but that similar techniques can be used to determine force densities in more complicated media; for example, extensions of the energy method should allow us to find the force density in materials that are electrically nonlinear. Certainly the energy methods of Chapter 3 are not confined to electrically linear systems. Most solids do not exhibit the simple linear isotropic constitutive laws used here. Nonetheless, energy methods can be employed to find the force density in such situations,* although the formalisms used may be somewhat different from those used here.†

* J. A. Stratton, *Electromagnetic Theory*, McGraw-Hill, New York, 1941, p. 140.

† P. Penfield and H. Haus, *Electrodynamics of Moving Media*, M.I.T. Press, Cambridge, Mass., 1967; W. F. Brown, Jr., "Theory of Magnetoelastic Effects in Ferromagnetism," *J. Appl. Phys.*, **36**, 994 (1965).

PROBLEMS

8.1. An identity $\nabla \cdot (\psi \mathbf{A}) = \psi \nabla \cdot \mathbf{A} + \mathbf{A} \cdot \nabla \psi$ is given, where $\psi =$ scalar, $\mathbf{A} =$ vector. Show by means of index notation that this identity is valid.

8.2. Show, by means of index notation, that the following vector equation is valid: $\mathbf{B} \cdot \nabla(\psi \mathbf{A}) = \psi \mathbf{B} \cdot \nabla \mathbf{A} + \mathbf{A} \mathbf{B} \cdot \nabla \psi$; $\psi =$ scalar and \mathbf{A} and \mathbf{B} are vectors.

8.3. Consider two orthogonal coordinate systems (x_1, x_2, x_3) and (x'_1, x'_2, x'_3) . The primed coordinate system is related to the unprimed system as follows: $x'_3 = x_3$; the x'_1 -axis makes an angle of 60° with the x_1 -axis as shown in Fig. 8P.3.

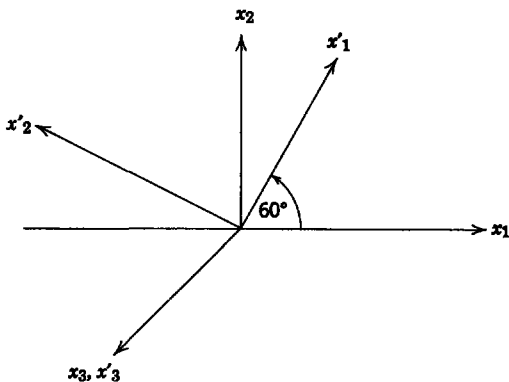


Fig. 8P.3

- (a) You are given the components of a vector \mathbf{A} in the (x_1, x_2, x_3) system: $A_1 = 1$; $A_2 = 2$; $A_3 = -1$. Find the components of \mathbf{A} in the (x'_1, x'_2, x'_3) system by using the transformation law for vectors, $A'_i = a_{ik} A_k$, where a_{ik} is the rotation matrix between (x_1, x_2, x_3) and (x'_1, x'_2, x'_3) .
- (b) A tensor T_{mn} in the (x_1, x_2, x_3) system has elements $T_{11} = 1$, $T_{22} = 2$, $T_{12} = T_{21} = 3$, $T_{33} = 1$, and $T_{13} = T_{31} = T_{23} = T_{32} = 0$. Find the elements of T_{mn} in the (x'_1, x'_2, x'_3) system by using $T'_{ij} = a_{ik} a_{jl} T_{kl}$.

8.4. A system has a stress tensor

$$T_{ij} = \begin{bmatrix} \frac{P_0^2}{2a^2} (x_1^2 - x_2^2) & -\frac{P_0^2}{a^2} x_1 x_2 & 0 \\ -\frac{P_0^2}{a^2} x_1 x_2 & \frac{P_0^2}{2a^2} (x_2^2 - x_1^2) & 0 \\ 0 & 0 & \frac{P_0^2}{2a^2} (-x_1^2 - x_2^2) \end{bmatrix}$$

Find the volume force density that results from this stress tensor.

8.5. A flat plate of infinite extent is parallel to the x_3 -axis and intersects the x_1 and x_2 -axes, as shown in Fig. 8P.5. In region (2) $\mathbf{E} = 0$, whereas in region (1) the electric field is given by $\mathbf{E} = E_0(\frac{2}{3}\mathbf{i}_1 + \mathbf{i}_2)$. Find the $x_1, x_2,$ and x_3 components of the force on the section of the

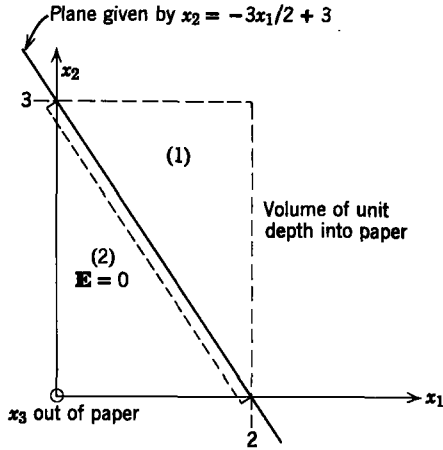


Fig. 8P.5

plate (per unit depth in the x_3 -direction) that extends from the x_1 - to the x_2 -axes. Do this by integrating the Maxwell stress tensor over the surface of the volume shown in Fig. 8P.5, which encloses this section of the plate.

8.6. A pair of parallel insulating sheets is shown in Fig. 8P.6. The sheet at $y = d$ supports a surface charge density $-\sigma_f$, whereas the sheet at $y = 0$ supports the image surface charge density σ_f . Hence the electric field between the plates *due to the charges* is $(\sigma_f/\epsilon_0)\mathbf{i}_y$. External

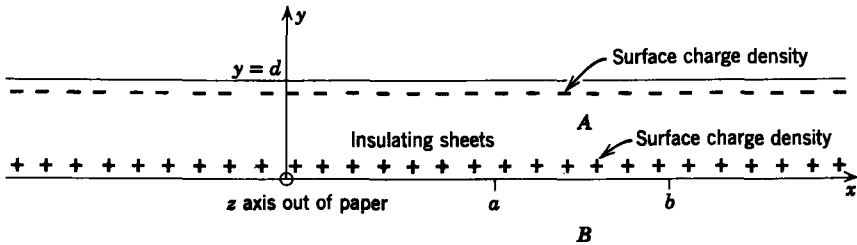


Fig. 8P.6

electrodes are used to impose an additional uniform electric field given everywhere by $\mathbf{E} = E_0\mathbf{i}_x + E_0\mathbf{i}_y$, where E_0 is a constant.

- (a) Write the components of the Maxwell stress tensor at points A and B in terms of σ_f and E_0 .
- (b) Use the Maxwell stress tensor to find the total electric force in each of the coordinate directions on the section of the lower sheet between $x = a$ and $x = b$ having depth D in the x_3 -direction.

8.7. Two perfectly conducting plates are arranged as shown in Fig. 8P.7. A magnetic field trapped between the plates is established in such a way that it does not penetrate the perfectly conducting plates. Also $H_3 = 0$ and $\partial/\partial x_3 = 0$. Under the assumption that $b \ll L$, find the x_1 -component of the force per unit x_3 on the section of the lower plate between $x_1 = L$ and $x_1 = -L$. You may assume that, when $x_1 = -L$, $\mathbf{H} = H_0\mathbf{i}_1$, where H_0 is a known constant.

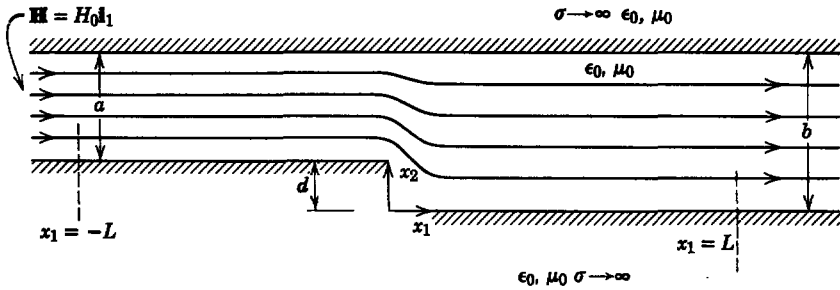


Fig. 8P.7

8.8. Three perfectly conducting plates are arranged as shown in Fig. 8P.8. A potential difference V_0 between the middle electrode and the outer electrodes is shown. Under the assumption that $a \ll l, b \ll l$, use the Maxwell stress tensor to find the force on the middle plate in the x -direction. Be sure to give all of your arguments.

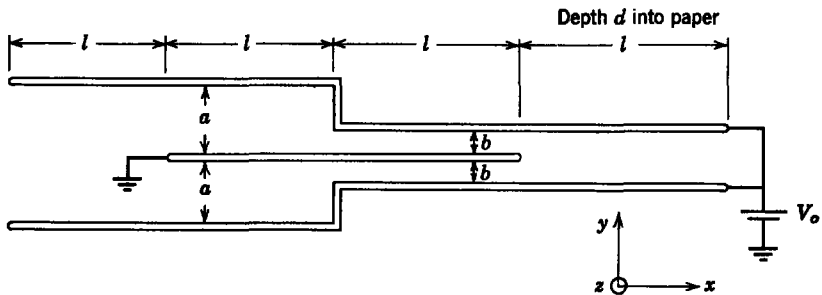


Fig. 8P.8

8.9. Capacitor plates with depth d (into the paper), length l , and spacing s are arranged as shown in Fig. 8P.9. Many of the plates are distributed along the x_1 -axis. The plates have, alternately, the potentials $+V_0$ and $-V_0$, as shown, so that an electric field exists between each pair of them. You are to find the force in the x_2 -direction on the section of plate enclosed by the volume V , which has a depth $w \ll d$ into the paper and encloses a section of the plate centered between its x_3 extremes.

8.10. Figure 8P.10 shows an electromechanical electrostatic voltmeter for measuring the relaxation time in liquids with very long relaxation times. The two outer conducting plates are fixed. The middle plate is constrained by a spring that is relaxed when $x = a$ but otherwise free to move in the x -direction. This plate (mass M) moves in a liquid dielectric of uniform conductivity σ and permittivity ϵ (the ϵ/σ to be measured). The liquid fills the region between the plates.

- Use Maxwell's stress tensor to find the total electric force on the middle plate in the x -direction as a function of the potential v of the middle plate and the position x . (Your answer should be exact, as $[s/(a-x)] \rightarrow 0$.)
- Use the energy method to check the result of part (a).
- The switch S has been closed for a long enough time to establish the middle plate in static equilibrium. Write the equations of motion for the plate position $x(t)$ (as many equations as unknowns) after the switch is opened.

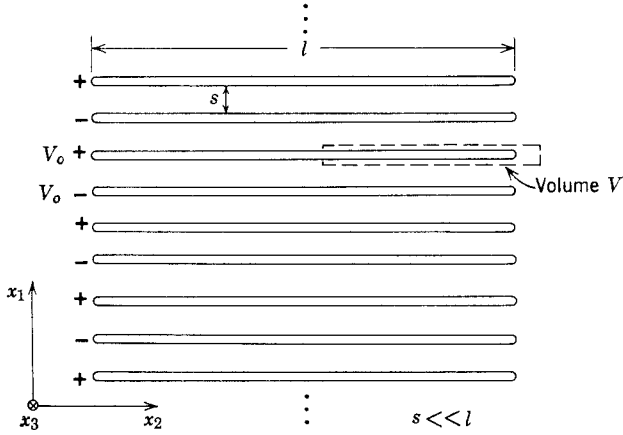


Fig. 8P.9

- (d) Assume that the inertial force on the plate can be ignored (that the plate moves very slowly) and find $x(t)$. Is your assumption that the inertial force can be ignored consistent with the liquid having a very long relaxation time?
- (e) How would you use this device to measure the relaxation time of the liquid?

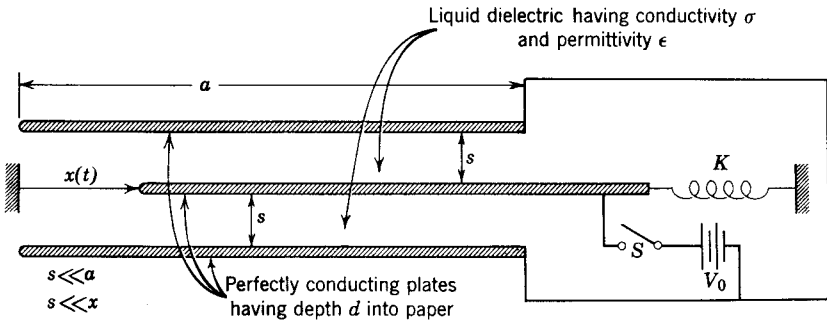


Fig. 8P.10

8.11. Two parallel conducting plates with a potential difference V_0 are shown in Fig. 8P.11. Assuming that $c < b < a \ll l \ll D$ and that the fringing fields are zero at the extreme points A and B , find the force in the x_1 -direction on the lower plate.

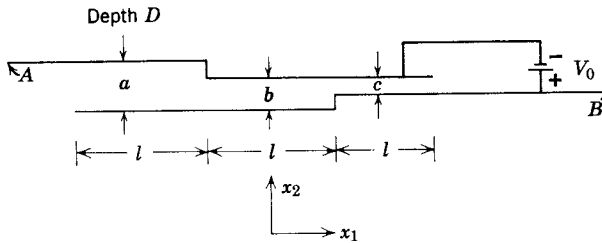


Fig. 8P.11

8.12. In Fig. 8P.12 two parallel perfectly conducting electrodes extend from $x_1 = 0$ to $x_1 = \infty$ and are infinite in the x_3 -direction. The separation of the electrodes in the x_2 -direction is a . A potential $\phi = \phi_0 \sin(\pi/a)x_2$ is established along the x_2 -axis at $x_1 = 0$.

- (a) Find the electric field intensity E everywhere between the plates and sketch.
- (b) Find the total force on the bottom plate per unit depth in the x_3 -direction.
- (c) Find the total force on the top plate per unit depth in the x_3 -direction.

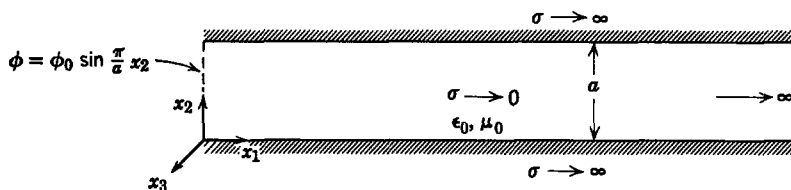


Fig. 8P.12

8.13. In the system in Fig. 8P.13 the geometry of two equipotentials is defined. These equipotentials are maintained at a potential difference V_0 by the battery, and the upper conductor has a movable section ($-a < x_1 < a$), as indicated. The system has a large width w in the x_3 -direction; thus we neglect any variations with x_3 and approximate the potential in the region between the conductors with the expression

$$\phi = \frac{V_0}{3a^2} (x_2^2 - x_1^2 - a^2);$$

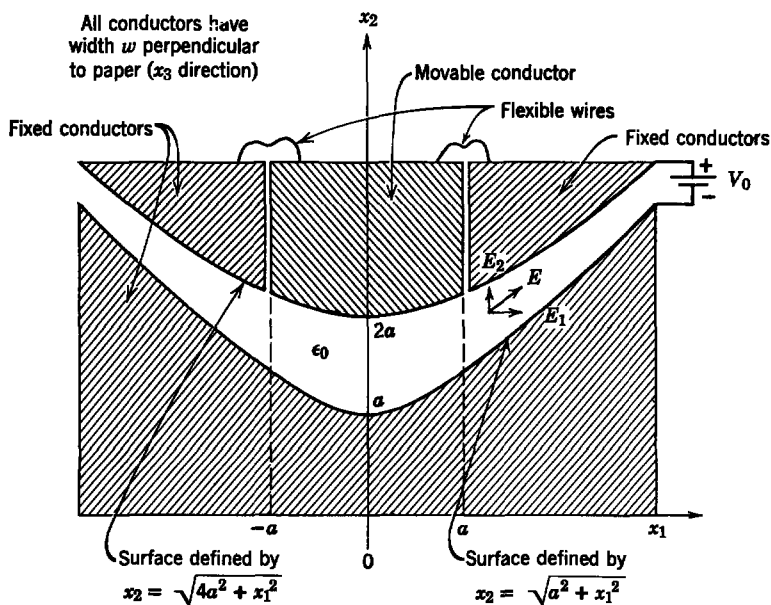


Fig. 8P.13

the two nonzero components of electric field intensity are then

$$E_1 = \frac{2V_0x_1}{3a^2}; \quad E_2 = -\frac{2V_0x_2}{3a^2}.$$

- Find the components T_{22} and T_{21} of the Maxwell stress tensor between the conductors in terms of ϵ_0 , V_0 , a , x_1 , and x_2 .
- Use the stress tensor to find the component f_2 of the force applied to the movable section of the upper conductor ($-a < x_1 < a$) by the electric field. Assume that the movable conductor is held in equilibrium in the position shown by externally applied forces.
- Prove that $f_1 = 0$ by using the stress tensor.
- Find f_2 by using the surface force density written in terms of the surface charge density σ_r (see Section 8.4.2).

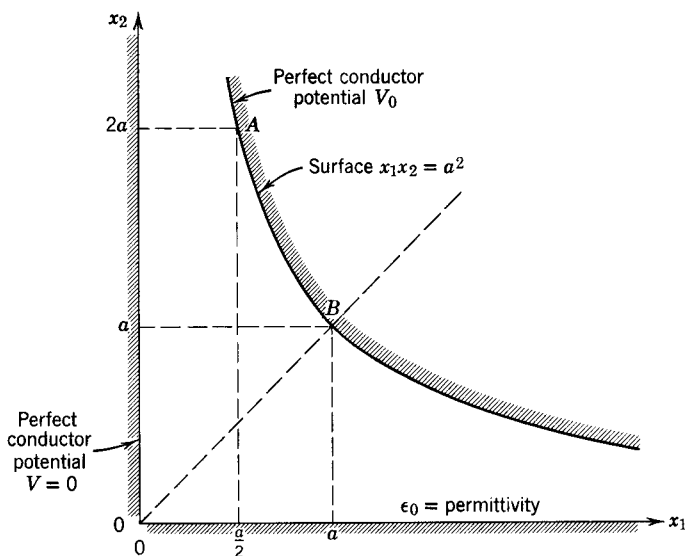


Fig. 8P.14

8.14. Figure 8P.14 shows two equipotential surfaces that are very long in the x_3 -direction. The electric potential is

$$\phi = \frac{V_0}{a^2} x_1 x_2,$$

where $\mathbf{E} = -\nabla\phi$.

- Evaluate all elements of the stress tensor for the region between the perfect conductors.
- Find the total force applied by the field to the segment of the curved conductor between points A and B and having depth D in the x_3 -direction.

8.15. A conducting block moves with the velocity V between plane-parallel, perfectly conducting electrodes, short-circuited as shown in Fig. 8P.15. A uniform magnetic field \mathbf{H}_0 is imposed. Ignore the magnetic field induced by currents flowing in the block,

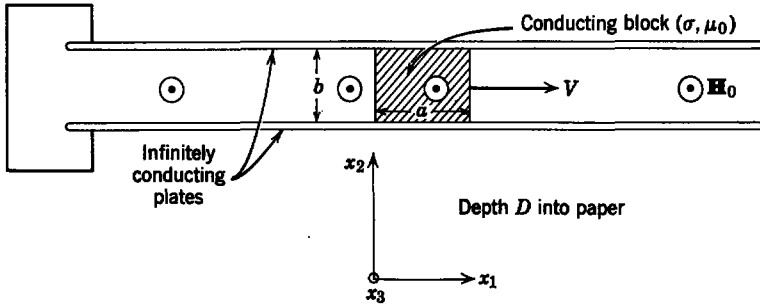


Fig. 8P.15

- (a) Compute the total force on the block using $\mathbf{J} \times \mu_0 \mathbf{H}$.
- (b) Show that in this case the Maxwell stress tensor gives zero force on the block.
- (c) Why do the results of (a) and (b) differ?

8.16. Figure 8P.16 shows a block of conducting material free to slide between two perfectly conducting plates that extend to infinity on the right. The conductivity of the block may be taken as $\sigma = \sigma_0(1 + \sin \pi x/2L)$ and the permeability as $\mu = \mu_0$. The conductivity σ_0 is a

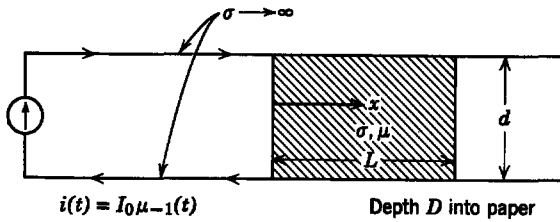


Fig. 8P.16

positive constant and x is the distance from the left-hand edge of the block. Find the total force of electromagnetic origin on the block as a function of time. Assume $d \ll D$, $d \ll L$.

8.17. A slab of conducting material (e.g., graphite) is sandwiched between perfectly conducting plates, as shown in Fig. 8P.17. The dimension a is much smaller than D and the x -dimension of the slab. In addition, the x -dimension is much larger than the skin depth at the frequency ω .

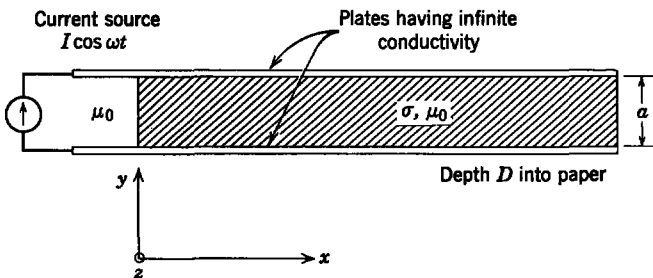


Fig. 8P.17

- Find the steady-state magnetic field \mathbf{H} and current density \mathbf{J} in the slab.
- Compute the total force on the slab in the x -direction by integrating $\mathbf{J} \times \mu_0 \mathbf{H}$ over a volume.
- Compute the total force on the slab in the x -direction by integrating the Maxwell stress tensor over a surface.

8.18. A rigid, perfectly conducting body of arbitrary shape is positioned between two perfectly conducting infinite plates, as shown in Fig. 8P.18. The plates are at a potential

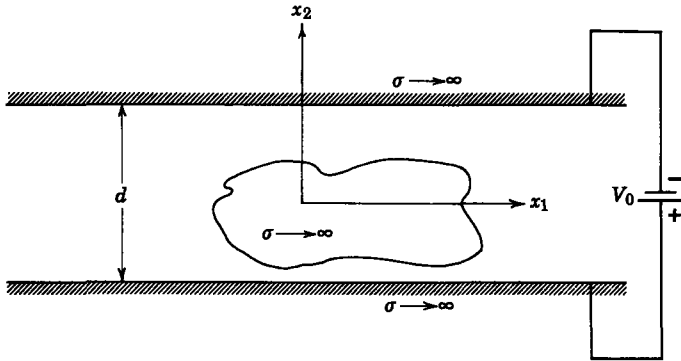


Fig. 8P.18

difference V_0 . Take advantage of the fact that far from the body $\mathbf{E} = \mathbf{i}_2(V_0/d)$ to calculate the x_1 -directed force on the body.

8.19. A pair of wires carries the constant current I as shown in Fig. 8P.19. The spacing $2a$ of the wires is much larger than the radius of either wire.

- Use the force density $\mathbf{J} \times \mathbf{B}$ to determine the force on a unit length of the right wire in the x_1 -direction.

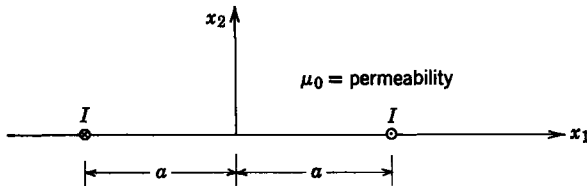


Fig. 8P.19

- Now enclose this section of wire with a convenient surface and integrate the Maxwell stress tensor over the surface to find the force in the x_1 -direction. Compare your answer with that found in (a).
Hint. A "convenient" surface might take advantage of the fact that the fields go to zero as x_1 and $x_2 \rightarrow \infty$ and that $x_1 = 0$ is a plane of symmetry.

8.20. Two line charges of strength $\pm\lambda$ per unit x_3 are located at $x_2 = +a$ and $x_2 = -a$ (see Fig. 8P.20). The line charges extend to $\pm\infty$ in the x_3 -direction.

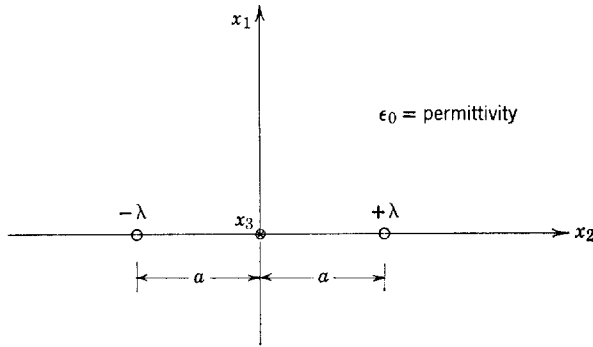


Fig. 8P.20

- (a) Use the Maxwell stress tensor to find the force in the x_2 -direction per unit depth in the x_3 -direction exerted by the electric field on the line charge at $x_2 = +a$.
- (b) Can you think of any other way of computing this force? If so, check it with part (a).

8.21. In Problem 7.14 a vehicle system was proposed in which a magnetic field provided both suspension (i.e., levitation) and propulsion forces. There it was assumed that the condition $ks \ll 1$ is valid and, to calculate the volume force density, $\mathbf{J} \times \mathbf{B}$ was applied. The Maxwell stress tensor provides an alternate and useful method for the calculation of

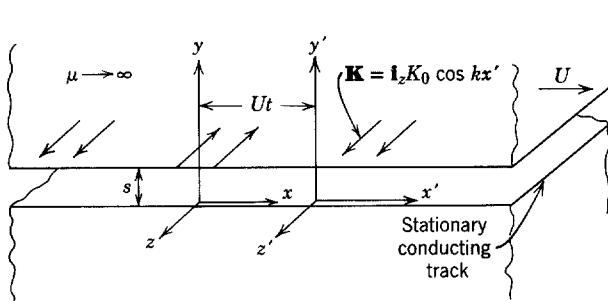


Fig. 8P.21

the forces per unit area (Fig. 8P.21). The solution for the magnetic field in the region $-\infty < y < 0$ is

$$B_x = \text{Re} [\mu_0 K_0 e^{\alpha y} e^{jk(x-Ut)}]$$

and

$$B_y = \text{Re} \left[\frac{-jk\mu_0 K_0}{\alpha} e^{\alpha y} e^{jk(x-Ut)} \right],$$

where

$$\alpha = k \left(1 - j \frac{\mu_0 \sigma U}{k} \right)^{1/2}.$$

- (a) Write the components of the Maxwell stress tensor explicitly in terms of B_x and B_y . Present your results in matrix form.
- (b) Using the stress tensor, compute the time average force per unit area (in the x - z plane) that holds the vehicle up. Take advantage of the periodic variation with x to define a suitable surface.
- (c) Again using the stress tensor, compute the time average force per unit area (x - z) that tends to propel the train.

8.22. A pair of perfectly conducting plane-parallel electrodes is shorted by a bar of metal with conductivity σ (a constant) (Fig. 8P.22). A source of constant current I_0 (amperes) is

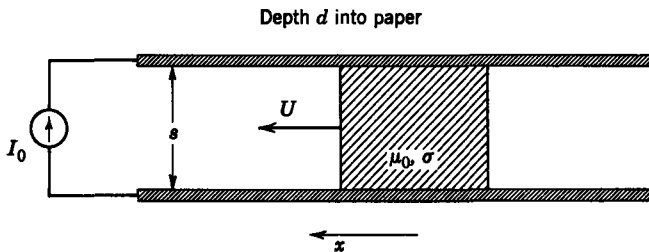


Fig. 8P.22

distributed along the left edges of the plates, and the block moves with the velocity U in the x -direction. What is the magnetic force on the block in the x -direction? Your answer should include the possibility that the magnetic Reynolds number is large or small.

8.23. A pair of perfectly conducting plane parallel electrodes “sandwich” a slab of lossy dielectric of thickness b and a region of free space of thickness $(a - b)$, as shown in Fig. 8P.23. The conductivity of the slab varies in the x -direction, and σ_0 and σ_1 are constants.

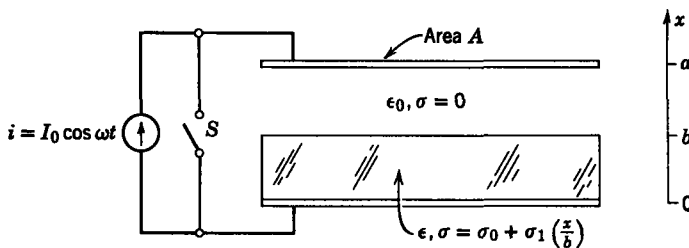


Fig. 8P.23

When $t < 0$, the switch S is closed and no electric fields exist between the plates. When $t = 0$, the switch S is opened. Neglect fringing fields and find the force in the x -direction on the upper plate as a function of time.

8.24. A pair of planar, diverging, perfectly conducting plates has a constant potential difference V_0 and the dimensions shown in Fig. 8P.24. What is the total electrical force on the lower plate in the x -direction? (Note that x is the radial direction half-way between the plates.)

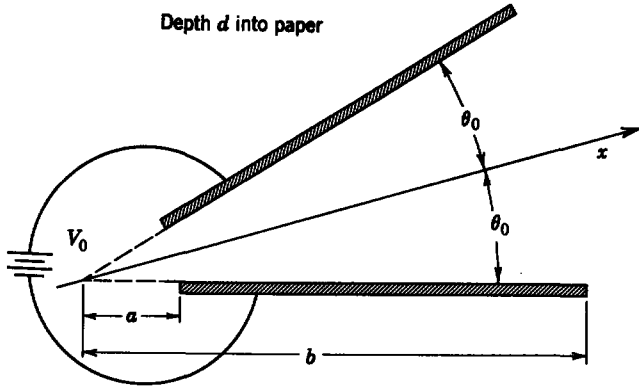


Fig. 8P.24

8.25. The dielectric slab shown in Fig. 8P.25 is free to slide in the x_1 -direction. The upper and lower surfaces of the slab are in contact with perfectly conducting plates. The remaining volume is free space. Find the x_1 -component of force on the slab. Use the Maxwell stress tensor.

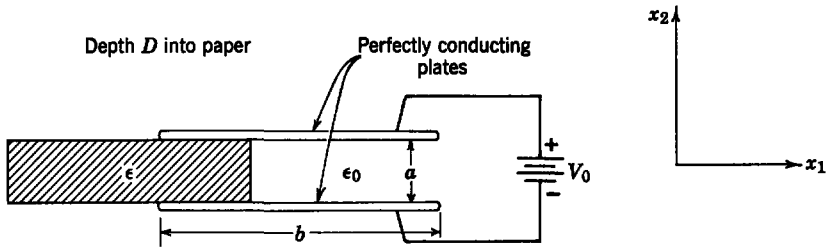


Fig. 8P.25

8.26. An elastic material is placed between two equipotential surfaces with its left-hand edge fixed to a rigid insulating wall, as shown in Fig. 8P.26. The right-hand edge of the elastic bulk is free and the permittivity of the material is a function of its mass density $\epsilon_1 = \epsilon_1(\rho)$. Free space fills the remaining volume. A potential difference (V_0) exists between the two plates.

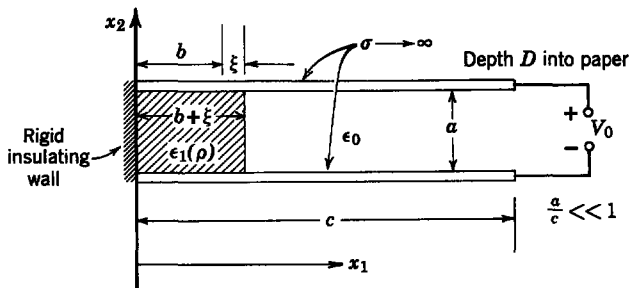


Fig. 8P.26

- (a) Using the Maxwell stress tensor for polarizable material, find the force on the right-hand edge of the elastic bulk.
- (b) Using energy methods, find the force on the right-hand edge of the elastic bulk.
- (c) Compare the answers of parts (a) and (b).

8.27. The force density on a polarized fluid with permittivity $\epsilon(x_1, x_2, x_3, t)$ is $\mathbf{F} = -\frac{1}{2}\mathbf{E} \cdot \mathbf{E} \nabla \epsilon + \frac{1}{2} \nabla(\epsilon \mathbf{E} \cdot \mathbf{E} b)$, where the free charge $\rho_f = 0$, $\nabla \times \mathbf{E} = 0$, and $b = (\rho/\epsilon) (\partial \epsilon / \partial \rho)$ is a parameter that accounts for the electrostriction of the fluid (Fig. 8P.27). The planar

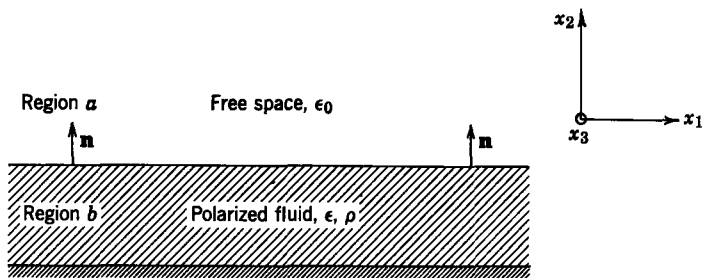


Fig. 8P.27

surface between dielectrics ϵ_0 and ϵ has a normal vector \mathbf{n} . Show that the polarization forces alone cannot exert a traction $\boldsymbol{\tau}$ on the interface between the two dielectrics which has a shear component. Remember that $T_m = [T_{mn}^a - T_{mn}^b]n_n$.

8.28. Use the electric force density of (8.5.45) to obtain the stress tensor of (8.5.46).

Chapter 9

SIMPLE ELASTIC CONTINUA

9.0 INTRODUCTION

The study of the effects of motion on electric and magnetic fields (Chapter 7) and of electromagnetic force densities (Chapter 8) provides the background necessary for an introduction to the electromechanics of continuous media. To someone familiar with the dynamics of continuous media this is a pretentious statement, for it implies that the description of distributed mechanical systems requires only a minor addition to the largely electromagnetic considerations so far introduced. In general, this is far from the case; for example, does the mechanical medium consist of a solid or a fluid? In either case the equations of motion vary considerably with the particular fluid or solid under study. These equations generally involve three-dimensional deformations, hence are likely to be at least as complicated as the electromagnetic field equations if not more so.

Fortunately, many of the most significant and practical interactions with continuous media can be modeled in terms of one or two-dimensional structures that *not only retain the salient features of the three-dimensional dynamics but represent idealizations that we should like to approach in practice.* In this and the next chapter attention is confined to situations in which the mechanical side of the electromechanical problem takes the form of one of two simple models: the thin rod subject to longitudinal motions and wires and membranes undergoing transverse motions. The derivation of the one- and two-dimensional equations of motion for these simple cases serves to illustrate the essential steps required to write the more general expressions for elastic media and fluids, as undertaken in Chapters 11 and 12. At the same time the continuum electromechanical dynamics studied in this and the next chapter give a preview of types of dynamics found in acoustics, fluid dynamics, electron beam-plasma dynamics, magnetohydrodynamics, electrohydrodynamics, and microwave magnetics.

In this chapter the discussion is limited to electromechanical interactions

with continuous media that occur through boundary conditions representable by terminal pairs. In Chapter 10 we consider physical situations in which the electromechanical coupling is itself distributed and in which our lumped parameter concept of a terminal pair can no longer account for the coupling.

9.1 LONGITUDINAL MOTION OF A THIN ROD

Longitudinal motion of a thin elastic rod provides a logical first topic in discussing the dynamics of elastic continua. This is true because we emphasize the wavelike nature of the dynamics; and in a thin rod longitudinal waves have a particularly simple form. As we shall see, waves in a thin rod can propagate without changing their shapes; hence they can be understood by means of comparatively simple mathematical techniques. This distortion-free behavior of the thin rod is used in applications such as acoustic delay lines and electromechanical filters in which the properties of the electromechanical system are especially attractive. We discuss some applications later in this section.

To describe longitudinal motion in an elastic rod we must make a mathematical model. This process consists essentially of two steps: (a) a mathematical description of force equilibrium for a small element of the rod and (b) a description of the elastic property of the rod.

We consider the long thin rod shown in Fig. 9.1.1a. The rod has a uniform cross section of area A perpendicular to the longitudinal (x_1)-direction. We apply forces in the x_1 -direction and observe motion in the x_1 -direction. By "thin" we mean that the dimensions of the rod perpendicular to x_1 are small enough that effects of any transverse motion are negligible. The

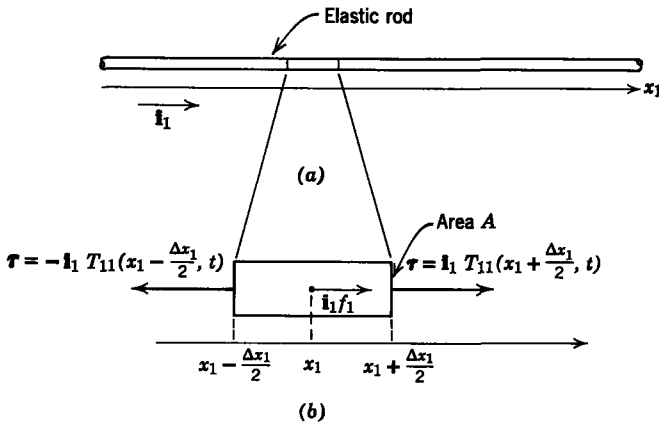


Fig. 9.1.1 Thin elastic rod with axis in the x_1 -direction and uniform cross section of area A : (a) the rod; (b) force and tractions applied to an element of length Δx_1 centered at x_1 .

criterion for making this assumption is obtained from the treatment of three-dimensional elasticity in Chapter 11.

To describe force equilibrium at each point along the rod we write Newton's second law for a small element of length Δx_1 centered at x_1 , as illustrated in Fig. 9.1.1*b*. There are two kinds of forces applied to this element of material: body forces, such as those due to gravity and electromagnetic fields, that act throughout the volume of the element and surface forces applied to the transverse surfaces of the element by the adjacent material.

When we specify a volume force density of magnitude F_1 in the x_1 -direction and require that over the length Δx_1 the force density shall not vary appreciably, we can write the total body force f_1 as

$$f_1 = F_1 A \Delta x_1. \tag{9.1.1}$$

This force is indicated in Fig. 9.1.1*b*

The forces applied at the surfaces of the element by adjacent matter are described in the following way. Consider first the situation in Fig. 9.1.2*a* in which a rod is at rest and subjected to equal and opposite forces of magnitude f . When an imaginary transverse cut is made in the rod, as illustrated in Fig. 9.1.2*b*, each segment must still be in equilibrium. If there are no externally applied body forces, the force f is applied to the two pieces of material at the cut, as shown. The vector force per unit area (or traction τ , as discussed in Section 8.2.1) applied to the left-hand segment by the right-hand segment is

$$\tau = \mathbf{i}_1 \frac{f}{A}. \tag{9.1.2}$$

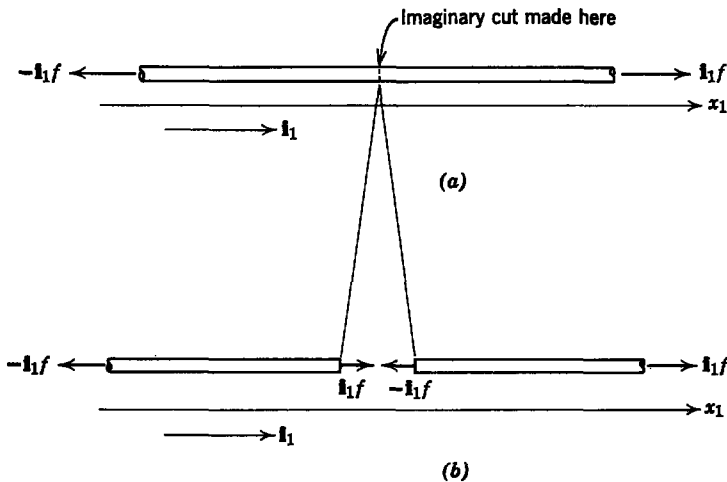


Fig. 9.1.2 An elastic rod in static equilibrium: (a) the rod with applied forces; (b) equilibrium conditions at an imaginary cut.

The traction applied to the right-hand segment by the left-hand segment is

$$\boldsymbol{\tau} = -\mathbf{i}_1 \frac{f}{A}. \quad (9.1.3)$$

We define the stress T_{11} (as in Section 8.2.1) transmitted by the rod as

$$T_{11} = \frac{f}{A}. \quad (9.1.4)$$

Then we obtain the x_1 -component of the mechanical traction τ_1 as

$$\tau_1 = T_{11}n_1, \quad (9.1.5)$$

where n_1 is the magnitude of the x_1 -component of the *outward* directed unit normal vector for the segment of rod to which the traction is applied. For this one-dimensional case, illustrated in Fig. 9.1.2, $n_1 = +1$ for the left-hand segment and $n_1 = -1$ for the right-hand segment. Equation 9.1.5 will be recognized as a simple special case of (8.2.8). Positive stress ($T_{11} > 0$) indicates tension and negative stress ($T_{11} < 0$) indicates compression.

Although our arguments have been based on a static experiment with no body forces applied, we can extend these definitions to the general case in which there are body forces that vary with space (x_1) and time. It is still true that a transverse cut must indicate force equilibrium, but the force transmitted at the cut will not be equal to the force applied at the ends. In this case we specify that the stress T_{11} is a function of space and time $T_{11}(x_1, t)$ and use (9.1.5) to calculate the surface traction applied to an element of material by the adjacent material. Thus the surface tractions are represented in Fig. 9.1.1*b*, and the net force due to the surface tractions, correct to first-order terms in Δx_1 , is

$$\mathbf{i}_1 A \left[T_{11} \left(x_1 + \frac{\Delta x_1}{2}, t \right) - T_{11} \left(x_1 - \frac{\Delta x_1}{2}, t \right) \right] = \mathbf{i}_1 \frac{\partial T_{11}}{\partial x_1} A \Delta x_1. \quad (9.1.6)$$

Note that the right side of (9.1.6) can be interpreted as the mechanical body force density ($\partial T_{11}/\partial x_1$) acting throughout the volume $A \Delta x_1$. The force density $\partial T_{11}/\partial x_1$ is a simple case of the general expression in (8.2.7). Here the stress T_{11} has a mechanical origin.

One of the forces applied to the small element of the rod illustrated in Fig. 9.1.1*b* is the acceleration force. To find this force we need to describe the instantaneous position of the element with respect to the inertial coordinate system (x_1). This is done conventionally by describing the displacement of the element with respect to its position in static equilibrium and with no applied forces. We illustrate it in Fig. 9.1.3. In Fig. 9.1.3*a* the rod is in static equilibrium with no forces applied. Then the element of material labeled a

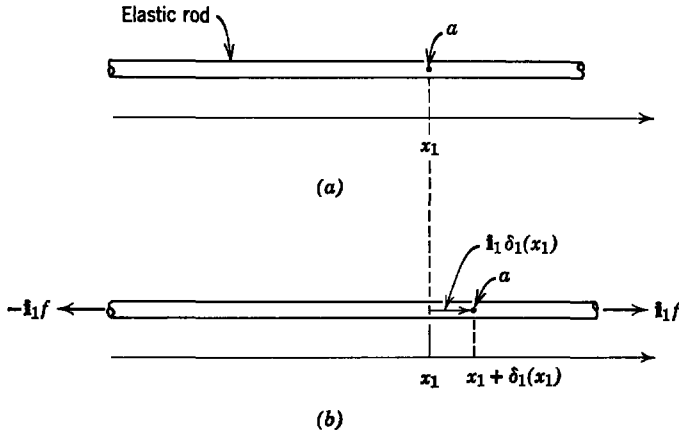


Fig. 9.1.3 Definition of displacement: (a) unstressed rod in static equilibrium; (b) stressed rod indicating definition of displacement δ_1 .

has the position x_1 . In Fig. 9.1.3b we apply forces of magnitude f at the ends of the rod, and it is stretched, thus moving the element a of material to the point $x_1 + \delta_1(x_1)$. With time-varying forces the displacement δ_1 from equilibrium will be the function of both space and time, $\delta_1(x_1, t)$.

Referring back to the element of the rod in Fig. 9.1.1b, we can describe the instantaneous displacement of the element as

$$\delta_1(x_1 - \delta_1, t),$$

that is, the equilibrium position of the matter that is instantaneously at position x_1 is $x_1 - \delta_1$. We now make the assumption, to be justified in Example 9.1.1, that the displacement δ_1 in an elastic material is usually small enough that we can use small-signal, linear differential equations with constant coefficients to describe the motion. Thus we expand the displacement δ_1 in a Taylor series about the value at x_1 and obtain

$$\delta_1(x_1 - \delta_1, t) = \delta_1(x_1, t) - \frac{\partial \delta_1(x_1, t)}{\partial x_1} \delta_1(x_1, t) + \dots \quad (9.1.7)$$

Usually, δ_1 and its space derivatives are small enough to allow us to neglect all but the first term on the right of (9.1.7). Thus the acceleration of the element centered at x_1 in Fig. 9.1.1b is

$$\frac{\partial^2 \delta_1(x_1, t)}{\partial t^2}.$$

Because the local displacement of the material is small, the fractional change in mass density will be small. Consequently, in the spirit of the

linearized theory we assume that the mass density ρ of the rod is constant and write the x_1 -component of Newton's second law for the element in Fig. 9.1.1*b* as

$$\rho A \Delta x_1 \frac{\partial^2 \delta_1}{\partial t^2} = \frac{\partial T_{11}}{\partial x_1} A \Delta x_1 + F_1 A \Delta x_1; \quad (9.1.8)$$

that is, the inertial force is equal to the mechanical force on the element from adjacent material plus any externally applied body forces. We divide this expression by the volume $A \Delta x_1$ of the element and obtain the desired equation of force equilibrium:

$$\rho \frac{\partial^2 \delta_1}{\partial t^2} = \frac{\partial T_{11}}{\partial x_1} + F_1. \quad (9.1.9)$$

Note that each term in this equation is a force density.

As the second step in finding the equations of motion for a thin elastic rod we introduce the elastic property of the material to relate stress T_{11} and displacement δ_1 . The form of this relation results from a mathematical description of experimental results obtained for a wide variety of elastic materials.

It is found experimentally that the elastic stress depends on how much the material is deformed, the stress increasing as the deformation increases. This is a statement for continuous media, analogous to the statement for lumped-parameter systems, that for an ideal spring the force is dependent on the relative displacement of the ends or on the deformation of the spring (see Section 2.2.1*a*).

To calculate the local deformation in a thin elastic rod we consider two grains of matter labeled a and b in Fig. 9.1.4. With no applied forces and static equilibrium these grains of matter are at positions x_1 and $x_1 + \Delta x_1$, as indicated in Fig. 9.1.4*a*. When forces are acting on the rod, the two grains of matter will have the positions indicated in Fig. 9.1.4*b*. Our objective is to find a unique relationship between the stress T_{11} and the displacement δ_1 . We expect that the *change* in the distance between the points a and b ,

$$\{[\delta_1(x_1 + \Delta x_1) + x_1 + \Delta x_1] - [\delta_1(x_1) + x_1]\} - \Delta x_1,$$

will be proportional to the applied stress. This change, however, is also proportional to the original distance Δx_1 between points a and b . To obtain a measure of the elongation that is independent of Δx_1 , we normalize the change in length to the unstretched length and take the limit $\Delta x_1 \rightarrow 0$. The resulting function e_{11} is called the *normal strain* and is

$$e_{11} = \lim_{\Delta x_1 \rightarrow 0} \frac{[\delta_1(x_1 + \Delta x_1) - \delta_1(x_1)]}{\Delta x_1} = \frac{\partial \delta_1}{\partial x_1}. \quad (9.1.10)$$

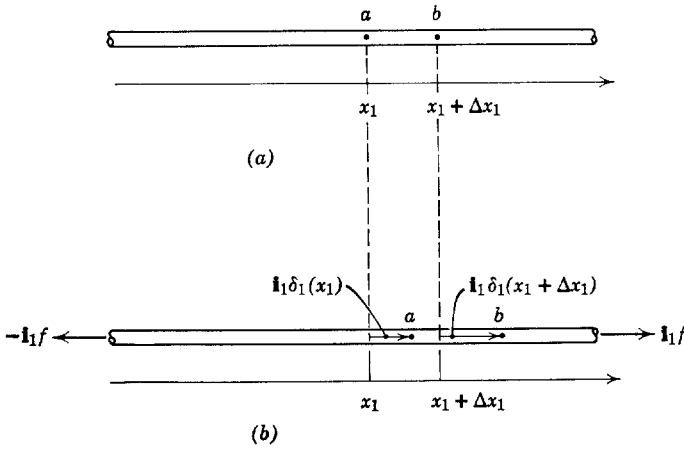


Fig. 9.1.4 Displacements of two adjacent particles: (a) unstretched; (b) stretched.

This geometrical relation is often called the *strain-displacement* relation and has its three-dimensional counterpart derived in Chapter 11.

We define an *ideal* elastic material as one in which the stress T_{11} is a function only of the strain e_{11} . This is analogous to the definition of an ideal spring in Section 2.2.1a. An ideal *linear* elastic material has a linear relation between stress and strain conventionally written as

$$T_{11} = E e_{11}. \tag{9.1.11}$$

The constant of proportionality E is called *Young's modulus* or the *modulus of elasticity* and (9.1.11) is often referred to as *Hooke's law*, or as the *stress-strain relation*. Equation 9.1.11, which introduces the physical properties of the material, is analogous to the constituent relations of electromagnetic theory, as discussed in Section 6.3. The modulus of elasticity E , like ϵ or σ , is found by laboratory measurements.

In our treatment we consider only ideal linear elastic media as described by (9.1.11). It is well to remember that the linear model holds over a limited range of strain and that some materials do not behave linearly.

We can now summarize the equations of motion that we use to describe longitudinal motion in a thin rod of linear elastic material. Force equilibrium is described by (9.1.9) and the stress-displacement equation is obtained by using (9.1.10) in (9.1.11).

$$\rho \frac{\partial^2 \delta_1}{\partial t^2} = \frac{\partial T_{11}}{\partial x_1} + F_1, \tag{9.1.9}$$

$$T_{11} = E \frac{\partial \delta_1}{\partial x_1}. \tag{9.1.12}$$

Table 9.1 Modulus of Elasticity E and Density ρ for Representative Materials*

| Material | E -units of 10^{11} N/m ² | ρ -units of 10^3 kg/m ³ | v_p -units† of m/sec |
|---------------------------------|---------------------------------------------|----------------------------------------------|---------------------------|
| Aluminum (pure and alloy) | 0.68–0.79 | 2.66–2.89 | 5100 |
| Brass (60–70% Cu, 40–30% Zn) | 1.0–1.1 | 8.36–8.51 | 3500 |
| Copper | 1.17–1.24 | 8.95–8.98 | 3700 |
| Iron, cast (2.7–3.6% C) | 0.89–1.45 | 6.96–7.35 | 4000 |
| Steel (carbon and low alloy) | 1.93–2.20 | 7.73–7.87 | 5100 |
| Stainless steel (18% Cr, 8% Ni) | 1.93–2.06 | 7.65–7.93 | 5100 |
| Titanium (pure and alloy) | 1.06–1.14 | 4.52 | 4900 |
| Glass | 0.49–0.79 | 2.38–3.88 | 4500 |
| Methyl methacrylate | 0.024–0.034 | 1.16 | 1600 |
| Polyethylene | $1.38\text{--}3.8 \times 10^{-3}$ | 0.915 | 530 |
| Rubber | $0.79\text{--}4.1 \times 10^{-5}$ | 0.99–1.245 | 46 |

* See S. H. Crandall, and N. C. Dahl, *An Introduction to the Mechanics of Solids*, McGraw-Hill, New York, 1959, for a list of references for these constants and a list of these constants in English units.

† Computed from average values of E and ρ .

The modulus of elasticity E and density ρ for common solids which can have elastic behavior (for small deformations) are given in Table 9.1. The equations of motion for a thin rod are summarized in Table 9.2 at the end of the chapter. The magnitude of the displacement resulting from a moderate applied stress is small, as illustrated in the following example.

Example 9.1.1. A metal rod is supported at one end by a rigid structure and subjected to a force $f = 100$ lb at the other end (Fig. 9.1.5). Using a rod made of aluminum ($E = 0.7 \times 10^{11}$ N/m²) in the dimensions shown, we wish to find the increase in length caused by the force f . The weight of the rod is small compared with f and can be neglected.

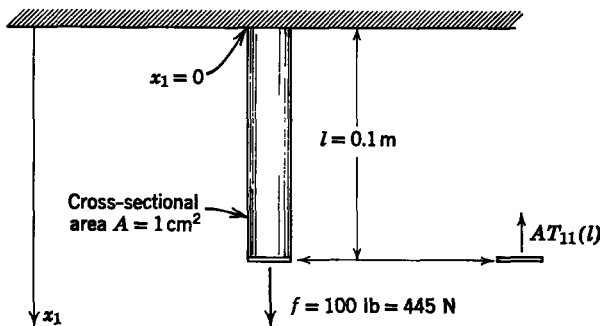


Fig. 9.1.5 Metal rod fixed at $x_1 = 0$ and subject to the force f at $x_1 = l$.

The rod is static. Hence (9.1.9) and (9.1.12) yield, with $F_1 = 0$,

$$\frac{d^2\delta_1}{dx_1^2} = 0. \quad (a)$$

with the solution

$$\delta_1 = Cx_1 + D. \quad (b)$$

Because $\delta(0) = 0$, the constant $D = 0$. The remaining constant is found from the boundary condition on the stress at $x_1 = l$; that is, the force equilibrium of a thin slice of the rod at $x_1 = l$ (see Fig. 9.1.5) requires that

$$AT_{11}(l) = f = AE \frac{d\delta_1}{dx_1}(l), \quad (c)$$

where A is the cross sectional area of the rod. Equations b and c show that $C = f/AE$ and that the displacement evaluated at $x_1 = l$, where it has its largest value, is

$$\delta_1 = \frac{fl}{EA} = \frac{(445)(0.1)}{(0.7 \times 10^{11})(10^{-4})} = 6.36 \times 10^{-6} \text{ m}, \quad (d)$$

or about 2.5×10^{-4} in. Note that although this displacement is extremely small it can be made arbitrarily large by increasing the length of the rod. It is the rate of change of the displacement, or the stress, that must be small if the linear stress-strain relation is to remain valid.*

9.1.1 Wave Propagation Without Dispersion

We consider a case in which the body force density F_1 in (9.1.9) is zero. Then (9.1.9) and (9.1.12) yield†

$$\frac{\partial^2 \delta}{\partial t^2} = \frac{E}{\rho} \frac{\partial^2 \delta}{\partial x^2}. \quad (9.1.13)$$

This is called the *wave equation* because it has solutions of the general form

$$\delta = \delta_+(x - v_p t) + \delta_-(x + v_p t), \quad (9.1.14)$$

where

$$v_p = \left(\frac{E}{\rho} \right)^{1/2}, \quad (9.1.15)$$

which can be verified by substituting (9.1.14) into (9.1.13). The function δ_+ represents a wave traveling in the $+x$ -direction and the function δ_- represents a wave traveling in the $-x$ -direction.

To an observer traveling with a velocity such that the phase (or argument) of δ_+ is constant the function δ_+ will have a space variation that does not vary with time. The required velocity is found by setting

$$x - v_p t = \text{constant} \quad (9.1.16)$$

* A discussion of inelastic behavior is given in most texts on the mechanics of solids; for example, G. Murphy, *Mechanics of Materials*, Ronald, New York, 1948, p. 23.

† In what follows the subscripts used in the preceding section are dropped. In the one-dimensional problems to be considered the subscripts are not needed.

and differentiating with respect to time to obtain

$$\frac{dx}{dt} = v_p. \quad (9.1.17)$$

Thus the observer must be traveling in the positive x -direction at the *phase velocity* v_p . Note that the phase velocity is the same for all x and all t . This justifies the interpretation of the function δ_+ as a wave traveling in the positive x -direction.

Similar reasoning shows that an observer must travel in the negative x -direction with speed v_p to observe a constant spatial distribution of δ_- .

Phase velocities for rods made of representative elastic materials are given in Table 9.1.

Because the waves δ_+ and δ_- propagate with constant speed and do not change their shape (or disperse) with time, they are referred to as non-dispersive. For any given problem the functions δ_+ and δ_- are determined by initial conditions and boundary conditions. This is illustrated with simple examples. In the process we introduce techniques that will prove useful in later sections in which the wave propagation will not be so simple as in the thin rod.*

9.1.1a Wave Propagation and Characteristics

We first consider the dynamics of a thin elastic rod of infinite length with general initial conditions given by

$$v(x, 0) = \frac{\partial \delta}{\partial t}(x, 0) = v_o(x), \quad (9.1.18)$$

$$T(x, 0) = E \frac{\partial \delta}{\partial x}(x, 0) = T_o(x), \quad (9.1.19)$$

* The reader may be familiar with waves in transmission lines, which are fully analogous to those considered here. To see this, note that (9.1.9) and (9.1.12) can be written (with $F_1 = 0$) as

$$\rho \frac{\partial v}{\partial t} = \frac{\partial T}{\partial x}; \quad \frac{\partial T}{\partial t} = E \frac{\partial v}{\partial x},$$

which are to be compared with the equations

$$L \frac{\partial I}{\partial t} = - \frac{\partial V}{\partial x}; \quad \frac{\partial V}{\partial t} = - \frac{1}{C} \frac{\partial I}{\partial x},$$

where I and V are the transmission line voltage and current and L and C are the inductance and capacitance per unit length. A discussion of wave transients on transmission lines is given in R. B. Adler, L. J. Chu, and R. M. Fano, *Electromagnetic Energy Transmission and Radiation*, Wiley, New York, 1960, p. 127.

where v is the local velocity $\partial\delta/\partial t$. Note that the two independent initial conditions necessary for the solution of the second-order differential equation (9.1.13) are specified as two independent derivatives of δ . The initial conditions can be specified in other ways.

In what follows we find it convenient to replace the two independent variables x and t by two new independent variables α and β defined by

$$\alpha = x - v_p t, \tag{9.1.20}$$

$$\beta = x + v_p t. \tag{9.1.21}$$

Thus we write (9.1.14) as

$$\delta = \delta_+(\alpha) + \delta_-(\beta), \tag{9.1.22}$$

and we use the definition of velocity v as $\partial\delta/\partial t$ and (9.1.12) to write the velocity and stress in terms of δ_+ and δ_- as

$$v(x, t) = -v_p \left[\frac{d\delta_+}{d\alpha} - \frac{d\delta_-}{d\beta} \right], \tag{9.1.23}$$

$$T(x, t) = E \left[\frac{d\delta_+}{d\alpha} + \frac{d\delta_-}{d\beta} \right]. \tag{9.1.24}$$

It is useful to view the behavior on an x - t plane, as illustrated in Fig. 9.1.6. Formally, we wish to find the values of v and T at any point (x, t) for $t > 0$, given the values of v and T at $t = 0$ (along the x -axis in Fig. 9.1.6). To achieve

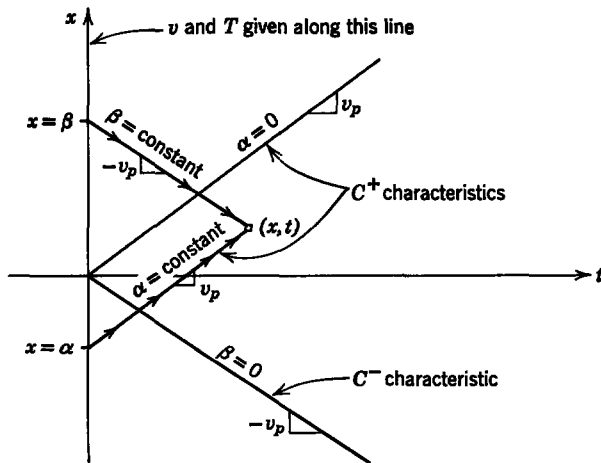


Fig. 9.1.6 The characteristic lines (9.1.20) and (9.1.21) in the x - t plane showing the C^+ and C^- characteristics that intersect at the point (x, t) .

this we solve (9.1.23) and (9.1.24) to obtain

$$\frac{d\delta_+}{d\alpha}(\alpha) = \frac{1}{2} \left[\frac{T(x, t)}{E} - \frac{v(x, t)}{v_p} \right], \quad (9.1.25)$$

$$\frac{d\delta_-}{d\beta}(\beta) = \frac{1}{2} \left[\frac{T(x, t)}{E} + \frac{v(x, t)}{v_p} \right]. \quad (9.1.26)$$

The left side of (9.1.25) is a function of α alone; consequently, for a particular value of α , $d\delta_+/d\alpha$ is constant. We find the value of the constant by recognizing that at $t = 0$, $x = \alpha$ (9.1.20), and the constant value of (9.1.25) is determined by using the initial conditions of (9.1.18) and (9.1.19) thus:

$$\frac{d\delta_+}{d\alpha}(\alpha) = \frac{1}{2} \left[\frac{T_o(\alpha)}{E} - \frac{v_o(\alpha)}{v_p} \right]. \quad (9.1.27)$$

In a similar manner we note that the left side of (9.1.26) is a function of β alone. For any value of β we determine $d\delta_-/d\beta$ by noting that at $t = 0$, $x = \beta$ (9.1.21) and using the initial conditions of (9.1.18) and (9.1.19) to obtain

$$\frac{d\delta_-}{d\beta}(\beta) = \frac{1}{2} \left[\frac{T_o(\beta)}{E} + \frac{v_o(\beta)}{v_p} \right]. \quad (9.1.28)$$

The value of T (or v) can now be found at any point (x, t) in the plane of Fig. 9.1.6 by using the facts that $d\delta_+/d\alpha$ is constant along a path of constant α and $d\delta_-/d\beta$ is constant along a path of constant β . As indicated by (9.1.20) and (9.1.21), $\alpha = \text{constant}$ and $\beta = \text{constant}$ are straight lines in the x - t plane. All lines of constant α are parallel with a positive slope of v_p and the line for $\alpha = 0$ passes through the origin as indicated. All lines of constant β are parallel with a slope $-v_p$ and the $\beta = 0$ line passes through the origin.

The lines $\alpha = \text{constant}$ and $\beta = \text{constant}$ in the x - t plane are called *characteristics*.* Because α is the argument of δ_+ , we refer to the family of lines $\alpha = \text{constant}$ as the C^+ characteristics. Similarly, the family of lines representing $\beta = \text{constant}$ are called the C^- characteristics.

A particular point (x, t) is the intersection of one C^+ and one C^- characteristic, as illustrated in Fig. 9.1.6. The particular values of α and β are given by (9.1.20) and (9.1.21) for the values of x and t at the point in question. Hence we can find the value of T or v at any point in the x - t plane by using these values of α and β in (9.1.27) and (9.1.28) and those results in (9.1.23) and (9.1.24) to find the stress $T(x, t)$ and the velocity $v(x, t)$; for example, the stress is found to be

$$T(x, t) = \frac{E}{2} \left\{ \left[\frac{T_o(x - v_p t)}{E} - \frac{v_o(x - v_p t)}{v_p} \right] + \left[\frac{T_o(x + v_p t)}{E} + \frac{v_o(x + v_p t)}{v_p} \right] \right\}. \quad (9.1.29)$$

* R. Courant and K. O. Friedrichs, *Supersonic Flow and Shock Waves*, Interscience, New York, 1948, Chapter II.

Physically we have found that the instantaneous value of the stress T (or velocity v) at the point (x, t) is determined by the initial ($t = 0$) values of stress and velocity at the positions $x = \alpha$ and $x = \beta$ along the rod. The initial conditions at $x = \alpha$ propagate (along the C^+ characteristic) in the positive x -direction with the velocity v_p and reach the point x under observation at the time t at which the measurement is to be made. Similarly, initial conditions at $x = \beta$ propagate (along the C^- characteristic) in the negative x -direction with velocity v_p and reach the point x at time t . Thus the values of T and v at (x, t) depend on the initial conditions at only two points. This is a property of nondispersive waves.

Before we consider a particular example we make one further observation. There is no mathematical reason why we could not find a solution to (9.1.13) for points to the left of the x -axis in Fig. 9.1.6. We could make an argument similar to the one just given to find the values of $d\delta_+/d\alpha$ and $d\delta_-/d\beta$ at a point $(x, t < 0)$ by following the characteristics from the x -axis to the point in question. In doing so, however, we would have assumed that the data at $t = 0$ can determine the dynamics before $t = 0$; that is, we would have made the present depend on the future. Implicit to our solution is the assumption, based on independent physical reasoning, that in terms of time the cause must come before the effect. When this physical reasoning is used to discriminate between solutions, we invoke the condition of causality.* We shall find it necessary to make further use of this condition to provide physically meaningful initial conditions and boundary conditions.

Example 9.1.2. As a special case, we consider the motions of the thin rod shown in Fig. 9.1.7. External forces are applied at the cross sections $x = a$ and $x = -a$ to produce an initial stress T_m over the length $-a < x < a$. With the rod in a static condition ($v = 0$), these forces are removed to give the initial stress distribution shown in Fig. 9.1.8. In this figure the x - t plane forms the "floor" of a three-dimensional plot, where the stress T provides the vertical axis. Hence at $t = 0$ the stress distribution is uniform along the x -axis between the points $x = \pm a$ and zero elsewhere. Because the initial conditions and

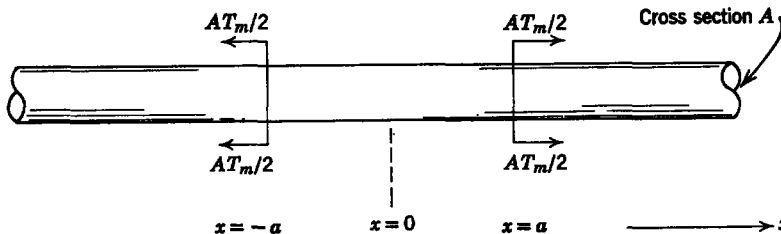


Fig. 9.1.7 Thin rod subject to an initial uniform static stress T_m over the section $-a < x < a$. At $t = 0$ the external forces $AT_m/2$ are removed.

* See, for example, P. M. Morse and H. Feshbach, *Methods of Theoretical Physics*, McGraw-Hill, New York, 1953, p. 834.

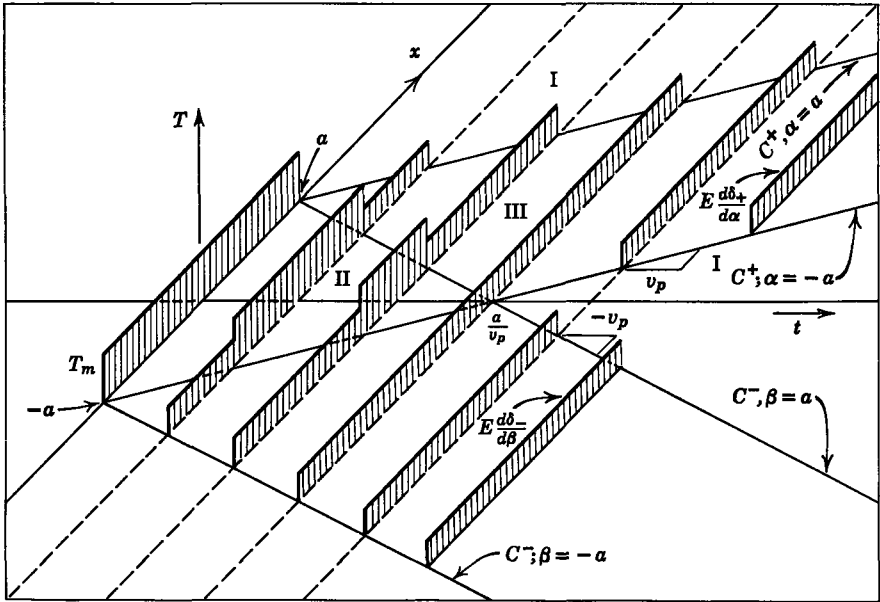


Fig. 9.1.8 Stress distribution T as a function of x at succeeding instants in time. When $t = 0$, the stress is uniform between $x = a$ and $x = -a$ and zero elsewhere; the velocity is zero.

the characteristics are symmetrical about the t -axis, we confine our attention to the half of the x - t plane in which $x \geq 0$.

The C^+ and C^- characteristics intersecting the x -axis at $x = \pm a$ are shown plotted in the x - t plane. We see that these particular characteristics divide the $x > 0$ half of the x - t plane into three types of regions, labeled I, II, and III in Fig. 9.1.8. These regions have the following properties:

- I The characteristics that cross at the point (x, t) originate on the x -axis, where $T = 0$ ($x > a, x < -a$). There are two of these regions.
- II The characteristics that cross at the point (x, t) originate on the x -axis, where $T = T_m$ ($-a < x < a$).
- III Of the characteristics that cross at the point (x, t) , C^+ originates when $t = 0$ where $T = T_m$ ($-a < x < a$), and C^- originates where $T = 0$ ($x > a$).

From (9.1.27) and (9.1.28) it follows that in

Region I

$$\frac{d\delta_+}{d\alpha} = 0, \quad \frac{d\delta_-}{d\beta} = 0.$$

Region II

$$\frac{d\delta_+}{d\alpha} = \frac{T_m}{2E}, \quad \frac{d\delta_-}{d\beta} = \frac{T_m}{2E}.$$

Region III

$$\frac{d\delta_+}{d\alpha} = \frac{T_m}{2E} \quad \frac{d\delta_-}{d\beta} = 0.$$

The stress distribution now follows from (9.1.24), and this is plotted at succeeding instants of time in Fig. 9.1.8. The edge of the initial stress distribution at $x = a$ propagates along the C^+ and C^- characteristics originating at $x = a$, and similarly the edge at $x = -a$ propagates along the C^+ and C^- characteristics originating at $x = -a$. In Region I the front edge of the forward traveling wave has not had time to arrive from $x = a$, hence the stress is still zero. In Region II the backward traveling wave from $x = a$ and the forward traveling wave from $x = -a$ have not had time to arrive and the stress is still T_m . In Region III, however, the forward wave has arrived from $x = a$ but the backward wave from $x = -a$ has not yet arrived. For time $t > a/v_p$ the waves are two separate pulses propagating with the velocity v_p in the $+x$ and $-x$ directions, respectively.

We have followed the development of the waves graphically to encourage a physical understanding of the relationship between the characteristics and the wave propagation. If we required an analytical result only, (9.1.29) could be used with the initial conditions

$$\begin{aligned} T_0(x) &= T_m[u_{-1}(x+a) - u_{-1}(x-a)], \\ v_0(x) &= 0, \end{aligned}$$

where $u_{-1}(x+a)$ is a unit step function defined as

$$\begin{aligned} 1 &\text{ for } x > -a, \\ 0 &\text{ for } x < -a, \end{aligned}$$

to obtain the result

$$T = \frac{T_m}{2} [u_{-1}(x - v_p t + a) - u_{-1}(x - v_p t - a) + u_{-1}(x + v_p t + a) - u_{-1}(x + v_p t - a)].$$

This expression is the same as that found with our graphical solution. When the initial conditions are given as complicated analytical functions of x , the analytical approach is more convenient than the graphical approach.

Attention has so far been confined to the dynamics near the center of a very long rod. In an actual rod the waves shown in Fig. 9.1.8 will eventually encounter ends or boundaries. The resulting dynamics are the subject of the next subsection.

9.1.1b Wave Reflection at a Boundary

Constraints imposed on the ends of the rod enter the mathematical description as boundary conditions; for example, an end may be free, as shown in Fig. 9.1.9a, in which case force equilibrium (for a thin slice of the material at the very end) requires that the instantaneous stress be zero. More obviously, if the end is fixed (Fig. 9.1.9b), the velocity must always be zero. In general, the ends can be attached to springs, masses, and dampers, or, as we shall see in Section 9.1.2, they can be excited by electromechanical transducers which act essentially as dependent mechanical sources.

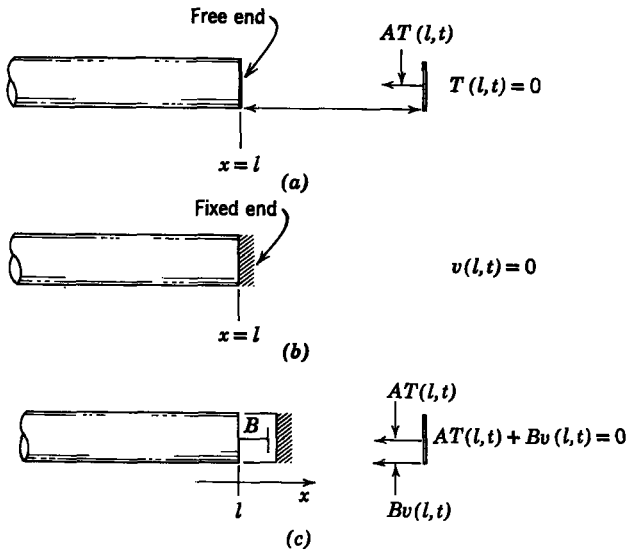


Fig. 9.1.9 Simple boundary conditions on the end of a thin rod: (a) free end; (b) fixed end; (c) end attached to a damper producing a total force Bv .

Force equilibrium on the end of an elastic rod attached to a linear damper, as illustrated in Fig. 9.1.9c, yields a boundary condition of the form

$$v(l, t) + CT(l, t) = 0, \quad (9.1.30)$$

where C is a constant ($C = A/B$ in Fig. 9.1.9c). This expression can also be used in its limiting forms to represent fixed and free end conditions; for example, if $C = 0$ (an infinitely stiff damper), we have the fixed end condition ($v = 0$) in Fig. 9.1.9b, whereas if $C \rightarrow \infty$ (limit of zero damping constant B) the free end condition ($T = 0$) in Fig. 9.1.9a results. A boundary condition of the form of (9.1.30) is used to illustrate the influence of boundary conditions on the dynamic behavior of a thin elastic rod.

We indicated in (9.1.14) that the motion in the rod is specified at any point by two waves, δ_+ propagating in the $+x$ -direction and δ_- which propagates in the $-x$ -direction. We further pointed out that the functions δ_+ and δ_- are determined by initial and boundary conditions. A wave that encounters a boundary is reflected; thus a forward wave δ_+ becomes a backward wave δ_- at a boundary. The relation between the incident and reflected waves depends on the boundary condition, as expressed by (9.1.30).

In Section 9.1.1a we learned that the δ_+ and δ_- waves propagate with constant amplitude along the C^+ and C^- characteristics. Hence a point in the x - t plane, such as A , shown in Fig. 9.1.10, is unaffected by the boundaries because it is the intersection of characteristics that do not originate on the

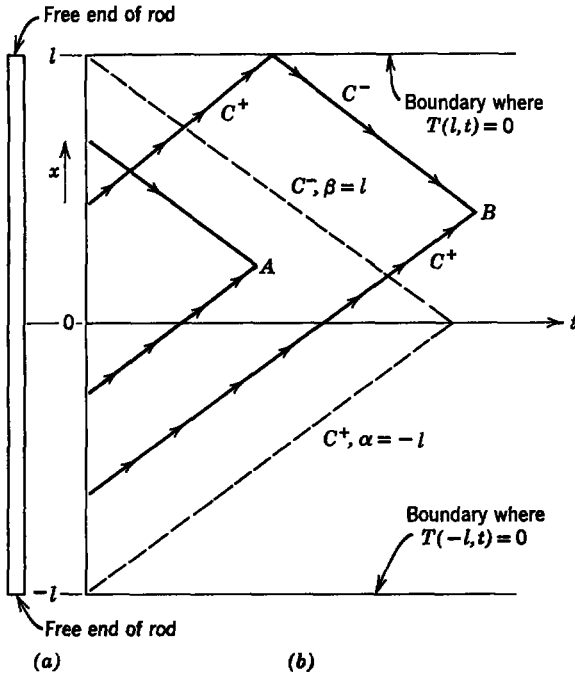


Fig. 9.1.10 (a) Thin rod of length $2l$ centered at $x = 0$; (b) an $x-t$ plot showing the characteristics relevant to the effect of the ends on the dynamics.

boundaries. At points such as B , however, outside the cone formed by the C^- characteristic $\beta = l$ and the C^+ characteristic $\alpha = -l$, one or both of the intersecting characteristics C^+ and C^- originates on a boundary; for example, the values of T and v at the point B shown in Fig. 9.1.10 are determined by a C^+ characteristic originating on the initial conditions at $t = 0$ and a C^- characteristic originating on the boundary at $x = l$. Hence we must use the boundary condition to determine the value of $(d\delta_-/d\beta)(\beta)$ along the C^- characteristic. To do this we set $x = l$ and substitute (9.1.23) and (9.1.24) into (9.1.30) and solve for $d\delta_-/d\beta$:

$$\frac{d\delta_-}{d\beta}(\beta) = -\frac{d\delta_+}{d\alpha}(\alpha) \left(\frac{CE - v_g}{CE + v_g} \right). \tag{9.1.31}$$

In this equation $d\delta_+/d\alpha$ is the value for the incident wave and thus is determined for this problem by the initial condition at $t = 0, x = \alpha$. As indicated by (9.1.31), the boundary condition and the incident wave determine completely the value of the reflected wave that propagates along the C^- characteristic. Analogous arguments can be made at the boundary $x = -l$, where the δ_- wave reflects as a δ_+ wave.

When a wave encounters more than one boundary before it reaches the point of interest in the $x-t$ plane, the boundary conditions must be applied at each reflection to find the properties of the wave at the point in question.

Example 9.1.3. As an example of the reflection of waves from the boundaries, we continue with Example 9.1.2, introduced in Section 9.1.1a. We found there that the initial distribution of stress near the center of the rod resolved itself into waves that propagated in the $+x$ and $-x$ -directions. When the rod is terminated in free ends, as shown in Fig. 9.1.10, these waves will be subject to boundary condition (9.1.30) in which $C \rightarrow \infty$ at $x = \pm l$.

$$T(l, t) = 0, \tag{a}$$

$$T(-l, t) = 0. \tag{b}$$

The use of either of these boundary conditions with (9.1.24) indicates that at a free boundary

$$\frac{d\delta_+}{d\alpha} = -\frac{d\delta_-}{d\beta}; \tag{c}$$

that is, the reflected stress wave must be equal in magnitude but opposite in sign to the incident wave to maintain the zero-stress boundary condition.

We use the condition of (c) with (9.1.24) to construct the solutions shown in Fig. 9.1.11. When we describe the two stress waves as T_+ and T_- , we find that a T_+ wave originating at point C at which $T = T_m$ and $T_+ = T_- = T_m/2$ is reflected at the boundary $x = l$ at point D as a negative traveling wave $T_- = -T_m/2$. Hence just after $t = (l - a)/v_p$ the leading edge of the T_+ wave is canceled by the reflected T_- wave.

It is clear from (9.1.31) that if $CE - v_p = 0$ no wave will be reflected by the boundary. With (9.1.15), this condition becomes

$$C = \frac{1}{\sqrt{\rho E}}, \tag{9.1.32}$$

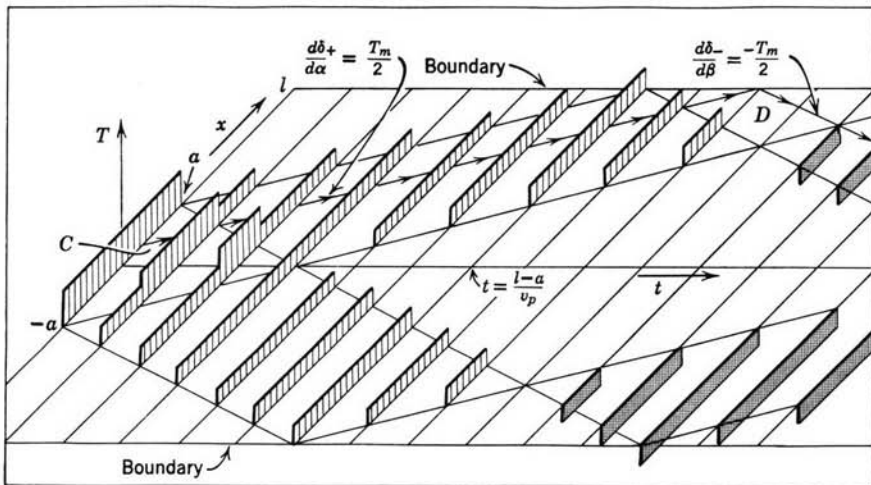


Fig. 9.1.11 Propagation of an initial pulse of stress on a rod terminated at $x = \pm l$ in free ends.

and the boundary condition 9.1.30 is

$$v(l, t) + \frac{1}{\sqrt{E\rho}} T(l, t) = 0. \tag{9.1.33}$$

One way in which this boundary condition can be obtained is shown in Fig. 9.1.9c, in which the rod is terminated in a viscous damper with a constant B . Force equilibrium for the end of the rod is the same as condition (9.1.33) if

$$B = A\sqrt{\rho E}; \tag{9.1.34}$$

that is, if the viscous damper has this coefficient, an incident wave will not be reflected*

Example 9.1.4. We can illustrate the significance of the boundary condition given by (9.1.33) by considering the dynamics that result if the end of a static rod is given the excitation $T(0, t) = T_0(t)$, as shown in Fig. 9.1.12. Because all the C^- characteristics either originate on the x -axis (at a time when there is no motion and no stress in the rod) or on the boundary at $x = l$, where no reflected waves can arise because of the boundary condition, we conclude that $d\delta_-/d\beta$ is zero everywhere in the portion of the x - t plane pertinent to the problem (Fig. 9.1.12). We can evaluate $d\delta_+/d\alpha$ at $x = 0$ from the excitation condition and (9.1.24); that is, the C^+ characteristic originating at $t = t'$ is given by [see (9.1.20)] $\alpha = -v_p t'$, hence we can write

$$\left. \frac{d\delta_+}{d\alpha} \right|_{\alpha=-v_p t'} = \frac{T_0(t')}{E}. \tag{a}$$

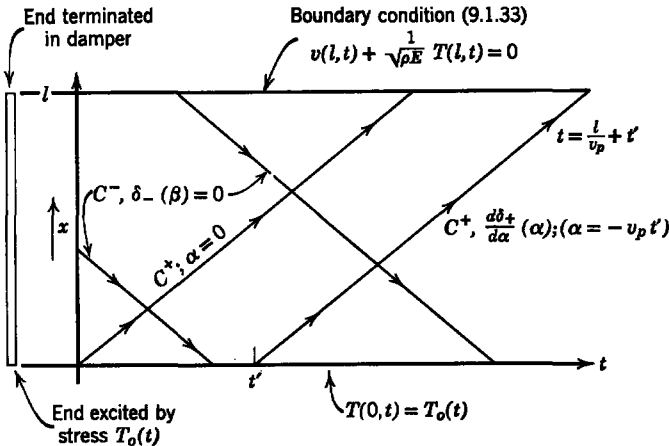


Fig. 9.1.12 Excitation $T_0(t)$ at one end of a thin rod transmitted to a matched end at $x = l$.

* In the terminology of transmission line theory we say that the termination is “matched” to the rod or that the rod is terminated in its “characteristic impedance.” See R. B. Adler, L. J. Chu, and R. M. Fano, *Electromagnetic Energy Transmission and Radiation*, Wiley, New York, 1960, pp. 88–90.

It follows that along the characteristic

$$\alpha = -v_p t' = x - v_p t \quad (b)$$

we have

$$T(x, t) = T_o(t'). \quad (c)$$

Equation b relates t' to t and allows us to write (c) as

$$T(x, t) = T_o\left(t - \frac{x}{v_p}\right). \quad (d)$$

In particular, at the end of the rod where $x = l$,

$$T(l, t) = T_o\left(t - \frac{l}{v_p}\right). \quad (e)$$

As we expected, we have found that a signal $T_o(t)$, introduced on the rod at the end where $x = 0$, appears at the opposite end delayed by the time l/v_p , or the time required for the signal (d) to travel the length of the rod. With the boundary condition of (9.1.33), a pulse introduced at one end will travel the length of the rod and leave no after effects in the form of reflections.

Wave propagation on a thin rod with a boundary condition in the form of (9.1.33) will play a basic role in the electromechanical delay line described in Section 9.1.2.

9.1.2 Electromechanical Coupling at Terminal Pairs

One of the most important ways in which coupling occurs between electric or magnetic fields and continuous media is through the boundary conditions. In the one-dimensional motions considered in this section the boundaries can be described in terms of the displacement (or velocity) and the stress evaluated at a fixed point in space (x). Because these boundary variables are only functions of time, they form a mechanical terminal pair; for example, if the end of the rod is at $x = 0$, the terminal pair of Fig. 9.1.13b can be used to describe the boundary condition applied to the thin rod in Fig. 9.1.13a.

Lumped-parameter electromechanical devices are often coupled to mechanical terminal pairs formed from boundary variables in much the same way as discussed in Chapters 2 and 5. As an example, Fig. 9.1.13a shows a plunger attached to the end of the rod (at $x = 0$, say). This plunger is subject to a force of electrical origin, as shown, and has the position $y(t)$. Other forces acting on the plunger are the forces $AT(0, t)$ from the attached rod and an inertial force. Within an arbitrarily defined constant, the displacement at the end of the rod is y or $y(t) = \delta(0, t)$.

Figure 9.1.13b formalizes the mechanical terminal pair. We write the force equilibrium equation as

$$M \frac{d^2 \delta(0, t)}{dt^2} = AT(0, t) + f^e. \quad (9.1.35)$$

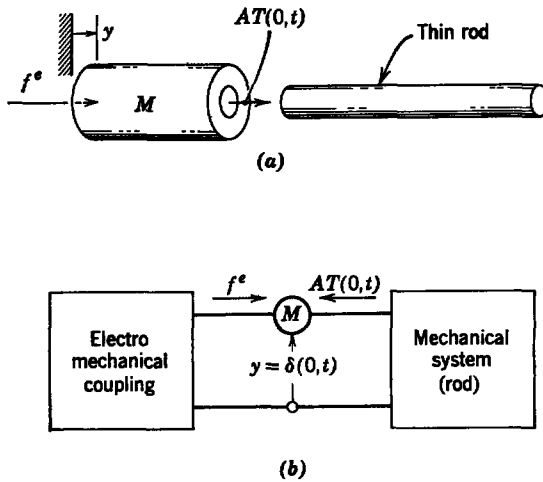


Fig. 9.1.13 Electromechanical coupling at the end of a thin rod: (a) physical system; end of rod attached to mass M acted on by the force of electric origin f^e ; (b) formal representation.

Note that, in general, f^e will involve the displacement $\delta(0, t)$ and electrical variables such as currents. The force equation (9.1.35) is the boundary condition presented by the coupling network to the distributed mechanical system. Its significance is demonstrated in the following example.

Example 9.1.5. Transmission systems that support nearly nondispersive waves are required to transmit a signal with a minimum of distortion. As we have pointed out, electromagnetic transmission lines have much the same dynamical behavior as the elastic rod that is the subject of this section. Because it takes a finite time for waves to propagate from one end of these systems to the other, a common application is to the production of time delays.

Acoustic waves propagate with velocities that are on the order of 4000 m/sec, as shown for various materials in Table 9.1. By contrast, electromagnetic waves propagate with velocities on the order of the speed of light in free space (3×10^8 m/sec). Hence the mechanical waves are useful in producing long time delays* (on the order of 10^{-3} sec). If, however, an electrical signal is required, it is necessary to use electromechanical coupling at the input and output of the mechanical structure. One system is shown in Fig. 9.1.14a. The input signal is the current $i_i(t)$ applied to the terminals of the transducer to the left. By proper design this current produces an electrical force on the left end of the elastic rod that is essentially proportional to the current i_i . This force is transmitted in the form of a stress wave to the right end of the rod, where it produces motion of the magnetic plunger in the output transducer hence an induced voltage $v_o(t)$. The conductance G and inductance L of the terminal pair (i_2, λ_2) are adjusted to absorb the transmitted wave without producing a reflected wave traveling in the $-x$ -direction. In this way the system is designed so that v_o is proportional to $i_i(t)$ delayed by l/v_p sec.

* See, for example, W. P. Mason, ed., *Physical Acoustics*, Academic, New York, 1964, Vol. 1, Part A, Chapters 6 and 7.

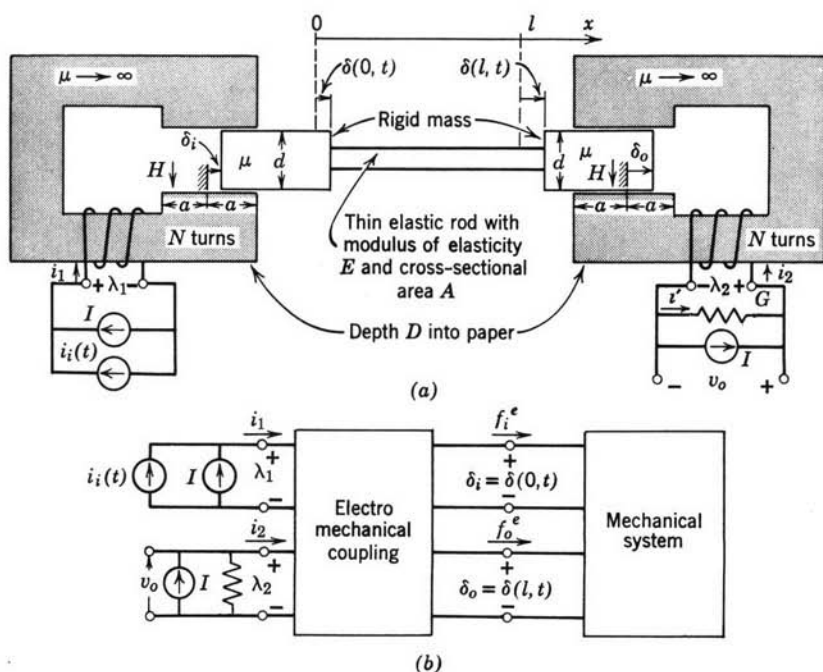


Fig. 9.1.14 (a) Electromechanical delay line designed to give an output signal $v_o(t)$ which is proportional to $i_i(t)$ delayed by l/v_p sec; (b) circuit representation of (a).

We begin by finding the force f_i^e of electrical origin on the plunger of the input transducer. This is a simple application of the ideas introduced in Chapters 2 and 3*. The magnetic field intensity in the gap of the magnetic circuit is assumed to be uniform so that in the gap

$$H = \frac{Ni_1}{d}. \quad (a)$$

Hence the flux density through the plunger is B_1 and through the air gap, B_2 , where

$$B_1 = \frac{\mu Ni_1}{d}, \quad (b)$$

$$B_2 = \frac{\mu_0 Ni_1}{d}.$$

The terminals (i_1, λ_1) link the total flux through the gap N times and we can write

$$\lambda_1 = N[(a - \delta_i)DB_1 + (a + \delta_i)DB_2], \quad (c)$$

where

$$\delta_i = \delta(0, t).$$

* Essential equations summarized in Tables 2.1 and 3.1, Appendix E.

We substitute (a) and (b) into (c) and arrange the result in the form

$$\lambda_1 = L_0 \left[\left(\frac{\mu + \mu_0}{\mu - \mu_0} \right) - \left(\frac{\delta_i}{a} \right) \right] i_1, \quad (d)$$

where

$$L_0 = \frac{N^2 D a (\mu - \mu_0)}{d} \quad (e)$$

The transducer is electrically linear; hence*

$$W'_m = \frac{1}{2} L_0 \left(\frac{\mu + \mu_0}{\mu - \mu_0} - \frac{\delta_i}{a} \right) i_1^2, \quad (f)$$

and†

$$f_i^e = \frac{\partial W'_m}{\partial \delta_i} = - \frac{L_0 i_1^2}{2a}. \quad (g)$$

Now, we want this force to be proportional to the driving current i_i , and this is the purpose of the biasing current I . From the circuit in Fig. 9.1.14 we write

$$(i_1)^2 = (I + i_i)^2 \approx I^2 + 2Ii_i, \quad (h)$$

where we are assuming that the bias current I is large enough to justify dropping the term i_i^2 . In practice, the bias field produced by I may be obtained from a permanent magnet placed in the magnetic circuit. The equivalence of the current excitation and the permanent magnet is discussed in Section 2.1.1.

We are now able to write the force equation for the plunger, which we recognize as (9.1.35) with $\delta = \delta_i$. A further approximation, justified by our design requirements, is made at this point. If we wish to make the stress $T(0, t)$ in (9.1.35) proportional to the applied force (hence to the input current), we must design the system with the mass M small enough to make the inertia force negligible under the desired operating conditions. This approximation becomes less accurate as the frequency is raised. The inertia force is a factor to be considered if the fidelity of the delay line is to be explored in detail.

With the assumption of *negligible inertia force*, (9.1.35) becomes

$$AT(0, t) - \frac{L_0}{2a} (I^2 + 2Ii_i) = 0, \quad (i)$$

where we have used (g) and (h) to write the force f^e . From this expression it is clear that the stress $T(0, t)$ will have a constant part due to the bias current I and a time-varying part due to the signal current i_i . Thus we write

$$T(0, t) = T_s + T'(0, t), \quad (j)$$

where

$$T_s = \frac{L_0 I^2}{2aA} \quad (k)$$

$$T'(0, t) = \frac{L_0 I}{aA} i_i(t). \quad (l)$$

The output transducer is identical to the input transducer and has the same bias current I . Consequently, under equilibrium conditions the output transducer applies a force AT_s to the end of the rod at $x = l$ equal in magnitude and opposite in direction to the force applied

* Equation k, Table 3.1, Appendix E.

† Equation g, Table 3.1, Appendix E.

at $x = 0$ by the input transducer. The result of this equilibrium stress T_s is a slight elongation of the rod, very much as described in Example 9.1.1. Our equations of motion are linear; thus we can superimpose the displacements due to T_s and T' . Because we are interested only in the response to T' , we ignore the equilibrium elongation due to T_s^* and assume that displacements δ_i and δ_o are the increments of displacement due to the driving signal $T'(0, t)$.

As stated at the outset, we wish to have no reflected waves at $x = l$; consequently, we must make (9.1.33) the boundary condition at $x = l$. We now specify the properties of the output transducer that are necessary to achieve this end. Because

$$v(l, t) = \frac{d\delta_o}{dt},$$

the desired form of the boundary condition is

$$\frac{d\delta_o}{dt} + \frac{1}{\sqrt{\rho E}} T(l, t) = 0. \quad (m)$$

We write the equation of motion for the plunger of the output transducer

$$M \frac{d^2\delta_o}{dt^2} = f_o^e - AT(l, t). \quad (n)$$

The inertia force must be negligible under the desired operating conditions to achieve the boundary condition of (m). For this case (n) reduces to

$$f_o^e - AT(l, t) = 0. \quad (o)$$

Next, we recognize that the two transducers are identical except for the definition of the plunger displacement. Thus we obtain the properties of the output transducer from (d) to (g) by replacing δ_i with $-\delta_o$ and i_1 with i_2 . The force f_o^e is

$$f_o^e = \frac{L_0 i_2^2}{2a}. \quad (p)$$

We write

$$i_2(t) = I + i'(t), \quad (q)$$

with $|i'(t)| \ll I$. Then, dropping equilibrium terms from (o), we can write the incremental (time-varying) boundary condition as

$$\frac{L_0 I}{a} i' - AT'(l, t) = 0. \quad (r)$$

From Fig. 9.1.14 we recognize that the current i' is that flowing through the conductance G and is therefore given by

$$i' = -G \frac{d\lambda_2}{dt} \quad (s)$$

y analogy with λ_1 (d), λ_2 is

$$\lambda_2 = L_0 \left(\frac{\mu + \mu_0}{\mu - \mu_0} + \frac{\delta_o}{a} \right) (I + i'),$$

*Care must be exercised in generalizing this assumption; for example, if the force f^e is dependent on δ_i (as it is not in this example) and the rod is very long, the equilibrium displacement can affect the behavior markedly. In any such case, however, a correct analysis can be obtained by exercising care in linearizing the force f^e in terms of equilibrium and perturbation variables.

and (s) can be written, correct to linear terms in time-varying quantities, as

$$i' = -G \left[L_0 \left(\frac{\mu + \mu_0}{\mu - \mu_0} \right) \frac{di'}{dt} + \frac{L_0 I d\delta_o}{a dt} \right]. \quad (t)$$

It is clear from (m) and (r) that the current i' must be proportional to $d\delta_o/dt$ if (m) is to be satisfied. Consequently, the output transducer must be operated in a regime such that

$$\frac{L_0 I d\delta_o}{a dt} \gg L_0 \left(\frac{\mu + \mu_0}{\mu - \mu_0} \right) \frac{di'}{dt}$$

Assuming that this condition is satisfied, (t) becomes

$$i' = - \frac{GL_0 I d\delta_o}{a dt} \quad (u)$$

and (m) and (r) become identical when

$$\frac{Aa^2}{GL_0^2 I^2} = \frac{1}{\sqrt{\rho E}}. \quad (v)$$

With the parameters thus adjusted, the conductance G absorbs the incident wave in the same way that the mechanical damper absorbed the incident wave in Section 9.1.1b.

With the driving stress $T'(0, t)$ given by (l) and with no reflected waves at $x = l$, the stress $T'(l, t)$ is

$$T'(l, t) = \frac{L_0 I}{aA} i_i \left(t - \frac{l}{v_p} \right), \quad (w)$$

where we have used the relation $T'(l, t) = T'(0, t - l/v_p)$ as shown in Example 9.1.4. The use of this result in r yields

$$i'(t) = i_i \left(t - \frac{l}{v_p} \right) \quad (x)$$

and the output voltage is

$$v_o = - \frac{i'(t)}{G} = - \frac{i_i(t - l/v_p)}{G} \quad (y)$$

Thus, with identical transducers and no reflected waves at $x = l$, the current i' is simply the driving current delayed by a time interval l/v_p and the output voltage $v_o(t)$ is a delayed replica of the input current $i_i(t)$.

In a practical device that uses wave propagation in an elastic material to obtain a time delay both electrical and mechanical damping are normally needed to obtain a matched condition and no reflections. Also, most practical electromechanical delay lines use magnetostrictive or piezoelectric transducers rather than the simple ones of our example.

9.1.3 Quasi-statics of Elastic Media

In the example of Fig. 9.1.14 the ends of the elastic rod are attached to plungers. In the analysis of Example 9.1.5 it is assumed that the plungers can be modeled as rigid masses but that the rod is deformable. Presumably, both the rod and the plungers are constructed of materials that exhibit elastic properties; consequently, the assumption is justified when signal transmission

(elastic wave propagation) through the plungers requires a time that is short compared with the time of transmission through the rod. In an intuitive way we recognize this as the condition that the plungers must be made of "stiffer" material than the rod; or, if both plungers and rod are made of the same material, the rod must be much longer than the plungers.

In this section we use the thin rod to illustrate the criteria that must be met in order to use lumped parameter models (see Section 2.2) for bodies made of elastic materials. The justification for lumped-parameter mechanical models is similar to the justification for using lumped-parameter electric circuit models. Hence our arguments in this section are similar to those presented in Section B.2.2.

Equations 9.1.9 and 9.1.12 are the equations of motion for the rod, which we write here in terms of the velocity $v(x, t) = \partial\delta/\partial t$ (with the body force density $F_1 = 0$):

$$\frac{\partial T}{\partial x} = \rho \frac{\partial v}{\partial t}, \quad (9.1.36)$$

$$\frac{\partial v}{\partial x} = \frac{1}{E} \frac{\partial T}{\partial t}. \quad (9.1.37)$$

If we have truly static solutions (a better name is time-independent solutions), we set the time derivatives equal to zero in (9.1.36) and (9.1.37) and obtain

$$\frac{\partial T}{\partial x} = 0, \quad (9.1.38)$$

$$\frac{\partial v}{\partial x} = 0. \quad (9.1.39)$$

Thus for static or steady systems the velocity v and stress T are independent of space x and time t , the values of v and T being determined by the boundary conditions.

The essence of a quasi-static analysis is the assumption that the static solutions are still valid with a time-varying excitation. The steady solutions are then used with the time derivatives on the right of (9.1.36) and (9.1.37) to calculate correction terms for T and v or to evaluate the accuracy of the approximation.

The quasi-static behavior of the thin rod is highly dependent on constraints imposed by boundary conditions. Two limiting cases (boundary conditions required by a fixed or a free end) result in systems in which the static solution for v or T is zero. In these cases single lumped-parameter elements can be used to represent the rod dynamics.

There is a complete analogy between the quasi-static behavior of the thin rod and the electromagnetic quasi-statics of plane-parallel electrodes driven

at one end and terminated in either an open circuit or a short circuit at the other. These electromagnetic problems are discussed in Appendix B (Section B.2.2), in which they are used to show the relationship between the quasi-static magnetic and electric field systems.

9.1.3a The Spring

Figure 9.1.15a shows a thin rod of cross-sectional area A , modulus of elasticity E , mass density ρ , and unstretched length l attached to a fixed support at $x = 0$ and driven by a force $f(t)$ at $x = l$. It is clear that for a static system ($f = \text{constant}$) the velocity v is zero and the stress T is uniform and given by

$$T(x) = \frac{f}{A}. \tag{9.1.40}$$

We now assume that this solution is still valid when the force is time varying; thus

$$T(x, t) = \frac{f(t)}{A} \tag{9.1.41}$$

To calculate the velocity v that results from this time-varying force we must use (9.1.41) in (9.1.37) to obtain

$$\frac{\partial v}{\partial x} = \frac{1}{EA} \frac{df}{dt}. \tag{9.1.42}$$

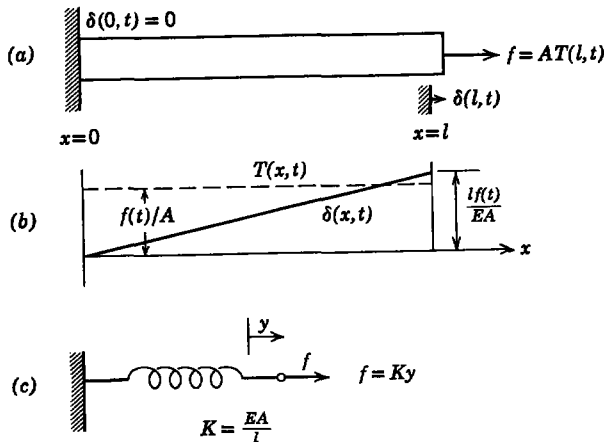


Fig. 9.1.15 (a) Thin elastic rod fixed at $x = 0$ and driven by $f(t)$ at $x = l$ showing (b) the quasi-static distribution of stress and displacement along the rod and (c) the equivalent lumped-parameter element.

Integration of this expression with respect to x and use of the boundary condition

$$v = 0 \quad \text{at} \quad x = 0$$

yields

$$v = \frac{x}{EA} \frac{df}{dt}. \quad (9.1.43)$$

We integrate this expression with respect to time and recognize that with $f = 0$, $\delta = 0$ to obtain

$$\delta(x, t) = \frac{x}{EA} f(t). \quad (9.1.44)$$

Thus, when we make the quasi-static approximation, the stress T and displacement δ are distributed along the rod, as illustrated in Fig. 9.1.15*b*.

We set

$$y(t) = \delta(l, t)$$

and write (9.1.44) as

$$y = \frac{1}{K} f, \quad (9.1.45)$$

where

$$K = \frac{EA}{l}.$$

This is the terminal relation of the spring illustrated in Fig. 9.1.15*c*. Thus we conclude that in the quasi-static approximation an elastic rod with a fixed end appears to a driving force at the other end as a massless spring.

It is worthwhile to explore the limitations on this ideal lumped-parameter model by evaluating correction terms that result from variations in stress caused by the time-varying velocity (9.1.36). This process is analogous to the evaluation of correction terms in the examples of Section B.2.2. We define the correction term for the stress as $T'(x, t)$ and write (9.1.36), using (9.1.43), as

$$\frac{\partial T'}{\partial x} = \frac{\rho x}{EA} \frac{d^2 f}{dt^2}. \quad (9.1.46)$$

We integrate with respect to x and use the boundary condition that $T' = 0$ at $x = l$ because the static solution for T accounts for the applied force. The result is

$$T' = \frac{\rho}{2EA} (x^2 - l^2) \frac{d^2 f}{dt^2}. \quad (9.1.47)$$

This correction term has a maximum magnitude at $x = 0$. Using this maximum value, we conclude that the quasi-static solution is valid, provided that

$$\left| \frac{T'}{T} \right| = \frac{\rho l^2}{2E} \frac{|d^2 f / dt^2|}{|f|} \ll 1. \quad (9.1.48)$$

We can interpret this result more effectively if we assume that

$$f = F_0 \cos \omega t.$$

Then (9.1.48) becomes

$$\left| \frac{T'}{T} \right| = \frac{l^2 \omega^2}{2v_p^2} \ll 1, \tag{9.1.49}$$

where the phase velocity $v_p = \sqrt{E/\rho}$. The wavelength of a longitudinal elastic wave of frequency ω and phase velocity v_p is

$$\lambda = \frac{2\pi v_p}{\omega}.$$

Thus we write (9.1.49) as

$$\frac{l^2 \omega^2}{2v_p^2} = 2\pi^2 \frac{l^2}{\lambda^2} \ll 1 \tag{9.1.50}$$

and conclude that the quasi-static approximation is valid, provided that the length of the rod is much shorter than an elastic wavelength at the frequency of interest. The condition of (9.1.48) can also be interpreted for transient systems by saying that the time of transmission of an elastic wave over the rod length l must be short compared with the shortest characteristic time of the driving force if the quasi-static approximation is to be valid.

9.1.3b The Mass

When the elastic rod is not fixed at $x = 0$, as it was in Fig. 9.1.15, but has a free end at $x = 0$ as shown in Fig. 9.1.16a, the quasi-static model is a

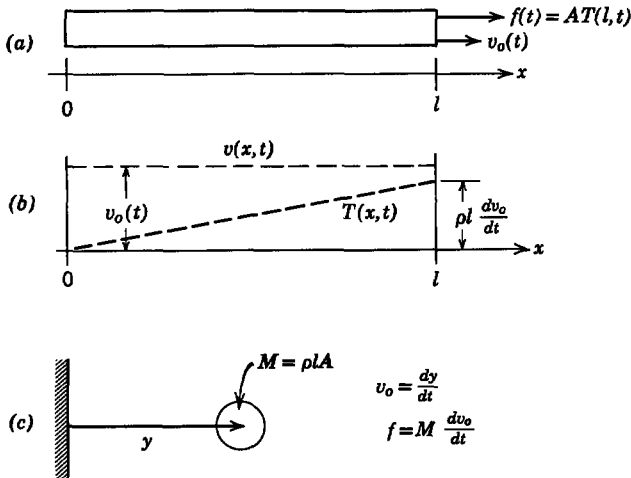


Fig. 9.1.16 (a) Thin elastic rod with free end at $x = 0$ and with end at $x = l$ driven by $v_0(t)$; (b) quasi-static distribution of stress and velocity; (c) equivalent lumped element.

rigid mass. This can be shown by specifying that at $x = l$ the rod is driven by a velocity source

$$v(l, t) = v_o(t) \quad (9.1.51)$$

For a steady solution with $v_o = \text{constant}$, the stress T is zero and the velocity is constant along the rod

$$v(x) = v_o \quad (9.1.52)$$

In a manner analogous to that of the preceding section, we now assume that v_o is time-varying but that (9.1.51) still describes the velocity distribution in the rod

$$v(x, t) = v_o(t). \quad (9.1.53)$$

We now use this velocity in (9.1.36) to write

$$\frac{\partial T}{\partial x} = \rho \frac{dv_o}{dt}, \quad (9.1.54)$$

which determines the stress. Integration of this expression and use of the free end condition ($T = 0$ at $x = 0$) yields

$$T(x, t) = \rho x \frac{dv_o}{dt} \quad (9.1.55)$$

The resulting quasi-static stress and velocity distributions are shown in Fig. 9.1.16*b*.

Evaluation of the total force supplied by the velocity source yields

$$f(t) = M \frac{dv_o}{dt}, \quad (9.1.56)$$

where $M = \rho l A$ is the total mass of the rod. This is the equation of motion for an ideal rigid mass for which the lumped element is given in Fig. 9.1.16*c*.

We could use (9.1.37) to evaluate a correction term in velocity and find the limit of accuracy of the quasi-static model. The process, however, is the same as that illustrated in the preceding section and the result, for an excitation frequency ω , is that given by (9.1.50). Thus we conclude that to model an elastic rod as a rigid mass the characteristic time of the motion must be long compared with the time taken for an elastic wave to travel from one end of the rod to the other.

Note that, because elastic waves propagate much less rapidly than electromagnetic waves, lumped-parameter mechanical models are likely to be inadequate at frequencies at which lumped electrical elements are an excellent approximation.

9.2 TRANSVERSE MOTIONS OF WIRES AND MEMBRANES

Among the most common structures used in connection with electro-mechanical systems are those that can be modeled as thin sheets or wires of elastic material subject to a large equilibrium tension. Acoustic devices are often characterized by lumped-parameter transducers coupled to wires or membranes (diaphragms). Current-carrying conductors under tension (and especially in the presence of large external magnetic fields) present continuum electromechanical problems that assume practical significance. These models also provide attractive vehicles for demonstrating many basic concepts, techniques, and phenomena of continuum electromechanics which have found application in more sophisticated configurations than are appropriate in our treatment. These applications are pointed out in the development.

The system to be considered is shown for equilibrium conditions in Fig. 9.2.1. The elastic sheet or membrane lies in the x - y plane ($z = 0$) and is assumed to be very thin in the z -direction*. It is stressed by a constant tension S (newtons per meter) applied along all four edges in the x - y plane. Thus the total force applied in the y -direction at the right-hand edge of the membrane is $S \Delta x$. The membrane has a surface mass density σ_m (kilograms per square meter).

We now wish to constrain the membrane of Fig. 9.2.1 in arbitrary ways along the edges, apply an arbitrary transverse force per unit area T_z , and describe the resulting motion. We assume that this transverse motion is small enough in amplitude that we can use a linear mathematical model. For such

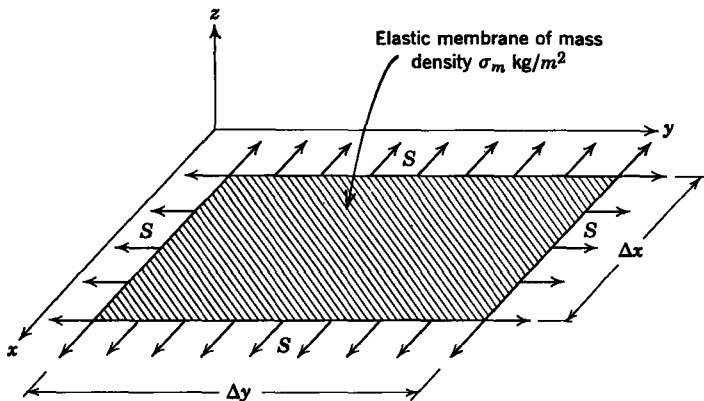


Fig. 9.2.1 A plane-elastic membrane in equilibrium subject to a tension S N/m along its edges.

* The mathematical model to be developed also describes accurately the motion of a thin sheet of fluid (bubble) whose dynamics are affected strongly by surface tension.

a case we find that the motion is independent of the elastic properties of the membrane but depends on the equilibrium tension S .

When the membrane is subjected to transverse (z -directed) excitations, it will undergo transverse motion. This motion is described by the transverse displacement $\xi(x, y, t)$ from equilibrium ($z = 0$). Thus to write the equation of motion we consider a rectangular section of membrane, with sides Δx and Δy and whose center is at position (x, y) , as illustrated in Fig. 9.2.2. We write the z -component of Newton's second law for this section and take the limit as Δx and Δy go to zero.

As stated earlier, the mathematical model is linear; consequently, we assume that the transverse displacement and its derivatives are small enough to justify the following assumptions:

1. The tension S is locally parallel to the surface of the membrane and constant in magnitude, independent of deformation.
2. The surface mass density σ_m is constant, independent of deformation.

With these assumptions we refer to Fig. 9.2.2 and write the z -component of Newton's second law as

$$\begin{aligned} \Delta x \Delta y \sigma_m \frac{\partial^2 \xi}{\partial t^2} = & S \Delta x \left[\frac{\partial \xi}{\partial y} \left(x, y + \frac{\Delta y}{2}, t \right) - \frac{\partial \xi}{\partial y} \left(x, y - \frac{\Delta y}{2}, t \right) \right] \\ & + S \Delta y \left[\frac{\partial \xi}{\partial x} \left(x + \frac{\Delta x}{2}, y, t \right) - \frac{\partial \xi}{\partial x} \left(x - \frac{\Delta x}{2}, y, t \right) \right] + T_z \Delta x \Delta y. \end{aligned} \quad (9.2.1)$$

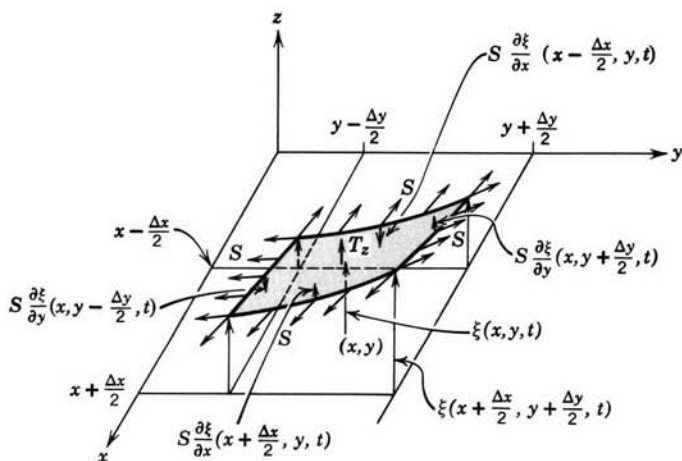


Fig. 9.2.2 Section of membrane having area $(\Delta x \Delta y)$ and subject to the uniform tension S . The displacement at the center of the section (x, y) is $\xi(x, y, t)$.

Division of this equation by the element of area $\Delta x \Delta y$ and taking the limit as $\Delta x \rightarrow 0$ and $\Delta y \rightarrow 0$ yield the desired result:

$$\sigma_m \frac{\partial^2 \xi}{\partial t^2} = S \left(\frac{\partial^2 \xi}{\partial x^2} + \frac{\partial^2 \xi}{\partial y^2} \right) + T_z. \quad (9.2.2)$$

Note that we have used essentially the same steps in deriving the equation of motion for the membrane as we used in Section 9.1 for the thin rod.

We recognize that the membrane can be excited by discrete terminal pairs (boundary conditions) or over the whole surface by the surface force density $T_z(x, y, t)$. In most cases considered in this book the surface force density T_z is of electrical origin and described mathematically as in Section 8.4. Attention is confined in this chapter to the case in which $T_z = 0$ and the membrane is excited through boundary conditions.

In the case in which the membrane is very thin in the y -direction or in which the deflection ξ does not depend on y , (9.2.2) becomes

$$\sigma_m \frac{\partial^2 \xi}{\partial t^2} = S \frac{\partial^2 \xi}{\partial x^2} + T_z. \quad (9.2.3a)$$

If we multiply this equation by a y -dimension l_y , $l_y \sigma_m$ is the mass per unit length, $S l_y$ is the total tension (newtons), and $T_z l_y$ is the z -component of an externally applied force per unit length. Written in this way, (9.2.3a) is also the equation of motion for a wire (or a "string") under large tension and constrained to move in only one transverse direction. To avoid problems with nomenclature we write the equation of motion of a string as

$$m \frac{\partial^2 \xi}{\partial t^2} = f \frac{\partial^2 \xi}{\partial x^2} + S_z, \quad (9.2.3b)$$

where m = mass per unit length (kilograms per meter),

f = total tension (newtons),

S_z = transverse force per unit length (newtons per meter).

The equations of motion for a membrane and for a string are summarized at the end of the chapter in Table 9.2.

9.2.1 Driven and Transient Response, Normal Modes

In the absence of an external force per unit length, (9.2.3a) and (9.2.3b) state that the deflections $\xi(x, t)$ of a membrane or a wire satisfy the wave equation

$$\frac{\partial^2 \xi}{\partial t^2} = v_p^2 \frac{\partial^2 \xi}{\partial x^2}, \quad (9.2.4)$$

where the phase velocity is

$$v_p = \left(\frac{S}{\sigma_m} \right)^{1/2} \text{ for a membrane,} \quad (9.2.5a)$$

$$v_p = \left(\frac{f}{m} \right)^{1/2} \text{ for a wire.} \quad (9.2.5b)$$

Hence the discussion of waves given in Section 9.1 applies equally well to the deflections of the wire shown by Fig. 9.2.3.

The sinusoidal steady-state response of physical systems is of general interest. This has been illustrated many times in the preceding chapters, both in the context of lumped-parameter systems (Chapters 4 and 5) and distributed systems (Chapter 7). The simple wire, described by (9.2.4), gives an opportunity to develop the basic relationship between the driven response of a continuous medium and its transient response. The insights afforded by the discussion that follows form a necessary prelude to understanding the continuum electromechanical examples undertaken in Chapter 10.

A wide class of problems is illustrated by considering the situation in which the wire is driven at one end ($x = -l$) by a sinusoidal excitation

$$\xi(-l, t) = \xi_a \sin \omega_a t \quad (9.2.6)$$

and fixed at the other end

$$\xi(0, t) = 0. \quad (9.2.7)$$

Physically, the excitation must be turned on at some time. For convenience we assume that this happens when $t = 0$, at which time the wire has the initial conditions

$$\xi(x, 0) = \xi_0(x), \quad (9.2.8)$$

$$\frac{\partial \xi}{\partial t}(x, 0) = \dot{\xi}_0(x). \quad (9.2.9)$$

The initial and boundary conditions are imposed along the contours shown in Fig. 9.2.4.

Now, we wish to determine the deflections $\xi(x, t)$ which satisfy these initial and boundary conditions. By analogy with the solution of lumped

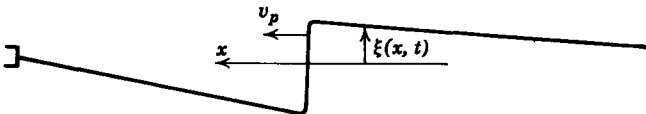


Fig. 9.2.3 Elastic wire or tightly wound helical spring under tension and plucked at one end. The wave is seen as it propagates to the left. The deflections of the spring provide a clear picture of the dynamics predicted by (9.2.4).

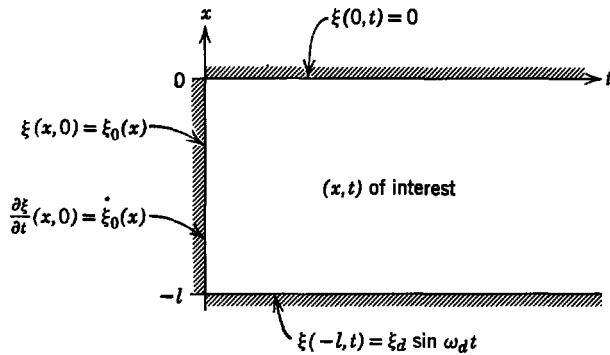


Fig. 9.2.4 Initial and boundary conditions in the x - t plane for wire fixed at $x = 0$, sinusoidally excited at $x = -l$, and having given initial conditions over the length of interest when $t = 0$.

parameter problems, discussed in Section 5.1.2, we divide the response into a part with the same sinusoidal steady-state character as the excitation and a transient part that is necessary to satisfy the initial conditions. In the discussion that follows we see a close connection between these two types of solution and their lumped-parameter counterparts.

In the analysis of lumped-parameter systems, defined by constant-coefficient ordinary differential equations, solutions take the form e^{st} . Similarly, distributed systems, defined by constant coefficient partial differential equations, have solutions that take the form*

$$\xi = \text{Re} [\hat{\xi} e^{j(\omega t - kx)}], \quad (9.2.10)$$

where the (angular) frequency ω and wavenumber k can, in general, be complex. This is shown by substituting (9.2.10) into (9.2.4), which requires that

$$\omega = \pm v_p k. \quad (9.2.11)$$

This relation between ω and k plays a role in continuum systems similar to that of the characteristic equation in lumped systems [see (5.1.6)]. Given the value of k (which represents the dependence of the deflection ξ on x), we obtain the possible frequencies of the solutions to (9.2.4). The relation between ω and k , given by (9.2.11), is referred to as the *dispersion equation*. We shall now see that it plays a fundamental role in determining both the sinusoidal steady-state and transient responses of continuous media.

* The general form of this solution could have been written as $e^{st} e^{\beta x}$, where s and β can be complex, to indicate the similarity to the e^{st} solution for total differential equations; however, (9.2.10) with ω and k real, represents a nondispersive wave which is our point of departure for studying continuum electromechanical dynamics in this context.

9.2.1a Sinusoidal Steady-State Response

It is assumed at the outset that the effects of initiating the excitation have died away,* hence it is appropriate to look for solutions with the same real frequency as the excitation. A plot of the dispersion equation (9.2.11) is shown in Fig. 9.2.5, in which it is made evident graphically that for a given frequency $\omega = \omega_d$, the dispersion equation will give two values of k , one the negative of the other ($k = \pm \omega_d/v_p$). Hence there are two possible solutions to (9.2.4) in the form of (9.2.10). A linear combination of these solutions is

$$\xi = \text{Re} \left\{ \xi_+ \exp \left[j\omega_d \left(t - \frac{x}{v_p} \right) \right] + \xi_- \exp \left[j\omega_d \left(t + \frac{x}{v_p} \right) \right] \right\}, \quad (9.2.12)$$

where ξ_+ and ξ_- are complex constants. Here it is evident that the response is composed of two waves propagating in opposite directions along the wire with equal phase velocities v_p .

For the particular problem at hand deflections are zero at $x = 0$ (9.2.7). This requires that the coefficients in (9.2.12) be negatives, so that solutions take the form

$$\xi = \text{Re} \left[\xi_- 2j \sin \frac{\omega_d x}{v_p} e^{j\omega_d t} \right]. \quad (9.2.13)$$

The coefficient ξ_- is, in turn, determined by the driving condition at $x = -l$ (9.2.6) (note that here we require the same frequency $\omega = \omega_d$ in the response as in the driving deflection).

$$\xi = -\xi_d \frac{\sin (\omega_d/v_p)x}{\sin (\omega_d/v_p)l} \sin \omega_d t. \quad (9.2.14)$$

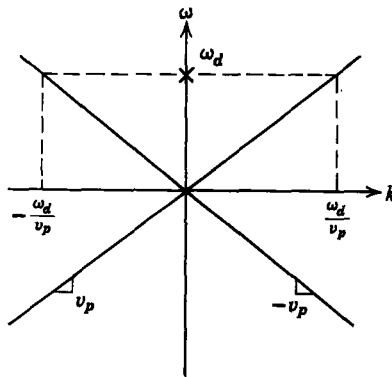


Fig. 9.2.5 Dispersion equation for ordinary waves on a wire.

* We return to this point later because, in fact, they may not “die away,” but rather grow with time.

This expression is the required sinusoidal steady-state response $\xi(x, t)$. It takes the form of a simple standing wave, as might be expected from the fact that it was obtained by superimposing two traveling waves of equal magnitude.

Remember that k is a linear function of ω_d , as shown in Fig. 9.2.5. Hence the shape of the deflection varies as the frequency is changed. At very low frequencies $\sin kx \rightarrow kx$, and (9.2.14) becomes

$$\xi = -\xi_a \left(\frac{x}{l} \right) \sin \omega_d t. \quad (9.2.15)$$

At any instant the low frequency deflections take the form of a straight line joining the fixed end to the instantaneous position of the sinusoidally varying deflection at $x = -l$. As the frequency is raised, the inertial effects of the wire come into play, and there is a tendency for it to bow outward. The response at low frequencies given by (9.2.15) would be found if the left-hand side of (9.2.4) (the inertial force on the wire) were ignored. This quasi-static behavior is completely analogous to the response of the elastic rod as described in Section 9.1.3a.

At frequencies such that

$$k = \pm \frac{\omega_d}{v_p} = \pm \frac{n\pi}{l}; \quad n = 1, 2, 3, \dots, \quad (9.2.16)$$

the denominator of (9.2.14) goes to zero and the response becomes infinite. This is an example of resonance, much as it is found in lumped-parameter systems. The salient feature of the continuum system is the infinite number of these resonances, each with a corresponding characteristic frequency and distribution of ξ in space. The relationship between the resonance frequencies and deflections is shown in Fig. 9.2.6. In this figure an experiment is sketched, wherein a taut spring is fixed at one end and excited at the other by attaching it to a rod with a sinusoidally varying position. In Fig. 9.2.6*a* the driving amplitude is very large to make evident the essentially linear distribution of the spring displacement at low frequencies. In Fig. 9.2.6*b, c, d* the excitation amplitude is kept the same and the resonances in the response are made evident. Of course, in the physical situation the finite mechanical losses limit the resonance amplitude to a finite value rather than the infinite value predicted by (9.2.14).

From the dynamics of lumped-parameter systems we know that a resonance peak indicates a driving frequency in the neighborhood of a natural frequency. In the actual experiment of Fig. 9.2.6 these natural frequencies are not purely real because mechanical damping adds an imaginary term; hence excitation at the purely real frequency ω_d gives rise to a bounded response. We see next that the natural frequencies predicted by our theory, which ignores the effects of damping, are indeed purely real. This we expect, in

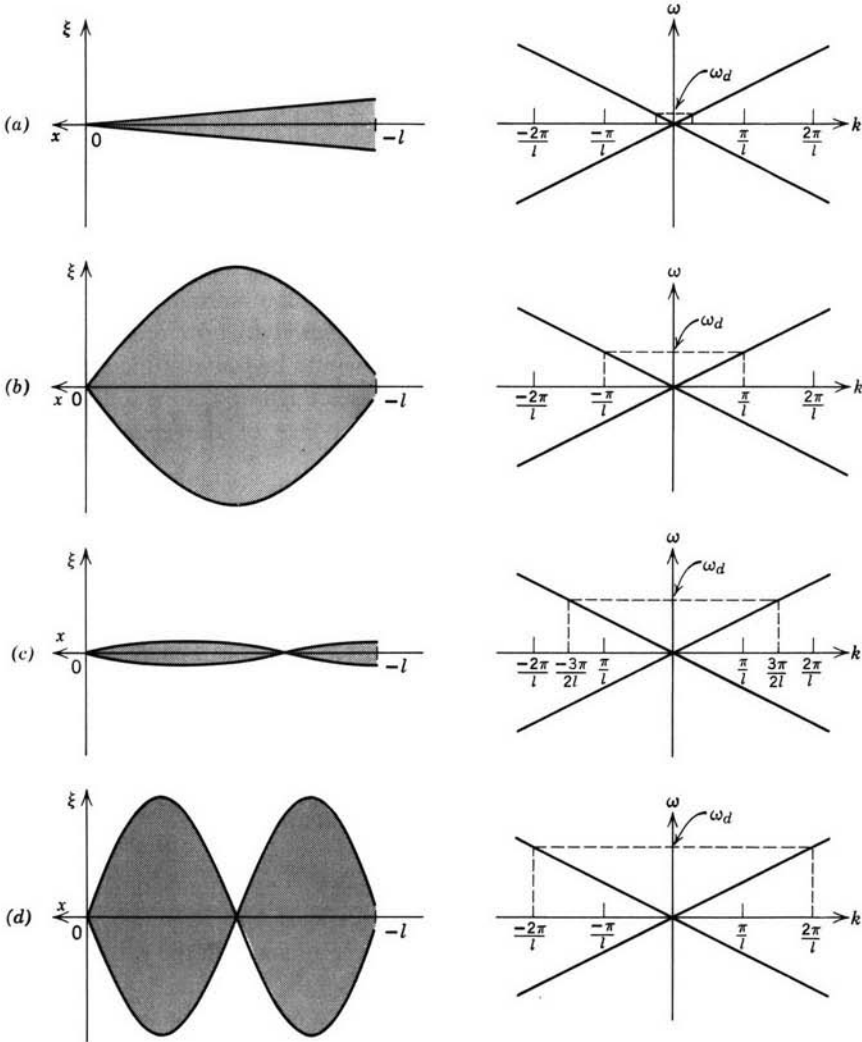


Fig. 9.2.6 Sketch of experiment in which a taut spring is fixed at the left end and deflected sinusoidally at the right end. (a) Deflections in the quasi-static limit at which the frequency is low compared with the reciprocal of the time required for a disturbance to propagate from one end of the spring to the other; (b) to (d) deflection as frequency is varied from value at which $k = \pi/l$ to $k = 2\pi/l$. The excitation amplitude is kept the same in going from (b) to (d). Actual experiment can be seen in film, "Complex Waves I" produced by Education Development Center for National Committee on Electrical Engineering Films.

view of the theoretically predicted resonances found in the response to the sinusoidal driving condition (9.2.14). Our ideal lossless model is accurate for predicting resonance frequencies, but not for calculating deflections at frequencies near resonance. The adequacy of our idealized model, which depends on the relative damping, must be ascertained for each physical situation and the purpose for which the model is to be used.

9.2.1b Transient Response

The steady-state solution given by (9.2.14) does not in general satisfy the initial conditions of (9.2.8-9). To satisfy these conditions, we require further solutions to (9.2.4) that can be added to the steady-state solution. Since the steady-state solution already satisfies the boundary conditions at $x = 0$ and $x = -l$, we require that these solutions satisfy the boundary conditions

$$\xi(0, t) = 0, \quad (9.2.17)$$

$$\xi(-l, t) = 0. \quad (9.2.18)$$

Again we resort to solutions in the form of (9.2.10). Now, however, ω is at the outset an unknown frequency to be determined from the boundary conditions. As in Section 9.2.1a, we take a linear combination of solutions that satisfy (9.2.17). This gives a solution in the form of (9.2.13) with $\omega_a \rightarrow \omega$.

$$\xi(x, t) = \text{Re}(A \sin kx e^{j\omega t}), \quad (9.2.19)$$

where A is a complex constant. The second boundary condition (9.2.18) is satisfied if

$$\sin kl = 0. \quad (9.2.20)$$

This is possible if

$$k = k_n = \frac{n\pi}{l}; \quad n = 1, 2, 3, \dots \quad (9.2.21)$$

Recall the procedure for finding the driven response. We used the dispersion equation to find the wavenumbers (the spatial behavior) by requiring that $\omega = \omega_a$. Now, to find the transient response we have used the boundary conditions to find the wavenumbers (9.2.21) and then used the dispersion equation (9.2.11) to find the possible frequencies of vibration.

$$\omega = \omega_n = \pm v_p k_n. \quad (9.2.22)$$

This relationship is shown graphically in Fig. 9.2.7.

We have found two solutions in the form of (9.2.19) for each value of k_n . Hence we write the n th *eigenmode**

$$\xi_n(x, t) = [A_n^+ e^{j\omega_n t} + A_n^- e^{-j\omega_n t}] \xi_n(x), \quad (9.2.23)$$

* C. R. Wylie, Jr., *Advanced Engineering Mathematics*, McGraw-Hill, New York, 1951, p. 234.

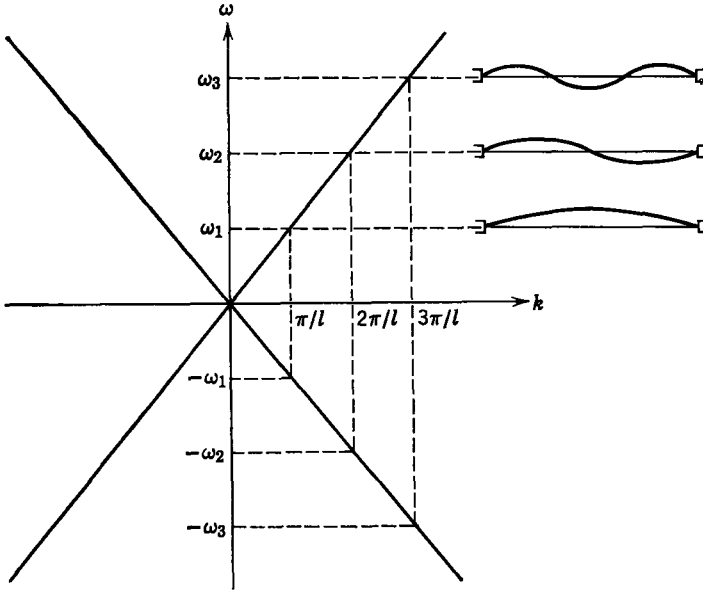


Fig. 9.2.7 Allowed wavenumbers (eigenvalues) $k = k_n$ as they are related to the eigenfrequencies ω_n by the dispersion equation.

where the “Re” has been dropped by requiring that the constant A_n^+ , if complex, be the complex conjugate of A_n^- and the *eigenfunction* $\xi_n(x)$ is

$$\xi_n(x) = \sin k_n x. \tag{9.2.24}$$

The constants k_n are called the *eigenvalues* of the problem, and the frequencies $\pm\omega_n$ are the *eigenfrequencies*. Specification of n fixes k_n , ω_n and the spatial dependence of the deflection mode.

The eigenfrequencies $\pm\omega_n$ are the natural frequencies of the distributed system, in the sense discussed for lumped systems in Section 5.1.1. In a distributed system the number of natural frequencies is infinite in contrast to the finite number that characterizes a finite number of interconnected lumped-parameter elements. The eigenfrequencies are placed in a familiar context by considering a time dependence of the form $e^{s_n t}$ [see (5.1.4)], where, in view of (9.2.10), $s_n = \pm j\omega_n$.

It has now been determined that the general deflection $\xi(x, t)$ is the sum of the transient solution, given by superimposing the modes of (9.2.23) and the driven response (9.2.14)*

$$\xi(x, t) = \sum_{n=1}^{\infty} (A_n^+ e^{j\omega_n t} + A_n^- e^{-j\omega_n t}) \xi_n(x) - \xi_a \frac{\sin(\omega_a/v_p)x}{\sin(\omega_a/v_p)l} \sin \omega_a t. \tag{9.2.25}$$

* It should be evident that this superposition is valid only when $\omega_a \neq \omega_n$.

The constants A_n^+ and A_n^- are determined by the initial conditions. To evaluate these constants observe that the eigenfunctions are *orthogonal*, in the sense that

$$\int_{-l}^0 \xi_n \xi_m dx = \begin{cases} 0; & n \neq m, \\ \frac{l}{2}; & n = m, \end{cases} \quad (9.2.26)$$

as can be seen by carrying out the integration for the particular functions at hand (9.2.24). (More general comments concerning the orthogonality relation are made in Section 9.2.1c.)

The orthogonality condition makes it possible to evaluate the constants A_n^+ and A_n^- , for when $t = 0$ (9.2.25) must give the initial deflection of (9.2.8):

$$\xi_0(x) = \sum_{n=1}^{\infty} (A_n^+ + A_n^-) \xi_n(x). \quad (9.2.27)$$

Now, if we multiply both sides of this expression by $\xi_m(x) = \sin k_m x$ and integrate over the length of the wire, it follows from (9.2.26) that

$$A_m^+ + A_m^- = \frac{2}{l} \int_{-l}^0 \xi_0(x) \sin k_m x dx, \quad (9.2.28)$$

for only one term in the infinite series is nonzero and that is the one in which $n = m$.

A second equation for the A_n 's is the result of the initial velocity condition in (9.2.9), which imposes the condition on the time derivative of (9.2.25):

$$\dot{\xi}_0(x) = \sum_{n=1}^{\infty} j\omega_n (A_n^+ - A_n^-) \xi_n(x) - \xi_a \omega_d \frac{\sin(\omega_d/v_p)x}{\sin(\omega_d/v_p)l}. \quad (9.2.29)$$

Now, when this equation is multiplied by $\xi_m(x)$ and integrated from $-l$ to 0, it follows that

$$A_m^+ - A_m^- = \frac{2}{j\omega_m l} \int_{-l}^0 \left[\dot{\xi}_0(x) + \xi_a \omega_d \frac{\sin(\omega_d/v_p)x}{\sin(\omega_d/v_p)l} \right] \sin k_m x dx. \quad (9.2.30)$$

The two expressions for the sum and difference of the A_n 's (9.2.28) and (9.2.30) are added and subtracted to obtain the explicit expressions

$$A_m^+ = \frac{1}{l} \int_{-l}^0 \left\{ \xi_0(x) + \frac{1}{j\omega_m} \left[\dot{\xi}_0(x) + \xi_a \omega_d \frac{\sin(\omega_d/v_p)x}{\sin(\omega_d/v_p)l} \right] \right\} \sin k_m x dx, \quad (9.2.31)$$

$$A_m^- = \frac{1}{l} \int_{-l}^0 \left\{ \xi_0(x) - \frac{1}{j\omega_m} \left[\dot{\xi}_0(x) + \xi_a \omega_d \frac{\sin(\omega_d/v_p)x}{\sin(\omega_d/v_p)l} \right] \right\} \sin k_m x dx. \quad (9.2.32)$$

For a given set of initial conditions we can now compute the constants A_n^{\pm} ; hence the solution given by (9.2.25) is now completed.

It is only in unusual situations that we become interested in the detailed transient response of a continuum system. Here we are primarily interested in the fact that the eigenmodes given by (9.2.23) can be used to represent the consequences of arbitrary initial conditions. Hence the development demonstrates that the eigenmodes play the same role in the distributed system as the homogeneous solutions of (5.1.11) played in lumped-parameter systems. For this reason it is not surprising that in Chapter 10 we use the eigenmodes to study the stability of continuum systems. If one of the eigenfrequencies has a negative imaginary part, the corresponding eigenmode is unstable and becomes unbounded in time. This is a case in which the transient solution does not die away but rather dominates the driven response. Even when all the eigenmodes are stable, as described here, the theoretical transient solution [the series in (9.2.25)] does not die away but continues to execute oscillatory motions. Of course, in any real system that involves the vibrations of a wire these transient modes would decay (due to damping), thus leaving just the driven response.

Example 9.2.1. It is important to recognize that the eigenmodes represent those oscillations of the continuous medium that can be independent of one another; that is, with appropriate initial conditions, we can initiate any one of the eigenmodes at $t = 0$ and the ensuing oscillations will involve it alone. This can be illustrated by considering the following situation:

1. There is no drive, $\xi_d = 0$.
2. When $t = 0$, the string is static, $\dot{\xi}_0(x) = 0$.
3. When $t = 0$, the string has the deflection $\xi_0 = \xi_m \sin 3\pi x/l$. Using these initial conditions, it follows from (9.2.31) and (9.2.32) that the constants A_m^+ and A_m^- are

$$A_m^+ = \frac{1}{l} \int_{-l}^0 \xi_m \sin \frac{3\pi x}{l} \sin k_m x \, dx, \quad (\text{a})$$

$$A_m^- = A_m^+, \quad (\text{b})$$

and the solution (9.2.25) becomes

$$\xi(x, t) = \xi_m \cos \omega_3 t \sin \frac{3\pi x}{l}. \quad (\text{c})$$

From this result it is clear that because the initial deflection has the same spatial distribution as the $n = 3$ eigenmode the motion persists as the single eigenmode $n = 3$, with the frequencies $\pm \omega_3$.

9.2.1c Orthogonality of Eigenmodes

A vector can be decomposed into three perpendicular components. We say that these components are orthogonal, in the sense that no part of one component is imbedded in another (i.e., the dot product of any pair of vectors is zero). It is in a sense analogous to this that eigenmodes are orthogonal. The orthogonality condition of (9.2.26) expresses the fact that there is no part of one of the eigenmodes imbedded in another. The decomposition of initial conditions into these modes is illustrated in Section 9.2.1b.

We were able to show that the orthogonality condition of (9.2.26) held by simply substituting the eigenfunctions of (9.2.24) into the integral, which could then be carried out. These functions are not always so easily integrated, and it is often necessary to use a less direct method of finding the orthogonality condition.

Because the solutions were found by using the differential equation, we expect that the orthogonality of two solutions is, in fact, a property of the differential equation and the boundary conditions. To show this observe that in terms of the eigenfunction ξ_n , solutions, as given by (9.2.23), take the form

$$\xi = \sum_{n=1}^{\infty} \hat{\xi}_n(x) e^{\pm j\omega_n t}. \tag{9.2.33}$$

It then follows from (9.2.4) that the eigenfunctions must satisfy the ordinary differential equation

$$\frac{d^2 \hat{\xi}_n}{dx^2} + k_n^2 \hat{\xi}_n = 0, \tag{9.2.34}$$

where k_n is introduced instead of the eigenfrequency ω_n because of (9.2.22), the dispersion equation.

In view of the form taken by the orthogonality condition (9.2.26), we now multiply (9.2.34) by another eigenmode $\hat{\xi}_m$ and integrate the expression over the length of the wire,

$$\int_{-l}^0 \hat{\xi}_m \frac{d^2 \hat{\xi}_n}{dx^2} dx + k_n^2 \int_{-l}^0 \hat{\xi}_m \hat{\xi}_n dx = 0. \tag{9.2.35}$$

The last term in this equation takes the form of the orthogonality condition. Further manipulations have the objective of eliminating the first term, which we integrate by parts* to obtain

$$\left[\hat{\xi}_m \frac{d \hat{\xi}_n}{dx} \right]_{-l}^0 - \int_{-l}^0 \frac{d \hat{\xi}_m}{dx} \frac{d \hat{\xi}_n}{dx} dx + k_n^2 \int_{-l}^0 \hat{\xi}_m \hat{\xi}_n dx = 0. \tag{9.2.36}$$

The second term in this equation is symmetric in m and n , which suggests that we now rederive this expression with the roles of m and n reversed to obtain (9.2.36) with $m \rightarrow n$. If this expression is then subtracted from (9.2.36), the terms that are symmetric in m and n subtract to zero and we obtain

$$\left[\frac{d \hat{\xi}_n}{dx} \hat{\xi}_m - \frac{d \hat{\xi}_m}{dx} \hat{\xi}_n \right]_{-l}^0 + (k_n^2 - k_m^2) \int_{-l}^0 \hat{\xi}_m \hat{\xi}_n dx = 0. \tag{9.2.37}$$

For the particular example undertaken in Section 9.2.1b the eigenfunctions were required to be zero at $x = 0$ and $x = -l$; hence the first term in

* $\int u dv = uv - \int v du$.

(9.2.37) vanishes to leave the desired orthogonality condition

$$(k_n^2 - k_m^2) \int_{-l}^0 \xi_m \xi_n dx = 0. \quad (9.2.38)$$

For differing eigenvalues ($m \neq n$) it is clear that the integral must vanish. This type of orthogonality proof is useful when the eigenfunctions are too complicated to make the performance of a direct integration easy.* Even when the continuum dynamics are governed by the simple wave equation, as illustrated here, the boundary conditions may be sufficiently complicated to warrant a proof of orthogonality in terms of the differential equation. The effect of boundary conditions on the normal modes is illustrated in the next section.

9.2.2 Boundary Conditions and Coupling at Terminal Pairs

The most common type of electromechanical coupling to continuous media can be modeled in terms of terminal pairs. The delay line analyzed in Example 9.1.5 illustrated this point. Mathematically, this class of situations is characterized by partial differential equations for the continuous media that do not involve electromechanical forces. Then the coupling is accounted for by means of boundary conditions, and when these boundary conditions can be formulated in terms of a finite set of variables (say forces and displacements) we can think of the problem formally in terms of coupling at terminal pairs.

The acoustic response of an auditorium to a public address system or the sonar sounding of the ocean floor exemplify this class of problem, in which electromechanical coupling occurs through the boundary conditions. In these examples the time required for an acoustic wave to propagate from one extreme to another in the continuous medium is significant compared with other times of interest, such as the period of excitation. Hence it is clear that in these cases many of the most significant aspects of the mechanics must be accounted for in terms of a continuum model. It is important to recognize, however, that the electromechanical aspects of the problem can often be modeled in terms of lumped parameters. We reserve the discussion of compressible fluids as a continuous medium and acoustic waves in fluids for Chapter 13 and use the simple wire and membrane models here to illustrate the basic considerations.

We have three objectives in this section: first, to see how the boundary conditions are written in the case of wires and membranes, including the possibility of electromechanical coupling; second, to see how the notions

* Our analysis lacks a proof that we have not left out a mode. The completeness of normal modes is discussed in R. V. Churchill, *Fourier Series and Boundary Value Problems*, McGraw-Hill, New York, 1941, p. 43.

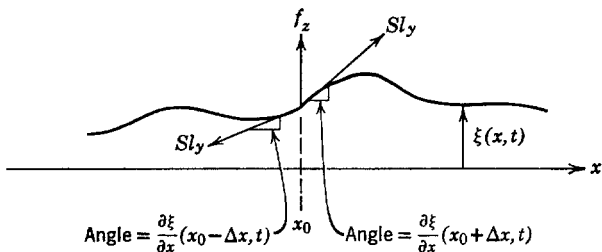


Fig. 9.2.8 Membrane with deflection ξ that depends only on (x, t) and is acted on by an externally applied force f_z at $x = x_0$. The force is distributed over the width l_y of the membrane.

introduced in Section 9.2.1 apply when the normal modes are more complicated than in a simple wire fixed at the ends; and finally, to compute the sinusoidal steady-state response of an electromechanical system, using as an example a simplified model of a loud speaker.

The one-dimensional motions of the membrane are defined by (9.2.3a), which we write as

$$\sigma_m l_y \frac{\partial^2 \xi}{\partial t^2} = S l_y \frac{\partial^2 \xi}{\partial x^2} + f_z(t) u_0(x - x_0). \tag{9.2.39}$$

Here the force acting on the membrane in the z -direction is concentrated at $x = x_0$; hence the force is the product of $f_z(t)$ (newtons) and a unit impulse at $x = x_0$.^{*} This physical situation is shown in Fig. 9.2.8.

A boundary condition for the effect of the force f_z on the membrane can be derived in two ways. The more physical method consists in writing a force balance equation for the mechanical node formed by the strip of membrane at $x = x_0$. In addition to the force f_z , other forces are due to the sections of membrane on either side of the node. Remember that the membrane is under the longitudinal tension S ; and when the membrane tilts there is a component of force in the z -direction which for small amplitude deflections is proportional to the slope of the deflection evaluated just to the right and left of the node. Hence the forces are as shown in Fig. 9.2.9.

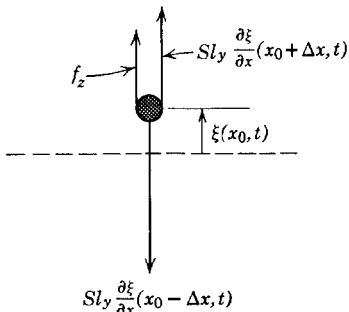


Fig. 9.2.9 Force balance for the strip of membrane at $x = x_0$ in Fig. 9.2.8.

^{*} The unit impulse function is most commonly used in circuit theory, in which its argument is time t rather than space x . See, for example, A. G. Bose, and K. N. Stevens, *Introductory Network Theory*, Harper & Row, New York, 1965.

If we designate

$$\lim_{\Delta x \rightarrow 0} (x_0 + \Delta x) = x^+ \quad \text{and} \quad \lim_{\Delta x \rightarrow 0} (x_0 - \Delta x) = x^-$$

the force balance equation becomes

$$f_z + Sl_y \left[\frac{\partial \xi}{\partial x}(x^+) - \frac{\partial \xi}{\partial x}(x^-) \right] = 0. \quad (9.2.40)$$

This equation represents a boundary condition for the membrane at $x = x_0$. Note the additional boundary condition on the deflection implied by the fact that ξ must be a continuous function at $x = x_0$.

An alternative procedure for finding the boundary condition is familiar because it is commonly used in connection with the electromagnetic field equations.* By use of this approach the equation of motion (9.2.39) is integrated from just to the left of x_0 to a point just to the right of x_0 .

$$\sigma_m l_y \int_{x_0 - \Delta x}^{x_0 + \Delta x} \frac{\partial^2 \xi}{\partial t^2} dx = Sl_y \int_{x_0 - \Delta x}^{x_0 + \Delta x} \frac{\partial}{\partial x} \left(\frac{\partial \xi}{\partial x} \right) dx + f_z(t) \int_{x_0 - \Delta x}^{x_0 + \Delta x} u_0(x - x_0) dx. \quad (9.2.41)$$

Because the deflection is a continuous function of x , the first term goes to zero in the limit where $\Delta x \rightarrow 0$. The first term on the right can be integrated to obtain the first derivative of ξ , whereas the last term is by definition simply $f_z(t)$. Hence we obtain

$$0 = Sl_y \left[\frac{\partial \xi}{\partial x}(x^+) - \frac{\partial \xi}{\partial x}(x^-) \right] + f_z(t). \quad (9.2.42)$$

in the limit in which $\Delta x \rightarrow 0$, which is the same as (9.2.40). Redefinition of Sl_y as the total tension f makes this expression useful for wires under tension.

The fact that the derivative is discontinuous at the point at which the force is applied is not surprising, in view of what we would expect to find if a taut wire were fixed at two ends and pulled upward at the center by a concentrated force. Force equilibrium for a concentrated force necessitates an abrupt change in the slope of the membrane or wire deflection.

The following example illustrates how normal modes and their eigenfrequencies are found in a case in which the boundary condition of (9.2.40) comes into play.

Example 9.2.2. A wire, with the tension f and mass per unit length m , is fixed at one end ($x = 0$) and attached to a pair of springs at the other end ($x = -l$), as shown in Fig.

* See, for example, Section 6.2.2, in which Gauss's theorem was used to derive the relationship between a singularity in volume charge density (the surface charge density) and the electric displacement vector.

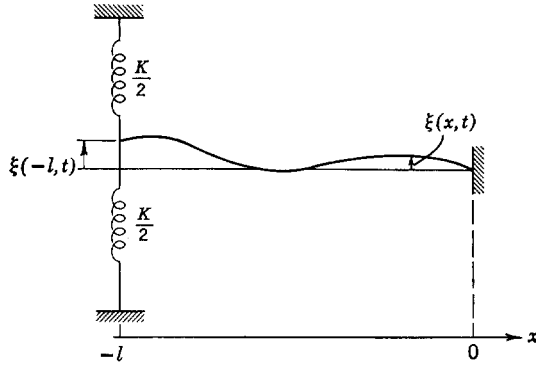


Fig. 9.2.10 A wire is fixed at one end and attached to a pair of springs; the combined spring constant is K .

9.2.10. We assume that the longitudinal tension on the wire is held in equilibrium at $x = -l$ by a constant longitudinal force, so that the end executes a purely transverse motion. The springs then exert a total force

$$f_z = -K\xi(-l, t). \tag{a}$$

Since there is no wire to the left of $x = -l$ to exert a transverse force on the node to which the springs are attached, boundary condition (9.2.40) becomes (here Sly is replaced by the wire tension f)

$$-K\xi(-l, t) + f \frac{\partial \xi}{\partial x}(-l, t) = 0 \tag{b}$$

for this particular case. Of course, the other boundary condition is

$$\xi(0, t) = 0. \tag{c}$$

Now, to find the eigenfrequencies we assume that solutions take the form

$$\xi = \text{Re} [\hat{\xi}(x)e^{j\omega t}], \tag{d}$$

where ω is an unknown frequency. Then the equation of motion [(9.2.3b) with $S_z = 0$] and boundary conditions require

$$\frac{d^2 \hat{\xi}}{dx^2} + k^2 \hat{\xi} = 0; \quad k^2 = \frac{\omega^2}{v_p^2}, \tag{e}$$

$$-K\hat{\xi}(-l) + f \frac{d\hat{\xi}}{dx}(-l) = 0, \tag{f}$$

$$\hat{\xi}(0) = 0. \tag{g}$$

The solution to (e) which satisfies boundary condition (g) is

$$\hat{\xi} = A \sin kx, \tag{h}$$

where A is an arbitrary constant. For this solution to satisfy (f)

$$KA \sin kl + fkA \cos kl = 0. \tag{i}$$

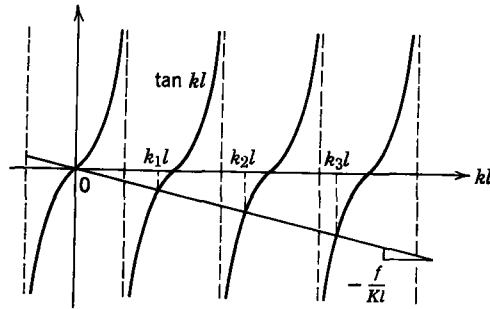


Fig. 9.2.11 A graphical solution of an eigenvalue equation [Example 9.2.2, (j)] shows the lowest three roots k_n .

Unless A is non-zero, there is no solution. Hence it follows from (i) that the eigenvalues k_n satisfy the equation

$$\tan kl = -\frac{f}{Kl}(kl), \quad (j)$$

which results from rearranging (i). This equation has an infinite number of solutions $k = k_n$, which can be designated by the index n and found graphically, as shown in Fig. 9.2.11. Once the eigenvalues k_n have been determined from the eigenvalue equation (j), the eigenfrequencies follow from the dispersion equation (e)

$$\omega_n = \pm k_n v_p. \quad (k)$$

Once again we have found modes in the form of (9.2.23). Note, however, that because of the boundary condition at $x = -l$ the eigenfrequencies ω_n are not harmonically related. Nevertheless, the modes are orthogonal in the sense of (9.2.38), as can be seen by evaluating (9.2.37) for the case at hand. It follows from (f) that each of the eigenfunctions satisfies a condition of the form

$$\frac{d\xi_n}{dx}(-l) = \frac{K}{f} \xi_n(-l). \quad (l)$$

Using this fact, the first term in (9.2.37) becomes

$$\frac{d\xi_n}{dx}(0)\xi_m(0) - \frac{d\xi_m}{dx}(0)\xi_n(0) - \frac{K}{f} [\xi_n(-l)\xi_m(-l) - \xi_m(-l)\xi_n(-l)]. \quad (m)$$

In view of boundary condition (g), it follows that this expression is zero, and from (9.2.37), that the modes (m) and (n) are orthogonal.

The purpose of the preceding example was to show how the boundary conditions can revise the character of the normal modes. As we saw in Section 9.2.1, these modes can be used to represent the response of a system to initial conditions. Also, the eigenfrequencies of the system, including any coupling as it occurs through the boundary conditions, play an important role in determining the nature of the sinusoidal steady-state driven response. This is illustrated by an example that involves electromechanical coupling to a membrane through the boundary condition.

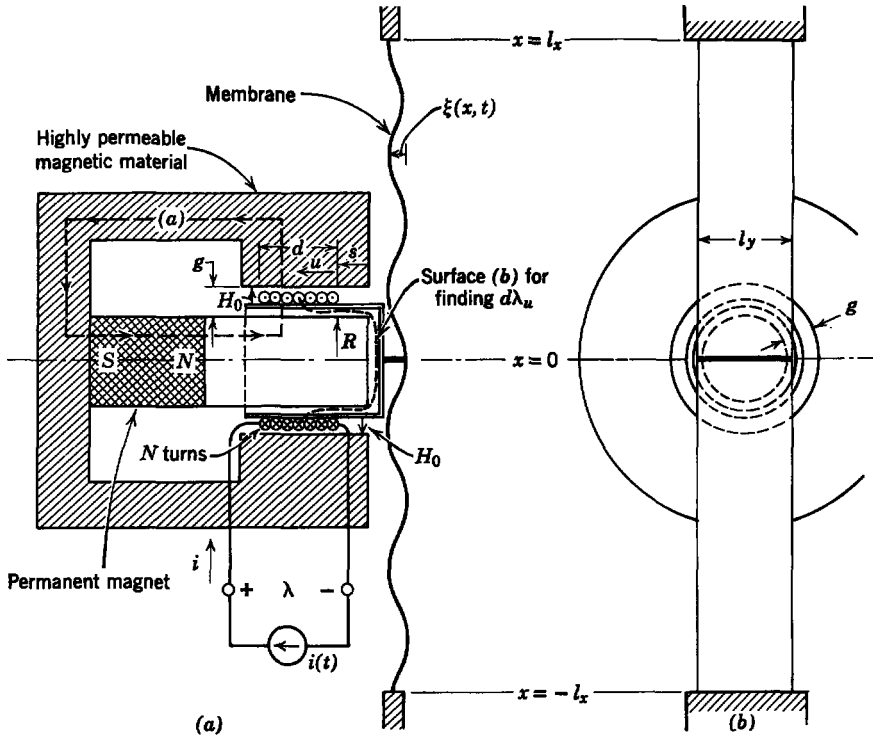


Fig. 9.2.12 One-dimensional model of a loud speaker used in Example 9.2.3. The N turns are attached to the plunger, which in turn is attached to the membrane at $x = 0$; (a) side view showing a cross section of the transducer; (b) end view of the membrane showing the width l_y .

Example 9.2.3. The system shown in Fig. 9.2.12 illustrates the basic construction of a loudspeaker in which the lumped-parameter transducer excites the one-dimensional membrane as a diaphragm. Of course, circular or elliptical diaphragms (or cones) are commonly used in practical speakers. The simple system of Fig. 9.2.12, however, illustrates much of the basic dynamics and pertinent techniques without the use of Bessel functions. Our objective here is to study the multiple-mode dynamics of the membrane and to ascertain how the motion of the membrane is reflected in such terminal characteristics as the input impedance of the transducer.

The transducer shown is characteristic of those commonly used in low-frequency speakers.* It is constructed coaxially about the center line and a permanent magnet provides a radial magnetic field in the gap g . The N -turn voice coil is attached to a cylindrical plunger which has the displacement s as shown. The plunger and voice coil assembly is treated as a rigid body of mass M and is attached to the membrane at $x = 0$. The membrane is fixed at the ends $x = \pm l_x$.

* F. E. Terman, *Radio Engineering*, McGraw-Hill, New York, 1947, pp. 870–877.

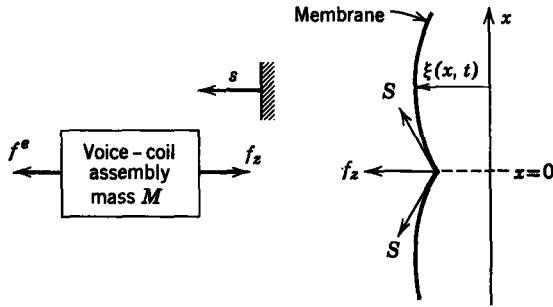


Fig. 9.2.13 Force equilibrium for the transducer plunger attached to the membrane at $x = 0$.

We can establish the boundary condition on the membrane at $x = 0$ by reference to Fig. 9.2.13 which shows the free-body diagram of the voice coil assembly and the membrane in the vicinity of $x = 0$. The force f^e is the force of electric origin applied to the voice coil and f_z is the force applied to the plunger by the membrane. The equation of motion for the mass M is then

$$M \frac{d^2 s}{dt^2} = f^e - f_z. \quad (a)$$

Recognizing that

$$\frac{ds}{dt} = \frac{\partial \xi}{\partial t}(0, t)$$

and using the boundary condition (9.2.40) to eliminate f_z , we obtain

$$M \frac{\partial^2 \xi}{\partial t^2}(0, t) = f^e + Sl_y \left[\frac{\partial \xi}{\partial x}(0^+, t) - \frac{\partial \xi}{\partial x}(0^-, t) \right]. \quad (b)$$

In addition the boundaries are fixed at $x = \pm l_x$; thus

$$\xi(l_x, t) = \xi(-l_x, t) = 0. \quad (c)$$

The problem can be simplified by recognizing that when the membrane is excited in the middle ($x = 0$) with both ends fixed, the response is symmetrical in x :

$$\xi(x, t) = \xi(-x, t).$$

Consequently, we recognize that

$$\frac{\partial \xi}{\partial x}(0^-, t) = -\frac{\partial \xi}{\partial x}(0^+, t)$$

and write (b) as

$$M \frac{\partial^2 \xi}{\partial t^2}(0, t) = f^e + 2Sl_y \frac{\partial \xi}{\partial x}(0^+, t). \quad (d)$$

Attention can now be confined to $0 < x < l_x$.

To complete the description of the system the force f^e must be related to the current $i(t)$ at the input terminals of the transducer. Thus we digress and use the techniques of Chapters 3, 6*, and 8 to make a mathematical model for the transducer.

* See Tables 3.1 and 6.1, Appendix E.

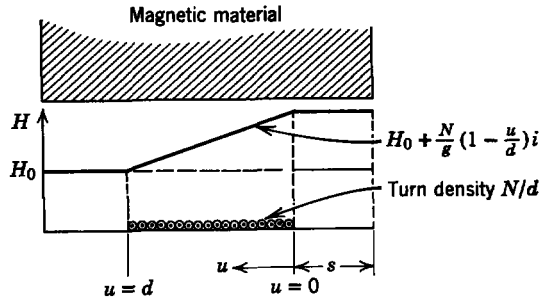


Fig. 9.2.14 Magnetic field intensity H in the gap g shows the uniform field H_0 that results from the permanent magnet and the distribution of field from the current i .

With reference to Fig. 9.2.12, the dimension g is assumed to be small enough that the radial variation of fields in the gap can be neglected. The magnetic field intensity in the gap is radial, independent of radius, and composed of a part H_0 due to the permanent magnet and a part due to current in the voice coil. The total field intensity in the gap can be found by using the integral form of Ampère's law with the contour (a) in Fig. 9.2.12 and assuming that the N voice-coil turns are uniformly distributed over the distance d . The field distribution is illustrated in Fig. 9.2.14.

To find the force of electric origin f^e we use the volume integration of $\mathbf{J} \times \mathbf{B}$ described in Section 8.1. The assumptions of no radial variation of magnetic field intensity and of a uniformly distributed voice coil with many turns N lead to the result that the contribution to f^e from a length (du) of the voice coil located at u is

$$df_u^e = 2\pi R \frac{Ni}{d} (du) \mu_0 \left[H_0 + \frac{N}{g} \left(1 - \frac{u}{d} \right) i \right].$$

Note that $\mathbf{J} \times \mathbf{B}$ is everywhere in the positive s -direction (see Fig. 9.2.12). Integration of this expression over the length d of the voice coil yields

$$f^e = 2\pi RN \left(\mu_0 H_0 i + \frac{\mu_0 N i^2}{2g} \right). \quad (e)$$

The first term represents the interaction between voice coil current and the field applied by the permanent magnet. The second term results from the current in one turn interacting with the field generated by current in all the other turns and is nonlinear in i . For good fidelity of sound reproduction a speaker is designed so that f^e is proportional to i ; consequently, good design results in the inequality

$$|H_0| \gg \left| \frac{Ni}{2g} \right|. \quad (f)$$

We assume in what follows that this inequality is satisfied and we can write f^e as

$$f^e = B_0 l i, \quad (g)$$

where

$$B_0 = \mu_0 H_0,$$

$$l = 2\pi RN.$$

The force produced by a voice coil is often written as in (g)* by ignoring the nonlinear term in (e) which can be eliminated only when condition (f) is satisfied.

The flux $d\lambda_u$ linked by an elemental coil at position u which has axial length du and therefore the number of turns $(N/d) du$ is found by using the surface of integration (b) shown in Fig. 9.2.12. This surface has the elemental coil as its boundary and extends through the air gap and over the end of the center pole piece. There is no contribution to the flux from that part of the surface at the end of the pole piece; consequently, the flux linked by the elemental coil at position u is

$$d\lambda_u = \left(\frac{N}{d}\right) du(2\pi R)\mu_0 \left\{ s \left(H_0 + \frac{Ni}{g} \right) + \int_0^u \left[H_0 + \frac{Ni}{g} \left(1 - \frac{u'}{d} \right) \right] du' \right\}$$

or

$$d\lambda_u = \left(\frac{N}{d}\right) du(2\pi R)\mu_0 \left[s \left(H_0 + \frac{Ni}{g} \right) + H_0 u + \frac{Ni}{g} \left(u - \frac{u^2}{2d} \right) \right]. \tag{h}$$

The total flux linked by the voice coil is found by summing the contributions $d\lambda_u$ of each coil. This amounts to integrating (h) over the length (d) of the coil

$$\lambda = 2\pi R\mu_0 \frac{N}{d} \int_0^d \left[H_0(s + u) + \frac{Ni}{g} \left(s + u - \frac{u^2}{2d} \right) \right] du$$

or

$$\lambda = 2\pi R\mu_0 N \left[H_0 \left(s + \frac{d}{2} \right) + \frac{Ni}{g} \left(s + \frac{d}{3} \right) \right]. \tag{i}$$

When we use condition (f), we can neglect the second term in (i) and write the terminal voltage of the voice coil as

$$v = \frac{d\lambda}{dt} = B_0 l \frac{ds}{dt}. \tag{j}$$

Recognizing that

$$\frac{ds}{dt} = \frac{\partial \xi}{\partial t} (0, t)$$

we write (j) as

$$v = B_0 l \frac{\partial \xi}{\partial t} (0, t). \tag{k}$$

Equations c, d, and g specify the boundary conditions applied to the membrane and (k) expresses the voltage seen by the input current source due to motion of the membrane.

We are interested in the steady-state response of the membrane to a sinusoidal voice-coil current

$$i(t) = \text{Re} (\hat{I} e^{j\omega t}) \tag{l}$$

where \hat{I} is a complex number that determines the amplitude and phase of the input current and ω is real and the angular frequency of the input signal. The equations of motion for the membrane and transducer are linear with constant coefficients; consequently, all dependent variables have the same time dependence as (l). Hence we assume that

$$\xi(x, t) = \text{Re} [\hat{\xi}(x) e^{j\omega t}], \tag{m}$$

where $\hat{\xi}(x)$ is the complex amplitude.

* H. H. Skilling, *Electromechanics*, Wiley, New York, 1962, p. 19.

The wave equation is satisfied by ξ everywhere on the membrane. Hence substitution of (m) into (9.2.3a), with $T_z = 0$, and cancellation of the exponential yields

$$\frac{d^2 \hat{\xi}}{dx^2} + k^2 \hat{\xi} = 0, \quad (\text{n})$$

where the wavenumber k is obtained from

$$k^2 = \frac{\omega^2 \sigma_m}{S}. \quad (\text{o})$$

The general solution for (n) can be written as

$$\hat{\xi}(x) = A \sin kx + B \cos kx, \quad (\text{p})$$

where we have taken k to be the positive root of (o).

We first use the boundary condition of (c) to eliminate B from (p) with the result that

$$\hat{\xi}(x) = A(\sin kx - \tan kl_x \cos kx). \quad (\text{q})$$

Next, we use (l) and (m) in (d), cancel out the time-dependent factor $e^{j\omega t}$, and obtain

$$-\omega^2 M \hat{\xi}(0) = B_0 \hat{I} + 2S l_y \frac{d\hat{\xi}}{dx}(0). \quad (\text{r})$$

Substitution of (q) into this expression and evaluation of the constant A yields

$$A = \frac{B_0 \hat{I}}{\omega^2 M \tan kl_x - 2kS l_y}, \quad (\text{s})$$

and it follows from (q) that

$$\hat{\xi}(x) = \frac{(\sin kx - \tan kl_x \cos kx)}{(\omega^2 M \tan kl_x - 2kS l_y)} B_0 \hat{I}. \quad (\text{t})$$

This result can be used with (m) to describe the motion at any point on the membrane.

When we write the terminal voltage of the voice coil as

$$v = \text{Re}(\hat{V} e^{j\omega t}),$$

we can use (k) and (t) to write the input admittance as

$$\frac{\hat{I}}{\hat{V}} = j \left[\frac{\omega M}{(B_0 l)^2} - \frac{2\sqrt{\sigma_m S} l_y}{(B_0 l)^2} \cot kl_x \right]. \quad (\text{u})$$

Note that the first term depends only on the lumped-parameter loading of the transducer by the voice-coil assembly mass M and that the second term depends on the properties of the membrane. Note further that the admittance is imaginary, which indicates a lossless system.

Equation u can be written in terms of two susceptances S_1 and S_2 ; thus

$$\frac{\hat{I}}{\hat{V}} = jS_1 + jS_2, \quad (\text{v})$$

where

$$S_1 = \frac{\omega M}{(B_0 l)^2},$$

$$S_2 = -\frac{2\sqrt{\sigma_m S} l_y}{(B_0 l)^2} \cot kl_x.$$

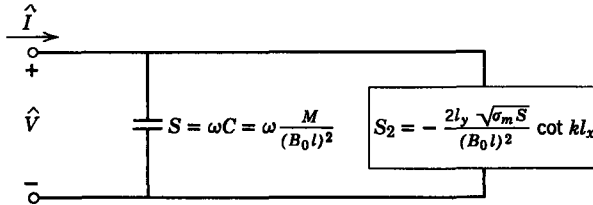


Fig. 9.2.15 Equivalent circuit seen by the current source $i(t)$ for the transducer shown in Fig. 9.2.12.

The susceptance S_1 appears capacitive with equivalent capacitance

$$C = \frac{M}{(B_0 l)^2}.$$

Thus we can draw the equivalent circuit of Fig. 9.2.15 to show separately the effects of the mass M and the membrane on the excitation source.

To study the effects of the membrane it is convenient to define a normalized frequency kl_x by

$$kl_x = \omega l_x \left(\frac{\sigma_m}{S} \right)^{1/2}.$$

The susceptances S_1 , S_2 and the total susceptance are plotted as functions of the normalized frequency in Fig. 9.2.16. The susceptance S_1 is linear with frequency, as indicated, but S_2

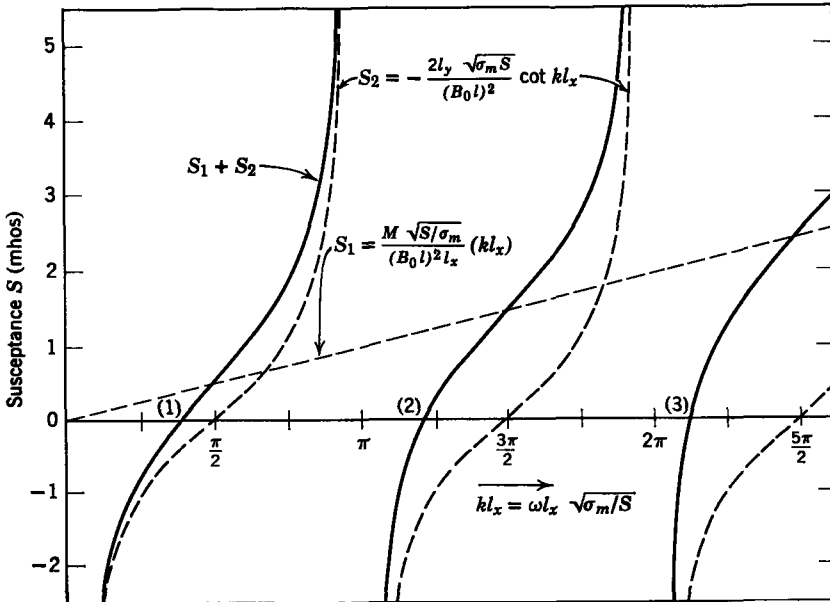


Fig. 9.2.16 The susceptance S of the system shown in Fig. 9.2.12 as a function of normalized frequency.

varies periodically with frequency, having zeros at $kl_x = \pi/2, 3\pi/2, 5\pi/2, \dots$, and poles at $kl_x = 0, \pi, 2\pi, 3\pi, \dots$. The addition of S_1 and S_2 to obtain the total input susceptance shows that the positions of the poles are the same as for S_2 but the zeros are reduced in frequency by the mass to values of kl_x indicated by points (1), (2), and (3) in Fig. 9.2.16. At a pole of the total susceptance the voltage is zero, regardless of the amplitude of the current, whereas at a zero of $(S_1 + S_2)$ zero current is required to obtain a finite voltage amplitude. This reflects our assumptions made initially that the membrane and transducer are not affected by electrical damping, viscous damping, or acoustic radiation. Of course, in loudspeakers the objective is to transfer as much energy as possible to an acoustic load (usually the air). The energy transfer, however, is usually comparatively small; consequently, our analysis gives a reasonably good first approximation to the behavior viewed from the electrical terminals. The resulting acoustic radiation can in many cases be computed under the assumption that the membrane motion derived here is not affected appreciably by the loading.* As we expect, the model is most in error at frequencies close to the singularities (poles and zeros) of admittance. The approximation can thus be improved by assuming small losses and treating the admittance in the vicinity of a singularity by the standard techniques of circuit theory.†

As indicated by the curves of Fig. 9.2.16, the system has multiple resonances due to the susceptance S_2 . This is a property of systems involving continuous media. The resonance of interest here results when a wave initiated at $x = 0$ travels to $x = l_x$, where it is reflected, and arrives back at $x = 0$ with a phase that reinforces the driving signal. Without the mass M , this occurs when the length l_x is an odd number of quarter wavelengths

$$l_x = \frac{1}{4}\lambda, \frac{3}{4}\lambda, \frac{5}{4}\lambda, \dots \quad (w)$$

We have defined the wavelength λ in the usual way as the phase velocity divided by the frequency

$$\lambda = \left(\frac{S}{\sigma_m}\right)^{1/2} \left(\frac{2\pi}{\omega}\right).$$

Each resonance described by (v) corresponds to a natural mode, each mode being characterized by a particular frequency. The natural modes have real frequencies and thus they appear as resonances in the transfer function.

With the mass M included, the resonances as given by points (1), (2), and (3) in Fig. 9.2.16 correspond to different modes on the membrane. We use the values of kl_x at each of these points (Fig. 9.2.16) in (t) to find the amplitude of the membrane displacement for the first three modes. The results are shown plotted in Fig. 9.2.17. Remember that from (m) the displacement is a sinusoidal function of time at any position x . Thus Fig. 9.2.17 represents what would be seen in a sideview snapshot taken at the instant of maximum deflection of the membrane. Alternatively, each curve of Fig. 9.2.17 can be interpreted as the envelope of a standing wave. The curves are plotted under the assumption that A is finite, as it is if the excitation I is decreased to zero as the resonance frequency is approached.

It should be clear from a study of Fig. 9.2.17 that the higher order modes will tend to excite acoustic signals that interfere with each other; for example, with the membrane in mode (3) an acoustic signal leaving the membrane at $x/l_x \approx 0.8$ is opposite in phase to the signal leaving the membrane at $x/l_x \approx 0.3$. When these two signals combine after having traveled the same distance, they interfere destructively. Such a property sets a design

* The applications of membranes to acoustic systems are discussed in W. P. Mason, *Electromechanical Transducers and Wave Filters*, Van Nostrand, 1942, p. 158.

† E. A. Guillemin, *Introductory Circuit Theory*, Wiley, New York, 1953, pp. 297–306.

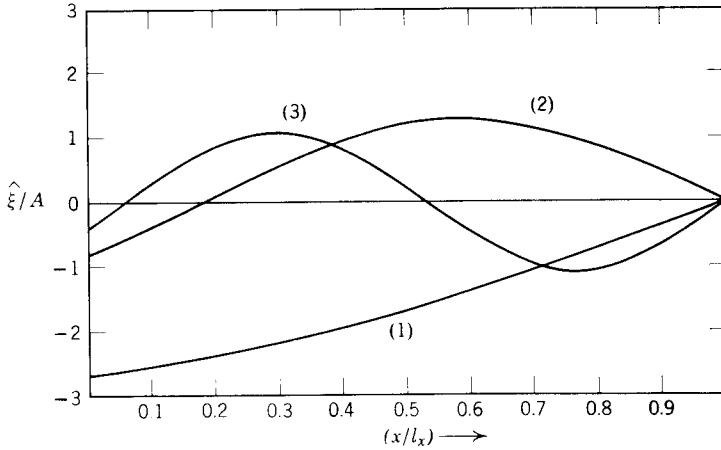


Fig. 9.2.17 Envelope of membrane deflection at the first three resonances of Fig. 9.2.16.

limitation on acoustic devices of this type. Moreover, when operation is in a higher order mode, the response function $[\hat{\xi}(x)/\hat{I}]$ varies violently with frequency. This effect is undesirable for most acoustic applications.

When the device is operated at low frequencies such that

$$kl_x \ll 1,$$

(t) shows that the response function is

$$\frac{\hat{\xi}}{\hat{I}} = \frac{(l_x - x)(B_0 l)}{2Sl_y - \omega^2 M l_x} \tag{x}$$

In this case all points on the membrane have the same relative phase indicated by the low-frequency limit in Fig. 9.2.18. The membrane acts quasi-statically or as a massless spring (in the sense of Section 9.1.3a) and resonates with the mass M at approximately the frequency given by point (1) in Fig. 9.2.16. Most loudspeakers are operated above this first resonance but below the second resonance. The effect of acoustic radiation resistance and cone geometry are important factors in the design of a high-fidelity device.*

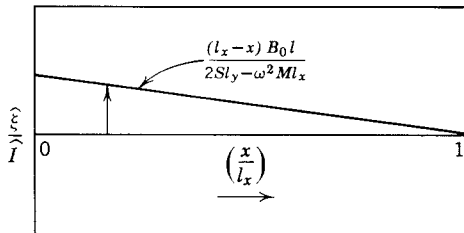


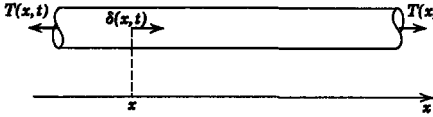
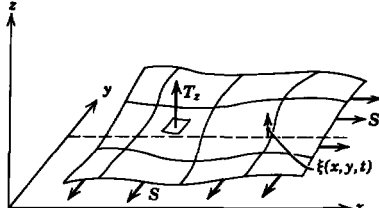
Fig. 9.2.18 Membrane deflection in the low-frequency limit at which the membrane behaves as a massless spring.

* F. E. Terman, *Radio Engineering*, McGraw-Hill, New York 1947, p. 872.

9.3 SUMMARY

Three practical, one-dimensional models introduced to illustrate the significance of continuum mechanical equations of motion are summarized in Table 9.2. The wire and membrane are used extensively in Chapter 10 to illustrate important types of continuum electromechanical behavior as they are found when fluids, plasmas, electron beams, or elastic media interact with electromagnetic fields. The wave dynamics studied in this chapter provide a background for understanding the more complicated dynamics that result in the presence of material convection and electromechanical coupling. The space-time behavior of waves, described in Section 9.1, is important in Chapter 10 for determining appropriate boundary conditions and visualizing

Table 9.2 Summary of One-Dimensional Mechanical Continua Introduced in Chapter 9

| | |
|-------------------------------------------------------------------------------------|-----------------------------------------------------------------------------------------------------------------------------------------------------------------------------------------------------------------------------------------------------------------------------------------------------------------------------------------------------------------------------------------------------------------------------------------------------|
| Thin Elastic Rod | |
|  | $\rho \frac{\partial^2 \delta}{\partial t^2} = E \frac{\partial^2 \delta}{\partial x^2} + F_x$ $T = E \frac{\partial \delta}{\partial x}$ <p> δ—longitudinal (x) displacement T—normal stress ρ—mass density E—modulus of elasticity F_x—longitudinal body force density </p> |
| Wire or "String" | |
|  | $m \frac{\partial^2 \xi}{\partial t^2} = f \frac{\partial^2 \xi}{\partial x^2} + S_z$ <p> ξ—transverse displacement m—mass/unit length f—tension (constant force) S_z—transverse force/unit length </p> |
| Membrane | |
|  | $\sigma_m \frac{\partial^2 \xi}{\partial t^2} = S \left(\frac{\partial^2 \xi}{\partial x^2} + \frac{\partial^2 \xi}{\partial y^2} \right) + T_z$ <p> ξ—transverse displacement σ_m—surface mass density S—tension in y- and z-directions (constant force per unit length) T_z—z-directed force per unit area </p> |

transient situations. At the same time the frequency-wavenumber picture of the dynamics, represented by the dispersion equation introduced in Section 9.2, provides the unifying theme for Chapter 10.

PROBLEMS

9.1. A long thin steel cable of unstressed length l is hanging from a fixed support, as illustrated in Fig. 9P.1. Assume that the origin of coordinates is at the support and that x measures positive as shown. Assume that the steel cable has the following constants:

| | |
|--------------------------|------------------------------------------------|
| Cross-sectional area | $A = 10^{-4} \text{ m}^2$ |
| Young's modulus | $E = 2.0 \times 10^{11} \text{ N/m}^2$ |
| Mass density | $\rho = 7.8 \times 10^3 \text{ kg/m}^3$ |
| Maximum allowable stress | $T_{\text{max}} = 2 \times 10^9 \text{ N/m}^2$ |

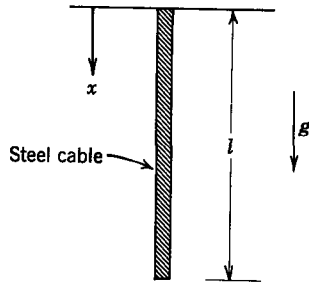


Fig. 9P.1

- (a) Find the length of cable l for which the maximum stress in the cable just equals the maximum allowable stress.
- (b) Find the displacement δ and stress T in the cable as functions of x .
- (c) Find the total elongation of the cable.

9.2. Two thin elastic rods are arranged as shown in Fig. 9P.2. The first rod has modulus of elasticity E_1 , density ρ_1 , and cross-sectional area A_1 . It is attached at one end to a rigid wall and at the other to a very thin rigid plate of mass m and area A_m . On the other side of

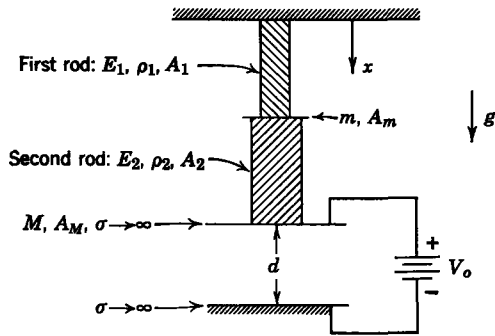


Fig. 9P.2

this plate is attached a second thin elastic rod with elastic modulus E_2 , density ρ_2 , and cross-sectional area A_2 . The other end of the second rod is fixed to a perfectly conducting thin plate with mass M and area A_M . This plate is held at a potential V_0 with respect to a second capacitor plate a distance d away. In the absence of gravity and with $V_0 = 0$, the length of the first rod is L_1 and the length of the second is L_2 . Assuming now that the system is immersed in a gravitational field g and that $V_0 \neq 0$, find the following:

- (a) The stress in the first rod $T^{(1)}(x)$ and the displacement in the first rod $\delta^{(1)}(x)$.
- (b) The stress in the second rod $T^{(2)}(x)$ and the displacement in the second rod $\delta^{(2)}(x)$.

9.3. In Fig. 9P.3 a thin elastic rod of cross-sectional area A , equilibrium length l , elastic modulus E , and mass density ρ is fixed at one end ($x = 0$) and attached to a rigid mass M

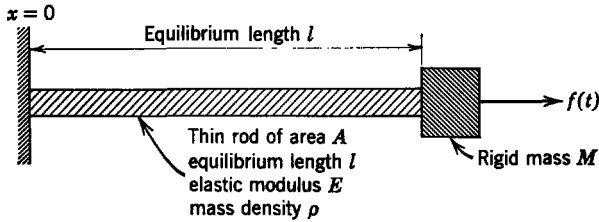


Fig. 9P.3

at the other ($x = l$). The mass is driven by a force source $f(t)$. The system constants are such that the mass M is much greater than the mass of the elastic rod; that is,

$$M \gg \rho Al.$$

The force source is constrained to be

$$f(t) = \text{Re} (f_0 e^{j\omega t}),$$

where f_0 and ω are positive real constants. The system is operating in the sinusoidal steady state. Neglect gravity.

- (a) Find the displacement $\delta(x, t)$ and stress $T(x, t)$ in the elastic rod.
- (b) Show a lumped-parameter mechanical system that represents the behavior of the system in Fig. 9P.3 for low frequencies (from $\omega = 0$ up to and including the lowest resonance frequency). Evaluate the equivalent elements in terms of the given parameters.

9.4. A long thin elastic rod with cross-sectional area A , unstressed length l , modulus of elasticity E , and mass density ρ is constrained at one end by the three ideal, lumped elements

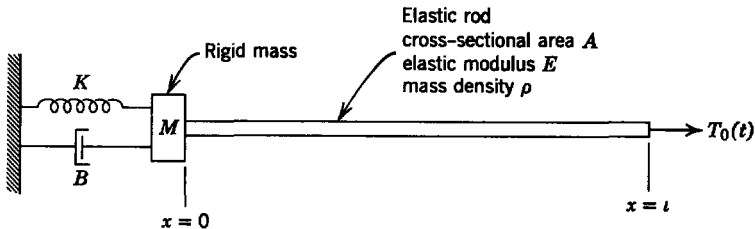


Fig. 9P.4

B , K , and M and at the other by a stress source $T_0(t)$, as shown in Fig. 9P.4. Determine the values of B , K , and M that are necessary for the response of the rod to $T_0(t)$ to be representable purely as a wave traveling in the negative x -direction. (Zero is an acceptable value for an element.)

9.5. A long thin rod of elastic modulus E , mass density ρ , and cross-sectional area A is fixed at one end ($x = 0$) and constrained at the other ($x = l$) by a force source $f(t)$ and a

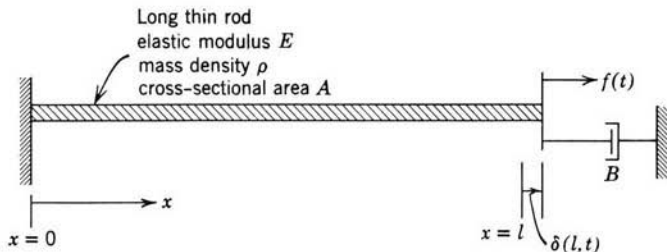


Fig. 9P.5

lumped linear damper of coefficient B , as illustrated in Fig. 9P.5. The applied force is sinusoidal $f(t) = \text{Re}(F_0 e^{j\omega t})$, where F_0 and ω are positive constants. The system is operating in the sinusoidal steady state.

- Write the boundary condition at $x = l$ in terms of the stress $T(l, t)$, the displacement $\delta(l, t)$, and the applied force $f(t)$.
- Assume that the displacement has the form $\delta(x, t) = \text{Re}[\hat{\delta}(x)e^{j\omega t}]$. Find the complex amplitude $\hat{\delta}(x)$ in terms of given data.
- If the damper coefficient B is positive and the frequency ω is real, can the system exhibit a resonance? That is, can the displacement δ be infinite with a zero applied force? Give justification for your answer.

9.6. A thin, circular magnetic rod is fixed at one end and constrained at the other end by a transducer (Fig. 9P.6). In the absence of an excitation, the transducer is simply biased by

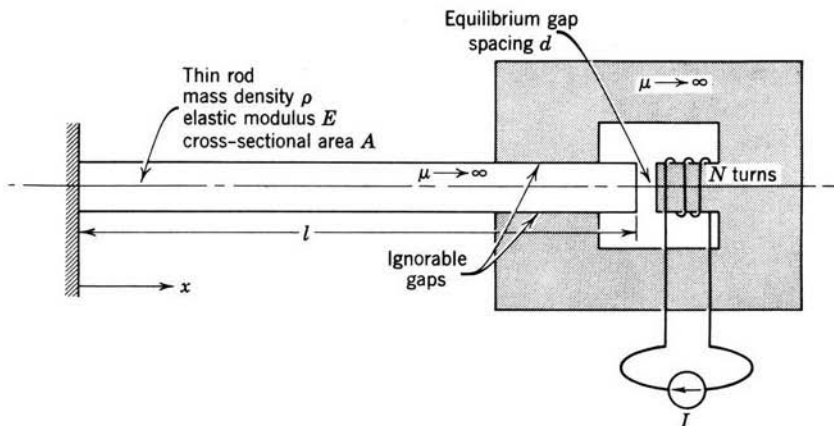


Fig. 9P.6

the constant current source I . When the rod is in static equilibrium, its length is l and the gap spacing is d . Compute the natural frequencies of the system under the assumption that the magnetization force on the rod acts on the end surface. A graphical representation of the eigenfrequencies is an adequate solution.

9.7. In Fig. 9P.7 two identical thin elastic rods are connected by a thin plate of mass M and area A_M . The plate is positioned between four springs, each having constant K . All

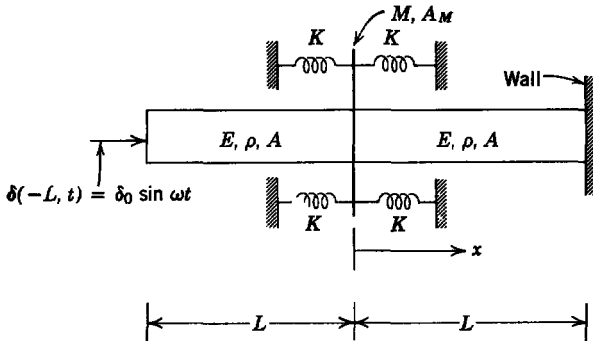


Fig. 9P.7

springs are relaxed when the plate is at $x = 0$. The system is driven on the left with a displacement $\delta(-L, t) = \delta_0 \sin \omega t$. Assume that steady state has been established.

- Write the general solution for the stress $\hat{T}(x)$ and the displacement $\hat{\delta}(x)$ everywhere in both rods in terms of arbitrary constants.
- What are the boundary conditions that determine the constants in (a)?
- Find the stress $T(x, t)$ everywhere in both rods.

9.8. Example 9.1.5 considers the response of the delay line shown in Fig. 9.1.14 to a transient input signal. In this example design approximations were made concerning the effect of the self-inductance in the output circuit [see approximation following (t)]. You wish to compute the sinusoidal steady-state response of this system without making this approximation. Confine your attention to the sinusoidal steady-state response $v_o = \text{Re}(\hat{v}_o e^{j\omega t})$, to the input $i_i = \text{Re}(\hat{i}_i e^{j\omega t})$, and find the transfer function $H(\omega) = \hat{v}_o / \hat{i}_i$.

9.9. A magnetic transducer is used to excite a thin elastic rod, as shown in Fig. 9P.9. The mass M is attached to the rod, which in turn is fixed to a rigid support at $x = 0$. The driving current $I(t)$ is much smaller than I_0 and is given by $I(t) = \text{Re}[\hat{I} \exp(j\omega t)]$. Under the assumption that the displacements of the mass from its equilibrium position are small, complete the following:

- Find an expression for the position of the mass $y(t)$. You may assume that when there is no applied current the mass is centered between the pole faces and the rod has a length L .
- Under what conditions would you say that it is meaningful to consider the magnetic yoke and plunger as rigid but to recognize that the rod is made of an elastic material?

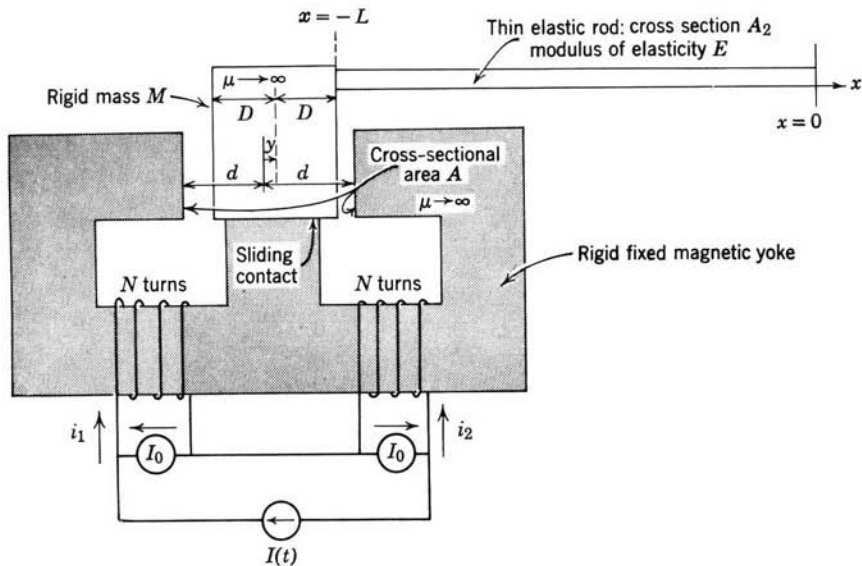


Fig. 9P.9

9.10. A long thin rod is fixed at $x = 0$ and driven at $x = l$, as shown in Fig. 9P.10. The driving transducer consists of a rigid plate with area A attached to the end of the rod, where it undergoes the displacement $\delta(l, t)$ from an equilibrium position exactly between two fixed plates. These fixed plates are biased by potentials V_0 and driven by the voltage $v = \text{Re}(\hat{V}e^{j\omega t})$, as shown. ($|\hat{V}| \ll V_0$)

- Derive a boundary condition relating $\delta(l, t)$, $(\partial\delta/\partial x)(l, t)$ and $v(t)$.
- Compute the driven deflection of the rod $\delta(x, t)$.

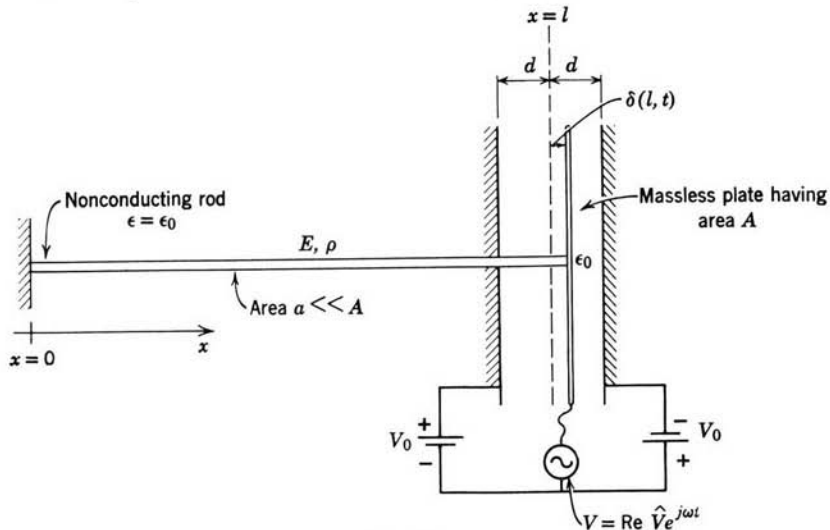


Fig. 9P.10

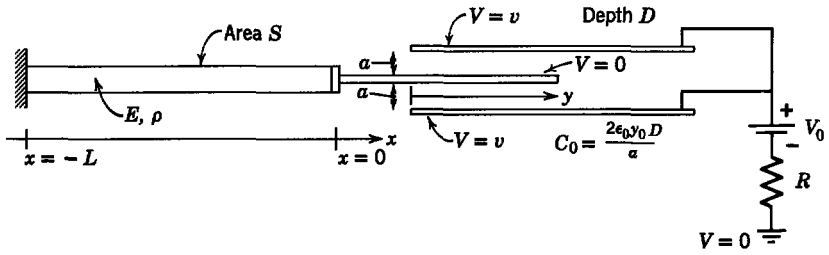


Fig. 9P.11

9.11. A long thin elastic rod (Fig. 9P.11) is fixed at $x = -L$. At $x = 0$ the rod is connected to a movable perfectly conducting plate which has negligible mass. The plate is electrically grounded and constrained to move only in the x -direction. Assume

$$v = V_0 + v_s, \quad v_s \ll V_0,$$

$$y = y_0 + y_s, \quad y_s \ll y_0,$$

where $y_s = \delta(t) =$ small signal displacement. Find the dc voltage (in terms of given parameters) for which there is no elastic wave reflection at the right-hand boundary for wave frequencies such that $\omega \ll 1/RC_0$.

9.12. The system of Fig. 9P.12 consists of two electric field transducers coupled mechanically by a long, thin rod of material with Young's modulus E , mass density ρ , and dielectric permittivity $\epsilon > \epsilon_0$. With the bias voltages V_0 applied and the system at rest, the rod has

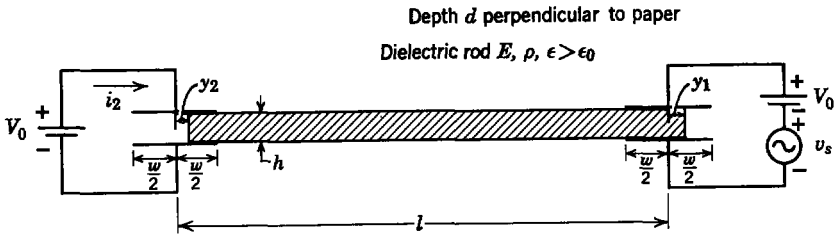


Fig. 9P.12

length l and is in the equilibrium position $y_1 = y_2 = 0$. The dimensions are defined in the figure and you can neglect fringing fields and mechanical friction. For sinusoidal excitation $v_s = \text{Re}(\hat{v}_s e^{j\omega t})$, such that $|\hat{v}_s| \ll V_0$ and steady-state operation about the equilibrium condition, assume that the current i_2 is given by $i_2(t) = \text{Re}(\hat{i}_2 e^{j\omega t})$.

- Find the transfer admittance $Y(j\omega) = \hat{i}_2/\hat{v}_s$.
- Specify the mathematical relation that defines the poles of this admittance. Find the lowest nonzero frequency at which a pole occurs.

9.13. Figure 9P.13 shows an electromechanical filter constructed with two magnetic transducers and a long (length L) thin rod. The transducers, which are alike, are symmetric about the axis of the rod. The ends of the rod form the plungers of magnetic circuits, with axially symmetric air gaps of length g . The left transducer is driven by a constant bias current I_0 and a small current $i = \text{Re}(j e^{j\omega t})$. This signal is transmitted by the rod to the right transducer, which is also biased by a constant current I_0 .

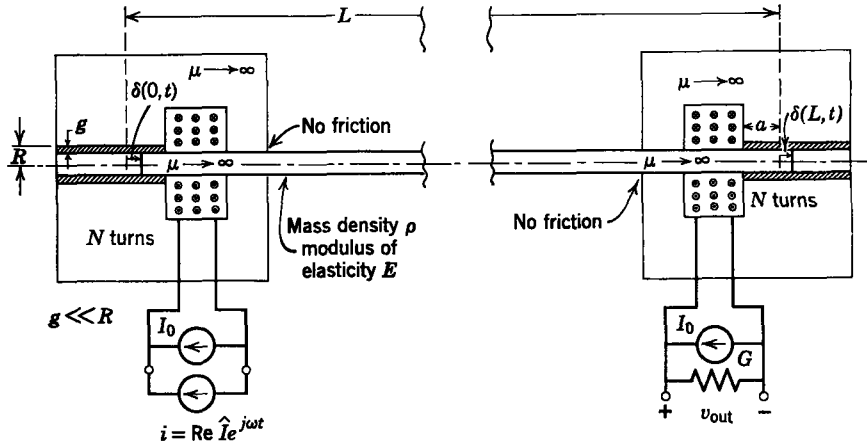


Fig. 9P.13

- (a) Use the energy method to find the magnetic forces acting on the ends of the rod.
- (b) Check the result of part (a) by using the magnetic stress tensor $T_{ij} = \mu H_i H_j - \frac{1}{2} \delta_{ij} \mu H_k H_k$ to find the forces acting on the ends of the rods.
- (c) Assume that the magnetic forces act just on the ends and compute the transfer function $G(\omega) = \hat{v}_{out} / \hat{I}$, where $v_{out} = \text{Re}(\hat{v}_{out} e^{j\omega t})$.
- (d) How would you adjust the system parameters so that $|\hat{v}_{out}|$ is proportional to $|\hat{I}|$, independent of frequency (over some range of frequencies)?

9.14. The electromechanical delay line shown in Fig. 9P.14 consists of a thin elastic rod terminated at both ends by capacitor plates that are massless and very thin. The elastic rod

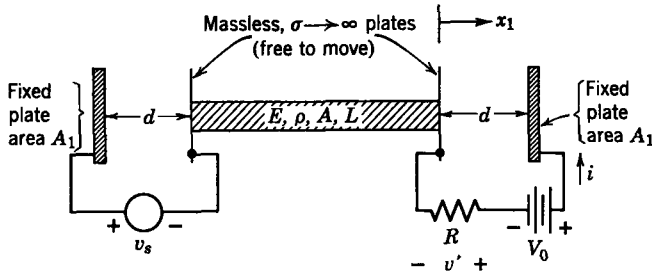


Fig. 9P.14

has length L in the absence of electrical excitations ($v_s = 0$ and $V_0 = 0$). Assume that $\delta(0) \ll d$ and that $\delta(-L) \ll d$.

- (a) If $v_s = V_0$ and the battery at the other capacitor is connected as shown, find the stress everywhere in the rod.
- (b) Suppose that $v_s = V_0 + v_o(t)$, where $v_o(t)$ is a short pulse. How long will it be before the signal is detected as a pulse in the output current i ? Compute a numerical value for the delay, assuming that the rod is steel with length 1 m.

- (c) What must the value of the resistance R be, so that if $v_s = V_0 + v_o(t)$, where v_o is again a short pulse, no pulse will travel back in the $-x_1$ -direction after encountering the capacitor plate at $x_1 = 0$? You may wish to do this by assuming that $v_o(t)$ is a sinusoid and requiring that there be no reflected wave in the rod for all frequencies of excitation. Assume that

$$v' \gg \frac{\epsilon_0 A_1 R}{d} \frac{dv'}{dt} \quad \text{or} \quad \frac{\omega \epsilon_0 A_1 R}{d} \ll 1,$$

where v' is the voltage across R .

9.15. This problem is intended to help you apply the techniques presented in Section 9.1 by considering an analogous situation, namely, the *torsional vibrations* of a thin, cylindrical elastic rod.

- (a) A static experiment is performed on the rod as follows. First, imagine that a line has been painted along one radius at every cross section of the rod when it is unstressed (see Fig. 9P.15). Now suppose that a *constant*, twisting torque τ is applied to the rod. If we single out a small length Δz of the rod (Fig. 9P.15b), we

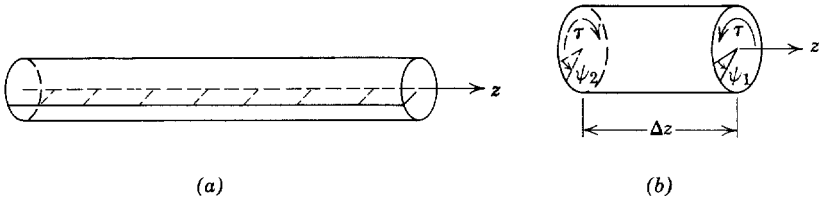


Fig. 9P.15

find that the *difference* between the angular deflections ψ_1 and ψ_2 of the painted line on the two faces is a constant β times the product of the applied torque and the length Δz . Find the relation between the torque τ and the deflection angle ψ in the limit as $\Delta z \rightarrow 0$.

- (b) We wish to find the dynamic equations for the rod. Assume that the twisting torque τ is now a function of z and t , $\tau = \tau(z, t)$. Also, $\psi = \psi(z, t)$. The rod has a moment of inertia J (per unit length) about the z -axis. Write an equation of motion for a length Δz of the rod. Then take the limit of this expression as Δz approaches zero.
- (d) Find a single partial differential equation for $\psi(z, t)$.
- 9.16.** The elastic bar shown in Fig. 9P.16a extends to infinity in the z -direction and has free surfaces at $y = 0$ and $y = a$. Shearing stresses T_{zx} are applied uniformly over the surface at $x = 0$ to set the bar into a mode of vibration, where the material is displaced from equilibrium by the amount $\delta_z(x, t)\mathbf{i}_z$. We wish to find a differential equation of motion for δ_z .
- (a) Write the differential force equation in the z -direction by using the differential slice of material shown in Fig. 9P.16b and the stress function $T_{zx}(x, t)$ N/m².
- (b) Define a shear strain e_{zx} and relate it to the displacement function δ_z . Your strain function should be defined such that we would expect $T_{zx} = 2Ge_{zx}$ (G -N/m²), where G is a constant property of the material. Figure 9P.16c provides a starting point in the derivation.
- (c) Combine the results of (a) and (b) to obtain a single differential equation for δ_z . What is the propagational velocity of disturbances in the x -direction?

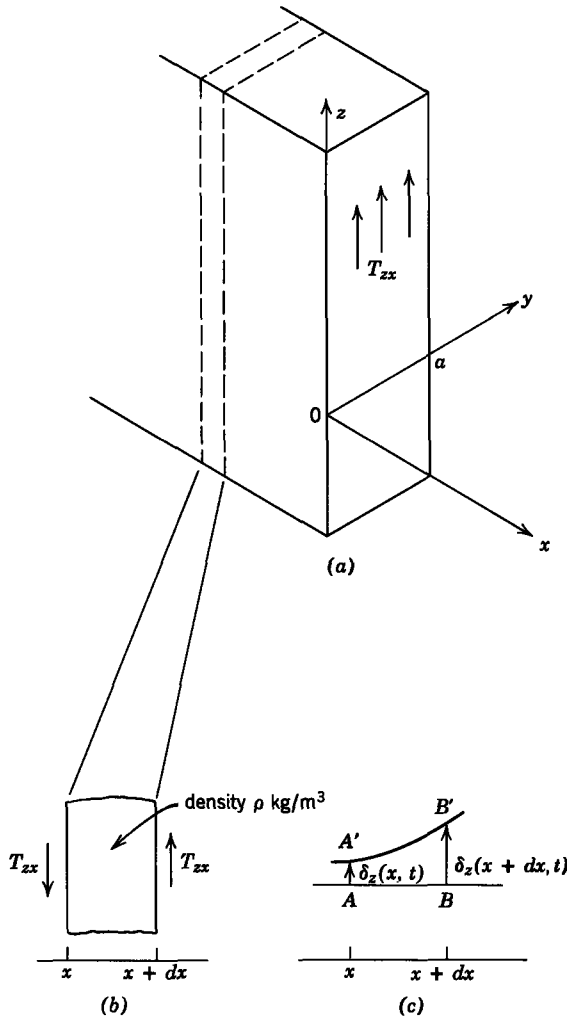


Fig. 9P.16

9.17. In general, an inviscid fluid differs grossly in its dynamics from an elastic solid. If, however, only normal stresses are involved and particle displacements are small, the dynamics of fluids and solids become similar. You are familiar with the derivation of the equation of motion for material in a thin elastic rod. The following derivation is somewhat similar. A tube filled with an initially stationary gas is shown in Fig. 9P.17a. We wish to derive an equation for the particle velocity $v(x, t)$ within the tube. To do this write an equation expressing conservation of mass for a slice of the material, as shown in Fig. 9P.17b. The fluid pressure $p(x, t)$ is a simple form of the stress tensor $T_{ij} = -\delta_{ij}p(x, t)$. We can write a differential equation to express conservation of momentum ($f = ma$) by using the slice of material shown in Fig. 9P.17c.

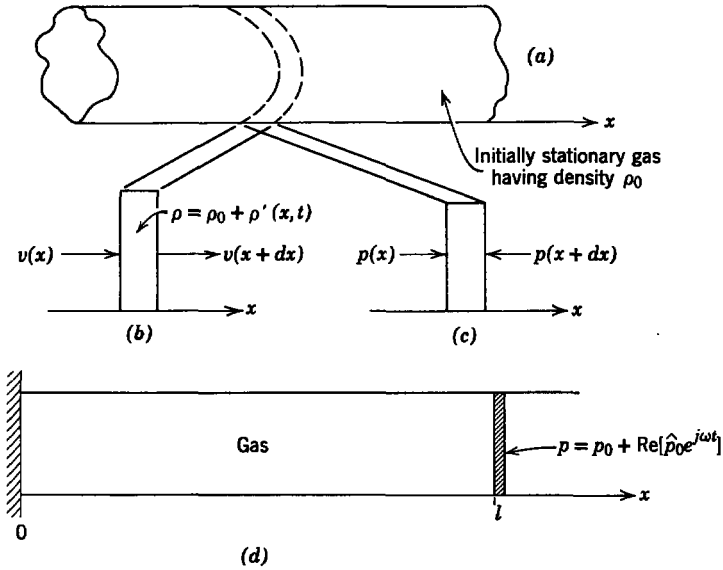


Fig. 9P.17

(a) Show that conservation of mass is expressed by

$$\rho_0 \frac{\partial v}{\partial x} = - \frac{\partial \rho'}{\partial t},$$

where we ignore products of perturbation quantities and $\rho = \rho_0 + \rho'(x, t)$; ρ_0 is the density of the gas when it is stationary.

(b) Show that conservation of momentum is expressed by

$$\rho_0 \frac{\partial v}{\partial t} = - \frac{\partial p'}{\partial x},$$

where $p = p_0 + p'(x, t)$ and p_0 is the pressure when the gas is stationary.

(c) Physical measurements show that the pressure and density are related by a given function $p = p(\rho)$ or

$$p = p_0(\rho_0) + \left(\frac{\partial p}{\partial \rho} \right)_{\rho_0} \rho'.$$

Use the results of (a) and (b) to find one equation for the velocity.

(d) Figure 9P.17d shows the tube driven at $x = l$ by a piston and terminated at $x = 0$ in a rigid wall. What is $v(x, t)$?

9.18. Figure 9P.18 shows the distribution of velocity $\partial \delta / \partial t$ at $t = 0$ in a thin elastic rod of infinite length. Assume that the rod is characterized by the constants E , ρ , and A , where E is Young's modulus, ρ is the density and A is the cross-sectional area of the rod. Given that $T(x, 0) = 0$, make a plot of $T(x, t)$ in the x - t plane. This plot should be similar to that shown in Fig. 9.1.8.

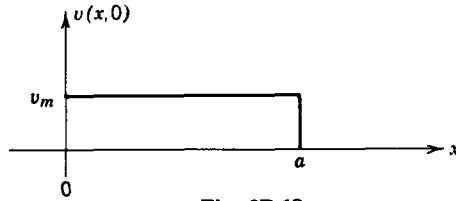


Fig. 9P.18

9.19. Figure 9P.19 shows the distribution of stress $T(x, 0) = E(\partial\delta/\partial x)$ at $t = 0$ in a thin elastic rod of infinite length. Assume that the rod is characterized by the constants E , ρ , and A , where E is Young's modulus, ρ is the density, and A is the cross-sectional area of the rod. Given that $v(x, 0) = 0 = \partial\delta/\partial t$, make a plot of $T(x, t)$ and $v(x, t)$ in the x - t plane. This plot should be similar to that shown in Fig. 9.1.8.

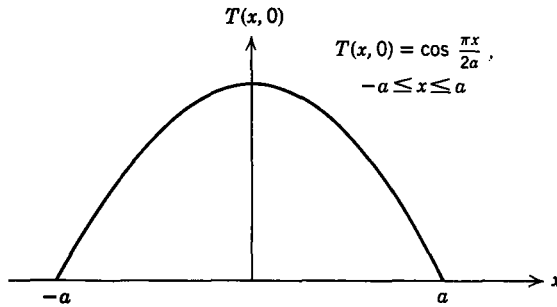


Fig. 9P.19

9.20. A long thin rod supports longitudinal motions $\delta(x, t)$.

- Consider first the case in which the material initially has the velocity distribution $(\partial\delta/\partial t)(x, 0)$ shown in Fig. 9P.20a and initially $(\partial\delta/\partial x)(x, 0) = 0$. The rod has a free end at $x = 0$ but extends to infinity in the positive x -direction. Sketch the resulting velocity $v(x, t)$ in the x - t plane.
- Now, in addition to the initial velocity of Fig. 9P.20a, the end of the rod at $x = 0$ is driven by a force that constrains the stress $T(0, t)$ as shown in Fig. 9P.20b. Sketch the resulting velocity $v(x, t)$ in the x - t plane.

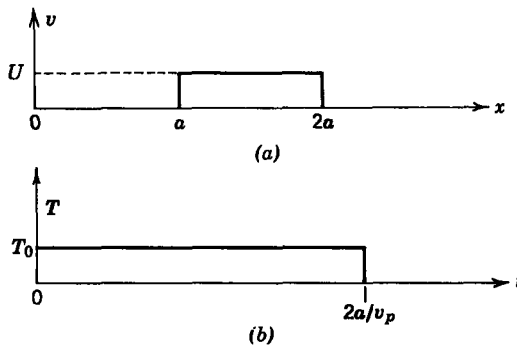


Fig. 9P.20

9.21. An electromechanical device that transduces a pulse of current $I(t)$ into a delayed stress pulse to rupture a diaphragm is shown in Fig. 9P.21. The current $I(t)$ passes through parallel, highly conducting plates shorted by a movable block with conductivity σ . The resulting motion initiates a stress at the left end of the rod, which propagates to the right end to provide the rupturing stress. The current has the form

$$I(t) = \begin{cases} \frac{I_0}{2} \left(1 - \cos \frac{2\pi t}{\tau} \right), & 0 < t < \tau, \\ 0, & t < 0, t > \tau. \end{cases}$$

The time required for the pulse to traverse the length of the rod is long compared with τ .

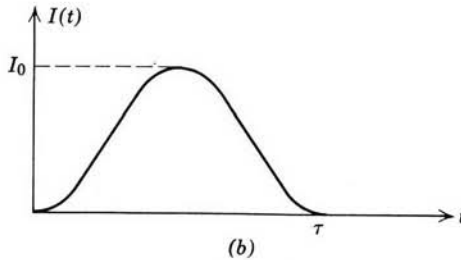
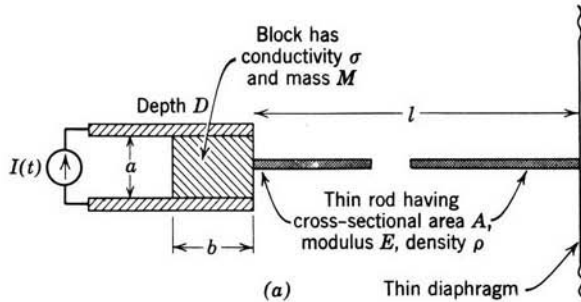


Fig. 9P.21

- Model the electromechanics by assuming that the current is returned on the inside surface of the block and write the boundary condition imposed on the left end of the rod by the magnetic force.
- For what values of τ (in terms of b , σ , etc.) would the surface current model be appropriate?
- Under what conditions can the mass M of the block be ignored in the boundary condition of (a)? Under this condition what is the current I_0 required to produce the peak stress T_r at the right end of the rod? (For this calculation assume that the right end of the rod is fixed in displacement.)

9.22. You are given the following pair of nonlinear differential equations:

$$\frac{\partial W}{\partial t} + W \frac{\partial W}{\partial x} + \frac{\partial U}{\partial x} + \frac{K}{U^3} \frac{\partial U}{\partial x} = 0, \quad (1)$$

$$\frac{\partial U}{\partial t} + \frac{\partial(UW)}{\partial x} = 0, \quad (2)$$

where K is a positive constant. In an equilibrium condition W is zero and U is a positive constant given by $U = C$.

- (a) Linearize (1) and (2), using the given equilibrium conditions.
- (b) By use of the equations of part (a), what is $W(x, t)$ if at $x = 0$, $W = 0$, at $x = -L$, $W = W_0 \cos \omega t$?

9.23. Two identical elastic membranes of mass σ_m per unit area and equilibrium tension S are joined together at $x = 0$ (Fig. 9P.23). Also attached to the membranes at $x = 0$ is a bar of mass M per unit width (kg/m). Both membranes are tied to rigid walls at their other ends ($x = \pm L$).

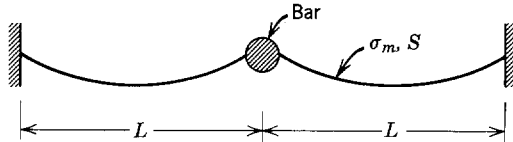


Fig. 9P.23

- (a) Compute the natural frequencies of the system.
- (b) Explain the effect of the mass/unit length M on the natural frequencies. In particular, give a physical reason for what happens when $M = 0$ and $M \rightarrow \infty$.

9.24. Figure 9P.24 shows an elastic membrane fixed at $x = L$ and $x = -L$ and coupled to a pair of capacitor plates at $x = 0$.

- (a) Find the natural frequencies of the system.
- (b) What is the effect on the natural frequencies of raising the voltage V_0 ?

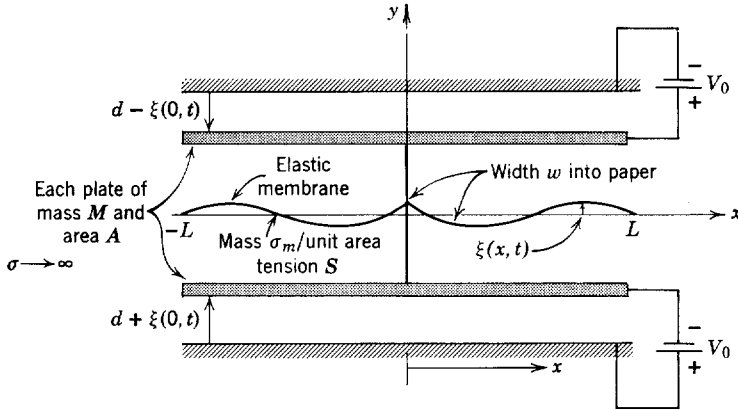


Fig. 9P.24

9.25. A wire is pinned at $x = 0$, where a potentiometer is attached. With the help of an amplifier G , this potentiometer produces a current i_1 proportional to the slope.

$$i_1 = G \frac{\partial \xi}{\partial x}(0, t), \quad G = \text{constant}.$$

The current i_1 is used to drive transducers, which in turn motivate the end of the spring at $x = -l$. The two transducers, which are alike, are connected so that in the absence of i_1

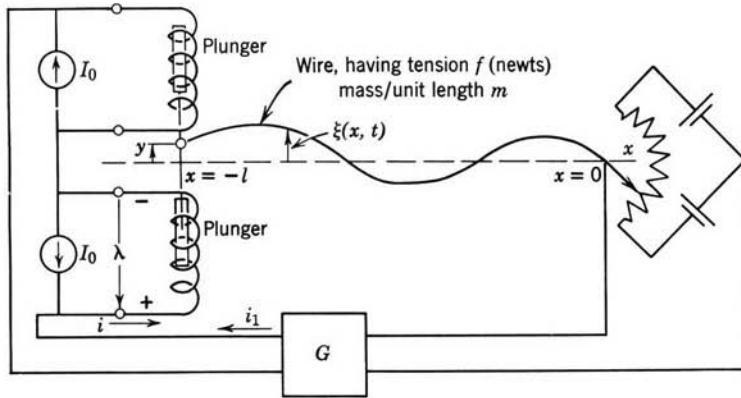


Fig. 9P.25

there is no net force on the wire. The terminal relation for the lower transducer is

$$\lambda = \left(\frac{L_0}{a} y \right) i,$$

where $y = \xi(-l, t)$ as shown in Fig. 9P.25.

- One boundary condition is $\xi(0, t) = 0$. What is the other condition? Ignore the mass of the plungers.
- Find a transcendental expression for the eigenfrequencies (natural frequencies) of the system. Make a plot that shows the graphical solution of this equation.
- What are the natural frequencies when $G = 0$?
- What is the effect of raising the gain G on the first and second nonzero eigenfrequencies?
- Is it possible that this system can be unstable? If so, for what values of G ?

9.26. A magnetic transducer is used to excite a thin elastic membrane of length L , as shown in Fig. 9P.26. The mass M is attached to the membrane, which in turn is fixed to a rigid support at $x = 0$. The driving current $I(t)$ is much smaller than I_0 and is given by

$$I(t) = \text{Re} [\hat{I} \exp(j\omega t)].$$

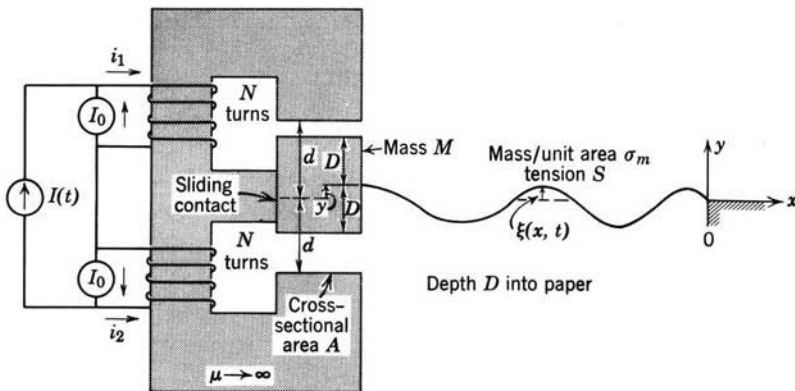


Fig. 9P.26

Work under the assumption that the displacements of the mass from its equilibrium position are small:

- Find an expression for the position of the mass, $y(t)$. You may assume that when there is no applied current the mass is centered between the pole faces.
- Find the resonance frequencies of the system. Your solution may be represented graphically (e.g., see Fig. 9.2.11).

9.27. A string with tension f and a mass per unit length m is fixed at $x = \pm l$, as shown in Fig. 9P.27. At $x = 0$ it is subject to the force $F(t)$ shown in Fig. 9P.27a.

- Write the boundary condition at $x = 0$ which relates $F(t)$ to ξ . For this purpose divide the function $\xi(x, t)$ into two functions valid to the left and to the right of $x = 0$.
- The displacement $\xi(x, t)$ can be divided into an odd and an even function of x . Show that the odd function $\xi(x, t) = -\xi(-x, t)$ is not excited by the driving force.
- We now confine ourselves to displacements that are even functions of x , $\xi(x, t) = \xi(-x, t)$. For $t < 0$ the string assumes a static shape with the force $F(t) = F_0$, where F_0 is a given constant (see Fig. 9P.27b). Use the equation of motion to find $\xi(x)$, $x > 0$, for $t < 0$.
- When $t = 0$, the force $F(t)$ becomes a cosinusoid, as shown in the figure. The string is initially static and has the dependence on x found in part (c). Find the displacement $\xi(x, t)$, $x > 0$, $t > 0$. (Reference. Section 9.2.1.)

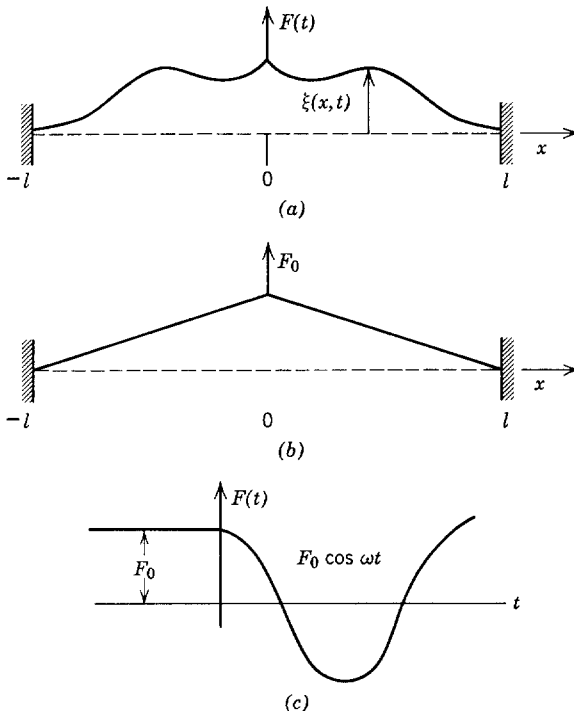


Fig. 9P.27

Chapter 10

DYNAMICS OF ELECTROMECHANICAL CONTINUA

10.0 INTRODUCTION

In Chapter 9 we treated simple examples of mechanical continua to establish the basic techniques of making mathematical models and to illustrate the kinds of dynamic behavior and the mathematical methods needed in analyses. In that chapter simple elastic continua at rest were excited at boundaries so that the resulting continuum dynamics were determined by mechanical characteristics alone.

In this chapter we still restrict our attention to simple elastic continua but we generalize on the treatment of Chapter 9 to include the effects of distributed forces of electric origin and material motion. By the use of simple models we illustrate the basic phenomena that occur in a wide variety of physical systems and the analytical techniques used in their mathematical description. In spite of the diversity of physical situations in which continuum electromechanical interactions are important, a unity results from mathematical techniques that are common to all of the situations. It is our purpose here to illuminate, in the simplest context possible, these mathematical techniques and the physical phenomena they describe.

As stated earlier, the techniques presented are fundamental to a wide variety of physical situations. It is therefore helpful for the purpose of appreciating our objectives to review some of the technical areas concerned with continuum electromechanics.

Magnetohydrodynamics (MHD) is concerned with the interactions of free currents and magnetic fields in fluids (liquids and gases) which have high enough electrical conductivity that a quasi-static magnetic field model is appropriate for describing the electromagnetic part of the system. To reflect more accurately the nature of the mechanical medium this area is sometimes referred to as *magnetogasdynamics (MGD)* or as *magnetofluidynamics (MFD)*. Areas of application include pumping and levitation of liquids (usually

metals), orientation and confinement of extremely hot ionized gases or plasmas, as, for example, in thermonuclear fusion experiments,* electric power generation from ionized gases produced by combustion of fossil fuels or from heat produced in a fission reactor,† and space propulsion achieved by electromagnetic acceleration of ionized gases.‡ Scientific interest in this area includes such geophysical and astrophysical topics as the origin of the earth's magnetic field in its liquid metal core and the dynamics of stellar structures composed of highly ionized gases.

A similar area is *ferrohydrodynamics*, which is concerned with magnetization interactions of magnetic fields with a ferromagnetic fluid.§

Electrohydrodynamics (EHD) is concerned with interaction between electric fields and free or bound (polarization) charges in fluids. The fluids may be extremely good insulators, slightly conducting, or even highly conducting. The distinguishing feature is that the electromagnetic part of the system is described by a quasi-static electric field model. Applications of EHD include pumping and levitation of liquids and gases, extraction of contaminants from gases such as smoke,** mixing of liquids, orientation of liquids in near-zero-gravity environments, augmentation of heat transfer, and property measurements in fluid systems. EHD interactions also occur in meteorology, in which charge distribution in the atmosphere (as in a thunderstorm) is important, and in surface physics, in which the distribution of charges at an interface is significant, as in frictional electrification.††

The engineering and scientific applications of *electron and ion beams* involve continuum electromechanical interactions. Electron beams, confined by magnetic fields and interacting through electric fields with distributed electric circuits, are commonly used to generate power at microwave frequencies.‡‡ In such applications the beam is represented by quasi-static equations, but the distributed electric circuits support electromagnetic waves and are not amenable to quasi-static analysis. Electron beams are also used for heating, welding, forming, and purifying metals. Charged particle beams, electrons and ions, are used for medical treatment, for measuring collision cross sections, and for heating plasmas.§§

* D. J. Rose and M. Clark, Jr., *Plasmas and Controlled Fusion*, M.I.T. Press and Wiley, New York, 1961.

† G. W. Sutton and A. Sherman, *Engineering Magnetohydrodynamics*, McGraw-Hill, New York, 1965.

‡ *Ibid.*, p. 447.

§ R. E. Rosensweig, "Magnetic Fluids," *Intern. Sci. Technol.*, **55**, 48-56, 90 (July 1966).

** H. J. White, *Industrial Electrostatic Precipitation*, Addison-Wesley, Reading, Mass., 1963.

†† L. B. Loeb, *Static Electrification*, Springer, Berlin, 1958.

‡‡ C. C. Johnson, *Field and Wave Electrodynamics*, McGraw-Hill, New York, 1965, p. 275.

§§ T. H. Stix, *The Theory of Plasma Waves*, McGraw-Hill, New York, 1962, p. 107.

*Plasma dynamics** is concerned with the behavior of gases composed at least in part of charged particles. Thus continuum electromechanical interactions will affect the behavior of a plasma. Probably the most common example of a plasma is the ionized gas in a fluorescent lamp. Other examples are gas-filled rectifiers, flames such as rocket exhausts, and the sun. The physical characteristics of ionized gases can assume many forms. In certain cases, such as proposed fusion devices and MHD generators, the plasma behaves as a highly conducting fluid and its dynamic behavior is described by a magnetohydrodynamic approximation. In other cases the plasma is only slightly ionized and the electrohydrodynamic equations are appropriate. In still other cases the plasma may be so tenuous that it is best described as a collection of noninteracting particles in imposed magnetic and electric fields. In all of these regimes the plasma exhibits the basic phenomena of wave propagation and instability, subjects that are treated in this chapter.

Electrons and holes in semiconductors, usefully modeled as plasmas, give rise to the name *solid-state plasmas*.† These charges behave collectively like gaseous plasmas and are thus amenable to analysis with the same types of mathematical model. Electromechanical interactions in solid-state plasmas are used to achieve microwave power generation and to make electronic components with a variety of useful terminal characteristics.

Electromechanical interactions of several types occur with elastic solids and lead to useful devices such as transducers. *Electroelasticity* and *piezoelectricity*‡ result from polarization interactions in elastic dielectrics and are modeled as quasi-static electric field systems. *Magnetoelasticity* and *piezomagnetism*§ result from magnetization interactions in elastic solids and are modeled as quasi-static magnetic field systems. Magnetoelastic phenomena have found applications in *microwave magnetism*** in which electromechanical interactions lead to useful microwave components.

The foregoing examples illustrate the diversity of physical situations, in which continuum electromechanical interactions are important, and the variety of applications resulting therefrom. We now proceed to study the kinds of dynamical phenomena that can result from these interactions.

In the study of lumped parameter systems defined by linear, constant-coefficient equations, the temporal behavior is characterized by e^{st} , as illustrated in Chapter 5. Similarly, the dynamics of a continuum with a single

* L. Spitzer, Jr., *Physics of Fully Ionized Gases*, Interscience, New York, 1956. (The plasma, as defined on p. 17 of this reference, is somewhat more specifically defined than in our discussion.)

† R. Bowers and M. C. Steele, *Proc. I.E.E.E.*, **52**, 1105 (1964).

‡ W. P. Mason, *Physical Acoustics*, Vol. 1, Part A, Academic, New York (1964, pp. 169–270).

§ *Ibid.*

** W. F. Brown, *Micromagnetism*, Interscience, New York, 1963.

space dependence x can be represented in terms of solutions in the form*

$$\xi = \text{Re } \hat{\xi} e^{j(\omega t - kx)}. \quad (10.0.1)$$

The (angular) frequency ω can, in general, be complex

$$\omega = \omega_r + j\omega_i, \quad (10.0.2)$$

just as s can be complex in the lumped-parameter case. As we shall see, the physical significance of a complex ω is not so clear as it is in the lumped-parameter case because the temporal dependence is only part of the story. The wavenumber k , which represents the spatial dependence, can also be complex:

$$k = k_r + jk_i. \quad (10.0.3)$$

The sections that follow have the objective of imparting some physical and mathematical insight as to how wave solutions in the form of (10.0.1) are used to describe the dynamics of one-dimensional continuous media.

10.1 WAVES AND INSTABILITIES IN STATIONARY MEDIA

It is the purpose of this chapter to illustrate the dynamics of electro-mechanical continua. This is done by making use of the one-dimensional model for the wire and membrane, introduced in Chapter 9. It should be evident from the introduction that the cases considered in the following sections illustrate the dynamics of a variety of purely mechanical and purely electrical as well as electromechanical systems. A salient feature of the dynamics of systems involving continuous media is the effect of material motion. Our development in this section is confined to the dynamics of systems in which the mechanical medium is at rest. The effect of convection, or gross material motion, on these systems is taken up in the next section.

It is helpful to associate fundamental types of dynamical behavior with a particular physical situation. One of the simplest we can imagine for this purpose is the "string" or wire under tension. If the wire has an equilibrium tension f and a mass per unit length m , its transverse deflections are governed by the equation

$$m \frac{\partial^2 \xi}{\partial t^2} = f \frac{\partial^2 \xi}{\partial x^2} + S_z, \quad (10.1.1)$$

where S_z is a transverse force per unit length (see Table 9.2). In the sections that follow we consider electromechanical coupling to the string through

* The use of $j\omega$ rather than s is simply a matter of convention.

S_z . Before embarking on this development it would be helpful to recall the essential features of the string dynamics in the absence of coupling.

10.1.1 Waves without Dispersion

In the absence of external forces the string deflections $\xi(x, t)$ must satisfy the wave equation [(10.1.1) with $S_z = 0$]

$$\frac{\partial^2 \xi}{\partial t^2} = v_s^2 \frac{\partial^2 \xi}{\partial x^2}, \quad (10.1.2)$$

where $v_s = \sqrt{f/m}$. In Section 9.2.1 we found both the sinusoidal steady-state and the transient response (normal modes) of the string by making appropriate use of solutions in the form of (10.0.1). Substitution of the assumed solution into the equation of motion (10.1.2) shows that ω and k must be related by the dispersion equation

$$\omega^2 = v_s^2 k^2. \quad (10.1.3)$$

Thus the ω - k plot for waves on the simple string appears as shown in Fig. 10.1.1. For the real value of frequency ω shown in the figure there are two solutions ($\pm\beta$) to (10.1.3) for the wavenumber k .

From the form of the wave solution (10.0.1) it follows that points of constant phase move along the x -axis with a phase velocity

$$v_p = \frac{\omega}{k}. \quad (10.1.4)$$

Figure 10.1.1 shows that for a given frequency there are two waves with phase velocities that are negatives. Note that the phase velocities of the waves are

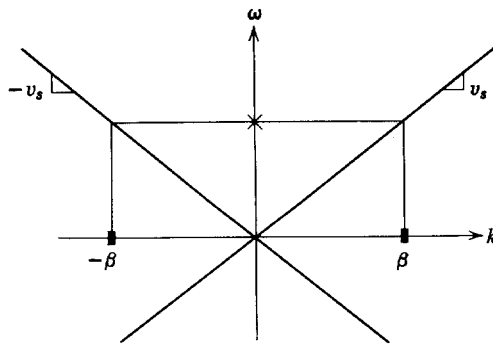


Fig. 10.1.1 Dispersion equation for waves on the simple string.

simply $\pm v_s$ and are independent of the frequency; that is, the dispersion equation for a given wave is a linear relationship between ω and k . For the simple string, waves with differing frequencies (or wavenumbers) propagate with the same phase velocity and are therefore said to propagate without dispersion.

10.1.2 Cutoff or Evanescent Waves

The string, described by (10.1.1), can be a taut conducting wire (or tightly wound helical spring) carrying a current that interacts with a magnetic field (Fig. 10.1.2). Here the string is stretched along the x -axis between two magnet coils arranged to give a null in magnetic field along the x -axis. The wire is free to vibrate in the horizontal plane of the magnet coils. For small excursions from the x -axis the wire experiences a magnetic flux density \mathbf{B} , which is essentially a linear function of ξ . Hence, when a current I is passed through the wire in the direction shown, a restoring force per unit length $\mathbf{I} \times \mathbf{B}$ tends to return the wire to the x -axis:

$$S_z \mathbf{i}_z = \mathbf{I} \times \mathbf{B} = -Ib \xi \mathbf{i}_z; \tag{10.1.5}$$

b is shown in Fig. 10.1.2b. This is the force-displacement relationship of a simple spring. The current \mathbf{I} and flux density \mathbf{B} interact to produce a spring-like force per unit length that tends to return the wire to its equilibrium position.

With the addition of coupling to the magnetic field, the equation of motion

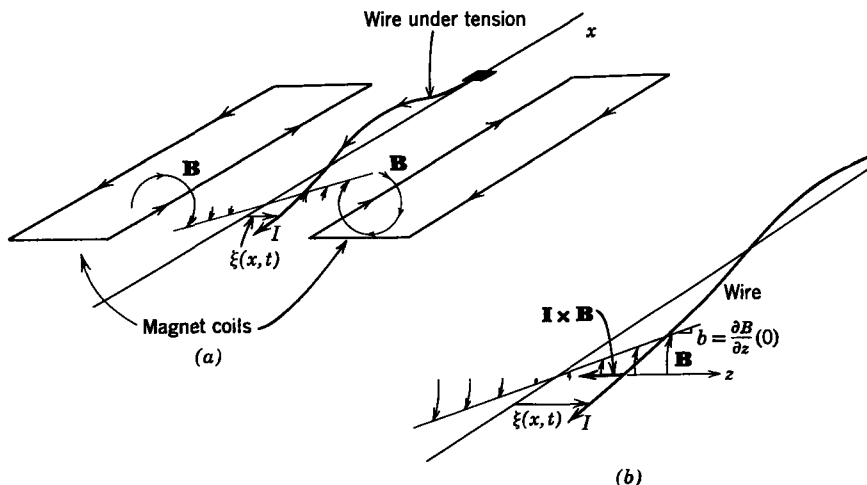


Fig. 10.1.2 (a) A conducting wire is stretched along the x -axis and is free to undergo transverse motions in the horizontal plane. Magnet coils produce a field \mathbf{B} which is zero along the x -axis; (b) the wire carries a current I so that deflections from the x -axis result in a force that tends to restore the wire to its equilibrium position.

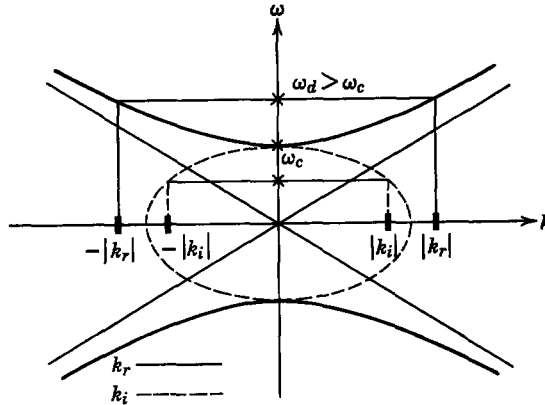


Fig. 10.1.3 Dispersion relation for the wire subject to a restoring force distributed along its length (for the case shown in Fig. 10.1.2). Complex values of k are shown as functions of real values of ω .

(10.1.1) becomes

$$\frac{\partial^2 \xi}{\partial t^2} = v_s^2 \frac{\partial^2 \xi}{\partial x^2} - \omega_c^2 \xi, \quad \omega_c^2 = \frac{Ib}{m}. \tag{10.1.6}$$

Now, substitution of solutions in the form of (10.0.1) gives a dispersion equation that is not simply the linear relationship between ω and k of (10.1.3). Rather

$$\omega^2 = v_s^2 k^2 + \omega_c^2. \tag{10.1.7}$$

For large values of k , ω does not depend significantly on ω_c , hence the asymptotes of an ω - k plot are simply the two straight lines of the ω - k plot with $\omega_c = 0$ (Fig. 10.1.1). If we note further that $\omega = \pm \omega_c$, where $k = 0$, the ω - k plot of Fig. 10.1.3 can be easily sketched. The effect of the current I is to evolve a pair of hyperbolas from the two straight lines of Fig. 10.1.1. As the current I is raised (with B fixed), the intersections ω_c move out along the ω -axis.

The dispersion equation is quadratic in both ω and k . Hence for each real value of k two values of ω can be seen from the solid curves of Fig. 10.1.3 always to be real. This relationship, however is not true if ω and k are interchanged. Real values of ω give real values of k only if $|\omega| > \omega_c$, as can also be seen in the figure. Solution of (10.1.7) shows that in the range $|\omega| < \omega_c$ the dispersion equation gives imaginary values of k represented by the dashed curve in Fig. 10.1.3. Note that when $k = jk_i$ in (10.1.7) the analytical geometric relation between ω and k_i is an ellipse; for example at the points at which $\omega = 0$ (10.1.7) shows that $k = \pm j\omega_c/v_s$.

The most evident consequences of introducing the additional force, which we can think of as resulting because of the current I , are illustrated by

considering the response to a sinusoidal, steady-state driving function. For purposes of illustration the spring is fixed at $x = 0$ and given a sinusoidal displacement at $x = -l$:

$$\xi(0, t) = 0, \quad (10.1.8)$$

$$\xi(-l, t) = \xi_a \sin \omega_d t. \quad (10.1.9)$$

These conditions are the same as those considered in Section 9.2.1*a* for the wire with no external force.

To match the driving condition the frequency ω of the dispersion equation is taken as ω_d , and solutions have the form of (10.0.1) for two values of k which can be found by solving (10.1.7).

$$k = \pm \frac{\sqrt{\omega_d^2 - \omega_c^2}}{v_s}. \quad (10.1.10)$$

These wavenumbers are shown graphically in Fig. 10.1.3.

To avoid ambiguity the wavenumbers consistent with the frequency $\omega = \omega_d$, given by (10.1.10) are written as

$$\begin{aligned} k &= \pm |k_r|, & \omega_d &> \omega_c, \\ k &= \pm j |k_i|, & \omega_d &< \omega_c. \end{aligned} \quad (10.1.11)$$

This is the notation used in Fig. 10.1.3. At this point we have established that there are two waves on the wire with the frequency ω_d , and the boundary conditions are satisfied by taking a linear combination of these waves. For $\omega_d > \omega_c$

$$\xi = \text{Re} (C e^{-j|k_r|x} + D e^{j|k_r|x}) e^{j\omega_d t} \quad (10.1.12)$$

and a similar equation with $|k_r| \rightarrow j |k_i|$ for $\omega_d < \omega_c$. The constants C and D are determined by the boundary conditions (10.1.8) and (10.1.9). It follows that for

$$\omega_d > \omega_c, \quad \xi = -\xi_a \frac{\sin |k_r| x}{\sin |k_r| l} \sin \omega_d t, \quad (10.1.13)$$

and for

$$\omega_d < \omega_c, \quad \xi = -\xi_a \frac{\sinh |k_i| x}{\sinh |k_i| l} \sin \omega_d t, \quad (10.1.14)$$

The significance of the imaginary wavenumbers is now apparent. Figure 10.1.4 shows the effect of raising the current I (i.e., ω_c) with the driving frequency ω_d fixed. With no current, waves on the wire have the same familiar appearance as in Section 9.2.1*a* (see Fig. 9.2.6). As long as $\omega_d > \omega_c$, this same general appearance prevails and the wire tends to bow outward and assume the shape usually found with standing waves. When ω_c has been raised to the point at which it coincides with ω_d , the wire takes on the appearance shown in Fig. 10.1.4*b*. Here the effect of inertia, which tends to make the wire bow outward,

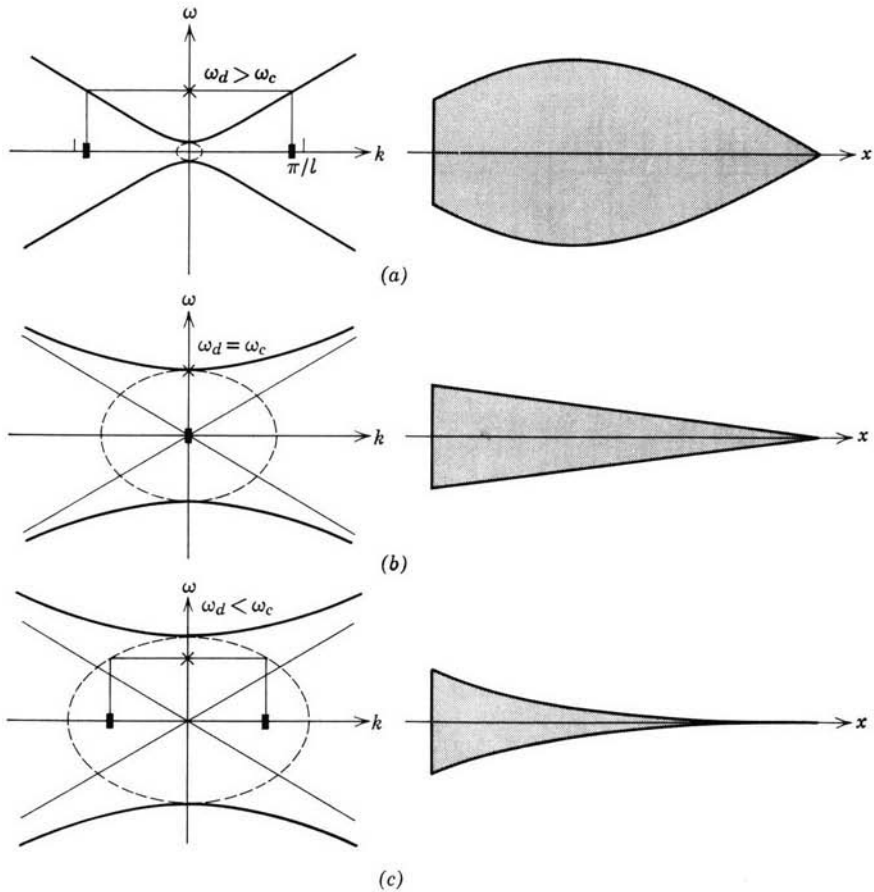


Fig. 10.1.4 Envelope of wire deflection in magnetic field. The wire is fixed at the right end and driven at a fixed sinusoidal frequency at the left end. The ω - k plots show the effect of the current I on the dispersion equation. The current I (or cutoff frequency ω_c) is being raised so that (a), $I \approx 0$, (b) I is sufficient just to cut off the propagation ($\omega_d = \omega_c$), and (c) the waves are evanescent, $\omega_d < \omega_c$. This experiment can be seen in the film "Complex Waves I," produced for the National Committee on Electrical Engineering films by Education Development Center, Newton, Mass.

is just canceled by the restoring force due to I . The wavenumbers are zero and the envelope of the wire deflection is a linear function of x . The limit of either (10.1.13) or (10.1.14) as $k \rightarrow 0$ yields

$$\xi = -\xi_d \left(\frac{x}{l} \right) \sin \omega_d t. \quad (10.1.15)$$

This is called the cutoff condition, hence ω_c is the *cutoff frequency*. As ω_c is raised still further, the wire bows inward, as shown in Fig. 10.1.4c. Here the

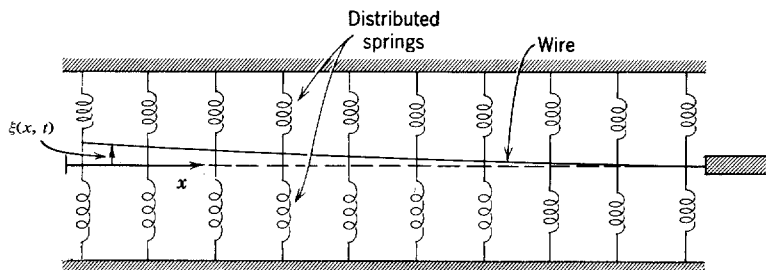


Fig. 10.1.5 With the current as shown, the system in Fig. 10.1.2 gives rise to forces on the wire that are equivalent to springs distributed along the length of the wire.

deflection amplitude simply decays spatially as we move away from the point of excitation. The spatial dependence of (10.1.14) is monotonic in x , so that the wire deflections have the same phase as the excitation. Note that these decaying or *evanescent* waves do not involve dissipation. They are present here because each segment of the wire is subject to a springlike restoring force that tends to push it toward the x -axis. An equivalent physical situation is shown in Fig. 10.1.5. Without recourse to mathematics we expect that when the left end of the wire is slowly displaced upward the wire tends to bow inward toward the x -axis. This is all that (10.1.14) is telling us. The restoring force that we would feel in slowly displacing the end of the wire would be the same as if we were displacing the end of a spring.

As we shall see, continuous media excited in the sinusoidal steady state can also support spatially decaying waves because of damping (dissipation of energy). Even more interesting are situations in which complex wavenumbers mean that waves grow spatially rather than decaying. Both cases, which are considered in later sections, involve dispersion equations that give complex values of k for real values of ω , just as we have here, and it is important to establish a physical picture of their significance.

Evanescent or cutoff waves are often found in studies of propagation through guiding structures. We shall see this in Section 10.4.1 in which waves that propagate in the x -direction on a membrane fixed along its edges at $y = 0$ and $y = b$ have a cutoff frequency below which they are evanescent. This is an example of a wide class of two- and three-dimensional situations in which propagation in a longitudinal (x) direction is restricted by boundary conditions in the transverse directions (y and z). The transverse boundaries restrict (or squash) the dynamical motions, just as they do in Fig. 10.1.5. Before propagation can take place the frequency of the drive must exceed some cutoff value in which the constraints produced by the transverse boundaries are canceled by a dynamic effect such as that resulting here from inertia. This is illustrated for waves in elastic structures in Sections 11.4.2b and 11.4.3.

Cutoff waves are found also in electromagnetic waveguides,* in which they are of considerable significance in establishing the propagation of a single mode (all modes but one are cutoff) and in which they are sometimes used to make microwave attenuators.

When an electromagnetic wave propagates through a medium, such as a plasma, it is possible that the medium will have the same effect on the waves as the springs of Fig. 10.1.5 have on waves propagating on the string. Hence cutoff or evanescent waves are of considerable importance in studies of wave propagation through plasmas.† Example 10.1.1 considers a situation, similar to that found in studies of the hydromagnetic equilibrium of fusion machines, in which evanescent waves account for the stabilizing (stiffening) influence of transverse boundaries.

Before considering what happens when I is reversed, it would be worthwhile to draw attention to the effect of the current I shown in Fig. 10.1.2 on the natural modes of vibration. Remember (from Section 9.2.1b) that it is these modes that characterize the response of the wire to initial conditions.

To find the eigenfrequencies with both ends ($x = 0$ and $x = -l$) of the string fixed, we once again take a linear combination of waves with wavenumbers k found from the dispersion equation (10.1.7) for a given value of ω . At the outset this frequency ω remains to be found.

$$\xi = \text{Re} (Ce^{-i\beta x} + De^{i\beta x})e^{j\omega t}. \quad (10.1.16)$$

For convenience we have written the two values of k as $k = \pm\beta$, with β defined as

$$\beta = \frac{\sqrt{\omega^2 - \omega_c^2}}{v_s}. \quad (10.1.17)$$

It is clear that to satisfy the boundary condition $\xi(0, t) = 0$, the constants C and D are related by $C = -D$, so that (10.1.16) becomes

$$\xi = \text{Re} \xi \sin \beta x e^{j\omega t}, \quad (10.1.18)$$

where ξ includes the remaining arbitrary constant. Then to satisfy the boundary condition $\xi(-l, t) = 0$ it follows from (10.1.18) that

$$\sin \beta l = 0. \quad (10.1.19)$$

* See R. B. Adler, L. J. Chu, and R. M. Fano, *Electromagnetic Energy Transmission and Radiation*, Wiley, New York, 1960, pp. 369–378, or S. Ramo, J. R. Whinnery, and T. Van Duzer, *Fields and Waves in Communications and Electronics*, Wiley, New York, 1965, p. 420.

† See T. H. Stix, *The Theory of Plasma Waves*, McGraw-Hill, New York, 1962, p. 13, or W. P. Allis, S. J. Buchsbaum, and A. Bers, *Waves in Anisotropic Plasmas*, M.I.T. Press, Cambridge, Mass., 1963, p. 13.

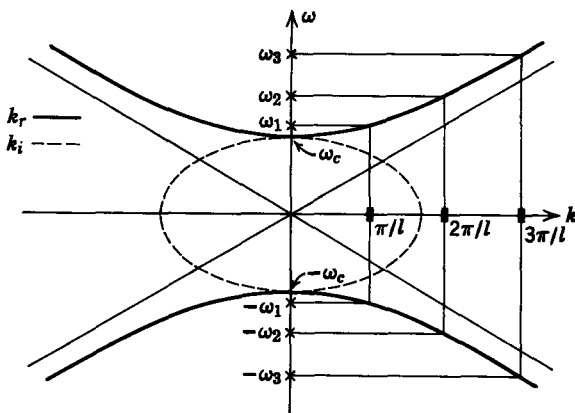


Fig. 10.1.6 A dispersion equation for waves on the wire in Fig. 10.1.2 showing the relationship between the eigenfrequencies ω_n and the eigenvalues $k = n\pi/l$.

This eigenvalue equation is the same as that for a wire without the magnetic force. It has solutions

$$\beta l = n\pi, \quad n = 1, 2, 3, \dots \tag{10.1.20}$$

Now that we have seen a case in which complex wavenumbers have physical significance it is worthwhile to observe that the solutions to (10.1.19), given by (10.1.20), are the only solutions and that they constrain β to be real. We have omitted negative values of n , for the modes represented by these roots are redundant. Note that $n = 0$ is not included because it leads to an eigenvalue $\beta = 0$; hence from (10.1.18) it leads to no deflection. Solutions to the eigenvalue equation of this type, which lead to a vanishing eigenfunction, are referred to as trivial solutions. Now that the eigenvalues have been determined, (10.1.20), we can solve (10.1.17) for the corresponding eigenfrequencies:

$$\omega = \pm\omega_n = \pm \left[\left(\frac{n\pi}{l} \right)^2 + \omega_c^2 \right]^{1/2}. \tag{10.1.21}$$

These are the natural frequencies of the wire in the presence of the magnetic force. The natural modes can be seen from (10.1.18) to have the same form as those for the wire with $I = 0$:

$$\xi = \text{Re} (A_n^+ e^{j\omega_n t} + A_n^- e^{-j\omega_n t}) \sin \frac{n\pi x}{l}. \tag{10.1.22}$$

Note, however, that the frequencies ω_n are affected by the current I . Their relationship to the dispersion equation is shown graphically in Fig. 10.1.6. The eigenvalues are indicated along the k -axis. (Note that taking negative values of k results in redundant frequencies.) The corresponding eigenfrequencies are increased in magnitude by an increase in the current (increase

in ω_c). As should be expected, the magnetic force has a tendency to stiffen the wire, with the largest effect on the longest wavelengths or lowest frequencies (those least affected by the tension of the wire). The most significant effect of the current is on the lowest eigenfrequency ω_1 , which approaches ω_c more rapidly than the other frequencies as the current is increased. Note that because of the current the eigenfrequencies are no longer harmonically related.

Because the natural frequencies are purely real, they appear as resonances of the driven response. This was discussed in detail in Section 9.2.1*a* for the wire without magnetic coupling. It could have been discerned earlier in this section by observing the possibility of a finite response from (10.1.13), even as $\xi_a \rightarrow 0$, if the denominator also approaches zero. This requires that

$$\sin |k_r| l = 0, \tag{10.1.23}$$

which is the same condition as that in (10.1.19) except that $|k_r|$ is a function of ω_a (the driving frequency) rather than an unspecified ω . Hence, if the frequency ω_a is tuned to one of the eigenfrequencies, there is a resonance in the response. The resonance frequencies of the wire are shifted upward by increasing the current I (or increasing the cutoff frequency ω_c).

Example 10.1.1. Magnetic fields are sometimes used to contain and orient highly conducting media; for example, in devices proposed to achieve thermonuclear fusion the magnetic field is used to make a “bottle” for the plasma. For many purposes this plasma, or highly ionized gas, can be considered as a perfectly conducting fluid. The example discussed here illustrates the continuum dynamics of a medium which, like the plasma, is assumed to have an infinite conductivity.

A perfectly conducting membrane forms the deformable part of the system shown in Fig. 10.1.7. When the membrane is undeformed, it lies in the x - y plane and is immersed in a uniform constant magnetic field $\mathbf{H} = H_0 \mathbf{j}_x$. We consider deformations of the membrane

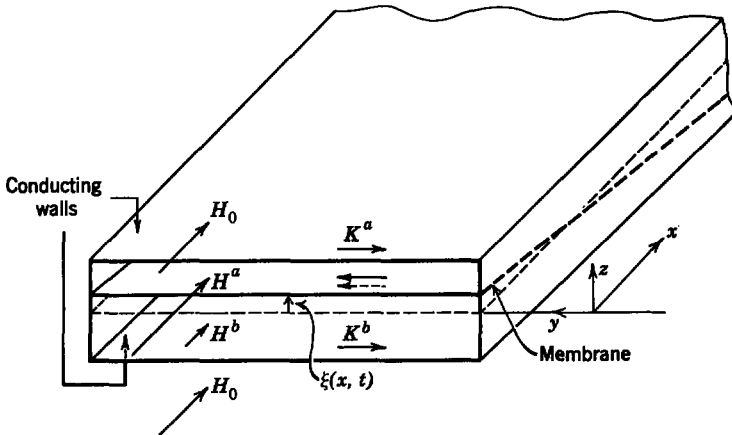


Fig. 10.1.7 A perfectly conducting membrane is bounded from above and below by fixed conducting walls and is immersed in an initially uniform magnetic field H_0 .

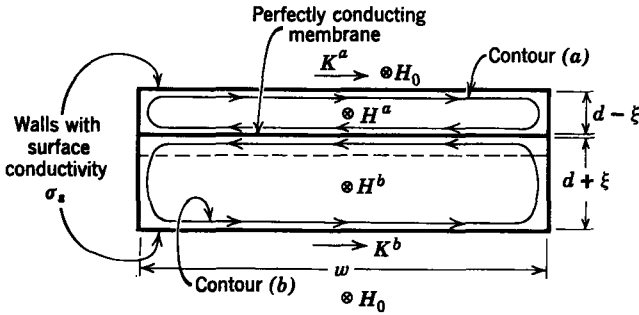


Fig. 10.1.8 Cross-sectional view of the apparatus shown in Fig. 10.1.7. The current loops (a) and (b), with the imposed magnetic field H_0 , couple the membrane to the upper and lower conducting walls.

$\xi(x, t)$ that do not depend on y ; hence the membrane has the general appearance shown in Fig. 10.1.7.

The membrane has a width w with its edges making electrical contact with the walls of a rectangular conducting conduit. Thus the membrane and the upper wall form a conducting loop [contour (a) shown in Fig. 10.1.8]. Similarly, the lower wall and membrane form the conducting loop (b). In the limit in which the conductivity of the walls (σ_s) is infinite the magnetic flux linked by each of these circuits must remain constant. Hence an upward deflection is accompanied by an increase in the field intensity above the membrane and a decrease in the field intensity below it. The conservation of flux is realized because of the flow of surface currents K^a and K^b as shown. This type of flux conservation dynamics is familiar from Section 5.1.3, in which it was encountered in the context of lumped-parameter dynamics.

The induced currents shown in Fig. 10.1.8 are responsible for creating a magnetic force on the membrane that tends to restore it to the plane of zero deflection. Therefore we can expect from the outset to obtain an equation of motion similar to (10.1.6).

The equation of motion for the membrane is

$$\sigma_m \frac{\partial^2 \xi}{\partial t^2} = S \frac{\partial^2 \xi}{\partial x^2} + T_z, \tag{a}$$

where T_z is the force per unit area acting in the z -direction (see Table 9.2). The magnetic field intensity above the membrane (a) and below the membrane (b) can be written as

$$\mathbf{H}^a = [H_0 + h^a(x, t)]\mathbf{i}_x, \tag{b}$$

$$\mathbf{H}^b = [H_0 + h^b(x, t)]\mathbf{i}_x, \tag{c}$$

where h^a and h^b represent perturbations from the equilibrium magnetic field intensity caused by deflections of the membrane. We assume that the transverse displacements $\xi(x, t)$ vary slowly enough with x that at each cross section of the system shown in Fig. 10.1.7 the magnetic field is essentially x -directed and is independent of y and z .

Ampère's law requires that the jump in magnetic field intensity on the upper and lower plates be equal to their respective surface currents. Hence

$$h^a = K^a, \tag{d}$$

$$h^b = -K^b, \tag{e}$$

and we can find the perturbation field intensities by writing circuit equations for the currents K^a and K^b . The integral law of induction used in conjunction with the contour (a) of Fig. 10.1.8 is

$$\oint_{C_a} \mathbf{E}' \cdot d\mathbf{l} = - \frac{\partial}{\partial t} \int_{S_a} \mu_0 \mathbf{H} \cdot \mathbf{n} \, da, \quad (\text{f})$$

where the time derivative is written as a partial because the flux is a function of the longitudinal position x of the cross-sectional surface of integration S_a enclosed by the contour C_a . To evaluate the integral on the left note that \mathbf{E}' is zero both in the perfectly conducting membrane and in the perfectly conducting end walls. In the upper plate the surface current density and electric field are related by Ohm's law, which takes the form

$$\mathbf{K}^a = \sigma_s \mathbf{E} \quad (\text{g})$$

because the upper wall is fixed. Equation f then becomes

$$\frac{wK^a}{\sigma_s} = - \frac{\partial}{\partial t} [w(d - \xi) \mu_0 (H_0 + h^a)]. \quad (\text{h})$$

Similar arguments, used with contour (b) in Fig. 10.1.8, produce the electrical equation

$$\frac{wK^b}{\sigma_s} = \frac{\partial}{\partial t} [w(d + \xi) \mu_0 (H_0 + h^b)]. \quad (\text{i})$$

We confine our attention to small displacements of the membrane so that it is appropriate to linearize these last two equations, which in view of (d) and (e) become

$$\frac{h^a}{\sigma_s} = - \frac{\partial}{\partial t} (\mu_0 d h^a - \mu_0 H_0 \xi), \quad (\text{j})$$

$$- \frac{h^b}{\sigma_s} = \frac{\partial}{\partial t} (\mu_0 d h^b + \mu_0 H_0 \xi). \quad (\text{k})$$

These expressions are the required electrical equations of motion that relate the field intensities above and below the membrane to the displacement ξ . The remaining equation is (a), with T_z written in terms of h^a and h^b .

To find T_z , the surface force density is related to the Maxwell stress T_{mn}^* by (8.4.2)

$$T_z = (T_{zm}^a - T_{zm}^b) n_m, \quad (\text{l})$$

where \mathbf{n} is the vector normal to the membrane surface. Because $\mathbf{n} \approx i_z$, the summation on m has only one contribution, $m = z$, and (l) reduces to

$$T_z = T_{zz}^a - T_{zz}^b = -\frac{1}{2} \mu_0 [(H^a)^2 - (H^b)^2]. \quad (\text{m})$$

Now, if we introduce (b) and (c), this expression can be linearized to obtain

$$T_z = -\mu_0 H_0 (h^a - h^b). \quad (\text{n})$$

* Alternatively, the surface force density can be derived by using the energy method of Chapter 3 and viewing each section of the membrane as forming a pair of parallel plate inductors with the side walls. If this is done, remember that in addition to the two terminal pairs for these inductors there is a third terminal pair, constrained to constant current, for the magnet that makes H_0 .

The effect of finite conductivity in the walls has been included up to this point because it offers the possibility of illustrating at least two important dynamical effects. These are discussed when this example is continued in Sections 10.1.4 and 10.2.4. For now, we consider the limit in which σ_s is large enough that the fluxes linked by contours (a) and (b) remain essentially constant. Because the quantities in parentheses in (j) and (k) are the flux perturbations, they must therefore be zero and it follows that

$$h^b = \frac{H_0 \xi}{d}, \tag{o}$$

$$h^a = \frac{-H_0 \xi}{d}. \tag{p}$$

If we combine these expressions with (n) and (a), an equation of motion results:

$$\frac{\partial^2 \xi}{\partial t^2} = v_s^2 \frac{\partial^2 \xi}{\partial x^2} - \omega_c^2 \xi, \tag{q}$$

where

$$v_s = \left(\frac{S}{\sigma_m} \right)^{1/2},$$

$$\omega_c^2 = \frac{2\mu_0 H_0^2}{\sigma_m d}.$$

This expression has the same form as (10.1.6), and we can conclude that in the limit in which $\sigma_s \rightarrow \infty$ the membrane of Fig. 10.1.7 will have the same dynamical behavior found for the wire shown in Fig. 10.1.5.

10.1.3 Absolute or Nonconvective Instability

When the current is reversed in the experiment of Fig. 10.1.2, the wire dynamics are found to be altogether different from those described in the preceding section. As the current I (shown in Fig. 10.1.9) is raised, there is a threshold beyond which the wire bows outward. Under this condition, no matter how carefully the wire is placed on the center line between the coils, it bows outward when it is released.

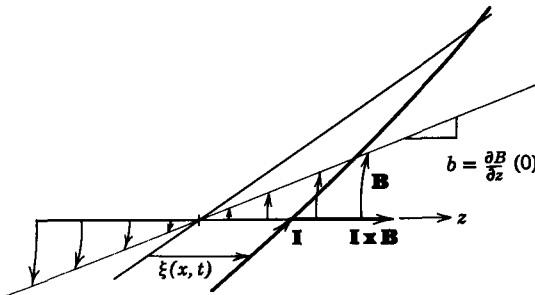


Fig. 10.1.9 Wire carrying current I in a magnetic field that is zero along the axis $\xi = 0$. Current is reversed from the situation shown in Fig. 10.1.2.

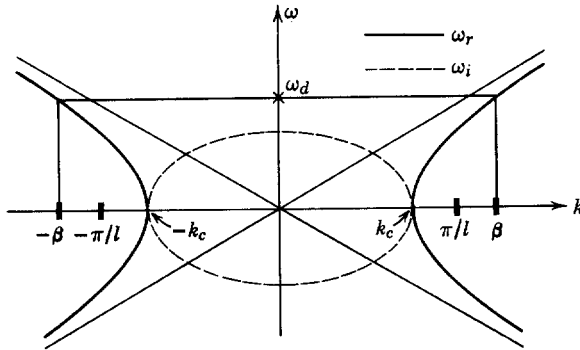


Fig. 10.1.10 Plot of the dispersion equation for physical situation shown in Fig. 10.1.2 with the current reversed, as in Fig. 10.1.9. Complex values of ω are shown for real values of k .

This might be expected. Reversing the current gives rise to a magnetic force, as in (10.1.5) with $I \rightarrow -I$, that tends to carry the wire in the same direction as the displacement. Hence it tends to produce an instability that is the continuum analogue of the static instability of lumped-parameter systems described in Section 5.1.2*a*. A transverse deflection, shown in Fig. 10.1.9, leads to a magnetic force that tends to make the deflection even larger.

The equation of motion is again (10.1.1), but now S_z is

$$S_z = Ib\xi \tag{10.1.24}$$

and the equation governing deflections of the wire is

$$\frac{1}{v_s^2} \frac{\partial^2 \xi}{\partial t^2} = \frac{\partial^2 \xi}{\partial x^2} + k_c^2 \xi, \tag{10.1.25}$$

where

$$k_c^2 = \frac{Ib}{f}.$$

Again, the dispersion equation is found by substituting (10.0.1) into this equation of motion to obtain

$$\omega^2 = v_s^2(k^2 - k_c^2). \tag{10.1.26}$$

The asymptotes of this expression, plotted in the ω - k plane, are again straight lines with slopes $\pm v_s$. The two branches of the plot, however, now pass through the k -axis, as can be seen by setting $\omega = 0$ and solving (10.1.26) to obtain $k = \pm k_c$. Hence the real values of ω , as a function of real values of k , appear as shown by the solid lines in Fig. 10.1.10. For each value of ω there is a corresponding pair of real wavenumbers k . This is evident either from Fig. 10.1.10 or from (10.1.26) solved for k . By contrast only real values of k with a magnitude greater than k_c lead to real values of ω .

Note that the roles of ω and k are the reverse of what they were in the preceding section. Now, it is appropriate to plot complex values of ω for real values of k , and this is the significance of the broken line in Fig. 10.1.10. In the range of wavenumbers $-k_c < k < k_c$ the frequency ω is purely imaginary. Substitution of $\omega = j\omega_i$ in (10.1.26) shows that the relation between ω_i and k is an ellipse (Fig. 10.1.10).

Consider first the sinusoidal steady-state vibrations with the same boundary conditions (10.1.8) and (10.1.9) used in the preceding section. Then the same steps used to compute (10.1.13) give

$$\xi = -\xi_a \frac{\sin \beta x}{\sin \beta l} \sin \omega_d t, \quad (10.1.27)$$

where

$$\beta = \left(\frac{\omega_d^2}{v_s^2} + k_c^2 \right)^{1/2}. \quad (10.1.28)$$

This solution to (10.1.25) is simply a linear combination of waves for which the two wavenumbers $k = \pm\beta$ are found by solving the dispersion equation (10.1.26) with $\omega = \omega_d$. These solutions are shown graphically in Fig. 10.1.10.

The sinusoidal steady-state vibrations have the same general spatial appearance as the wire with no magnetic force. The frequency response, however, has been altered by the current I . As in Section 10.1.2, there are resonances in this response at the natural frequencies. They occur when the denominator of (10.1.27) goes to zero or when $\beta l = n\pi$, $n = 1, 2, 3, \dots$. It follows from (10.1.28) that the resonance frequencies are

$$\omega_d = \pm v_s \left[\left(\frac{n\pi}{l} \right)^2 - k_c^2 \right]^{1/2}, \quad n = 1, 2, 3, \dots \quad (10.1.29)$$

Remember that k_c can be increased by increasing the current I . The equation shows that the response frequencies are reduced by the interaction with the magnetic field. This is just the opposite of the effect found in the preceding section, in which these resonance frequencies were increased by the magnetic interaction.

As the current I is increased, the point is reached at which the lowest resonance frequency is reduced to zero. From (10.1.29) this critical condition occurs when

$$k_c = \frac{\pi}{l} \quad (10.1.30)$$

For larger values of k_c the lowest resonance frequency is no longer real. Because this resonance results when the driving frequency is tuned to the natural frequency, we suspect that the lowest natural frequency is complex after k_c exceeds π/l . Note that the driven response given by (10.1.27) is still perfectly valid even if k_c is larger than the critical value given by (10.1.30).

It is of crucial importance to recognize that once k_c exceeds π/l the sinusoidal steady-state response is of little significance. The lowest natural mode of the system is unstable and the transient solution, initiated by the initial conditions, eventually dominates the driven response. To see this we now consider the natural modes of the wire with both ends fixed.

The steps used in Section 10.1.2 in going from (10.1.18) to (10.1.22) are equally valid here. Hence the eigenmodes are given by (10.1.22). Now, however, the eigenfrequencies are given by the revised dispersion equation (10.1.26) with $k^2 = (n\pi/l)^2$.

$$\omega = \pm \omega_n = \pm v_s \left[\left(\frac{n\pi}{l} \right)^2 - k_c^2 \right]^{1/2}. \tag{10.1.31}$$

These eigenfrequencies are shown in Fig. 10.1.11, in which a graphical representation of the dispersion equation shows how the discrete values of k allowed by the fixed ends of the spring are related to the ω_n 's. From the figure it can readily be visualized how the frequencies of each mode shift inward as $k_c(l)$ is increased. As k_c is increased beyond $n\pi/l$, the frequencies of the n th mode move onto the ellipse and take the form

$$\omega_n = j |\omega_i|,$$

as can be seen from (10.1.31). The negative imaginary eigenfrequency gives rise to an eigenmode (10.1.22) that has an exponentially increasing amplitude.

In Section 9.2.1*b* we saw that the eigenmodes were orthogonal. Physically this meant that if initial conditions were such that only one of the modes was excited that mode would persist indefinitely without involving the others. [See Example (9.2.1) for a particular illustration of this point.] Suppose that

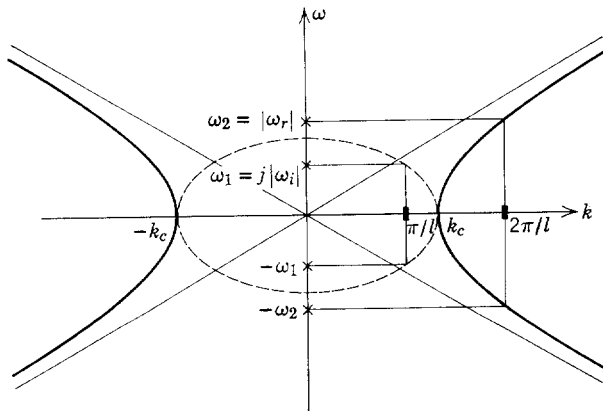


Fig. 10.1.11 The dispersion equation for the system of Fig. 10.1.2 with current as shown in Fig. 10.1.9. Complex values of ω are shown for real values of k . The allowed values of k give rise to the eigenfrequencies as shown.

the A_n 's in (10.1.22) were adjusted so that just the lowest mode was initiated. Then, with $k_c < \pi/l$, the vibrations of the wire would have the oscillatory dependence on x and t shown in Fig. 10.1.12a. With $k_c > \pi/l$, wire displacements would appear as the instability shown in Fig. 10.1.12b. This is an example of an absolute or nonconvective instability because, unlike instabilities that we shall study in Section 10.2, it involves deflections that become unbounded as time increases at a fixed point in space; That is, if the wire extended to $x = \pm \infty$ and a pulse were initiated at $x = 0$, the deflection at $x = 0$ would become unbounded with time.

The "unboundedness" of the unstable deflections is, of course, a prediction of the mathematical model that sooner or later is not accurate because of nonlinear effects that were neglected in both the derivation of the equation of motion for the wire and in writing S_z as in (10.1.24). This same limitation was involved in the lumped-parameter, linear stability theory of Section 5.1.2.

The dynamics that determine when the deflections will become large vary from the mundane to the spectacular and from the disastrous to the useful. In the system of Fig. 10.1.9 the deflections may increase until the wire encounters one of the magnet coils or they may simply reach some saturation

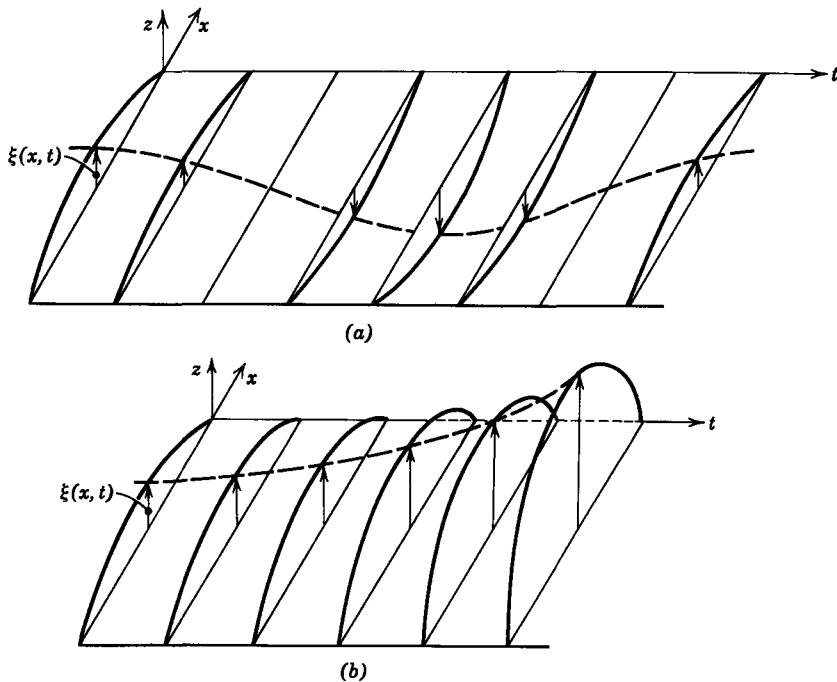


Fig. 10.1.12 Space-time dependence of lowest eigenmode: (a) $k_c < \pi/l$, stable; (b) $k_c > \pi/l$, unstable.

amplitude dictated by the large amplitude variation of the magnetic field. In Section 10.4.3 we shall see a grossly nonlinear consequence of absolute instability—the destruction of the system. On the other hand, as discussed later, instabilities of some types form the basis for making oscillators.

The example of instability presented in this section has the virtue of being extremely simple to understand mathematically, by comparison with instabilities often found in continuous media.* Nevertheless, there are practical situations in which this model has engineering significance. Example 10.1.2 considers how instability, predicted by this simple model, imposes a limitation on the levitation of continuous media with an electric field.

Absolute instability is of great interest to those concerned with fluid dynamics and the dynamics of elastic media. A classic example in the first category, which is closely related to the case considered in this section, is shown in Fig. 10.1.13. In Fig. 10.1.13*a* a heavy fluid (which is dark) is supported on a lighter fluid (which is clear) by hydrostatic pressure. In this initial equilibrium state each element of the fluid is in force equilibrium. With the heavy fluid on top, however, the equilibrium is unstable in the same sense that the wire of Fig. 10.1.9 was unstable. The only reason that the heavy fluid holds the position shown in Fig. 10.1.13*a* is that it is subject to an electric field, which induces polarization forces (discussed in Section 8.5) that stabilize the equilibrium. When this electric field is removed, the equilibrium becomes unstable, as shown in Figs. 10.1.13*b–e*, and the heavier fluid falls to the bottom of the tank. This is called a Rayleigh-Taylor† instability, and although the three-dimensional fluid motions are more complicated mathematically than those of the wire considered here the properties of these instabilities are in many ways similar. Both are absolute instabilities, and both instabilities have small amplitude motions characterized by a purely exponential growth with time.

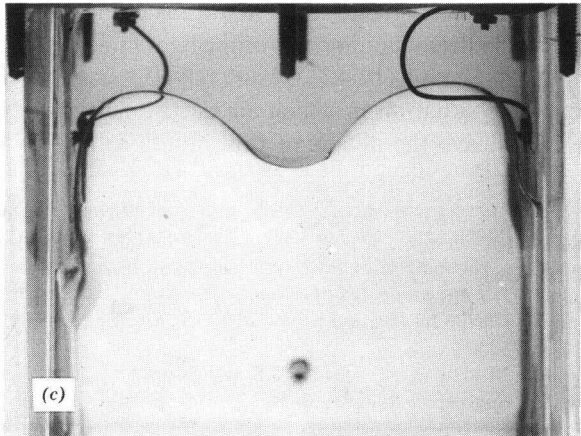
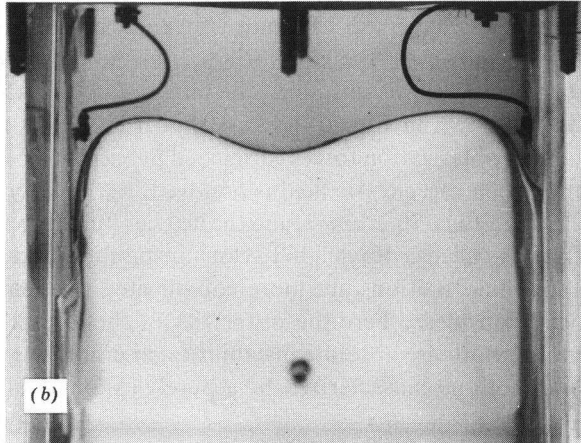
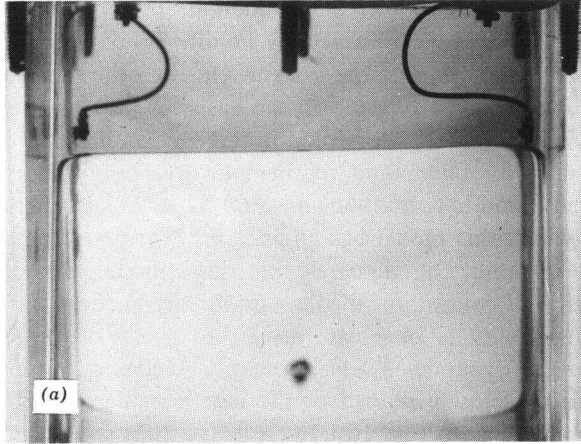
Rayleigh-Taylor types of instability are found in a variety of situations. Many found in the hydromagnetic equilibria of fusion machines have characteristics similar to the heavy fluid on top of the light fluid.‡ This connection is explored further in Section 10.4.3. Figure 10.1.13 actually illustrates an electrohydrodynamic situation in which an electric field prevents instability (although we must leave the details of this situation for further reading§).

* The downward shift of the natural frequencies and instability of the lowest mode are illustrated in the film "Complex Waves I" produced by the Education Development Center, Newton, Mass., for the National Committee on Electrical Engineering Films.

† S. Chandrasekhar, *Hydrodynamic and Hydromagnetic Stability*, Oxford, 1961, p. 428.

‡ D. J. Rose and M. Clark, Jr., *Plasmas and Controlled Fusion*, M.I.T. Press and Wiley, New York, 1961, p. 258.

§ J. R. Melcher and M. Hurwitz, "Gradient Stabilization of Electrohydrodynamically Oriented Liquids," *J. Spacecraft Rockets*, 4, No. 7, 864–881 (July 1967).



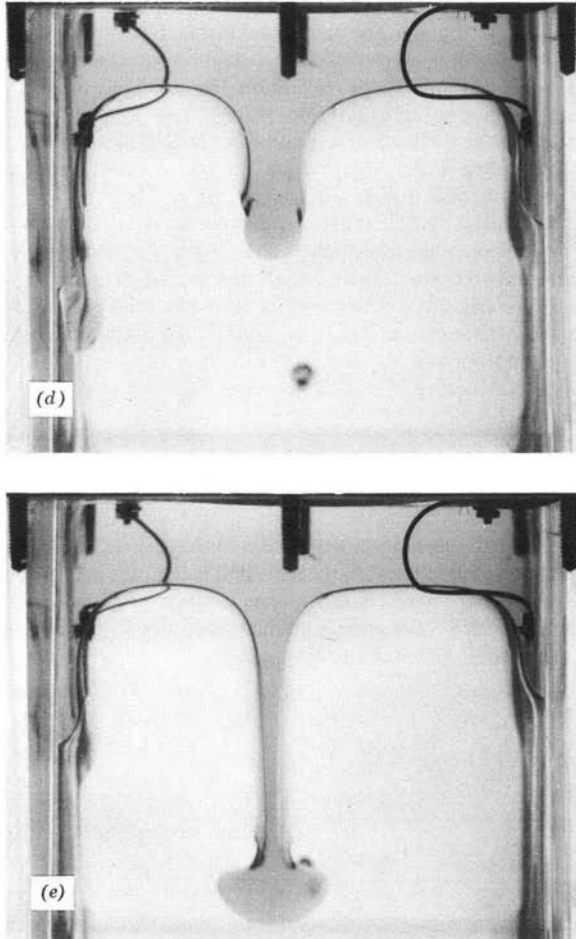


Fig. 10.1.13 (a) A heavy (dark) liquid is supported above a light (clear) liquid by hydrostatic pressure; (b – e) show growth of Rayleigh-Taylor instability resulting after stabilizing electric polarization forces in (a) are removed. (Photograph courtesy of Dynatech Corp., Cambridge, Mass.) This phenomenon can be seen in the film, “Complex Waves II,” available from Education Development Center, Inc., Newton, Mass.

Courtesy of Education Development Center, Inc. Used with permission.

Electric fields most often produce instabilities. The literature of plasma dynamics abounds in illustrations of absolute instabilities.*

Example 10.1.2. Electric and magnetic fields are often used to separate, levitate, or confine continuous media. A simple example of levitation is given in Fig. 10.1.14. An electrically conducting elastic film (membrane), with a mass per unit area σ_m , is stretched horizontally with equilibrium tension S between two rigid supports. With no other forces acting, the gravitational force makes the membrane sag in the middle. We propose to remove the sag without making physical contact with the membrane by placing a parallel conducting electrode, as shown in Fig. 10.1.14, and applying a potential difference between the membrane and the fixed plate. The membrane can be placed in a perfectly horizontal static equilibrium by providing an electrostatic attraction force per unit area between the plate and the membrane just equal to the gravitational force per unit area $\sigma_m g$. An important question, however, is this: Is the equilibrium stable? That is, can we expect that small transverse deflections of the surface due to noise will not become continuously larger? The electromechanical coupling occurs everywhere on the surface; hence to answer this question we must analyze a distributed surface-coupled problem.

It is assumed at the outset that the transverse displacements of the membrane, which are critical, do not depend on the y -coordinate. This is justified if the y -dimension of the membrane is small compared with l . In an actual situation this would mean that the tension in the y -direction of the membrane shown in Fig. 10.1.14 would be considerably less than the tension S in the x -direction, a fact that would make a one-dimensional membrane equation even more appropriate.

Because there is a gravitational force per unit area $\sigma_m g$ acting in the $-z$ -direction, the equation of motion (9.2.3a) becomes

$$\sigma_m \frac{\partial^2 \xi}{\partial t^2} = S \frac{\partial^2 \xi}{\partial x^2} - \sigma_m g + T_z^e, \quad (a)$$

where T_z^e is the transverse force per unit area due to the electric field.

The electric field in the region between the plate and membrane is in general a function of both x and z . We restrict our interest here, however, to the "long-wave limit" (see Example 6.2.4) in which the slope $\partial \xi / \partial x$ is small enough that the electric field is essentially z -directed. Hence we write the electric field intensity as

$$\mathbf{E} = \frac{V}{d - \xi} \mathbf{i}_z. \quad (b)$$

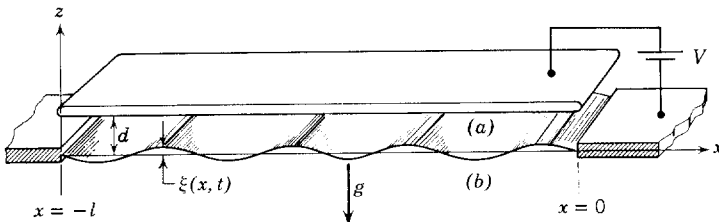


Fig. 10.1.14 Conducting elastic membrane held horizontal in a gravitational field by an electrostatic force.

* J. G. Linhart, *Plasma Physics*, North-Holland, Amsterdam, 1960, p. 101.

We have used the assumption that the membrane and the fixed plate are equipotentials; that is, the conductivities are high enough to allow charges to relax from one position to another on the conductors in a time that is short compared with a characteristic time of the mechanical motions (e.g., period of oscillation of the membrane or, as we shall see, time constant for instability). This is the idealization of the zero electric Reynolds number discussed in Section 7.2.

The force per unit area in the z -direction on a surface with the normal vector \mathbf{n} is in general [from (8.4.2)]

$$T_z^e = (T_{zm}^a - T_{zm}^b)n_m. \quad (c)$$

Because $n_m \cong n_z \cong 1$ and there is no electric field below the membrane, this reduces to

$$T_z^e = T_{zz}^{(a)}. \quad (d)$$

Recall from (8.3.10) that because $E_x \approx 0$ and $E_y \approx 0$ the component of the stress tensor T_{zz} is

$$T_{zz} = \frac{1}{2}\epsilon_0 E_z^2, \quad (e)$$

and it follows from (b), (d), and (e) that

$$T_z^e = \frac{1}{2}\epsilon_0 \left(\frac{V}{d - \xi} \right)^2. \quad (f)$$

Expansion of this surface force density in a Taylor series about the equilibrium position $\xi = 0$ and retention of only linear terms in displacement yield

$$T_z^e = \frac{\epsilon_0}{2d^2} V^2 + \frac{\epsilon_0}{d^3} V^2 \xi. \quad (g)$$

This result is now substituted into (a) to obtain the differential equation of motion

$$\sigma_m \frac{\partial^2 \xi}{\partial t^2} = S \frac{\partial^2 \xi}{\partial x^2} - \sigma_m g + \frac{\epsilon_0 V^2}{2d^2} + \frac{\epsilon_0}{d^3} V^2 \xi. \quad (h)$$

It is desired that the voltage V be adjusted so that in static equilibrium the membrane has no sag ($\xi = 0$). In this case, (h) reduces to

$$-\sigma_m g + \frac{\epsilon_0 V^2}{2d^2} = 0, \quad (i)$$

which simply states that the net electrical force upward (the upward attraction of the upper plate) must balance the downward force of gravity.

Subtraction of the equilibrium equation (i) from (h) gives an expression that must be satisfied by the perturbation deflections

$$\frac{1}{v_s^2} \frac{\partial^2 \xi}{\partial t^2} = \frac{\partial^2 \xi}{\partial x^2} + k_c^2 \xi, \quad (j)$$

where

$$v_s = \left(\frac{S}{\sigma_m} \right)^{1/2} \quad (k)$$

$$k_c^2 = \frac{\epsilon_0 V^2}{Sd^3}. \quad (l)$$

This equation has the same form as (10.1.25). We can immediately conclude that because the boundary conditions are also the same as those considered in writing (10.1.30) the equilibrium is stable if

$$\frac{\epsilon_0 V^2}{Sd^3} < \left(\frac{\pi}{l}\right)^2. \quad (m)$$

This institutes an upper bound on the voltage V consistent with stability. If we recognize that a requirement is also imposed on the voltage by the levitation condition (i), it follows that a largest mass-per-unit-area σ_m can be levitated by an apparatus with given dimensions and membrane tension S . This follows by eliminating V^2 from (m) and (i):

$$\sigma_m < \left(\frac{\pi}{l}\right)^2 \frac{Sd}{2g}. \quad (n)$$

It is a limitation of this kind that absolute instability often imposes on practical systems.

In an actual design a further restriction on allowable voltages arises because the material between the plate and membrane in Fig. 10.1.14 will be able to withstand only a finite electric field intensity; for example, if this region is filled with air at atmospheric pressure, the electric field intensity cannot exceed about 3×10^6 V/m.*

10.1.4 Waves with Damping, Diffusion Waves

Any real system is affected to some extent by energy dissipative effects, whether they take the form of mechanical friction or are caused by resistive heating. This fact alone would justify at least brief attention to the dynamics of a continuum influenced by losses. Even more important, however, are the physical situations in which the effect of energy dissipation is essential. This was seen in Chapter 7, in which magnetic diffusion and charge relaxation were governed by loss-dominated continuum equations. The discussion presented in this section adds further physical significance to the diffusion equation, which in Chapter 7 represented the dynamics of the magnetic field in a conducting material and in this section the dynamics of a string in a viscous fluid. One of our reasons for introducing this topic here becomes even more evident in Section 10.2.4, in which the simple ideas introduced are extended to show how losses, in conjunction with material convection, can give rise to a class of instabilities. These "resistive wall" instabilities assume importance in a variety of situations.

For purposes of illustration suppose that the wire is immersed in a viscous liquid. Then transverse deflections ξ produce a viscous drag on each section of the wire which is analogous in its effect to the viscous damper (see Section 2.2.1b) of lumped-parameter systems. A small section of the wire, shown in Fig. 10.1.15, experiences a (retarding) force per unit length to oppose the

* A. E. Knowlton, *Standard Handbook for Electrical Engineers*, McGraw-Hill, 9th ed., 1957, p. 416.

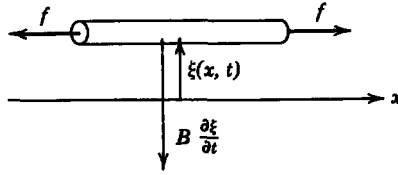


Fig. 10.1.15 A viscous drag per unit length acts to retard the motion of each element of the wire.

motion. If the velocity is low enough (or the viscosity is high enough*), this force is simply proportional to the transverse velocity; that is,

$$S_z = -B \frac{\partial \xi}{\partial t}, \quad (10.1.32)$$

where B is a damping coefficient per unit length.

With this type of force acting on the string, the equation of motion (10.1.1) becomes

$$\frac{\partial^2 \xi}{\partial t^2} = v_s^2 \frac{\partial^2 \xi}{\partial x^2} - \nu \frac{\partial \xi}{\partial t}, \quad (10.1.33)$$

where, as before,

$$v_s = \left(\frac{f}{m} \right)^{1/2} \quad (10.1.34)$$

and a normalized “damping frequency” has been defined as

$$\nu = \frac{B}{m}. \quad (10.1.35)$$

Now substitution of the standard form of solution (10.0.1) into (10.1.33) gives the dispersion equation

$$\omega^2 = v_s^2 k^2 + j\nu\omega. \quad (10.1.36)$$

This equation, like those considered in the preceding sections, is a simple quadratic either for ω or for k . Note that by contrast with the preceding cases, which did not involve dissipation, the dispersion equation now has a complex coefficient. Although the problem is formally no more complicated than it was before, the complex coefficient is responsible for making the algebra more involved.

First of all, consider the driven response to a sinusoidal steady-state excitation with the frequency $\omega = \omega_a$. Then it is appropriate to solve the dispersion

* The drag on a cylinder in a liquid obeys this law, provided the Reynolds number is small enough. See H. Rouse, *Elementary Mechanics of Fluids*, Wiley, New York, 1946, p. 247.

equation (10.1.36) for k , given that the frequency is ω_d :

$$k = \pm \frac{\sqrt{\omega_d^2 - j\nu\omega_d}}{v_s} \tag{10.1.37}$$

The radical makes it convenient to recognize that this expression has the form

$$k = \pm (|k_r| - j|k_i|). \tag{10.1.38}$$

The graphical construction in the complex plane (Fig. 10.1.16) shows how $|k_r|$ and $|k_i|$ are related to the driving frequency ω_d . The vectors provide a convenient way to picture the result of taking the square root of (10.1.37).

In view of the possible wavenumbers expressed by (10.1.38), the driven response is made up of two waves with amplitudes A^+ and A^- determined by the boundary conditions.

$$\xi = \text{Re} [A^+ e^{-j(|k_r| - j|k_i|)x} + A^- e^{j(|k_r| - j|k_i|)x}] e^{j\omega_d t}. \tag{10.1.39}$$

Remember that the real part of the wavenumber contains information about the periodicity and the phase velocity of the wave. Hence the first term in (10.1.39) represents a wave with the wavelength (measured between points of zero phase)

$$\lambda = \frac{2\pi}{|k_r|} \tag{10.1.40}$$

and a phase velocity (again for points of zero phase) of

$$v_p = \frac{\omega_d}{|k_r|}. \tag{10.1.41}$$

These points of zero phase propagate in the positive x -direction. From the form of (10.1.39) it is also clear that this wave decays in the positive x -direction at a rate determined by $|k_i|$. The A^- wave has a similar physical significance,

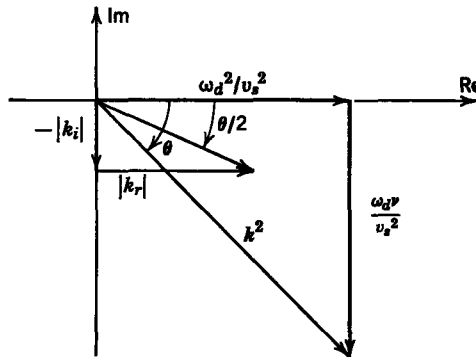


Fig. 10.1.16 Graphical solution of (10.1.37) to show complex nature of k .

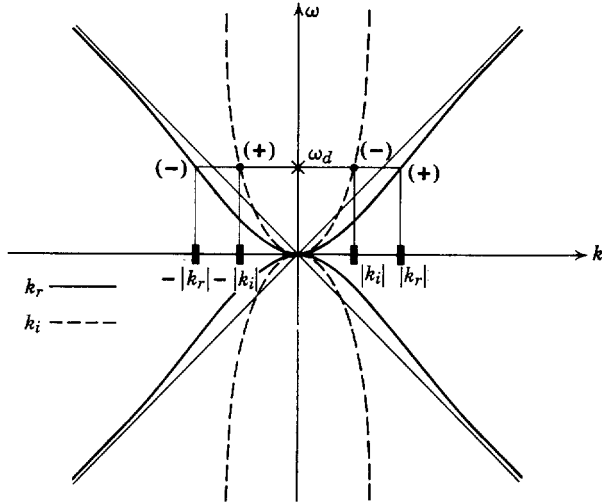


Fig. 10.1.17 Dispersion equation (10.1.37) for a string immersed in a viscous liquid, showing complex values of k for real values of ω .

with points of zero phase propagating in the $-x$ -direction and an amplitude that decays also in the $-x$ -direction.

What we have found is not too surprising. The effect of the damping on the driven waves is to produce a spatial decay in the direction of propagation. Figure 10.1.17 shows the ω - k plot predicted by (10.1.37). Here we are considering the driven response and plot complex values of k for real values of ω . Note that the positive real part of k (corresponding to a given frequency $\omega = \omega_d$) goes with a negative imaginary part of k on this diagram. As the driving frequency is raised, the real parts of k approach the same values they would have in the absence of damping whereas the imaginary parts (which reflect the spatial rate of decay) reach the asymptotic value $|k_i| = \nu/2v_s$.

The terms in (10.1.36) have the same physical significance as the corresponding terms in (10.1.33); that is, the ω^2 on the left represents the effects of inertia, whereas $v_s^2 k^2$ and $j\nu\omega$, respectively, symbolize effects of the tension and viscous drag. If the damping is sufficiently large that

$$\nu \gg \omega_d, \tag{10.1.42}$$

the effect of damping dominates that of the inertia and the ω^2 term in (10.1.36) can be ignored. (This is similar to the class of dynamics discussed in Section 5.2.2 in the context of lumped parameters.) The resulting dispersion equation takes the form

$$k^2 = -\frac{j\omega_d \nu}{v_s^2} \tag{10.1.43}$$

In this simple form the radical found in solving for k [as in (10.1.37)] can be taken to obtain

$$k = \pm \left(\frac{-j\omega_d v}{v_s^2} \right)^{1/2} = \pm \left(\frac{\omega_d v}{2v_s^2} \right)^{1/2} (1 - j). \quad (10.1.44)$$

This simplified dispersion equation is familiar from Section 7.1.3a [see (7.1.70)], where it was found in discussing the sinusoidal steady-state behavior of a magnetic field in a conducting medium. Instead of the magnetic skin depth δ , we now have $\delta \rightarrow \sqrt{2v_s^2/\omega_d v}$. The mathematical analogy between the viscous dominated spring and the magnetic diffusion could have been seen at the outset by comparing the one-dimensional form of (7.1.11) with (10.1.33), with the inertia term omitted. Both systems are represented by the diffusion equation.*

The value in recognizing the analogy between the deflection of the spring as it “oozes” through the viscous liquid and the magnetic diffusion through a conducting material is not confined to the mathematics. We can obtain a good physical “feel” for the diffusion process as it occurs in a diversity of situations by keeping in mind that the dynamics are similar to those found in the experiment shown in Fig. 10.1.18. Here a tightly wound helical spring (which is equivalent to a wire or string with a small tension f) is fixed at one end and driven up and down in a sinusoidal fashion at the other. The spring is immersed in glycerin. If we were to produce this excitation by hand, we would be most aware of a viscous retarding force. This is in contrast to the force required to excite the evanescent waves of Section 10.1.2, which was of the same nature as that required to compress a spring. (The comparison is worthy of note, for in both cases we are concerned with waves that decay spatially away from the point of excitation.)

The dispersion relation for the diffusion wave is characterized by equal real and imaginary parts of k for real values of ω . This is the region near the origin in Fig. 10.1.17, as is evident either from the ω - k plot or from the condition of (10.1.42).

In the preceding sections reference has been made to the effect of damping on the natural frequencies. This effect was clearly necessary for an accurate picture of the transient dynamics over many oscillations of the string. With the ends of the string fixed (as in the last two sections), the natural modes are found by again recognizing that solutions for k have the form $k = \pm\beta$ (where ω is now unknown and (10.1.36) is solved for k) and writing solutions in the form of (10.1.16). The same arguments used then, lead to the conclusion that

$$\beta = \frac{n\pi}{l}, \quad n = 1, 2, 3, \dots, \quad (10.1.45)$$

* Reference to other systems represented by this equation was made in the footnote to (7.1.11).

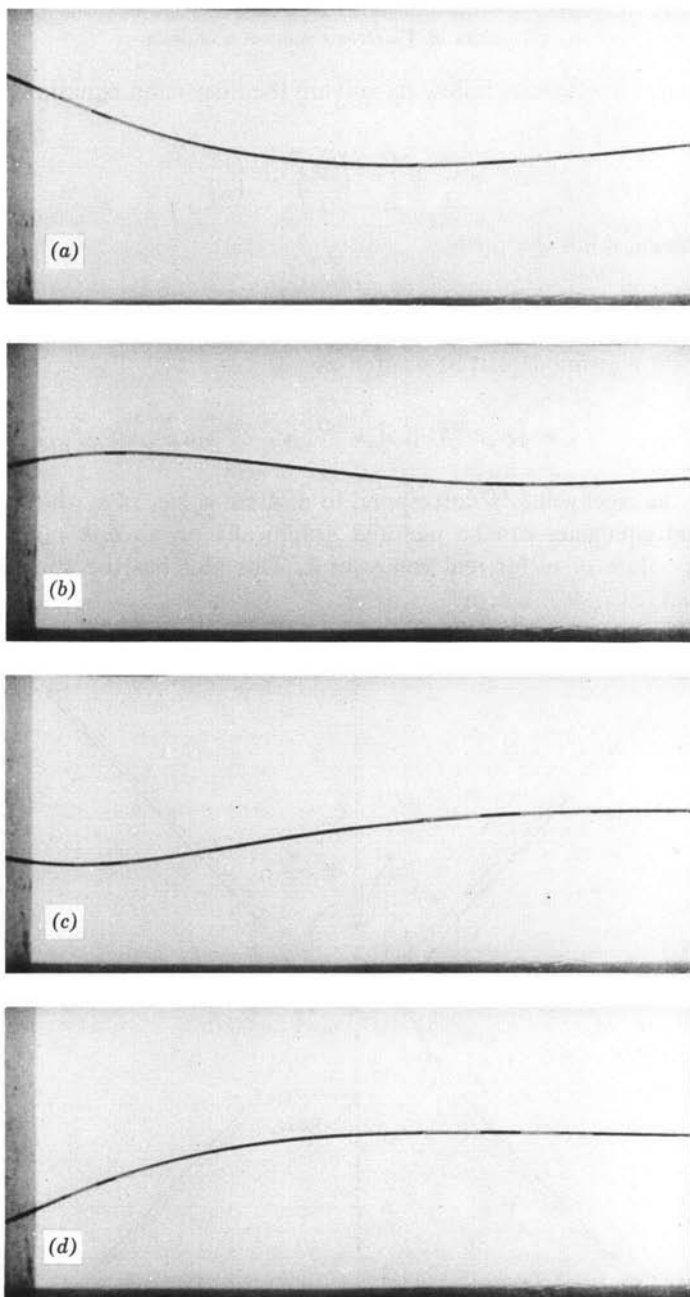


Fig. 10.1.18 A spring under tension is driven sinusoidally at the left end and fixed at the right end. It is immersed in glycerine which is sufficiently viscous that the effect of damping exceeds that of inertia. Hence the resulting motions which are shown in sequence over about one half cycle exemplify diffusion waves (or skin effect waves) in the sinusoidal steady state. (From four-minute film "Diffusion Waves" made for M.I.T. by Education Development Center, Inc., Newton, Mass.)

and the eigenfrequencies follow by solving the dispersion equation (10.1.36) with $k^2 = (n\pi/l)^2$.

$$\omega_n^\pm = \frac{j\nu}{2} \pm \left[v_s^2 \left(\frac{n\pi}{l} \right)^2 - \left(\frac{\nu}{2} \right)^2 \right]^{1/2}. \tag{10.1.46}$$

This expression has the form

$$\omega_n^\pm = \frac{j\nu}{2} \pm \Omega_n, \tag{10.1.47}$$

and the n th eigenmode can be written as

$$\xi = [A_n^+ e^{j\Omega_n t} + A_n^- e^{-j\Omega_n t}] e^{-(\nu/2)t} \sin \frac{n\pi x}{l}. \tag{10.1.48}$$

Because the eigenvalues β correspond to discrete values of k which are real, the eigenfrequencies can be pictured graphically on an ω - k plot to show complex values of ω for real values of k . This plot has the appearance of Fig. 10.1.19.

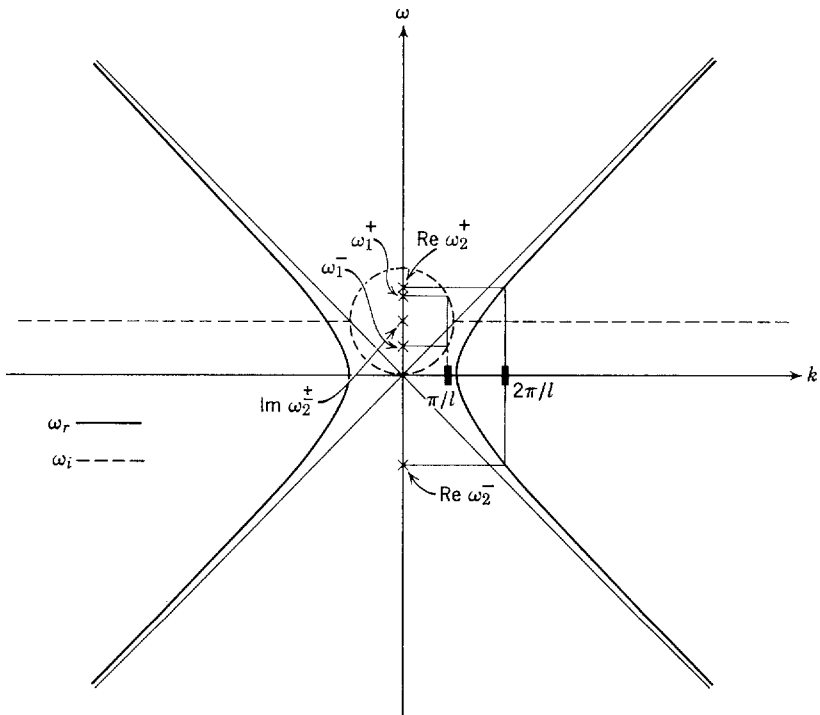


Fig. 10.1.19 Dispersion equation for string in a viscous liquid showing complex values of ω for real values of k . The lowest pairs of eigenfrequencies for a string fixed at each end are shown.

Note that for a given mode n both eigenfrequencies are imaginary (and represent pure damping) if the second (viscous drag) term under the radical in (10.1.46) exceeds the first (tension) term; for example, in Fig. 10.1.19 the $n = 1$ mode is characterized by two exponentially decaying deflections whereas the $n = 2$ mode takes the form of two oscillating deflections with amplitudes with a temporally decaying envelope. In this case we say that the lowest mode is overdamped and the others are underdamped.

Example 10.1.3. Of course, the damping can occur because of electrical as well as mechanical dissipation. The system introduced in Example 10.1.1 serves as an illustration of this fact. Suppose that the conducting top and bottom walls in Fig. 10.1.7 are so highly resistive that the voltage induced by the motion of the membrane is entirely absorbed by the resistance of the plates. This is the opposite extreme to the case considered in Example 10.1.1 in which this voltage was absorbed by the self-inductance of the current loops (a) and (b) shown in Fig. 10.1.8. (These extremes were discussed in the context of lumped parameters in Section 5.1.3.) Then, in writing the electrical loop equations (j) and (k) of Example 10.1.1, we can make the approximation that

$$\left| \frac{h^a}{\sigma_s} \right| \gg \left| \frac{\partial}{\partial t} \mu_0 dh^a \right|, \quad (a)$$

$$\left| \frac{h^b}{\sigma_s} \right| \gg \left| \frac{\partial}{\partial t} \mu_0 dh^b \right|, \quad (b)$$

to obtain

$$h^a = \sigma_s \mu_0 H_0 \frac{\partial \xi}{\partial t}, \quad (c)$$

$$h^b = -\sigma_s \mu_0 H_0 \frac{\partial \xi}{\partial t}. \quad (d)$$

The equation of motion is obtained by combining (a) and (n) in Example 10.1.1 with the last two equations:

$$\frac{\partial^2 \xi}{\partial t^2} = v_s^2 \frac{\partial^2 \xi}{\partial x^2} - \nu \frac{\partial \xi}{\partial t}, \quad (e)$$

where

$$v_s = \left(\frac{S}{\sigma_m} \right)^{1/2} \quad (f)$$

$$\nu = \frac{2\sigma_s(\mu_0 H_0)^2}{\sigma_m}. \quad (g)$$

Hence in the limit in which the upper and lower walls in Fig. 10.1.7 are very lossy, the effect of the magnetic field is to damp the transverse motions of the perfectly conducting membrane. It is clear from (e) that the discussion of this section applies equally well to the resistively loaded membrane in which the damping is of electrical origin.

This example is continued in Section 10.2.4, in which the effects of electrical damping are exhibited in a considerably less obvious way than found here.

10.2 WAVES AND INSTABILITIES IN THE PRESENCE OF MATERIAL MOTION

We are concerned in this chapter with continuous media and have confined our interest so far to cases in which the continuum is initially at rest or in

static equilibrium. Gross motion of a medium can have a profound effect on the dynamics found, for example, when attempts are made to carry on a conversation in a high wind. In this section we use strings and membranes as models for introducing concepts related to the dynamics of media initially in a state of uniform motion. Again, our remarks are related to particular physical situations chosen for their simplicity, but with implications for a wide range of physical situations; for example, the string might be replaced by a beam of electrons in vacuum, by a stream of holes in a semiconductor, or by a streaming gas or plasma.

The systems to be considered now have the same basic physical nature as those in Section 10.1. The mechanical continuum is a string or a membrane undergoing one-dimensional transverse displacements $\xi(x, t)$. Now we introduce a new ingredient and specify that the continuum is moving in the longitudinal (x) direction with an equilibrium velocity U . Although the remarks that follow use the string as an example, it should be clear that they also apply directly to the one-dimensional motion of a membrane.

Our interest here is in exciting the moving string at a fixed point and in describing the dynamical behavior as viewed from a fixed frame. Consequently, the equation of motion developed in Section 9.2 is not adequate because it does not account for the equilibrium velocity (convection) of the continuum. It does, however, give a proper description of the string viewed from a reference frame moving in the x -direction with a velocity U because in that frame the string has no velocity in the x -direction. We denote variables (both independent and dependent) measured in this moving frame by primes and write (10.1.1) for string deflections ξ' in the moving frame as

$$m \frac{\partial^2 \xi'}{\partial t'^2} = f \frac{\partial^2 \xi'}{\partial x'^2} + S'_z. \quad (10.2.1)$$

We are dealing with velocities much lower than the velocity of light; consequently we use Fig. 10.2.1 to relate the coordinates and time in the two frames by the Galilean transformation*:

$$x = x' + Ut', \quad (10.2.2)$$

$$z = z' \quad (10.2.3)$$

$$t = t'. \quad (10.2.4)$$

It follows from (10.2.3) that $\xi = \xi'$ and because the moving frame is not accelerating, we can also say that $S'_z = S_z$. Hence to write (10.2.1) in the fixed

* This discussion represents a review of ideas developed in Section 6.1, now applied to transforming mechanical rather than electrical equations of motion. Hence once again we encounter the substantial or convective derivative.

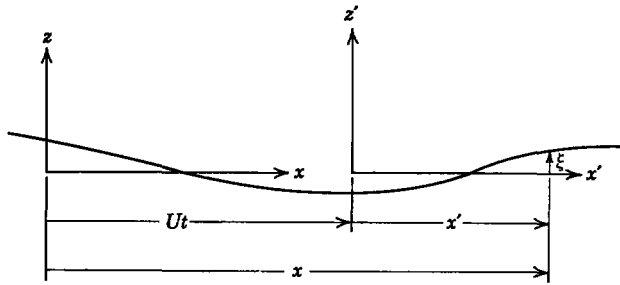


Fig. 10.2.1 The fixed coordinate system x, y, z or the moving coordinate system x', y', z' can be used to define a given position along the equilibrium axis of the string. Because the moving coordinate system has the same velocity U in the x -direction as the string, the string appears to move only in the z' -direction when viewed from the primed frame.

frame we need only compute the derivatives in terms of (x, t) ; that is

$$\frac{\partial \xi}{\partial t'} = \frac{\partial \xi}{\partial t} \frac{\partial t}{\partial t'} + \frac{\partial \xi}{\partial x} \frac{\partial x}{\partial t'} = \frac{\partial \xi}{\partial t} + U \frac{\partial \xi}{\partial x}. \tag{10.2.5}$$

Repeating this procedure, we have

$$\frac{\partial^2 \xi}{\partial t'^2} = \frac{\partial}{\partial t} \left(\frac{\partial \xi}{\partial t} + U \frac{\partial \xi}{\partial x} \right) + U \frac{\partial}{\partial x} \left(\frac{\partial \xi}{\partial t} + U \frac{\partial \xi}{\partial x} \right). \tag{10.2.6}$$

The space derivative is found in the same way to be

$$\frac{\partial^2 \xi}{\partial x'^2} = \frac{\partial^2 \xi}{\partial x^2}, \tag{10.2.7}$$

hence (10.2.1) becomes

$$m \left(\frac{\partial}{\partial t} + U \frac{\partial}{\partial x} \right)^2 \xi = f \frac{\partial^2 \xi}{\partial x^2} + S_z, \tag{10.2.8}$$

where the quantity in brackets on the left is recognized as the one-dimensional form of the substantial or convective derivative operating twice on ξ .* Remember from Section 6.1 (6.1.19) that the substantial or convective derivative is the time rate of change viewed from a frame moving with the velocity U . Our derivation of (10.2.8) makes this interpretation apparent once again. Here the convective derivative provides the means of expressing the equation of motion in the fixed frame.

* From the derivation $\left(\frac{\partial}{\partial t} + U \frac{\partial}{\partial x} \right)^2 \xi \equiv \frac{\partial^2 \xi}{\partial t^2} + 2U \frac{\partial^2 \xi}{\partial x \partial t} + U^2 \frac{\partial^2 \xi}{\partial x^2}$.

10.2.1 Fast and Slow Waves

Before introducing further complications, it is worthwhile to consider the nature of waves that propagate on a convecting string with no electro-mechanical coupling. Thus we set $S_z = 0$ and (10.2.8) becomes

$$\left(\frac{\partial}{\partial t} + U \frac{\partial}{\partial x}\right)^2 \xi = v_s^2 \frac{\partial^2 \xi}{\partial x^2}, \tag{10.2.9}$$

where once again $v_s = \sqrt{f/m}$.

10.2.1a Traveling Waves

Now, if $U = 0$, the problem is mathematically identical to the one discussed in Section 9.1.1 in which we also found that the wave equation was pertinent and that deflections took the form of waves (9.1.14). We expect that in the moving frame shown in Fig. 10.2.1 solutions will have this same form and that we can now write solutions as

$$\xi = \xi_+(\alpha) + \xi_-(\beta), \tag{10.2.10}$$

where

$$\alpha = x' - v_s t', \quad C^+, \tag{10.2.11}$$

$$\beta = x' + v_s t', \quad C^-. \tag{10.2.12}$$

The parameters α and β can be written in terms of the fixed frame variables (x, t) by using the transformation equations (10.2.2) to (10.2.4):

$$\alpha = x - (v_s + U)t, \quad C^+, \tag{10.2.13}$$

$$\beta = x + (v_s - U)t, \quad C^-, \tag{10.2.14}$$

and direct substitution into (10.2.9) shows that (10.2.10) is indeed a solution.

Equations 10.2.13 and 10.2.14 for α and β are recognized as the characteristics discussed in Section 9.1.1a but altered by the convection. The convection increases the velocity of waves propagating in the positive x -direction along C^+ characteristic lines and decreases the velocity of waves propagating in the negative x -direction along C^- characteristics.

The characteristic lines that originate at $x = 0$ when $t = 0$ (α and β equal to zero in (10.2.13) and (10.2.14)) are shown in Fig. 10.2.2. In (a) of this figure waves propagate relative to the string with a velocity exceeding U ($v_s = 2U$). Note that the slopes of the characteristics are the velocities of propagation for the forward and backward waves ξ_+ and ξ_- . Hence the wave propagating in the $+x$ -direction does so more rapidly than the wave propagating against the convection in the $-x$ -direction.

By contrast Fig. 10.2.2b shows the case in which the convection makes both characteristics point downstream ($+x$ -direction) as time increases. Hence a

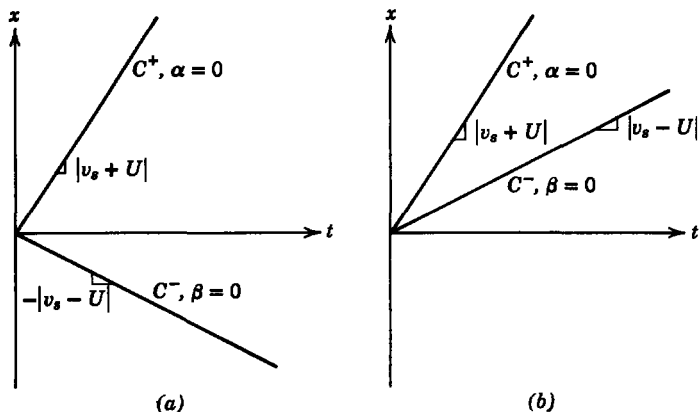


Fig. 10.2.2 Characteristic lines in the space-time plane along which a disturbance at $x = 0$ when $t = 0$ will propagate: (a) when $v_s = 2U$; (b) when $v_s = U/2$.

disturbance at $x = 0$ when $t = 0$ will result in two waves that propagate in the $+x$ -direction. There is no effect from such a disturbance on that part of the string in which $x < 0$. As we shall find in Chapter 13, sound waves in a gas have a behavior analogous to that of the elastic waves considered here. In the language of gas dynamics we say that the two cases of Fig. 10.2.2 are “subsonic” and “supersonic,” respectively.

An example serves to clarify further the effect of material convection on waves.

Example 10.2.1. In Example 9.1.2 of Section 9.1.1a we studied the behavior of an initially static pulse propagating on an elastic rod. A mathematically similar problem is now considered in which the string is given an initial displacement and velocity and we inquire about the resulting motions; that is, we are given

$$\xi(x, 0) = \xi_0(x), \quad (a)$$

$$\frac{\partial \xi}{\partial t}(x, 0) = \dot{\xi}_0(x). \quad (b)$$

We can evaluate ξ_+ and ξ_- by using the initial conditions. This is done by taking the derivative of (10.2.10) with respect to x and using (a). (Here we use the fact that $\partial \alpha / \partial x = \partial \beta / \partial x = 1$.)

$$\frac{d\xi_+}{d\alpha} + \frac{d\xi_-}{d\beta} = \frac{d\xi_0}{dx}. \quad (c)$$

Similarly, the use of the time derivative of (10.2.10) with (b) gives

$$-(v_s + U) \frac{d\xi_+}{d\alpha} + (v_s - U) \frac{d\xi_-}{d\beta} = \dot{\xi}_0(x). \quad (d)$$

Simultaneous solution of (c) and (d) yields

$$\frac{d\xi_+}{d\alpha} = \left(\frac{v_s - U}{2v_s} \right) \frac{d\xi_0}{dx} - \frac{1}{2v_s} \dot{\xi}_0(x), \quad (e)$$

$$\frac{d\xi_-}{d\beta} = \left(\frac{v_s + U}{2v_s} \right) \frac{d\xi_0}{dx} + \frac{1}{2v_s} \dot{\xi}_0(x). \quad (f)$$

Remember that in (e) and (f) x is the position along the string when $t = 0$. To find the solution at a general point C in space and time, as shown in Fig. 10.2.3, we use (e) with x evaluated at A , where $x = \alpha$. In the same way (f) is evaluated at point B , where $x = \beta$. Then (e) provides $d\xi_+/d\alpha$ anywhere along the C^+ characteristic shown in Fig. 10.2.3. The particular values of α and β required to give characteristics passing through the point $C(x, t)$ are given by (10.2.13) and (10.2.14). The space derivative of (10.2.10) can now be evaluated in terms of the initial conditions by using (e) and (f).

$$\frac{\partial \xi}{\partial x}(x, t) = \left(\frac{v_s - U}{2v_s} \right) \frac{d\xi_0}{dx}(\alpha) + \left(\frac{v_s + U}{2v_s} \right) \frac{d\xi_0}{dx}(\beta) - \frac{\dot{\xi}_0(\alpha) - \dot{\xi}_0(\beta)}{2v_s}. \quad (g)$$

Suppose that when $t = 0$ the string is static ($\dot{\xi}_0 = 0$) and the displacement is a uniform pulse of magnitude A distributed between $x = -a$ and $x = a$. Then we have

$$\frac{d\xi_0}{dx}(x) = A[u_0(x + a) - u_0(x - a)], \quad (h)$$

where $u_0(x + a)$ is a unit impulse at the position $x = -a$. The resulting space derivative of the displacement follows from (g) which becomes

$$\frac{\partial \xi}{\partial x}(x, t) = A \left\{ \frac{(v_s + U)}{2v_s} [u_0(\beta + a) - u_0(\beta - a)] + \frac{(v_s - U)}{2v_s} [u_0(\alpha + a) - u_0(\alpha - a)] \right\}. \quad (i)$$

Remember that α and β are given by (10.2.13) and (10.2.14). The first two terms in this expression are recognized as impulses propagating along the C^- characteristics originating

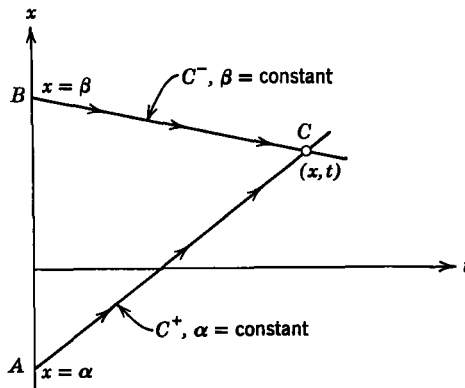


Fig. 10.2.3 Characteristics that intersect at a general point in space and time (x, t) showing the points A and B at which the initial conditions determine the dependent variables at C .

at $x = -a$ and $x = a$, respectively. The last two terms are impulses propagating along the C^+ characteristics. We can obtain the displacement ξ by integrating this equation with respect to x . The resulting values of ξ in two cases are shown in Figs 10.2.4 and 10.2.5. In the first of these figures U is less than v_s and we see that the original pulse divides into a part propagating slowly in the $-x$ -direction (upstream) and a part that is propagating rapidly in the $+x$ -direction. In Fig. 10.2.5 the convection velocity U is greater than the propagation velocity v_s and, although the pulse divides into two parts, both parts are carried downstream by the convection. Note that the convection also makes the ξ_+ and ξ_- waves unequal in magnitude. In fact, when U exceeds v_s , the ξ_+ wave is inverted, as shown in Fig. 10.2.5.

We are now in a position to make an important observation about the appropriate initial conditions and boundary conditions when the differential equation of motion is (10.2.9). We first observe that this expression is a partial differential equation that is second-order in both time (t) and space (x). Consequently, we need two initial conditions and two boundary conditions to evaluate all the constants in the solution. Where these conditions can be applied depends on whether the convection velocity U is greater or less than the propagation velocity v_s and is essentially the question whether a disturbance can propagate upstream (in the negative x -direction).

Consider first the case in which $U < v_s$ and disturbances can propagate upstream. As an example, assume that the string deflection is fixed at $x = l$. Then we can say that $\xi = 0$ along the line $x = l$ in the x - t plane. This is one boundary condition. A second boundary condition is that at $x = 0$ the string position is driven independently

$$\xi(0, t) = \xi_a(t). \quad (10.2.15)$$

It is helpful to picture these conditions as shown in Fig. 10.2.6. The two initial conditions can be specified as the initial displacement $\xi(x, 0)$ and the initial transverse velocity $(\partial\xi/\partial t)(x, 0)$. The solution for $\xi(x, t)$ at an arbitrary point C can be found as follows. First, the value of $\xi_+(\alpha)$ that propagates from A to B along a C^+ characteristic is determined by the initial conditions at point A . Similarly, the $\xi_-(\beta)$ wave propagating along a C^- characteristic from E to D is found from the initial conditions at point E . These incident waves, together with the boundary conditions at B and D , determine the reflected waves that travel from B to C along a C^- characteristic [a $\xi_-(\beta)$ wave] and from D to C along a C^+ characteristic [a $\xi_+(\alpha)$ wave] described in Section 9.1.1*b*. Hence we have found the solution for the displacement at point C . From similar arguments, perhaps involving many reflections of the waves, we can find the solution at any point in the x - t plane in the interval of space $0 < x < l$.

Consider next the case in which $U > v_s$. As indicated by Fig. 10.2.6*b*) both the C^+ and C^- characteristics point downstream (positive x -direction) as t increases and no disturbances can propagate upstream. Consequently, we expect that initial conditions and boundary conditions applied downstream

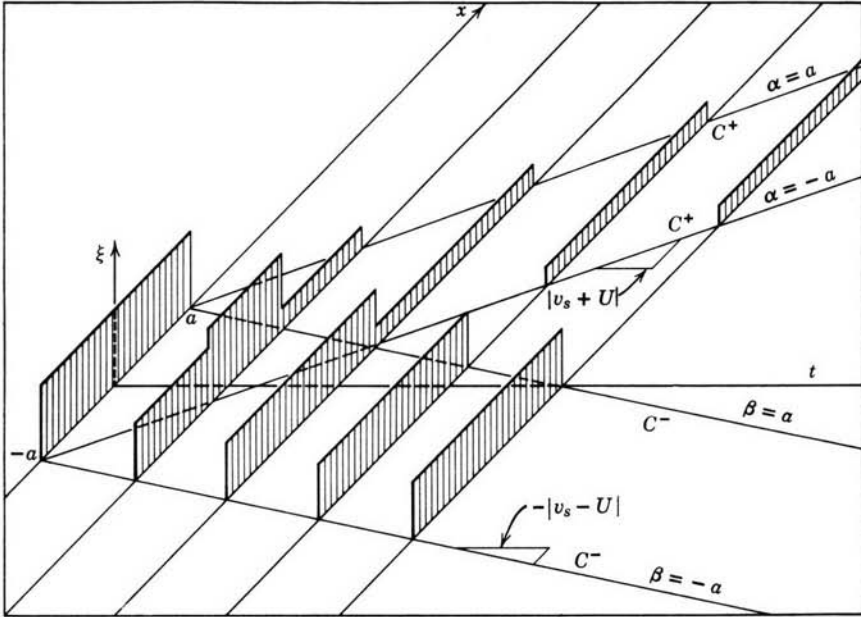


Fig. 10.2.4 Propagation of an initially static displacement pulse on a string moving with the velocity $U = v_s/2$.

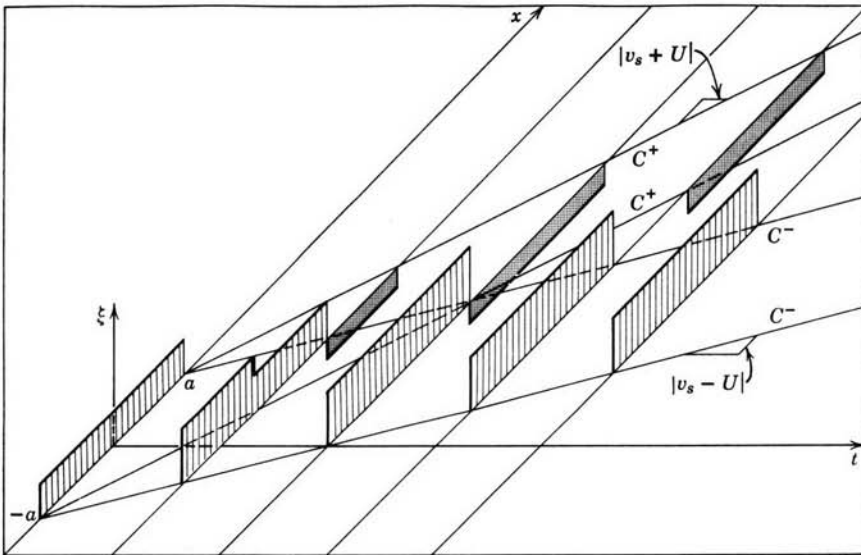


Fig. 10.2.5 Propagation of an initially static displacement pulse on a string moving with the velocity $U = 2v_s$.

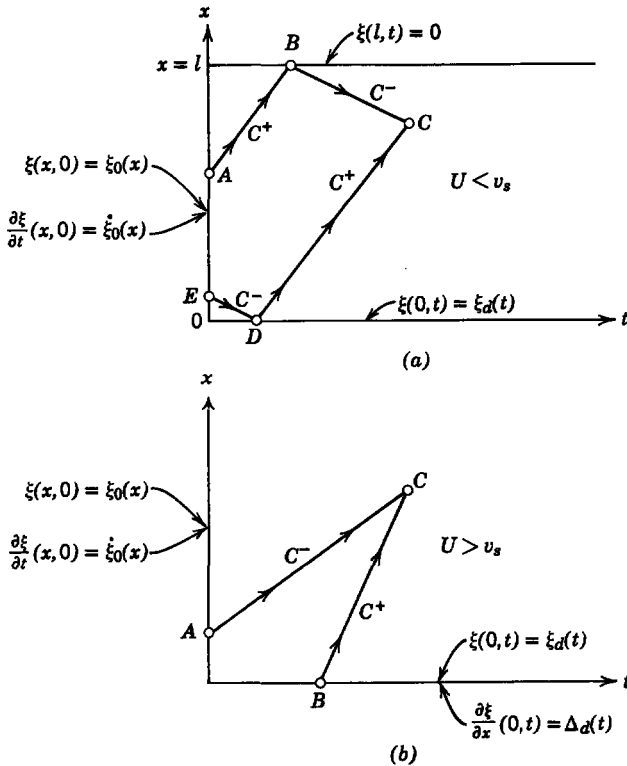


Fig. 10.2.6 Boundary and initial conditions to establish solution $\xi(x, t)$ at a point C : (a) $U < v_s$; (b) $U > v_s$.

from point C will not affect the displacement ξ at point C because the effects of initial and boundary conditions are transmitted in space and time by waves that propagate along the characteristics. To make this discussion explicit we refer to Fig. 10.2.6b and ask for the displacement at an arbitrary point C . Note that the solution at C can depend on only conditions at A and B . Hence causality is introduced as a physical law that must be obeyed by our mathematical solution, and we assume that solutions evolve from left to right (in the direction of increasing time) in Fig. 10.2.6. Hence it is necessary to impose two conditions at A and two conditions at B . Note that this means that boundary conditions along the $(x = 0)$ -axis have the same nature as initial conditions along the $(t = 0)$ -axis. In addition to the two initial conditions when $t = 0$, we can impose

$$\xi(0, t) = \xi_d(t) \tag{10.2.16}$$

and the slope at $x = 0$,

$$\frac{\partial \xi}{\partial x}(0, t) = \Delta_d(t). \tag{10.2.17}$$

With the initial and boundary conditions thus specified, we can calculate the $\xi_+(\alpha)$ wave that propagates along the C^+ characteristic from B to C and the $\xi_-(\beta)$ wave that propagates along the C^- characteristic from A to C in Fig. 10.2.6*b*. Thus we have found the displacement at point C .

A comparison of Figs. 10.2.6*a* and *b* shows that the essential difference between the two cases is that with $U < v_s$ boundary conditions must be specified both upstream and downstream from the point in question because waves propagate in both directions. For the case $U > v_s$, waves propagate downstream only; thus the boundary conditions must be specified upstream from the point in question.

In the supersonic case ($U > v_s$) it would violate causality to impose only one boundary condition at $x = 0$ and the second condition at $x = l$. Waves propagating along the C^+ and C^- characteristics would have to know in advance that they had to satisfy a boundary condition at C in Fig. 10.2.6*b*. This is an important point because there can be no mathematical objection to a solution to (10.2.9) with $U > v_s$ which satisfies one upstream and one downstream boundary condition. Rather our objection is based on the physical requirement of causality.*

10.2.1*b* Sinusoidal Steady State

To appreciate fully the drastic effect of the convection it is important to recognize the manner in which a sinusoidal steady-state condition is established on the “supersonic” string. Suppose that with $U > v_s$ a sinusoidal excitation is applied when $t = 0$ at $x = 0$. This is shown in Fig. 10.2.7, in

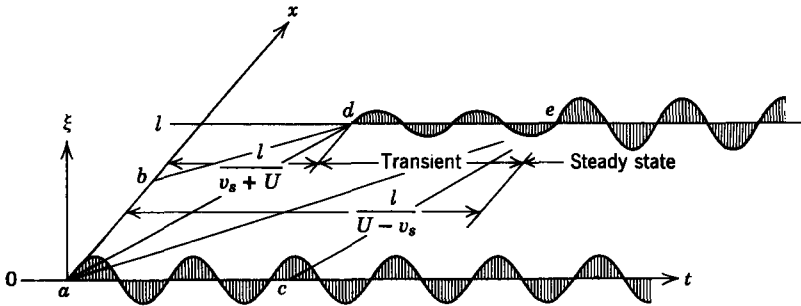


Fig. 10.2.7 A sinusoidal excitation turned on at $x = 0$ when $t = 0$ is applied to a moving string ($U > v_s$). At the downstream position $x = l$ the sinusoidal steady state is established when the slow wave arrives [$t = l/(U - v_s)$].

* Nonlinear disturbances can propagate upstream even when $U > v_s$. In the language of gas dynamics these are “shock waves” that travel faster than the speed v_s of small amplitude disturbances. These nonlinear phenomena are beyond the scope of this work and are not predicted by our simple, linear model. See, for example, R. Courant and K. O. Friedrichs, *Supersonic Flow and Shock Waves*, Interscience, New York, 1948, Part II.

which two sinusoidal driving conditions are imposed along the t -axis when $t > 0$ and when $t = 0$ the string has a dynamical state specified by the initial conditions.

Consider the string deflections that would be observed at the downstream position $x = l$. We have learned in this section that the solution at any given time is determined by a superposition of fast and slow waves propagating downstream on the C^+ and C^- characteristics, respectively. These characteristics originate either on the x -axis, where the initial conditions are arbitrary, or on the t -axis, where the boundary conditions are in the sinusoidal steady state. From this it follows that there is no response to the sinusoidal drive observed at $x = l$ until the fast wave initiated by the excitation at (a) in Fig. 10.2.7 arrives at (d) . Hence, if the initial conditions are zero, there is no response until $t = l/(U + v_s)$. In the interval of time between the points d and e at $x = l$ the slow wave is determined by the initial conditions, whereas the fast wave is determined by the sinusoidal driving conditions. After the slow wave arrives when $t = l/(U - v_s)$, however, both characteristic lines, which determine the solution at a given point along the line $x = l$, originate in the sinusoidal steady-state driving condition. Because the conditions that determine the solution are then periodic in time, it follows that so also is the solution; that is, after the time $t = l/(U - v_s)$ when the slow wave arrives at $x = l$ the sinusoidal steady-state condition has been established. After this time there is no evidence of the initial conditions.

Recall the nature of the response to the initial conditions, as described in Section 10.1, in which the string has no longitudinal velocity. There the effect of initial conditions was described in terms of the normal modes, and the consequences of the initial conditions persisted in the form of these modes for an indefinite period of time. As we saw in the examples of Section 10.1, these modes are purely oscillatory unless other effects, such as damping, are introduced.

In the sections that follow we introduce additional forces on the string, with the longitudinal convection included ($U > v_s$). Hence the examples considered involve the same transverse forces that are developed in Section 10.1 but in addition include the effect of convection. With this in mind, remember that in the examples in Section 10.1 the normal modes, with amplitudes specified by the initial conditions, determine whether the string deflections become unbounded in time. In any of these cases the sinusoidal steady-state solution can be found, but in cases in which the system is unstable this steady-state solution is eventually dominated by the unstable normal modes. With the convection, this dominance of the transient resulting from the initial conditions is not possible. The sinusoidal steady-state solution is all that remains after the time $l/(U - v_s)$, which means that in the supersonic case ($U > v_s$) it is not possible for deflections to become unbounded with time at a given position x .

The significance of these remarks becomes more evident in Section 10.2.3. In any case it should be evident that with $U > v_s$ the driven response assumes primary importance

If once again we assume complex waves (10.0.1) as solutions, substitution into (10.2.9) shows that the dispersion relation between the frequency ω and wavenumber k is

$$(\omega - kU)^2 = v_s^2 k^2. \tag{10.2.18}$$

Note that this is the relation obtained in Section 10.1.1, except that now $\omega \rightarrow \omega - kU$, which reflects the fact that the effect of the convection is to replace the time derivative with the convective derivative. (As we emphasize in Section 10.2.4, care must be taken in transforming from one frame of reference to another using this simple substitution by noting the parts of the system that are moving.)

The dispersion equation has the graphical form of two straight lines, as can be seen by solving (10.2.18) for ω :

$$\omega = k(U \pm v_s). \tag{10.2.19}$$

The subsonic and supersonic cases are shown in Fig. 10.2.8. The effect of increasing U is to rotate the two straight lines of Fig. 10.1.1 until finally, when $U > v_s$, as shown in Fig. 10.2.8b, both straight lines are in the first and third quadrants of the ω - k plane.

The dispersion equation can be used to find the response of the string to a drive with the frequency ω_d by solving (10.2.19) for the wavenumbers k , given that $\omega = \omega_d$:

$$k = \eta \pm \gamma, \tag{10.2.20}$$

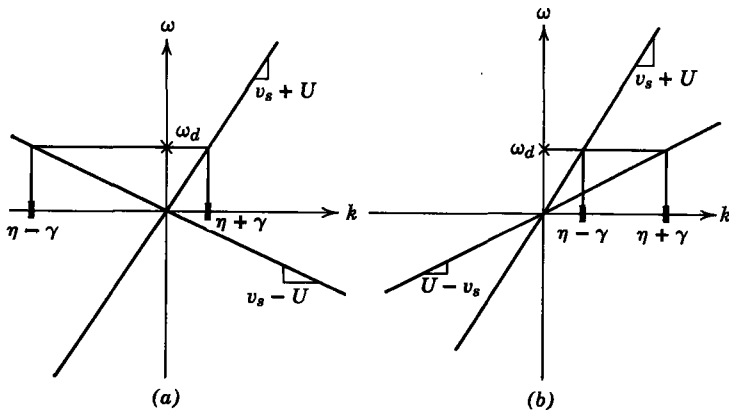


Fig. 10.2.8 Dispersion relations for waves on a string moving with the equilibrium velocity U in the positive x -direction. Although the geometry for the subsonic and supersonic cases is the same as that for the characteristic lines in Fig. 10.2.2, the axes here are ω - k , whereas in Fig. 10.2.2 they are x - t : (a) $U < v_s$; (b) $U > v_s$.

where for the string without additional forces

$$\eta = \frac{U}{v_s} \gamma, \quad (10.2.21)$$

$$\gamma = \frac{\omega_d v_s}{U^2 - v_s^2}$$

A graphic representation of these two wavenumbers corresponding to the frequency ω_d is given in Fig. 10.2.8. Remember that the phase velocity of a wave is ω/k . With $U < v_s$, phases of one wave propagate rapidly downstream with the velocity $v_p = U + v_s$, whereas those of the other propagate upstream at the lesser velocity $v_p = v_s - U$. With $U > v_s$, as shown in Fig. 10.2.8b, phases of both waves propagate downstream. These results are not surprising in view of the wave dynamics found in Section 10.2.1a.

Consider the sinusoidal steady-state dynamics resulting when $U > v_s$. Then, upstream boundary conditions in the form of (10.2.16) and (10.2.17) are appropriate. In particular, suppose that

$$\xi(0, t) = 0 \quad (10.2.22)$$

$$\frac{\partial \xi}{\partial x}(0, t) = \Delta_0 \cos \omega_d t. \quad (10.2.23)$$

Then we can take a linear combination of waves with wavenumbers given by (10.2.20) to satisfy the first of these conditions:

$$\xi(x, t) = \text{Re } A e^{j(\omega_d t - \eta x)} \sin \gamma x. \quad (10.2.24)$$

The remaining arbitrary constant A is determined by the second condition to be $A = \Delta_0/\gamma$, and so the required sinusoidal steady-state driven response is

$$\xi(x, t) = \frac{\Delta_0}{\gamma} \cos(\omega_d t - \eta x) \sin \gamma x. \quad (10.2.25)$$

We have found that when sinusoidal steady-state waves are excited on the supersonic string they combine to form an envelope with nulls spaced by the distance $\pi/\gamma = \pi(U^2 - v_s^2)/\omega_d v_s$. Within this envelope points of zero phase on the string move in the x -direction with the velocity $\omega_d/\eta = (U^2 - v_s^2)/U$. The deflections are shown at an instant in time in Fig. 10.2.9.

The periodic envelope of the waves is stationary in space and therefore has the same character as the standing waves found for the stationary string. These peaks and nulls in the deflection are sometimes referred to as beats*

* The beating of two sinusoidal signals is commonly encountered in demodulation processes, such as those that occur in the ear when tuning two musical instruments. Tones that differ slightly in frequency beat together at the difference frequency. This illustrates how phenomena observed as functions of time are found as functions of space when the supersonic motion of a medium is involved.

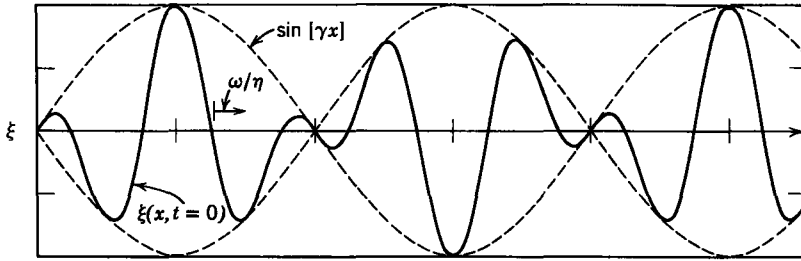


Fig. 10.2.9 Fast and slow waves interfere to form beats in space when $U > v_s$. The deflection is as the string appears if illuminated once each period of excitation $2\pi/\omega_a$.

because they result from interference between the two waves propagating downstream. At some positions the deflections from the two waves tend to add, whereas at others the deflections cancel.

In the sections that follow we undertake to show the effect of convection on each of the classes of interactions developed in Section 10.1. In cases in which the convection is equivalent to the entire system being in a state of uniform translation this is a simple matter, since the effect of the convection is represented by replacing the time derivatives in the differential equation with convective derivatives.

10.2.2 Evanescence and Oscillation with Convection

The developments of Section 10.2.1 pertained to the effect of convection on the dynamics of an ordinary string. In the absence of convection this string supports waves that propagate without dispersion. In this section we begin a discussion of the effects of convection on dispersive waves. In particular, we reconsider the systems that support the cutoff or evanescent waves described in Section 10.1.2. Now the system is as shown in Fig. 10.1.2, except that the wire has an equilibrium longitudinal velocity U . Because the magnetic restoring force is the same, whether evaluated in the frame moving with the string or in a fixed frame, the equation of motion found in Section 10.1.2 (10.1.6) is valid in a frame moving with the velocity U in the x -direction. As illustrated in Section 10.2, the equation of motion in the fixed frame is obtained by replacing the time derivative with the convective derivative. From this it follows that the dispersion equation with convection is obtained by simply replacing ω in the dispersion equation for the fixed system (10.1.7) with $\omega - kU$. Hence the required dispersion equation with convection is

$$(\omega - kU)^2 = v_s^2 k^2 + \omega_c^2. \tag{10.2.26}$$

The graphical representation of this equation is shown in Fig. 10.2.10, in which $U < v_s$ and $U > v_s$ are shown. These plots give complex values of k

for real values of ω . It should be clear from the plots and the fact that the dispersion equation is quadratic in ω that only real values of ω are given by (10.2.26) for real values of k .

The asymptotes of the dispersion equation are the two straight lines of Fig. 10.2.8*a, b*. Hence the result of increasing the velocity U is to rotate the hyperbolas in a counterclockwise direction. To make further deductions about the dispersion equation, it is helpful to solve (10.2.26) for k .

$$k = \eta \pm \gamma, \tag{10.2.27}$$

where

$$\eta = \frac{\omega_d U}{U^2 - v_s^2}, \tag{10.2.28}$$

$$\gamma = \frac{\sqrt{v_s^2 \omega_d^2 + (U^2 - v_s^2) \omega_c^2}}{U^2 - v_s^2}.$$

This makes it evident that in the case in which $U < v_s$, there is a range of driving frequencies over which the wavenumbers are complex. From the last two equations, this is the range of ω_d over which the quantity under the radical is negative.

$$|\omega_d| < \left| \frac{(v_s^2 - U^2) \omega_c^2}{v_s^2} \right|^{1/2}. \tag{10.2.29}$$

The complex values of k are shown in Fig. 10.2.10*a*, in which the imaginary part of k takes the form of an ellipse and the real part of k (the straight line) is the same for both waves.

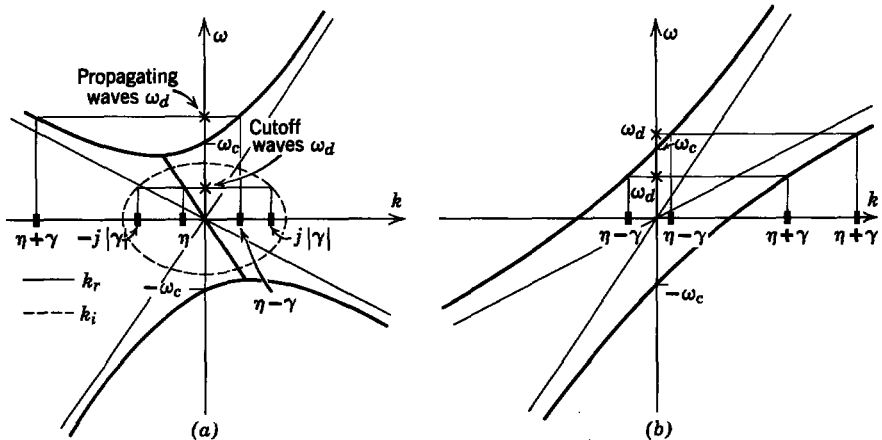


Fig. 10.2.10 Dispersion relations for system of Section 1.2, with the addition of a longitudinal velocity U . When U exceeds v_s , both waves propagate without decay, regardless of the frequency, and the effect of the convection is to eliminate the evanescence. (a) $U < v_s$; (b) $U > v_s$.

Two cases are shown in Fig. 10.2.10a. At the lower of the two driving frequencies waves with wavenumbers whose real part is η and imaginary parts, $\pm j|\gamma|$ are cutoff. At the larger driving frequency both wavenumbers are real. Note that the effect of the convection has been to make the cutoff wavenumbers complex rather than purely imaginary, as they were when the string was stationary.

As U is raised, the ellipse of Fig. 10.2.10a becomes smaller, until under the critical condition that $U = v_s$ it disappears and only real values of k are possible. Hence in Fig. 10.2.10b there are two real wavenumbers corresponding to a given driving frequency ω_a .

It is evident from what we have found that the effect of the convection has been to eliminate the evanescence. Two cases are illustrated in Fig. 10.2.10b. At the larger of the two driving frequencies both wavenumbers are positive and points of constant phase on the waves propagate downstream. At the lower driving frequency, however, the phase velocity of the slow wave is in the negative x -direction (upstream). This is perhaps our first disenchantment with the physical significance of the phase velocity. In fact, a pulse initiated at some point along the moving string would not propagate upstream in the face of the convection. The phase velocity does *not* indicate the manner in which a wavefront would propagate.

We introduced a discussion of the propagation of pulses on the moving string in Section 10.2 because it clearly indicated the direction in which a disturbance would propagate on the string. The string alone, however, is a rather special case in that such sinusoidal steady-state quantities as the phase velocity are identical with the actual propagational velocity of wavefronts. This is why the string merits the designation "dispersionless medium." In general, the phase velocity has no more significance than that associated with the dynamics of the sinusoidal steady state. We return to a discussion of propagational velocities in Section 10.3. For now, suffice it to say that regardless of the types of dispersion introduced with the examples of this and the preceding section wavefronts propagate with the velocities $U + v_s$ and $U - v_s$. Hence boundary conditions are imposed in accordance with the relative values of U and v_s , just as they are with the string alone.

If U is less than v_s , a pulse on the string can propagate upstream. Hence in Fig. 10.2.10a it is appropriate to use the wavenumbers to provide solutions that satisfy one upstream and one downstream boundary condition. Just as in the case considered in Section 10.1.2 the complex wavenumbers indicate that the deflections excited at one end decay spatially from the point of excitation. In the supersonic case shown in Fig. 10.2.10b it is appropriate to impose two boundary conditions at an upstream position. The sinusoidal steady state is then established in essentially the same way as for the moving string alone (Fig. 10.2.7). In fact, the wavenumbers now have the same form

considered in Section 10.2.1 (10.2.20), except that η and γ are defined by (10.2.27). Without any further mathematical developments, we can see that driving conditions in the sinusoidal steady-state form of (10.2.22) and (10.2.23) lead to the deflections given by (10.2.24) and shown in Fig. 10.2.9. The waves combine to form spatial beats as an envelope. The most salient consequences of the dispersion introduced by the addition of the magnetic restoring force can be seen if we consider the limit in which the tension on the string is of negligible importance. Then $v_s \rightarrow 0$ and η and γ , as given by (10.2.28), reduce to

$$\begin{aligned}\eta &= \frac{\omega_d}{U}, \\ \gamma &= \frac{\omega_c}{U}.\end{aligned}\tag{10.2.30}$$

It follows that the string deflections for the sinusoidal steady-state solution of (10.2.25) become

$$\xi(x, t) = \frac{\Delta_0 U}{\omega_c} \cos \left[\omega_d \left(t - \frac{x}{U} \right) \right] \sin \frac{\omega_c x}{U}.\tag{10.2.31}$$

The envelope of the waveform is determined by the cutoff frequency ω_c , whereas the phase velocity of the waves within this envelope is simply the convection velocity U .

In the absence of a tension f each section of the string is subject only to the spring like restoring force of the magnetic field. Because each section has a mass, the resulting dynamics can be pictured in terms of the mechanical model shown in Fig. 10.2.11. Here the mass has been lumped at discrete positions so that it is clear that each section of the string behaves as a simple mass-spring oscillator. As in Section 10.1.2, the spring represents the effect of the field. The convection carries these oscillators in the x -direction with the velocity U .

The resonance frequency of the mass-spring oscillators is ω_c . We can see this by recognizing that in the moving frame the equation of motion takes the form found with a simple harmonic oscillator.

$$\frac{\partial^2 \xi}{\partial t'^2} = -\omega_c^2 \xi.\tag{10.2.32}$$

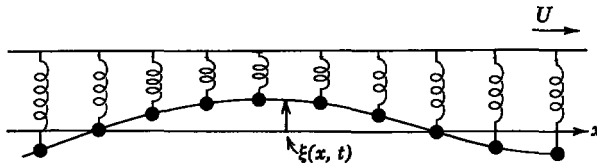


Fig. 10.2.11 When $f \rightarrow 0$ ($v_s \rightarrow 0$), the moving string subject to the restoring force of the magnetic field is equivalent to a distribution of mass-spring oscillators with the resonance frequency ω_c and moving with the velocity U in the x -direction.

The example that follows illustrates how this type of dynamics develops in dealing with electron beams.

Example 10.2.2. The dynamics of moving oscillators is of importance in dealing with interactions between streaming electrons and various media, such as distributed circuits, plasmas, and solid-state lattice structures. The similarity between the electron and string dynamics treated in this section can be illustrated by considering a simple one-dimensional example.

Suppose that a given region of space is filled with electrons with the number density n_e and ions with the number density n_i . We assume that these particles do not interact with one another, except through their electric fields. In the equilibrium situation both the electrons and the ions are static. Moreover, the ion charge density is equal to the electron charge density, so that there is no net charge so long as the system of particles is in equilibrium; for example, if both the ions and electrons have a single electronic charge e , the ion charge density en_i just balances the electron charge density $-en_e$ when the system is in equilibrium.

We are concerned here about the dynamics of the electrons, which have a much smaller mass than the ions. For this reason, it is a good approximation to consider the more massive ions as fixed, hence as having a constant number density. Then the perturbation from equilibrium charge density is

$$\rho_e = (n_i - n_e)e = -ne, \quad (a)$$

where $n(x, t)$ is the amount by which the number density of electrons exceeds the equilibrium value n_e at any given (x, t) .

To describe the electric part of this interaction it is recognized that the charge density is related to the electric field intensity by Gauss's law. In one dimension this is

$$\frac{\partial E}{\partial x} = -\frac{ne}{\epsilon_0}. \quad (b)$$

In addition, conservation of charge in one dimension becomes

$$\frac{\partial J_f}{\partial x} + \frac{\partial \rho_e}{\partial t} = 0, \quad (c)$$

where J_f is the current density. In the present case currents arise only because of the motion of the electrons in the x -direction; hence

$$J_f = -(n_e + n)ev \simeq -n_e ev, \quad (d)$$

where v is the longitudinal (x) electron velocity and the last approximate equality results from a linearization.

The mechanical equation of motion is Newton's law expressed for each of the electrons (having the mass m).

$$m \frac{\partial v}{\partial t} = -eE. \quad (e)$$

Now, a combination of (a) through (e) gives

$$\frac{\partial^2 n}{\partial t^2} + \omega_p^2 n = 0, \quad (f)$$

where

$$\omega_p = \left(\frac{n_e e^2}{\epsilon_0 m} \right)^{1/2}. \quad (g)$$

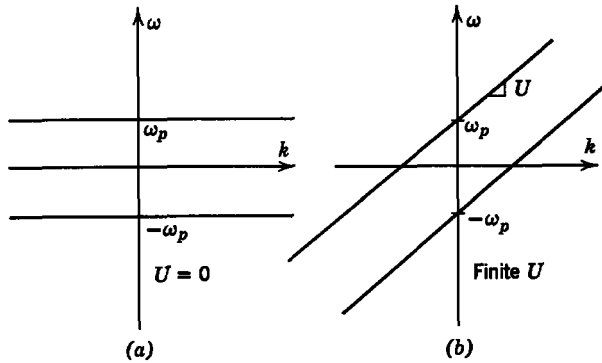


Fig. 10.2.12 Dispersion plot for electron oscillations having the plasma frequency ω_p : (a) the electrons with a fixed equilibrium state; (b) electrons with an equilibrium velocity U in the x -direction.

On the basis of the developments in this and the preceding section, it is a simple matter to see that if the electrons have an equilibrium state of motion in the x -direction with the velocity U (f) is altered to

$$\left(\frac{\partial}{\partial t} + U \frac{\partial}{\partial x}\right)^2 n + \omega_p^2 n = 0. \quad (\text{h})$$

The dispersion equations for these two situations are shown in Fig. 10.2.12. The plasma frequency ω_p plays the same role here as the cutoff frequency ω_c in the discussion of this section. The string dynamics in the magnetic field are described by the same dispersion equation found here in the limit in which $v_s \rightarrow 0$. Note, however, that the electron motions considered here are longitudinal, whereas the deflections of the oscillators (Fig. 10.2.11) are transverse.

In electron beam devices similar oscillations are obtained on a beam with finite cross-sectional dimensions by imposing a large longitudinally directed magnetic field. The Lorentz force $-ev \times \mathbf{B}$ then tends to confine these space-charge oscillations to the longitudinal direction.*

10.2.3 Convective Instability or Wave Amplification

Continuum instability is the subject of Section 10.1.3, in which the simple string, under the influence of a destabilizing magnetic force (Fig. 10.1.9), sustained deflections that grew exponentially with time.

In this section we shall find that if the unstable medium moves fast enough the instability will be carried downstream and a perturbation can grow in amplitude, but not at the same point in space at which it originated. This

* For a discussion of electron beam dynamics, see C. C. Johnson, *Field and Wave Electrodynamics*, McGraw-Hill, 1965, p. 277. The analogy between the moving string and the electron beam should make it clear to those who are familiar with the two-cavity klystron that the moving string with $U > v_s$ can be used to make a "stringtron" or amplifier using the longitudinal kinetic energy of the string as a source of energy.

type of instability can be excited in the sinusoidal steady state, in which case it appears as a spatially growing wave. Hence this *convective instability* is also called an *amplifying wave*, since it can be used to amplify a driving signal.

Some electron-beam devices, such as traveling wave tubes (TWT), make practical use of amplifying waves. In addition, convective instabilities play important roles in a variety of physical situations, ranging from fluid dynamics (boundary layer dynamics) to physical acoustics (ultrasonic amplification). In some cases the convective instability can be put to work, and in others the convective instability occurs inherently in a system and must be understood.

We can illustrate the basic nature of the amplifying wave by considering the effect of convection on the instability studied in Section 10.1.3. We now include the fact that the string is moving in the x -direction with the velocity U .

The effect of the convection is accounted for by replacing the time derivative in the equation of motion by the convective derivative. Hence (10.1.25) becomes

$$\frac{1}{v_s^2} \left(\frac{\partial}{\partial t} + U \frac{\partial}{\partial x} \right)^2 \xi = \frac{\partial^2 \xi}{\partial x^2} + k_c^2 \xi. \quad (10.2.33)$$

Remember, k_c^2 is proportional to the current I in the wire and the gradient of the imposed magnetic field.

Substitution of the traveling wave solution (10.0.1) into this equation of motion yields

$$(\omega - kU)^2 = v_s^2(k^2 - k_c^2). \quad (10.2.34)$$

We could just as well have obtained this dispersion equation by replacing ω in the dispersion equation of Section 10.1.3 with $\omega - kU$. The effect of the convection is simply to translate the entire system in the x -direction with the velocity U . As in Section 10.2.2, however, the excitations and frame of observation remain fixed, and it is this fact that makes the situation inherently different from the case with no convection.

Equation 10.2.34 is quadratic in either ω or k . Solving it for ω shows that there are “unstable” values of ω for real values of k ($|k| < |k_c|$)

$$\omega = kU \pm \sqrt{v_s^2(k^2 - k_c^2)}. \quad (10.2.35)$$

We have seen situations in which a negative imaginary value of ω resulting from a real value of k indicates that the deflections become unbounded with time (Section 10.1.3). In fact, if $U = 0$ and the string is fixed at each end, the allowed values of $k = n\pi/l$, and the associated eigenfrequencies are given by (10.2.35). With the string moving with a velocity U that exceeds v_s , it is no longer consistent with causality to impose a downstream boundary condition. This means that the response to initial conditions is no longer defined in terms of eigenmodes, but rather that it has the character described

in Section 10.2.1. With $U > v_s$, we impose two boundary conditions at $x = 0$. At any downstream position the transient response to the initial conditions is over when a slow wavefront arrives from $x = 0$. Hence the deflections of the string can no longer become unbounded with time at a fixed position x . If the boundary conditions at $x = 0$ are both zero, the response will be zero once the transient is completed.

Consider the consequences of a sinusoidal steady-state boundary condition at $x = 0$. Solution of the dispersion equation shows that for $\omega = \omega_d$, the wavenumbers k are

$$k = \eta \pm j\gamma, \tag{10.2.36}$$

where

$$\eta = \frac{\omega_d U}{U^2 - v_s^2},$$

$$\gamma = \frac{v_s \sqrt{(U^2 - v_s^2)k_c^2 - \omega_d^2}}{U^2 - v_s^2}.$$

The dispersion equation is shown graphically in Fig. 10.2.13. In this ω - k plot complex values of k are shown as functions of real values of ω . As can be seen from (10.2.36), over the range of frequencies

$$\omega_d^2 < (U^2 - v_s^2)k_c^2, \tag{10.2.37}$$

the wavenumbers are complex. Each wavenumber has the same real part over this range, which depends linearly on ω , as shown by the straight line in Fig. 10.2.13. As a function of ω , the imaginary part of k forms an ellipse. Of

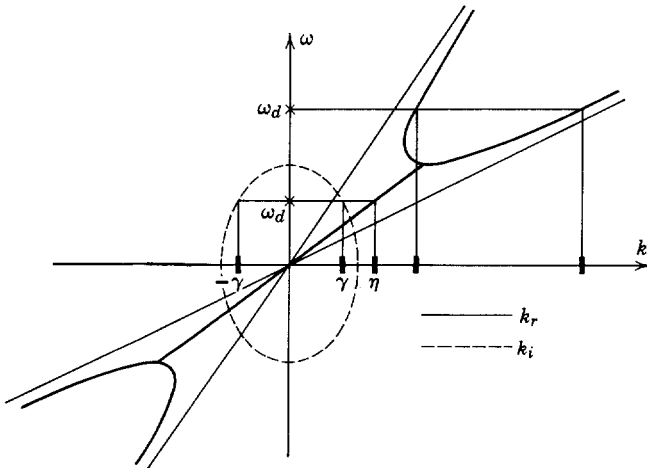


Fig. 10.2.13 Dispersion plot for supersonic string with a destabilizing magnetic force that shows complex values of k for real values of ω .

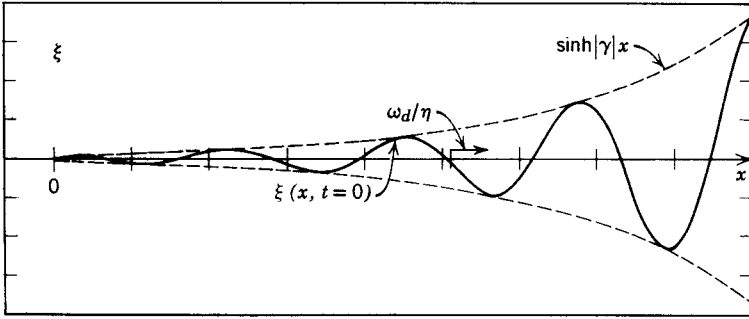


Fig. 10.2.14 Instantaneous view of string deflections when they are convectively unstable.

course, if the driving frequency exceeds a maximum value (10.2.37), both wavenumbers become real and the driven response takes on the form discussed in Section 10.2.1b.

To appreciate the significance of what we have found, consider once again the sinusoidal steady-state response to the boundary conditions of (10.2.22) and (10.2.23). Following the procedures outlined in Section 10.2.1b, we take a linear combination of the two waves which satisfies the boundary conditions at $x = 0$.

$$\xi(x, t) = \frac{\Delta_0}{|\gamma|} \sinh |\gamma|x \cos (\omega_d t - \eta x). \tag{10.2.38}$$

Here we have assumed that the driving frequency ω_d is the lower of the two shown in Fig. 10.2.13 so that the wavenumbers are complex.

The displacement given by (10.2.38) is shown as a function of x at a given instant of time in Fig. 10.2.14.*

Points of zero deflection move downstream with the phase velocity ω_d/η . Most important, the displacements have an envelope that grows exponentially with increasing x . The effect of the motion on the instability is now apparent. Rather than having an amplitude that is a monotonically increasing function of time at a given point in space, the displacements are now bounded in time but exhibit an exponential growth in space. The convection is responsible for washing the instability downstream.

The convective and absolute instabilities impose very different limitations on the engineering of systems. The largest amplitude obtained by the string within a given length is determined by the input of signals, perhaps in the form of noise, to the system. The more nearly the excitations are eliminated from the system, the more nearly will the string maintain its equilibrium

* The reason for the term “amplifying wave” is that an output transducer downstream from the excitation can extract a signal of the same frequency as the excitation but at a higher power level. The source of power is the moving medium.

position. This is by contrast to the case of absolute instability, in which, inadvertently, no matter how carefully the conditions of the string are set, initial noise will result in displacements that become unbounded in time.

The following example affords an opportunity to gain further physical insight into the nature of the convective instability.

Example 10.2.3. In Section 10.1.3 (on absolute instability) an example was considered in which a highly conducting membrane stressed by an electric field was found to be absolutely unstable (Example 10.1.2). Figure 10.2.15 shows a somewhat similar situation in which a jet of water passes between plane-parallel electrodes. The jet moves in the x -direction with the equilibrium velocity U . Transverse or kinking motions of the stream can be modeled by the string equation with the effect of convection included. In the jet the tension f is due to surface tension.

The jet is grounded, but the plates are at the same constant potential V shown in the figure. This is an electric field system, and because the time required for free charges to

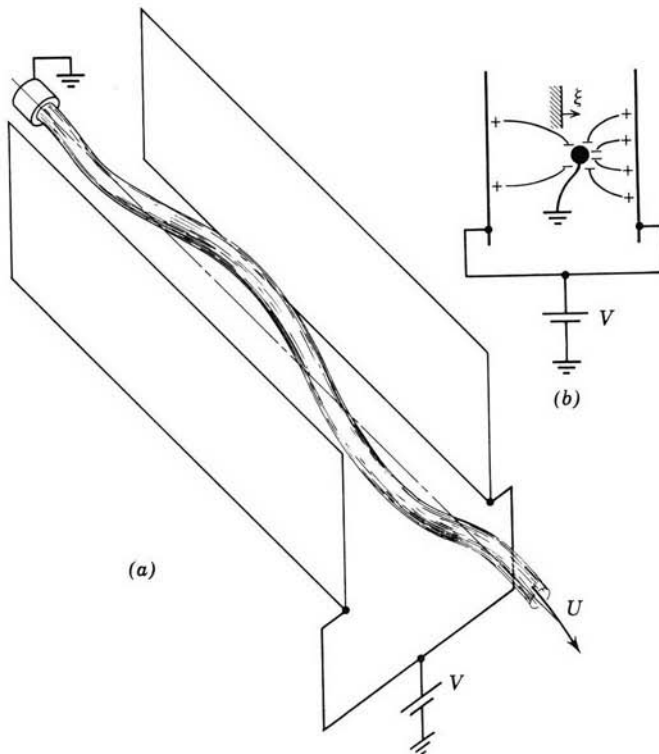


Fig. 10.2.15 (a) A jet of water has a streaming velocity U midway between plane-parallel electrodes. A potential difference V is applied between the plates and the jet. (b) As the jet is deflected toward one of the plates, an unbalance in the electric force of attraction tends to carry it even farther in the direction of deflection. The instability resulting from this force is washed downstream to form the convective instability sketched in Fig. 10.2.16.

relax from one point to another on the water jet is extremely short compared with dynamical times of interest, the jet can be regarded as perfectly conducting; that is, the potential difference between any point on the jet and either of the electrodes is the constant V . This is the same electrical situation as in Example 10.1.2, in which the membrane and electrodes retained a constant potential difference even as the membrane deflected. The dependence of the electric force on the jet displacement is much the same as in the membrane.

A cross section of the jet and plates is shown in Fig. 10.2.15*b*. When the jet is centered, charges induced on its surface are attracted equally toward their images on each of the plates. Hence there is no net transverse force on the jet so long as it remains centered. If, however, it moves off center by the amount ξ , there is a net force. More charges are induced on the side of the jet that is nearer one of the plates (remember that the potential difference is constant and so the jet and plates form a constant potential capacitor). This surplus of

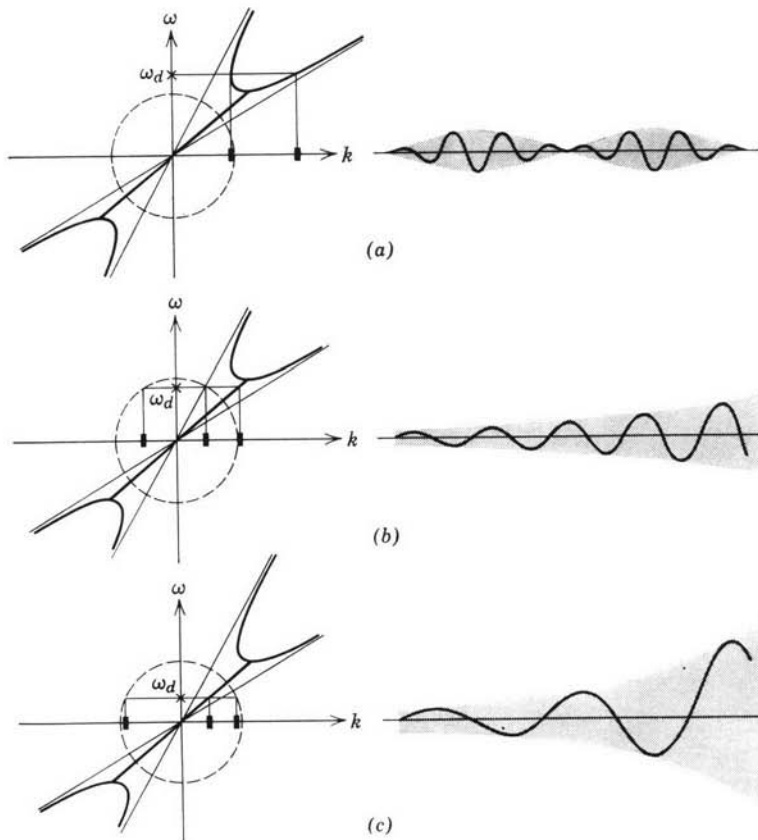


Fig. 10.2.16 Sinusoidal excitation of jet shown in Fig. 10.2.15. Driving frequency decreases from (a) to (c). This experiment together with animated ω - k plots can be seen in the film "Complex Waves II," produced for the National Committee on Electrical Engineering Films by the Education Development Center, Newton, Mass.

charge is attracted toward its image on the plate. Hence the force is (to linear terms) proportional to ξ and in the same direction as ξ . Both the amount of surface charge and the electric field are proportional to V , hence the force, which is proportional to the product of these quantities, is proportional to V^2 . We conclude that the force per unit length acting on the jet transverse to its direction of streaming has the form

$$S_z = bV^2\xi, \quad (a)$$

where b is a geometric constant.

If we combine the electric force of (a) with the equation of motion for the jet alone (10.2.9), it follows that the equation for the jet in the electric field will take the form of (10.2.33) with

$$k_c^2 = \frac{bV^2}{f}. \quad (b)$$

A jet of tap water with the diameter of a pencil and moving with a longitudinal velocity of 2 m/sec has a convection velocity U that exceeds v_s by a factor of 10 or more. Hence in the presence of the electric field the jet is subject to convective instability. It can be excited in the sinusoidal steady state at the upstream end to obtain the response illustrated by (10.2.38) and sketched in Fig. 10.2.16.

In the sequence of sketches the driving frequency ω_d is reduced, as indicated on the corresponding ω - k plots. Hence in Fig. 10.2.16*a* the frequency is high enough that wavenumbers are real and beats form on the jet, as described in Section 10.2.2. In Fig. 10.2.16*b,c* the frequency is reduced to the point at which the wavenumbers are complex and the waves exhibit spatial growth. Note that as the frequency is reduced the wavelength is increased and the rate of spatial growth is increased. This is consistent with the prediction of the ω - k plot, since the rate of growth is proportional to the imaginary part of k , whereas the wavelength is inversely proportional to the real part of k .

The physical significance of the complex wavenumbers found in this section is altogether different from that for the evanescent waves. In Section 10.1.2 complex wavenumbers were used to represent waves that decayed spatially away from the point of excitation. Here the deflection amplitude grows as a function of distance from the excitation.

The contrast between evanescent and amplifying waves must be emphasized, for even though these waves are physically very different they can be confused mathematically; for example, we could arbitrarily impose two upstream sinusoidal steady-state boundary conditions on the evanescent waves found in Section 10.1.2. The resulting mathematical solution would exhibit spatial growth and would appear to be an amplifying wave. Similarly, we could use the waves represented by (10.2.34) with $U > v_s$ to satisfy boundary conditions at two points in space and to conclude that waves decay away from the point of excitation. What we have called a convective instability in this section would then appear to be an evanescent wave. Both sinusoidal steady-state solutions, however, would be inconsistent with causality. The boundary conditions would make it impossible to establish the sinusoidal steady-state solution with the past always affecting the future and not vice versa.

The dispersion equation, as we have used it here, simply guarantees that solutions with the form $\exp j(\omega t - kx)$ satisfy the equation of motion. To make appropriate use of these solutions requires that proper regard be taken of the physical realizability of boundary conditions imposed on the solutions. The examples considered here are so simple that we could use physical intuition or a knowledge of how the system behaves without dispersion effects to establish the correct boundary conditions. Our arguments hinge essentially on observing how the system responds from the moment it is "turned on" until the sinusoidal steady state has been established. If the sinusoidal steady state can be established without violating conditions of causality, it is physically significant. We return to this topic in Section 10.3, in which propagation in the presence of dispersion is considered.*

10.2.4 "Resistive Wall" Wave Amplification

As shown in Section 10.2.3, the instability of continuous media in motion can give rise to amplifying waves. In the frame of reference attached to the moving medium the convective instability appears to grow in time, but in the fixed frame it is bounded in time. Hence it can be excited in the sinusoidal steady state with an attendant spatial growth.

Although the combination of material convection and absolute instability is one way of obtaining a convective instability, it is by no means true that this is the only way in which convective instabilities arise. Convective instabilities or amplifying waves often result when a stream interacts with a fixed structure. This is how amplifying waves are obtained in a traveling wave (electron beam) tube. A beam of electrons is coupled to a fixed electromagnetic transmission line. Similarly, beams of electrons or holes can couple to solid-state crystal structures to produce amplifying waves. These systems are more complicated than those introduced in this section because they involve more than two waves. Not only do the beams support waves, but so also do the fixed structures. Here we can illustrate this class of phenomenon by coupling the moving continuum to a fixed structure that does not support waves—simply a resistive wall. In fact, resistive wall instabilities are also found in electron beam devices and particle accelerators.†

With the developments of Section 10.1.4 in view, it is a simple matter to illustrate how convection, in conjunction with the damping, can produce wave amplification. Consider once again the situation in which the string is

* For a general discussion of this topic see A. Bers and R. J. Briggs, "Criteria for determining absolute instabilities and distinguishing between amplifying and evanescent waves," *Bull. Amer. Phys. Soc.*, Ser 2, 9, 304 (1964) or R. J. Briggs, *Electron-Stream Interaction With Plasmas*, M.I.T. Press, Cambridge, Mass., 1964, pp. 8–46.

† F. H. Clauser, *Symposium on Plasma Dynamics*, Addison-Wesley, Reading, Mass., 1960, pp. 78–118.

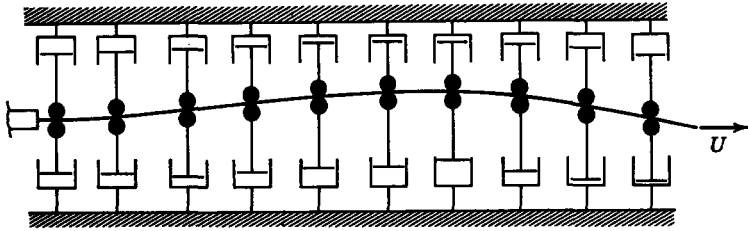


Fig. 10.2.17 The string moves unimpeded in the x -direction with the velocity U , and transverse motions are retarded by dashpots that interact with the string through rollers. The dashpots are fixed to the laboratory frame of reference.

immersed in a viscous liquid. Now, however, the string has a longitudinal velocity U . We assume that the convection of the string in the x -direction is unimpeded by the viscous fluid, even though the transverse motions lead to transverse viscous retarding forces. For conceptual purposes it is helpful to think of the system as being equivalent to that shown in Fig. 10.2.17.

The damping remains in the fixed frame. This means that the effect of the string motion is not simply accounted for by replacing time derivatives in (10.1.33) with convective derivatives, as would be appropriate with the total system in motion. We do, however, know the equation of motion for the string alone (10.2.8). Because the damping force does not depend on the motions, it remains as given by (10.1.32). Hence the equation of motion is (10.1.33) with the second time derivative (acceleration term) replaced by the second convective derivative but with the damping term left unaltered.

$$\left(\frac{\partial}{\partial t} + U \frac{\partial}{\partial x}\right)^2 \xi = v_s^2 \frac{\partial^2 \xi}{\partial x^2} - \nu \frac{\partial \xi}{\partial t}. \quad (10.2.39)$$

As in Section 10.1.4, the wavefront velocity v_s , and damping frequency ν are

$$v_s = \left(\frac{f}{m}\right)^{1/2},$$

$$\nu = \frac{B}{m}.$$

It follows from (10.2.39) that traveling wave solutions must satisfy the dispersion equation

$$(\omega - kU)^2 = v_s^2 k^2 + j\omega\nu, \quad (10.2.40)$$

which has the same form as (10.1.36), except that the ω on the left has been replaced by $\omega - kU$. Now, this dispersion equation, like others introduced in this and the preceding section, is simply quadratic in ω and k . Hence we

can solve for either ω or k . Observe first that $\omega(k)$ is

$$\omega = kU + \frac{j\nu}{2} \pm \left[\left(kU + \frac{j\nu}{2} \right)^2 - (U^2 - v_s^2)k^2 \right]^{1/2}. \quad (10.2.41)$$

If U exceeds v_s , this result shows that for real values of k there are negative imaginary values of ω . The ω - k plot, which shows complex values of ω for real values of k , is sketched in Fig. 10.2.18. This plot should be compared with Fig. 10.1.19 to appreciate the effect of convection. The convection is responsible for replacing the damping found (in Section 10.1.4) with $U < v_s$ by an instability. It would be erroneous, however, to assume on the basis of (10.2.41) that deflections of the string would become unbounded with time at a fixed position x . As in Section 10.2.3, the fact that U exceeds v_s requires that two upstream boundary conditions be imposed. In a manner similar to that discussed in Section 10.2.1*b*, the response to initial conditions vanishes in a finite time at a given position. Hence a sinusoidal steady state can be established, and the corresponding mathematical solution is found by solving (10.2.40) for k as a function of ω .

$$k = \frac{\omega U \pm \sqrt{v_s^2 \omega^2 + (U^2 - v_s^2)(j\omega\nu)}}{(U^2 - v_s^2)}. \quad (10.2.42)$$

This dispersion equation is shown in Fig. 10.2.19, in which complex values of k are shown for real values of ω . Note that the phase velocity of both waves is now downstream. More significant is the fact that because $U > v_s$ the wave with a positive imaginary wavenumber grows spatially. With the

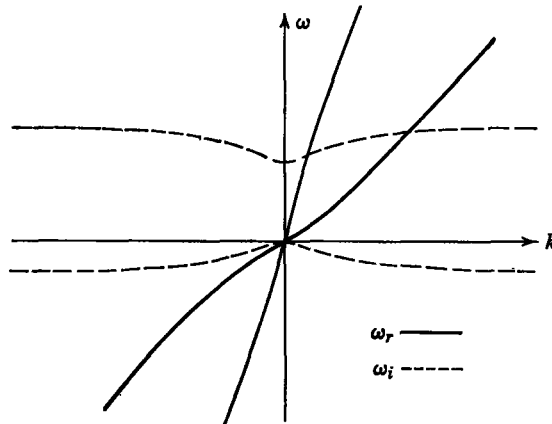


Fig. 10.2.18 Dispersion equation for resistive wall instability. Complex values of ω are shown for real values of k . Although this plot indicates that the string deflections are unstable, the instability is exhibited as a growth in space rather than in time.

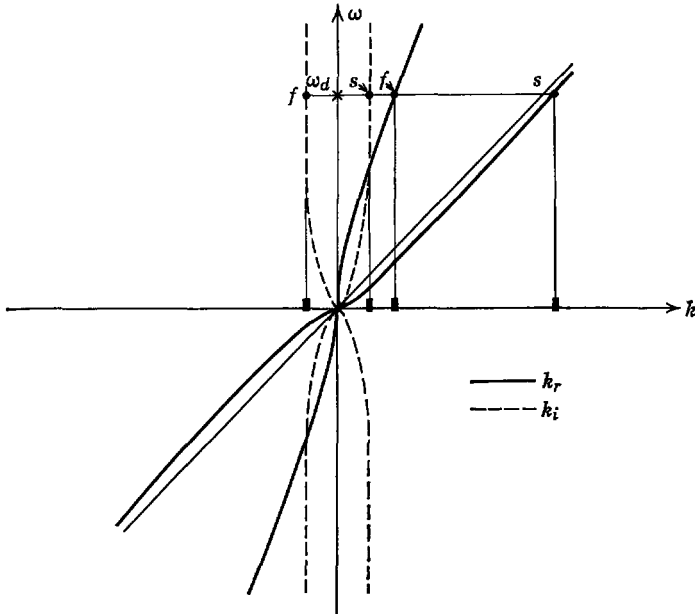


Fig. 10.2.19 Dispersion relation for resistive wall instability. Complex values of k are shown as functions of real values of ω . The effect of convection is apparent if this plot is compared with that shown in Fig. 10.1.17 (where $U = 0$).

damping removed, this is the wave that tries to buck the convection and, because $U > v_s$, propagates slowly downstream. The amplifying slow wave is denoted by (s) in Fig. 10.2.19; the spatially decaying fast wave is labeled (f). This amplifying wave has been termed a resistive wall instability because it is often found in electron beam devices when the beam is coupled to a resistive wall. The mechanical dampers might also be viewed as a resistive wall. The same effect as the dampers, however, is produced by coupling the continuum through a magnetic field to a dissipative structure, as shown in Example 10.1.3. With motion, that example quite literally illustrates a resistive wall instability, as discussed in the following example.

Example 10.2.4. Consider once again the perfectly conducting membrane shown in Fig. 10.1.7. Recall that the membrane is immersed in a longitudinal magnetic field that is uniform when the membrane is undeflected. Because the edges of the membrane make contact with side walls, which in turn form electric circuits above and below the membrane, deformations are accompanied by currents that tend to conserve the total flux above and below the membrane. We consider here the effect of convection when the resistance of the walls is so high that the self-inductance of the external current loops is unimportant. This limit was discussed in Example 10.1.3, in which it was found that the wall had the effect of damping the transverse motions.

We now introduce the additional complication that the membrane is moving in the x -direction with a velocity $U > v_s$. The resistive walls remain fixed. Consequently, the equation of motion, which for the membrane without convection takes the form of (e) in Example 10.1.3, becomes

$$\left(\frac{\partial}{\partial t} + U \frac{\partial}{\partial x}\right)^2 \xi = v_s^2 \frac{\partial^2 \xi}{\partial x^2} - \nu \frac{\partial \xi}{\partial t}, \tag{a}$$

where $v_s = \sqrt{S/\sigma_m}$ and $\nu = 2\sigma_s(\mu_0 H_0)^2/\sigma_m$. The left-hand side of this equation reflects the effect of convection on the moving membrane, whereas the damping force on the right remains unaffected. This can be shown by using a contour of integration for Faraday's law [contour (a) or (b) in Fig. 10.1.8] just as in Example 10.1.1 but with the segment through the membrane moving in the x -direction with velocity U . Because the membrane is perfectly conducting $\mathbf{E}' = 0$ over that segment and, moreover, there is no addition to the rate of change of the flux linked by the contour.

Because (a) has the same form as (10.2.39), we conclude that the moving membrane coupled to the resistive wall is subject to convective instability.

A physical picture of the variety of convective instability studied in Section 10.2.3 is not difficult to obtain. In a frame of reference moving with the string the amplitude becomes unbounded with time for the same reason that it does when the string is stationary. Without the motion, however, the system we consider in this section is stable. In fact, we normally think of damping as a stabilizing influence. Yet the combination of the convection and damping leads to instability!

An understanding of this instability can be obtained by considering string deflections in a frame of reference moving with the string, represented by Fig. 10.2.20. In this frame the string appears to have no longitudinal velocity but the resistive wall (the dampers) moves in the $-x$ -direction with the velocity U . The viscous force, expressed in terms of the coordinates (x', t') , is

$$S_z = -B \left(\frac{\partial}{\partial t'} - U \frac{\partial}{\partial x'}\right) \xi. \tag{10.2.43}$$

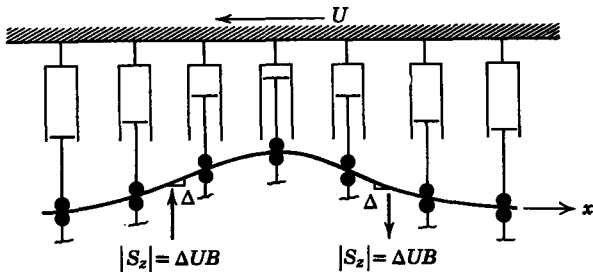


Fig. 10.2.20 A pulse is initially stationary when viewed from a frame moving with the string. Then, as the dashpots move to the left, they produce a force with a sign determined by the slope of the string.

The first term, familiar as the retarding force due to the transverse velocity, will always act in a direction opposite to that in which ξ is temporally increasing. The second term enters because, with the dashpots moving to the left, the plungers must change their positions at a rate determined by U and the slope of the string; for example, suppose that the pulse is instantaneously stationary in the x' -frame. The moving dampers will tend to increase the deflection when the slope is positive and decrease it when the slope is negative. Hence the back of the pulse tends to grow, whereas the front of the pulse is flattened by the moving dampers. As the regions of positive slope grow, they move to the right when viewed in the fixed frame, and we have the ingredients of a convective instability.

10.3 PROPAGATION

The situations developed in the last two sections provide an ample background for embarking on a discussion of wave propagation in distributed systems exhibiting dispersive waves. In retrospect, it is clear that we have either confined attention to sinusoidal steady-state behavior or, when transient conditions were considered, to nondispersive waves (with and without convection); for example, in Section 10.2.1 we used the moving string without external forces to illustrate how conditions of causality restrict the boundary conditions that can be imposed. Throughout our discussion we have assumed that even with dispersive waves (an extreme example is the convective instability) we are justified in imposing two upstream conditions if $U > v_s$ and one upstream and one downstream condition if $U < v_s$. In fact, our assumption is correct but this is not obvious. One way to ask the question is this: if a pulse is initiated on the string, does any part of it propagate upstream? If so, we must impose a downstream boundary condition. We have illustrated that the phase velocity of a periodic wave is not a reliable basis for answering this question. We begin by reviewing this point.

10.3.1 Phase Velocity

Suppose that we restrict attention to waves that are purely sinusoidal in space and time so that both ω and k are real. Then points of constant phase propagate with the velocity,

$$v_p = \frac{\omega}{k}. \quad (10.3.1)$$

On an ω - k plot this phase velocity has the geometrical significance shown in Fig. 10.3.1. As long as we are dealing with nondispersive waves, the phase velocity is identical with the velocity of propagation of wavefronts, which is

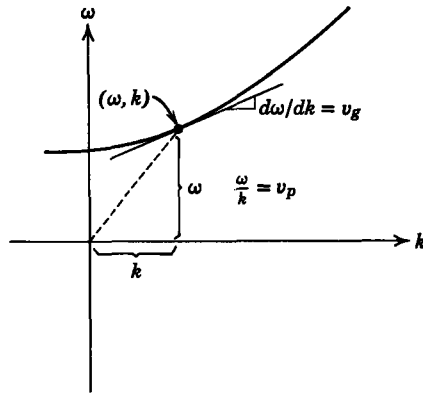


Fig. 10.3.1 The slope of the line joining the point (ω, k) and the origin is the phase velocity. The tangent of the ω - k curve at this same point is the group velocity.

why the ω - k plots of Fig. 10.2.8 appear so similar to the characteristic lines in the x - t plane, shown in Fig. 10.2.2. For the moving string without external forces wavefronts propagate with the velocities $U \pm v_s$ (the slopes of the characteristics), and these are the phase velocities of the fast and slow waves in the sinusoidal steady state.

It would be an assumption to say that the phase velocity is always the velocity of propagation of a wavefront, and we have examples from which to choose to show that this assumption is not well founded. In the case in which we have the possibility of evanescent waves (Fig. 10.1.3) the phase velocity approaches infinity as $k \rightarrow 0$, and it is certainly unreasonable to assume that a pulse will propagate with this velocity. Even more obvious, since v_p is a function of ω or k , which value do we select as the velocity of a wavefront? Considerations of this type lead us to consider other velocities such as the group velocity.

10.3.2 Group Velocity

The group velocity of waves with frequencies in the neighborhood of ω is defined as

$$v_g = \frac{d\omega}{dk} \quad (10.3.2)$$

or as the slope shown in Fig. 10.3.1. The velocity v_g has the physical significance of being the velocity of propagation of a group of waves with essentially the same wavenumber and frequency.

A straightforward way to show the dynamical meaning of the group velocity is to consider an excitation in the form of

$$\xi(0, t) = \xi_0[1 + \cos \omega_m t] \cos \omega_s t, \quad (10.3.3)$$

which is recognized as amplitude modulation of a sinusoidal excitation with a frequency ω_s . The amplitude of the excitation varies between $2\xi_0$ and 0 with a frequency ω_m . The nature of the resulting waves is most easily demonstrated if it is assumed that the string has an infinite extent in the x -direction and excitations are applied in such a way that only one of the two possible waves is excited.

A trigonometric identity* converts (10.3.3) to

$$\xi(0, t) = \xi_0 \cos \omega_s t + \frac{1}{2} \xi_0 [\cos (\omega_s + \omega_m)t + \cos (\omega_s - \omega_m)t], \quad (10.3.4)$$

which is the familiar statement that a sinusoidal signal with a frequency ω_s , amplitude modulated at the frequency ω_m , is equivalent to three signals with frequencies ω_s , $\omega_s + \omega_m$, and $\omega_s - \omega_m$. Because the wavenumber depends on the frequency of excitation, each of the terms in (10.3.4) excites a wave with a different wavelength.

Attention is confined to situations in which $\omega_m \ll \omega_s$. Then the wavenumbers corresponding to $\omega_s \pm \omega_m$ are given approximately by $k = k_s \pm \omega_m/v_g$. Figure 10.3.2 shows graphically the relationship between frequencies and wavenumbers. The wavenumbers adjacent to k_s are obtained by assuming that in the vicinity of the point (ω_s, k_s) the dispersion equation can be approximated by a straight line whose slope v_g is the same as that in the ω - k plot.

If only one wave is excited, the first term in (10.3.4) gives rise to the string deflections

$$\xi(x, t) = \xi_0 \cos (\omega_s t - k_s x). \quad (10.3.5)$$

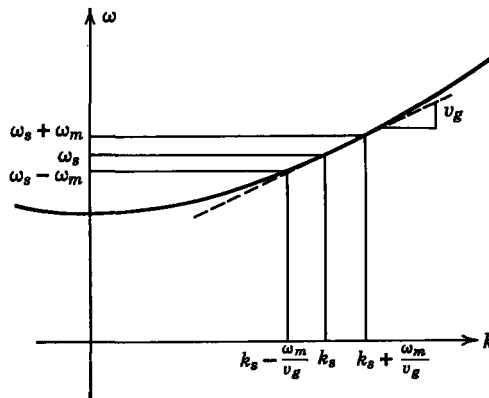


Fig. 10.3.2 For waves with very nearly the same frequency the group velocity v_g can be used to represent the dispersion.

* $\cos A \cos B = \frac{1}{2}[\cos (A + B) + \cos (A - B)]$.

The excitations at the sum and difference frequencies $\omega_s \pm \omega_m$ lead to similar waves with wavenumbers $k_s \pm \omega_m/v_g$ which are now superimposed to find waves resulting from the total excitation.

$$\begin{aligned} \xi(x, t) = & \xi_0 \cos(\omega_s t - k_s x) \\ & + \frac{1}{2} \xi_0 \cos \left[(\omega_s t - k_s x) + \omega_m \left(t - \frac{x}{v_g} \right) \right] \\ & + \frac{1}{2} \xi_0 \cos \left[(\omega_s t - k_s x) - \omega_m \left(t - \frac{x}{v_g} \right) \right]. \end{aligned} \tag{10.3.6}$$

We again use a trigonometric identity* to write this expression as

$$\xi(x, t) = \xi_0 \left[1 + \cos \omega_m \left(t - \frac{x}{v_g} \right) \right] \cos(\omega_s t - k_s x), \tag{10.3.7}$$

so that it is clear that displacements take the form of a wave, with a frequency ω_s , which is modulated by another wave with a frequency ω_m . At an instant of time the string appears as shown in Fig. 10.3.3. A point of constant phase (a zero crossing) moves to the right with the phase velocity ω_s/k_s . By contrast, a point of constant phase on the *envelope* moves to the right with group velocity v_g . The group velocity is therefore interpreted as the velocity at which the group of waves, defined by the envelope, propagates in the x -direction. Note that because the phase and group velocities are different the waves will appear to move with respect to the envelope. In the ω - k plot of Fig. 10.1.3 (which was the subject of Section 10.1.2) the group velocity is less than the phase velocity; hence the phases move downstream more rapidly than the envelope.

Our analysis presumes that the wavetrain of Fig. 10.3.3 extends to infinity in the x -direction and that the sinusoidal steady state has been established.

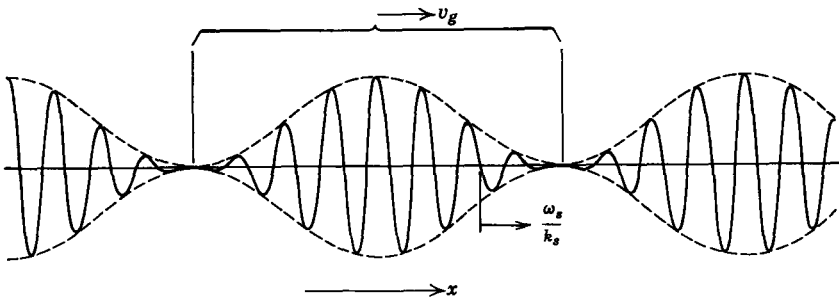


Fig. 10.3.3 Wavetrain amplitude modulated at a frequency that is much lower than the wave frequency. The string appears as shown by the solid line at an instant in time.

* $\cos(A + B) = \cos A \cos B - \sin A \sin B$.

Hence it does not directly indicate the manner in which a pulse propagates. Suppose, however, that we were concerned with the propagation of the pulse obtained by eliminating all the wavetrain except the one full pulse in Fig. 10.3.3 bounded on either end by the nulls in the envelope. It is not possible to describe this signal as the superposition of three sinusoidal signals, but, if we take the Fourier transform of this signal*

$$\hat{\xi}(\omega, k) = \int_{-\infty}^{+\infty} \int_{-\infty}^{+\infty} \xi(x, t) e^{-j(\omega t + kx)} dx dt, \quad (10.3.8)$$

we find that its major frequency and wavenumber components are in the neighborhood of (ω_s, k_s) . Provided that the spectrum of frequency (hence, because of the dispersion equation, the wavenumbers) of a pulse is confined essentially to a small region, the group velocity gives a measure of the velocity of the pulse. In terms of (x, t) this pulse is almost a pure sinusoid, except for a slowly varying envelope.

From this discussion it should be clear that the group velocity can be used to ascertain the "over-all" velocity of a high-frequency pulse, but because only those portions of the pulse that have a slowly varying envelope can be so described the group velocity is not the velocity of a wavefront. As we have seen, in the region of a wavefront deflections vary rapidly and, in fact, can be discontinuous. Hence the group velocity is not appropriate for determining the boundary conditions consistent with causality. As for the phase velocity, we might have suspected this limitation from the outset, since the group velocity is a function of ω or k . We hope that the question whether two upstream boundary conditions or one upstream and one downstream boundary condition should be used is independent of the dynamical quantities ω and k .

We must make one further reservation concerning the physical significance of the group velocity. It does not give a reliable indication of pulse propagation, even subject to the limitations outlined, if the system is unstable.† This is true whether the instability is convective or nonconvective. We have not attempted to prove this here but have used the examples of the two previous sections to make this further limitation plausible. The ω - k plot for the unstable string is shown in Fig. 10.1.11. Note that as $k \rightarrow k_e$ the group velocity approaches infinity. It would be unreasonable to conclude that a pulse could be made to propagate with an arbitrarily large velocity.

With convection (Fig. 10.2.13) the insignificance of v_g becomes even more apparent. In this case we can select ω or k to give any value of v_g , positive,

* R. G. Brown and J. W. Nilsson, *Introduction to Linear Systems Analysis*, Wiley, New York, 1962, p. 209.

† R. J. Briggs, *Electron-Stream Interaction With Plasmas*, M.I.T. Press, Cambridge, Mass., 1964, p. 33.

negative, zero, and infinite! From this it is clear that the notion of a group velocity must be used with care. Cases in which instability can develop make this particularly clear. A pulse of finite extent contains all wavenumbers. The group velocity is meaningful if the dynamics are dominated by signal components confined to a small range of wavenumbers. The wavenumber spectrum that is unstable tends to amplify and cannot be ignored.

10.3.3 Characteristics and the Velocity of Wavefronts

Wavefronts propagate along the characteristic lines in the $x-t$ plane. This is illustrated by considering a convecting string with a destabilizing force, discussed in Section 10.2.3. The equation of motion (10.2.33) is

$$\left(\frac{\partial}{\partial t} + U \frac{\partial}{\partial x}\right)^2 = v_s^2 \left[\frac{\partial^2 \xi}{\partial x^2} + k_c^2 \xi \right]. \quad (10.3.9)$$

A general discussion of how characteristics can be found for a given differential equation would lead us afield.* Thus for our purposes we view the characteristics as a convenient transformation of independent variables from the coordinate system (x, t) to the new coordinate system (α, β) according to the relations

$$\alpha = x - (U + v_s)t, \quad (10.3.10)$$

$$\beta = x - (U - v_s)t. \quad (10.3.11)$$

The resulting simplification in the differential equation and its interpretation and solution justify the transformation.

Note that the characteristic lines are the same as those used in Sections 9.1.1a and 10.2.1, in which nondispersive waves were studied.

To write (10.3.9) in terms of the new independent variables α and β , we use (10.3.10) and (10.3.11) to evaluate the partial time derivative as

$$\frac{\partial \xi}{\partial t} = \frac{\partial \xi}{\partial \alpha} \frac{\partial \alpha}{\partial t} + \frac{\partial \xi}{\partial \beta} \frac{\partial \beta}{\partial t} = -(U + v_s) \frac{\partial \xi}{\partial \alpha} - (U - v_s) \frac{\partial \xi}{\partial \beta}. \quad (10.3.12)$$

In a similar manner

$$\frac{\partial \xi}{\partial x} = \frac{\partial \xi}{\partial \alpha} \frac{\partial \alpha}{\partial x} + \frac{\partial \xi}{\partial \beta} \frac{\partial \beta}{\partial x} = \frac{\partial \xi}{\partial \alpha} + \frac{\partial \xi}{\partial \beta}. \quad (10.3.13)$$

* For a general discussion of the method of characteristics see, for example, R. Courant and K. O. Friedrichs, *Supersonic Flow and Shock Waves*, Interscience, New York, 1948, Chapters, II, III, and IV.

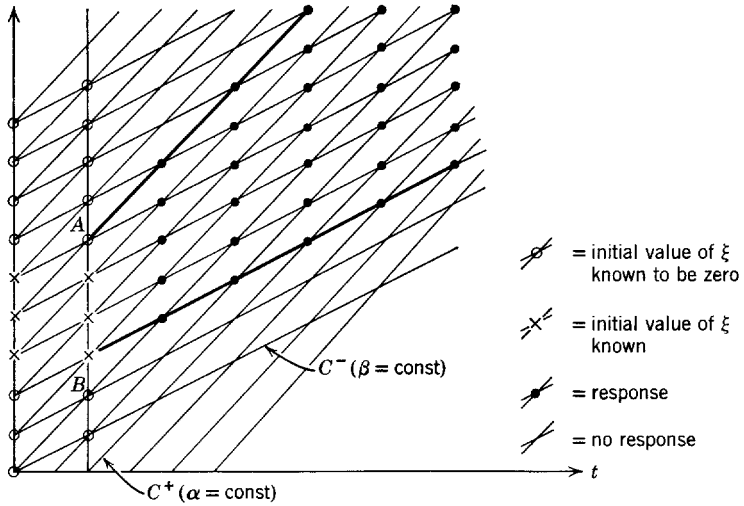


Fig. 10.3.4 Grid of characteristics in the $x-t$ plane for $U > v_s$.

A repetition of the process and transformation of the derivatives in (10.3.9) yields

$$\frac{\partial^2 \xi}{\partial \alpha \partial \beta} + \frac{k_c^2}{4} \xi = 0. \tag{10.3.14}$$

This form of the equation of motion makes it particularly clear why $\xi(\alpha)$ and $\xi(\beta)$ are both solutions when $k_c = 0$.

In the $x-t$ plane the C^+ characteristics ($\alpha = \text{constant}$) are parallel straight lines with the slope $U + v_s$ and the C^- characteristics ($\beta = \text{constant}$) are parallel straight lines with slope $U - v_s$. These characteristics fill the $x-t$ plane as illustrated in Fig. 10.3.4. In Fig. 10.3.5 the four intersections of two pairs of closely spaced characteristics are shown. This configuration can be used to obtain an approximate integral of (10.3.14). The solution thus obtained yields both numerical answers and insight into how disturbances propagate.

We assume that the displacements at points A , B , and D in Fig. 10.3.5 are

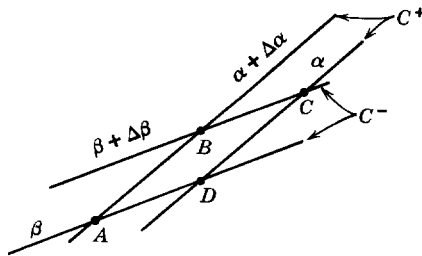


Fig. 10.3.5 Intersections A , B , C , and D of two pairs of characteristics with $U > v_s$.

known and we wish to evaluate the displacement at point C (at some future time at a downstream point) When $\Delta\alpha$ and $\Delta\beta$ are small, we can write

$$\frac{\partial \xi}{\partial \alpha}(\alpha, \beta + \Delta\beta) \approx \frac{\xi(\alpha + \Delta\alpha, \beta + \Delta\beta) - \xi(\alpha, \beta + \Delta\beta)}{\Delta\alpha} = \frac{\xi_B - \xi_C}{\Delta\alpha}, \quad (10.3.15)$$

$$\frac{\partial \xi}{\partial \alpha}(\alpha, \beta) \approx \frac{\xi(\alpha + \Delta\alpha, \beta) - \xi(\alpha, \beta)}{\Delta\alpha} = \frac{\xi_A - \xi_D}{\Delta\alpha} \quad (10.3.16)$$

Continuation of this process one step further yields

$$\frac{\partial^2 \xi}{\partial \alpha \partial \beta}(\alpha, \beta) \approx \frac{(\partial \xi / \partial \alpha)(\alpha, \beta + \Delta\beta) - (\partial \xi / \partial \alpha)(\alpha, \beta)}{\Delta\beta} \quad (10.3.17)$$

or

$$\frac{\partial^2 \xi}{\partial \alpha \partial \beta}(\alpha, \beta) \approx \frac{(\xi_B - \xi_C) - (\xi_A - \xi_D)}{\Delta\alpha \Delta\beta} \quad (10.3.18)$$

The use of this approximate derivative in (10.3.14) and solution for ξ_C yield the desired result*:

$$\xi_C = \xi_B + \xi_D - \xi_A \left(1 - \frac{k_c^2 \Delta\alpha \Delta\beta}{4} \right). \quad (10.3.19)$$

The solution to our problem $\xi(x, t)$ or $\xi(\alpha, \beta)$ can be viewed in a three-dimensional plot as the height of a surface above the $x-t$ or $\alpha-\beta$ plane. Hence the initial conditions $\xi(x, 0)$ and $(\partial \xi / \partial t)(x, 0)$ give the height of the surface and its slope in the t -direction near the x -axis. In approximate terms this is equivalent to giving the value of ξ at the intersections of characteristics on and adjacent to the x -axis, as shown in Fig. 10.3.4. From this initial data (10.3.19) can be used to find ξ at the next (third) vertical column of intersections in the $x-t$ plane of Fig. 10.3.4. These values, in turn, can be used to calculate ξ at the next vertical column of intersections.

In Fig. 10.3.4 we have indicated an initial pulse by an \times at the characteristic intersections; that is, ξ has some finite value at these points. The initial displacements are zero at intersections marked \circ . The approximate solution (10.3.19) of the equation of motion then shows that there is no deflection ξ except possibly at the intersections marked. Hence the initial deflection in the interval AB results in wavefronts propagating within the region in the $x-t$ plane bounded by the C^+ characteristic originating at A and the C^- characteristic originating at B . Because $U > v_s$, the initial disturbance propagates downstream, as we assumed in Section 10.2.3.

* Note that the term $k_c^2 \xi_A / 4$ has been approximated by $k_c^2 \xi_A / 4$. The error implicit in this approximation becomes more and more significant as iterative use is made of (10.3.19).

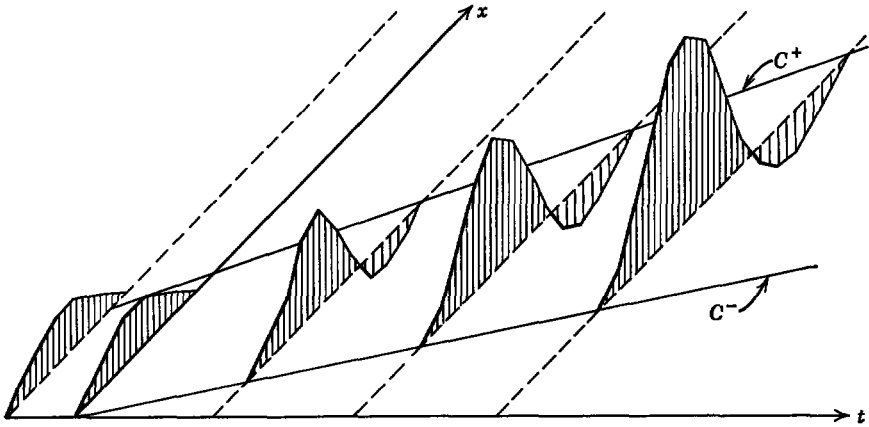


Fig. 10.3.6 Transient deflection following the initiation of a static pulse on a moving unstable string ($U = 3v_s$). The deflection is convectively unstable.

It can be seen that as long as both families of characteristics go downstream as t increases, a driving condition (along the t -axis) that involves two conditions on ξ is no different mathematically from the two initial conditions along the x -axis considered here.

Our approximate solution for the equation of motion shows also that waves are likely to grow. Consider the case in which points A , B , and D all have the deflection $\xi = \xi_0$ (the initial condition of a static, spatially uniform pulse of height ξ_0). Then

$$\xi_C = \xi_0 \left(1 + \frac{k_c^2 \Delta\alpha \Delta\beta}{4} \right), \quad (10.3.20)$$

and the amplitude has increased by the time the pulse reaches the point C .

A numerical example is shown in Fig. 10.3.6. For all values of $t < 0$ the initial pulse has the same x -dependence, as shown; that is, the pulse is initially static. For this transient solution seven grid points have been used to describe the initial pulse and $k_c^2 \Delta\alpha \Delta\beta / 4 = 0.1$. The pulse grows in amplitude but propagates downstream. At any given position x , the deflection remains bounded. These are the salient features of a convective instability.

The leading edge of the pulse becomes inverted, as is expected from the results found in Example 10.2.1 for an initially static pulse in a stable situation but with $U > v_s$ (see Fig. 10.2.5).

10.4 DYNAMICS IN TWO DIMENSIONS

The techniques described for dealing with continuum electromechanical interactions are not limited to a single space dimension, as implied by the

examples given. In this section we consider several cases that show how the dispersion equation also accounts for motions that depend on two or three dimensions.

10.4.1 Membrane Dynamics: Two-Dimensional Modes

A classic demonstration of wave propagation, as it depends on two dimensions, is given by considering a membrane. In the absence of external surface forces the equation of motion (as derived in Section 9.2) is

$$\frac{\partial^2 \xi}{\partial t^2} = v_s^2 \left(\frac{\partial^2 \xi}{\partial x^2} + \frac{\partial^2 \xi}{\partial y^2} \right), \quad (10.4.1)$$

where

$$v_s = \left(\frac{S}{\sigma_m} \right)^{1/2}.$$

Solutions to this equation have the general form

$$\xi = \text{Re } \hat{\xi} e^{j(\omega t - k_x x - k_y y)}, \quad (10.4.2)$$

where we must now distinguish between the wavenumber k_y , which indicates the dependence on y , and k_x , which indicates the x -dependence. Substitution of (10.4.2) into (10.4.1) shows that ω is related to k_y and k_x by the dispersion equation

$$\omega^2 = v_s^2 (k_x^2 + k_y^2). \quad (10.4.3)$$

Now suppose that the edges of the membrane at $y = 0$ and $y = b$ are fixed, as shown in Fig. 10.4.1; that is, deflections satisfy the boundary conditions

$$\xi(x, 0, t) = 0, \quad (10.4.4)$$

$$\xi(x, b, t) = 0. \quad (10.4.5)$$

Any linear combination of solutions with the traveling waveform of (10.4.2) and (ω, k_x, k_y) satisfying the dispersion equation (10.4.3) will satisfy the equation of motion. In particular, we take the linear combination

$$\xi = \text{Re } [\hat{\xi}_1 \sin k_y y + \hat{\xi}_2 \cos k_y y] e^{j(\omega t - k_x x)}. \quad (10.4.6)$$

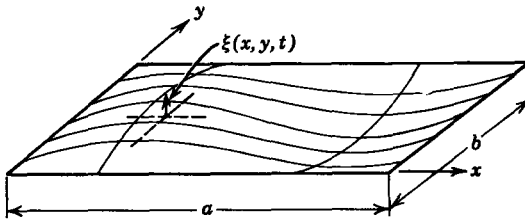


Fig. 10.4.1 Membrane having static equilibrium in x - y plane.

Here it is more convenient to write the complex exponential dependence on y in terms of trigonometric functions because it is clear from (10.4.4) that $\hat{\xi}_2 = 0$. Moreover, if boundary condition (10.4.5) is to be satisfied,

$$k_y = \frac{n\pi}{b}. \quad (10.4.7)$$

We have found that modes satisfying the transverse boundary conditions take the form

$$\xi(x, y, t) = \text{Re } \hat{\xi}_1 \sin\left(\frac{n\pi y}{b}\right) e^{j(\omega t - k_x x)}, \quad (10.4.8)$$

where in view of (10.4.7) the dispersion equation relating (ω, k_x) for any given mode (n) is

$$\omega^2 = v_s^2 \left[k_x^2 + \left(\frac{n\pi}{b}\right)^2 \right]. \quad (10.4.9)$$

This expression takes the same form as the dispersion equation (10.1.7) developed in Section 10.1.2, in which evanescent waves were studied. Hence for each mode the dispersion equation takes the geometrical form shown in Fig. 10.1.3. The cutoff frequency is [compare (10.1.7) and (10.4.9)]

$$\omega_c^2 = v_s^2 \left(\frac{n\pi}{b}\right)^2. \quad (10.4.10)$$

Suppose that the membrane is driven at one end by a sinusoidal steady-state excitation with a frequency $\omega = \omega_a$. Then we have found that the response is composed of an infinite number of waves, each having n half-wavelengths in the y -direction. If $\omega_a < \omega_c$, the waves in the x -direction are evanescent. Hence for any given driving frequency a finite number (or, if $\omega_a < v_s \pi/b$, none) of the waves will propagate (have real values of k_x), whereas all others will be evanescent.

The evanescent or cutoff waves are a consequence of the stiffening effect of the transverse boundaries. Curvature of the membrane leads to an elastic restoring force (remember the membrane is under the longitudinal and transverse tension S). Because of the transverse boundaries, the membrane cannot deform without incurring a curvature. Waves are cutoff if the elastic restoring force resulting from this curvature (proportional to k_y^2) outweighs the effect of inertia.

If, in addition to the boundary conditions already imposed, the membrane is fixed at $x = 0$ and $x = a$, it is appropriate to look for the natural modes or eigenmodes of the membrane. This time we take a linear combination of solutions in the form of (10.4.8) to determine that

$$\xi(x, y, t) = \text{Re } \hat{\xi}_3 \sin\left(\frac{n\pi y}{b}\right) \sin\left(\frac{m\pi x}{a}\right) e^{j\omega t}, \quad (10.4.11)$$

where k_x has been made $m\pi/a$; hence the dispersion equation gives the eigenfrequencies as

$$\omega_{mn} = \pm v_s \left[\left(\frac{n\pi}{b} \right)^2 + \left(\frac{m\pi}{a} \right)^2 \right]^{1/2}. \quad (10.4.12)$$

The indices (n, m) can have any integer values. Note, however, that if both n and m are zero the solution is trivial, since (10.4.11) then shows that the deflections are zero.

The eigenfrequencies of the membrane constrained on all of its edges have the same physical significance as those of the simple string; for example, if the membrane is driven in some manner by a sinusoidal steady-state forcing function, there will be a resonance in the response at the eigenfrequencies, with the membrane assuming the corresponding deflections given by (10.4.11). Figure 10.4.2 is a graphic example of membrane modes $n = 1$. A soap film is attached to a rectangular wire frame by surface tension. Each of the modes is then excited by vibrating the frame by hand.

10.4.2 Moving Membrane: Mach Lines

We have seen that convection can have a marked effect on the dynamics of one-dimensional continua. This is especially true if the motion is supersonic, in the sense that the convection velocity (U) is greater than the propagation velocity (v_s) of small disturbances. The moving membrane provides an opportunity to determine how these effects are displayed in two dimensions.

With the membrane moving in the x -direction with the velocity U , the equation of motion is

$$\left(\frac{\partial}{\partial t} + U \frac{\partial}{\partial x} \right)^2 \xi = v_s^2 \left(\frac{\partial^2 \xi}{\partial x^2} + \frac{\partial^2 \xi}{\partial y^2} \right). \quad (10.4.13)$$

Here we have replaced the time derivative with the convective derivative, as justified in Section 10.2.

Now suppose we consider the case in which the *Mach number* M is greater than unity,

$$M = \frac{U}{v_s} > 1, \quad (10.4.14)$$

and in which steady-state conditions prevail ($\partial/\partial t = 0$). Then (10.4.13) becomes

$$(M^2 - 1) \frac{\partial^2 \xi}{\partial x^2} = \frac{\partial^2 \xi}{\partial y^2}. \quad (10.4.15)$$

This expression has the same familiar form as the wave equation. The time dependence, however, has been replaced by a dependence on the second dimension y . With this in mind, we expect that deformations of the membrane,

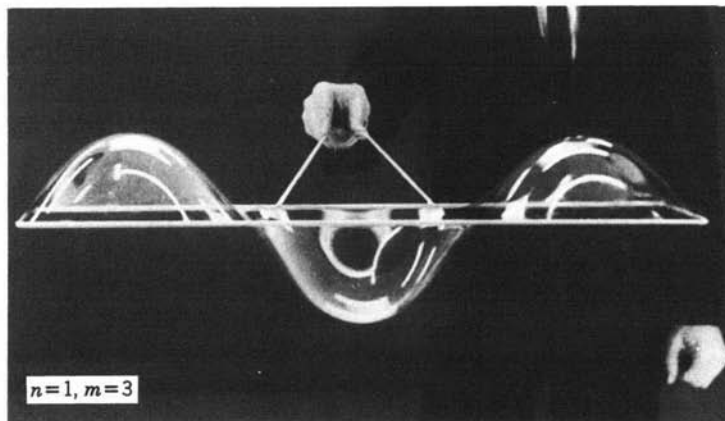
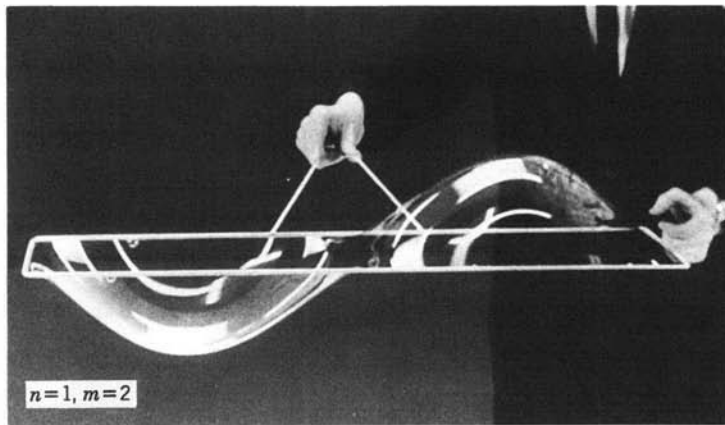
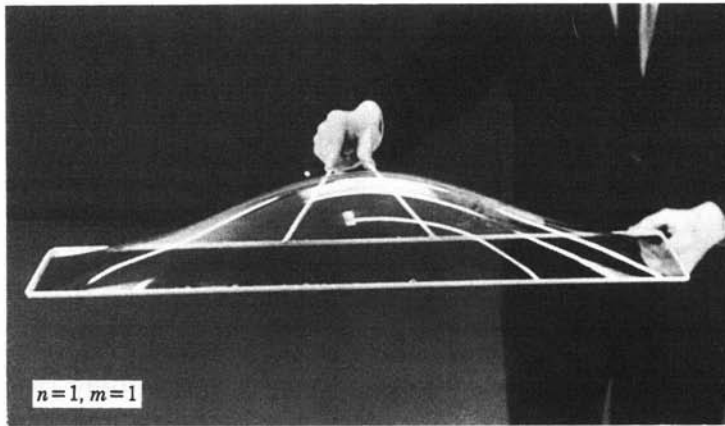


Fig. 10.4.2 Membrane motions illustrated by soap film on a vibrating wire frame. Pictures from film "Soap Film Oscillations." Courtesy of A. M. Hudson, Occidental College and Film Studio, Education Development Center, Inc., Newton, Mass.

as they depend on (x, y) , will assume the same wavelike character found in Section 9.1.1a.

Solution of (10.4.15) is completely analogous to the solution of the wave equation in (x, t) coordinates. Reference to Section 9.1.1a shows that we have solutions

$$\xi = \xi_+(\alpha) + \xi_-(\beta), \tag{10.4.16}$$

where

$$\alpha = x - \sqrt{M^2 - 1} y, \tag{10.4.17}$$

$$\beta = x + \sqrt{M^2 - 1} y. \tag{10.4.18}$$

The lines $\alpha = \text{constant}$ and $\beta = \text{constant}$ are again the characteristic lines along which we expect that the membrane can undergo abrupt deformations. These lines along which the equivalent of wavefronts in the x - y space can exist are referred to as *Mach lines*.* Their physical significance is more apparent in the context of a simple example.

Example 10.4.1. A sheet of molten plastic is to be given the cross-sectional shape shown in Fig. 10.4.3a. It is proposed that this be done by ejecting the molten plastic as a sheet

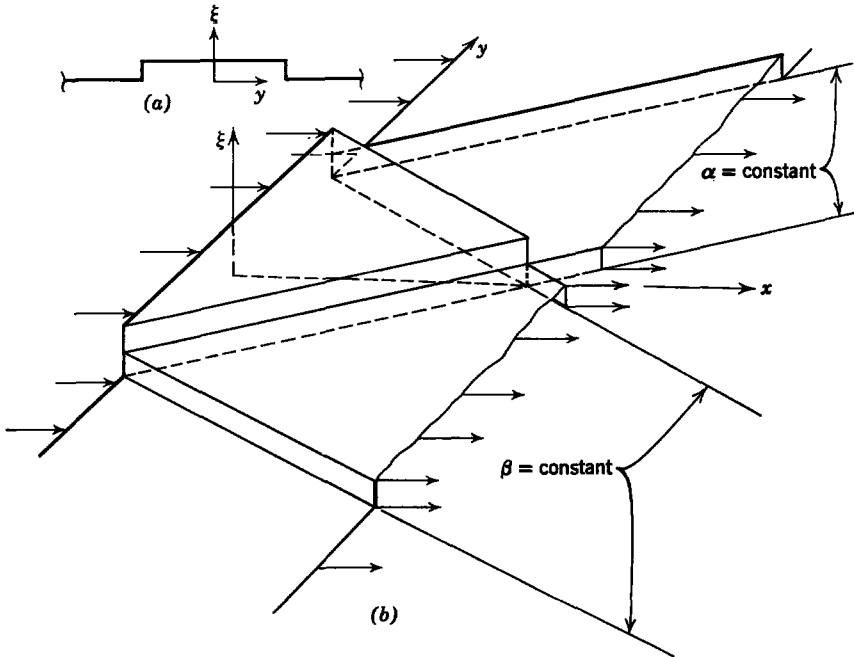


Fig. 10.4.3 (a) A membrane is constrained to have the shape shown at $x = 0$; (b) the resulting deflections for $M > 1$.

* A. H. Shapiro, *The Dynamics and Thermodynamics of Compressible Fluid Flow*, Ronald, New York, 1953, Vol. I, p. 462.

through an orifice in the shape of Fig. 10.4.3a. As long as the sheet is molten and thin, it is reasonable to obtain an idea of the likely success of our method by modeling the sheet as a membrane with $M > 1$ because the effect of surface tension, hence v_s , is small. The membrane is constrained at $x = 0$ so that $\xi(0, y)$ has the form shown in Fig. 10.4.3a and

$$\frac{\partial \xi}{\partial x}(0, y) = 0. \quad (\text{a})$$

This problem then reduces to one that is essentially the same as that discussed in Example 9.1.2. The deformations of the membrane, as they depend on (x, y) , are shown in Fig. 10.4.3b. The pulse that originates at $x = 0$ divides into two pulses that tend toward infinity in the $\pm y$ -directions as x increases. On the basis of this finding, we expect that our technique of forming the plastic would not be a good one unless the plastic could be made to solidify within a distance short compared with that required for the pulses to separate from one another.

10.4.3 A Kink Instability

Two-dimensional motions of a wire are very different from those of a membrane and provide an excellent model for demonstrating electro-mechanical coupling between propagating modes. A wire is shown in Fig. 10.4.4. It is now free to deflect in the x - or y -direction; hence we can, in general, find the wire at the transverse position

$$\xi = u(z, t)\mathbf{i}_x + v(z, t)\mathbf{i}_y. \quad (10.4.19)$$

Note that the motions still involve only two independent variables (z, t) by contrast with the two-dimensional motions of the membrane. Now,

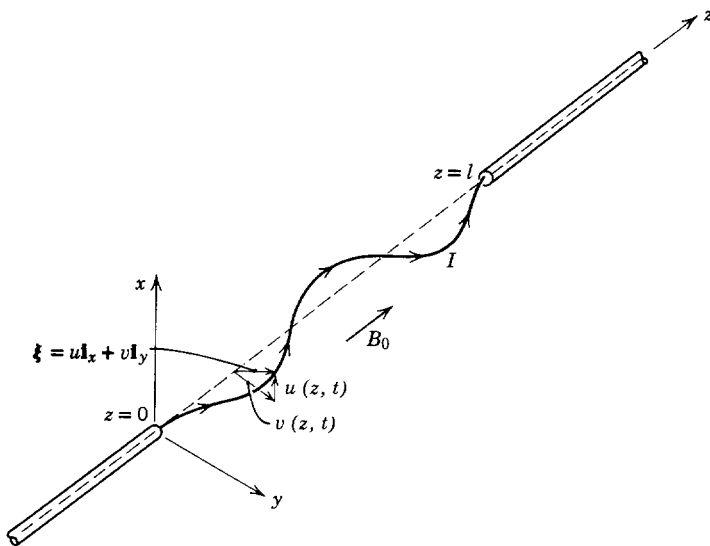


Fig. 10.4.4 A wire stretched along the z -axis.

however, there are two dependent variables $u(z, t)$ and $v(z, t)$, the displacements along the x - and y -axes, respectively.

We have already found that motions in the x - or y -direction are defined by the string equation (Table 9.2). To linear terms deflections v in the y -direction do not produce an x -directed force on the wire, and vice versa; hence the string equation remains valid for two-dimensional motions. A force equation for deflections in the x - and y -directions is

$$m \frac{\partial^2 \xi}{\partial t^2} = f \frac{\partial^2 \xi}{\partial z^2} + S. \quad (10.4.20)$$

The external force per unit length S has components S_x and S_y . With $S = 0$ motions in the x - and y -directions are uncoupled. In either case they are governed by a simple wave equation and disturbances propagate with the velocity $v_s = \sqrt{f/m}$.

We now use a magnetic field interaction to couple the motions in the x - and y -directions. In the process the continuum model of a constant-current constraint is illustrated.

The elastic wire is assumed to be conducting and is stretched between the pole pieces of a magnet (along the z -axis). As shown in Fig. 10.4.4, a current I is carried by the wire. In static equilibrium this current is in the same direction as an imposed magnetic flux density B_0 ; hence there is no magnetic force per unit length $\mathbf{I} \times \mathbf{B}_0$. Any slight perturbation of the current path (the wire position), however, will result in a radial component of current, and this component produces an $\mathbf{I} \times \mathbf{B}$ force that tends to rotate the wire about the z -axis. We see that motions of the wire cannot be purely in the x - z or y - z plane but must involve all three space dimensions.

Our constant current approximation is implicit in the statement that the current in the wire has the same direction as the wire. To linear terms we write

$$\mathbf{I} = \mathbf{i}_x \frac{\partial u}{\partial z} I + \mathbf{i}_y \frac{\partial v}{\partial z} I + \mathbf{i}_z I. \quad (10.4.21)$$

Here we have assumed that the cross section of the wire is small enough to make currents induced by the motion negligible. In general, the motion would produce currents that close on themselves in the x - y plane (eddy currents), and they could be crossed with the imposed magnetic field to give a transverse force on the wire. In Section 7.1 we obtained the condition that the currents induced by the motion of a conductor (conductivity σ) in a magnetic field are small if

$$R_m = \frac{\mu_0 \sigma \omega d^2}{2} \ll 1, \quad (10.4.22)$$

where in our case d is the diameter of the wire and ω is the frequency of vibration. Our constant current approximation is the limit of small R_m .

We make the additional assumption that the magnetic flux density B_0 imposed by the external magnet is much larger than the equilibrium flux density generated by the current I . This allows us to compute the force on the wire as

$$\mathbf{S} = \mathbf{I} \times B_0 \mathbf{i}_z \quad (10.4.23)$$

or from Eq. (10.4.21)

$$\mathbf{S} = B_0 I \frac{\partial v}{\partial z} \mathbf{i}_x - B_0 I \frac{\partial u}{\partial z} \mathbf{i}_y. \quad (10.4.24)$$

We now use these forces, and the components of (10.4.20) become

$$\frac{\partial^2 u}{\partial t^2} = v_s^2 \frac{\partial^2 u}{\partial z^2} + \frac{B_0 I}{m} \frac{\partial v}{\partial z}, \quad (10.4.25)$$

$$\frac{\partial^2 v}{\partial t^2} = v_s^2 \frac{\partial^2 v}{\partial z^2} - \frac{B_0 I}{m} \frac{\partial u}{\partial z}. \quad (10.4.26)$$

This pair of equations is sufficient to describe the dynamics of the current-carrying wire. As our intuition suggested, the magnetic field produces a force in the x -direction [the last term in (10.4.25)] in proportion to the tilt of the wire in the y -direction. The equations are now coupled. A motion in one transverse direction cannot occur without involving a motion in the other transverse direction. Put another way, waves polarized in either the x - or y -directions are now coupled as they propagate along the z -axis, and we expect that the coupling will affect the dynamics of both waves.

There are still two waves that propagate in each direction on the wire. We can find them if we assume solutions with the variable separable form

$$u = \text{Re} [\hat{u} \exp j(\omega t - kz)] \quad \text{and} \quad v = \text{Re} [\hat{v} \exp j(\omega t - kz)].$$

The equations of motion are satisfied by these solutions if

$$\hat{u}(\omega^2 - v_s^2 k^2) - \hat{v} \left(\frac{jkB_0 I}{m} \right) = 0, \quad (10.4.27)$$

$$\hat{u} \left(\frac{jkB_0 I}{m} \right) + \hat{v}(\omega^2 - v_s^2 k^2) = 0. \quad (10.4.28)$$

These equations are homogeneous in the amplitudes \hat{u} and \hat{v} . Unless both amplitudes are zero (not an interesting situation), the determinant of the coefficients must be zero. It is concluded that ω and k are related by

$$(\omega^2 - v_s^2 k^2) = \pm \left(\frac{kB_0 I}{m} \right). \quad (10.4.29)$$

We have found the dispersion equation for waves on the wire, and the nature of these waves is made evident by solving (10.4.29) for ω^2 :

$$\omega^2 = k^2 \left[v_s^2 \pm \left(\frac{B_0 I}{km} \right) \right]. \quad (10.4.30)$$

Evidently four waves can propagate on the wire, which is consistent with what we find if there is no magnetic field.

Equation 10.4.30 shows that one pair of waves (+ sign) has a phase velocity that increases with the magnetic field, whereas the other pair has a phase velocity that decreases with the magnetic field. The slower waves can, in fact, be unstable if

$$\left| \frac{B_0 I}{v_s^2 m} \right| > k, \quad (10.4.31)$$

for then $\omega = \pm j\alpha$, where α is a real number. If all real values of k were allowed by the boundary conditions, the wire would be unstable, no matter how small $B_0 I$, since there would always be a small enough wavenumber (long enough wave) to satisfy the condition for instability. The boundary conditions, however, are satisfied only by certain discrete values of k , which we enumerate shortly.

For the purpose of establishing the physical significance of the waves we have found, consider the case in which the wire is excited in the sinusoidal steady state at the (real) frequency ω . Then (10.4.29) is

$$k^2 \pm k \left(\frac{B_0 I}{v_s^2 m} \right) - \frac{\omega^2}{v_s^2} = 0, \quad (10.4.32)$$

and we can solve this relation to find four possible wavenumbers. Using the + sign in (10.4.32), we obtain

$$k = k_2, -k_1, \quad (10.4.33)$$

and using the minus sign we obtain

$$k = k_1, -k_2, \quad (10.4.34)$$

where k_1 and k_2 are the positive real numbers

$$k_1 = \frac{B_0 I}{2v_s^2 m} + \left[\left(\frac{B_0 I}{2v_s^2 m} \right)^2 + \frac{\omega^2}{v_s^2} \right]^{1/2}, \quad (10.4.35)$$

$$k_2 = -\frac{B_0 I}{2v_s^2 m} + \left[\left(\frac{B_0 I}{2v_s^2 m} \right)^2 + \frac{\omega^2}{v_s^2} \right]^{1/2}. \quad (10.4.36)$$

(Just to keep things straight, we assume for now that $B_0 I > 0$.) Note that $k_1 > k_2$. The dispersion equation (10.4.29), together with (10.4.27) or (10.4.28), shows that

$$\hat{v} = \pm j\hat{u} \quad (10.4.37)$$

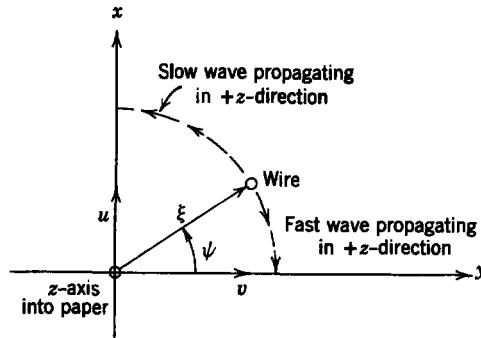


Fig. 10.4.5 Polar coordinates of wire deflection. At a given position along the z -axis the wire appears to rotate about it. The fast and slow waves have opposite directions of rotation.

We must remember to use the upper sign with those waves with wavenumbers given by (10.4.33) and the lower sign with those given by (10.4.34). Hence, if we have a wave given by

$$u = \text{Re} [\hat{u}_+^a e^{j(\omega t - k_1 z)} + \hat{u}_+^b e^{j(\omega t - k_2 z)} + \hat{u}_-^a e^{j(\omega t + k_1 z)} + \hat{u}_-^b e^{j(\omega t + k_2 z)}], \quad (10.4.38)$$

it follows from (10.4.37) that

$$v = \text{Re} j[\hat{u}_+^a e^{j(\omega t - k_1 z)} - \hat{u}_+^b e^{j(\omega t - k_2 z)} - \hat{u}_-^a e^{j(\omega t + k_1 z)} + \hat{u}_-^b e^{j(\omega t + k_2 z)}]. \quad (10.4.39)$$

The first two terms in these equations are waves with points of constant phase propagating in the $+z$ -direction. Because $k_1 > k_2$, the (a) wave propagates more slowly than the (b) wave. The third and fourth terms are similar waves propagating in the $-z$ -direction.

To obtain some insight into the nature of these waves, consider the first wave alone with $\hat{u}_+^a = -ju_0$. Then

$$\xi = u\mathbf{i}_x + v\mathbf{i}_y = u_0[\sin(\omega t - k_1 z)\mathbf{i}_x + \cos(\omega t - k_1 z)\mathbf{i}_y]. \quad (10.4.40)$$

This deflection is easier to interpret if we consider the magnitude ξ and angle ψ defined in Fig. 10.4.5. Then

$$\begin{aligned} \xi &= \sqrt{u^2 + v^2}, \\ \psi &= \tan^{-1}\left(\frac{u}{v}\right) = \omega t - k_1 z. \end{aligned} \quad (10.4.41)$$

At an instant in time the deflection given by this wave is a spiral that circles the z -axis in the clockwise direction, as shown in Fig. 10.4.6b. Points of constant phase advance in the z -direction with the velocity ω/k_1 . The phases of the (b) wave, which propagates in the $+z$ -direction, move more rapidly with the velocity ω/k_2 . If we repeat the arguments that led to (10.4.41),

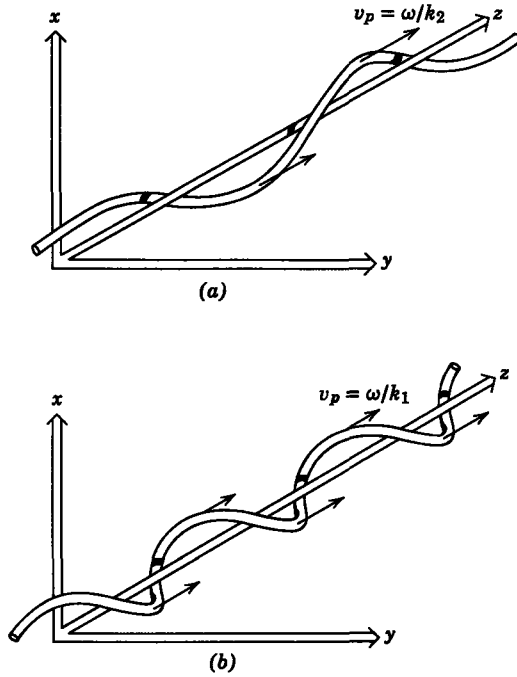


Fig. 10.4.6 Waves propagating in the $+z$ -direction: (a) fast wave with a wavelength $2\pi/k_2$; and (b) slow wave with a wavelength $2\pi/k_1$.

using the u_+^b wave, we obtain a spiral that at an instant in time circles the z -axis in the counterclockwise direction (Fig. 10.4.6a). At any position z the wire will circle the z -axis in the counterclockwise direction for the slow wave and in the clockwise direction for the fast wave. Except that the propagation is in the opposite direction, the u_- waves have the same physical appearance.

We address ourselves now to superimposing these four wave solutions to find the free modes that satisfy the boundary conditions of Fig. 10.4.4 in which the wire is fixed at $z = 0$ and at $z = l$. This is done by finding the allowed eigenvalues k and then using (10.4.30) to find the associated eigenfrequencies.

In a boundary value problem of this type it is easier to work with trigonometric functions than with the complex exponentials. Hence we use the fact that $e^{j\theta} = \cos \theta + j \sin \theta$ and write the solution given by (10.4.38) as

$$u = \text{Re} \{ e^{j\omega t} [A \sin k_1 z + B \cos k_1 z + C \sin k_2 z + D \cos k_2 z] \}, \quad (10.4.42)$$

where we have defined a new set of four constants as

$$\begin{aligned} A &= j(\hat{u}_-^a - \hat{u}_+^a), & C &= j(\hat{u}_-^b - \hat{u}_+^b), \\ B &= (\hat{u}_+^a + \hat{u}_-^a), & D &= (\hat{u}_+^b + \hat{u}_-^b). \end{aligned} \quad (10.4.43)$$

In terms of these same constants the solution for the y -deflection becomes (10.4.39)

$$v = -\operatorname{Re} \{e^{j\omega t} [A \cos k_1 z - B \sin k_1 z - C \cos k_2 z + D \sin k_2 z]\}. \quad (10.4.44)$$

The four constants are, of course, determined by the boundary conditions

$$\begin{aligned} u(0, t) &= 0, & v(0, t) &= 0, \\ u(l, t) &= 0, & v(l, t) &= 0. \end{aligned} \quad (10.4.45)$$

The advantage of the trigonometric form that we have used for our solution is the simplicity of the relation among the constants that results from the boundary conditions at $z = 0$. Because the sine functions are zero at the origin,

$$\begin{aligned} B &= -D, \\ A &= C. \end{aligned} \quad (10.4.46)$$

The remaining two conditions at $z = l$ require that

$$\begin{aligned} A(\sin k_1 l + \sin k_2 l) + B(\cos k_1 l - \cos k_2 l) &= 0, \\ A(\cos k_1 l - \cos k_2 l) - B(\sin k_1 l + \sin k_2 l) &= 0. \end{aligned} \quad (10.4.47)$$

Because A and B are not zero, the determinant of the coefficients must be zero; that is,

$$(\sin k_1 l + \sin k_2 l)^2 + (\cos k_1 l - \cos k_2 l)^2 = 0. \quad (10.4.48)$$

Recall that $\sin^2 \theta + \cos^2 \theta = 1$ and $\cos \theta \cos \gamma - \sin \theta \sin \gamma = \cos(\theta + \gamma)$, and (10.4.48) reduces to the simple condition

$$\cos l(k_1 + k_2) = 1. \quad (10.4.49)$$

It follows that the argument $l(k_1 + k_2)$ must have values $0, 2\pi, 4\pi, \dots, 2n\pi, \dots$. If $k_1 + k_2$ is replaced by the sum of (10.4.35) and (10.4.36), we obtain an expression that determines the eigenfrequencies ω_n :

$$\omega_n^2 = \frac{v_s^2}{4} \left[\left(\frac{2n\pi}{l} \right)^2 - \left(\frac{B_0 I}{v_s^2 m} \right)^2 \right], \quad n = 1, 2, \dots \quad (10.4.50)$$

We have left out the case $n = 0$ because this solution is trivial; that is, there is no deflection when $n = 0$, as can be seen by taking the limiting case in which there is no magnetic field.

We have found that if we set the wire into vibration in one of its natural modes and then turn on the magnetic field and current, the frequency will decrease in magnitude. As we raise the magnetic field, the equilibrium is first unstable in the $n = 1$ mode. The system is unstable if

$$\left| \frac{B_0 I}{v_s^2 m} \right| > \frac{2\pi}{l}. \quad (10.4.51)$$

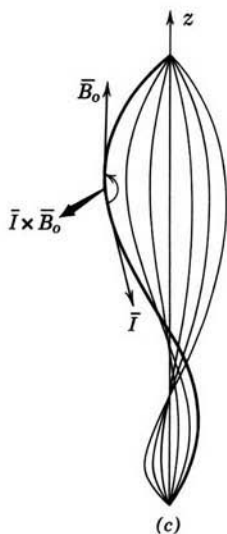
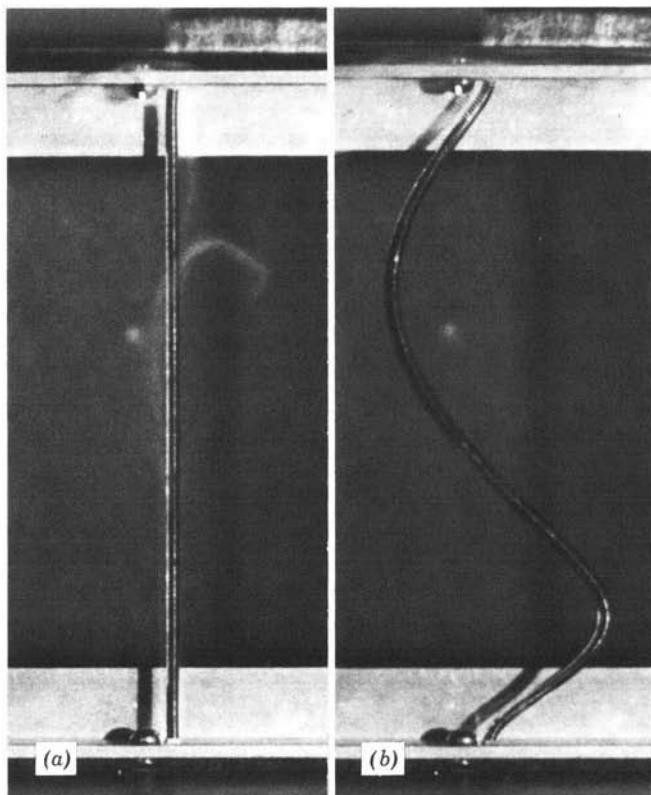


Fig. 10.4.7 (a) Experiment in which a conducting spring is stretched between pole faces of a magnet. There is a vertical field B_0 and a current has just been applied to the spring. (b) A moment later instability occurs. (c) Predicted $n = 1$ mode at point of impending instability. (From Film "Complex Waves I, Propagation, Evanescence and Instability," produced by Education Development Center, Inc., Newton, Mass., for the National Committee on Electrical Engineering Films.)

We have established that the value of k that should be used in (10.4.31) is $2\pi/l$.

Finally, it is worthwhile to see what the physical form of a natural mode is. Given one of the constants, the other three can be determined from (10.4.46) and (10.4.47). For this particular problem, however, the compatibility condition (10.4.49) ensures that the coefficients of both A 's and B 's in (10.4.47) are zero, as can be determined by using trigonometric identities. This means that all conditions are satisfied if A and B are specified independently. Consider the case in which A , hence [from (10.4.46)] C is zero. Then, since $B = -D$, if we determine the time phase by taking B as a real number, (10.4.42) and (10.4.44) become [here, use is made of (10.4.35) and (10.4.36) and the fact that $k_1 + k_2 = 2n\pi/l$]

$$\begin{aligned} u &= -2B \cos \omega t \sin \frac{n\pi z}{l} \sin \frac{B_0 I}{2v_s^2 m} z, \\ v &= 2B \cos \omega t \sin \frac{n\pi z}{l} \cos \frac{B_0 I}{2v_s^2 m} z. \end{aligned} \quad (10.4.52)$$

In terms of the polar variables of (10.4.41) and Fig. 10.4.5,

$$\begin{aligned} \psi &= -\frac{B_0 I}{2v_s^2 m} z, \\ \xi &= 2B \cos \omega t \sin \frac{n\pi z}{l}. \end{aligned} \quad (10.4.53)$$

If we had used the constant A , rather than B , it would have shifted this deflection by 90° about the z -axis.

A plot of (10.4.53) is shown in Fig. 10.4.7c for the first eigenmode with $B_0 I < 0$. Note that because of the condition for instability (10.4.51) the maximum twist ψ that the standing wave can undergo is 180° . Hence the mode shown in Fig. 10.4.7c is at the point at which instability occurs for the $n = 1$ mode.

The wave dynamics that we have found in this section are related to several types of electromechanical interaction. The "pinch" confinement of a plasma, proposed as a scheme for containing a controlled thermonuclear reaction, suffers from an instability with the same kinked property as the one found here.* The plasma is likely to behave more nearly as a perfectly conducting medium or as one with a high rather than a low magnetic Reynolds number. If, however, a current is passed through a liquid column of mercury (where R_m is small) in the presence of an axial magnetic field, an instability with

* D. J. Rose and M. Clarke, Jr., *Plasmas and Controlled Fusion*, M. I. T. Press and Wiley, New York, 1961, p. 336.

essentially the same features as that described here will result.* Often the twisting motions that characterize the dynamics of the wire are found in other electromechanical systems that involve an imposed magnetic field. An example is the cyclotron wave of electron beam theory.†

10.5 DISCUSSION

In this chapter we have explored the consequences of continuum electro-mechanical coupling with simple elastic continua. This has produced mathematical analyses and physical interpretations of evanescent waves, absolute instabilities, and waves and instabilities in convecting systems. The unifying mathematical concept is the dispersion relation presented graphically in the ω - k plots.

Although our examples have been framed in terms of simple physical situations, the phenomena we have discussed occur in the wide variety of practical situations indicated in Section 10.0 and throughout the chapter.

PROBLEMS

10.1. The current-carrying wire described in Section 10.1.2 is attached to a pair of dashpots with damping coefficients B and driven at $x = -l$, as shown in Fig. 10P.1.

- (a) What is the boundary condition at $x = 0$?
- (b) Compute the power absorbed in the dashpots for $\omega < \omega_e$, given the amplitude ξ_0 and other system parameters.

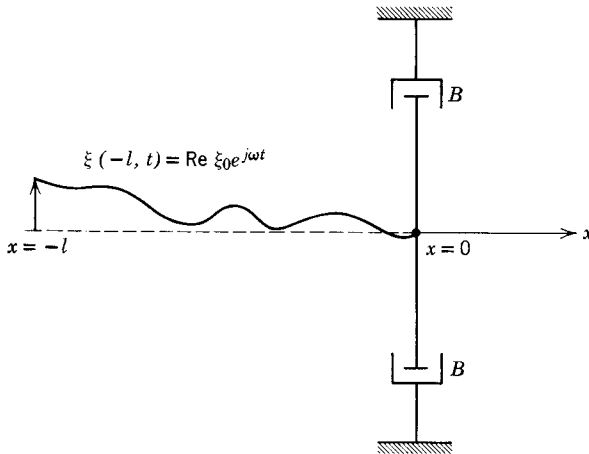


Fig. 10P.1

* Film Cartridge, produced by the National Committee for Fluid Mechanics Films, *Current-Induced Instability of a Mercury Jet*, may be obtained from Education Development Center, Inc., Newton, Mass. The instability seen in this film is convective, as would be the case here if the string were in motion with $U > v_s$.

† W. H. Louisell, *Coupled Modes and Parametric Electronics*, Wiley, 1960, p. 51.

10.2. Consider the same physical situation as that described in Section 10.1.2, except with the current-carrying wire constrained at $x = 0$, so that $(\partial\xi/\partial x)(0, t) = 0$, and driven at $x = -l$ such that $\xi(-l, t) = \xi_a \cos \omega_a t$.

- (a) Find analytical expressions for $\xi(x, t)$ with $\omega_a > \omega_c$ and $\omega_a < \omega_c$.
- (b) Sketch the results of (a) at an instant in time for cases in which $\omega_a = 0$, $\omega_a < \omega_c$, $\omega_a > \omega_c$.
- (c) How could the boundary condition at $x = 0$ be realized physically?

10.3. The ends of the spring shown in Fig. 10.1.2 and discussed in Sections 10.1.2 and 10.1.3 are constrained such that

$$\frac{\partial \xi}{\partial x}(0, t) = 0,$$

$$\frac{\partial \xi}{\partial x}(-l, t) = 0.$$

- (a) What are the eigenfrequencies of the spring with the current as shown in Fig. 10.1.2?
- (b) What are these frequencies with I as shown in Fig. 10.1.9?
- (c) What current I is required to make the equilibrium with $\xi = 0$ unstable? Give a physical argument in support of your answer.

10.4. In Section 10.1.2 a current-carrying wire in a magnetic field was described by the equation of motion

$$m \frac{\partial^2 \xi}{\partial t^2} = f \frac{\partial^2 \xi}{\partial x^2} - Ib\xi + F(x, t), \tag{a}$$

where F is an externally applied force/unit length. We wish to consider the flow of power on the string. Because $F \partial\xi/\partial t$ is the power input/unit length to the string, we can find a conservation of power equation by multiplying (a) by $\partial\xi/\partial t$. Show that

$$P_{\text{in}} = \frac{\partial W}{\partial t} + \frac{\partial P}{\partial x}, \tag{b}$$

where $P_{\text{in}} = F \partial\xi/\partial t$,

$W =$ energy stored/unit length

$$\frac{1}{2}m \left(\frac{\partial \xi}{\partial t} \right)^2 + \frac{1}{2}f \left(\frac{\partial \xi}{\partial x} \right)^2 + \frac{1}{2}Ib\xi^2,$$

$P =$ power flux

$$= -f \frac{\partial \xi}{\partial x} \frac{\partial \xi}{\partial t}.$$

10.5. Waves on the string in Problem 10.4 have the form

$$\xi(x, t) = \text{Re}[\xi_+ e^{j(\omega t - kx)} + \xi_- e^{j(\omega t + kx)}].$$

This problem makes a fundamental point of the way in which power is carried by ordinary waves in contrast to evanescent waves. The instantaneous power P carried by the string is given in Problem 10.4. Sinusoidal steady-state conditions prevail.

- (a) Compute the time average power carried by the waves under the assumption that k is real. Your answer should show that the powers carried by the forward and

backward waves are independent; that is,

$$\langle P \rangle = \frac{\omega k f}{2} (\xi_+^* \xi_+ - \xi_-^* \xi_-),$$

where ξ^* is the complex conjugate of ξ .

(b) Show that if $k = j\beta$, β real we obtain by contrast

$$\langle P \rangle = \frac{-j\omega\beta f}{2} (\xi_+^* \xi_- - \xi_-^* \xi_+).$$

A single evanescent wave cannot carry power.

(c) Physically, how could it be argued that (b) must be the case rather than (a) for an evanescent wave?

10.6. Use the results of Problem 10.4 to show that the group velocity $v_g = d\omega/dk$ is given by the ratio of the time average power to the time average energy/unit length: $v_g = \langle P \rangle / \langle W \rangle$. Attention should be confined to the particular case of Problem 10.4 with $F = 0$.

10.7. A pair of perfectly conducting membranes has equilibrium spacing d from each other and from parallel rigid walls (Fig. 10P.7). The membranes and walls support currents such

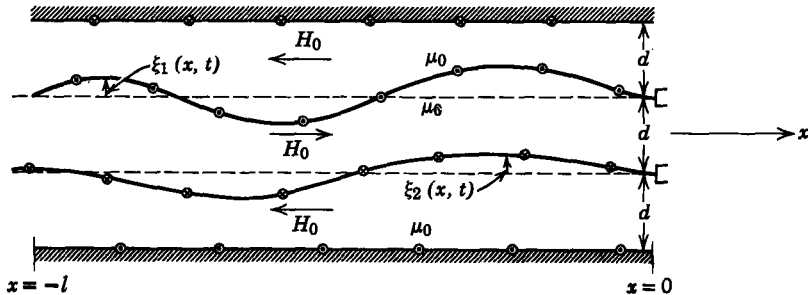


Fig. 10P.7

that with $\xi_1 = 0$ and $\xi_2 = 0$ the static uniform magnetic field intensities H_0 are as shown. As the membranes deform, the flux through each of the three regions between conductors is conserved.

- (a) Assume that both membranes have tension S and mass/unit area σ_m . Write two equations of motion for ξ_1 and ξ_2 .
- (b) Assume that $\xi_1 = \text{Re } \xi_1 \exp j(\omega t - kx)$ and $\xi_2 = \text{Re } \xi_2 \exp j(\omega t - kx)$ and find the dispersion equation.
- (c) Make an ω - k plot to show complex values of k for real values of ω . Show which branch of this plot goes with $\xi_1 = \xi_2$ and which with $\xi_1 = -\xi_2$. What are the respective cutoff frequencies for these odd and even modes?
- (d) The membranes are fixed at $x = 0$ and given the displacements $\xi_1(-l, t) = -\xi_2(-l, t) = \text{Re } \xi_0 \exp j\omega t$. Find ξ_1 and ξ_2 and sketch for $\omega = 0$.

10.8. An electromagnetic wave can be transmitted through or reflected by a plasma, depending on the frequency of the wave relative to the plasma frequency ω_p . This phenomenon, which is fundamental to the propagation of radio signals in the ionosphere, is illustrated by the following simple example of a cutoff wave. In dealing with electromagnetic waves, we require that both the electric displacement current in Ampère's law and the

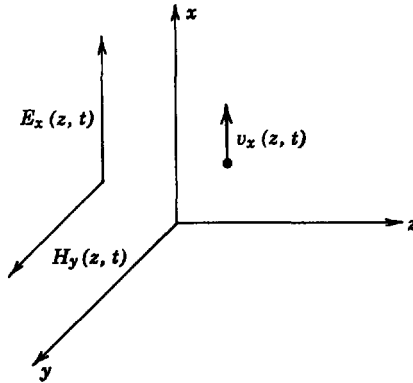


Fig. 10P.8

magnetic induction in Faraday's law (see Section B.2.1) be accounted for. We consider one-dimensional plane waves in which $\mathbf{E} = \mathbf{i}_x E_x(z, t)$ and $\mathbf{H} = \mathbf{i}_y H_y(z, t)$.

(a) Show that Maxwell's equations require that

$$\frac{\partial E_x}{\partial z} = -\frac{\partial \mu_0 H_y}{\partial t}, \quad -\frac{\partial H_y}{\partial z} = \frac{\partial \epsilon_0 E_x}{\partial t} + J_x.$$

- (b) The space is filled with plasma composed of equal numbers of ions and electrons. Assume that the more massive ions remain fixed and that n_e is the electron number density, whereas e and m are the electronic charge and mass. Use a linearized force equation to relate E_x and v_x , where v_x is the average electron velocity in the x -direction.
- (c) Relate v_x and J_x to linear terms.
- (d) Use the equations of (a)–(c) to find the dispersion equation for waves in the form of $\exp j(\omega t - kz)$.
- (e) Define the plasma frequency as $\omega_p = \sqrt{n_e e^2 / \epsilon_0 m}$ and describe the dynamics of a wave with $\omega < \omega_p$.
- (f) Suppose that a wave in free space were to be normally incident on a layer of plasma (such as the ionosphere). What would you expect to happen? (See Problem 10.9 for a similar situation.)

10.9. A current-carrying string extends from $x = -\infty$ to $x = +\infty$. The section $-l < x < 0$ is subjected to a magnetic field with the distribution shown in Fig. 10.1.2. Hence the sections of string to the left of $x = -l$ and to the right of $x = 0$ support ordinary waves, whereas the section in between can support cutoff waves. Sinusoidal steady-state conditions

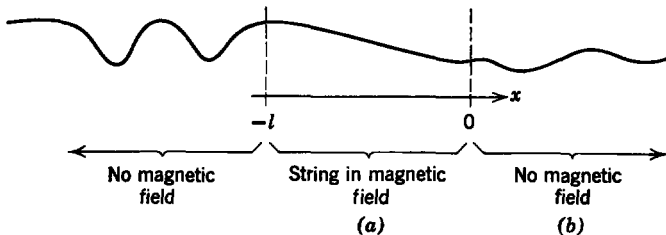


Fig. 10P.9

prevail, with waves incident from the left producing a deflection $\xi(-l, t) = \text{Re } \xi_0 e^{j\omega t}$, $\omega < \omega_c$. Assume that waves propagating to the right are completely absorbed at $x \rightarrow \infty$ so that in interval (b) $\xi_b = \text{Re } \xi_0 e^{j(\omega t - k_b x)}$, $k_b = \omega/v_s$.

- (a) Find the attenuation factor ξ_b/ξ_0 for a wave passing through the cutoff section.
- (b) What is ξ_b/ξ_0 as $l \rightarrow 0$? As $l \rightarrow \infty$?

10.10. A rigid straight rod supports a charge Q coulombs per unit length and is fixed. Just below this rod an insulating string is stretched between fixed supports, as shown in Fig.

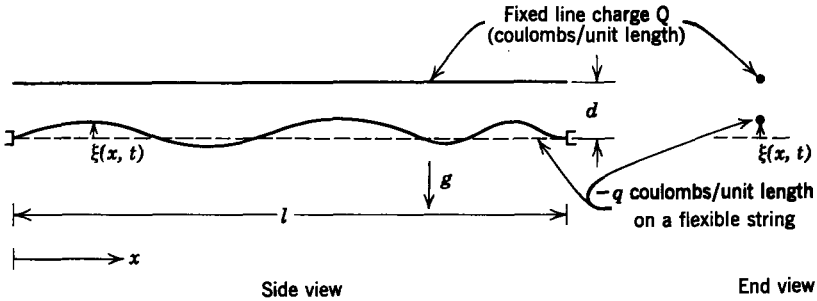


Fig. 10P.10

10P.10. This string, which has a tension f and mass per unit length m , supports a charge per unit length $-q$, where $q \ll Q$ and both Q and q are positive.

- (a) What should qQ be in order that the string have the static equilibrium $\xi = 0$ in spite of the gravitational acceleration g ?
- (b) What is the largest value of m that is consistent with the equilibrium of part (a) being stable?
- (c) How would you alter this physical situation to make the static equilibrium stable even with m larger than given by (b)?

10.11. A wire with the mass/unit length m and tension f is stretched between fixed supports, as shown in Fig. 10P.11. The wire carries a current I and is subject to the gravitational

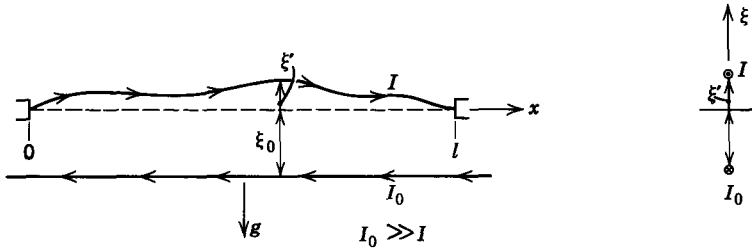


Fig. 10P.11

acceleration g . An adjacent wire carries the much larger current I_0 . Because $I_0 \gg I$, the magnetic field produced by I can be ignored.

- (a) Given all other system parameters, what value of I is required to hold the wire in static equilibrium with $\xi' = 0$?
- (b) Write the differential equation of motion for vertical displacements $\xi'(x, t)$ of the wire from a horizontal equilibrium at $\xi = \xi_0$.
- (c) Under what conditions will the equilibrium be stable?

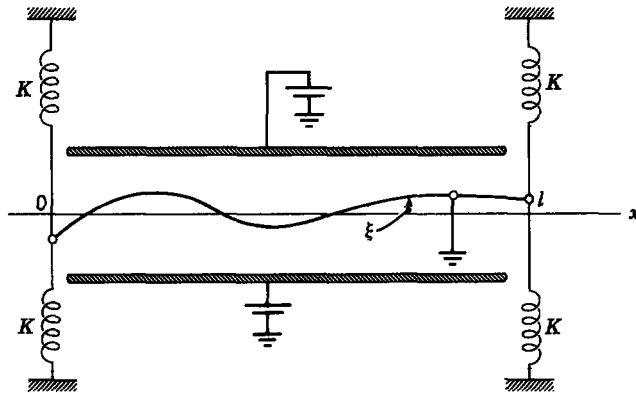


Fig. 10P.12

10.12. The conducting wire shown in Fig. 10P.12 is stressed by a transverse electric field and hence has transverse displacements that satisfy the force equation :

$$m \frac{\partial^2 \xi}{\partial t^2} = f \frac{\partial^2 \xi}{\partial x^2} + P \xi,$$

where m , f , and P are known constants. (P arises from the electric field.) The ends of the string are constrained by springs, but are otherwise free to move in the transverse direction.

- (a) Write the boundary conditions in terms of $\xi(x, t)$ at $x = 0$ and $x = l$.
- (b) Find an expression for the natural frequencies and illustrate its solution graphically. What effect does raising P have on the lowest eigenfrequency?
- (c) What is the largest value of P consistent with stability in the limit where $K \rightarrow 0$?

10.13. A pair of perfectly conducting membranes are stretched between rigid supports at $x = 0$ and $x = L$, as shown in Fig. 10P.13. The membranes have the applied voltage V_0 with respect to each other and with respect to plane-parallel electrodes.

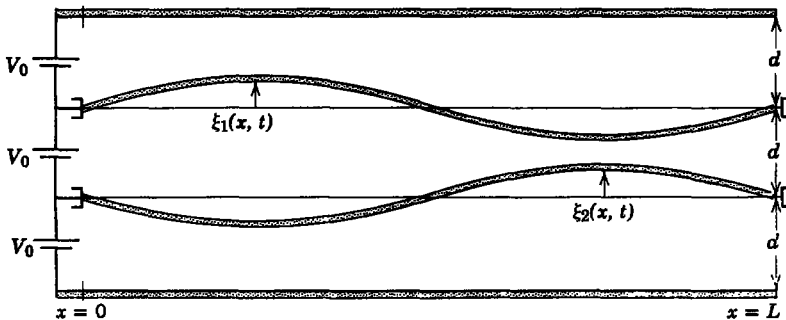


Fig. 10P.13

- (a) Write a pair of differential equations in $\xi_1(x, t)$ and $\xi_2(x, t)$ which describe the membrane motions. Assume that ξ_1 and ξ_2 are small enough to warrant linearization and that the wavelengths are long enough that the membranes appear flat to the electric field at any one value of x .

(b) Assume that

$$\xi_1 = \operatorname{Re} \xi_1^{\dot{}} e^{j(\omega t - kx)}$$

$$\xi_2 = \operatorname{Re} \xi_2^{\dot{}} e^{j(\omega t - kx)}$$

and find a dispersion equation relating ω and k .

(c) Make an ω - k plot showing the results of part (b), including imaginary values of ω for real values of k . (This equation should be biquadratic in ω .)

(d) At what potential V_0 will the static equilibrium $\xi_1 = 0$ and $\xi_2 = 0$ first become unstable? Describe the mode of instability.

10.14. A spring is immersed in a viscous fluid so that damping forces of the type discussed in Section 10.1.4 are important. The spring is fixed at $x = 0$ and $x = -l$. When $t = 0$, it is static and released from the initial deflection shown.

(a) Find $\xi(x, t)$ in terms of the system normal modes and ξ_0 .

(b) Compare this physical situation with that developed in Section 7.1.1.

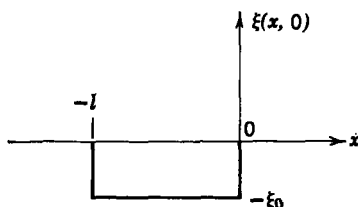


Fig. 10P.14

10.15. A string with tension f and mass/unit length m moves in the x -direction with the velocity $U > \sqrt{f/m}$. The string may be regarded as infinitely long. When $t = 0$, the string has no deflection: $[\xi(x, 0) = 0]$. It has, however, the transverse velocity $(\partial \xi / \partial t)(x, 0)$ given in Fig. 10P.15. Find an analytical expression for $\xi(x, t)$ and sketch it as a function of (x, t) . (Your sketch should have an appearance similar to that of Figs. 10.2.4 and 10.2.5.)

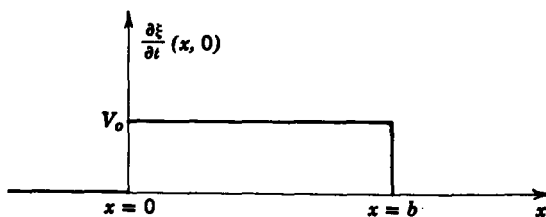


Fig. 10P.15

10.16. A string with the tension f and mass/unit length m has an equilibrium velocity U in the x -direction, where $U > \sqrt{f/m}$. At $x = 0$ it is constrained such that

$$\xi(0, t) = \xi_0 \cos \omega t,$$

$$\frac{\partial \xi}{\partial x}(0, t) = 0.$$

(a) Find the sinusoidal steady-state response $\xi(x, t)$.

(b) Sketch the results of (a) at an instant in time.

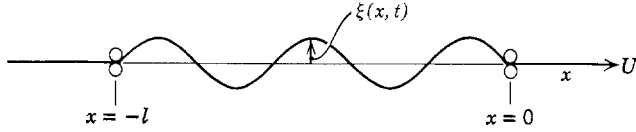


Fig. 10P.17

10.17. A string with the longitudinal velocity U is excited sinusoidally at $x = -l$, $\xi(-l, t) = \text{Re } \xi_0 e^{j\omega t}$, and constrained to zero deflection at $x = 0$ by pairs of rollers.

- (a) Find the driven response $\xi(x, t)$ in the interval $-l < x < 0$.
- (b) What are the natural frequencies of the system? How do they depend on U ?
- (c) For what values of U are the results of (a) and (b) physically meaningful?

10.18. A wire under the tension f is closed on itself as shown. The resulting loop rotates with the constant angular velocity Ω . We consider deflections ξ from a circular equilibrium which have short wavelengths compared with the radius R . Hence each section of the wire is essentially straight and effects of the curvature on the dynamics can be ignored.

- (a) Show that the partial differential equation of motion is

$$m \left(\frac{\partial}{\partial t} + \Omega \frac{\partial}{\partial \theta} \right)^2 \xi = \frac{f}{R^2} \frac{\partial^2 \xi}{\partial \theta^2}$$

where m , f , and R are given constants.

- (b) For $t < 0$ the pulse of deflection (Fig. 10P.18b) is imposed externally and is stationary when $t = 0$. At $t = 0$ this pulse is released. You are given that $\Omega R = 2\sqrt{f/m}$. Plot the deflection $\xi(0, t)$ for $0 \leq t \leq 2\pi R/\sqrt{f/m}$.

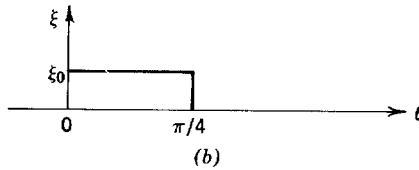
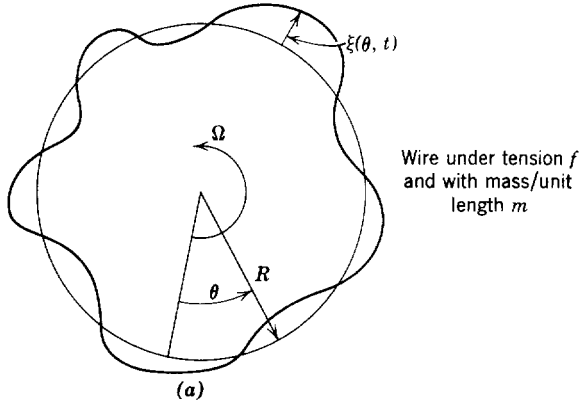


Fig. 10P.18

10.19. A string has the velocity U in the x -direction and is subject to arbitrary inputs of energy from a distributed force $F(x, t)$. Use the equation of motion to find a conservation of power equation in the form $P_{\text{in}} = \frac{\partial W}{\partial t} + \frac{\partial P}{\partial x}$. (See Problem 10.4.)

10.20. Find the sinusoidal steady-state response for the conditions outlined in Problem 10.16 with the additional effect of a destabilizing force included (see Section 10.2.3). Sketch the deflections at an instant in time under conditions in which the response takes the form of an amplifying wave.

10.21. A perfectly conducting membrane with the tension S and mass per unit area σ_m is ejected from a nozzle along the x -axis with a velocity U . Gravity acts as shown in Fig.

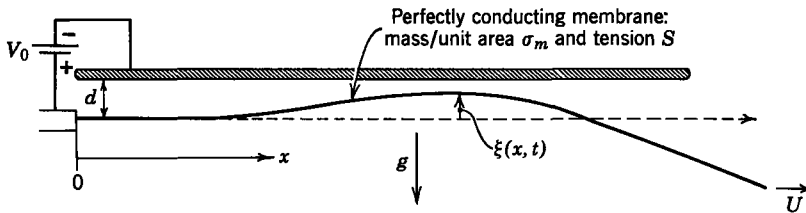


Fig. 10P.21

10P.21. A planar electrode above the membrane has the constant potential V_0 relative to the membrane.

- What value of V_0 is required to make the membrane assume an equilibrium parallel to the electrode?
- Now, under the conditions in (a), the membrane is excited at the frequency ω_d ; what is the lowest frequency of excitation that will not lead to spatially growing deflections? Assume that $U > \sqrt{S/\sigma_m}$.

10.22. An elastic membrane with tension S and mass/unit area σ_m is closed on itself, as shown in Fig. 10P.22. When it is in a steady-state equilibrium, the membrane has radius R

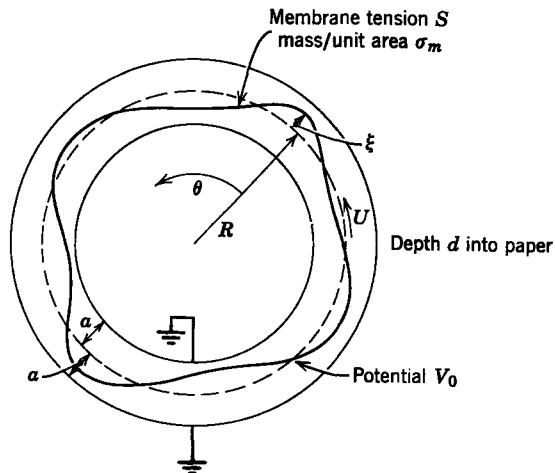


Fig. 10P.22

and rotates with angular velocity Ω . Any point on its surface has an azimuthal velocity $U = \Omega R$. At a distance a to either side of the membrane are coaxial electrodes which, like the membrane, are perfectly conducting. There is a constant potential difference V_0 between the membrane and each of the electrodes. The radius R is very large, so that effects of the membrane and electrode curvatures can be ignored. In addition, wavelengths on the membrane are much greater than a .

- (a) Show that the equation of motion for membrane deflections takes the form

$$\left(\frac{\partial}{\partial t} + \Omega \frac{\partial}{\partial \theta}\right)^2 \xi = \Omega_s^2 \left(\frac{\partial^2 \xi}{\partial \theta^2} + m_c^2 \xi\right); \quad \Omega_s \text{ and } m_c = ?$$

- (b) Assume that solutions have the form $\xi = \text{Re } \hat{\xi} \exp j(\omega t - m\theta)$ and find the ω - m relation. Plot complex ω for real m and complex m for real ω .
 (c) Under what conditions is this system absolutely stable?

10.23. A pair of perfectly conducting membranes move in the x -direction with the velocity U . The membranes have the applied voltage V_0 with respect to one another and to plane-parallel electrodes. They enter the region between the plates from rollers at $x = 0$.

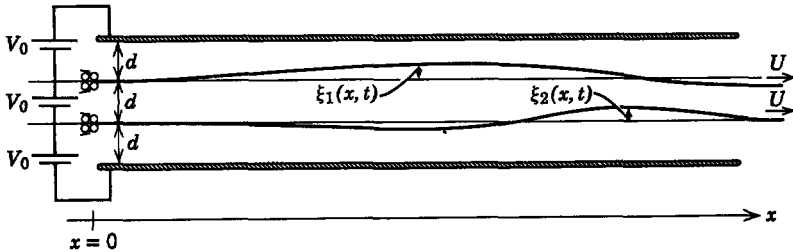


Fig. 10P.23

- (a) Write a pair of differential equations in $\xi_1(x, t)$ and $\xi_2(x, t)$ to describe the membrane motions. Assume that ξ_1 and ξ_2 are small enough to warrant linearization and that the wavelengths are long enough for the membrane to appear flat to the electric field at any one value of x .
 (b) Assume that

$$\begin{aligned} \xi_1 &= \text{Re } \hat{\xi}_1 e^{j(\omega t - kx)}, \\ \xi_2 &= \text{Re } \hat{\xi}_2 e^{j(\omega t - kx)} \end{aligned}$$

and find a dispersion equation relating ω and k .

- (c) Make an ω - k plot to show the results of part (b), including complex values of k for real values of ω . This equation can be factored into two quadratic equations for k . Assume that $U > \sqrt{S/\sigma_m}$.
 (d) One of the quadratic factors in part (c) describes motions in which $\xi_1(x, t) = \xi_2(x, t)$, whereas the other describes motions in which $\xi_1(x, t) = -\xi_2(x, t)$. Show that this is true by assuming first that $\xi_1 = \xi_2$ and then that $\xi_1 = -\xi_2$ in parts (a) and (b).
 (e) Now suppose that the rollers at $x = 0$ are given the sinusoidal excitation $\xi_1(0, t) = \text{Re } \hat{\xi} e^{j\omega t} = -\xi_2(0, t)$, where $\hat{\xi}$ is the same real constant for each excitation. Also, $0 = \partial \xi_1 / \partial x = \partial \xi_2 / \partial x$ at $x = 0$. Find $\xi_1(x, t)$ and $\xi_2(x, t)$.
 (f) What voltage V_0 is required to make the waves excited in part (e) amplify?
 (g) Sketch the spatial dependence of ξ_1 and ξ_2 at an instant in time with $V_0 = 0$ and with V_0 large enough to produce amplifying waves.

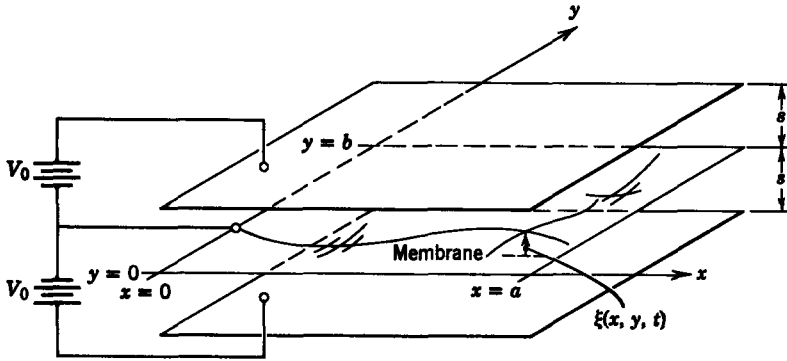


Fig. 10P.24

10.24. A perfectly conducting membrane with tension S and mass/unit area σ_m is fixed at $x = 0$ and $x = a$ and at $y = 0$ and $y = b$. Perfectly conducting plane-parallel electrodes have an equilibrium distance s from the membrane and a potential V_0 relative to the membrane.

- (a) What is the largest value of V_0 that will still allow the membrane to be in a state of stable static equilibrium? You may assume that $a \gg s$ and $b \gg s$.
- (b) What are the natural frequencies of the membrane?
- (c) Given that the membrane is stationary when $t = 0$ and that

$$\xi(x, y, 0) = J_0 \mu_0 \left(x - \frac{a}{2}\right) \mu_0 \left(y - \frac{b}{2}\right),$$

where μ_0 is the unit impulse and J_0 is an arbitrary constant, find the response $\xi(x, y, t)$.

10.25. A membrane with tension S and mass/unit area σ_m is fixed along its edges at $y = 0$ and $y = a$. It is also fixed along the edge $x = b$. At $x = 0$ it is driven and has the displacement shown in Fig. 10P.25b. Find the sinusoidal steady-state driven response $\xi(x, y, t)$.

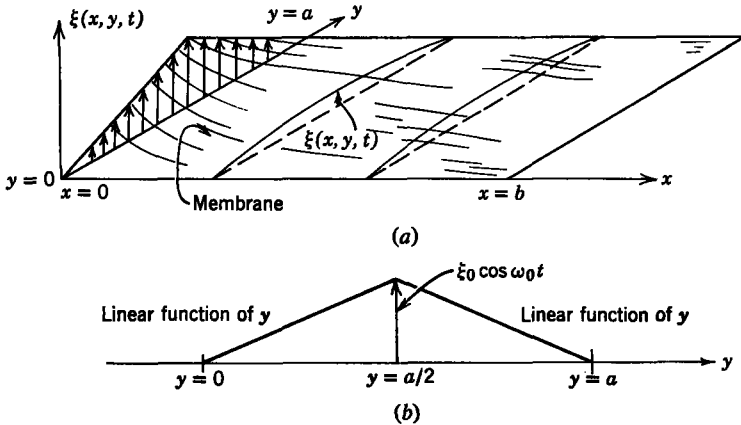


Fig. 10P.25

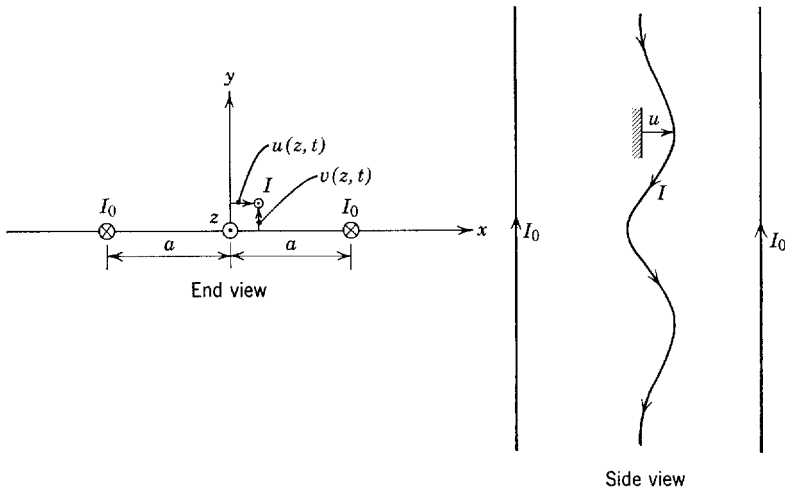


Fig. 10P.26

10.26. A pair of conductors, separated by a distance $2a$, carries currents I_0 (amperes) in the $-z$ -direction, as shown in Fig. 10P.26. A conducting wire of mass density/unit length m is stretched along the z -axis and carries a current I ($I \ll I_0$). Deflections of the wire from the z -axis are given by $u(z, t)\mathbf{i}_x + v(z, t)\mathbf{i}_y$.

- (a) Show that the equations of motion for the wire in the magnetic field have the form

$$m \frac{\partial^2 u}{\partial t^2} = f \frac{\partial^2 u}{\partial z^2} - Ibu,$$

$$m \frac{\partial^2 v}{\partial t^2} = f \frac{\partial^2 v}{\partial z^2} + Ibv,$$

under the assumption that deflections u and v are small. What is the constant b in terms of I_0 and a ? What fundamental law requires that if Ibu appears with a positive sign in the second equation it must appear with a negative sign in the first equation?

- (b) Consider solutions that have the form $u = \text{Re } \hat{u}e^{j(\omega t - kz)}$ and $v = \text{Re } \hat{v}e^{j(\omega t - kz)}$ and find the relationship between ω - k for x and for y displacements. Make dimensioned plots in each case of real and imaginary values of k for real values of ω . Make dimensioned plots in each case of real and imaginary values of ω for real values of k . (Throughout this problem consider $I_0 > 0$, $I > 0$.)
- (c) The wire is now fixed at $z = 0$ and, given the deflection

$$u(-l, t)\mathbf{i}_x + v(-l, t)\mathbf{i}_y = u_0 \cos \omega_0 t \mathbf{i}_x + v_0 \sin \omega_0 t \mathbf{i}_y \quad (\omega_0 \text{ is real}).$$

Find $u(z, t)$ and $v(z, t)$.

- (d) For what values of the currents (I, I_0) will it be possible to establish the sinusoidal steady-state solution of part (c)? For what values of ω_0 , in terms of f, m , and l , will the wire support evanescent waves as x -deflections and remain stable?
- (e) The frequency ω_0 is set $\omega_0 = (\pi/2l)\sqrt{flm}$. Sketch the peak deflections u and v as functions of z for several values of I (starting with $I = 0$). Summarize in words how the deflections will change as the current I is raised.

10.27. This is a continuation of Problem 10.26. Now the wire has an equilibrium velocity U along the z -axis with $U > \sqrt{f/m}$.

- (a) Write the differential equations for the deflections $u(z, t)$ and $v(z, t)$, including the effect of U .
- (b) Consider solutions $u = \text{Re } \hat{u}e^{j(\omega t - kz)}$ and $v = \text{Re } \hat{v}e^{j(\omega t - kz)}$ and find the relationship between $\omega - k$ for x and y displacements. Make dimensioned plots in each case of real and imaginary values of k for real values of ω . Make dimensioned plots in each case of real and imaginary values of ω for real values of k ($I_0 > 0, I > 0$).
- (c) Why would it not be possible to impose the boundary conditions of part (c) in Problem 10.26 to solve this problem? The wire is driven at $z = 0$ by the deflection $u(0, t)\mathbf{i}_x + v(0, t)\mathbf{i}_y = u_0 \cos \omega_0 t \mathbf{i}_x + v_0 \sin \omega_0 t \mathbf{i}_y$ with the slopes

$$\frac{\partial u}{\partial z}(0, t) = 0, \quad \frac{\partial v}{\partial z}(0, t) = 0.$$

Find $u(z, t)$ and $v(z, t)$.

- (d) For a given driving frequency ω_0 sketch the peak deflections u and v as functions of z for several values of I (starting with $I = 0$). Summarize in words how the deflections would change as the current I is raised.
- (e) How would you devise an experiment to demonstrate the results of the preceding parts (i.e., what would you use as the moving “wire” and how would you excite it?).

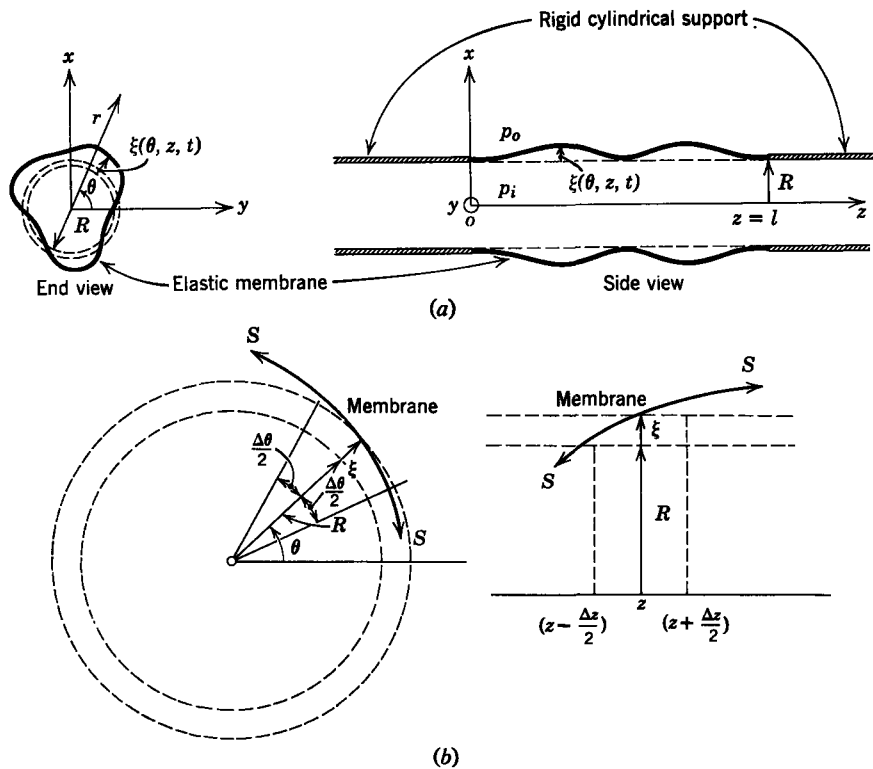


Fig. 10P.28

10.28. An elastic membrane with constant tension S has a circular cylindrical equilibrium geometry, as shown in Fig. 10P28a. It is supported at $z = 0$ and at $z = l$ by circular rigid tubes. Intuitively, we expect that the membrane will collapse inward if the pressure inside the membrane (p_i) is not larger than that outside (p_o). We could imagine stopping up one of the supporting tubes and pushing a cork into the end of the other tube just far enough to maintain the required pressure difference, as might be done in extruding a hollow section of molten glass or plastic or a soap film.

- (a) Show that for a static equilibrium to exist with $\xi = 0$, $p_i - p_o = S/R$.
- (b) There is, of course, no guarantee that if we establish this pressure difference the equilibrium will be stable. To examine this question write a linearized equation of radial force equilibrium for a small section of the membrane. The sketches of surface deformation shown in Fig. 10P.28b should be helpful in writing the force per unit area due to the tension S . Your equation of motion should be

$$\sigma_m \frac{\partial^2 \xi}{\partial t^2} = S \left(\frac{\xi}{R^2} + \frac{1}{R^2} \frac{\partial^2 \xi}{\partial \theta^2} + \frac{\partial^2 \xi}{\partial z^2} \right)$$

- (c) Under what conditions is the equilibrium stable?
- (d) Describe the lowest modes of oscillation for the membrane.
- (e) Reconsider Problem 10.22, taking into account the effect of the curvature.

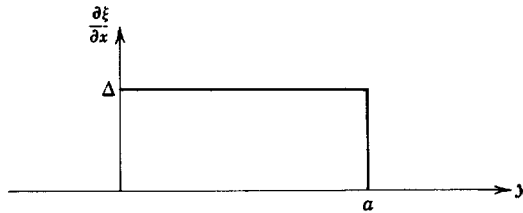


Fig. 10P.29

10.29. A membrane has the velocity $U > v_s$ in the x -direction, as described in Section 10.4.2. At $x = 0$, $\xi = 0$, and $\partial \xi / \partial x$ has the distribution shown. Assume that the membrane is infinitely wide in the y -direction.

- (a) Find and sketch $\xi(x, y)$ for $x > 0$. Assume that $M^2 = 2$.
- (b) Describe how you would physically produce the postulated excitation at $x = 0$.

10.30. A membrane moves with the velocity $U > v_s$ in the x -direction (see Section 10.4.2). Its edges are prevented from undergoing transverse motions along boundaries at $y = 0$ and

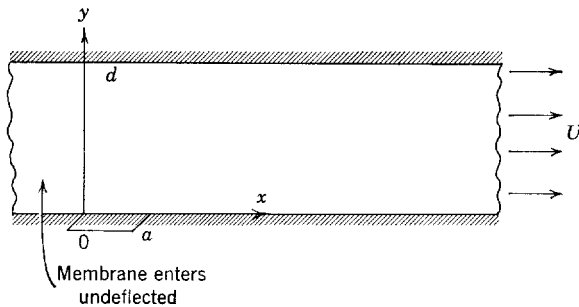


Fig. 10P.30

$y = d$, except for the segment $0 < x < a$, where the membrane is constrained to have the constant amplitude ξ_0 . Assume that $M^2 = 2$ and find the resulting deflection $\xi(x, t)$. Your answer should be presented as a sketch similar to Fig. 10.4.3.

10.31. Plot the ω - k relation (10.4.30) for the example described in Section 10.4.3 to show complex ω for real k and complex k for real ω . Indicate the modes (fast wave or slow wave) represented by each branch of the curves.

10.32. Consider the example of Section 10.4.3, but with the wire having a longitudinal velocity $U > v_s$.

- (a) Find the revised dispersion equation.
- (b) Sketch the ω - k relation and show complex values of k for real values of ω .
- (c) Describe the response of the wire to a sinusoidal excitation.

Appendix D

GLOSSARY OF COMMONLY USED SYMBOLS

Section references indicate where symbols of a given significance are introduced; grouped symbols are accompanied by their respective references. The absence of a section reference indicates that a symbol has been applied for a variety of purposes. Nomenclature used in examples is not included.

| Symbol | Meaning | Section |
|---------------------------------|-------------------------------------------------------------|----------------------|
| A | cross-sectional area | |
| A_i | coefficient in differential equation | 5.1.1 |
| (A_n^+, A_n^-) | complex amplitudes of components of n th mode | 9.2.1 |
| A_w | cross-sectional area of armature conductor | 6.4.1 |
| a | spacing of pole faces in magnetic circuit | 8.5.1 |
| $a, (a_c, a_s)$ | phase velocity of acoustic related waves | 13.2.1, 11.4.1 |
| a_b | Alfvén velocity | 12.2.3 |
| (a, b, c) | Lagrangian coordinates | 11.1 |
| a_i | constant coefficient in differential equation | 5.1.1 |
| \mathbf{a}_p | instantaneous acceleration of point p fixed in material | 2.2.1c |
| B, B_r, B_s | damping constant for linear, angular and square law dampers | 2.2.1b, 4.1.1, 5.2.2 |
| $\mathbf{B}, \mathbf{B}_i, B_0$ | magnetic flux density | 1.1.1a, 8.1, 6.4.2 |
| B_i | induced flux density | 7.0 |
| $(B_r, B_{ra}, B_{rb}, B_{rm})$ | radial components of air-gap flux densities | 4.1.4 |
| $[B_{rf}, (B_{rf})_{av}]$ | radial flux density due to field current | 6.4.1 |
| b | width of pole faces in magnetic circuit | 8.5 |
| b | half thickness of thin beam | 11.4.2b |
| C | contour of integration | 1.1.2a |
| $C, (C_a, C_b), C_o$ | capacitance | 2.1.2, 7.2.1a, 5.2.1 |
| C | coefficient in boundary condition | 9.1.1 |
| \mathbf{C} | the curl of the displacement | 11.4 |
| (C^+, C^-) | designation of characteristic lines | 9.1.1 |

| Symbol | Meaning | Section |
|-------------------------------------------------------------------------------------------------------------|-----------------------------------------------------------------------------------|----------------------------------------------|
| c_p | specific heat capacity at constant pressure | 13.1.2 |
| c_v | specific heat capacity at constant volume | 13.1.2 |
| D | electric displacement | 1.1.1a |
| d | length | |
| da | elemental area | 1.1.2a |
| $d\mathbf{f}_n$ | total elemental force on material in rigid body | 2.2.1c |
| $d\mathbf{l}$ | elemental line segment | 1.1.2a |
| $d\mathbf{T}_n$ | torque on elemental volume of material | 2.2.1c |
| dV | elemental volume | 1.1.2b |
| E | constant of motion | 5.2.1 |
| E | Young's modulus or the modulus of elasticity | 9.1 |
| \mathbf{E}, E_0 | electric field intensity | 1.1.1a, 5.1.2d |
| E_f | magnitude of armature voltage generated by field current in a synchronous machine | 4.1.6a |
| E_i | induced electric field intensity | 7.0 |
| e_{11}, e_{ij} | strain tensor | 9.1, 11.2 |
| \dot{e}_{ij} | strain-rate tensor | 14.1.1a |
| F | magnetomotive force (mmf) | 13.2.2 |
| F | force density | 1.1.1a |
| \hat{F} | complex amplitude of $f(t)$ | 5.1.1 |
| F_0 | amplitude of sinusoidal driving force | 9.1.3 |
| f | equilibrium tension of string | 9.2 |
| f | driving function | 5.1.1 |
| $f, \mathbf{f}, f^e, f^s, f_j, f_i, f_1$ | force | 2.2.1, 2.2.1c, 3.1, 5.1.2a, 3.1.2b, 8.1, 9.1 |
| f | arbitrary scalar function | 6.1 |
| f' | scalar function in moving coordinate system | 6.1 |
| f | three-dimensional surface | 6.2 |
| f | integration constant | 11.4.2a |
| G | a constant | 5.1.2c |
| G | shear modulus of elasticity | 11.2.2 |
| G | speed coefficient | 6.4.1 |
| G | conductance | 3.1 |
| g | air-gap length | 5.2.1 |
| g, \mathbf{g} | acceleration of gravity | 5.1.2c, 12.1.3 |
| $(\mathbf{H}, H_x, H_y, H_z)$ | magnetic field intensity | 1.1.1a |
| h | specific enthalpy | 13.1.2 |
| I, I, (I_r, I_s), I_f | electrical current | 10.4.3, 12.2.1a, 4.1.2, 6.4.1 |
| $(i, i_1, i_2, \dots, i_k), (i_{ar}, i_{as}, i_{br}, i_{bs}), i_a, (i_a, i_b, i_c), (i_f, i_t), (i_r, i_s)$ | electrical current | 2.1, 4.1.3, 6.4.1, 4.1.7, 6.4.1, 4.1 |

| Symbol | Meaning | Section |
|------------------------------------------------------------------------------------|---------------------------------------------------------------|---------------------------------------------|
| i_n | unit vector perpendicular to area of integration | 6.2.1 |
| i_s | unit vector normal to surface of integration | 6.2.1 |
| $(i_x, i_y, i_z), (i_1, i_2, i_3)$ | unit vectors in coordinate directions | 2.2.1c |
| J, J_f | current density | 7.0, 1.1.1a |
| $J, J_r, (J_x, J_y, J_z)$ | moment of inertia | 5.1.2b, 4.1.1, 2.2.1c |
| J_{xx}, J_{yz} | products of inertia | 2.2.1c |
| j | $\sqrt{-1}$ | 4.1.6a |
| K | loading factor | 13.2.2 |
| K, K_f | surface current density | 7.0, 1.1.1a |
| K | linear or torsional spring constant | 2.2.1a |
| K_i | induced surface current density | 7.0 |
| $k, k_c, (k_r, k_t)$ | wavenumber | 7.1.3, 10.1.3, 10.0 |
| k | summation index | 2.1.1 |
| k | maximum coefficient of coupling | 4.1.6b |
| k_n | n th eigenvalue | 9.2 |
| $(L, L_1, L_2), (L_a, L_f),$ $L_m, (L_0, L_2),$ $(L_r, L_s, L_{sr}), L_{ss}$ | inductance | 2.1.1, 6.4.1, 2.1.1, 4.2.1, 4.1.1, 4.2.4 |
| L | length of incremental line segment | 6.2.1 |
| l | value of relative displacement for which spring force is zero | 2.2.1a |
| l, l_w, l_y | length | |
| M | Hartmann number | 14.2.2 |
| M | mass of one mole of gas in kilograms | 13.1.2 |
| M | Mach number | 13.2.1 |
| M | mass | 2.2.1c |
| M | number of mechanical terminal pairs | 2.1.1 |
| M, M_s | mutual inductance | 4.1.1, 4.2.4 |
| M | magnetization density | 1.1.1a |
| m | mass/unit length of string | 9.2 |
| N | number of electrical terminal pairs | 2.1.1 |
| N | number of turns | 5.2.2 |
| n | number density of ions | 12.3.1 |
| n | integer | 7.1.1 |
| n | unit normal vector | 1.1.2 |
| P | polarization density | 1.1.1a |
| P | power | 12.2.1a |
| p | number of pole pairs in a machine | 4.1.8 |
| p | power per unit area | 14.2.1 |
| p | pressure | 5.1.2d and 12.1.4 |
| P_e, P_g, P_m, P_r | power | 4.1.6a, 4.1.6b, 4.1.2, 4.1.6b |
| Q | electric charge | 7.2.1a |
| q, q_i, q_k | electric charge | 1.1.3 and 2.1.2, 8.1, 2.1.2 |
| R, R_i, R_o | radius | |

| Symbol | Meaning | Section |
|---------------------------------------------|------------------------------------------------------------------------------------------------------------------------------|----------------------------------------------------|
| $R, R_a, R_b, R_f, R_r, R_s$ | resistance | |
| (R, R_ρ) | gas constant | 13.1.2 |
| R_e | electric Reynolds number | 7.0 |
| R_m | magnetic Reynolds number | 7.0 |
| r | radial coordinate | |
| \mathbf{r} | position vector of material | 2.2.1c |
| \mathbf{r}' | position vector in moving reference frame | 6.1 |
| \mathbf{r}_m | center of mass of rigid body | 2.2.1c |
| S | reciprocal modulus of elasticity | 11.5.2c |
| S | surface of integration | 1.1.2a |
| S | normalized frequency | 7.2.4 |
| S | membrane tension | 9.2 |
| S_z | transverse force/unit length acting on string | 9.2 |
| s | complex frequency | 5.1.1 |
| (s, s_{mT}) | slip | 4.1.6b |
| s_i | i th root of characteristic equation, a natural frequency | 5.1.1 |
| T | period of oscillation | 5.2.1 |
| T | temperature | 13.1.2 |
| $\mathbf{T}, T, T^e, T_{em}, T_m, T_0, T_1$ | torque | 2.2.1c, 5.1.2b, 3.1.1, 4.1.6b, 4.1.1, 6.4.1, 6.4.1 |
| \mathbf{T} | surface force | 8.4 |
| T_{ij}^m | mechanical stress tensor | 13.1.2 |
| T_{mn} | the component of the stress-tensor with m th-direction on a cartesian surface with a normal vector in the n th-direction | 8.1 |
| T_{or} | constant of coulomb damping | 4.1.1 |
| T_0 | initial stress distribution on thin rod | 9.1.1 |
| T | longitudinal stress on a thin rod | 9.1.1 |
| T_z | transverse force per unit area on membrane | 9.2 |
| T_2 | transverse force per unit area acting on thin beam | 11.4.2b |
| t | time | 1.1.1 |
| t' | time measured in moving reference frame | 6.1 |
| U | gravitational potential | 12.1.3 |
| U | longitudinal steady velocity of string or membrane | 10.2 |
| u | internal energy per unit mass | 13.1.1 |
| u | surface coordinate | 11.3 |
| $u_0(x - x_0)$ | unit impulse at $x = x_0$ | 9.2.1 |
| u | transverse deflection of wire in x -direction | 10.4.3 |
| $u_{-1}(t)$ | unit step occurring at $t = 0$ | 5.1.2b |
| V, V_m | velocity | 7.0, 13.2.3 |
| V | volume | 1.1.2 |
| V, V_a, V_f, V_o, V_s | voltage | |
| V | potential energy | 5.2.1 |

| Symbol | Meaning | Section |
|----------------------------------------------|--------------------------------------------------------------------------------|--------------------|
| v, \mathbf{v} | velocity | |
| (v, v_1, \dots, v_k) | voltage | 2.1.1 |
| $v', (v_a, v_b, v_c),$ v_f, v_{oc}, v_t | voltage | |
| v_n | velocity of surface in normal direction | 6.2.1 |
| v_o | initial velocity distribution on thin rod | 9.1.1 |
| v_p | phase velocity | 9.1.1 and 10.2 |
| \mathbf{v}^r | relative velocity of inertial reference frames | 6.1 |
| v_s | $\sqrt{f/m}$ for a string under tension f and having mass/unit length m | 10.1.1 |
| v | longitudinal material velocity on thin rod | 9.1.1 |
| v | transverse deflection of wire in y -direction | 10.4.3 |
| (W_e, W_m) | energy stored in electromechanical coupling | 3.1.1 |
| (W'_e, W'_m, W') | coenergy stored in electromechanical coupling | 3.1.2b |
| W'' | hybrid energy function | 5.2.1 |
| w | width | 5.2.2 |
| w | energy density | 11.5.2c |
| w' | coenergy density | 8.5 |
| X | equilibrium position | 5.1.2a |
| $(x, x_1, x_2, \dots, x_k)$ | displacement of mechanical node | 2.1.1 |
| x | dependent variable | 5.1.1 |
| x_p | particular solution of differential equation | 5.1.1 |
| $(x_1, x_2, x_3), (x, y, z)$ | cartesian coordinates | 8.1, 6.1 |
| (x', y', z') | cartesian coordinates of moving frame | 6.1 |
| (α, β) | constants along C^+ and C^- characteristics, respectively | 9.1.1 |
| (α, β) | see (10.2.20) or (10.2.27) | |
| α | transverse wavenumber | 11.4.3 |
| (α, β) | angles used to define shear strain | 11.2 |
| (α, β) | constant angles | 4.1.6b |
| α | space decay parameter | 7.1.4 |
| α | damping constant | 5.1.2b |
| α | equilibrium angle of torsional spring | 2.2.1a |
| γ | ratio of specific heats | 13.1.2 |
| γ | piezoelectric constant | 11.5.2c |
| $\gamma, \gamma_0, \gamma'$ | angular position | |
| $\Delta_a(t)$ | slope excitation of string | 10.2.1b |
| Δ_0 | amplitude of sinusoidal slope excitation | 10.2.1b |
| Δr | distance between unstressed material points | 11.2.1a |
| Δs | distance between stressed positions of material points | 11.2.1a |
| $\delta()$ | incremental change in () | 8.5 |
| $\delta, \delta_1, \delta_0$ | displacement of elastic material | 11.1, 9.1, 11.4.2a |
| δ | thickness of incremental volume element | 6.2.1 |
| δ | torque angle | 4.1.6a |

| Symbol | Meaning | Section |
|------------------------------------------------------------|-------------------------------------------------------------|----------------------|
| δ_{ij} | Kronecker delta | 8.1 |
| (δ_+, δ_-) | wave components traveling in the $\pm x$ -directions | 9.1.1 |
| ϵ | linear permittivity | 1.1.1b |
| ϵ_0 | permittivity of free space | 1.1.1a |
| η | efficiency of an induction motor | 4.1.6b |
| η | second coefficient of viscosity | 14.1.1c |
| $\theta, \theta_i, \theta_m$ | angular displacement | 2.1.1, 3.1.1, 5.2.1 |
| θ | power factor angle; phase angle between current and voltage | 4.1.6a |
| θ | equilibrium angle | 5.2.1 |
| $\dot{\theta}$ | angular velocity of armature | 6.4.1 |
| θ_m | maximum angular deflection | 5.2.1 |
| $(\lambda, \lambda_1, \lambda_2, \dots, \lambda_k)$ | magnetic flux linkage | 2.1.1, 6.4.1, 4.1.7, |
| λ_a | | 4.1.3, 4.1 |
| $(\lambda_a, \lambda_b, \lambda_c)$ | | |
| $(\lambda_{ar}, \lambda_{as}, \lambda_{br}, \lambda_{bs})$ | | |
| (λ_r, λ_s) | | |
| λ | Lamé constant for elastic material | 11.2.3 |
| λ | wavelength | 7.1.4 |
| μ | linear permeability | 1.1.1a |
| $\mu, (\mu_+, \mu_-)$ | mobility | 12.3.1, 1.1.1b |
| μ | coefficient of viscosity | 14.1.1 |
| μ_d | coefficient of dynamic friction | 2.2.1b |
| μ_0 | permeability of free space | 1.1.1a |
| μ_s | coefficient of static friction | 2.2.1b |
| ν | Poisson's ratio for elastic material | 11.2.2 |
| ν | damping frequency | 10.1.4 |
| (ξ, ξ) | continuum displacement | 8.5 |
| ξ_0 | initial deflection of string | 9.2 |
| ξ_d | amplitude of sinusoidal driving deflection | 9.2 |
| $(\xi_n(x), \xi_n(x))$ | n th eigenfunctions | 9.2.1b |
| (ξ_+, ξ_-) | amplitudes of forward and backward traveling waves | 9.2 |
| $\dot{\xi}_0(x)$ | initial velocity of string | 9.2 |
| ρ | mass density | 2.2.1c |
| ρ_f | free charge density | 1.1.1a |
| ρ_s | surface mass density | 11.3 |
| Σ | surface of discontinuity | 6.2 |
| σ | conductivity | 1.1.1a |
| σ_f | free surface charge density | 1.1.1a |
| σ_m | surface mass density of membrane | 9.2 |
| σ_o | surface charge density | 7.2.3 |
| σ_s | surface conductivity | 1.1.1a |
| σ_u | surface charge density | 7.2.3 |
| τ | surface traction | 8.2.1 |
| τ, τ_d | diffusion time constant | 7.1.1, 7.1.2a |
| τ | relaxation time | 7.2.1a |

| Symbol | Meaning | Section |
|--------------------------------|------------------------------------------------------------------------------------|---------------|
| τ_e | electrical time constant | 5.2.2 |
| τ_m | time for air gap to close | 5.2.2 |
| τ_o | time constant | 5.1.3 |
| τ_t | traversal time | 7.1.2a |
| ϕ | electric potential | 7.2 |
| ϕ | magnetic flux | 2.1.1 |
| ϕ | cylindrical coordinate | 2.1.1 |
| ϕ | potential for H when $J_f = 0$ | 8.5.2 |
| ϕ | flow potential | 12.2 |
| χ_e | electric susceptibility | 1.1.1b |
| χ_m | magnetic susceptibility | 1.1.1a |
| ψ | the divergence of the material displacement | 11.4 |
| ψ | angle defined in Fig. 6.4.2 | 6.4.1 |
| ψ | angular position in the air gap measured from stator winding (a) magnetic axis | 4.1.4 |
| ψ | electromagnetic force potential | 12.2 |
| ψ | angular deflection of wire | 10.4.3 |
| Ω | equilibrium rotational speed | 5.1.2b |
| Ω | rotation vector in elastic material | 11.2.1a |
| Ω_n | real part of eigenfrequency (10.1.47) | 10.1.4 |
| $\omega, (\omega_r, \omega_s)$ | radian frequency of electrical excitation | 4.1.6a, 4.1.2 |
| ω | natural angular frequency (Im s) | 5.1.2b |
| ω, ω_m | angular velocity | 2.2.1c, 4.1.2 |
| ω_c | cutoff frequency for evanescent waves | 10.1.2 |
| ω_d | driving frequency | 9.2 |
| ω_n | n th eigenfrequency | 9.2 |
| ω_o | natural angular frequency | 5.1.3 |
| (ω_r, ω_t) | real and imaginary parts of ω | 10.0 |
| ∇ | nabla | 6.1 |
| ∇_Σ | surface divergence | 6.2.1 |

Appendix E

SUMMARY OF PARTS I AND II AND USEFUL THEOREMS

IDENTITIES

$$\mathbf{A} \times \mathbf{B} \cdot \mathbf{C} = \mathbf{A} \cdot \mathbf{B} \times \mathbf{C},$$

$$\mathbf{A} \times (\mathbf{B} \times \mathbf{C}) = \mathbf{B}(\mathbf{A} \cdot \mathbf{C}) - \mathbf{C}(\mathbf{A} \cdot \mathbf{B})$$

$$\nabla(\phi + \psi) = \nabla\phi + \nabla\psi,$$

$$\nabla \cdot (\mathbf{A} + \mathbf{B}) = \nabla \cdot \mathbf{A} + \nabla \cdot \mathbf{B},$$

$$\nabla \times (\mathbf{A} + \mathbf{B}) = \nabla \times \mathbf{A} + \nabla \times \mathbf{B},$$

$$\nabla(\phi\psi) = \phi \nabla\psi + \psi \nabla\phi,$$

$$\nabla \cdot (\psi\mathbf{A}) = \mathbf{A} \cdot \nabla\psi + \psi \nabla \cdot \mathbf{A},$$

$$\nabla \cdot (\mathbf{A} \times \mathbf{B}) = \mathbf{B} \cdot \nabla \times \mathbf{A} - \mathbf{A} \cdot \nabla \times \mathbf{B},$$

$$\nabla \cdot \nabla\phi = \nabla^2\phi,$$

$$\nabla \cdot \nabla \times \mathbf{A} = 0,$$

$$\nabla \times \nabla\phi = 0,$$

$$\nabla \times (\nabla \times \mathbf{A}) = \nabla(\nabla \cdot \mathbf{A}) - \nabla^2\mathbf{A},$$

$$(\nabla \times \mathbf{A}) \times \mathbf{A} = (\mathbf{A} \cdot \nabla)\mathbf{A} - \frac{1}{2}\nabla(\mathbf{A} \cdot \mathbf{A}),$$

$$\nabla(\mathbf{A} \cdot \mathbf{B}) = (\mathbf{A} \cdot \nabla)\mathbf{B} + (\mathbf{B} \cdot \nabla)\mathbf{A} + \mathbf{A} \times (\nabla \times \mathbf{B}) + \mathbf{B} \times (\nabla \times \mathbf{A})$$

$$\nabla \times (\phi\mathbf{A}) = \nabla\phi \times \mathbf{A} + \phi \nabla \times \mathbf{A},$$

$$\nabla \times (\mathbf{A} \times \mathbf{B}) = \mathbf{A}(\nabla \cdot \mathbf{B}) - \mathbf{B}(\nabla \cdot \mathbf{A}) + (\mathbf{B} \cdot \nabla)\mathbf{A} - (\mathbf{A} \cdot \nabla)\mathbf{B}.$$

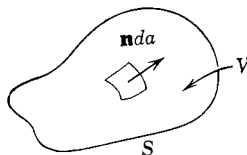
THEOREMS

$$\int_a^b \nabla \phi \cdot d\mathbf{l} = \phi_b - \phi_a.$$



Divergence theorem

$$\oint_S \mathbf{A} \cdot \mathbf{n} \, da = \int_V \nabla \cdot \mathbf{A} \, dV$$



Stokes's theorem

$$\oint_C \mathbf{A} \cdot d\mathbf{l} = \int_S (\nabla \times \mathbf{A}) \cdot \mathbf{n} \, da$$

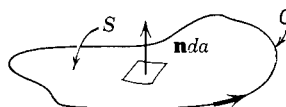
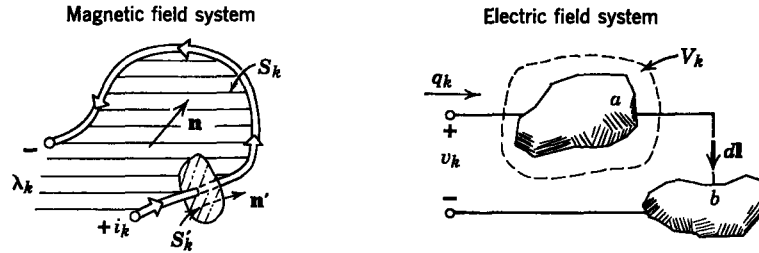


Table 1.2 Summary of Quasi-Static Electromagnetic Equations

| | Differential Equations | | Integral Equations | |
|-----------------------|------------------------------------------------------------------------------------|-----------------------------------------------------------|-----------------------------------------------------------------------------------------------------------------------------------------------|----------|
| Magnetic field system | $\nabla \times \mathbf{H} = \mathbf{J}_f$ | (1.1.1) | $\oint_C \mathbf{H} \cdot d\mathbf{l} = \int_S \mathbf{J}_f \cdot \mathbf{n} \, da$ | (1.1.20) |
| | $\nabla \cdot \mathbf{B} = 0$ | (1.1.2) | $\oint_S \mathbf{B} \cdot \mathbf{n} \, da = 0$ | (1.1.21) |
| | $\nabla \cdot \mathbf{J}_f = 0$ | (1.1.3) | $\oint_S \mathbf{J}_f \cdot \mathbf{n} \, da = 0$ | (1.1.22) |
| | $\nabla \times \mathbf{E} = -\frac{\partial \mathbf{B}}{\partial t}$ | (1.1.5) | $\oint_C \mathbf{E}' \cdot d\mathbf{l} = -\frac{d}{dt} \int_S \mathbf{B} \cdot \mathbf{n} \, da$ | (1.1.23) |
| | | | where $\mathbf{E}' = \mathbf{E} + \mathbf{v} \times \mathbf{B}$ | |
| Electric field system | $\nabla \times \mathbf{E} = 0$ | (1.1.11) | $\oint_C \mathbf{E} \cdot d\mathbf{l} = 0$ | (1.1.24) |
| | $\nabla \cdot \mathbf{D} = \rho_f$ | (1.1.12) | $\oint_S \mathbf{D} \cdot \mathbf{n} \, da = \int_V \rho_f \, dV$ | (1.1.25) |
| | $\nabla \cdot \mathbf{J}_f = -\frac{\partial \rho_f}{\partial t}$ | (1.1.14) | $\oint_S \mathbf{J}'_f \cdot \mathbf{n} \, da = -\frac{d}{dt} \int_V \rho_f \, dV$ | (1.1.26) |
| | $\nabla \times \mathbf{H} = \mathbf{J}_f + \frac{\partial \mathbf{D}}{\partial t}$ | (1.1.15) | $\oint_C \mathbf{H}' \cdot d\mathbf{l} = \int_S \mathbf{J}'_f \cdot \mathbf{n} \, da + \frac{d}{dt} \int_S \mathbf{D} \cdot \mathbf{n} \, da$ | (1.1.27) |
| | | where $\mathbf{J}'_f = \mathbf{J}_f - \rho_f \mathbf{v}$ | | |
| | | $\mathbf{H}' = \mathbf{H} - \mathbf{v} \times \mathbf{D}$ | | |

Table 2.1 Summary of Terminal Variables and Terminal Relations



Definition of Terminal Variables

Flux

$$\lambda_k = \int_{S_k} \mathbf{B} \cdot \mathbf{n} \, da$$

Current

$$i_k = \int_{S'_k} \mathbf{J}_f \cdot \mathbf{n}' \, da$$

Charge

$$q_k = \int_{V_k} \rho_f \, dV$$

Voltage

$$v_k = \int_a^b \mathbf{E} \cdot d\mathbf{l}$$

Terminal Conditions

$$v_k = \frac{d\lambda_k}{dt}$$

$$i_k = \frac{dq_k}{dt}$$

$$\lambda_k = \lambda_k(i_1 \cdots i_N; \text{geometry})$$

$$q_k = q_k(v_1 \cdots v_N; \text{geometry})$$

$$i_k = i_k(\lambda_1 \cdots \lambda_N; \text{geometry})$$

$$v_k = v_k(q_1 \cdots q_N; \text{geometry})$$

and M Mechanical Terminal Pairs*

Magnetic Field Systems

Electric Field Systems

Conservation of Energy

$$dW_m = \sum_{j=1}^N i_j d\lambda_j - \sum_{j=1}^M f_j^e dx_j$$

(a)

$$dW_e = \sum_{j=1}^N v_j dq_j - \sum_{j=1}^M f_j^e dx_j$$

(b)

$$dW'_m = \sum_{j=1}^N \lambda_j di_j + \sum_{j=1}^M f_j^e dx_j$$

(c)

$$dW'_e = \sum_{j=1}^N q_j dv_j + \sum_{j=1}^M f_j^e dx_j$$

(d)

Forces of Electric Origin, $j = 1, \dots, M$

$$f_j^e = - \frac{\partial W_m(\lambda_1, \dots, \lambda_N; x_1, \dots, x_M)}{\partial x_j}$$

(e)

$$f_j^e = - \frac{\partial W_e(q_1, \dots, q_N; x_1, \dots, x_M)}{\partial x_j}$$

(f)

$$f_j^e = \frac{\partial W'_m(i_1, \dots, i_N; x_1, \dots, x_M)}{\partial x_j}$$

(g)

$$f_j^e = \frac{\partial W'_e(v_1, \dots, v_N; x_1, \dots, x_M)}{\partial x_j}$$

(h)

Relation of Energy to Coenergy

$$W_m + W'_m = \sum_{j=1}^N \lambda_j i_j$$

(i)

$$W_e + W'_e = \sum_{j=1}^N v_j q_j$$

(j)

Energy and Coenergy from Electrical Terminal Relations

$$W_m = \sum_{j=1}^N \int_0^{\lambda_j} i_j(\lambda_1, \dots, \lambda_{j-1}, \lambda'_j, 0, \dots, 0; x_1, \dots, x_M) d\lambda'_j \quad (k)$$

$$W_e = \sum_{j=1}^N \int_0^{q_j} v_j(q_1, \dots, q_{j-1}, q'_j, 0, \dots, 0; x_1, \dots, x_M) dq'_j \quad (l)$$

$$W'_m = \sum_{j=1}^N \int_0^{i_j} \lambda_j(i_1, \dots, i_{j-1}, i'_j, 0, \dots, 0; x_1, \dots, x_M) di'_j \quad (m)$$

$$W'_e = \sum_{j=1}^N \int_0^{v_j} q_j(v_1, \dots, v_{j-1}, v'_j, 0, \dots, 0; x_1, \dots, x_M) dv'_j \quad (n)$$

* The mechanical variables f_j and x_j can be regarded as the j th force and displacement or the j th torque T_j and angular displacement θ_j .

Table 6.1 Differential Equations, Transformations, and Boundary Conditions for Quasi-static Electromagnetic Systems with Moving Media

| | Differential Equations | | Transformations | | Boundary Conditions | |
|---------------------------------------------------|------------------------------------------------------------------------------------|----------------------------|-------------------------------------------------------------|----------|-------------------------------------------------------------------------------------------------------------------------------------------------------------|----------|
| Magnetic field systems | $\nabla \times \mathbf{H} = \mathbf{J}_f$ | (1.1.1) | $\mathbf{H}' = \mathbf{H}$ | (6.1.35) | $\mathbf{n} \times (\mathbf{H}^a - \mathbf{H}^b) = \mathbf{K}_f$ | (6.2.14) |
| | $\nabla \cdot \mathbf{B} = 0$ | (1.1.2) | $\mathbf{B}' = \mathbf{B}$ | (6.1.37) | $\mathbf{n} \cdot (\mathbf{B}^a - \mathbf{B}^b) = 0$ | (6.2.7) |
| | $\nabla \cdot \mathbf{J}_f = 0$ | (1.1.3) | $\mathbf{J}'_f = \mathbf{J}_f$ | (6.1.36) | $\mathbf{n} \cdot (\mathbf{J}_f^a - \mathbf{J}_f^b) + \nabla_{\Sigma} \cdot \mathbf{K}_f = 0$ | (6.2.9) |
| | $\nabla \times \mathbf{E} = -\frac{\partial \mathbf{B}}{\partial t}$ | (1.1.5) | $\mathbf{E}' = \mathbf{E} + \mathbf{v}^r \times \mathbf{B}$ | (6.1.38) | $\mathbf{n} \times (\mathbf{E}^a - \mathbf{E}^b) = v_n(\mathbf{B}^a - \mathbf{B}^b)$ | (6.2.22) |
| | $\mathbf{B} = \mu_0(\mathbf{H} + \mathbf{M})$ | (1.1.4) | $\mathbf{M}' = \mathbf{M}$ | (6.1.39) | | |
| Electric field systems | $\nabla \times \mathbf{E} = 0$ | (1.1.11) | $\mathbf{E}' = \mathbf{E}$ | (6.1.54) | $\mathbf{n} \times (\mathbf{E}^a - \mathbf{E}^b) = 0$ | (6.2.31) |
| | $\nabla \cdot \mathbf{D} = \rho_f$ | (1.1.12) | $\mathbf{D}' = \mathbf{D}$ | (6.1.55) | $\mathbf{n} \cdot (\mathbf{D}^a - \mathbf{D}^b) = \sigma_f$ | (6.2.33) |
| | | | $\rho'_f = \rho_f$ | (6.1.56) | | |
| | $\nabla \cdot \mathbf{J}_f = -\frac{\partial \rho_f}{\partial t}$ | (1.1.14) | $\mathbf{J}'_f = \mathbf{J}_f - \rho_f \mathbf{v}^r$ | (6.1.58) | $\mathbf{n} \cdot (\mathbf{J}_f^a - \mathbf{J}_f^b) + \nabla_{\Sigma} \cdot \mathbf{K}_f = v_n(\rho_f^a - \rho_f^b) - \frac{\partial \sigma_f}{\partial t}$ | (6.2.36) |
| | $\nabla \times \mathbf{H} = \mathbf{J}_f + \frac{\partial \mathbf{D}}{\partial t}$ | (1.1.15) | $\mathbf{H}' = \mathbf{H} - \mathbf{v}^r \times \mathbf{D}$ | (6.1.57) | $\mathbf{n} \times (\mathbf{H}^a - \mathbf{H}^b) = \mathbf{K}_f + v_n \mathbf{n} \times [\mathbf{n} \times (\mathbf{D}^a - \mathbf{D}^b)]$ | (6.2.38) |
| $\mathbf{D} = \epsilon_0 \mathbf{E} + \mathbf{P}$ | (1.1.13) | $\mathbf{P}' = \mathbf{P}$ | (6.1.59) | | | |

INDEX

Numbers preceded by letters are Appendix references. Appendices A, B, and C are in Part One; Appendices D and E, Part Two; and Appendices F and G, Part Three.

- Acceleration, centrifugal fluid, 729
 - centripetal, 59
 - Coriolis, 59
 - Eulerian variable, 727
 - fluid, 727
 - instantaneous, 45
- Accelerator, electric field, 776
 - MHD, 825
 - particle, 608
- Acoustic delay lines, 480
- Acoustic waves, compressional in solid, 673
 - dilatational in solid, 673
 - elastic media, 671
 - fluid, 544
 - gases, 845
 - guided, 679, 683, 693
 - magnetic fields and, 846
 - membrane, 509
 - shear elastic, 675
 - string, 509
 - thin beam, 683
 - thin rod, 487, 681
- Acyctic machine, 286
- Air-gap magnetic fields, 114
- Alfvén velocity, 763
- Alfvén waves, 759
 - compressible fluids and, 841
 - cylindrical geometry, 767
 - effect of conductivity on, 772
 - mechanical analogue to, 766
 - nature of, 764
 - numerical example of, 771
 - resonances and, 771
 - standing, 771
 - torsional, 765
- Amortisseur winding, 164
- Ampère, 1
- Ampère's law, B6, C3, E3, G3
 - dynamic, B9
 - electromechanical, 304
 - example of, B7
 - integral form of, B36, C3, E3, G3
 - magnetization and, B26
- Amplifying wave, coupled system and, 608
 - electric field induced, 605
 - evanescent wave and, 607
 - space-time behavior of, 604, 606
- Angular frequency, 513
- Angular momentum, 248
- Angular velocity, 47
- Applications of electromechanics, 2
- Approximations, electromechanical, 206
- Armature, ac machine, 120
 - dc machine, 141, 293
- Armature reaction, 297
- Astrophysics and MHD, 552
- Attenuation, microwave, 561
- Average power converted, salient pole machine, 155
 - smooth-air-gap machine, 124
- Beats in space, 595
- Bernoulli's equation, 738
 - example of, 752
- Bessel functions, 408
 - roots of, 409
- Bias, linear transducer operation and, 201
 - piezoelectricity and, 711
- Bode plot, 206
- Boundary, analytic description of, 269, 668
 - examples of moving, 269, 276, 279, 280, 364, 392, 397, 451, 460, 563, 574, 605, 627, 704, 783
 - moving, 267
 - well defined, 267
- Boundary condition, Alfvén waves, 769
 - causality and, 491, 592, 607
 - conservation of charge, 279, 374, 376, 394, 399
 - convection and, 267, 587, 598
 - dispersion and, 618
 - elastic media, 671, 676
 - electric displacement, 278
 - electric field intensity, 275, 278
 - electric field systems, 277, E6, G6
 - electromagnetic field, 267
 - electromechanical, 668
 - field transformations and, 275
 - geometric effect of, 280
 - initial condition and, 513
 - inviscid fluid, 752
 - inviscid fluid slip, 740
 - longitudinal and transverse, 680
 - magnetic field intensity, 273, 280
 - magnetic field systems, 270, E6, G6
 - magnetic field system current, 272
 - magnetic fluid, 774
 - magnetic flux density, 271
 - MHD, 769
 - motion and, 267, 491, 587, 592, 598, 607
 - string and membrane, 522
 - summary of electromagnetic, 268, E6, G6
 - thin rod, 493
 - viscous fluid, 873
- Boundary layer dynamics, 602
- Brake, induction, 134
 - MHD, 744
- Breakdown, electrical, 576, 782
- Breakdown strength of air, 576

- Brush, dc machine, 292
 - liquid-metal, 316, 878
 - metal-graphite, 883
- Bullard's equation, 336
- Cables, charge relaxation in high voltage, 380
 - nonuniform conductivity in, 380
- Capability curve of synchronous generator, 170
- Capacitance, electrical linearity and, 30
 - example for calculation of, 32, 33
 - generalized, 28
 - quasi-static limit and, B18
- Causality, boundary conditions and, 592, 607
 - condition of, 491, 592, 607
- Center of mass, 46
- Channel, variable-area MHD, 751
- Characteristic dynamical times, excitation and, 332
 - material motion and, 332
- Characteristic equation, 181
- Characteristics, wave fronts and, 618
 - wave propagation and, 488, 490
 - waves with convection and, 586
- Charge, B1
 - conservation of, B5
 - net flow and flow of net, B6
 - test, 12
 - total, 29
- Charge-average velocity, B5
- Charge carriers, effect of motion on, 290
- Charge conservation, differential form of, B5
 - integral form of, B5
- Charge density, B1
 - effect of motion on, 290, 334, 382, 387, 388, 392, 397, 401
 - free, 7, B28
 - magnetic field system and, 288
- Charge distribution, effect of motion on, 334, 382, 387, 388, 392, 397, 401
- Charge relaxation, 330, 370
 - electrical transient, 372
 - examples of, 372, 375
 - excitation frequency and, 378, 400
 - frequency in frame of material and, 399
 - general equation for, 371
 - lumped-parameter models for, 331, 375
 - magnetic diffusion and, 401
 - motion sinusoidal excitation with, 392
 - moving frame and, 381
 - nonuniform properties and, 378
 - sources of charge and, 372
 - spatially and temporally periodic fields and, 397
 - steady motion and, 380
 - thunder storms, and, 388
 - traveling wave in a moving material and, 397
 - uniform properties and, 372
- Choking, constant area flow, 824
- Circuit breaker, transducer for a, 22
- Circuit theory, 16
- Coefficient, of sliding friction, 42
 - of static friction, 42
- Coefficients of viscosity, independence of, 870
- Coenergy, 73, E5, G5
 - electrical linearity and, 76
 - potential well motions and, 217
- Coenergy density, electric field system, 464, 714
 - magnetic field system, 456
- Collector rings, 120
- Commutation in dc machines, 296
- Commutator, 140
 - of dc machines, 292
- Commutator bars, 142
- Commutator machines, 140
 - ac generator, 329
 - brake operation of, 306
 - compound wound, 310
 - electrical power input of, 303
 - equation for armature of, 300
 - equation for field of, 297
 - equation of motion for, 297
 - generator operation of, 306
 - linear amplifier, 304
 - mechanical power output of, 303
 - motor operation of, 306
 - operation with alternating currents and, 312
 - properties of, 303
 - separately excited, 306
 - series excitation of, 309
 - shunt excitation of, 309
 - speed curves of, shunt excited, 310
 - speed regulation of, 307
 - summary of equations for, 303
 - torque-current curves of series excited, 311
 - torque-speed curves of shunt excited, 310
 - transient performance of, 306
- Compensating networks, 198
- Compensation in feedback loops, 198
- Compressibility constant, 845
- Compressibility of fluid, 725
- Compressible fluids, 813
 - electromechanical coupling to, 820
- Conduction, electrical, 7, B30
 - in electric field system, effect of motion on, 371
 - heat, 815
 - motion and electrical, 284, 289
- Conduction current, B6
 - absence of net free charge and, 374
- Conduction machine, MHD, 740
 - variable area, MHD, 753
 - see also* Commutator machine; DC machine:
- Conductivity, air and water, 388
 - electrical, 7
 - electrical surface, 7
 - mechanical strength and, 698
 - nonuniform, 380
 - numerical values of, 345, 377
- Conductor, electric field perfect, 29, 213,

- 390, 400, 401
 magnetic field perfect, 18, 211, 223, 354, 401, 563
- Confinement, electromechanical, 4, 407
- Conservation, of charge, B5
 displacement current and, B9
 integral form of, B37
 of energy, 63, 66
 continuum, 456, 464
 continuum coupling and, 455
 equation, steady state, 820
 fluid, 814
 incompressible fluid, 757
 integral form of, 819
 of flux, lumped-parameter, 211, 220
 perfectly conducting fluid and, 761
 of mass, differential law of, 731
 example of, 730
 fluid, 729, 814
 integral form of, 730
 of momentum, fluid, 731, 814
 integral form of, 733, 734
 interfacial, 671
 stress and, 733
- Conservative systems, 213
- Constant charge dynamics, 205, 213
- Constant-current constant-flux dynamics, 220
- Constant-current constraint, continuum, 628
- Constant-current dynamics, 220
- Constant flux, lumped and continuum, 212
- Constant flux dynamics, fluid, 761
 lumped-parameter, 211, 220
- Constant of the motion, fluid, 738
- Constant voltage dynamics, 204, 212, 226
- Constituent relations, electromagnetic, 283, B25
 fluid, 815
 fluid mechanical, 735
 materials in motion and, 283
 moving media in electric field systems and, 289
 moving media in magnetic field systems and, 284
- Constitutive law, mobile ion, 778
 piezoelectric slab, 712
- Contact resistance, MHD, 750
- Contacts, sliding, 42
- Continuity of space, 35
- Continuum and discrete dynamics, 553
- Continuum descriptions, 727
- Continuum electromechanical systems, 251
- Contour, deforming, 11, B32
- Control, dc machines and, 291
- Controlled thermonuclear reactions, 354
- Convection, dynamical effect of, 584
 and instability, 593
- Convection current, B6
- Convective derivative, 259, 584
 charge relaxation and, 381
 example of, 729
 magnetic diffusion and, 357
see also Substantial derivative
- Convective second derivative, 585
- Coordinate system, inertial, 254
- Corona discharge, 776, 782
- Corona wind, demonstration of, 782
- Couette flow, plane, 876
- Coulomb's law, B1
 point charge, B2
- Coupling, electromechanical, 15, 60
- Coupling to continuous media at terminal pairs, 498
- Coupling network, lossless and conservative, 63
- Creep, failure in solids by, 704
- Critical condition for instability, 568
- Crystals, electromechanics of, 651
 piezoelectric materials as, 711
- Current, balanced two-phase, 113
 conduction, B6
 convection, B6
 displacement, B9
 electric field system, 29
 free, B25
 magnetization, B25
 polarization, B29
- Current density, B5
 diffusion of, 343
 distribution of, 332
 free, 7
- Current law, Kirchhoff's, 16
- Currents as functions of flux linkages, 26
- Current transformation, examples of, 226
- Cutoff condition, 559
- Cutoff frequency, 559
 elastic shear waves, 695
 membrane, 623
- Cutoff waves, 556
 electromagnetic plasma, 638
 membrane, 623
 power flow and, 637
 thin beam, 684
see also Evanescent wave
- Cyclic energy conversion processes, 79
- Cylindrical coordinates, stress components in, 437
- Cylindrical modes, 648
- Damped waves, driven response of, 577
- Damper, linear ideal, 40
 lumped element, 36, 40
 square-law, 43, 229
- Damper winding in rotating machine, 164
- Damping, magnetic fluid, 750
 negative, 198
 spatial decay and, 560
 wave dynamics with, 576
- Damping constant, 41
- Damping frequency, 577
- DC generator, magnetic saturation in, 310
 self-excited, 310
- DC machines, 140; *see also* Commutator machines
- DC motor, self-excited, 308
 series excited, 311

- starting torque of, 310
- torque-speed curves for, 306
- Definitions, electromagnetic, 7, B1
- Deforming contours of integration, 10, 18, 262, B32, 761
- Degree of freedom, 49
- Delay line, acoustic, 480
 - acoustic magnetostrictive, 708
 - fidelity in, 501
 - mechanical, 499
 - shear waves and, 696
- Delta function, B2
 - Kronecker, 421
- Derivative, convective, 259, 584, 726
 - individual, 728
 - particle, 728
 - Stokes, 728
 - substantial, 259, 584, 728
 - total, 728
- Dielectrophoresis, 783
- Difference equation, 620
- Differential equation, order of, 180
 - linear, 180
- Differential operators, moving coordinates and, 257
- Diffusion, magnetic, 576
 - magnetic analogous to mechanical, 580
 - of magnetic field and current, 335
- Diffusion equation, 337
- Diffusion time constant, 341
 - numerical values of, 344
- Diffusion wave, magnetic, 358
 - picture of, 581
 - space-time behavior of, 359
- Dilatational motion of fluid, 866
- Direction cosines, definition of, 435
 - relation among, 439
- Discrete systems, electromechanics of, 60
- Discrete variables, mechanical, 36
 - summary of electrical, 35
- Dispersion equation, absolutely unstable wire, 567
 - Alfvén wave, 769
 - amplifying wave, 602
 - convective instability, 602
 - damped waves, 577
 - elastic guided shear waves, 695
 - electron oscillations, 601
 - evanescent wave, 557
 - kink instability, 629
 - magnetic diffusion with motion, 357
 - membrane, 623
 - moving wire destabilized by magnetic field, 602
 - moving wire stabilized by magnetic field, 596
 - ordinary waves, 513
 - with convection, 594
 - on wire, 555
 - on wires and membranes, 513
 - resistive wall interactions, 609
 - sinusoidal steady-state, and 514
 - wire with convection and damping, 609
- Displacement, elastic materials, 486
 - elastic media, 652
 - lumped parameter systems, 36
 - one-dimensional, 483
 - relative, 657
 - and rotation, 657
 - and strain, 658
 - transformation of, 659
 - translational, 657
- Displacement current, B9
- Displacement current negligible, B19
- Distributed circuits, electromechanical, 651
- Divergence, surface, 272
 - tensor, 422, G9
 - theorem, B4, C2, E2, G2, G9
- Driven and transient response, unstable system, 569
- Driven response, one-dimensional continuum, 511
 - unstable wire, 568
- Driving function, differential equation, 180
 - sinusoidal, 181
- Dynamics, constant charge, 205, 213
 - constant current, 220
 - constant flux, 211, 220
 - constant voltage, 204, 212, 226
 - lumped-parameter, 179
 - reactance dominated, 138, 211, 220, 242, 336, 354, 368, 563
 - resistance dominated, 138, 209, 233, 242, 336, 354, 368, 503, 583, 611
 - two-dimensional, 621
- Dynamics of continua, x - t plane, 488, 586
 - omega- k plane, 511, 554
- Dynamo, electrohydrodynamic, 388
- Eddy currents, 342, 628
- Efficiency of induction machine, 134
- EHD, 3, 552, 776
- EHD pump, demonstration of, 783
- Eigenfrequencies, 518
 - electromechanical filter, 707
 - magnetic field, shift of, 562
 - not harmonic, 563, 684
 - wire stiffened by magnetic field, 562
- Eigenfunction, 518
- Eigenmode, 517
 - complex boundary conditions and, 533
 - orthogonality of, 341, 519, 520
- Eigenvalues, 518
 - dispersion and, 562
 - graphic solution for, 526
 - kink instability, 630
- Elastic beam, resonant circuit element, 688
- Elastic constants, independence of, 664
 - numerical values of, 486
- Elastic continua, 479
- Elastic failure, example of electromechanical, 701
- Elastic force density, 667
- Elastic guiding structures, 693
- Elasticity, summary of equations of, 666, 668
- Elasticity equations, steps in derivation of, 651

- Elastic material, ideal, 485
 linear, 485
- Elastic media, 651
 electromechanical design and, 697
 electromechanics of, 696
 equations of motion for, 653
 quasi-statics of, 503
- Elastic model, membrane, 509
 thin rod, 480
 wire, 509
- Elastic waves, lumped mechanical elements and, 507
 shear, 543
 thin rod, 543
see also Acoustic waves
- Electrical circuits, 16
- Electric displacement, 7, B28
- Electric field, effect of motion on, 334, 382, 387, 388, 392, 397, 401
- Electric field coupling to fluids, 776
- Electric field equations, periodic solution to, 281
- Electric field intensity, 7, B1
- Electric field system, B19
 differential equations for, 8, E3, G3
 integral equations for, 11, E3, G3
- Electric field transformation, example of, 262
 Faraday's law and, 262
- Electric force, field description of, 440
 fluids and, 776
 stress tensor for, 441
- Electric force density, 418, 463
- Electric Reynolds number, 335, 370, 381, 383, 395, 399, 401, 575, 780
 mobility model and, 780
- Electric shear, induced surface charge and, 400
- Electric surface force, 447
- Electrification, frictional, 552
- Electroelasticity, 553
- Electrostatic generator, 782
- Electrohydrodynamic orientation, 785
- Electrohydrodynamic power generation, 782
- Electrohydrodynamics, 3, 552, 776
- Electrohydrodynamic stabilization, 786
- Electromagnetic equations, differential, 6, B12, B19, E3, G3
 integral, 9, B32, E3, G3
 quasi-static, 5, B19, B32, E3, G3
 summary of quasi-static, 13, E3, G3
- Electromagnetic field equations, summary of, 268, E6, G6
- Electromagnetic fields, moving observer and, 254
- Electromagnetic theory, 5, B1
 summary of, 5, E6, G6
- Electromagnetic waves, B13
 absorption of, B25
- Electromechanical coupling, field description of, 251
- Electromechanics, continuum, 330
 of elastic media, 651
 incompressible fluids and, 737
 lumped-parameter, 60
- Electron beam, 4, 552, 600, 608
 magnetic field confinement of, 601
 oscillations of, 600
- Electrostatic ac generator, 415
- Electrostatic self-excited generator, 388
- Electrostatic voltmeter, 94
- Electrostriction, incompressibility and, 784
- Electrostriction force density, 465
- Elements, lumped-parameter electrical, 16
 lumped-parameter mechanical, 36
- Energy, conservation of fluid, 814
 electrical linearity and, 76
 electric field system conservation of, 66
 internal or thermal gas, 813
 internal per unit mass, 815
 kinetic per unit mass, 815
 magnetic field system conservation of, 63
 magnetic stored, 64
 potential and kinetic, 214
- Energy conversion, cyclic, 79, 110
 electromechanical, 79
 lumped-parameter systems, 79
- Energy density, B23
 equal electric and magnetic, B24
- Energy dissipated, electromagnetic, B22
- Energy flux, B22
- Energy function, hybrid, 220
- Energy method, 60, 450, E5, G5
- Energy relations, summary of, 68, E5, G5
- Enthalpy, specific, 820
- Equation of motion, elastic media, 668
 electromechanical, 84
 examples of lumped-parameter, 84, 86
 incompressible, irrotational inviscid flow, 738
 linearized, 183
 lumped mechanical, 49
- Equilibrium, of continuum, stability of, 574
 dynamic or steady-state, 188
 hydromagnetic, 561
 kink instability of, 633
 potential well stability of, 216
 static, 182
- Equipotentials, fluid, 752
- Eulerian description, 727
- Evanescence with convection, 596
- Evanescence wave, 556
 appearance of, 559
 constant flux and, 563
 dissipation and, 560
 elastic shear, 695
 equation for, 557
 example of, 556
 membrane, 560, 623
 physical nature of, 560
 signal transmission and, 639
 sinusoidal steady-state, 558
 thin beam, 684
- Evil, 697
- Failure in solids, fatigue and creep, 704
- Faraday, 1

- Faraday disk, 286
 Faraday's law, B9
 deforming contour of integration and, 262, 300, 315, 565, B32, E3, G3
 differential form, 6, B10, E3, G3
 example of integral, 262, 276, 286, 297, 315
 integral form of, B10, B32
 perfectly conducting fluid and, 761
 Fatigue, failure in solids by, 704
 Feedback, continuous media and, 548
 stabilization by use of, 193
 Ferroelectrics, B29
 piezoelectric materials and, 711
 Ferrohydrodynamics, 552, 772
 Field circuit of dc machine, 141
 Field equations, moving media, generalization of, 252
 Fields and moving media, 251
 Field transformations, 268, E6, G6;
 see also Transformations
 Field winding, ac machine, 120
 dc machine, 293
 Film, *Complex Waves I*, xi, 516, 559, 571, 634
 Film, *Complex Waves II*, xi, 573, 606
 Filter, electromechanical, 2, 200, 480, 704
 First law of thermodynamics, 63
 Flow, Hartmann, 884
 irrotational fluid, 737
 laminar, 725
 turbulent, 725
 Flowmeter, liquid metal, 363
 Fluid, boundary condition for, 725
 boundary condition on, inviscid, 752
 compressibility of, 725
 effect of temperature and pressure on, 724
 electric field coupled, 776
 electromechanics of, 724
 ferromagnetic, 552, 772
 highly conducting, 760
 incompressible, 724, 735
 inhomogeneous, 735
 internal friction of, 724
 inviscid, 724, 725
 laminar and turbulent flow of, 725
 magnetic field coupling to incompressible, 737
 magnetizable, 772
 Newtonian, 861
 perfectly conducting, 563
 solids and, 724
 static, 735
 viscous, 861
 Fluid dynamics, equations of inviscid compressible, 813
 equations of inviscid, incompressible, 726
 equations of viscous, 871
 Fluid flow, accelerating but steady, 753
 around a corner, 751
 potential, 751
 unsteady, 746
 variable-area channel, 751
 Fluid-mechanical examples with viscosity, 875
 Fluid orientation systems, 785
 Fluid pendulum, electric-field coupled, 784
 magnetic damping of, 750
 Fluid pump or accelerator, 776
 Fluid stagnation point, 752
 Fluid streamlines, 752
 Fluid transformer, variable-area channel as, 756
 Flux amplification, plasmas and, 354
 Flux conservation, lumped-parameter, 211, 220
 magnetic fields and, 352
 perfectly conducting gas and, 849
 Flux density, mechanical amplification of, 354
 Flux linkage, 19, E4, G4
 example of, 22, 23
 Force, charge, B1
 derivative of inductance and, 453
 electric origin, 67, E5, G5
 electromagnetic, 12
 field description of, 418
 fluid electric, 776
 Lorentz, 12, 255, 419
 magnetic, B6
 magnetization with one degree of freedom, 451
 physical significance of electromagnetic, 420
 polarized fluids, 463, 572, 784
 single ion, 778
 surface integral of stress and, 422
 Force-coenergy relations, 72, E5, G5
 Force density, 7
 averaging of electric, 440
 averaging of magnetic, 419
 divergence of stress tensor and, 422, 427, G9
 effect of permeability on, 455, 456
 elastic medium, 667
 electric, 12, B3, 440, G11
 magnetic field systems, 419, 462, G11
 electromagnetic fluid, 732
 electrostriction, 465, G11
 fluid mechanical, 732
 fluid pressure, 736
 free current, 419, G11
 inviscid fluid mechanical, 737
 lumped parameter model for, 455
 magnetic, 12, 419, B9
 magnetization, 448, 450, 462, G11
 magnetostriction, 461, 462, G11
 polarization, 450, 463, G11
 summary of, 448, G11
 Forced related to variable capacitance, 75
 Force-energy relations, 67, E5, G5
 examples of, 70
 Force equations, elastic media, 653
 Force of electric origin, 60, E5, G5
 Fourier series, 340
 Fourier transform, two-dimensional, 617
 Fourier transforms and series, diffusion

- equation and, 340
- eigenmodes as, 517
- linear continuum systems and, 511, 554, 617
- linear lumped systems and, 200
- mutual inductance expansions and, 108, 153
- Frame of reference, laboratory, 254
- Free-body diagram, 49
- Free charge density, B28
- Free charge forces, avoidance of, 787
- Frequency, complex, 181, 554
 - complex angular, 554
 - natural, 181, 515
 - voltage tuning of, 704
- Frequency conditions for power conversion, 111, 155
- Frequency response of transducer, 204
- Friction, coulomb, 42
- Frozen fields, perfectly conducting gas and, 849
- Fusion machines, instability of, 571
- Galilean transformation, 584
- Gamma rays, B13
- Gas, perfect, 816
- Gas constant, 816
 - universal, 816
- Gases, definition of, 724
 - ionized, 813
- Gauss's law, differential form of, B5
 - example of, B4
 - integral form of, B3
 - magnetic field, B12
 - polarization and, B28
- Gauss's theorem, tensor form of, 423, G9
- Generators, electric field, 778
 - electrohydrodynamic applications of, 3
 - hydroelectric, 152
 - induction, 134
 - magnetohydrodynamic applications of, 3
 - MHD, 744
 - Van de Graaff, 3, 383, 385
- Geometrical compatibility, 53
- Geophysics and MHD, 552
- Gravitational potential, 733
- Gravity, artificial electric, 785
 - force density due to, 732
 - waves, 794
- Group velocity, 614
 - power flow and, 638
 - unstable media and, 617
- Guiding structures, evanescence in, 560
- Hartmann flow, 884
- Hartmann number, 887
- Heat transfer, EHD and, 552
- Homogeneity, B27
- Homogeneous differential equation, solution of, 180
- Homopolar machine, 286, 312
 - armature voltage for, 314
 - speed coefficient for, 314
 - summary of equations for, 316
 - torque for, 316
- Hunting transient of synchronous machine, 192
- Hydraulic turbine, 151
- Hydroelectric generator, 152
- Hydrodynamic equilibria, 561, 571
- Hysteresis, magnetic, B27
- Identities, C1, E1, G1
- Impedance, characteristic, 497
- Incompressibility, fluid, 735
- Incompressible fluids, MHD, 737
- Incompressible media, 380
- Incremental motions, *see* Linearization
- Independence of variables, 69, 97 (*see* Problem 3.16)
- Independent variables, change of, 72
- Index notation, 421, G7
- Inductance, calculation of, 22
 - electrical linearity and, 20
 - generalized, 17
 - quasi-static limit and, B18
- Induction, demonstration of motional, 253
 - law of, B9; *see also* Faraday's law
- Induction brake, 134
- Induction generator, 134
 - electric, 400
- Induction interaction, 367
- Induction law, integral, B32; *see also* Faraday's law
- Induction machine, 127
 - coefficient of coupling for, 135
 - distributed linear, 368
 - efficiency of, 134
 - equivalent circuit for, 131
 - loading of, 137
 - lumped-parameter, 368
 - MHD, 745
 - power flow in, 133
 - reactance and resistance dominated, 137
 - single phase, 138
 - squirrel-cage, 129
 - starting of, 137, 139
 - torque in, 132
 - torque-slip curve of, 135
 - variable resistance in, 136
 - wound rotor, 106
- Induction motor, 134
- Inductor, 17
- Inelastic behavior of solids, 699
- Influence coefficients, MHD, 822
 - variable-area MHD machine, 832
- Initial and boundary conditions, 513
- Initial conditions, convection and, 587
 - one-dimensional continuum, 488, 512
- Initial value problem, continuum, 488
- Instability, absolute, 566
 - and convective, 604
 - aeroelastic absolute, 793
 - convective, 601
 - dynamic, 192
 - electrohydrodynamic, 571
 - engineering limitations from convective, 604

- and equilibrium, example of, 185
- failure of a static argument to predict, 192
- fluid pendulum, 785
- fluid turbulence and, 725
- graphical determination of, 184
- heavy on light fluid, 571
- and initial conditions, 184
- kink, 627
- linear and nonlinear description of, 216
- nonconvective, 566
- nonlinearity and, 570
- omega- k plot for, 569
- plasma, 553
- in presence of motion, 583
- Rayleigh-Taylor, 571
- resistive wall, 576, 608
- space-time dependence of absolute, 570
- static, 182
- in stationary media, 554
- Integral laws, electromagnetic, 9, B32, E3, G3
- Integrated electronics, electromechanics and, 688
- Integration contour, deforming, 11, B32
- Internal energy, perfect gas, 816
- Invariance of equations, 256
- Inviscid fluid, boundary condition for, 752
- Ion beams, 552
- Ion conduction, moving fluid and, 778
- Ion drag, efficiency of, 782
- Ion-drag phenomena, 776
- Ionized gases, acceleration of, 746
- Ion source, 776
- Isotropic elastic media, 660
- Isotropy, B27

- Kinetic energy, 214
- Kirchhoff's current law, 16
- Kirchhoff's laws, 15
 - electromechanical coupling and, 84
- Kirchhoff's voltage law, 16
- Klystron, 601
- Kronecker delta function, 421, G7

- Lagrangian coordinates, 652
 - surface in, 669
- Lagrangian description, 727
- Lagrangian to Eulerian descriptions, 483
- Lamé constant, 667
 - numerical values of, 677
- Laplace's equation, fluid dynamics and, 737
 - two-dimensional flow and, 751
- Leakage resistance of capacitors, 377
- Legendre transformation, 73
- Length expander bar, equivalent circuit for, 716
 - piezoelectric, 712
- Levitating force, induction, 369
- Levitation, electromechanical, 4, 195, 365, 370
 - demonstration of magnetic, 370
 - and instability, 574
 - of liquids, EHD, 552
 - MHD, 552
 - solid and liquid magnetic, 365
- Light, velocity of, B14
- Linearity, electrical, 20, 30, B27
- Linearization, continuum, 483, 510, 556, 652, 842
 - error from, 224
 - lumped-parameter, 182
- Linear systems, 180
- Line integration in variable space, 64, 67
- Liquid drops, charge-carrying, 388
- Liquid level gauge, 416
- Liquid metal brush, 878
 - numerical example of, 883
- Liquid metal MHD, numerical example of 750
- Liquid metals, pumping of, 746
- Liquid orientation in fields, 785
- Liquids, definition of, 724
- Liquids and gases, comparison of, 724
- Loading factor, MHD machine, 833
- Lodestone, B25
- Long-wave limit, 283, 574
 - thin elastic rod and, 683
- Lord Kelvin, 389
- Lorentz force, 419
- Loss-dominated dynamics, continuum, 576
- Loss-dominated electromechanics, 229, 249
- Loss-dominated systems, 227
- Losses, fluid joule, 815
- Loudspeaker, model for, 527
- Lumped-parameter electromechanics, 60
- Lumped-parameter variables, summary of, 35, E4, G4

- Mach lines, 624
- Mach number, 624, 823
- Macroscopic models, electromagnetic, B25
- Magnet, permanent, 27
- Magnetic axes of rotating machines, 105
- Magnetic circuit, example of, 22, 23
- Magnetic diffusion, 330, 335
 - charge relaxation compared to, 401
 - competition between motion and, 351
 - cylindrical geometry and, 408
 - effect of motion on, 354
 - electrical transient, 338
 - induction machines and, 746
 - initial conditions for, 339
 - limit, of infinite conductivity in, 343
 - of small conductivity in, 343
 - liquid metals and, 354
 - lumped-parameter models for, 331, 334, 336
 - sinusoidal steady-state, 358
 - sinusoidal steady-state with motion, 355
 - steady-state, 337, 347
 - steady-state in the moving frame, 351
 - traveling-wave moving media, 364
- Magnetic diffusion time, 341, 772
- Magnetic field, air-gap, 114
 - induced and imposed, 212, 286, 332
 - origin of earths, 336, 552
- Magnetic field compression, 354
- Magnetic field equations, insulating me-

- dium, 773
 Magnetic field intensity, 7, B25
 Magnetic field system, 6, B19
 differential equations for, 6, B20, E6, G6
 integral equations for, 10, B32, E3, G3
 Magnetic field transformation, example of, 266; *see also* Transformations
 Magnetic fluid, demonstration of, 777
 Magnetic flux density, 7, B6
 Magnetic flux lines, frozen, 763
 Magnetic force, field description of, 418, G11
 stress tensor for, 422, G11
 Magnetic forces and mechanical design, 697
 Magnetic induction negligible, B19
 Magnetic piston, 354
 Magnetic pressure, 369
 Magnetic Reynolds numbers, 333, 349, 351, 353, 357, 401, 628, 741, 821
 MHD flow, 754
 numerical value of, 354
 Magnetic saturation in commutator machines, 297
 Magnetic surface force, 447
 Magnetic tension, 767
 Magnetization, B25
 effect of free current forces on, 455
 Magnetization currents, B25
 Magnetization density, 7, B25
 Magnetization force, fluids and, 772
 one degree of freedom and, 451
 Magnetization force density, changes in density and, 461
 example of, 460
 inhomogeneity and, 460
 in moving media, 285
 summary of, 448, G11
 Magnetoacoustic velocity, 850
 Magnetoacoustic wave, 846
 electrical losses and, 860
 flux and density in, 851
 numerical example, in gas, 852
 in liquid, 853
 Magnetoelasticity, 553
 Magnetofluid dynamics, 551
 Magnetogasdynamics, 551
 Magnetohydrodynamic conduction machine, 740
 Magnetohydrodynamic generator, constant-area, 821
 variable-area, 828
 Magnetohydrodynamics, 551
 constant-area channel, 740
 viscosity and, 725
 Magnetohydrodynamics of viscous fluids, 878
 Magnetostriction, 697
 one degree of freedom and, 452
 Magnetostriction force, incompressible fluid and, 776
 Magnetostrictive coupling, 707
 Magnetostrictive transducer, terminal representation of, 711
 Mass, conservation of fluid, 729
 elastic continua, quasi-static limit of, 507
 lumped-parameter, 36, 43
 total, 46
 Mass conservation, 731
 Mass density, 45
 elastic materials, numerical values of, 486
 of solid, 486
 numerical values of, 486, G12
 Mass per unit area of membrane, 509
 Mass per unit length of wire, 511
 Matched termination, 497
 Material motion, waves and instabilities with, 583
 Matter, states of, 724
 Maxwell, 1
 Maxwell's equations, B12
 limiting forms of, B14
 Maxwell stress tensor, 420, 441, G7, G11
 Mechanical circuits, 36
 Mechanical continuum, 479
 Mechanical equations, lumped-parameter, 49
 Mechanical input power, fluid, 756
 variable-area channel, 756
 Mechanical lumped-parameter equations, examples of, 49, 51, 53
 Mechanics, lumped-parameter, 35
 rigid body, 35
 transformations and Newtonian, 254
 Membrane, elastic continua and, 509, 535, electric field and, 574
 equations of motion for, 511, 535, G13
 two-dimensional modes of, 622
 Membrane dynamics with convection, 584
 Mercury, density and conductivity of, 750
 properties of, 883
 Meteorology, EHD and, 552
 MFD, 551; *see also* MHD
 MGD, 551; *see also* MHD
 MHD, 551
 compressible fluids and, 813
 liquid metal numerical example of, 750
 magnetic damping in, 750
 transient effects in, 746, 759
 transient example of, 750
 variable-area channel in, 751
 of viscous fluids, 878
 MHD conduction machine, 821, 828
 equivalent circuit for, 742
 pressure drop in, 742
 terminal characteristics of, 742
 MHD constant-area channel, 740, 820
 MHD flows, dynamic effects in, 746
 MHD generator, comparison of, 839
 compressibility and, 820
 constant voltage constrained, 743
 distribution of properties in, 827
 end effects in, 797
 examples of, 840, 841
 Mach number in, 823
 numerical example of, 826
 temperature in, 823
 variable-area channel, 828
 viscosity and, 725, 884

- MHD machine, compressible and incompressible, 825
 constant velocity, loading factor and aspect ratio, 834
 dynamic operation of, 746
 equivalent circuit for variable area, 756
 loading factor of, 833
 operation of brake, pump, generator, 744
 quasi-one-dimensional, 828
 steady-state operation of, 740
 velocity profile of, 891
- MHD plane Couette flow, 884
 MHD plane Poiseuille flow, 878
 MHD pressure driven flow, 884
 MHD pump or accelerator, 824
 MHD transient phenomena, 759
- MHD variable-area channel equations, conservation of energy and, 831, 833
 conservation of mass and, 831, 833
 conservation of momentum and, 831, 833
 local Mach number and, 823, 833
 local sound velocity and, 822, 833
 mechanical equation of state and, 816, 833
 Ohm's law and, 830, 833
 thermal equations of state and, 820, 833
- MHD variable-area machine, equations for, 833
- MHD variable-area pumps, generators and brakes, 751
- Microphone, capacitor, 201
 fidelity of, 204
 Microphones, 200
- Microwave magnetics, 553
 Microwave power generation, 552
- Mobility, 289, B31
 ion, 778
- Model, engineering, 206
- Modulus of elasticity, 485
 numerical values of, 486, G12
- Molecular weight of gas, 816
- Moment of inertia, 36, 48
- Momentum, conservation of, *see* Conservation of momentum
- Momentum density, fluid, 734
- Motor, commutator, 140, 291
 induction, 134
 reluctance, 156
 synchronous, 119
- Moving media, electromagnetic fields and, 251
- Mutual inductance, calculation of, 22
- Natural frequencies, 515
 dispersion equation and, 517
- Natural modes, dispersion and, 561
 kink instability, 635
 of membrane, 624, 625
 overdamped and underdamped, 583
 of unstable wire, 569
- Navier-Stokes equation, 872
- Negative sequence currents, 144
- Networks, compensating, 198
- Newtonian fluids, 861
- Newton's laws, 15, 35
 elastic media and, 653
- Newton's second law, 44, 50
 electromechanical coupling and, 84
 fluid and, 729, 731
- Node, mechanical, 36, 49
- Nonlinear systems, 206, 213
- Nonuniform magnetic field, motion of conductor through, 367
- Normal modes, 511
 boundary conditions and, 524
- Normal strain and shear stress, 662
- Normal stress and normal strain, 661
- Normal vector, analytic description of, 269
- Oerstad, 1, B25
- Ohm's law, 7, B30
 for moving media, 284, 298
- Omega- k plot, absolutely unstable wire, 567
 amplifying wave, 603
 convective instability, 603
 damped waves, complex k for real omega, 579
 elastic guided shear waves, 695
 electron oscillations, 601
 evanescent wave, 557, 559, 597, 615, 695
 moving wire, with destabilizing magnetic force, 603
 with resistive wall, complex k for real omega, 611
 with resistive wall, complex omega for real k , 610
- ordinary wave, with convection, 594
 on wires and membranes, 514
- ordinary waves, 514, 555
- unstable eigenfrequencies and, 569
- waves with damping showing eigenfrequencies, 582
- wire stabilized by magnetic field, 557
- Orientation, electrohydrodynamic, 571
 electromechanical, 4
 of liquids, dielectrophoretic, 785
 EHD, 552
- Orthogonality, eigenfunctions and, 341, 519, 520
- Oscillations, nonlinear, 226
 with convection, 596
- Oscillators in motion, 599
- Overstability, 192
- Particles, charge carriers and, 782
- Particular solution of differential equation, 180
- Pendulum, hydrodynamic, 746
 simple mechanical, 214
- Perfect conductor, no slip condition on, 769
- Perfect gas law, 816
- Perfectly conducting gas, dynamics of, 846
- Perfectly conducting media, *see* Conductor
- Permanent magnet, in electromechanics, 27
 example of, 28
 as rotor for machine, 127
- Permanent set, solids and, 700

- Permeability, 7, B27
 - deformation and, 459
 - density dependence of, 454
 - free space, 7, B7
- Permittivity, 9, B30
 - free space, 7, 9, B2
- Perturbations, 183
- Phase sequence, 144
- Phase velocity, 613
 - diffusion wave, 358
 - dispersive wave, 598
 - membrane wave, 512
 - numerical elastic compressional wave, 677
 - numerical elastic shear wave, 677
 - numerical thin rod, 486, G12
 - ordinary wave, 487
 - thin rod, 487
 - wire wave, 512
- Physical acoustics, 553, 651
- Piezoelectric coupling, 711
 - reciprocity in, 712
- Piezoelectric devices, example of, 717
- Piezoelectricity, 553, 711
- Piezoelectric length expander bar, 712
- Piezoelectric resonator, equivalent circuit for, 716
- Piezoelectric transducer, admittance of, 714
- Piezomagnetism, 553
- Plane motion, 44
- Plasma, confinement of, 552
 - electromechanics and, 4
 - evanescent waves in, 561, 638
 - heating of, 552
 - lumped-parameter model for, 223
 - magnetic bottle for, 563
 - magnetic diffusion and, 408
 - MHD and, 553
 - solid state, 553
- Plasma dynamics, 553
- Plasma frequency, 600
- Poiseuille flow, plane, 878
- Poisson's ratio, 662
 - numerical values of, 666
- Polarization, effect of motion on, 290
 - current, B29
 - density, 7, B28
 - electric, B27
 - force, 463, 571, G11
- Polarization force, one degree of freedom, 464
- Polarization interactions, liquids and, 783
- Polarization stress tensor, 463, G11
- Pole pairs, 148
- Poles in a machine, 146
- Polyphase machines, 142
- Position vector, 45
- Positive sequence currents, 144
- Potential, electric, B9
 - electromagnetic force, 738
 - gravitational, 733
 - mechanical, 214
 - velocity, 737
- Potential difference, B10
- Potential energy, 214
- Potential flow, irrotational electrical forces and, 738
- Potential fluid flow, two-dimensional, 751
- Potential plot, 214
- Potential well, electrical constraints and, 217
 - electromechanical system and, 217
 - temporal behavior from, 224
- Power, conservation of, 64
- Power density input to fluid, 818
- Power factor, 126
- Power flow, group velocity and, 638
 - ordinary and evanescent waves and, 638
 - rotating machines and, 110
- Power generation, ionized gases and, 552
 - microwave, 552, 553
- Power input, electrical, 64
 - fluid electrical, 818
 - mechanical, 64
 - mechanical MHD, 743
- Power input to fluid, electric forces and, 819
 - electrical losses and, 818, 819
 - magnetic forces and, 818
 - pressure forces and, 818
- Power output, electric MHD, 743
- Power theorem, wire in magnetic field, 637, 644
- Poynting's theorem, B22
- Pressure, density and temperature dependence of, 816
 - hydrostatic, 735
 - hydrostatic example of, 736
 - incompressible fluids and significance of, 753
 - isotropic, 735
 - magnetic, 369
 - normal compressive stress and, 735
 - significance of negative, 753
 - velocity and, 753
- Principal axes, 49
- Principal modes, 681
 - elastic structure, 679
 - shear wave, 695
- Principle of virtual work, *see* Conservation, of energy
- Products of inertia, 48
- Propagation, 613
- Propulsion, electromagnetic, 552
 - electromechanical, 4
 - MHD space, 746
- Pulling out of step for synchronous machine, 125
- Pump, electric field, 776
 - electrostatic, 778
 - liquid metal induction, 365
 - MHD, 744, 746
 - variation of parameters in MHD, 825
- Pumping, EHD, 552
 - MHD, 552
- Quasi-one-dimensional model, charge relaxa-

- tion, 392, 394
- electron beam, 600
- gravity wave, 794
- magnetic diffusion, 347
- membrane, 509, 648
 - and fluid, 793
- MHD generator, 828
- thin bar, 712
- thin beam, 683
- thin rod, 480, 681
- wire or string, 509
 - in field, 556, 563, 574, 605, 627
- Quasi-static approximations, 6, B17
- Quasi-static limit, sinusoidal steady-state
 - and, 515, 534
 - wavelength and, B17
 - wire and, 534
- Quasi-statics, conditions for, B21
 - correction fields for, B21
 - elastic media and, 503
 - electromagnetic, B19
- Quasi-static systems, electric, 8
 - magnetic, 6
- Radiation, heat, 815
- Rate of strain, 864
- Reactance-dominated dynamics, 138, 211, 220, 242, 336, 354, 368, 563, 759
- Reciprocity, electromechanical coupling
 - and, 77
 - piezoelectric coupling and, 713
- Reference system, inertial, 44
- Regulation, transformer design and, 699
- Relative displacement, rotation, strain and, 658
- Relativity, Einstein, 254
 - Galilean, 255
 - postulate of special, 261
 - theory of, 44
- Relaxation time, free charge, 372
 - numerical values of, 377
- Relay, damped time-delay, 229
- Reluctance motor, 156
- Resistance-dominated dynamics, 138, 209, 233, 242, 336, 354, 368, 503, 583, 611
 - MHD, 750
- Resistive wall damping, continuum, 583
- Resistive wall instability, nature of, 612
- Resistive wall wave amplification, 608
- Resonance, electromechanically driven
 - continuum and, 533
 - response of continua and, 515
- Resonance frequencies, magnetic field
 - shift of, 563
 - membrane, 624
 - natural frequencies and, 515
- Resonant gate transistor, 688
- Response, sinusoidal steady-state, 181, 200, 514
- Rigid body, 44
- Rigid-body mechanics, 35
- Rotating machines, 103
 - air-gap magnetic fields in, 114
 - applications of, 3
 - balanced two-phase, 113
 - classification of, 119
 - commutator type, 140, 255, 292
 - computation of mutual inductance in, 22
 - dc, 140, 291
 - differential equations for, 106
 - effect of poles on speed of, 149
 - electric field type, 177
 - energy conversion conditions for, 110
 - energy conversion in salient pole, 154
 - equations for salient pole, 151
 - hunting transient of synchronous, 192
 - induction, 127
 - losses in, 109
 - magnetic saturation in, 106
 - mutual inductance in, 108
 - number of poles in, 146
 - polyphase, 142
 - power flow in, 110
 - salient pole, 103, 150
 - single-phase, 106
 - single-phase salient-pole, 79
 - smooth-air-gap, 103, 104
 - stresses in rotor of, 697
 - superconducting rotor in, 92
 - synchronous, 119
 - two-phase, smooth-air-gap, 111
 - winding distribution of, 108
- Rotating machines, physical structure,
 - acyclic generator, 287
 - commutator type, 292
 - dc motor, 293
 - development of dc, 295
 - distribution of currents and, 166, 169
 - four-pole, salient pole, 164
 - four-pole, single phase, 147
 - homopolar, 313
 - hydroelectric generator, 152
 - multiple-pole rotor, 146
 - rotor of induction motor, 107
 - rotor of salient-pole synchronous, 151
 - synchronous, salient-pole, 152
 - salient-pole, two phase, 158
 - salient-pole, single phase, 150
 - smooth-air-gap, single phase, 104
 - stator for induction motor, 106
 - three-phase stator, 145
 - turboalternator, 120
 - two-pole commutator, 294
- Rotation, fluid, 865
- Rotation vector, 658
- Rotor of rotating machines, 104, 107, 112, 120, 146, 147, 150, 151, 152, 158, 164, 166, 169
- Rotor teeth, shield effect of, 301
- Saliency in different machines, 156
- Salient-pole rotating machines, 103, 150
- Salient poles and dc machines, 293
- Servomotor, 140
- Shading coils in machines, 139
- Shear flow, 862, 864, 875

- magnetic coupling, 878
- Shear modulus, 664
 - numerical values of, 666
- Shear rate, 866
- Shear strain, 543, 655
 - normal strain and, 663
 - shear stress and, 664
- Shear stress, 543
- Shear waves, elastic slab and, 693
- Shearing modes, beam principal, 683
- Shock tube, example related to, 276
- Shock waves, supersonic flow and, 592
- Sinusoidal steady-state, 181, 200, 514
 - convection and establishing, 592
- Sinusoidal steady-state response, elastic continua, 514
- Skin depth, 357
 - numerical values of, 361
- Skin effect, 358
 - effect of motion on, 361
- Slip of induction machine, 131
- Slip rings, 120
 - ac machines and, 120
- Slots of dc machine, 296
- Sodium liquid, density of, 771
- Solids, definition of, 724
- Sound speed, gases, 844
 - liquids, 845
- Sound velocity, *see* Velocity
- Sound waves, *see* Acoustic waves
- Source, force, 37
 - position, 36
 - velocity, 37
- Space charge, fluid and, 780
- Space-charge oscillations, 601
- Speakers, 200
- Specific heat capacity, constant pressure, 817
 - constant volume, 816
 - ratio of, 817
- Speed coefficient, of commutator machine, 300
 - torque on dc machine and, 302
- Speed control of rotating machines, 149
- Speedometer transducer, 170
- Speed voltage in commutator machine, 299
- Spring, linear ideal, 38
 - lumped element, 36, 38
 - quasi-static limit of elastic continua and, 505
 - torsional, 40
- Spring constant, 39
- Stability, 182, 566, 583
- Stagnation point, fluid, 752
- Standing waves, electromagnetic, B16
 - electromechanical, 516, 559, 596, 771
- State, coupling network, 61, 65
 - thermal, 816
- Stator, of rotating machines, 104, 106, 120, 145, 147, 150, 152, 158, 164, 166, 169
 - smooth-air-gap, 103
- Stinger, magnetic, 193
- Strain, formal derivation of, 656
 - geometric significance of, 654
 - normal, 654
 - permanent, 700
 - shear, 543, 654
 - as a tensor, 659
 - thin rod, normal, 484
- Strain components, 656
- Strain-displacement relation, 653
 - thin-rod, 485
- Strain rate, 724, 864
 - dilatational, 869
- Strain-rate tensor, 864
- Streaming electron oscillations, 600
- Streamline, fluid, 752
- Stress, fluid isotropy and, 868
 - fluid mechanical, 872
 - hydrostatic, 724
 - limiting, 700
 - normal, 432
 - shear, 432, 543
 - and traction, 424, G9
- Stress components, 425
- Stress-strain, nonlinear, 700
- Stress-strain rate relations, 868
- Stress-strain relation, 660, 668
 - thin-rod, 485
- Stress-tensor, elastic media and, 667
 - example of magnetic, 428
 - magnetization, 462, G11
 - Maxwell, 420
 - physical interpretation of, 425, G7
 - polarization, 463, G11
 - pressure as, 735
 - properties of, 423, G7
 - surface force density and, 446, G9
 - symmetry of, 422
 - total force and, 444, G9
- Stress tensors, summary of, 448, G11
- String, convection and, 584
 - equation of motion for, 511, 535
 - and membrane, electromechanical coupling to, 522
 - see also* Wire
- Subsonic steady MHD flow, 823
- Subsonic velocity, 587
- Substantial derivative, 259, 584, 726; *see also* Convective derivative
- Summation convention, 421, G7
- Superconductors, flux amplification in, 354
- Supersonic steady MHD flow, 823
- Supersonic steady-state dynamics, 524
- Supersonic velocity, 587
- Surface charge density, free, 7
- Surface conduction in moving media, 285
- Surface current density, free, 7
- Surface force, example of, 449
 - magnetization, 775
- Surface force densities, summary of, 448, G11
- Surface force density, 445, G11
 - free surface charge and, 447, G11
 - free surface currents and, 447, G11
- Surface tension, 605
- Susceptance, electromechanical driving, 531
- Susceptibility, dielectric, 9, B30
 - electric, 9, B30
 - magnetic, 7, B27
- Suspension, magnetic, 193

- Symbols, A1, D1, F1
- Symbols for electromagnetic quantities, 7
- Synchronous condenser, 127
- Synchronous machine, 119
 - equivalent circuit of, 123
 - hunting transient of, 192
 - phasor diagram for, 124, 162
 - polyphase, salient-pole, 157
 - torque in, 122, 123, 125
 - torque of salient-pole, two-phase, 160, 162
- Synchronous motor, performance of, 126
- Synchronous reactance, 123
- Synchronous traveling-wave energy conversion, 117
- Tachometer, drag-cup, 363
- Taylor series, evaluation of displacement with, 483
 - multivariable, 187
 - single variable, 183
- Teeth of dc machine, 296
- Temperature, electrical conductivity and, 380
- Tension, of membrane, 509
 - of wire, 511
- Tensor, first and second order, 437
 - one-dimensional divergence of, 482
 - surface integration of, 428, 441, 444, G9
 - transformation law, 437, G10
 - transformation of, 434, G9
- Tensor strain, 659
- Tensor transformation, example of, 437
- Terminal pairs, mechanical, 36
- Terminal variables, summary of, 35, E4, G4
- Terminal voltage, definition of, 18
- Theorems, C2, E2, G2
- Thermonuclear devices, electromechanics and, 4
- Thermonuclear fusion, 552
- Theta-pinch machine, 408
- Thin beam, 683
 - boundary conditions for, 687
 - cantilevered, 688
 - deflections of, 691, 692
 - eigenvalues of, 692
 - electromechanical elements and, 688, 691, 701, 704
 - equation for, 687
 - resonance frequencies of, 692
 - static loading of, 701
- Thin rod, 681
 - boundary conditions for, 494
 - conditions for, 683
 - equations of motion for, 485, G13
 - force equation for, 484
 - longitudinal motion of, 480
 - transverse motions of, 682
- Three-phase currents, 143
- Time constant, charge relaxation, 372
 - magnetic diffusion, 341
- Time delay, acoustic and electromagnetic, 499
- Time-delay relay, electrically damped, 249
- Time derivative, moving coordinates and, 258
- Time rate of change, moving grain and, 727
- Torque, dc machine, 302
 - electrical, 66
 - Lorentz force density and, 301
 - pull-out, 124
- Torque-angle, 123
- Torque-angle characteristic of synchronous machine, 125
- Torque-angle curve, salient-pole synchronous machine, 163
- Torque-slip curve for induction machine, 135
- Torque-speed curve, single phase induction machine, 139
- Torsional vibrations of thin rod, 543
- Traction, 424, 432
 - pressure and, 735
 - stress and, 432, G9
- Traction drives, 310
- Transducer, applications of, 2
 - continuum, 704
 - example of equations for, 84, 86
 - fidelity of, 203
 - incremental motion, 180, 193, 200
 - Magnetostrictive, 708
- Transfer function capacitor microphone, 204
- electromechanical filter, 706
- Transformations, electric field system, 264
 - Galilean coordinate, 254, 256
 - integral laws and, 11, 276, 300, 315, B32
 - Lorentz, 254
 - Lorentz force and, 262
 - magnetic field system, 260
 - primed to imprimed frame, 439
 - summary of field, 268, E6, G6
 - vector and tensor, 434, G9
- Transformer, electromechanical effects in, 697
 - step-down, 698
 - tested to failure, 698
- Transformer efficiency, mechanical design and, 699
- Transformer talk, 697
- Transient response, convective instability, 621
 - elastic continua, 517
 - MHD system, 751
 - one-dimensional continua, 511
 - superposition of eigenmodes in, 518
 - supersonic media, 593
- Transient waves, convection and, 587
- Transmission line, electromagnetic, B16
 - parallel plate, B15
 - thin rod and, 488
- Transmission without distortion in elastic structures, 696
- Traveling wave, 487
 - convection and, 586
 - magnetic diffusion in terms of, 357
 - single-phase excitation of, 118
 - standing wave and, 116
 - two-dimensional, 622
 - two-dimensional elastic, 694
 - two-phase current excitation of, 116
- Traveling-wave induction interaction, 368
- Traveling-wave MHD interaction, 746
- Traveling-wave solutions, 554
- Traveling-wave tube, 602
- Turboalternator, 120
- Turbulence in fluids, 725
- Turbulent flow, 43

- Ultrasonic amplification, 602
- Ultrasonics in integrated electronics, 688
- Units of electromagnetic quantities, 7
- Van de Graaff generator, example of, 383, 385
 - gaseous, 778
- Variable, dependent, 180
 - independent, differential equation, 180
 - thermodynamic independent, 64
- Variable capacitance continuum coupling, 704
- V curve for synchronous machine, 125
- Vector, transformation of, 434, 659
- Vector transformation, example of, 435
- Velocity, absolute, 44
 - acoustic elastic wave, 673, 677
 - acoustic fluid wave, 844, 846
 - Alfvén wave, 763, 772
 - charge-average, B5
 - charge relaxation used to measure, 396
 - charge relaxation wave, 395
 - compressional elastic wave, 673, 677
 - dilatational elastic wave, 673, 677
 - elastic distortion wave, 675, 677
 - fast and slow wave, 586
 - light wave, B14
 - magnetic diffusion wave, 358
 - magnetic flux wave, 114
 - magnetoacoustic wave, 850, 852
 - measurement of material, 356, 362
 - membrane wave, 512
 - phase, 488
 - shear elastic wave, 675, 677
 - thin rod wave, 486, 487, 682
 - wavefront, 618
 - with dispersion, 598
 - wire or string wave, 512
- Velocity potential, 737
- Viscosity, 862
 - coefficient of, 863
 - examples of, 875
 - fluid, 724
 - mathematical description of, 862
 - second coefficient of, 871
- Viscous flow, pressure driven, 877
- Viscous fluids, 861
- Viscous losses, turbulent flow, 725
- Voltage, definition of, B10
 - speed, 20, 21
 - terminal, 18
 - transformer, 20, 21
- Voltage equation, Kirchhoff, 16
- Ward-Leonard system, 307
- Water waves, 794
- Wave amplification, 601
- Wave equation, 487
- Wavenumber, 357, 513
 - complex, 554, 607
- Wave propagation, 487
 - characteristics and, 487, 586, 618
 - group velocity and, 616
 - phase velocity and, 613
- Wave reflection at a boundary, 493
- Waves, acoustic elastic, 673
 - acoustic in fluid, 544, 841, 842, 845
 - Alfvén, 759
 - compressional elastic, 673
 - convection and, 586
 - cutoff, *see* Cutoff waves
 - damping and, 576
 - diffusion, 355, 576
 - dilatational, 672
 - dispersionless, 555
 - dispersion of, 488
 - of distortion, 675
 - elastic shear, 678
 - electromagnetic, B13, 488
 - electromechanical in fluids, 759
 - evanescent, *see* Evanescent waves
 - fast and slow, 586
 - fast and slow circularly polarized, 631
 - fluid convection and, 860
 - fluid shear, 760
 - fluid sound, 813
 - incident and reflected at a boundary, 494
 - light, B13
 - longitudinal elastic, 673
 - magnetoacoustic, 841, 846
 - motion and, 583
 - plasma, 553, 600, 638
 - radio, B13
 - rotational, 671
 - shear elastic, 675
 - stationary media and, 554
 - surface gravity, 794
 - thin rod and infinite media, 673
- Wave transients, solution for, 490
- Wind tunnel, magnetic stinger in, 193
- Windings, balanced two-phase, 113
 - dc machine, 292
 - lap, 296
 - wave, 296
- Wire, continuum elastic, 509, 535
 - convection and dynamics of, 584
 - dynamics of, 554
 - equations of motion for, 511, G13
 - magnetic field and, 556, 566, 627
 - two-dimensional motions of, 627
- Yield strength, elastic, 700
- Young's modulus, 485, G12
- Zero-gravity experiments, KC-135 trajectory and, 787